GEOLOGICAL SURVEY OF CANADA
COMMISSION GÉOLOGIQUE DU CANADA

**PAPER/ÉTUDE**
**92-1C**

# CURRENT RESEARCH, PART C
# CANADIAN SHIELD

# RECHERCHES EN COURS, PARTIE C
# BOUCLIER CANADIEN

Energy, Mines and Resources Canada
Énergie, Mines et Ressources Canada

Canada

THE ENERGY OF OUR RESOURCES - THE POWER OF OUR IDEAS

L'ÉNERGIE DE NOS RESSOURCES - NOTRE FORCE CRÉATRICE

## NOTICE TO LIBRARIANS AND INDEXERS

The Geological Survey's Current Research series contains many reports comparable in scope and subject matter to those appearing in scientific journals and other serials. Most contributions to Current Research include an abstract and bibliographic citation. It is hoped that these will assist you in cataloguing and indexing these reports and that this will result in a still wider dissemination of the results of the Geological Survey's research activities.

## AVIS AUX BIBLIOTHÉCAIRES ET PRÉPARATEURS D'INDEX

La série Recherches en cours de la Commission géologique contient plusieurs rapports dont la portée et la nature sont comparables à ceux qui paraissent dans les revues scientifiques et autres périodiques. La plupart des articles publiés dans Recherches en cours sont accompagnés d'un résumé et d'une bibliographie, ce qui vous permettra, on l'espère, de cataloguer et d'indexer ces rapports, d'où une meilleure diffusion des résultats de recherche de la Commission géologique.

GEOLOGICAL SURVEY OF CANADA
COMMISSION GÉOLOGIQUE DU CANADA

**PAPER / ÉTUDE**
**92-1C**

# CURRENT RESEARCH, PART C
# CANADIAN SHIELD

---

# RECHERCHES EN COURS, PARTIE C
# BOUCLIER CANADIEN

**1992**

Available in Canada through

authorized bookstore agents and other bookstores

or by mail from

Canada Communication Group — Publishing
Ottawa, Canada K1A 0S9

and from

Geological Survey of Canada offices:

601 Booth Street
Ottawa, Canada K1A 0E8

3303-33rd Street N.W.,
Calgary, Alberta T2L 2A7

100 West Pender Street,
Vancouver, B.C. V6B 1R8

A deposit copy of this publication is also available for
reference in public libraries across Canada

Cat. No. M44-92/1C
ISBN 0-660-57064-5

Price subject to change without notice

**Cover description**

Ductilely folded high-strain zone in mafic and quartzofeldspathic gneisses showing "sheath fold" geometry, Barbour Bay, south shore of Chesterfield Inlet, Northwest Territories. Photo by M. Schau.

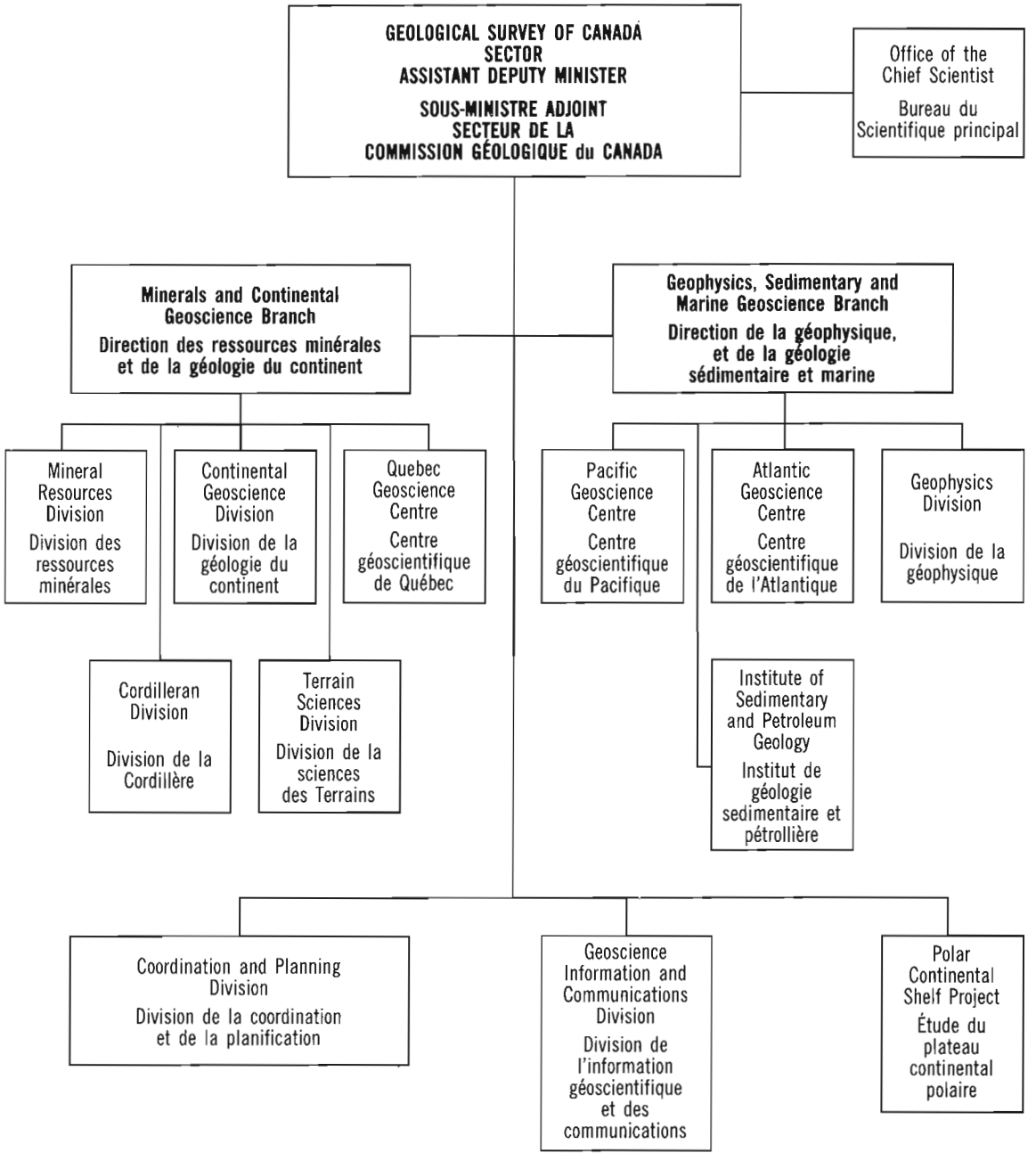
GEOLOGICAL SURVEY OF CANADA
SECTOR
ASSISTANT DEPUTY MINISTER
SOUS-MINISTRE ADJOINT
SECTEUR DE LA
COMMISSION GÉOLOGIQUE du CANADA
Office of the Chief Scientist
Bureau du Scientifique principal
Minerals and Continental Geoscience Branch
Direction des ressources minérales et de la géologie du continent
Geophysics, Sedimentary and Marine Geoscience Branch
Direction de la géophysique, et de la géologie sédimentaire et marine
Mineral Resources Division
Division des ressources minérales
Continental Geoscience Division
Division de la géologie du continent
Quebec Geoscience Centre
Centre géoscientifique de Québec
Pacific Geoscience Centre
Centre géoscientifique du Pacifique
Atlantic Geoscience Centre
Centre géoscientifique de l'Atlantique
Geophysics Division
Division de la géophysique
Cordilleran Division
Division de la Cordillère
Terrain Sciences Division
Division de la sciences des Terrains
Institute of Sedimentary and Petroleum Geology
Institut de géologie sedimentaire et pétrollière
Coordination and Planning Division
Division de la coordination et de la planification
Geoscience Information and Communications Division
Division de l'information géoscientifique et des communications
Polar Continental Shelf Project
Étude du plateau continental polaire

## Separates

A limited number of separates of the papers that appear in this volume are available by direct request to the individual authors. The addresses of the Geological Survey of Canada offices follow:

601 Booth Street
OTTAWA, Ontario
K1A 0E8
(FAX: 613-996-9990)

Institute of Sedimentary and Petroleum Geology
3303-33rd Street N.W.
CALGARY, Alberta
T2L 2A7
(FAX: 403-292-5377)

Cordilleran Division
100 West Pender Street
VANCOUVER, B.C.
V6B 1R8
(FAX: 604-666-1124)

Pacific Geoscience Centre
P.O. Box 6000
9860 Saanich Road
SIDNEY, B.C.
V8L 4B2
(Fax: 604-363-6565)

Atlantic Geoscience Centre
Bedford Institute of Oceanography
P.O. Box 1006
DARTMOUTH, N.S.
B2Y 4A2
(FAX: 902-426-2256)

Québec Geoscience Centre
2700, rue Einstein
C.P. 7500
Ste-Foy (Québec)
G1V 4C7
(FAX: 418-654-2615)

When no location accompanies an author's name in the title of a paper, the Ottawa address should be used.

## Tirés à part

On peut obtenir un nombre limité de «tirés à part» des articles qui paraissent dans cette publication en s'adressant directement à chaque auteur. Les adresses des différents bureaux de la Commission géologique du Canada sont les suivantes:

601, rue Booth
OTTAWA, Ontario
K1A 0E8
(facsimilé : 613-996-9990)

Institut de géologie sédimentaire et pétrolière
3303-33rd St. N.W.,
CALGARY, Alberta
T2L 2A7
(facsimilé : 403-292-5377)

Division de la Cordillère
100 West Pender Street
VANCOUVER, British Columbia
V6B 1R8
(facsimilé : 604-666-1124)

Centre géoscientifique du Pacifique
P.O. Box 6000
9860 Saanich Road
SIDNEY, British Columbia
V8L 4B2
(facsimilé : 604-363-6565)

Centre géoscientifique de l'Atlantique
Institut océanographique Bedford
B.P. 1006
DARTMOUTH, Nova Scotia
B2Y 4A2
(facsimilé : 902-426-2256)

Centre géoscientifique de Québec
2700, rue Einstein
C.P. 7500
Ste-Foy (Québec)
G1V 4C7
(facsimilé : 418-654-2615)

Lorsque l'adresse de l'auteur ne figure pas sous le titre d'un document, on doit alors utiliser l'adresse d'Ottawa.

## CONTENTS

# Precambrian geology and economic potential of the Meliadine Lake-Barbour Bay region, District of Keewatin, Northwest Territories

**S. Tella, Mikkel Schau, A.E. Armitage[1], B.E. Seemayer[2], and D. Lemkow**
**Continental Geoscience Division**

*Tella, S., Schau, M., Armitage, A.E., Seemayer, B.E., and Lemkow, D., 1992: Precambrian geology and economic potential of the Meliadine Lake-Barbour Bay region, District of Keewatin, Northwest Territories; in Current Research, Part C; Geological Survey of Canada, Paper 92-1C, p. 1-11.*

***Abstract***

*The Meliadine Lake area is underlain by an Archean (ca 2.63 Ga) supracrustal sequence which forms a regional scale, Archean $F_2$ syncline. Along the north limb, three sets of pre-$F_2$ mesoscopic folds are present in a turbidite-hosted, locally auriferous oxide iron-formation. An assemblage of biotite + chlorite in silicate-rich layers of the iron-formation is overprinted by random intergrowths of fine grained grunerite + hornblende + carbonate with pyrrhotite, and coarse hornblende +/- biotite with arsenopyrite. Textures suggest that gold mineralization is associated with S, Ca and $CO_2$ metasomatism, and is controlled by the youngest set of pre-$F_2$ folds.*

*The Archean lithologies in the Barbour Bay region are dominated by polydeformed quartzofeldspathic gneiss, migmatite, granitoid plutons, paragneiss, amphibolite, and garnetiferous, silicate iron-formation. Folded high-strain zones containing tectonized remnants of anorthosite, gabbro, and pegmatite transect the gneisses. Four sets of folds and one event of amphibolite grade metamorphism are recognized. The distribution of lithologies is controlled by west-plunging $F_3$ folds. The mapping indicates the presence of flat-lying, crustal-scale tectonic slabs.*

***Résumé***

*La région du lac Meliadine repose sur une séquence supracrustale archéenne (2,63 Ga environ) qui forme un synclinal $F_2$ archéen d'échelle régionale. Le long du flanc nord, trois séries de plis mésoscopiques antérieurs à $F_2$ se sont formées dans une formation ferrifère à faciès oxydé et, par endroits, aurifère logée dans des turbidites. Sur un assemblage de biotite + chlorite contenu dans des couches silicatées de la formation ferrifère, se superposent des enchevêtrements à orientation aléatoire au hasard de grunérite + hornblende + carbonate à grain fin, accompagnés de pyrrhotine, et de hornblende +/- biotite à grain grossier accompagnées d'arsénopyrite. Les textures indiquent que la minéralisation aurifère est associée à un métasomatisme de S, Ca et $CO_2$ et qu'elle est régie par le plus récent groupe de plis antérieurs à $F_2$.*

*Les lithologies archéennes dans la région de la baie Barbour sont surtout composées de gneiss quartzofeldspathique, de migmatite, de plutons granitoïdes, de paragneiss, d'amphibolite polydéformés et de formation ferrifère silicatée et grenatifère. Les zones très plissés contenant des restes tectonisés d'anorthosite, de gabbro et de pegmatite recoupent les gneiss. On distingue quatre séries de plis et un épisode de métamorphisme d'intensité correspondant au faciès des amphibolites. La répartition des lithologies est régie par des plis $F_3$ plongeant vers l'ouest. La cartographie révèle la présence de lambeaux tectoniques subhorizontaux d'échelle crustale.*

[1] Department of Geology, Laurentian University, Sudbury, Ontario, P3E 2C6
[2] Department of Geology, Lakehead University, Thunder Bay, Ontario, P7B 5E1

## INTRODUCTION

This report summarizes results of bedrock mapping (1:250 000 and 1:50 000 scales), undertaken during the 1991 field season in parts of Gibson Lake east-half (55N), Rankin Inlet (55K/16), and Meliadine Lake (55J/13) map areas. The study area (Fig. 1) is part of a region previously mapped by Wright (1967) at a scale of one inch to eight miles. The results of more recent regional mapping in areas surrounding the study area were previously reported by Reinhardt et al. (1980), Schau and Ashton (1980), Schau et al (1982), Tella and Annesley (1987,1988), and Tella et al. (1986,1989,1990). For a more comprehensive list of references to previous studies, the reader is referred to the above publications. Previous structural, stratigraphic, thermobarometric, and geochronological studies to the east and northeast within an Archean and Proterozoic granite-greenstone-gneiss terrane outlined several crustal-scale ductile, high-strain zones that separate and expose different levels of crust (Tella et al., 1990). Tectonic juxtaposition of these crustal segments is believed to have occurred in the early Proterozoic prior to emplacement of 1.85 Ga fluorite granites. The highlights of previous structural work are summarized in a schematic section (transect A-B, Fig. 1,2). For a more comprehensive account of tectonic synthesis, the reader is referred to the publications cited in the caption to Figure 2. The present study area is the western extension of a part of the Rankin Inlet – Chesterfield segment (Fig. 2). The objectives of this study are to upgrade the reconnaissance mapping and to extend the more recent work to address outstanding structural, metamorphic, and metallogenic problems in the region, thereby providing a better framework for regional correlation and tectonic synthesis in this part of the Churchill Structural Province.

A pilot study showing the feasibility of generating digital working and compilation of maps using FIELDLOG (Brodaric and Fyon, 1989) and AutoCAD software applications was successfully completed as a part of the field component. Field-based portable PC and pocket computers were used for data input.


### *Acknowledgments*

We extend our thanks to the following: A. Meldrum for field assistance; B. Brodaric, Continental Geoscience Division, for introducing the authors to Fieldlog and AutoCad software applications; Bert Struik and coworkers at the Geological Survey of Canada, Vancouver for the use of an early version of the GEOF(Geological Editor Of Fieldnotes) program to facilitate data input on the outcrop; A.R. Miller, Mineral Resources Division for discussions on gold metallogeny of


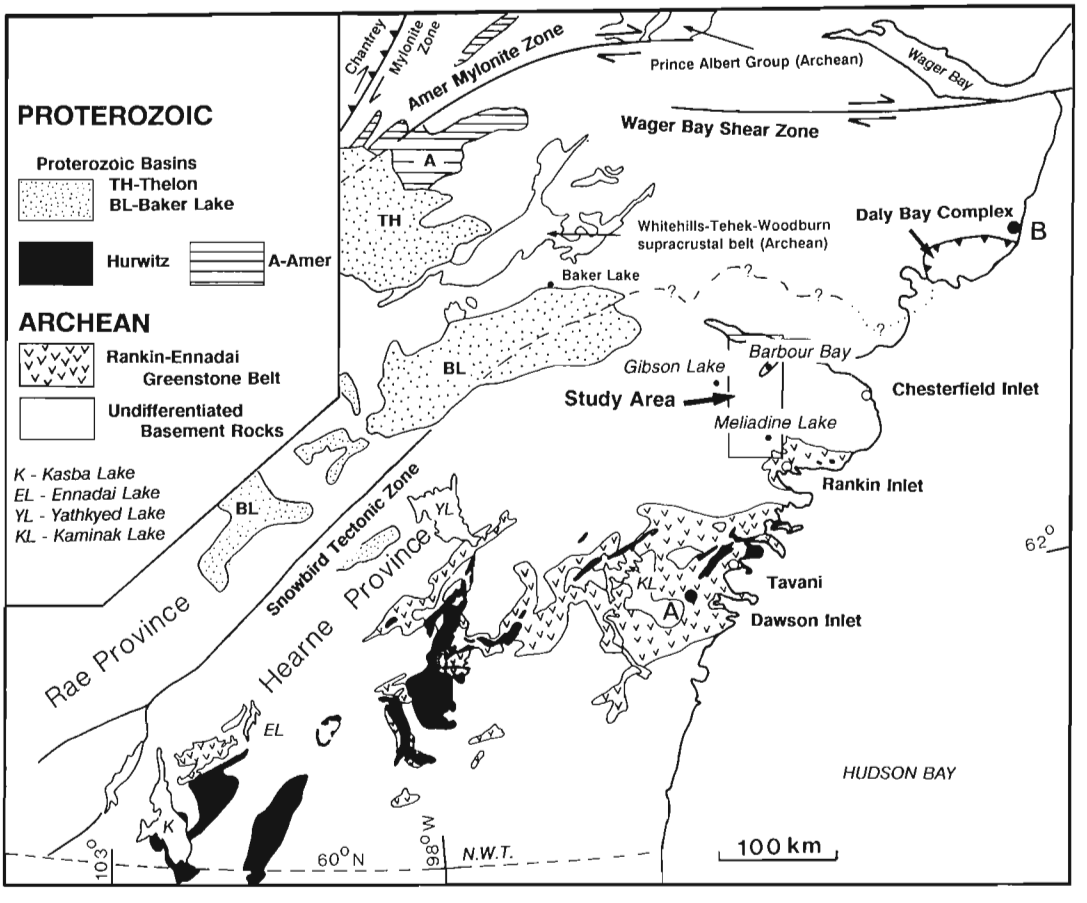


**Figure 1**. Sketch map showing location of the Meliadine Lake-Barbour Bay region, and the distribution of major supracrustal belts,and shear zones, District of Keewatin.

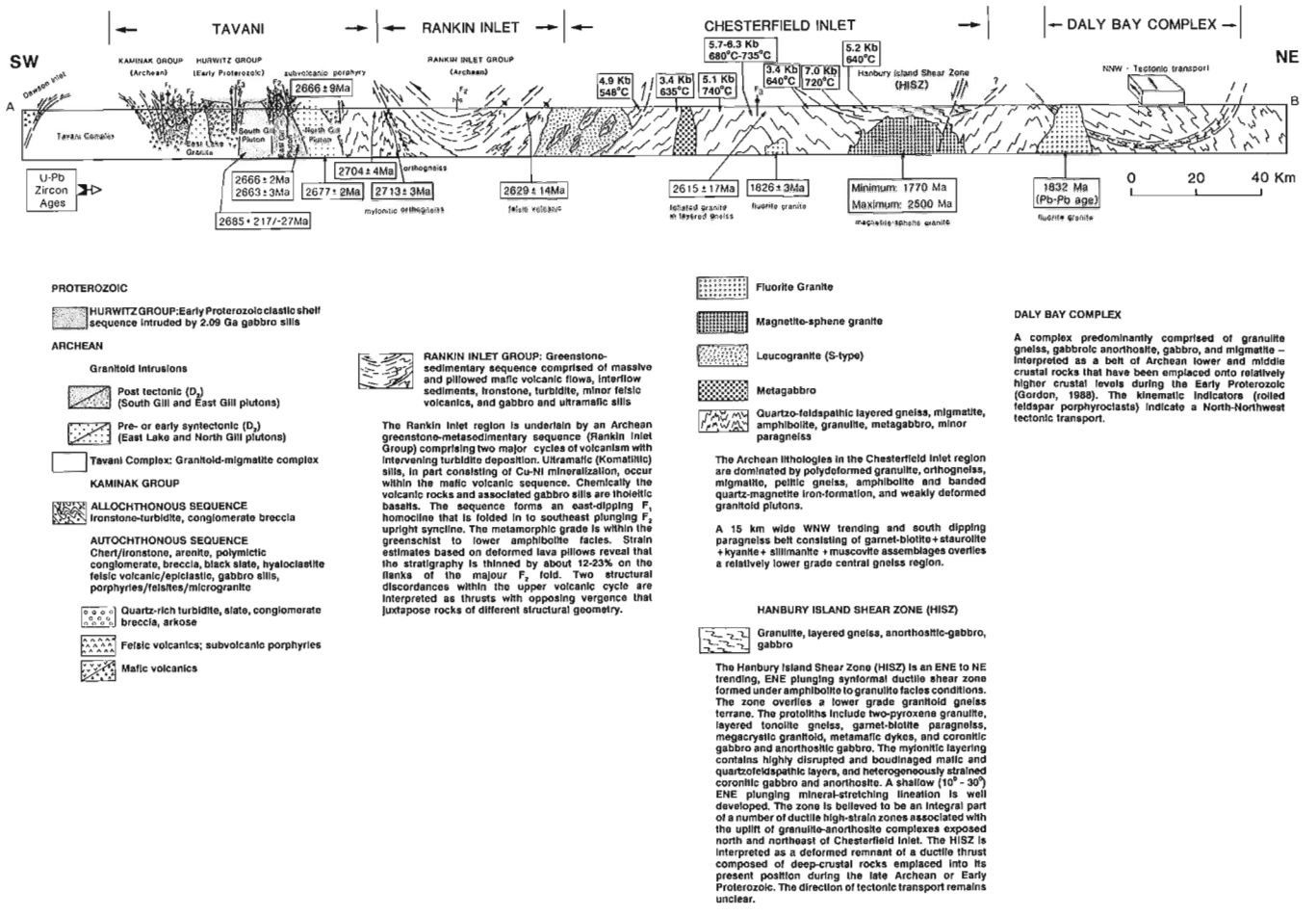


**Figure 2.** Schematic crustal transect (A-B, Fig.1) from Tavani to Daly Bay. Compiled from previous work (Tella et al., 1986,1989,1990; Tella and Annesley, 1987,1988; Gordon, 1988; Park and Ralser, 1990, in press).

the region; G. Dixon of Asamara Minerals Inc. and his crew for making available the core samples from the Meliadine prospect; Robin Ostertag of Frontier Helicopters, Vancouver, for rotary-wing support; M. Tatty and R. Mercer, M&T Enterprises Ltd., Rankin Inlet, for expediting services. K.D. Card, T. Frisch, A.N. LeCheminant, and A.R. Miller critically reviewed the manuscript.

## LITHOLOGY, STRUCTURE, AND METAMORPHISM

### *General statement*

The distribution of rock units and their regional structural framework in the Meliadine Lake-Barbour Bay area are shown in Figures 3 and 4 respectively, and the orientation of planar and linear fabric elements are shown in Figure 5. The Archean lithologies in the Meliadine Lake – Peter Lake region (Fig. 3) are dominated by polydeformed and regionally metamorphosed supracrustal rocks of the Rankin Inlet Group (unit 1). Active gold exploration in the region is focussed on turbidite-hosted, auriferous oxide-iron formation of the Rankin Inlet Group (Tella et al., 1986). The region between Meliadine Lake and Barbour Bay (Fig. 3), is underlain by polydeformed and metamorphosed amphibolite, pelitic gneiss, migmatite, and quartzofeldspathic granitoid rocks (units 2 to 6). Several generations of relatively undeformed mafic intrusions (gabbro, diabase, pyroxenite; unit 7) of probable early Proterozoic age occur sporadically as plugs and dykes throughout the region. Post-tectonic Early Proterozoic activity is recorded by several phases of granite intrusions (unit 8). A two-mica granite (unit 9) of uncertain age intrudes rocks of units 2 and 3, but its relationship to other rock units is not known. South-southeast-trending biotite lamprophyre dykes (unit 10) and north-northwest-trending Mackenzie dykes (unit 11) are present in a few localities, but are too small to be represented on the accompanying maps. At least three sets of late brittle faults (E-, NE-, and NW-trending) transect the region.

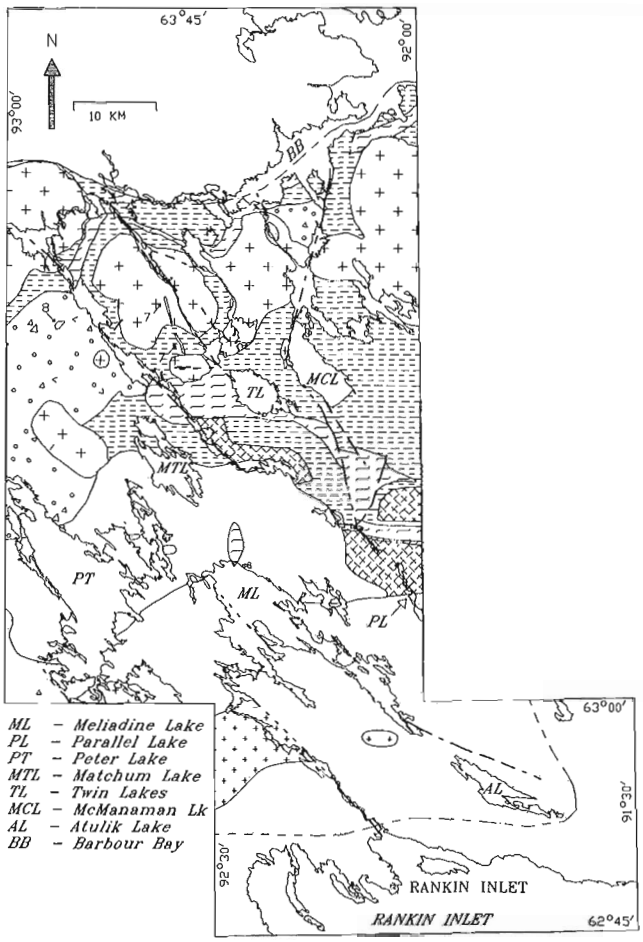


**Figure 3.** Simplified geological sketch map of the Barbour Bay-Meliadine Lake region.

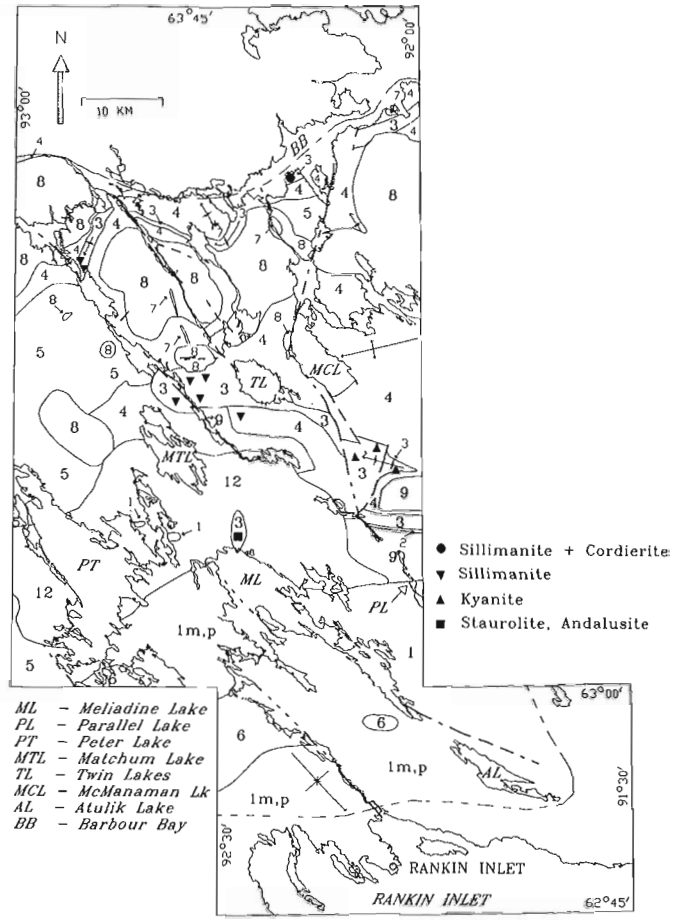


**Figure 4.** Major structural features: Meliadine Lake-Barbour Bay region.

### *Meliadine Lake – Peter Lake area*

This area is underlain by the Archean (ca 2.63 Ga) Rankin Inlet Group (unit 1), a deformed and metamorphosed supracrustal sequence composed of massive and pillowed mafic volcanic flows, interflow sediments, quartz-magnetite iron-formation, and minor mafic and felsic tuffs, pyroclastics, and volcanic breccia. Gabbro sills occur throughout the sequence. Previous stratigraphic and structural studies (Tella et al., 1986) to the south established that the sequence forms an $F_1$ homocline which is folded into a southeast-plunging $F_2$ syncline, and identified pre-$F_2$ ductile thrusts. In the Meliadine Lake-Peter Lake area, the Archean sequence forms part of an east-southeast-trending northern limb of a regional $F_2$ fold. Several limb-parallel, ductile, high-strain zones are present between Peter Lake and Atulik Lake (Fig. 3,4), some of which are interpreted as pre-$F_2$ thrust faults that show oblique-dextral, northside-down sense of displacement. The deformation and greenschist grade metamorphism are considered to be Archean.

The main rock types exposed in the region southeast of Peter Lake are sheared and carbonatized mafic metavolcanics (chlorite schist, amphibolite), gabbro sills, and minor intercalated mafic tuffs, pyroclastics, and pillowed flows. All rock types are fine- to medium-grained, well layered, and massive to well cleaved. Altered metamafic rocks contain blue-green amphibole, chlorite, biotite and carbonate. They are locally garnetiferous adjacent to granite intrusions. Numerous quartz and quartz-carbonate-chlorite veins, some containing arsenopyrite, pyrite, and chalcopyrite mineralization, occur within and transecting the mafic layers. Pyritiferous gossans, with or without sphalerite, are spatially related to late brittle faults. At least three separate layers of east-trending, banded, quartz-magnetite iron-formation are present southeast of Peter Lake, each separated by 10-20 m thick amphibolite. The iron-formation can be traced for over 200 m easterly along strike. Most of these lithologies can be traced along strike to the east and southeast beyond Meliadine Lake. The bands of iron-formation show pronounced aeromagnetic signatures (Geological Survey of Canada, 1966a,b,c). South of Meliadine Lake, minor amounts of felsic volcanics, agglomerate, and impure quartzite are intercalated with chlorite schists and mafic volcanics. The metasedimentary component consisting of mafic and felsic tuffs, and biotite turbidites, increases to the east of Meliadine Lake and to the north of Atulik Lake (Fig. 3). Gabbro sills and dykes are common. Two sets of planar fabrics at an acute angle (<15°) to each other are present in the rocks of this sequence (Fig. 5a,b). Both fabrics contain down-dip quartz

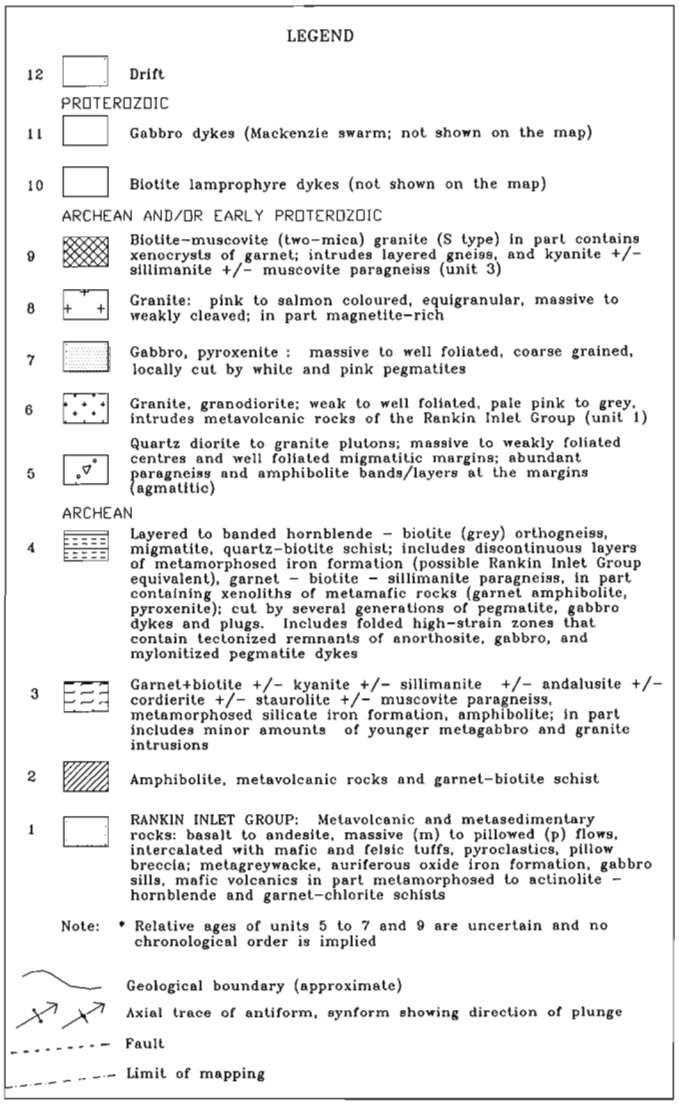


**Legend for Figures 3 and 4**

and carbonate rodding lineations which suggest layer-parallel slip. North of Atulik Lake, auriferous oxide iron formation occurs in several bands, some of which are repeated by folding. Adjacent to one of the pre-$F_2$ ductile thrusts, three sets of pre-$F_2$ mesoscopic folds (Fig. 6) with well developed interference patterns are present in locally auriferous oxide iron formation. The earlier two sets ($F_a$ and $F_b$) are coaxially folded structures that plunge shallowly towards the east (Fig. 5b). The youngest set ($F_c$), with Z-asymmetry, plunges moderately (30°-45°) northeast. The $F_c$ fold axes are parallel to the regionally pervasive pre-$F_2$ mineral stretching lineation (Fig. 7). A locally developed, but well expressed, axial planar cleavage is present in the $F_c$ folds. A prograde assemblage of biotite+chlorite in silicate-rich layers of the iron formation is overprinted by random to weakly oriented intergrowths of fine grained grunerite+hornblende+carbonate with pyrrhotite, and coarse hornblende+biotite with arsenopyrite.

Textural relations suggest that gold mineralization is associated with S, Ca, $CO_2$ metasomatism. The sulphidized and auriferous oxide iron-formation is hosted in a biotite turbidite sequence, and the epigenetic gold mineralization appears to be controlled by the youngest set of pre-$F_2$ folds with Z-asymmetry which acted as structural traps. The timing of mineralization is probably late syn- to post-$F_c$ and may have been related to movements on pre-$F_2$ thrusts. Geochronology of hornblende and biotite is planned to constrain the age of mineralization.

Southwest of Meliadine Lake and west of Peter Lake, the mafic volcanic rocks and associated schists are intruded by a white to pink, fine- to medium-grained granite (unit 6). The granite contains disseminated magnetite (<2%) and a few mafic minerals (<10%), and is weakly foliated at the margins. Adjacent mafic volcanic rocks contain garnet, perhaps a product of contact metamorphism.

Northeast of Meliadine Lake, a 10 m wide, fine grained, diabase dyke with 1-8 cm size phenocrysts of plagioclase cuts the mafic volcanic sequence. The dyke trends 160° and is texturally similar to the Kaminak dykes in the Kaminak Lake area (Davidson, 1970).

### *Parallel Lake area*

Amphibolite, minor metavolcanic rocks, and garnet-biotite schist (unit 2) form an east trending, steeply south dipping belt north of Parallel Lake (Fig. 3). Structurally they overlie a pelitic gneiss unit (3), and are believed to be higher grade equivalents of the Rankin Inlet Group metavolcanics. The belt is intruded by dykes and plugs of two-mica granite (unit 9). The belt extends east into the Chesterfield Inlet map area and is truncated to the west by a northwest-trending, late brittle fault.

### *Meliadine Lake – Barbour Bay area*

A west-northwest trending paragneiss belt (unit 3), consisting of garnet+biotite +/- muscovite +/- Al-silicate + plagioclase + quartz assemblages, is exposed to the south and southeast of Twin Lakes (Fig. 3). The belt overlies the layered quartzofeldspathic gneiss (unit 4). Gneissosity in the paragneiss is concordant with that in the layered gneiss for the most part, but discontinuous, layer-parallel, ductile, high-strain zones (metres to tens of metres wide) are present along the entire length of the contact, suggesting a tectonic break between the two units (3&4). The rocks in this belt are commonly fine- to medium-grained iron-rich pelites that are compositionally well banded with quartz, quartz+feldspar, and garnet+biotite +/- staurolite +/- Al-silicate +/- cordierite rich layers. Porphyroblasts of kyanite upto 8 cm long are present in the region southeast of McManaman Lake. Several discontinuous interlayers of silicate iron-formation consisting of magnetite, garnet, grunerite, and hornblende occur in the paragneiss belt. They show prominant aeromagnetic anomalies (Geological Survey of Canada, 1966a,b,c,d). The iron-formation is finely banded on a millimetre to centimetre scale, and thickness seldom exceeds more than a few tens of metres. Some multiple bands represent

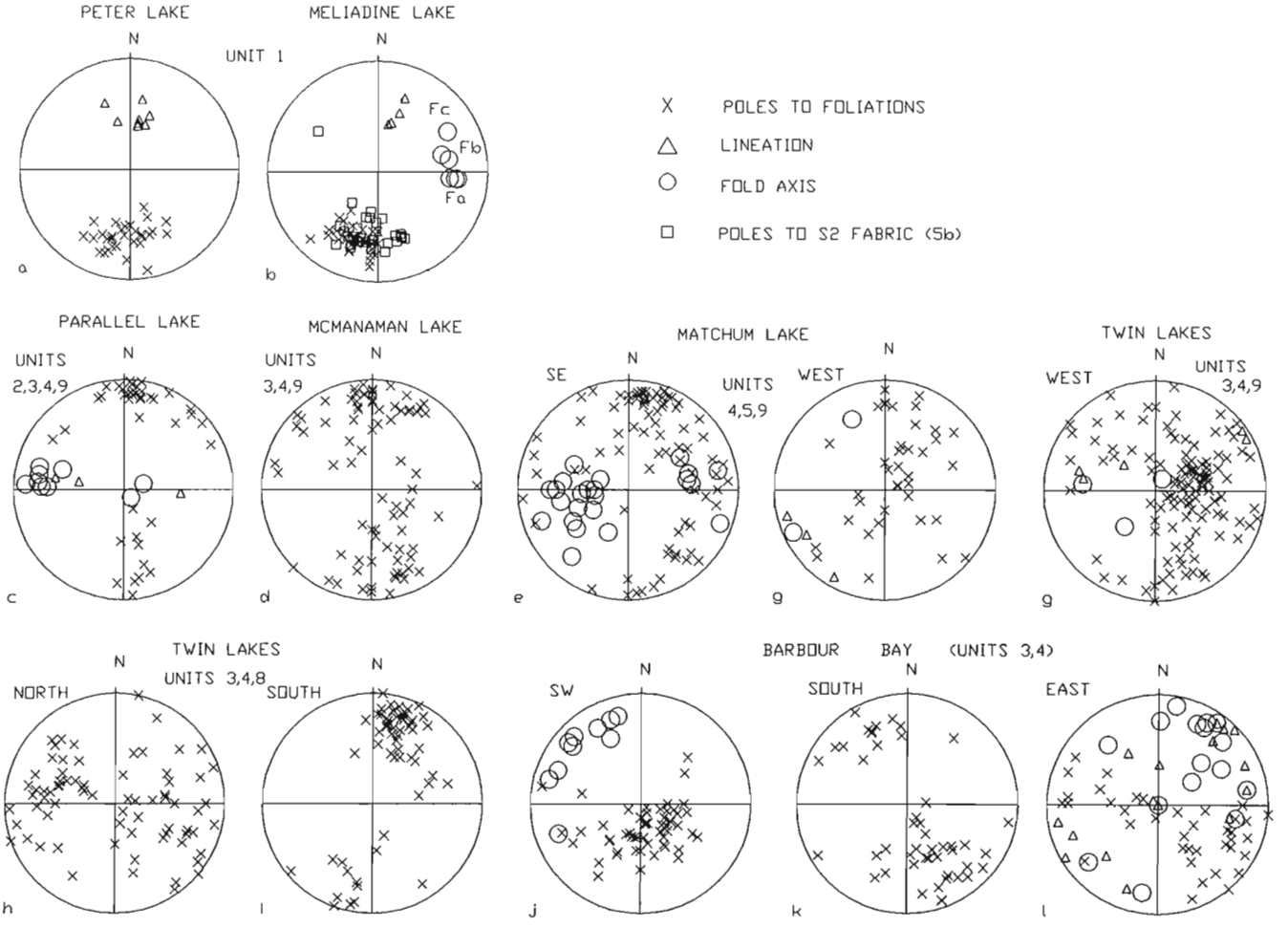


**Figure 5**. Orientation of planar and linear fabric elements from Meliadine Lake-Barbour Bay region.

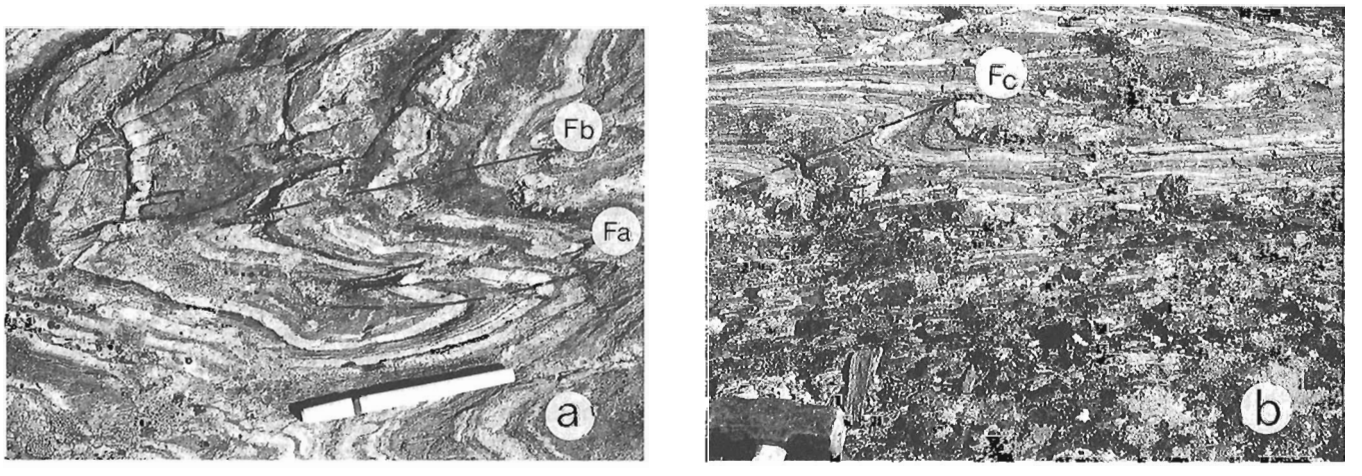


**a)** Coaxially refolded folds ($F_a$ and $F_b$); both plunge shallowly to the east. GSC1991-574K

**b)** Fold ($F_c$) in iron-formation (top centre) with Z-asymmetry and locally developed axial plane cleavage. Fold plunge is 40° towards 045. GSC1991-574F

**Figure 6**. Fold interference patterns in iron-formation, Rankin Inlet Group, northwest of Atulik Lake.

the same stratigraphic horizons, repeated by tight isoclinal folds that are common in the paragneiss. The iron-formation appears to have limited economic potential. The paragneiss belt extends west towards Matchum Lake, where the trend progressively changes through northwest to north, and becomes northeasterly south of Barbour Bay (Fig. 3). The paragneiss belt wraps around, and dips away from, domal masses of younger felsic plutons (unit 8). Most rocks in the gneiss belt are stromatic migmatites. The melanosome is biotite-quartz- feldspar schist with or without Al-silicates, and the leucosome is composed of quartz and feldspar. The leucosome is either layer-parallel or cuts the schistosity at low angles. For the most part, the rocks form part of a high-strain zone between units 3 and 4. The pelitic rocks extend into the Chesterfield Inlet map area where they have similar lithological and structural characteristics (Tella and Annesley, 1987).

At least four sets of folds are present in the paragneiss belt. An early isoclinal, doubly plunging, recumbent fold set ($F_1$) is refolded by a northwest-plunging open to tight fold set ($F_2$), which in turn, is modified by moderately (<45°) west plunging open $F_3$ folds (see Fig. 5e), and north plunging $F_4$ folds (Fig. 5l). The map distribution of the paragneiss belt (unit 3) appears to be controlled by regional $F_3$ fold geometry.

The distribution of Al-silicate polymorphs, staurolite, and cordierite is shown in Figure 4. Staurolite and andalusite are restricted to the southernmost parts of the belt, north of Meliadine and Parallel lakes. South of McManaman Lake, garnet-kyanite pelites are juxtaposed against sillimanite-muscovite pelites along a north-northwest- trending, late brittle fault. There the pelitic belt forms a moderate, west-plunging synform. The abrupt change of Al-silicate polymorph along strike appears to be due to a combination of changes in structural relief and vertical or oblique displacements along the fault. South of Barbour Bay, the paragneiss belt contains muscovite + sillimanite +/- cordierite +/- garnet + plagioclase + quartz assemblages. There, the gneissic layers are interlayered with garnetiferous metamafic rocks, and metagabbro pods. Metamorphic mineral assemblages indicate middle to upper amphibolite facies conditions of regional metamorphism.

Rocks within unit 3 are considered to be higher grade equivalents of aluminous and iron-rich sedimentary successions of the Rankin Inlet Group (unit 1). Thermobarometric calculations, based on a number of different mineral equilibria, from the adjoining region to the east, yielded P-T estimates of ca 3.4kb and 635°C for the assemblages in this unit (Tella et al., 1990; see also Fig. 2).

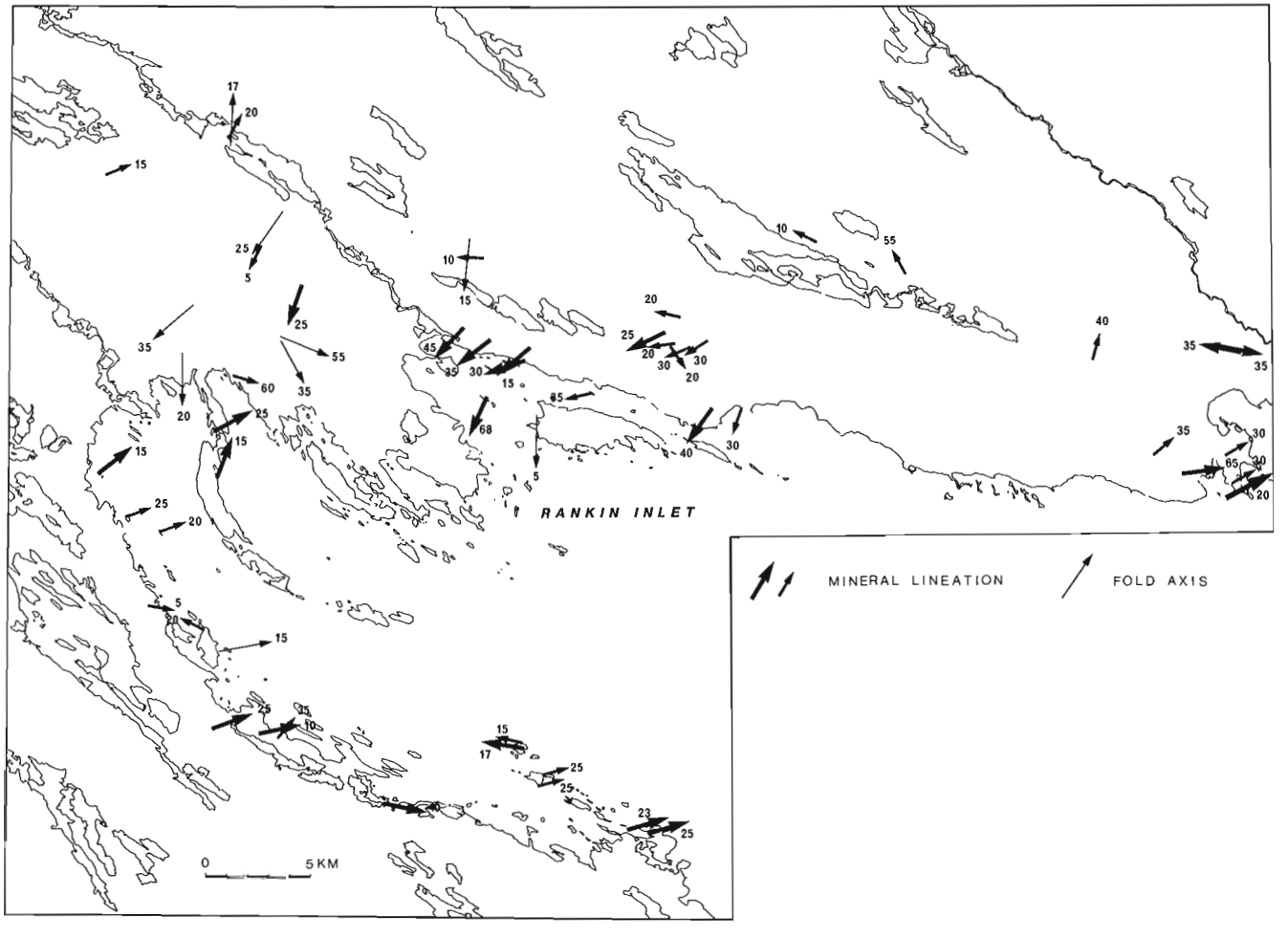


**Figure 7.** Orientation of pre $F_2$ mineral stretching lineations, Rankin Inlet region.





**Figure 8. a**) Ductilely folded layered gneiss, unit 4. GSC1991-574C **b**) ductilely folded, high-strain zone displaying rolled porphyroclasts of K-feldspar; Barbour Bay. GSC1991-574B **c**) Sheath folds in ductile, high-strain zone, southeast of Barbour Bay. GSC1991-574E **d**) High-strain zone with porphyroclasts of K-feldspar, unit 4, Twin Lakes region. GSC1991-574I

Rocks of unit 4 (Fig.3) comprise mixed assemblages of polydeformed, amphibolite grade orthogneiss, migmatite, biotite-muscovite-sillimanite +/- cordierite +/- garnet gneiss, minor proportions of iron-rich metasediments, and different generations of mafic dykes, now transformed into garnetiferous amphibolites. Granite dykes of several ages cut the rocks of this unit on all scales. South of Barbour Bay, the orthogneiss is fine- to medium-grained, light- to dark- grey to pink, well banded and layered rock (Fig. 8a) consisting of several distinct compositional phases that range from tonalite to granite. The gneissic layers contain variable proportions of quartz-plagioclase-K-feldspar-biotite-amphibole assemblages. Less deformed granite protoliths show gradational contacts with the orthogneiss. The layered gneiss contains xenoliths of metamafic rocks consisting of garnet-hornblende-clinopyroxene assemblages, agmatite, and rafts of anorthosite and gabbro. North of Twin Lakes (Fig. 3), the most common rock types are foliated metagabbro, garnetiferous amphibolites, and well layered quartzofeldspathic gneiss. Epidote alteration is common throughout. Plagioclase reaction rims around garnet are locally present in the amphibolites. Coarse, pink pegmatite dykes, related to a large granite body (unit 9), cut all rock types in this area. The pegmatite contains muscovite, biotite, garnet, and tourmaline as accessory phases. Northwest of Twin Lakes, cordierite knots are present in the amphibolites adjacent to a granite pluton (unit 9), and appear to be related to contact metamorphic effects of the granite. Mylonitic rocks containing coarse K-feldspar porphyroclasts form concordant layers (tens of metres wide) within quartzofeldspathic gneiss.

In the Barbour Bay region, foliation in unit 4 strikes northeasterly and dips 35°-70° to the northwest. Foliations strike north-south in the central part of the region around

McManaman Lake, and become southeasterly to the south. The map distribution of this unit defines a broad, west-plunging antiform.

Numerous discontinuous, folded, ductile, high-strain zones, which display excellent mylonitic textures (Fig. 8b,d), are an integral part of unit 4. They are well exposed southeast of Barbour Bay and extend southwest towards the Twin Lakes, where their trend swings from south to southeast. High-strain zones, a few metres to over hundreds of metres wide, are separated by low-strain segments. Protoliths include deformed orthogneiss, migmatite, paragneiss, anorthosite, gabbro, and different generations of metamafic and granite dykes. The high-strain zones are folded into tight, upright, shallow (<30°) doubly plunging isoclines that are coaxially refolded into moderate to open, northeast-plunging upright folds. Fold hinges in rootless, steep (70°) doubly plunging folds in pelitic and mafic layers are parallel to tight isoclines developed in the high-strain zones. Sheath folds are locally developed in the high-strain zones (Fig. 8b,c). In some localities, the mylonitic fabric is partially or completely annealed, and is clearly overgrown by K-feldspar porphyroblasts. Mineral stretching lineations are generally less well developed, but where present, they plunge shallowly (<30°) north-northeast, northeast, or southwest (Fig. 5l). Kinematic indicators (rotated feldspars) indicate both sinistral and dextral senses of shear due to folding. The ductile shear zones appear to have a complex deformational history of multiple periods of development, each punctuated by injection and subsequent mylonitization of different sets of mafic and granitic dykes. The age of deformation, metamorphism of the country rock, and subsequent development and folding of ductile strain zones, are all believed to be Archean.

Rocks of unit 5 are well exposed in the central part of the map area northwest of Matchum Lake, and to a lesser extent in areas south of Barbour Bay and southwest of Peter Lake. The dominant lithologies consist of white- to pale-pink, gneissic quartz diorite and granodiorite that form large plutons. They show well foliated migmatitic margins that contain abundant, but discontinuous, amphibolite layers up to 100 m wide. The margins in part are agmatitic and contain lenses and centimetre-scale layers of sillimanite-muscovite schist. The central portions of the pluton, northwest of Matchum Lake, are relatively undeformed. Rare rounded xenocrysts of garnet were noted west of Matchum Lake. The large pluton is truncated to the east by a northwest-trending fault that extends from Parallel Lake to the northwestern edge of the study area. Regional foliation strikes northeast and dips northwest in the northern portions, and southeast in the southern portions. Amphibolite and migmatite layers wrap around the pluton.

South of Barbour Bay, rocks of unit 5 consist of banded quartzofeldspathic gneiss and gneissic granodiorite, minor garnet-sillimanite schist, and pink granite. The gneisses are fine- to medium-grained and well banded (up to 300 m wide), and are grey to pink on the weathered surface. The banding is defined by biotite-poor and biotite-rich layers. The banded gneiss contains numerous inclusions of biotite+/-garnet schists, and garnetiferous amphibolites. Remnants of banded iron-formation, traceable along strike for only a few metres, are noted in a few localities. Regional foliation strikes northeast with variable dips to the northwest. The unit is bounded to the north by a ductile, high-strain zone (Fig. 8b), a part of unit 4, and intruded by gabbro (unit 7) to the west and granite (unit 8) to the south. The contact with the granite is gradational, with pink granite dyke and blocks of country rock forming a ca. 100 m wide contact zone. The unit is truncated to the east by a northeast-trending fault. Southwest of Peter Lake, the granitoid rocks are leucocratic, weakly foliated, and poorly exposed. There the contact with the Rankin Inlet Group is an inferred fault (Fig. 3).

Scattered outcrops of medium- to coarse-grained, weakly foliated white granite (unit 6) occur in the region north and northwest of Rankin Inlet . The granite is commonly poor in mafics (<5% biotite, <1% disseminated magnetite). Related sills and dykes cut the metavolcanic rocks of the Rankin Inlet Group.

A number of medium- to coarse-grained, massive to weakly foliated gabbro intrusions (unit 7) of probable early Proterozoic age, are sporadically distributed throughout the region. Although they are grouped in a single map unit, they may represent several generations of mafic intrusions. Two large gabbro bodies are exposed in the region south and southeast of Barbour Bay. They are undeformed, relatively fresh, locally contain hornblende oikocrysts and numerous inclusions of older gneissic rocks (unit 4). Pink granite dykes, related to unit 8, intrude the gabbro. Approximately 20 km north of Matchum Lake, a northwest-trending, weakly altered, deformed gabbro dyke cuts the layered gneiss (unit 4). The dyke is discontinuous over a strike-length of 5 km, also occurs as a remnant within a granite pluton (unit 8, Fig. 3), although its trend is maintained. A number of gabbro plugs and east-trending dykes (up to 300 m wide) also occur as isolated outcrops between Matchum Lake and McManaman Lake. They cut the layered gneiss, pelitic gneiss, and two-mica granite (units 3,4,9). Southeast of McManaman Lake, scattered exposures of gabbro are aligned in an easterly direction for more than 20 km distance. They may represent multiple sets of east-trending dykes. The gabbros clearly intrude the polydeformed rocks of unit 4, and are overprinted by a weak, later deformation.

A coarse grained, massive and fresh, 150 m wide, pyroxenite dyke of uncertain age cuts gneissic rocks (unit 4) 5 km southwest of Barbour Bay. The dyke trends northerly and can be traced along strike for over 5 km to the north.

A number of granite plutons (unit 8) that intrude the layered and pelitic gneisses (units 3,4) are widely distributed in an east-northeast belt between Barbour Bay and McManaman Lake (Fig.3). Individual plutons range in composition from quartzmonzonite to granite. They are equigranular to massive, pink to salmon coloured bodies that contain abundant inclusions and rafts of layered gneiss, paragneiss, metagabbro, and rare bands of iron-formation. The plutons are in part magnetite-rich, and show high aeromagnetic signatures. Southeast of Barbour Bay, the easternmost pluton contains mega-rafts of anorthositic gabbro (Fig. 9), and remnants of the ductile, high-strain zones

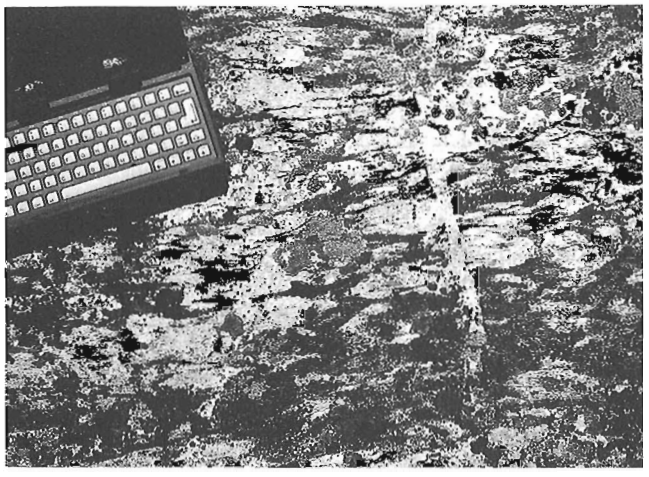

**Figure 9.** Tectonized anorthositic gabbro; mega-inclusion in granite, unit 8; computer (18x10 cm) for scale. GSC1991-574D

described previously. Gradational colour variations, on an outcrop scale, from pink to pale pink and white are common. However, a distinct salmon variety that intrudes the white granite is also present southeast of Barbour Bay. Pegmatite and aplite dykes, related to the plutons, are widespread throughout the region. The plutonic rocks are undeformed in the cores, but show a weak to well developed foliation at the margins, migmatitic aureoles (up to 100 m wide), and gradational contacts with the country rocks. The abundance of inclusions of country rocks increases towards the margins of the plutons. The above lithological characteristics are similar to those described in the Gibson Lake west-half map area (Reinhardt and Chandler, 1973; Reinhardt et al. 1980), and to those noted in the Chesterfield Inlet to the east (Tella and Annesely, 1987). Although all plutons are grouped into one single unit(8), they may not all be coeval.

A well foliated, biotite-muscovite leucogranite (unit 9), which forms west-northwest-trending elongate masses, is extensively exposed in the central part of the map area between Twin Lakes and Parallel Lakes (Fig. 3). Northwest of Matchum Lake, the granite is truncated to the west by a northwest-trending fault, and extends into the Chesterfield Inlet map area to the east. The granite is coarse- to medium-grained, grey to white weathering, and weakly to well foliated. The regional foliation within the unit trends west-northwest and dips steeply (60°-75°) to the south, although local reversals to the north are noted. Abundant garnet and muscovite xenocrysts, inclusions of pelitic gneiss (unit 3) and orthogneiss (unit 4), and minor metagabbro are present within the granite. Textural and mineralogical characteristics suggest the granite is peraluminous S-type.

Lamprophyre dykes (unit 10) are relatively rare in the region. Southeast of McManaman Lake, two discontinuous, 1-3 m thick, dykes with 130°-140° trend are present in the pelitic gneiss unit (3). They are dark grey to black, relatively undeformed, medium- to fine-grained rocks with large biotite/phlogopite phenocrysts. They are texturally similar to lamprophyre dykes described from the Rankin Inlet region (Tella et al., 1986) and from the Kaminak Lake area (Davidson, 1970), and probably are related to the ca. 1.85 Ga alkaline igneous suite in the central Keewatin (LeCheminant et al., 1987).

Northwest trending gabbro dykes (unit 11, not shown on the map), probably part of the 1.27 Ga Mackenzie swarm, were noted in a few localities in the central part of the gneiss terrane. They are massive, relatively fresh, and coarse grained.

## SUMMARY

1. All rocks in the Meliadine Lake – Barbour Bay region, with the exception of units 7,8,10, and 11, have been polydeformed and regionally metamorphosed under greenschist to amphibolite facies conditions. The age of deformation and metamorphism is believed to be Archean, but definitive geochronology is required to establish time relations between deformation, metamorphism, and plutonism.

2. In the Meliadine Lake area, gold mineralization in the oxide-iron formation (unit 1) is structurally controlled by a widespread northeast-plunging, pre $F_2$ set of folds ($F_C$). Metamorphic textures suggest that mineralization is associated with local S, Ca, and $CO_2$ metasomatism.

3. Metamorphic mineral assemblages in the polydeformed pelitic gneisses (unit 3) indicate amphibolite facies conditions, but awaits critical evaluation of polymetamorphic textures.

4. The contact between units 3 and 4, is marked by a well developed, but poorly exposed, high-strain zone. Discontinuous segments of the zone wrap around a west-plunging, regional-scale antiform ($F_3$). The southeastern extension of the zone links with a tectonic break that juxtaposes two crustal levels in the Chesterfield Inlet region (Fig. 2).

5. Ductile high-strain zones in the layered gneisses (unit 4) show structural and lithological similarities to those described from adjoining regions (Schau and Ashton, 1980; Gordon, 1988; Tella et al. 1986, Tella and Annesley, 1987, 1988). Their geometry is consistent with those documented from the Rankin Inlet-Chesterfield Inlet region (Fig. 2), and may represent several interleaved, flat-lying, crustal-scale tectonic slabs. Detailed kinematic analysis of the zones requires new mapping in the region north of Barbour Bay, where the dominant lithologies appear to be anorthosite complexes, and granulite grade orthogneisses.

## REFERENCES

**Brodaric, B. and Fyon, J.A.**
1989: OGS FIELDLOG: A microcomputer-based methodology to store, process and display map-related data; Ontario Geological Survey, Open File Report 5709, 73 p. and 1 magnetic diskette.

**Davidson, A.**
1970: Precambrian geology, Kaminak Lake map area, District of Keewatin; Geological Survey of Canada, Paper 69-51, 27p.

**Geological Survey of Canada**
1966a: Gibson Lake; Geophysical Series (Aeromagnetic) Map 7299G.
1966b: Tavani; Geophysical Series (Aeromagnetic) Map 7296G.
1966c: Marble Island; Geophysical Series (Aeromagnetic) Map 7295G.
1966d: Chesterfield Inlet; Geophysical Series (Aeromagnetic) Map 7298G.

**Gordon, T.M.**
1988: Precambrian geology of the Daly Bay Area, District of Keewatin; Geological Survey of Canada, Memoir 422, 21p.

**LeCheminant, A.N., Miller, A.R. and LeCheminant, G.M.**
1987: Early Proterozoic alkaline igneous rocks, District of Keewatin, Canada; in Petrogenesis and Mineralization of Proterozoic Volcanic Suites; (ed.) T.C. Pharaoh, R.D. Beckinsale, and D. Rickard; Geological Society Special Publication, No. 33, p. 219-240.

**Park, A.F. and Ralser, S.**
1990: Geology of the southwestern part of the Tavani map area (55K/3,4,5,6), District of Keewatin, N.W.T.; Geological Survey of Canada, Open File 2265.
in press: Precambrian geology of the southwestern part of the Tavani map area, District of Keewatin, N.W.T.; Geological Survey of Canada, Bulletin 416.

**Reinhardt. E.W. and Chandler, F.W.**
1973: Gibson-MacQuiod Lake map area, District of Keewatin; in Report of Activities, Part A; Geological Survey of Canada, Paper 73-1A, p. 162-165.

**Reinhardt, E.W., Chandler, F.W., and Skippen, G.B.**
1980: Geological map of the MacQuoid Lake (NTS 55M, E1/2) and Gibson Lake (NTS 55N, W1/2) map area, District of Keewatin; Geological Survey of Canada, Open File 703; compiled by G.B. Skippen.

**Schau, M. and Ashton, K.E.**
1980: Geological map of the granulite and anorthosite complex at the southeast end of Baker Lake, 56D1, 56C4, parts of 55M16 and 55N13; Geological Survey of Canada, Open File 712.

**Schau, M., Tremblay, F., and Christopher, A.**
1982: Geology of Baker Lake map area, District of Keewatin: a progress report; in Current Research, Part A; Geological Survey of Canada, Paper 82-1A, p. 143-150.

**Tella, S. and Annesley, I.R.**
1987: Precambrian geology of parts of the Chesterfield Inlet map area, District of Keewatin; in Current Research, Part A; Geological Survey of Canada, Paper 87-1A, p. 25-36.
1988: Hanbury Island Shear Zone, a deformed remnant of a ductile thrust, District of Keewatin, N.W.T.; in Current Research, Part C; Geological Survey of Canada, Paper 88-1C, p. 283-289.

**Tella, S., Roddick, J.C., Park, A.F., and Ralser, S.**
1990: Geochronological constraints on the evolution of the Archean and Early Proterozoic terrane in the Tavani-Rankin Inlet region, Churchill Structural Province, N.W.T.; Geological Society of America, Abstracts with Programs, v. 22, no. 7, p. A174.

**Tella, S., Roddick, J.C., Bonardi, M., and Berman, R.G.**
1989: Archean and Proterozoic tectonic history of the Rankin Inlet - Chesterfield Inlet region, District of Keewatin, N.W.T. (abstract); Geological Society of America, Abstracts with Programs, v. 21, no. 6, p. 22.

**Tella, S., Annesley, I.R., Borradaile, G.J., and Henderson, J.R.**
1986: Precambrian geology of parts of Tavani, Marble Island and Chesterfield Inlet map areas, District of Keewatin, N.W.T.; Geological Survey of Canada, Paper 86-13, 20 p.

**Wright, G.M.**
1967: Geology of the southeastern barren grounds, parts of the District of Mackenzie and Keewatin; Geological Survey of Canada, Memoir 350, 91 p.

Geological Survey of Canada Project 850002

# An application of reflection seismology to mineral exploration in the Matagami area, Abitibi Belt, Quebec

**B. Milkereit, E. Adam[1], A. Barnes[1], C. Beaudry[2], R. Pineault[2], and A. Cinq-Mars[3]**
**Continental Geoscience Division**

*Milkereit, B., Adam, E., Barnes, A., Beaudry, C., Pineault, R., and Cinq-Mars, A., 1992: An application of reflection seismology to mineral exploration in the Matagami area, Abitibi Belt, Quebec; in Current Research, Part C; Geological Survey of Canada, Paper 92-1C, p. 13-18.*

***Abstract***

*As part of the LITHOPROBE Abitibi-Grenville transect, a high-frequency Vibroseis survey was conducted in the Matagami mining camp located on the southern part of the Matagami anticlinorium, a gently dipping crustal structure. In the study area, the location of all contact between the predominantly felsic Watson Lake Group and the overlying Wabassee basalts is important since it accommodates most known economic deposits discovered in the camp. Correlation of the seismic data with existing borehole information suggests that this contact can be mapped with the reflection seismic method. In addition, a complex reflection pattern, diagnostic of multiple faulting and tilted crustal blocks, has been imaged in the vicinity of the Daniel fault zone.*

***Résumé***

*Dans le cadre du transect Abitibi-Granville du projet LITHOPROBE, un levé Vibro-sismique à haute fréquence a été effectué dans le camp minier de Matagami pour sonder le flanc sud de l'anticlinal de Matagami, une structure crustale à faible pendage. Dans la région étudiée, le contact entre les laves surtout felsiques du groupe de Watson Lake et les basaltes du groupe de Wabassee est recherché puisque la plupart des gisements à valeur commerciale du camp y sont associés. L'interprétation de la section sismique basée sur les trous de forages semble indiquer que le contact minéralisé peut être identifié au moyen de la sismique réflexion. De plus, les réflexions complexes observées dans la zone de failles de Daniel mettent en évidence des fractures multiples de même que des blocs basculés.*

[1] École Polytechnique de Montréal, Montreal
[2] Noranda Exploration Ltd., Rouyn-Noranda
[3] Mineral Resources Division

## INTRODUCTION

The Matagami felsic volcanic complex (Fig. 1) is part of the Abitibi belt, the largest Archean greenstone terrane on earth. The volcanic complex extends beyond the limits of the mining camp, it may cover more than 1,500 square kilometres and it is bounded by major crustal deformation zones across which stratigraphic relationships are not known. The Matagami area is host to one of the most productive base metal mining camps in Canada and has seen uninterrupted production since 1963.

The volcanic complex is subdivided into a lower, felsic Watson Lake Group and an upper, mafic-felsic Wabassee Group. The contact between the two groups is marked by the Key Tuffite, a thin but areally extensive exhalite horizon which hosts most of the massive sulphide deposits in the camp. The volcanics have been intruded by the Bell River layered igneous complex and numerous gabbro and tonalite sills, and are folded into the shallow west-plunging Galinée anticline. A number of faults have disrupted the volcanic stratigraphy.

### *Regional setting*

Across the south limb of the Galinée anticline, nearly 2,000 m of continuous stratigraphy have been established by surface drilling. The base of the section is composed of spherulitic rhyolite of the Watson Lake Group, overlain by the Key Tuffite. The overlying Wabassee Group consists of a lower 500 m unit of mafic and felsic volcanics and an upper unit composed of andesitic lavas. Both units are cut by several sub-concordant gabbro sills, some of which could be thick massive flows. The Daniel Fault (DF) is a major NW-SE trending, moderately NE dipping, syntectonic thrust which

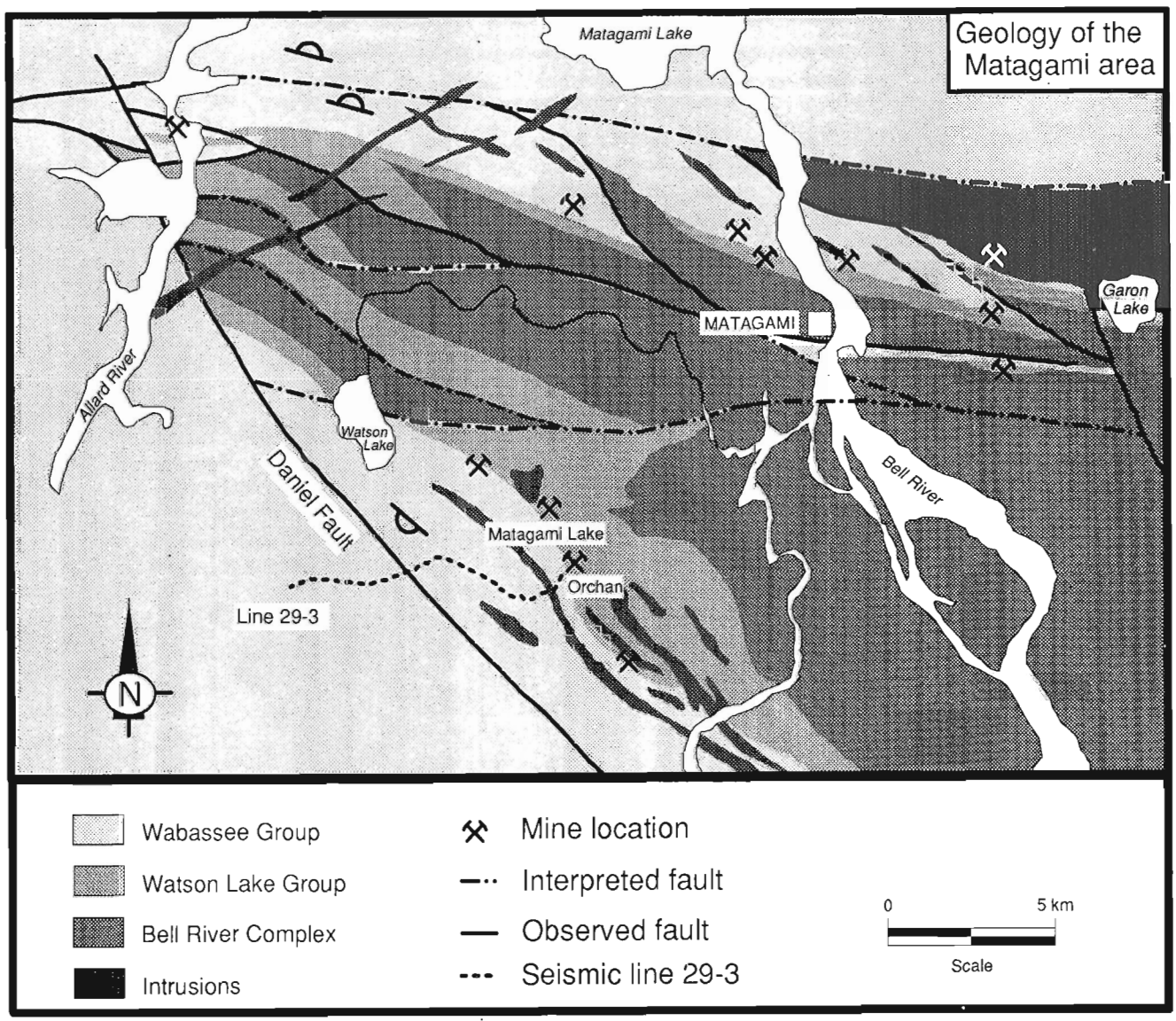


**Figure 1.** Geological map of the Matagami mining camp showing main lithological units crossed by LITHOPROBE seismic reflection profile 29-3 (modified after Piché et al., 1990).

bounds the southern flank of the mining camp. The DF has a dip-slip displacement of 1 to 2 km. Available drill data suggest the structure consists of several, coalescing fault zones. To the southwest of the DF, the area between the Matagami camp and the Phelps Dodge volcanic belt is underlain by mafic to intermediate volcanic rocks of the Wabassee Group. In this area the geology is poorly known and only a few deep holes have intersected the Key Tuffite.

### *Objectives*

In the study area, conventional geophysical methods failed to map the known volcanic sequence at depths greater than 300 m. Recent seismic surveys conducted across the Buchans mine in central Newfoundland (Spencer et al., 1992) and across the southern part of the Abitibi greenstone belt (Green et al., 1990) have demonstrated the potential of high-frequency seismic reflection profiling for delineating lithology and structure at depth. LITHOPROBE's high-frequency vibroseis study was carried out across the south limb of the Galinée anticline (Fig. 1; line 29-3) where mildly deformed rocks dip moderately to the southwest and where a large number of drill holes offer excellent geological control. In addition, significant density and seismic impedance contrasts were expected at the contact between the lower, predominantly felsic, Watson Lake Group and the overlying Wabassee basalts. The goal of the LITHOPROBE study was to map the attitude of the contact along an east-west transect, using the seismic reflection method adapted to mineral exploration.

## REFLECTION SEISMIC PROFILING

The seismic reflection survey was conducted using the same equipment as used for hydrocarbon exploration; however, acquisition parameters were modified to improve lateral resolution and fold, as well as vertical resolution. The Rayleigh resolution limit is defined as one-quarter of the dominant wavelength (e.g. Sheriff and Geldart, 1982), where the amplitude is at a maximum because of constructive interference. A layer with a thickness of less than one-quarter wavelength may still produce reflections although its thickness cannot be reliably determined from the wave shape. Given that the average velocity of basement rocks in the survey area is about 6000 m/s, and taking the centre frequency of the sweep, 85 Hz, to be the dominant frequency, the vertical resolution of our data is about 18 m. Thus, no significant reflection response can be expected from lateral thickness variations associated with the thin (<<18 m) Key Tuffite layer.

### *Data acquisition*

In the course of the survey 8 km of high-frequency vibroseis data were collected along an east-west line using a multichannel telemetry acquisition system with in-field stacking, noise-rejection, and correlation capabilities. The source consisted of two vibroseis trucks with 40,000 lbs peak force rating. Vibrator points were spaced every 20 m and a 20 m weighted source array was formed by the two vibrators during move-ups between individual sweeps. Four 12 s linear sweeps from 30 to 140 hz (2.22 octaves) were generated at every vibration point. The receiver spread employed 240 receiver groups spaced every 20 m resulting in a nominal fold of 120. The source-receiver spread geometry was almost evenly split-spread, with a near offset of 0 m and a far offset of 2400 m. No bandpass or notch filters were applied to the data during acquisition except for an anti-alias filter. For any individual "shot" record, successive sweeps were recorded such that external 60 Hz powerline noise was effectively attenuated in the vertical sum of all four sweeps. Vibroseis correlation was accomplished in the field, yielding fully-correlated records of length 4 s. Data acquisition parameters are summarized in Table 1.

### *Data processing*

Corrections for highly varied overburden conditions and imaging of steeply dipping crustal structures are among the challenges encountered during the processing of the high frequency data from the Matagami area.

Accurate static corrections are required to overcome problems associated with variations in overburden thicknesses along the seismic profile. First arrival times were automatically picked on more than 200 shot gathers and used in a tomographic inversion process to determine overburden thickness variations. Final static corrections were derived by removing the delay time associated with the 1500 m/s near-surface material and replacing with the delay time through 6000 m/s material. Total static corrections vary by more than 80 ms along the transect. It is important to note that, without application of these corrections, subsequent

**Table 1.** Acquisition parameters

| | |
|---|---|
| SOURCE | |
| Source type | Vibroseis, MERTZ Model 18 |
| Source interval | 20 m |
| Source length | 12 s |
| Source frequencies | 30 - 140 Hz linear |
| Sweep repetition | 4 |
| Source pattern | 2 Vibrators |
| RECEIVERS | |
| Geophone type | 30 Hz MARK PRODUCTS L-25 |
| Geophone interval | 20 m |
| Geophone layout | 9 over 20 m |
| Spread | 120/120 split, no gap |
| ACQUISITION SYSTEM | |
| Instrumentation | 240 Channel SERCEL SN368 |
| Gain type | Floating point |
| Field filter | 178 Hz High-cut |
| Record length | 4 s |
| Sample rate | 2 ms |

processing steps (such as velocity analysis, stacking, trim-static corrections, etc.) resulted in low quality seismic images with poor signal-to-noise ratios.

Normal moveout corrections, applied in a conventional seismic processing sequence, assume horizontal reflectors; dipping reflection events exhibit higher apparent stacking velocities and do not stack correctly with the flat dip rms-stacking velocities. Thus, a conventional processing sequence often results in poor stacking of dipping events and diffraction patterns. This phenomenon is highlighted in Fig. 2. Although amplitudes of dipping events can be large, they may be attenuated by conventional processing (stacking is an effective dip-filter). Such difficulty can be overcome by pre-stack migration or by dip-moveout (DMO) processing (e.g. Milkereit et al., 1990). Compared to full prestack migration of shot gathers, DMO-processing (e.g. Yilmaz, 1987) operates on a limited offset range and requires less computing time. For each offset range, dipping events are repositioned along a hyperbolic path to their zero-offset equivalent. DMO-processing followed by a second round of stacking velocity analysis is capable of imaging horizontal and dipping events (see Fig. 2). However, dipping reflections and diffraction patterns do not appear at their correct lateral position in the stacked section. Such events are always defocused, their dips are underestimated, and subsequent application of post-stack migration is required to correct these effects. The complete data processing sequence is summarized in Table 2.

## INTERPRETATION

The interpreted seismic section across the Matagami volcanic center is shown in Figure 3. After DMO- processing and post-stack migration, prominent west- dipping reflections can be traced with confidence from the Orchan mine area towards the Daniel Fault. Interpretation of the seismic data is constrained by information from four deep boreholes (marked B1 to B4) along the eastern portion of transect. In addition, downhole geophysical measurements were made to a depth of 1150 m in hole B4. Based on the seismic image and supporting drill information the interpreted crustal model can be divided into three parts.

**Table 2.** Data processing

| | |
|---|---|
| BASIC PROCESSING SEQUENCE | |
| Crooked Line Geometry | |
| Deconvolution | Spiking (1% Pre-Whitening) |
| Trace Editing | |
| Bandpass Filter | 0.0-1.0s : 35/40-135/104 Hz |
| | 1.0-4.0s : 30/35-135/140 Hz |
| Scale | 200 ms (AGC) |
| Refraction Statics | |
| First Break Analysis | Automatic |
| Datum | 400 m Above Sea Level |
| Stacking Velocity Analysis | Every 1.2 km for 30 CDPs |
| NMO Corrections | |
| Mute Control | Every 50 CDPs |
| DMO PROCESSING SEQUENCE | |
| Dip Moveout | |
| Stacking Velocity Analysis | Every 1.2 km for 30 CDPs |
| CDP Residual Statics | Window : 150-3500 ms |
| | Maximum shift : 20 ms |
| Stack | |
| DISPLAY | |
| Spectral Whitening | 0.0-4.0s : 25/30-110/115 Hz |
| Scale | 0.0-1.0s : 300 ms (AGC) |
| | 1.0-4.0s : 1000 ms (AGC) |
| FK Migration | 6000 m/s |
| Coherency Enhancement | |

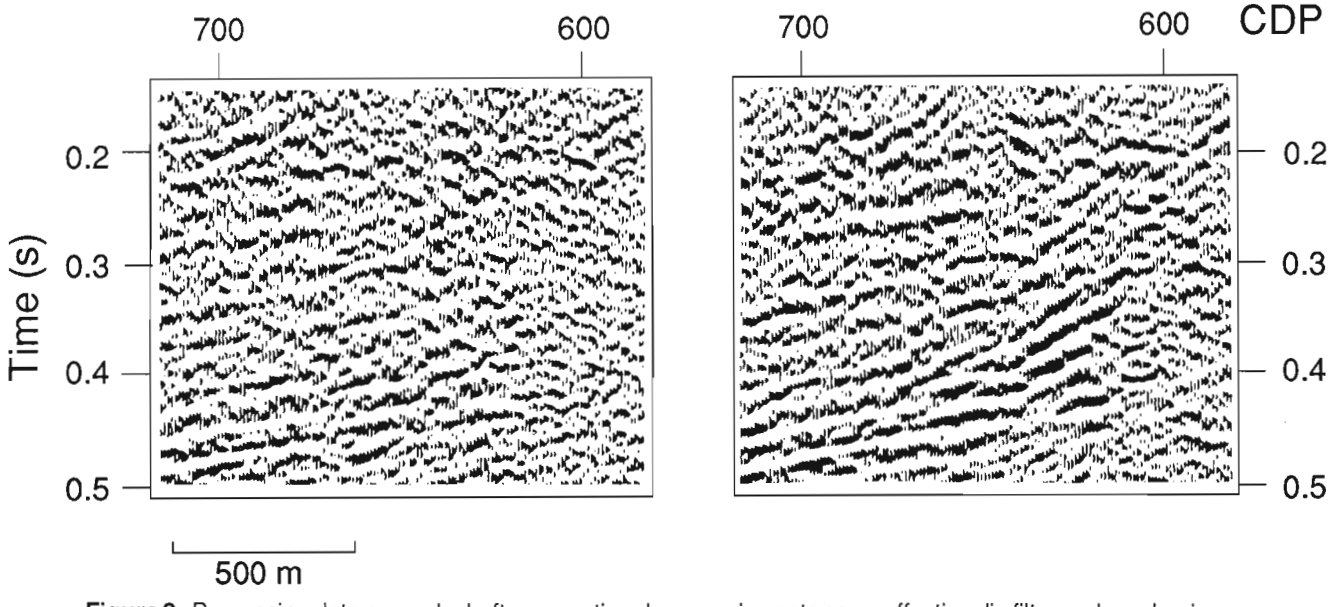


**Figure 2.** Processing data example. Left: conventional processing acts as an effective dip filter and emphasizes horizontal reflections. Right: dip-moveout (DMO) processing sequence preserves horizontal and dipping

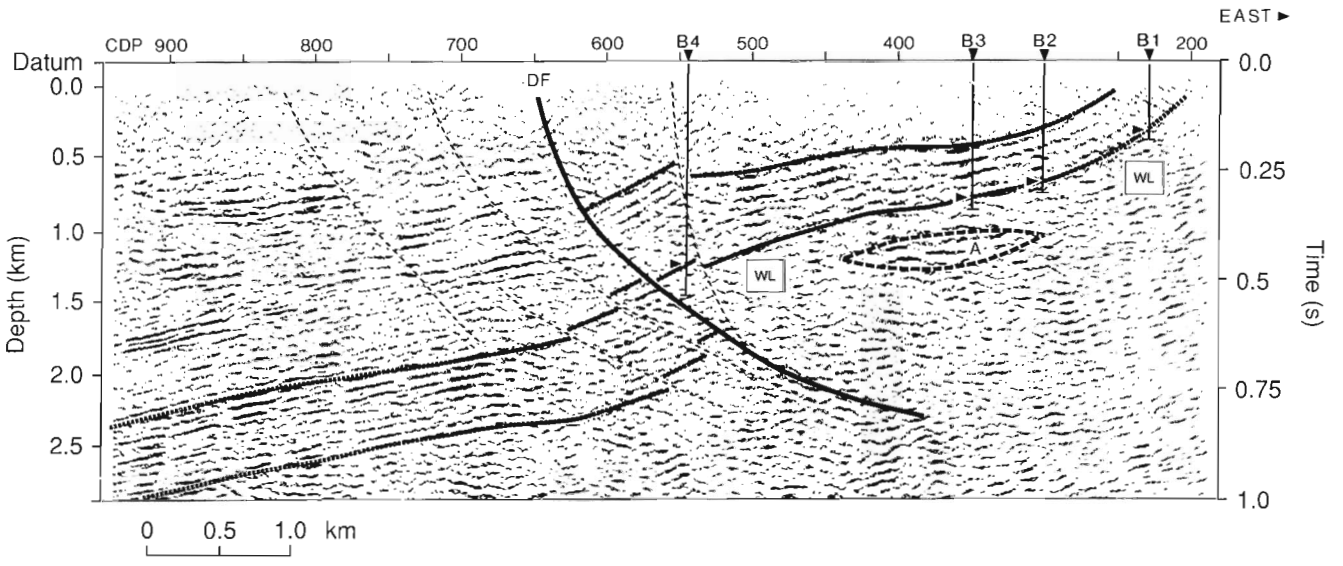


**Figure 3.** Interpretation of main features revealed by migrated seismic data with information from deep diamond drilling superimposed. Top and bottom of the reflective lower Wabassee Group and faults are marked by dashed lines. A 6000 m/s average crustal velocity was used to convert borehole information into equivalent reflection times (triangles mark Key Tuffite at the contact between Wabassee and Watson Lake Group). WL: Watson Lake Group; A: local amplitude anomaly within the Watson Lake Group; DF: Daniel Fault with splays; B1-4: boreholes.

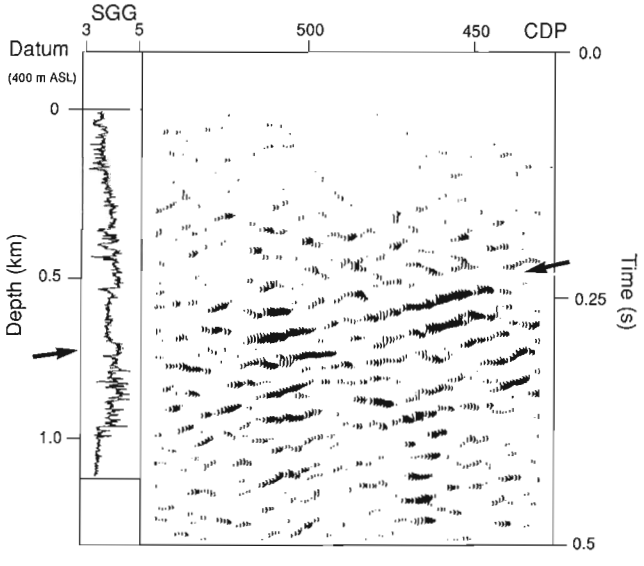


**Figure 4.** Seismic reflection and borehole spectral gamma-gamma (SGG) data from hole B4 for the Wabassee Group. Prominent reflections from near the top of the lower Wabassee Group (indicated by the arrows) show a good correlation with high SGG ratio indicating significant variations in the bulk rock chemistry.

The easternmost part of the seismic profile, between CDP 190 and 525, is characterized by a sequence of strong, west-dipping reflections that is overlain by a seismically transparent zone. The top and bottom of the reflective sequence clearly define the lower Wabassee Group. However, it is difficult to identify individual reflectors or marker horizons within the reflective sequence. The overlying upper Wabassee Group appears to be non-reflective. Borehole geophysical data from hole B4 (Fig. 4) confirm the proposed subdivision of the Wabassee Group. Spectral gamma-gamma (SGG) ratios (the ratio of high energy and low energy count rates) provide information about the elemental composition (changes in the rock equivalent atomic numbers) and density variations of rock formations; density variations are directly related to impedance contrasts and seismic reflection coefficients. High SGG ratios are observed for the 740 to 1000 m depth interval. The SGG anomaly correlates well with prominent reflections associated with a basalt-gabbro sequence from near the top of the lower Wabassee Group. The Key Tuffite and the underlying Watson Lake Group are characterized by their low reflectivity and can be traced with confidence at the base of the lower Wabassee Group. A 6000 m/s average crustal velocity was used to obtain reflection time estimates for comparison with the borehole data along the profile. The reflection image shows clear evidence for faulting in the lower Wabassee Group. In the underlying Watson Lake Group, a pronounced seismic amplitude anomaly can be observed at about 450 ms time (approximately 1300 m depth) beneath CDPs 300 to 425.

The central part of the profile, between CDP 525 and 750, contains information about the Daniel fault zone. A splay of the DF truncates the west-dipping reflections at about CDP 550. A highly reflective, west-dipping sequence can be observed at 650-750 ms west of the DF. This sequence may be equivalent to the reflective lower Wabassee Group identified at the eastern end of the seismic profile. Our preferred interpretation shows that the DF is not a single fault but a complex zone within which the reflective sequence appears to be down-faulted to the west. That reflections

associated with the lower Wabassee Group can be correlated across the DF zone suggests no major component of lateral movement or strike-slip faulting.

The western part of the profile, between CDP 750 and 1000, contains information about the upper Wabassee Group. Several bands of west-dipping reflections are observed west of the DF, but can not be correlated across DF. Our interpretation indicates significant thickening of the upper Wabassee Group west of the DF, where as much as 2500 m of continuous volcanic stratigraphy may be present. The reflective lower Wabassee Group is shown at the bottom of the seismic section with gentle westward dips of about 10 to 15 degrees.

## DISCUSSION AND CONCLUSIONS

LITHOPROBE's high-frequency vibroseis reflection profile was carried out across a portion of a well known Matagami mining camp. An important factor in the success of this reconnaissance survey was the availability of deep borehole information for the calibration of the seismic data. Our results confirm that seismic data acquisition and processing parameters can be tailored to image volcanic stratigraphy and structures. In particular, the high frequency reflection data defined the location and attitude of the Daniel fault zone and revealed a sequence of prominent reflections that can be correlated with the lower Wabassee Group. This group has been imaged at depth well beyond the limits of existing diamond drilling. The lower Wabassee Group may be used as a marker sequence to outline and map the western part of the Matagami volcanic center in three dimensions.

High-frequency reflection profiling may help to extend the limits of the Matagami mining camp, but more research is required to integrate this new mapping technique into normal exploration procedures.

## ACKNOWLEDGMENT

The seismic data for this experiment were collected by JRS Exploration of Calgary and preliminary data processing was done by Seismic Data Processors (SDP) of Calgary. Downhole geophysical measurements were conducted by the borehole geophysics section of the Geological Survey of Canada. We thank Noranda Exploration Ltd. for permission to publish this case history.

## REFERENCES

**Green, A.G., Milkereit, B., Mayrand, L.J., Ludden, J.N., Hubert, C., Jackson, C.L., Sutcliffe, R.H., West, G.F., and Verpaelst, P.**
1990: Deep structure of an Archean greenstone terrane, Nature, v. 344, p. 327 - 330.

**Milkereit, B., Green, A.G., Lee, M.W., Agena, W.F., and Spencer, C.**
1990: Pre- and post-stack migration of GLIMPCE reflection data, Tectonophysics, v. 173, p. 1-13.

**Piché, M., Guha, J., Gaigneault, R., Sullivan, J.R., and Bouchard, G.**
1990: Les gisements volcanogènes du camp miner de Matagami: structure, stratigraphie et implications métallogéniques; in: The northwestern Quebec polymetallic belt; edited by M. Rive, P. Verpaelst, Y. Gagnon, J.M. Lulin, G. Riverin, and A. Simard; The Canadian Institute of Mining and Metallurgy, Special Volume 43, p. 327 - 335.

**Sheriff, R.E. and Geldart, L.P.**
1982: Exploration Seismology: history, theory and data acquisition; Cambridge University Press, Cambridge, 253 p.

**Spencer, C., Thurlow, G., Wright, J., White, D., Carroll, P., Milkereit, B., and Reed, L.**
1992: A Vibroseis reflection survey at the Buchans mine in central Newfoundland; Geophysics; in press.

**Yilmaz, Ö.**
1987: Seismic data processing, Society of Exploration Geophysics, Tulsa, 526 p.

Geological Survey of Canada Project 870046

# The East Athabasca mylonite zone : an Archean segment of the Snowbird tectonic zone in Northern Saskatchewan

**Simon Hanmer, Mark Darrach[1], and Chris Kopf[2]**
**Continental Geoscience Division**

*Hanmer, S., Darrach, M., and Kopf, C., 1992: The East Athabasca mylonite zone : an Archean segment of the Snowbird tectonic zone in Northern Saskatchewan; in Current Research, Part C; Geological Survey of Canada, Paper 92-1C, p. 19-29.*

***Abstract***

*The East Athabasca mylonite zone is a triangular segment of the Snowbird tectonic zone, characterized by a complex flow pattern. Polyphase deformation occurred under transitional to granulite facies conditions at ca. 3.2 and ca. 2.6 Ga.*

***Résumé***

*La zone mylonitique d'East Athabasca forme un tronçon de la zone tectonique de Snowbird. Les épisodes de déformation polyphasée ont eu lieu, au faciès des granulites, à ca. 3,2 et ca. 2,6 Ga.*

[1] Department of Geology and Geography, U. Mass., Amherst, Massachussetts
[2] Earth Science Board, U.C.S.C., Santa Cruz, California

## INTRODUCTION

The Snowbird tectonic zone, clearly delimited as a pronounced linear anomaly in the horizontal gravity gradient map of the Canadian Shield, is well exposed as a triangle of high grade mylonitic rocks (125 by 80 by 75 km) in the Stony Rapids area, northern Saskatchewan (Fig. 1). The triangular structure (Tantato Domain of Gilboy, 1980; Slimmon, 1989) lies at the northeast end of the largest (300 by 100 km) of a chain of magnetically defined elliptical domains which may represent relatively stiff, crustal-scale 'boudins' (see Hanmer et al., 1991 for references).

Tantato Domain is divided into two structural decks (Fig. 2; Hanmer et al., 1991). The fan-shaped lower deck is characterised by upright foliations and shallowly to moderately SW plunging extension lineations. The upper deck is arcuate. Foliations parallel to its northwest-southeast trending margin dip shallowly to the southwest at an high angle to the upright foliations of the lower deck, whereas those parallel to the northeast-southwest trending margin are upright. All extension lineations in the upper deck plunge shallowly, toward either the southwest or the northwest. Preliminary geochronological data (unpublished; U/Pb zircon), quoted in this report, have been obtained by R. Parrish (Geochronology Laboratory, Geological Survey of Canada). In order to more clearly convey the structural nature of the Snowbird tectonic zone in the map area (Fig. 3), we suggest that the name East Athabasca mylonite zone (EAmz) should replace the non-genetic term 'Tantato Domain'.

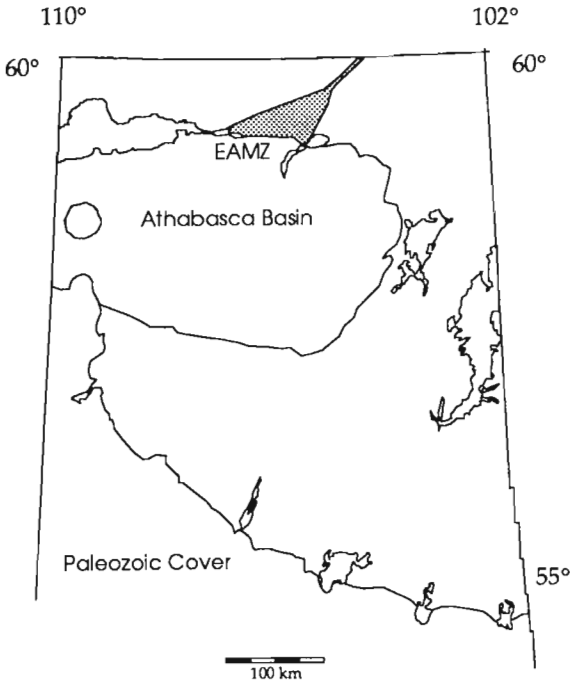


**Figure 1.** Location of East Athabasca mylonite zone (EAmz).

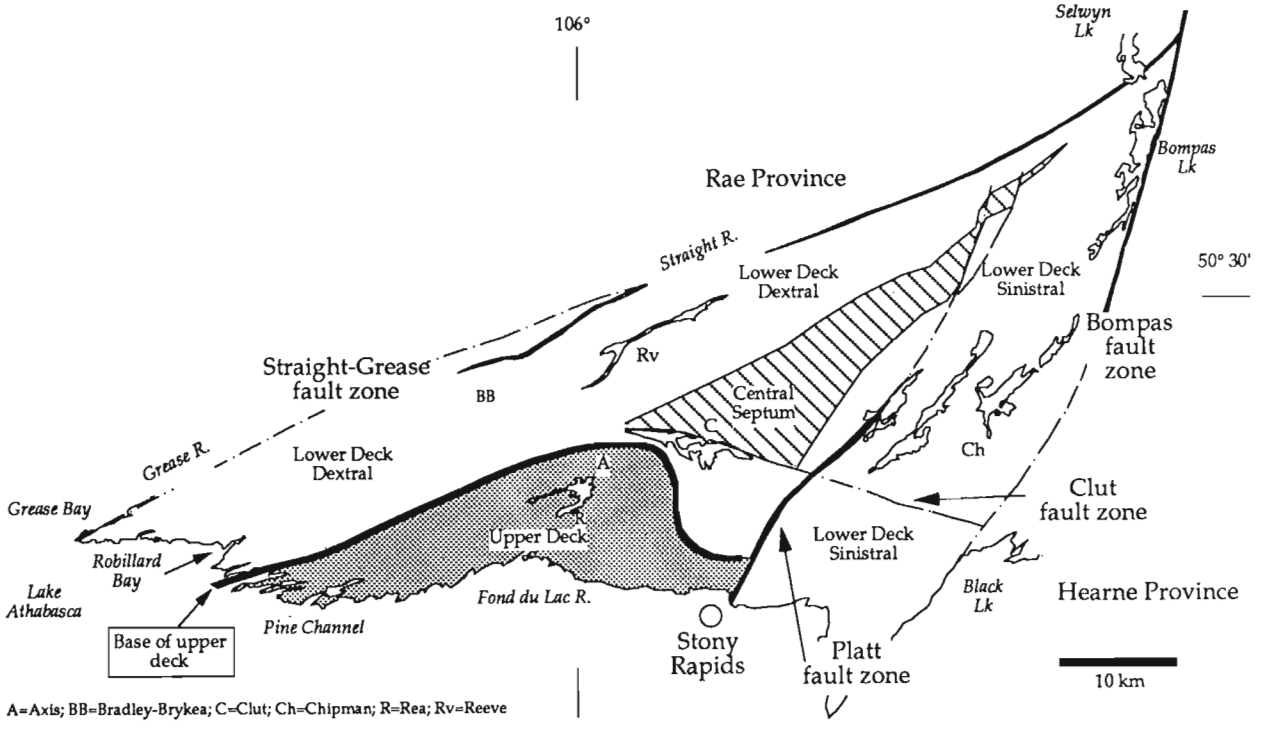


**Figure 2.** Structural framework of East Athabasca mylonite zone.

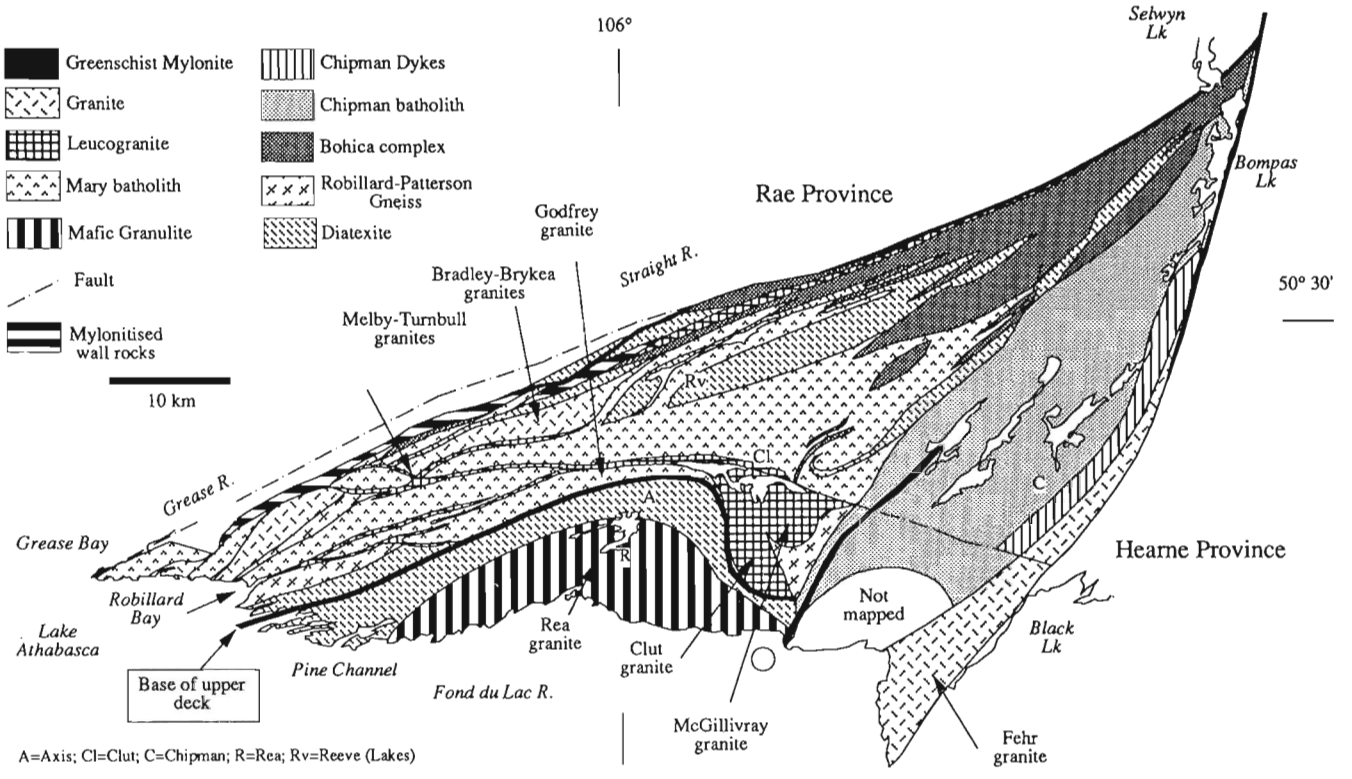


**Figure 3.** Geology of East Athabasca mylonite zone.

## UPPER DECK

### *Pine Channel diatexite*

The Pine Channel diatexite, 4 km thick, is banded, leucocratic and quartzo-feldspathic with an highly variable content of lilac to delicate pink garnets, orthopyroxene, graphite and sillimanite. Mylonitic to ultramylonitic ribbon fabrics are penetratively developed throughout the Pine Channel diatexite, except near Pine Channel. There, kilometric lenses of often highly irregular, folded migmatite (Fig. 4), with cross-cutting garnet-orthopyroxene granitoid sheets, form a stack of steeply SE dipping 'horses', bounded above and below by their highly attenuated ultramylonitised equivalents (Figs. 5 and 6).

### *Fond du Lac mafic granulites*

The Fond du Lac mafic granulites are a 5 km thick stack of sheets (each up to 2 km thick), essentially orthopyroxene-plagioclase-magnetite ± garnet in composition, separated from one another by thin, often mappable, horizons of diatexite ribbon mylonite. The mafic granulites (meta-gabbro/norite), which preserve ophitic igneous textures throughout a thickness of more than a kilometre south and east of Axis Lake, grade into the annealed mylonites which predominate throughout this map unit. An hitherto unknown, compositionally homogeneous, locally clinopyroxene-bearing leucocratic granite outcrops along the south shore of Axis Lake and west of Rea Lake; the Rea granite. Contact relations with the mafic granulites are not exposed, and the granite is penetratively mylonitised with an excellent ribbon fabric.

**Figure 4.** Structurally complex migmatite, Pine Channel diatexite. Large dimension of illustration is 1m.

## LOWER DECK

Diatexite in the lower deck is petrologically and structurally very similar to the Pine Channel diatexite. We propose the name Reeve diatexite.

**Figure 5.** Core-and-mantle structure in orthopyroxene in orthopyroxene ribbon mylonite after granite, Pine Channel diatexite.

**Figure 6.** Mylonitised diatexite with orthopyroxene ribbons, Pine Channel diatexite.

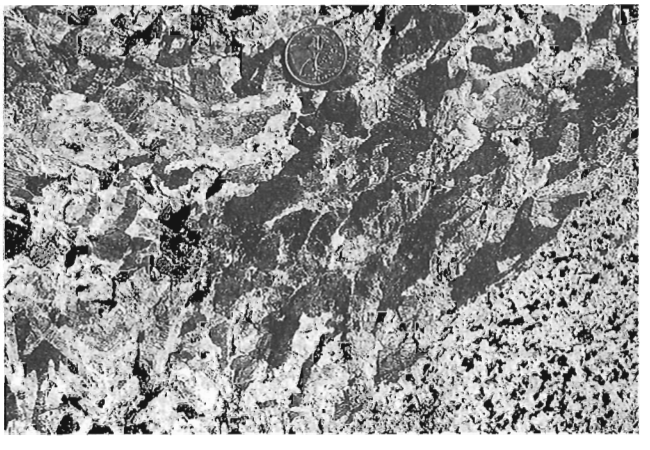

**Figure 7.** Isotropic norite, Bohica complex.

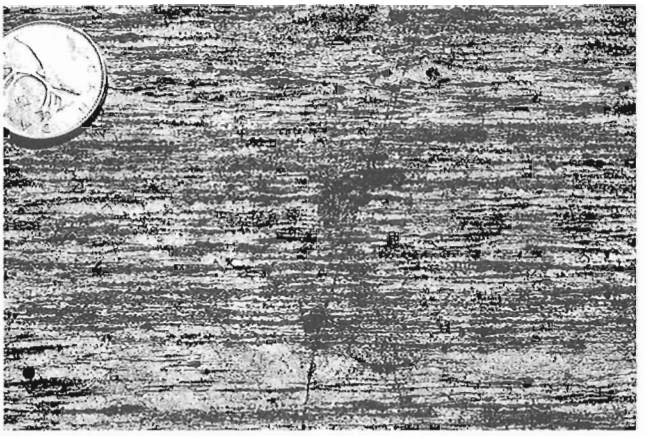

**Figure 8.** Noritic ribbon ultramylonite, Bohica complex.

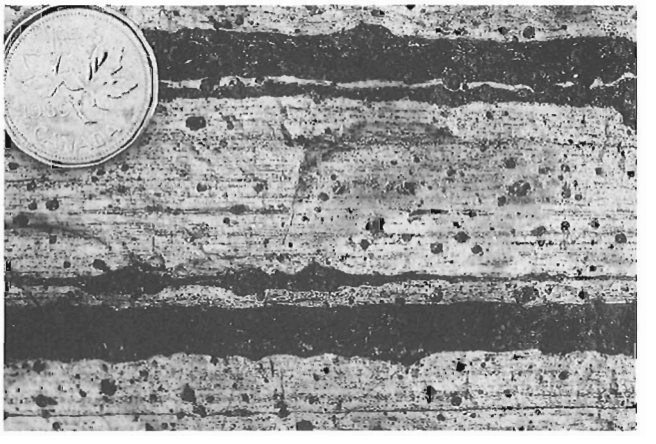

**Figure 9.** Anorthositic ribbon ultramylonite with garnet-clinopyroxene bands.

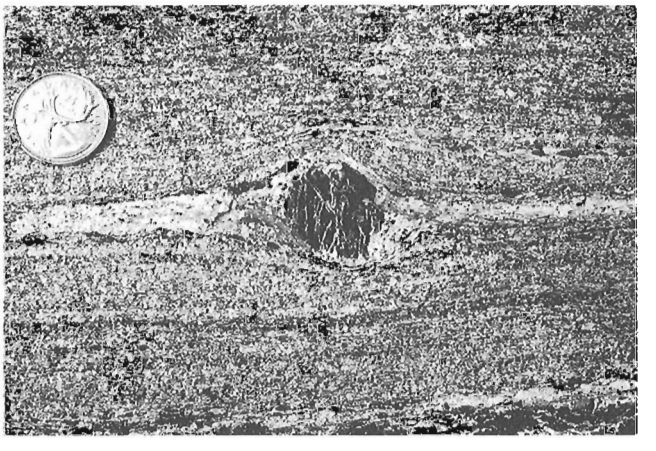

**Figure 10.** Plagioclase porphyroclast in annealed tonalite straight gneiss (mylonite), Chipman batholith.

### *Bohica complex*

Very coarse primary ophitic textures to strongly flattened flaser fabrics are locally preserved in norite, gabbro, anorthosite and diorite, especially in the central part of the EAmz. The norite may contain xenoliths of Reeve diatexite. The coarse igneous textures can be followed progressively into garnet-two pyroxene to garnet-hornblende (± pyroxene) mylonites (Figs. 7 and 8). Two large bodies of anorthosite and gabbroic anorthosite ultramylonite with splendid ribbon fabrics (Fig. 9), locally strongly annealed, outcrop on the SE side of the complex.

### *Chipman batholith*

In the tonalitic Chipman batholith, Hanmer et al. (1991) identified a coarse grained, low strain central core, flanked to the SE by strongly annealed tonalitic straight gneisses (mylonites; Fig. 10), and to the northwest by clinopyroxene-bearing tonalite ribbon mylonites and ultramylonites. Widespread xenoliths and rafts represent the remains of a dismembered layered mafic-anorthositic-ultramafic complex. The Chipman batholith also contains concordant, transposed slices of Reeve diatexite along its western margin. We suggest that these are xenolithic rafts of country rock within the batholith, whereas the Bohica complex is a potential source of the dispersed mafic inclusions within the Chipman batholith. Accordingly the Reeve diatexite and the Bohica complex should be older than the Chipman batholith.

A regionally concordant swarm of Chipman dykes (garnet-hornblende and garnet-clinopyroxene; Fig. 11) was emplaced throughout the batholith. However, east of a line through Chipman Lake, and spatially coincident with the strongly annealed tonalitic straight gneisses, the dykes may form up to 70+% of the map unit in belts up to 1.5 km thick. The dykes show a complete range of deformation, from early transposed components of the tonalite gneissosity, to later cross-cutting, dykes with pristine igneous contacts. The earlier, strongly foliated dykes and the tonalitic straight gneisses are cross-cut by an array of 1-10 m thick leucogranite veins (Hanmer et al., 1991; ca. 3.2 Ga.).

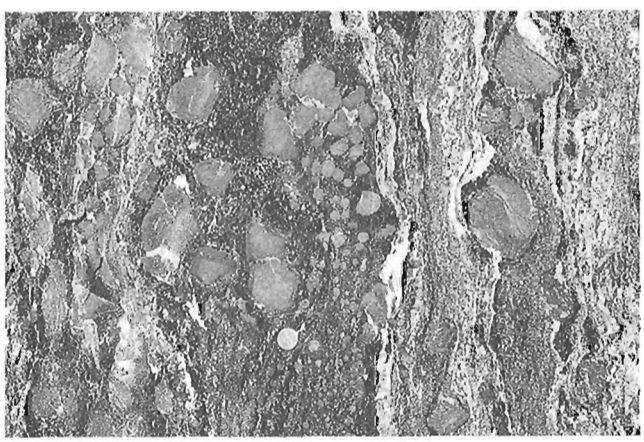

**Figure 11.** Garnet-hornblende meta-dyke with tonalitic melt, Chipman dykes.

### *Mary batholith*

Hanmer et al. (1991) first distinguished the Mary batholith as a compositionally monotonous, garnet-hornblende-clinopyroxene granite to granodiorite (ca. 2.6 Ga.). The abundance of mafic minerals lends a mesocratic aspect to the granitoids in the western part of the batholith. By contrast, granitoid rocks in the eastern part are distinctly leucocratic (ca. 2.6 Ga.), yet contain the same mineral assemblages as found in the west. The garnet-hornblende-clinopyroxene content of the batholith rocks is highly variable, both between and within individual outcrops. The mechanical disaggregation of fist to football sized garnet-pyroxene aggregates within the host granitoid suggests that the mineralogical heterogeneity may reflect variation in the xenocryst population at all scales.

In the western part of the batholith (Fig. 12), two distinctive types of tectonite were derived from the same, locally preserved, very coarse grained (5 cm+) hornblende-pyroxene? granitoid protolith. One is a coarse ribbon gneiss, wherein the igneous feldspars have been tectonically drawn out into thick polycrystalline ribbons, 100 by 5 mm, and which contains very few feldspar porphyroclasts (Fig. 13). The other is a very fine grained, annealed porphyroclastic mylonite, with 5-50 mm feldspar porphyroclasts, and smaller ones of hornblende and garnet (± pyroxene; Fig. 14). By contrast, tectonic fabrics in the eastern part of the batholith vary from isotropic to protomylonites, with locally developed, but nevertheless voluminous, mylonite to ultramylonite. Our field observations suggest that (i) the leucocratic eastern granitoids are a relatively late component of the Mary batholith, (ii) the mesocratic western granitoids were syntectonically emplaced during regionally pervasive mylonitisation, whereas (i) was emplaced during the waning stages of the deformation.

### *Other granites*

Discrete, map-scale plutons and sheets of generally leucocratic granite occur throughout the lower deck of the EAmz. They may not represent a related suite of granites and are only grouped here for clarity of presentation.

The Godfrey granite was described by Hanmer et al. (1991) as a coarse grained, garnet-pyroxene granite, lining the base of the upper deck in the Clut Lakes area. We cannot exclude the possibility that this granite is related to the Mary batholith. The Brykea granite is a strikingly salmon pink granite ultramylonite with abundant, 1 mm cherry red garnets set in a fine grained, sugary annealed matrix with variable proportions of small feldspar porphyroclasts. The Bradley granite is a splendid ribbon ultramylonite derived from a very coarse grained protolith. The Fehr granite (ca. 2.6 Ga.) is generally isotropic and extremely coarse grained. To the SE, the granite is charged with abundant amoeboid clots of coarse, polycrystalline hornblende ± orthopyroxene, visibly derived by the disaggregation of larger, metre size xenoliths, reminiscent of the inferred xenocrystic mafic phases of the Mary batholith.

The granite is cut by a swarm of regionally strike-parallel mafic dykes, 1-10's of metres wide, which may locally account for 20% of the Fehr granite outcrop. Some of the dykes contain abundant 2-4 mm garnets, often replaced by plagioclase. Although its intrusive contact with the Chipman batholith is abrupt, veins of Fehr granite cut across both the batholith structure and the Chipman dykes. Accordingly, there are at least two dykes swarms in the eastern part of the EAmz.

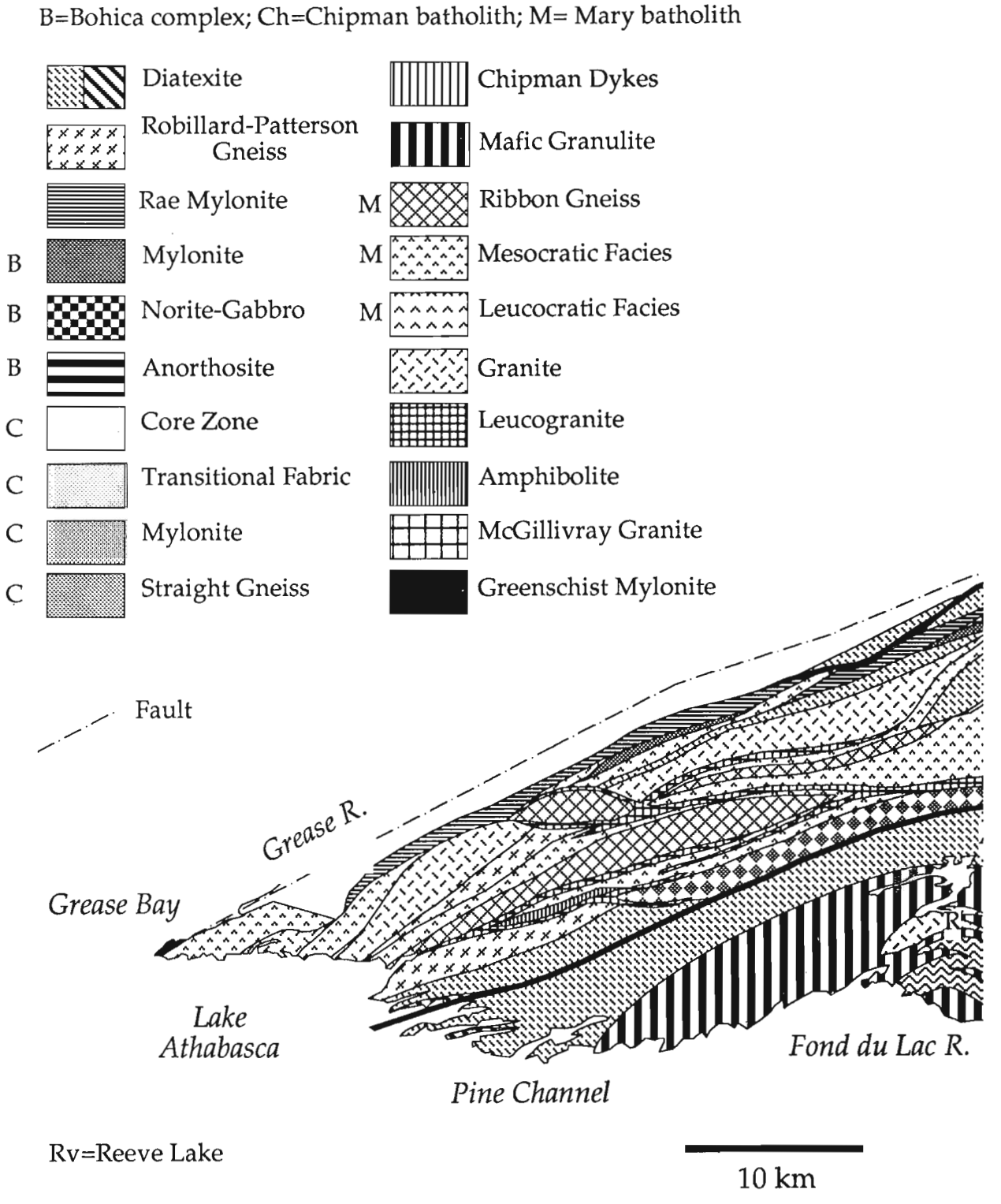


**Figure 12.** Detail of SW corner of Fig. 3.

The Clut granite (ca. 2.62 Ga.) is a voluminous biotite-hornblende leucogranitic protomylonite which occupies the Clut Lakes area. The late-syntectonic McGillivray granite (ca. 2.62 Ga.) intruded the already deformed Clut granite (Hanmer et al., 1991).

Along strike to the southwest of the Clut Lakes granite is a suite of biotite-hornblende leucogranite sheets, each one up to several hundreds of metres thick, or more; the Melby-Turnbull granites. They lie preferentially within the belts of porphyroclastic mylonite which enclose the map-scale lozenges of ribbon gneiss and Reeve diatexite. Although the poorly foliated parts of the granite sheets have abrupt intrusive contacts and contain misoriented xenoliths of the adjacent porphyroclastic mylonites, they are themselves locally to extensively mylonitised. We suggest that they were emplaced during the waning stages of mylonitisation.

### *Robillard-Patterson gneiss*

Two map-scale slices of white granitoid gneiss, with included rafts of rhythmically layered garnet-sillimanite metapelite, occur within the lower deck, east of Robillard Bay and west of Patterson Creek. The granitoid component, is well banded, coarsely rodded and irregularly folded. At the grain-scale, the rock is coarsely recrystallised and generally lacks a shape fabric. Pegmatite veins in a variety of strain states are common and may cross-cut both banding and folding in the gneiss. In the eastern exposures, the gneiss is distinctly migmatitic, although it includes a very coarse grained granitoid which intrudes a large mass of isotropic gabbro. We suggest that the fabrics in the Robillard-Patterson gneiss may be older than the deformation and metamorphism of the adjacent mylonite zone rocks.

## STRUCTURE AND METAMORPHISM

Our completed mapping allows us to confirm and elaborate upon the broad structural geometry outlined by Hanmer et al (1991). Foliations within the fan-shaped lower deck are generally steeply dipping and concordant with the EAmz boundaries, except in the southwest, along the shore of Lake Athabasca. Here, the foliation is often very shallow dipping and highly variable in orientation. Nonetheless, extension lineations tend to plunge moderately to shallowly toward the southwest, irrespective of foliation attitude.

The distribution, development and preservation of high-strain fabrics in the lower deck are complex. Relatively low-strain fabrics in granitic and mafic lithologies are characterised by moderately flattened plates of polycrystalline quartz or plagioclase. More rarely, isotropic igneous fabrics are preserved with coarse equant quartz grains or coarse ophitic pyroxenes.

The principal low strain zone is the Central Septum (Fig. 2) of heterogeneously deformed Bohica complex mafic rocks and leucocratic Mary batholith granites. It is flanked on either side by regional-scale strain gradients, passing into extremely attenuated Reeve diatexite, Chipman batholith and Bohica complex ribbon mylonites.

Outside of the relatively low strain zones, the rocks of the lower deck are highly attenuated mylonites or straight gneisses, with the exception of the Robillard-Patterson gneiss. To the northwest of the Central Septum, garnet-hornblende-pyroxene (± sillimanite) ribbon mylonites are developed from Reeve diatexite, Bohica complex and Mary batholith lithologies. Within 2 km of the northwest margin of the EAmz, mylonites are so fine grained that the ribbon structure is difficult to discern in the field. To the southeast of the Central Septum, garnet-two pyroxene ribbon mylonites are developed from Reeve diatexite, anorthosite and mafic rocks of the Bohica complex and from the Chipman batholith. A narrow belt, less than a kilometre thick, of garnet-hornblende ribbon mylonites is developed along the eastern margin of the EAmz in rocks of the Chipman batholith and the northern part of the Fehr granite.

Between the garnet-hornblende ribbon mylonites to the east, and the relatively low strain central core to the west (Hanmer et al., 1991), the Chipman batholith and the earlier components of the Chipman dyke swarm have been folded

**Figure 13.** Ribbon gneiss, Mary batholith .

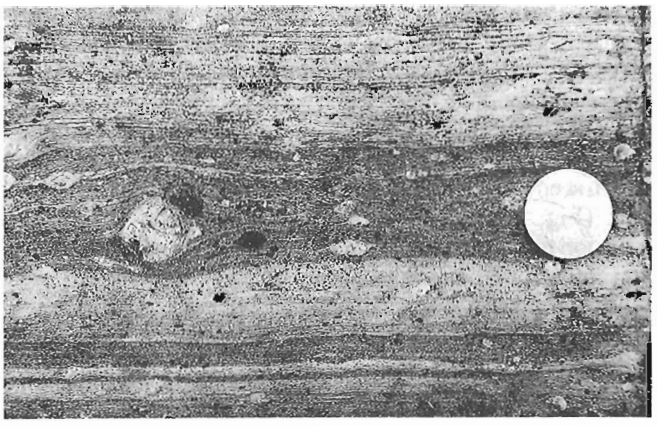

**Figure 14.** Porphyroclastic mylonite, with hornblende porphyroclasts.

and transposed to form a coarsely recrystallised, annealed hornblende (± garnet) straight gneiss, totally lacking in shape fabrics. The straight gneiss banding has been locally disrupted and folded, and intruded by syntectonic, locally mylonitised leucogranite veins, all cross-cut by the later components of the Chipman dyke swarm. A magmatic crystallisation age of ca. 3.2 Ga., obtained from one of the syntectonic granite veins which cross-cuts the straight gneiss banding, indicates that the straight gneiss fabric is ca. 3.2 Ga. or older. It also indicates that the Chipman dyke swarm was emplaced at ca. 3.2 Ga., and that transitional granulite facies metamorphic conditions prevailed at that time. In contrast, the high grade ribbon mylonites in the rest of the lower deck developed at the expense of a suite of protoliths ranging in age from pre-3.2 Ga. to 2.6 Ga. If all of these ribbon fabrics are approximately contemporaneous, as the field mapping suggests, then the ribbon mylonites may be at least 0.6 Ga. younger than the straight gneisses.

Within the upper deck, the strike of the foliation in the penetratively developed orthopyroxene-plagioclase, garnet-orthopyroxene and sillimanite-orthopyroxene ribbon mylonites is concordant with respect to the deck margin. In the west, steeply southeast dipping to upright foliations trend NE and carry subhorizontal to gently SW plunging longitudinal extension lineations. In the east, foliations dip west at ca. 25° and carry steeply pitching, transverse extension lineations. Although the base of the lower deck coincides with a lithological boundary in the east, in the west it lies within the Pine Channel diatexite. The boundary is everywhere the limit of penetrative, *completely transposed* ribbon mylonites. Within the adjacent lower deck, although the Pine Channel diatexite is a ribbon mylonite, it contains abundant cross-cutting and open to tight folded granite veins. At the boundary of the upper deck, the granite sheets are totally transposed and the ribbon fabric becomes even more extremely attenuated.

### *Greenschist Fault Zones*

Hanmer et al. (1991) described both discrete brittle faults and narrow (100 m) belts of greenschist mylonite along the eastern and northwestern margins of the EAmz (Black Lake and Grease River - Straight River shear zones, respectively; Gilboy, 1980; Slimmon, 1989). Previous workers have over emphasised the mylonitic nature of these complex fault zones. For example, the principal exposures of the "Black Lake shear zone" at Black Lake are not mylonites at all. The western shore of Black Lake is formed of intensely crenulated pelitic schists with coarse (5 cm) porphyroblasts which we have traced along strike to the northeast into the eastern wall rock (Fig. 15). The porphyroblasts contain fossilised inclusion trails representing preserved open fold hinges of the first foliation, preserved from transposition within the relatively stiff crystals. The contact with the Fehr granite, exposed in the cliff section, is a discrete fault.

Our mapping suggests that significant volumes of greenschist mylonite are only preserved along these marginal fault zones in the northern part of the EAmz, except for a 500 m thick belt at Grease Bay. Elsewhere, they are cut out by later brittle faulting. Furthermore, the geometry of the discrete fault strands, mylonitic or otherwise, is complex. Between Reeve Lake and Grease Bay, the fault zone is made of a number of anastomosing strands, some of which lie to the SE of the Straight River. Accordingly, we propose to call the eastern structure the Bompas fault zone, and the northwestern structure the Straight-Grease fault zone.

**Figure 15.** Crenulated porphyroblastic schist, Black Lake.

Within the EAmz, the eastern contact between the upper and lower decks is the narrow (<500 m) greenschist facies mylonitic Platt Creek fault zone (Platt Creek shear zone of Gilboy, 1980). We have traced the chlorite-actinolite fault zone mylonites to the northeast where they form discontinuous lenses distributed en-echelon along slices of relatively stiff anorthosite. North of the latitude of Clut Lakes, the greenschist mylonites occur only sporadically along a discrete fault, which splays and terminates within the EAmz. The Taylor fault zone is a narrow (<100 m) belt of west dipping, dip-lineated, top-down to the west hornblende-bearing mylonites developed along the western flank of the McGillivray granite (Hanmer et al., 1991). It either roots into, or is truncated by, the Platt Creek fault zone. In either case, the Plat Creek fault zone is dip-lineated in the vicinity of the possible junction.

The Clut fault zone outcrops as a narrow (<50 m) belt of steeply south dipping, dip-lineated actinolitic mylonites along the north shore of west Clut Lake. It may be extended to the east along a topographic lineament. Although the geology of the Chipman batholith shows significant differences across this lineament, the fault is nowhere exposed east of the Clut Lakes, nor does it appear to off-set any of the northeast-southwest trending map-unit boundaries. While it is possible that a dip-slip fault cutting across steeply dipping markers may not displace them in the map plane, we maintain a degree of scepticism concerning the validity of the inferred extended fault trace.

### *Kinematics*

The distribution patterns of both strain rate and shear-sense are complex within the EAmz. As we shall demonstrate, both show a causal relationship to the emplacement of leucogranite sheets, especially in the southern part of the lower deck.

We confirm the suggestion of Hanmer et al. (1991) that the lower deck is divided into two shear-sense sectors, dextral in the northwest and sinistral in the east (Fig. 2). A full range of mechanically independent shear-sense (winged porphyroclasts and inclusions, asymmetrical extensional shear bands, C/S fabrics) and kinematic indicators (boudinaged oblique veins) occurs throughout both sectors (Fig. 16; e.g. Hanmer and Passchier, 1991). This flow pattern applies equally to the greenschist mylonites of the Straight-Grease and Bompas fault zones. Note also that the kinematically complex Platt Creek fault zone, geometrically parallel to the sinistral Bompas fault zone is, at least in its northeast part, a sinistral strike-slip structure. Hanmer et al. (1991) suggested that top-down to the SW displacement of the upper deck was accommodated by sub-granulite facies shearing within the underlying, apparently concordant, Godfrey and Clut granites. They further suggested that the penetrative development of the upper deck granulite facies mylonites was related to initial thrust emplacement of the deck. We have found few, but widespread, shear-sense indicators within the upper deck mylonites. All without exception, indicate that the mylonite fabrics formed during top-down to the southwest shearing. Moreover, preliminary geothermobarometric data do not lend support to the suggestion of Hanmer et al. (1991) that the granulites of the upper deck necessarily formed at higher temperatures than those of the lower deck. Finally, mapping shows that the lithologies of the upper deck are not exotic with respect to the lower deck. Accordingly, we can no longer advance the hypothesis of initial thrust emplacement.

Shear-sense indicators, principally asymmetrical extensional shear bands, are common within the Central Septum. Both sinistral and dextral shear-sense indicators occur in similar proportions. If these structures are contemporaneous, the Central Septum has followed an approximately coaxial deformation path. Nevertheless, an highly variable sense of shear is locally developed in the Central Septum, often as a direct function of the orientation of the plane along which the local shearing was resolved. This is remarkably well illustrated in the case of xenolithic rafts and screens of Reeve diatexite and Bohica complex gabbro?-norite within the leucocratic eastern part of the Mary batholith (Fig. 17). Northeast of Clut Lakes, where the principal gabbroic raft is oriented ca. 070° parallel to the dextral boundary of the EAmz, the shear-sense is dextral. Along strike to the SW, where the orientation of the gabbroic raft swings to ca. 020° parallel to the sinistral margin of the EAmz, the shear-sense is sinistral. To the southeast, in the axial zone of the large southwest plunging fold marked by the screen of Reeve diatexite, top-down to the southwest dip-slip displacements occurred along the axis-parallel extension lineation within diatexite ultramylonites. The ultramylonites can be followed around the fold into the 070° trending fold limb where the mylonitic foliation is upright and the extension lineation coaxial with that in the axial zone. We suggest that the upright mylonites formed during transcurrent (dextral?) shear and are kinematically compatible with the displacements observed in the axial zone. The point to retain here is that appropriately oriented components of the fold structure resolved the same shear-sense as the southwest dipping base of the upper deck and the ENE trending margin of the EAmz.

Hanmer et al. (1991) noted the spatial coincidence of granulite facies mylonites, unusually rich in porphyroclasts, and the development of a map-scale anastomosing pattern of mylonitic belts in the Reeve Lake area of the lower deck. This structural pattern extends from Reeve Lake to the shore of Lake Athabasca and corresponds, for the most part, to the lozenges of coarse ribbon gneiss of Mary batholith affinity, enclosed by belts of annealed porphyroclastic mylonite (Fig. 12). The bulk strain experienced by of most of the lozenge material is lower than that of the enclosing porphyroclastic mylonites. Locally, as at Reeve Lake, diatexite is coarse grained and isotropic. Deformation fabrics in Mary batholith protolith are either heterogeneous from outcrop to outcrop, or remarkably homogeneous at all scales down to the hand-specimen, as in the ribbon gneisses. The ribbon gneiss and porphyroclastic mylonites are particularly significant. Although both were derived from the same protolith, at the same metamorphic grade, the porphyroclast-poor ribbon gneisses cannot represent an

**Figure 16.** Dextral rotated winged inclusion, Mary batholith.

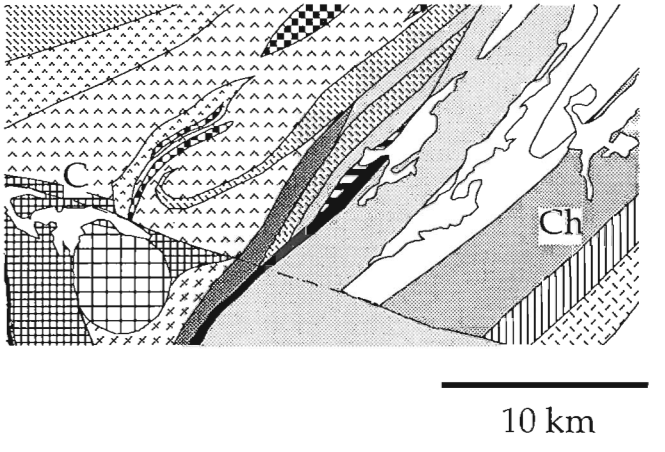


**Figure 17.** Detail of Clut Lakes area of Fig. 3. Legend as in Fig. 12.

intermediate step in the fabric path leading to the porphyroclastic mylonites. We suggest that these different fabric paths were determined by differences in strain rate, whereby slower rates would favour homogeneous crystal plasticity of the constituent feldspars at all scales. At faster strain rates, plastic deformation mechanisms in the feldspars would not have been able to keep up with the imposed deformation and the feldspars developed as stiff porphyroclasts.

If our hypothesis is correct, then the anastomosing pattern of porphyroclastic mylonite belts in the southwest part of the lower deck represents the spatial distribution of strain rate at the map-scale. However, this begs the question of the cause of the heterogeneous deformation. We note that the volume of heterogeneous flow is located adjacent to the northeast-southwest oriented lateral ramp of the upper deck (Fig. 18), where the bulk shear planes and extension lineations in both the lower and upper decks are mutually coplanar and collinear. Hanmer et al. (1991) suggested that the dextral and sinistral sectors in the lower deck represent a complex bulk coaxial flow located at the northeast end of a relatively stiff crustal-scale boudin. In 2D, this flow pattern would represent a response to horizontal, northwest-southeast shortening (Fig., 19). The top-down to the southwest shear-sense developed throughout the upper deck may represent a response to vertical shortening. If the two principal shortening directions represent *contemporaneous active loads*, they would each generate northeast-southwest oriented dextral shear along steeply dipping planes. This would result in mutually reinforcement, and an anomalously elevated rate of dextral shear strain should occur adjacent to the lateral ramp of the upper deck. In contrast, because the shear planes in the upper and lower decks are oriented at an high angle to each other, there can be little or no shear strain rate reinforcement in the vicinity of the trailing edge of the upper deck.

Hanmer et al. (1991) suggested that the Clut and McGillivray granites were emplaced into a zone of potential dilation adjacent to the trailing edge of the upper deck. We would further suggest that the displacements associated with the upper deck were also influential in the emplacement into the lower deck of the eastern leucocratic components of the Mary batholith and the Melby-Turnbull granite sheets. In the former case, the granitoids are located opposite the trailing edge of the upper deck and our interpretation is analogous to that for the Clut granite. However, we note that the Melby-Turnbull granite sheets were preferentially, and syntectonically, emplaced into what we interpret as relatively high strain rate mylonite belts. We suggest that belts of elevated strain rate are ideal sites for transient excursion into the brittle deformation field, in response to short lived increase either in pore fluid pressure, or in strain rate. In either case, brittle fracture and dilation would favour the emplacement of sheet-like bodies of granite magma. With decay of the transient perturbation, the deformation would return to the plastic regime, with continued mylonitisation. Accordingly, we propose that the displacements of the upper deck in the EAmz have controlled much of the syntectonic emplacement of granitoid magmas within the adjacent lower deck.

## ECONOMIC IMPLICATIONS

Current exploration and drilling activity (nickel and gold; Devex Exploration Inc. and Noranda Exploration Co. Ltd) is focussed on the classic sites at Axis and Rea Lakes. During the past decade, there has been some exploration and drilling along the northwest margin of the EAmz, particularly between Reeve and Selwyn Lakes. In this context, it is perhaps significant that (i) an hitherto unknown body of (Rea) granite outcrops within gabbroic-noritic and paragneissic

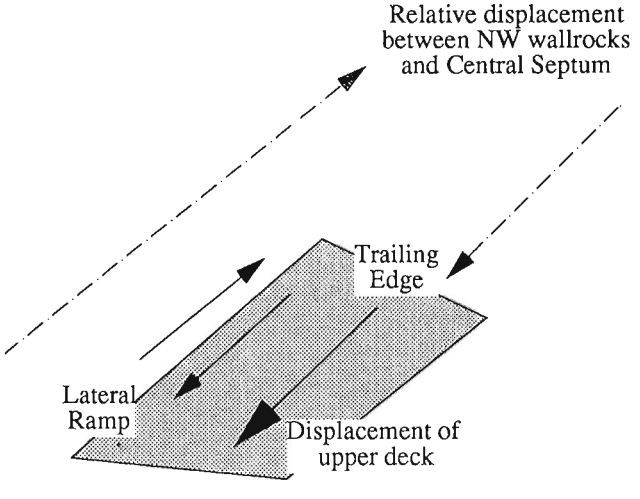


**Figure 18.** Sketch of geometrical relations between displacements of the lateral ramp of the upper deck and the dextral shear in the lower deck.

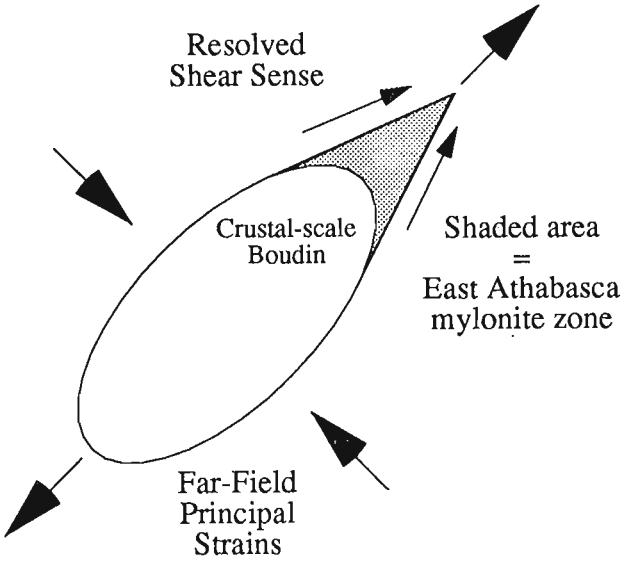


**Figure 19.** Sketch of the 2D geometrical and kinematical relations at the NE end of a crustal-scale boudin subjected to bulk progressive pure shear. See text.

rocks between the targets of economic interest in the upper deck, and that (ii) an important volume of mylonitised, hitherto unidentified mafic plutonic material (Bohica complex), in spatial association with paragneissic rocks occurs in the vicinity of exploration sites in the lower deck.

## SYNTHESIS

A pile of pelitic metasediments, located between the Rae and Hearne Provinces, was intruded by the Bohica layered mafic complex, and subsequently by the tonalitic Chipman batholith pre-ca. 3.2 Ga. At ca. 3.2 Ga, the Chipman batholith was strongly deformed (mylonitised during strike-slip sinistral shear), annealed under transitional granulite facies conditions and invaded by the voluminous Chipman mafic dyke swarm. The metamorphic fate of the metasediments at that time is unknown, but the Bohica complex was apparently not strongly deformed. The significance of the Robillard-Patterson gneiss is uncertain. At ca. 2.6 Ga., the metasediments, Bohica complex and Chipman batholith underwent progressive bulk pure shear, extreme migmatisation, transitional to granulite facies metamorphism and the syntectonic emplacement of the granitoids of the Mary batholith. The bulk pure shear flow was partitioned into dextral and sinistral shear-sense sectors, separated by a Central Septum of relatively low finite strain which experienced approximately pure shear flow. As the Central Septum was translated to the southwest *relative to the wall rocks* outside of the EAmz, an overlying upper deck of penetrative mylonites was transported downwards to the southwest *relative to the Central Septum* and the rest of the lower deck. Deformation within the upper deck was remarkably homogeneous compared to that in the lower deck. This could reflect a difference in strain rate. Alternatively, it could reflect a potentially paradoxical difference in temperature; paradoxical inasmuch as it would imply that the upper deck was warmer than the lower deck in an extensional regime. According to one possible scenario, the plutonic precursor to the voluminous Fond du Lac mafic granulites could have been emplaced at ca. 2.6 Ga. and represent a significant heat source within the upper deck.

Low pressure zones beneath the trailing edge of the upper deck, and transiently brittle zones adjacent to its lateral ramp, were sites of preferential emplacement of relatively late syntectonic leucogranites. Continued top-down to the southwest movement, focussed on the interface between the upper and lower decks, generated low grade extensional fault zones below the trailing edge of the upper deck (Hanmer et al., 1991). Continued displacements of the wall rocks with respect to the lower deck resulted in complex greenschist fault zones along the lateral margins of the EAmz.

High grade deformation in this segment of the Snowbird tectonic zone occurred at and prior to ca. 2.6 Ga. If later, Early Proterozoic movements have occurred (Hoffman, 1988), they were confined to narrow greenschist fault zones, marginal to the high grade mylonites.

## ACKNOWLEDGMENTS

We are indebted to Melanie Kells, Brent Loney, Mike Peshko and Dave Ross for their enthusiasm and unflagging contribution to this summer's fieldwork, regardless of bush, terrain or weather. We also thank Janet King and Randy Parrish for critically reading the manuscript. We acknowledge support from NSF grants EAR 9105284 and 91061 to Ken Collerson and Mike Williams.

## REFERENCES

**Gilboy, C.F.**
1980: Bedrock compilation geology: Stony Rapids area (NTS 74-P); Preliminary Geological Map, scale 1: 250 000, Saskatchewan Geological Survey, Saskatchewan Energy and Mines.

**Hanmer, S., Ji, S., Darrach, M., and Kopf, C.**
1991: Tantato domain, northern Saskatchewan: a segment of the Snowbird tectonic zone; Current Research Part A, Geological Survey of Canada Paper 91-1A, p. 121-133.

**Hanmer, S. and Passchier, C.W.**
1991: Shear-sense indicators: a review; Geological Survey of Canada Paper 90-17, 72 p.

**Hoffman, P.F.**
1988: United plates of America, the birth of a craton: Early Proterozoic assembly and growth of Laurentia; Annual Review of Earth & Planetary Sciences, v. 16, p. 543-603.

**Slimmon, W.L.**
1989: Bedrock compilation geology: Fond du Lac (NTS 74-O); Geological Map, scale 1: 250 000, Saskatchewan Geological Survey, Saskatchewan Energy and Mines.

Geological Survey of Canada Project 830008

# New insight on the crustal structure and tectonic history of the Ungava Orogen, Kovik Bay and Cap Wolstenholme, Quebec

**M.R. St-Onge and S.B. Lucas**
**Continental Geoscience Division**

*St-Onge, M.R., and Lucas, S.B., 1992: New insight on the crustal structure and tectonic history of the Ungava Orogen, Kovik Bay and Cap Wolstenholme, Quebec; in Current Research, Part C; Geological Survey of Canada, Paper 92-1C, p. 31-41.*

***Abstract***

*Fieldwork in the northwestern part of the Ungava orogen has documented a crustal architecture in which autochthonous footwall basement is exposed in an antiformal window through the south-verging thrust belt. Similarities in lithology and structural-metamorphic history between the structural basement and the Superior Province exposed in the eastern part of the orogen suggest that rocks in the northwestern basement window also belong to the Archean Superior Province. The basement window is overthrust on its south side by Parent Group intermediate to felsic lavas and volcaniclastic sedimentary rocks, and on its north side by the Narsajuaq arc. The Narsajuaq arc is a distinct terrane (ca. 1.86-1.83 Ga) comprised of a layered calc-alkaline plutonic sequence and relatively deepwater sedimentary rocks cut by voluminous plutons. Syn-magmatic, granulite-grade metamorphic assemblages in all Narsajuaq arc lithologies are overprinted by amphibolite-grade assemblages associated with the collision between the arc and the Superior Province margin.*

***Résumé***

*La cartographie géologique dans la partie nord-ouest de l'orogène de l'Ungava a démontré la présence d'une structure d'échelle crustale comprenant un socle autochthone affleurant au coeur d'une fenêtre structurale en forme d'antiforme et entouré par les unités de la zone de chevauchement à charriage vers le sud. Des similitudes lithologiques entre le socle de la fenêtre stucturale et les unités de la province du lac Supérieur affleurant dans la partie est de l'orogène, ainsi qu'une histoire structurale-métamorphique semblabe, semblent indiquer que le socle structural du nord-ouest fait aussi partie de la province du lac Supérieur. La fenêtre structurale est chevauchée sur son versant sud par les laves de composition intermédiaire à felsique et par les roches sédimentaires volcanoclastiques du Groupe de Parent. Le versant nord est chevauché par l'arc de Narsajuaq. L'arc de Narsajuaq est un terrane distinct (ca. 1,86-1,83 Ga) qui comprend une série de roches plutoniques calco-alcalines rubanées et des roches sédimentaires de faciès relativement profond recoupées par des plutons volumineux. Des cortèges de minéraux métamorphiques syn-magmatiques appartenant au faciès des granulites caractérisent toutes les unités de l'arc de Narsajuaq. Ces cortèges sont repris par des assemblages métamorphiques du faciès des amphibolites, associés à la collision entre l'arc magmatique et la province du lac Supérieur.*

## INTRODUCTION

The Ungava orogen, an early Proterozoic arc-continent collisional belt in northern Quebec (St-Onge and Lucas, 1990a; St-Onge et al., in press) has been the focus of two major Geological Survey of Canada (GSC) mapping projects since 1985. The present project, initiated in 1989, was undertaken to examine the rocks in the internal zone of the Ungava orogen (i.e., north of the Cape Smith Belt, Fig. 1) through regional bedrock mapping and associated multidisciplinary research studies. Fieldwork, completed during the summer of 1991, resulted in significant discoveries concerning the architecture, tectonostratigraphy and tectonic history of the orogen. This report of activities focuses on the discoveries of the 1991 field season (for results of previous field seasons *see* St-Onge and Lucas, 1990b; Lucas and St-Onge, 1991, in press; St-Onge et al., in press). In the following sections, results are presented using the framework of principal tectonic subdivisions of the orogen: Superior Province, Cape Smith Belt and Narsajuaq arc (Fig. 1).

## SUPERIOR PROVINCE

### *Tectonostratigraphy*

The structurally-bound assemblage of rocks observed east of Kovik Bay and interpreted as belonging to the Archean Superior Province (Fig. 2) comprises predominantly felsic plutonic units and locally abundant sedimentary rocks. The most dominant lithology is a medium grained, equigranular biotite hornblende tonalite. The tonalite is in general well foliated and/or lineated, and contains m-scale enclaves to kilometre-scale rafts of quartz diorite, amphibolite, pyroxenite and siliciclastic sedimentary rocks . On an outcrop-scale, mafic and ultramafic rocks occur in two distinct relationships with the tonalite: (1) quartz diorite interlayered and apparently comagmatic with tonalite; and (2) amphibolite and pyroxenite forming angular, low-aspect-ratio enclaves in tonalite (agmatitic texture). The mafic rocks are interlayered with siliciclastic rocks (see below) at the outcrop-scale, but their origin (extrusive vs. intrusive) remains equivocal. The larger rafts within the tonalite units (or alternatively, country rock units forming screens or roof pendants between tonalite intrusive bodies) are illustrated in Figure 2.

Sedimentary rocks are volumetrically minor but locally form mappable bands with significant strike lengths (Fig. 2). The sedimentary sequence is dominated by pelite and semipelite, which are rarely interlayered with quartzite. The sequence suggests a deeper water depositional environment, while field relations indicate that the sedimentary rocks are preserved as screens between and/or within tonalite plutons. The sedimentary sequence is cut by granitoid veins derived from adjacent or enveloping plutonic bodies, and apparently also by local partial melting.

The heterogeneous tonalite bodies are intruded by metre- to kilometre-scale sheets of granodiorite to monzogranite (Fig. 2). The granitoid rocks are generally medium-grained but vary from equigranular to K-feldspar porphyritic. While the granites clearly intrude the tonalites, they contain a variably developed foliation parallel to that in the tonalites, mafic and sedimentary rocks. This foliation is truncated at the fault separating this assemblage from the overlying early Proterozoic rocks (Fig. 2), suggesting that the granites form an integral part of this assemblage which pre-dates the early Proterozoic deformation event (see below). The tonalite bodies are interlayered on a m-scale with cm- to m-thick veins of granodiorite to syenogranite. These veins locally cut the tonalite foliation at a range of angles but are themselves foliated, consistent with a model of syn-tectonic intrusion and variable post-emplacement, deformation-induced rotation (Lucas and St-Onge, 1991). The relative absence of granite veins cutting the granite bodies and the similar variable bulk deformation states of the granite veins and plutons suggest that veining may in part be related to the plutonism.

The plutonic-dominated assemblage coring the antiformal structure east of Kovik Bay is remarkably similar, in terms of lithologies and cross-cutting relations, to the autochthonous Superior Province basement mapped in continuity from south of the Cape Smith Belt to the area south of Sugluk Inlet (Fig. 2; St-Onge and Lucas, 1990b; Lucas and St-Onge, 1991). The Superior Province in the eastern part of the map area is marked by voluminous tonalite bodies emplaced in mafic to ultramafic intrusive units and clastic metasedimentary rocks and subsequently intruded by granite plutons (Lucas and St-Onge, 1991). U-Pb geochronology on the basement to the eastern Ungava orogen has yielded 2780 and 2882 Ma ages for tonalite samples (Parrish, 1989). The combination of lithological similarities, structural position and structural-metamorphic history (see below) provides a

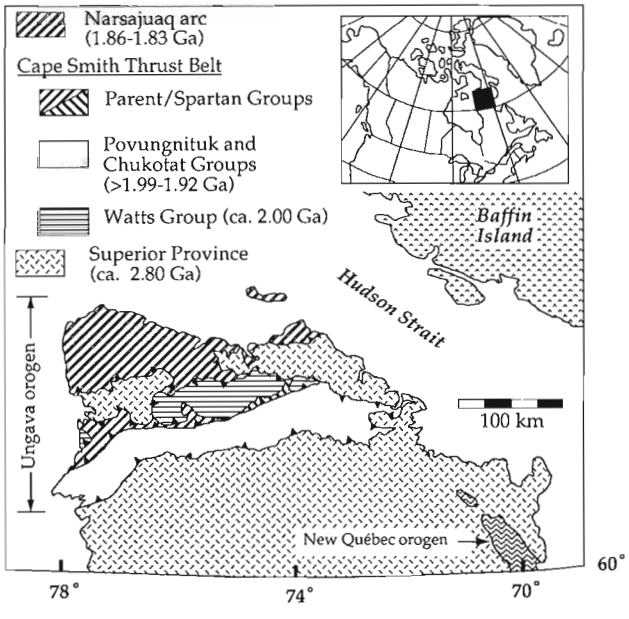


**Figure 1.** Map illustrating the tectonic elements in the entire Ungava orogen and highlighting the location of the 1991 map area (outlined with box). U-Pb ages are from Parrish (1989, pers. comm. 1991; see St-Onge et al., in press) and Machado et al. (1990).

compelling argument for an interpretation of the structurally-bound assemblage east of Kovik Bay (Fig. 2) as autochthonous Superior Province basement.

### *Structural-metamorphic history*

The oldest structure in the proposed basement is a pervasive gneissic foliation defined by compositional layering and the alignment of constituent minerals. The foliation often contains a stretching lineation marked by quartz-feldspar rodding or the alignment of hornblende, and locally predominates over the foliation. The relative timing of this early penetrative deformation is indicated by two observations: (1) granite plutons are variably foliated and related veins are variably transposed into the regional gneissosity; and (2) foliations are defined by granulite facies minerals (e.g., orthopyroxne) in relatively rare patches of preserved high-grade assemblages. Together these observations suggest that deformation was synchronous with granulite-facies metamorphism and granite plutonism and, if the correlation with the demonstrable Superior Province basement to the east is correct, then the deformation event is late Archean in age.

The regional gneissic foliation was reworked both penetratively and "passively" during two distinct deformation events interpreted as being early Proterozoic in age. Structures related to the first of these events are restricted to (1) within several metres of the contact between the basement assemblage and the overlying early Proterozoic rocks; (2) narrow shear zones within the basement which contain relatively high pressure/low temperature mineral assemblages consistent with assemblages in the overlying early Proterozoic rocks; and (3) an interpreted thrust slice of basement rocks interleaved with early Proterozoic supracrustal rocks ("A", Fig. 3). The basement rocks immediately adjacent to the contact with Povungnituk Group metabasalts and metasedimentary rocks (Figs. 2, 3) are marked by a mylonitic foliation and transverse stretching lineation parallel to that in the cover rocks. The fabrics are defined by amphibolite grade assemblages consistent with those in the overlying Povungnituk Group, and notably, by the presence of muscovite and deformed quartz veins otherwise unobserved in the structural basement. These observations suggest that a fault separates the Povungnituk Group rocks from the proposed basement assemblage. At the east end of the orogen, this contact has been interpreted as the basal décollement (Fig. 2) along which the early Proterozoic rocks moved southward across the autochthonous basement in a thrust sense (Lucas, 1989; St-Onge and Lucas, 1990a). Outcrop-scale kinematic indicators associated with the basement-cover contact were not observed in the western part of the orogen.

Geological mapping has documented that the proposed western Superior Province assemblage lies in the core of a major, regional-scale antiform found north of the Cape Smith Belt (Fig. 1) and corresponds to the appropriately named Kovik antiform of Hoffman (1985). Lucas (1989) and St-Onge and Lucas (1990a) have shown that folding of basement, Cape Smith Belt rocks and Narsajuaq arc about east-trending axes followed the thrusting event documented in the Cape Smith Belt. The basement-cored antiform appears to be a first-order fold of this generation. While this event did not generate a new regional foliation in the basement, it appears to have "passively" reoriented the pre-existing Archean gneissosity and overprinting Proterozoic fabrics such that they now define a broad antiform (Fig. 3). The structural height attained by the basement-cored antiform is a consequence of constructive interference of the east-trending antiform with an approximately north-trending antiform generated during a second basement-involved folding event. The regional (first-order) fold geometry related to this younger event defines a U-shaped profile with a synformal saddle in the central part of the orogen passing up-plunge into the two basement-cored antiforms (Fig. 1). Lucas (1989) estimated the structural relief on the eastern flank of the synformal saddle to be on the order of 20 km. Higher-order north-trending folds can be recognized in the outline of the basement-cover contact (5-15 km wavelength; Figs. 2, 3) and are responsible for the varying plunge of the basement antiform's axis (Fig. 3).

## CAPE SMITH BELT

### *Tectonostratigraphy*

Four Cape Smith Belt units were mapped during the 1991 field season (Figs. 2, 3): the Povungituk, Chukotat, Parent and Watts groups. The Povungnituk Group in this area consists principally of highly deformed mafic rocks (Fig. 4), probably including both basalt flows and gabbro sills (St-Onge and Lucas, 1990b). Siliciclastic sedimentary rocks, in general semipelite and quartzite, are common at the base of the Povungnituk Group thrust imbricate (Fig. 3). The Chukotat Group is restricted to the footwall of the orogen-scale Bergeron Fault (Fig. 2), and is characterized by little deformed, plagioclase-phyric pillowed basalts (e.g., Francis et al., 1983; Picard et al., 1990). The Watts Group studied in the 1991 map area occurs in the hanging wall of a major fault which overrides units of the Narsajuaq arc, the Povungnituk Group and the Parent Group (Figs. 2, 3). The fault carries layered mafic and ultramafic cumulate rocks of the ophiolitic suite which are intruded to the east by younger granitic and dioritic plutons (St-Onge et al., in press).

The northwestern part of the Cape Smith Belt contains a sequence of volcanic and sedimentary rocks (Parent Group; Figs. 2, 3) sandwiched between thrust sheets of Povungnituk and Chukotat Group rocks and the Watts Group ophiolite. The Parent Group is a succession of felsic to intermediate volcanic rocks, associated volcaniclastic deposits and siliciclastic sedimentary rocks recently mapped by the MERQ (Lamothe, 1986; Barrette, 1989; Picard et al., 1990). The volcanic rocks vary in composition from rhyolite to basalt with andesite and andesitic basalt being most common. Flows are either equigranular or contain plagioclase, carbonate and/or biotite porphyroblasts (after phenocrysts?). Both massive and pillowed flows (Fig. 5) were observed in outcrops where primary features are not obliterated by the

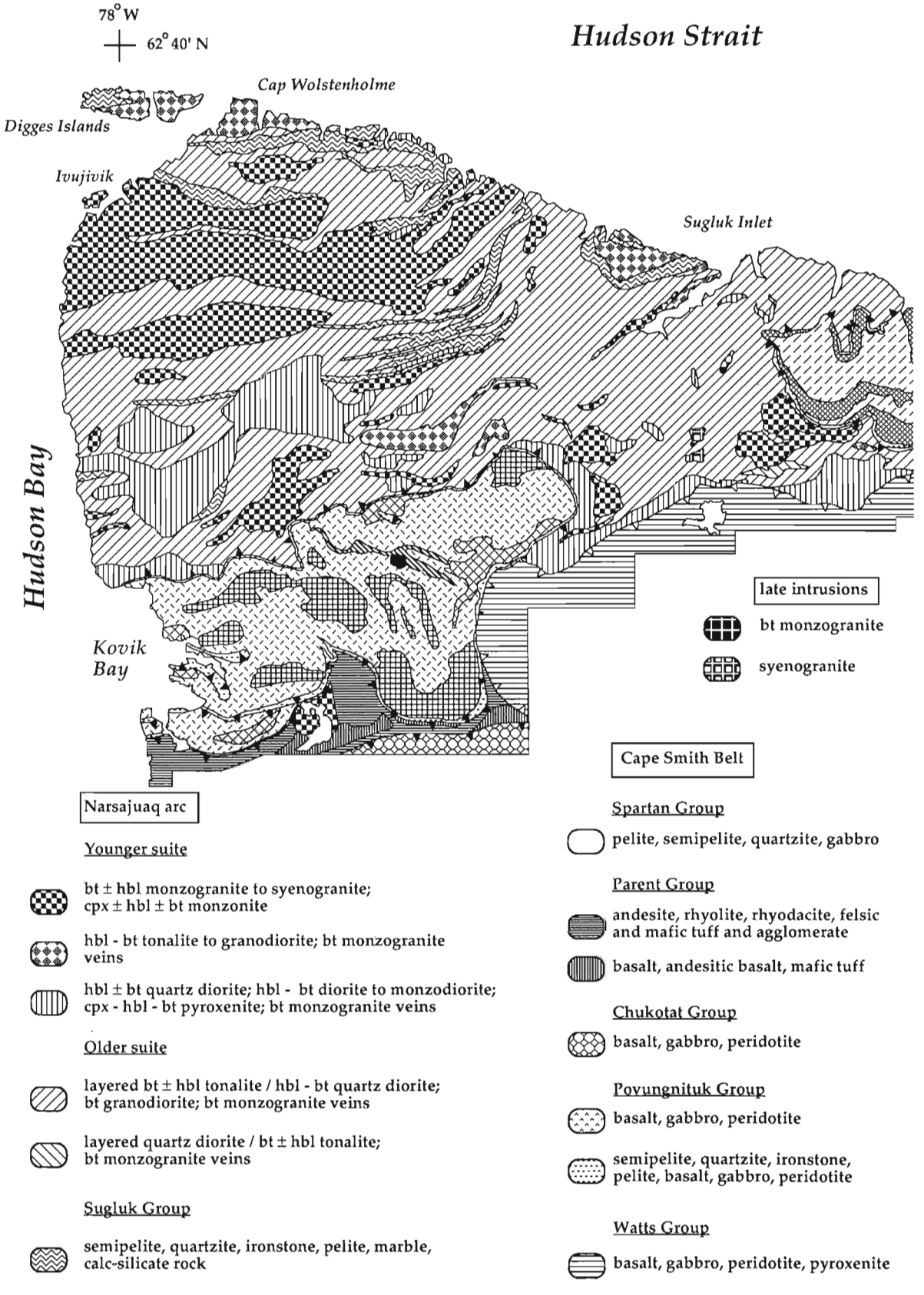


**Figure 2.** Geological compilation map for the northern and eastern portions of the Ungava orogen, incorporating the results of GSC mapping during the summers of 1985-87 and 1989-91.

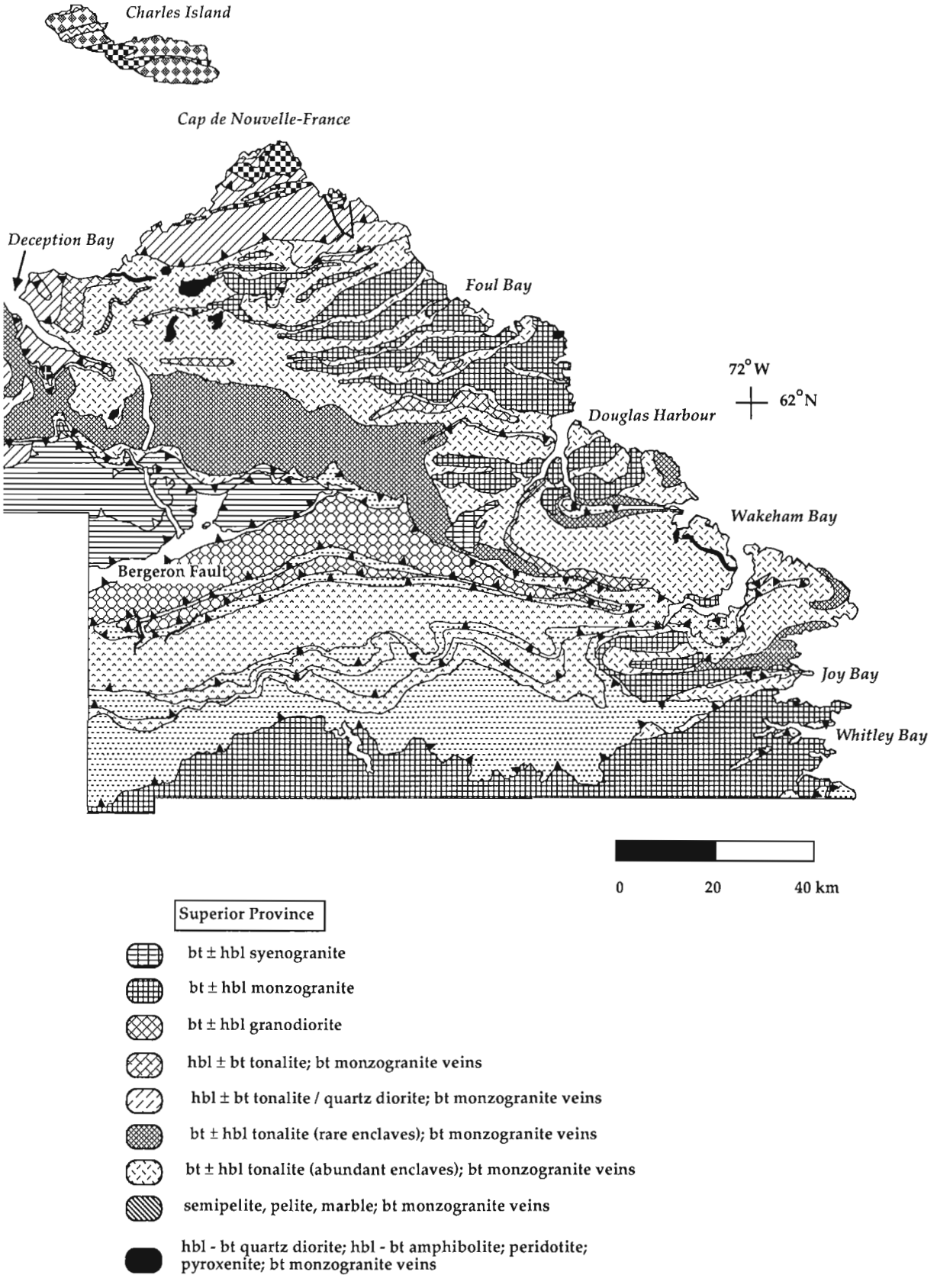


**Figure 2.** (cont.)

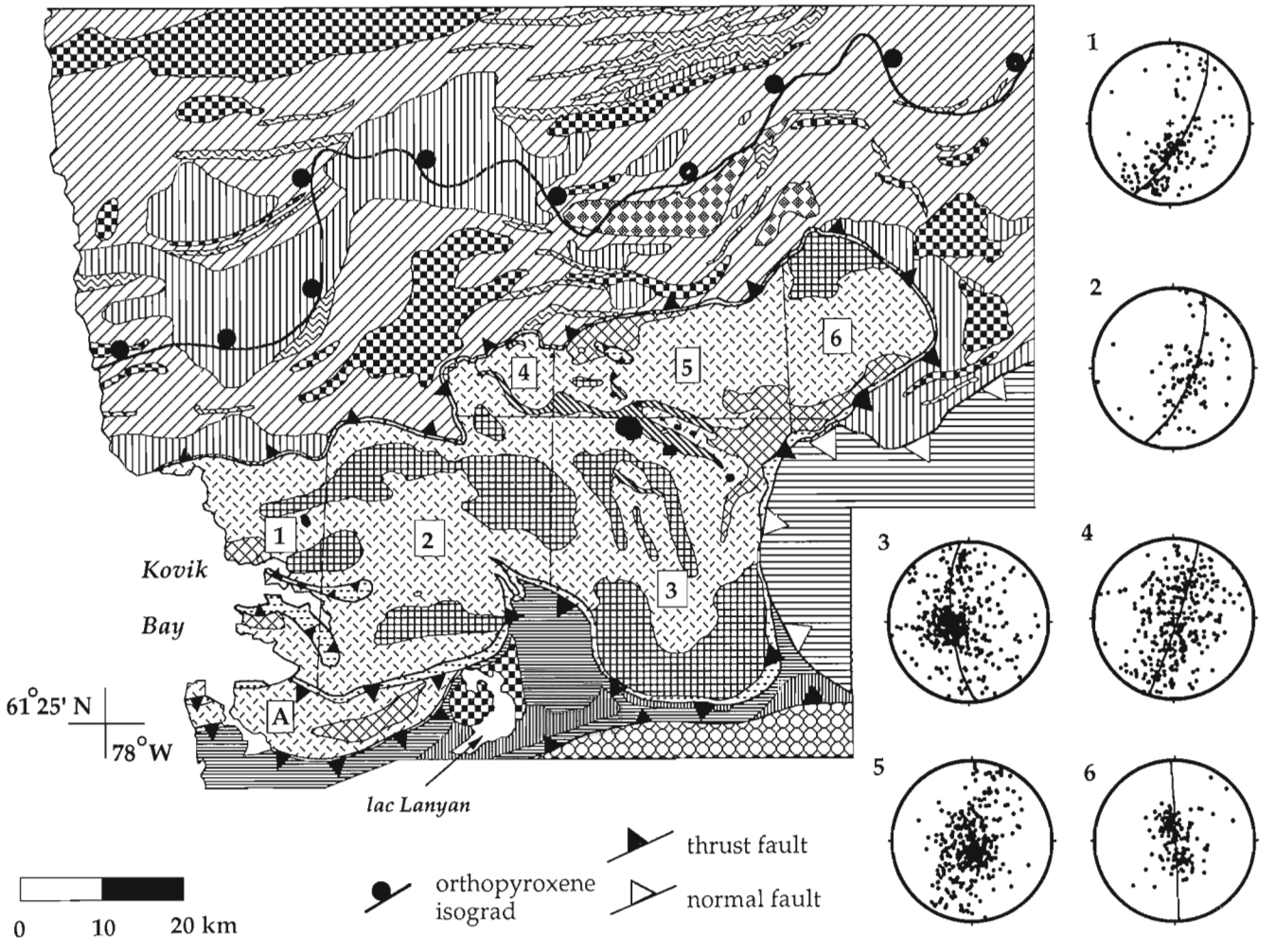


**Figure 3.** Detailed map of the proposed Superior Province basement window east of Kovik Bay (Fig. 2) illustrating the (1) basement-cover relationships, (2) basement imbricate ("A"), (3) the variably plunging antiformal geometry of the basement rocks (stereonet projections of poles to basement foliation and the derived fold axes) and the (4) field-defined orthopyroxene isograd in Narsajuaq arc rocks. Legend is given in Fig. 2.

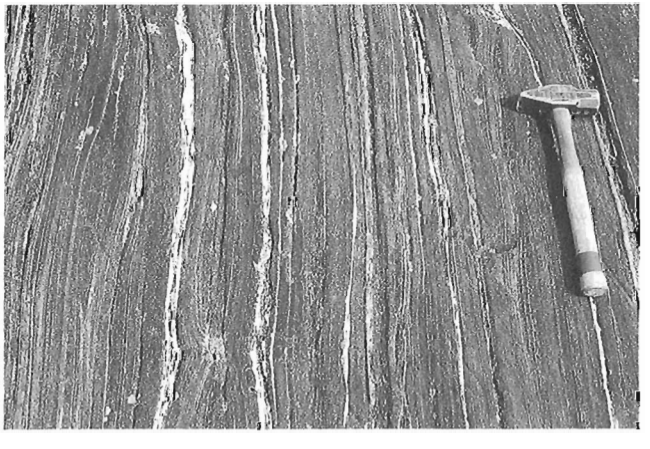

**Figure 4.** Highly deformed Povungnituk Group metabasites from the north side of the basement-cored antiform. The strain is interpreted to have accumulated during the thrusting event related to arc-continent collision. Hammer for scale is 45 cm long. (GSC 1991-562-O)

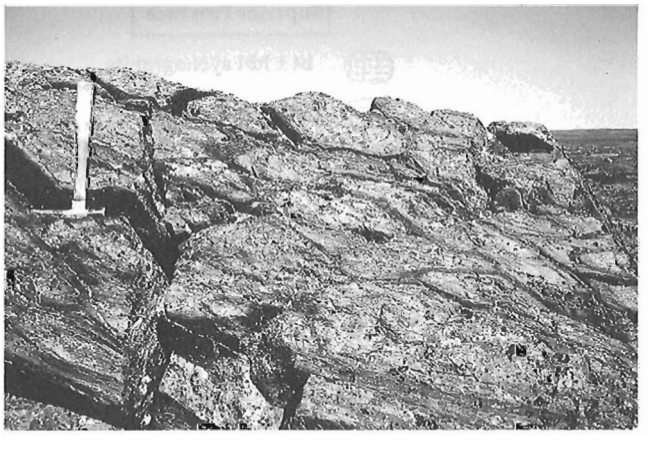

**Figure 5.** Pillowed mafic flows of the Parent Group. Hammer for scale is 34 cm long. (GSC 1991-562-D)

layer-parallel foliation. A Parent Group rhyolite collected by MERQ has recently been dated at 1860 Ma (N. Machado, pers. comm., 1991).

Volcaniclastic rocks form an integral part of the Parent Group. These units vary from felsic tuffs and agglomerates, with rhyolite, rhyodacite and porphyry clasts, to more intermediate and mafic tuffs. The volcaniclastic rocks are well foliated metamorphic rocks, and tuffs of intermediate composition are often marked by cm-scale, radiating sprays of hornblende. The laterally discontinuous nature of Parent Group units and the intertonguing of volcanic and volcaniclastic rocks (Fig. 3) suggests an environment dominated by subaerial volcanic edifices and erosion and deposition of volcanic detritus in adjacent basins. Furthermore, lateral and vertical changes in the composition and volume of volcanic rocks appears to indicate that distinct eruptive centres existed during Parent Group volcanism.

The Parent Group is intruded by granodiorite, granite and quartz diorite plutons with dimensions ranging from metres to kilometres. A granodioritic phase of a large composite pluton centred on lac Lanyan (Fig. 3) has been dated at about 1848 Ma (Machado et al., 1990). The limited geochronological data suggests that Parent Group volcanism was broadly synchronous with plutonism in the Watts and Parent groups (1898-1839 Ma; Parrish, 1989; Machado et al., 1990). In addition, compositional similarities appear to indicate that the plutons are intrusive equivalents to the Parent Group volcanic rocks (Picard et al., 1990; J. Dunphy, pers. comm., 1991). Furthermore, the ages of the both the granite and the felsic flow overlap with U/Pb ages derived for plutonic rocks in the Narsajuaq arc (1863-1826 Ma; St-Onge et al., in press). The Parent Group appears to have formed in a magmatic arc environment (Picard et al., 1990) and may be the supracrustal cap for at least part of the Narsajuaq arc plutonic core (St-Onge et al., in press).

### *Structural-metamorphic history*

The structural history of the Cape Smith Belt has been previously described by Lucas (1989) and St-Onge and Lucas (1990a) and will not be reviewed here. The principal new results from mapping in the northwestern part of the belt concern the geometry and nature of faults bounding the Parent and Watts groups. These faults (Fig. 3) are folded by both the east- and north-trending structures which are responsible for the basement-cored antiform east of Kovik Bay, and can be linked with documented collision-related faults to the east (Fig. 1). They are consequently interpreted to be related to the arc-continent collision (Lucas and St-Onge, in press). The structurally lowest fault separates highly foliated Povungnituk Group rocks in the footwall (Fig. 4) from mylonitic Parent Group volcaniclastic rocks in the immediate hanging wall. Bulk strain decreases up section in the Parent Group such that primary structures can be recognized in more competent lithologies (e.g., Fig. 5). The nature and movement sense of the fault could not be determined as a result of (1) an absence of mesoscopic kinematic indicators; (2) no significant change in fault position or geometry over tens of kilometres of strike length; and (3) similar amphibolite-facies mineral assemblages in both hanging wall and footwall. However, this fault is tentatively interpreted as a south-directed thrust fault, given that the equivalent fault in the eastern part of the Cape Smith Belt (carrying Spartan Group rocks; Fig. 2; see also Lucas, 1989) is a thrust fault.

The fault carrying the Watts Group layered cumulate rocks is a relatively late structure of regional extent (Fig. 2) which cuts off all pre-existing faults in its footwall, including the thrust faults carrying the Narsajuaq arc and the Parent Group (Fig. 3). The relative age of the fault is indicated by the retrograde metamorphism (greenschist over amphibolite grade assemblages; Lucas, 1989; St-Onge and Lucas, 1990a) which characterizes the hanging wall. The Narsajuaq arc footwall truncation is repeated on both sides of the north-trending synformal saddle which characterizes the central longitudes of the orogen and is cored by the Watts Group (Fig. 2). Based on structural, metamorphic and geochronological arguments, Lucas and St-Onge (in press) proposed that the Watts Group fault is a normal fault with a top-to-the south movement sense.

## NARSAJUAQ ARC

### *Tectonostratigraphy*

The oldest plutonic unit in the Narsajuaq arc is a layered sequence of tonalite and quartz diorite (Fig. 2). Layering is on a metre-scale, with tonalite predominating, although the relative proportions of tonalite and quartz diorite vary locally. The unit shows a remarkable consistency in composition and texture across the entire width of the internal zone (Fig. 2; St-Onge and Lucas, 1990b; Lucas and St-Onge, 1991). This layered unit contains a variety of older to comagmatic mafic and ultramafic rocks in a number of different relationships: (1) amphibolite and pyroxenite form low-aspect-ratio enclaves and larger xenolithic rafts; (2) concordant layered sequences of quartz diorite, amphibolite, pyroxenite and peridotite occur locally in the arc; and (3) metre to kilometre-scale peridotite bodies apparently intrude the layered tonalite-quartz diorite unit. The relatively fine-scale layering in the unit, coupled with locally preserved intrusive relationships (St-Onge and Lucas, 1990b), suggest that it may be a primary magmatic feature which has subsequently been enhanced by high temperature deformation (Lucas and St-Onge, in press).

Sedimentary rocks in the Narsajuaq arc (Sugluk Group, Lucas and St-Onge, 1991) comprise predominantly graphitic, sulphidic semi-pelites. These rocks are locally interlayered with pelite, quartzite (often arkosic) and minor carbonate units. All of the sedimentary rocks experienced intense deformation and high grade metamorphism, and as such their depositional environment(s) is difficult to constrain. The predominance of semi-pelites and the relative paucity of shelf-type units suggest that the sedimentary rocks were deposited in a relatively deepwater environment. While the quartzite and carbonate units could be interpreted as basinal deposits (distal turbidites and marls), the absence of primary sedimentary structures makes this interpretation equivocal.

The sedimentary rocks occur in bands of relatively limited width (<1 km) but significant strike lengths (up to 65 km; Figs. 2, 3).

The layered plutonic and sedimentary rocks in the Narsajauq arc were intruded by tonalite, granite and quartz diorite plutonic bodies (Fig. 2). These bodies, equivalent to the younger suite intrusions (1844-1826 Ma) of St-Onge et al. (in press), are variably foliated but in general are characterized by relatively low bulk deformation states (Figs. 6, 7, 8). The younger intrusive bodies (1) vary in diameter from <1 km to tens of kilometres; (2) generally have irregular shapes which crosscut both outcrop- and regional-scale layering (Fig. 2); and (3) include xenolithic blocks (Fig. 8) and large-scale screens of country rock (Fig. 2). The large screens commonly parallel regional layering, suggesting that the plutons may have been emplaced passively as concordant sheets. However, the size and homogeneity of the younger plutons contrasts markedly with the finely layered aspect of the older plutonic rocks, and suggests that the younger plutons may have been emplaced at higher crustal levels.

Narsajuaq arc rocks are cut by a variety of granite veins ranging in nature from layer-parallel and foliated to cross-cutting and massive (Fig. 9). Characterization of the significance, distribution and age (relative and absolute) of the vein generations is clearly a key to unravelling the tectonic history of the arc. The oldest veins are close in age to the host rock (1861 Ma granodiorite vein in 1863 Ma

**Figure 6.** Unfoliated biotite-hornblende monzogranite from the pluton south of Ivujivik (Fig. 2). The pluton contains a number of phases, varying from granodiorite to syenogranite in composition and from equigranular to K-feldspar megacrystic in texture. Pen for scale is 15 cm long. (GSC 1991-562-N)

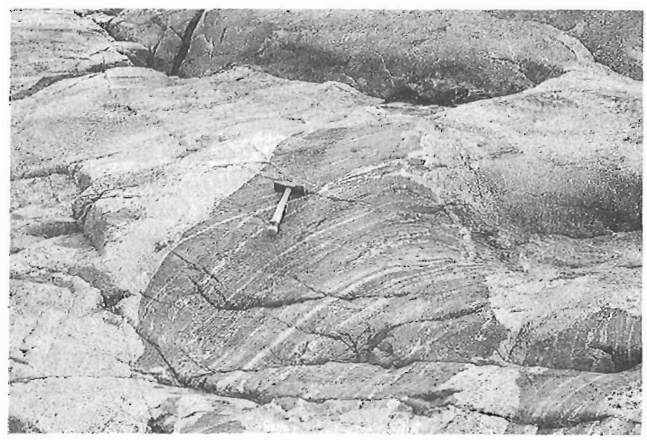

**Figure 8.** Misoriented enclaves of the older layered tonalite-quartz diorite unit in a younger, weakly foliated monzogranite body west of Ivujivik. Hammer for scale is 45 cm long. (GSC 1991-562-E)

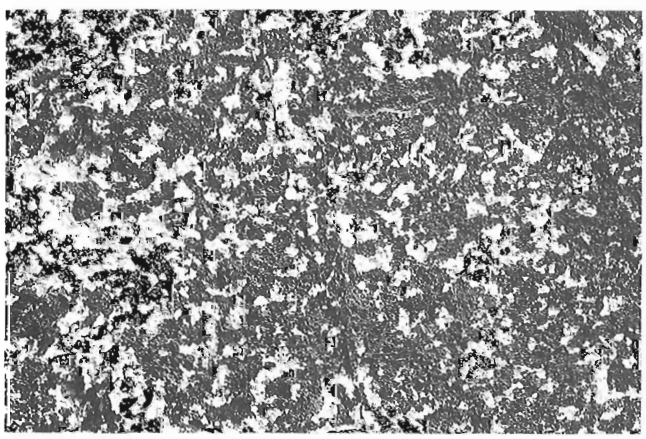

**Figure 7.** Unfoliated quartz diorite from the large pluton found north of the basement window (Fig. 2). The mineral assemblage of the pluton (hornblende-biotite ± orthopyroxene ± clinopyroxene garnet) reflects variable retrogression of granulite-grade assemblages. Grain size is approximately 0.5-1 cm. (GSC 1991-562-I)

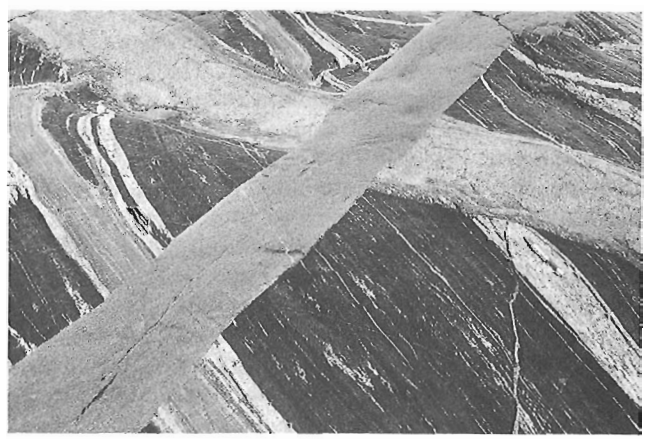

**Figure 9.** Granitic veins cutting the layered tonalite-quartz diorite unit in Narsajuaq arc. At least 5 generations of vein are present, and range in deformation state from well foliated (layer-parallel veins) to undeformed (vein cutting diagonally from bottom left to top right). Pen for scale is 15 cm long. (GSC 1991-562-G)

tonalite; St-Onge et al., in press), are layer-parallel and generally have experienced similar bulk strain as the host rock (Fig. 10). Successive generations of veins cut these older plutonic units, both at low and high angles to the pre-existing layering, and record variable amounts of deformation (Figs. 10, 11). Some of the less deformed veins are probably related to the younger granitic plutons (ca. 1.83 Ga; Fig. 11). Cross-cutting syenogranite veins (Fig. 12) are part of a regional set, dated at 1759 Ma (Parrish, 1989), which stitch together all tectonic elements of the orogen (St-Onge et al., in press).

While the relationship between the younger plutons and older plutonic and sedimentary rocks is clearly illustrated on the geological map (Figs. 2, 3), the nature of the contact between the older layered plutonic sequence and the sedimentary rocks remains in question. At the outcrop scale, well foliated bands of Sugluk Group rocks are concordant with layering in the tonalite-quartz diorite unit, making it difficult to distinguish between intrusive, depositional and/or tectonic contacts. The regional distribution of sedimentary rock bands argues against a simple depositional contact interpretation (Figs. 2, 3). Resolution of this question in part rests on detailed geochronological study of detrital zircon populations in Sugluk Group rocks and further study of the crystallization ages of the plutonic rocks. In one such study, Parrish (1989) has shown that rapid deposition, burial and metamorphism of a quartzite sample occurred at ca. 1830 Ma, approximately 30 Ma younger than dated older plutonic units (St-Onge et al., in press). However, field relations suggest that much of the sedimentary rock was interlayered with the older plutonic rocks prior to the emplacement of the voluminous younger plutons (Fig. 2). As such, at least some of the older plutonic bodies may have been emplaced in Sugluk Group sedimentary rocks, which could then be interpreted as country rock screens and roof pendants in the plutonic domain.

**Figure 10.** Variably deformed granitic veins cutting the layered tonalite-quartz diorite unit of Narsajuaq arc. Pen for scale is 15 cm long. (GSC 1991-562-Q)

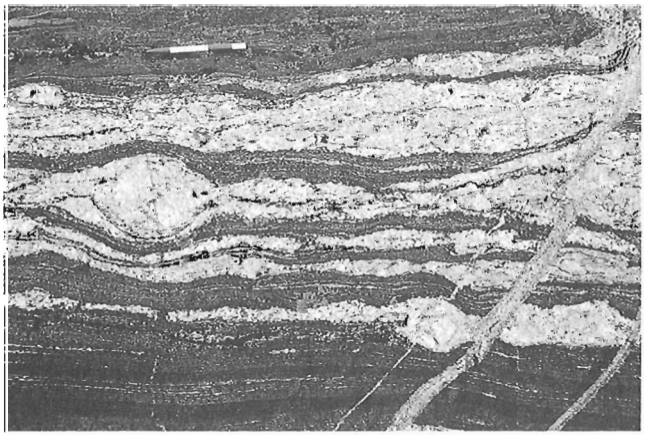

**Figure 11.** Relatively coarse-grained, layer-parallel veins of monzogranite emplaced in the layered tonalite-quartz diorite unit of Narsajuaq arc. The foliated veins are themselves obliquely cut by undeformed granite veins. Pen for scale is 15 cm long. (GSC 1991-562-F)

### *Structural-metamorphic history*

Narsajuaq arc units are characterized by a penetrative foliation which parallels the outcrop-scale compositional layering (Figs. 10, 11). The generally steep, east-trending foliations in both the older Narsajuaq arc units and the younger plutons are defined by amphibolite- to granulite-facies metamorphic assemblages. However, the presence of granulite-grade assemblages in all lithologies, the heterogeneous distribution of the metamorphic facies and thin-section observations indicate that the regional foliation developed during granulite metamorphism (Lucas and St-Onge, in press). This high grade deformation event is coeval with plutonism in the Narsajuaq arc, and is thus constrained to pre-date accretion of the arc to the Superior Province continental margin (St-Onge et al., in press). Two principal collision-related features were documented in the 1991 map area: (1) the basal fault along which the Narsajuaq arc was accreted (Figs. 2, 3); and (2) an orthopyroxene

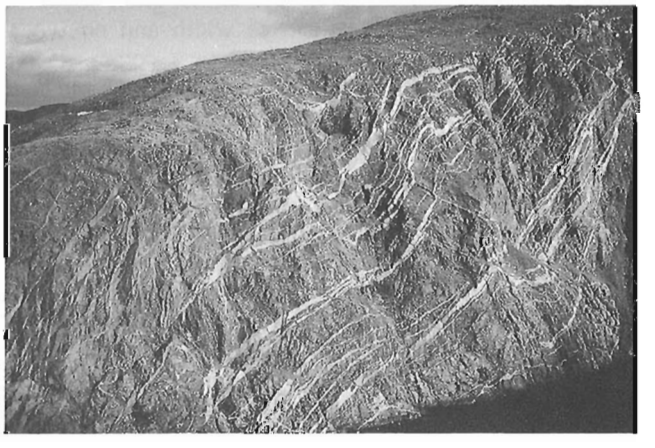

**Figure 12.** Syenogranite veins cutting well foliated plutonic rocks of Narsajuaq arc. Height of cliff is approximately 300 m. (GSC 1991-562-M)

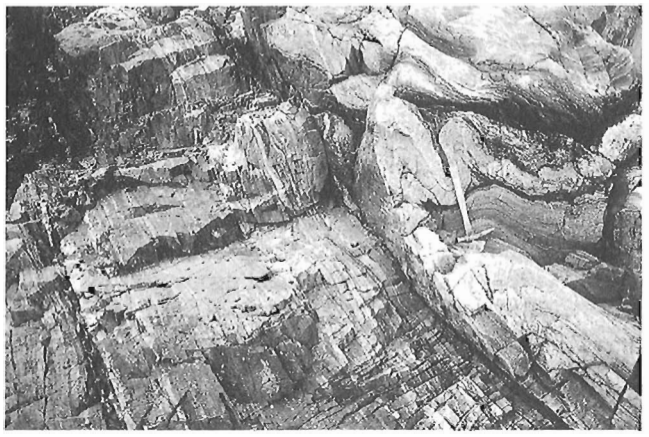

**Figure 13.** Greenschist-grade mylonites cutting foliated and folded Narsajuaq arc rocks on the eastern Digges Island (Fig. 2). Hammer for scale is 34 cm long. (GSC 1991-562-B)

isograd which parallels the basal accretion fault (Fig. 3) and which appears to mark the limit of preservation (heading up structural section) of pre-collisional orthopyroxene (see also Lucas and St-Onge, in press). No unequivocal evidence for collision-related faulting within the Narsajauq arc was documented in the course of mapping.

Folding of the Narsajuaq arc, the Cape Smith Belt units and the Superior Province basement about east-trending axes succeeded collisional deformation, and was followed by folding about northwest-trending axes (see above; Lucas, 1989; Lucas and St-Onge, in press). Outcrop-scale deformation structures possibly related to the first folding event are well developed in the most northwestern portion of the Narsajuaq arc (Digges Islands, Fig. 2), and are characterized by folding and shearing of plutonic and sedimentary units. A deformation gradient has been documented from the northwestern peninsulas of the mainland to the Digges Islands in which the regional (pre-collisional) foliation becomes progressively reoriented through non-cylindrical folding about east-west trending axes of highly variable plunge. On the Digges Islands (Fig. 2), map-scale folds are cut by greenschist-grade mylonite zones of metres to tens-of-metres width and equivocal kinematics (Fig. 13; D.M. Carmichael, pers. comm., 1991). While the principal mylonite zones trend east-west and have a sub-vertical foliation (Fig. 13), some lower-strain domains between mylonite bands are marked by northwest-trending, map-scale shear bands. These structures accommodated north-south shortening and east-west extension of the chiefly sedimentary (marble and calc-silicate units) domains through dextral slip and anticlockwise block rotation (D.M. Carmichael, pers. comm., 1991). In total, the deformation event appears to be associated with north-south compression accompanied by east-west extension and a possible dextral asymmetry, and may be coeval with the east-trending, basement-involved folding event (Lucas and St-Onge, in press).

## DISCUSSION

Regional mapping and complementary structural, metamorphic, geochronological and isotopic studies by the MERQ and GSC since 1983 have dramatically changed the map of the northern Ungava Peninsula. In addition, this work has shown that (1) the Cape Smith Belt was thrust southward over the Superior Province basement, (2) autochthonous basement is exposed in two half-windows coring a large-scale antiform north of the belt, (3) the belt contains a 2.00 Ga ophiolite, and (4) the internal zone is characterized by a 1.86-1.83 Ga magmatic arc terrane which collided with the Superior Province continental margin after 1.83 Ga (Ungava orogeny). Oblique exposure of a Superior Province crustal section in the two internal basement half-windows represents an important opportunity for study of the mid to lower crust of a late Archean magmatic arc terrane. The "suture" between suspect and Superior-Province-margin rocks in the Ungava orogen is interpreted to be the faults which juxtapose Narsajuaq arc, Parent or Spartan Group rocks against the Povungnituk or Chukotat Group rocks (Figs. 2, 3). In addition, a lower crustal "suture" along which Superior Province crust abuts Narsajuaq arc crust (or the crust of a block that trailed behind it) must also be present to the north of the basement windows . Fieldwork on southern Baffin Island and/or offshore seismic reflection surveys should be able to delineate the extent of Superior Province as well as Narsajuaq arc crust to the north of the Ungava Peninsula.

No obvious new economic targets were revealed in the course of mapping in the internal zone of the orogen. The sedimentary rocks of the Sugluk Group are often rusty weathering, sulphidic and graphitic semipelites, but significant concentrations of sulphide minerals were not observed. While two magmatic arc terranes have been documented through systematic mapping and laboratory research, neither the Narsajuaq arc plutonic core nor the Superior Province basement represent good targets for classic porphyry-type deposits because of the apparent preservation of only middle to lower crustal levels. However, the Parent Group's volcanic, sedimentary and/or intrusive rocks may contain mineralization related to hydrothermal circulation systems driven by magmatic heat within the proposed arc.

## ACKNOWLEDGMENTS

The successful mapping program in the unprecedentedly sunny summer of 1991 was made possible by the high calibre fieldwork of our assistants Kathy Bethune (Queen's University), Jan Dunphy (Université de Montréal), John Ketchum (Dalhousie University) and Patrick Monday (Queen's University). Robin Roots is commended for her fine cuisine, superb camp management and unfailing spirit. Once again, we enjoyed the excellent service and company of our helicopter crew, Pierrette Paroz (pilot) and Michel Meloche (engineer). The Polar Continental Shelf Project is gratefully acknowledged for their generous helicopter support. Quaternary expertise and pleasant camaraderie were provided by Robert-André Daigneault (CGQ) and Sheila Petrie (Université Laval). The mapping program benefitted from the field visits of Bob Baragar

(GSC), Dugald Carmichael (Queen's University), Sandy Colvine (GSC), John Ludden (Université de Montréal), Urs Mader (GSC) and Randy Parrish (GSC). Randy Parrish and John Percival are thanked for their comments on a first version of this manuscript.

## REFERENCES

**Barrette, P.D.**
1989: Géologie de la région du lac Bolduc, Fosse de l'Ungava; Ministère de l'Énergie et des Ressources du Québec, carte préliminaire, DP 88-17.

**Francis, D.M., Ludden, J., and Hynes, A.J.**
1983: Magma evolution in a Proterozoic rifting environment; Journal of Petrology, v. 24, p. 556-582.

**Hoffman, P.F.**
1985: Is the Cape Smith Belt (northern Quebec) a klippe?; Canadian Journal of Earth Sciences, v. 22, p. 1361-1369.

**Lamothe, D.**
1986: Développements récents dans la Fosse de l'Ungava; In Exploration en Ungava: données récentes sur la géologie et la gîtologie. D. Lamothe, R. Gagnon, and T. Clark (eds.), Ministère de l'Energie et des Ressources du Québec, DV 86-16, p. 1-6.

**Lucas, S.B.**
1989: Structural evolution of the Cape Smith Thrust Belt and the role of out-of-sequence faulting in the thickening of mountain belts; Tectonics, v. 8, p. 655-676.

**Lucas, S.B. and St-Onge, M.R.**
1991: Evolution of Archean and early Proterozoic magmatic arcs in northeastern Ungava Peninsula, Quebec; In Current Research, Part C; Geological Survey of Canada, Paper 91-1C, p. 109-119.

**Lucas, S.B. and St-Onge, M.R.**
in press: Terrane accretion in the internal zone of the Ungava orogen, northern Québec; Part 2: Structural and metamorphic history; Canadian Journal of Earth Sciences.

**Machado, N., Gariépy, C., Philippe, S., and David, J.**
1990: Géochronologie U-Pb du territoire québécois: Fosses du Labrador et de l'Ungava et sous-province de Pontiac; In Ministère de l'Energie et des Ressources du Québec, MB 91-07, p. 19-29.

**Parrish, R .R.**
1989: U-Pb geochronology of the Cape Smith Belt and Sugluk block, northern Quebec; Geoscience Canada, v. 16, p. 126-130.

**Picard, C., Lamothe, D., Piboule, M., and Olivier, R.**
1990: Magmatic and geotectonic evolution of a Proterozoic oceanic basin system: the Cape Smith Thrust-Fold Belt (New Quebec); Precambrian Research, v. 47, p. 223-249.

**St-Onge, M.R., and Lucas, S.B.**
1990a: Evolution of the Cape Smith Belt: Early Proterozoic continental underthrusting, ophiolite obduction and thick-skinned folding; In The early Proterozoic Trans-Hudson Orogen of North America. J.F. Lewry and M.R. Stauffer (eds), Geological Association of Canada, Special Paper v. 37, p. 313-351.

**St-Onge, M.R. and Lucas, S.B.**
1990b: Early Proterozoic collisional tectonics in the internal zone of the Ungava (Trans-Hudson) orogen, Lacs Nuvilik and Sugluk map areas, Québec; In Current Research, Part C. Geological Survey of Canada, Paper 90-1C, p. 119-132.

**St-Onge, M.R., Lucas, S.B., and Parrish, R.R.**
in press: Terrane accretion in the internal zone of the Ungava orogen, northern Québec, Part 1: Tectonostratigraphic assemblages and their tectonic implications; Canadian Journal of Earth Sciences.

Geological Survey of Canada Project 890010

# Paleomagnetism of units P1-P3 of the Late Precambrian Shaler Group, Brock Inlier, Northwest Territories

**John K. Park**
**Continental Geoscience Division**

*Park, J.K., 1992: Paleomagnetism of units P1-P3 of the Late Precambrian Shaler Group, Brock Inlier, Northwest Territories; in Current Research, Part C; Geological Survey of Canada, Paper 92-1C, p. 43-52.*

***Abstract***

*This paper uses paleomagnetic results from the Late Precambrian rocks of the Brock Inlier, N.W.T., to test whether these sedimentary rocks are correlative with units of the Mackenzie Mountains Supergroup, 500 km to the southwest. Paleomagnetic analysis of units P1, P2, and P3 revealed four stable magnetic components. The closely similar, mainly reverse, A components of all units, probably residing largely in magnetite, are considered to be primary. Considering the limited data, the best defined primary component in upper unit P3, yields a paleopole ($P3_A$: 191°W, 12°N; 10 samples) that is reasonably close to a pole from the geologically correlative Tsezotene Formation/Katherine Group of the Mackenzie Mountains. It is often difficult to distinguish A from a secondary component B, which is thought to have been acquired during intrusion of the Franklin diabase sills, prior to quartz cementation. Younger magnetic components, C1 and C2, reside in secondary hematite developed after the quartz cement.*

***Résumé***

*Dans le présent document, on utilise les données paléomagnétiques recueillies dans les roches du Précambrien tardif de la boutonnière de Brock (T.N.-O.) pour vérifier si ces roches sédimentaires sont équivalentes aux unités du supergroupe de Mackenzie Mountains, situé à 500 km au sud-ouest. L'analyse paléomagnétique des unités P1, P2 et P3 a révélé la présence de quatre composantes magnétiques stables. Dans toutes les unités, les composantes A principalement inverses, très semblables et probablement surtout présentes dans la magnétite sont considérées primaires. Compte tenu du nombre limité de données, la composante primaire la mieux définie dans l'unité supérieure P3 donne un paléopôle ($P3_A$: 191 °W, 12 °N; 10 échantillons) qui est raisonnablement proche d'un pôle de la formation de Tsezotene, formation géologiquement équivalente, faisant partie du Groupe de Katherine dans les monts Mackenzie. Il est souvent difficile de faire la distinction entre une composante A et une composante secondaire B qui aurait été acquise durant l'intrusion des filons-couches de diabase de Franklin, avant la cimentation du quartz. Les composantes magnétiques plus récentes, C1 et C2, résident dans une hématite secondaire formée après la cimentation du quartz.*

## INTRODUCTION

In 1977 sedimentary units P1, P2, and P3, and diabasic unit P6 that intrudes them, were sampled for paleomagnetic study from the Upper Proterozoic rocks of the Brock Inlier, north of Great Bear Lake. It was hoped to determine whether P6 was related to the Franklin diabases - in particular to the Coronation suite to the southeast (Young, 1977), - to sills intruding the Tsezotene Formation in the Mackenzie Mountains to the southwest, or to both (Fig. 1). Paleomagnetic results from P6 showed that the unit correlated with diabases of the widespread Franklin igneous episode (Park, 1981c) and not with sills of the Mackenzie Mountains (Park, 1981b). That conclusion was recently confirmed by radiometric age-dating of U-Pb, which revealed precise ages of 723 ± 3 Ma (Heaman et al., 1990) from baddeleyite of the Franklin diabases and 777.7 + 2.5/- 1.8 Ma (Jefferson and Parrish, 1989) from zircon of a diorite plug in the Mackenzie Mountains.

It remained to complete the paleomagnetic study of units P1, P2, and P3, of which P2 and P3 on geological grounds had been respectively correlated with several units intruded by the diabases of the Mackenzie Mountains (Aitken et al., 1978), namely, the H1 unit and the Tsezotene Formation/Katherine Group (units K1-K6) (Table 1). Because paleomagnetic results were available from the Tsezotene (Park and Aitken, 1986b) and Katherine (units K1-K5) (Park and Aitken, 1986a), it was important to see whether these results correlated with those of the Brock Inlier, in view of the geological correlation. Paleomagnetism revealed that a paleopole calculated from the best-defined probable primary magnetization of unit P3 is similar to that from the Tsezotene/Katherine units, consistent with the geological correlation.

## GEOLOGY

The Precambrian succession in the Brock Inlier consists of five unmetamorphosed sedimentary units (P1 - P5) of marine and (or) fluvial-deltaic origin that are intruded by diabasic and gabbroic dykes and sills (P6) (Cook and Aitken, 1969). Units P1-P5 have been assigned to the Shaler Group of Victoria Island, because they lie on trend with the type locality and have a similar lithology and stratigraphic position (Thorsteinsson and Tozer, 1962). They have also been correlated with units of the Mackenzie Mountains Supergroup generally by Aitken et al. (1978) and in more detail by Jefferson and Young (1989) and Jefferson and Jones (1991) (Table 1).

The structural history of the region is not completely understood. At least four tectonic episodes are documented (Cook and Aitken, 1969). These are evidenced by fault movement that possibly predated and definitely postdated deposition of P5; by faulting and folding of the lower Paleozoic succession (in part along reactivated Proterozoic faults) in post-Early Devonian time; by tectonism along the Coppermine Arch in pre-Middle Devonian time; and by folding in post-Cretacious time.

We collected 10 sites from beds dipping less than 6° (Fig. 1a). P1 sites (17-19) consist of shale; P2 sites (2), of pink dolomite; and P3 sites (4, 11-13, 15, 16), of quartzite.

## METHODS

Cores or hand samples collected in the field were oriented by sun and magnetic compasses. Standard cylindrical specimens for study (2.2 cm height, 2.5 cm diameter) were prepared in the laboratory. Magnetizations of specimens were measured with a Geofyzika Instruments JR-4 fast spinner magnetometer. Toward the end of the study some measurements were made within a magnetically-shielded room (residual fields ca. 1000 nT).

The natural remanent magnetization (NRM) was analyzed with alternating field (AF), thermal (TH), and chemical (CH) demagnetization techniques, or a combination of them, either AF or CH followed by TH. AF experiments were conducted with an 'in-house' 3-axis tumbling device (Roy et al., 1973), and specimens were measured after each 5 to 10 mT increment of field, up to a total of 290 mT. Thermal experiments were done in both a large in-house instrument (Roy et al., 1972) and small commercial ovens (Schonstedt TSM-1), and specimens were measured after incremental steps of 5° to 100°C to a maximum temperature of 680°C. Residual fields in the in-house instruments were generally less than 2 nT, but ranged up to 30 nT in the commercial furnaces.

CH demagnetization was carried out on only five specimens from several of the quartzite sites using the methods of Park (1970) and Roy and Park (1974). Leaching was discontinued after remanences ceased to change significantly, generally after 770 h in acid. Vector diagrams, vector subtraction, the LINEFIND paleomagnetic analysis program (Kent et al., 1983), and the DIPS program (Hoek and

**Table 1.** Lithostratigraphic correlation between Mackenzie Mountains and Brock Inlier[1]

| Mackenzie Mountains Supergroup | Shaler Group |
|---|---|
| Little Dal Group | |
| Upper Carbonate fm. | |
| Rusty Shale fm. | |
| Gypsum fm. | P5 |
| Grainstone fm. | P4C,D |
| Basinal sequence | P4C,D |
| Mudcracked fm. | P4C,D |
| Katherine Group, K8 | P4B |
| Katherine Group, K7 | P4A |
| Katherine Group, K1-K6 | P3 |
| Tsezotene Fm. | P3 |
| H1 unit | P2 |
| unexposed unit | P1 |

[1] After Aitken et al. (1978), Jefferson and Young (1989), and Jefferson and Jones (1991).

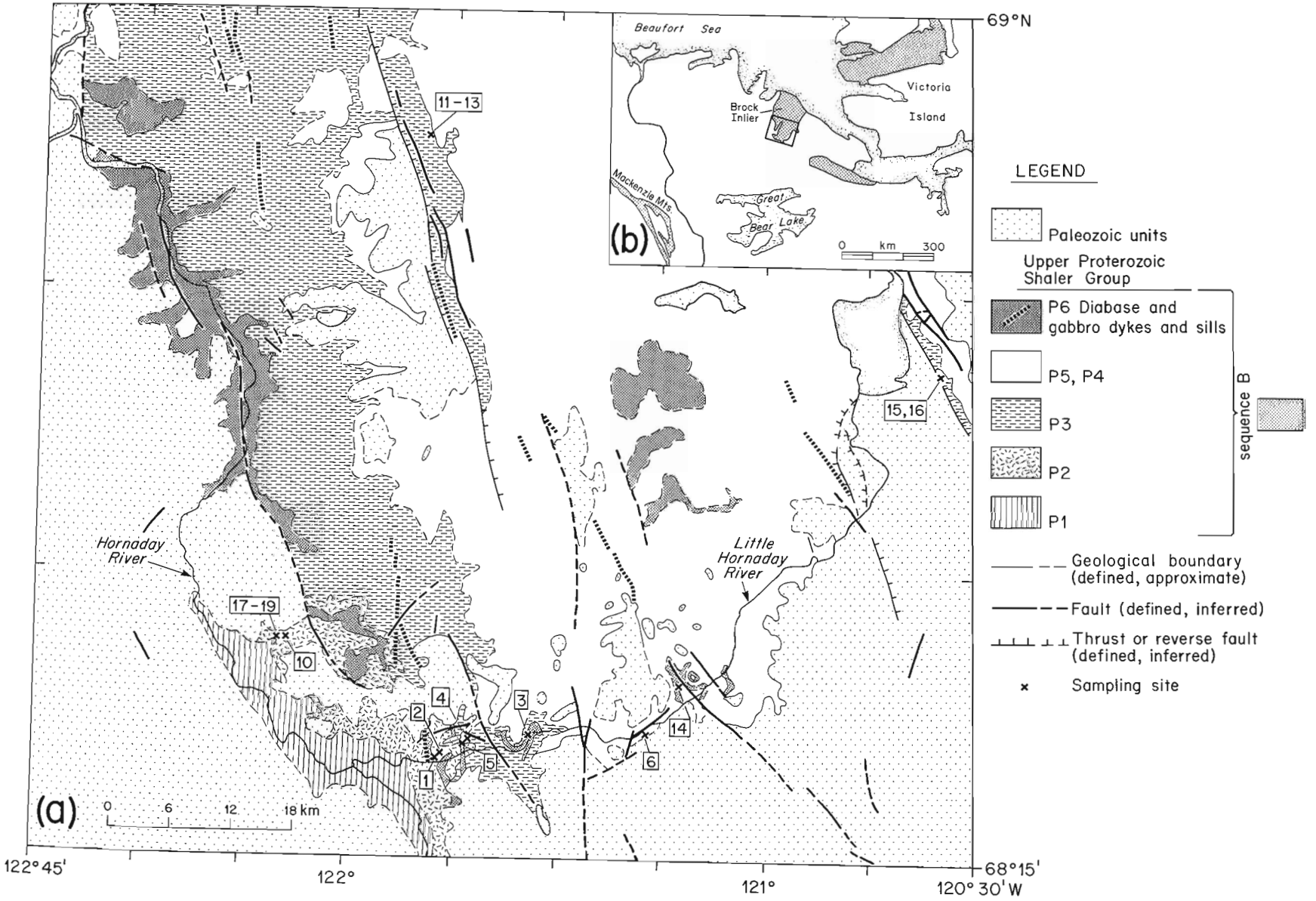


**Figure 1.** (**a**) Geological map after Cook and Aitken (1969) showing the paleomagnetic sampling sites. (**b**) Regional map showing areas of probable correlative Late Proterozoic units in the time range ~1.2 to ~0.8 Ga, designated sequence B (Young et al., 1979). The rectangle in the regional map is the sampling area.

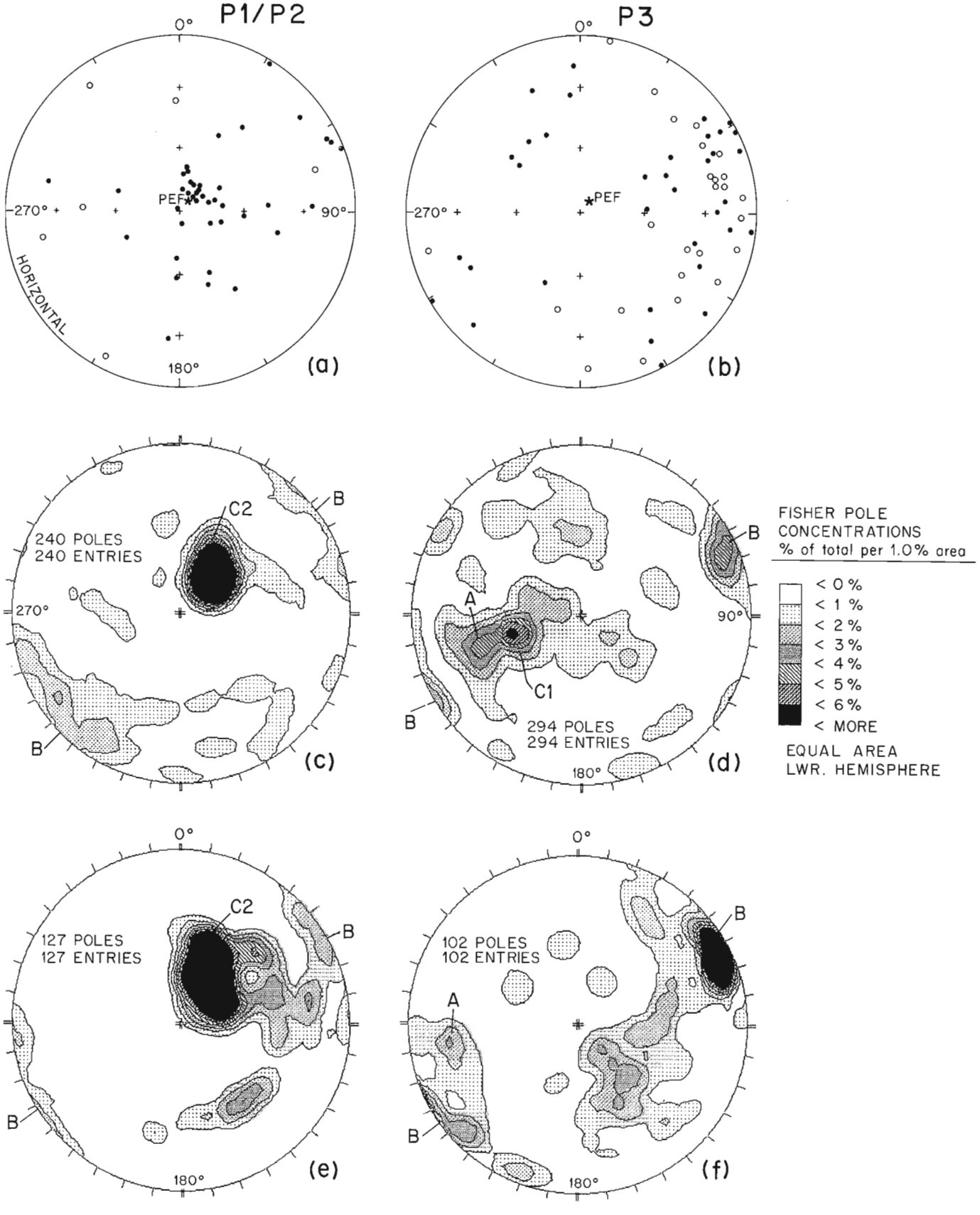


**Figure 2.** Natural remanent magnetization directions of individual specimens from units P2 (**a**) and P3 (**b**). (**c**)-(**f**) show contour plots of directions from all thermal measurements: (**c**) and (**d**), for measurements between 200° and 580°C, and (**e**) and (**f**), for measurements greater than 580°C. Component C2 of parts (**c**) and (**e**) is only found in unit P2. Closed symbols represent downward directions and open symbols, upward directions.

Diederichs, 1989) helped to determine magnetic components. The DIPS program allows directional data to be contoured, thus revealing concentrations of directions.

Subscripts identify magnetic components. A is generally used for the primary or original magnetization; B and C, for secondary or later magnetizations. For consistency with other studies in the region, C is reserved for high-inclination components, no matter when formed.

## RESULTS

NRMs have weak intensities ranging from 0.1-2 mA/m and directions that tend to be steep and downward for P2 (Fig. 2a) and shallow and westerly for P3 (Fig. 2b). Demagnetization experiments generally serve to decompose NRMs into several components: a temporary viscous component D, which is removed at AFs below about 5 mT (Fig. 3) and temperatures below about 200°C (Fig. 4), and more stable components, A, B, C1, and C2, which were revealed at higher temperatures (Fig. 3, 4, 5). Contour plots of the thermal measurements indicate the approximate positions of components that were analyzed using vector diagrams and the LINEFIND program (Fig. 2c-2f).

Components C1 and C2 (most apparent in unit P2) are steeply directed (Fig. 2c-2e), either up (Fig. 4) or down. The downward directed component (C2) was revealed over two unblocking temperature ($T_{UB}$) and resistive coercive force (rcf) ranges (e.g. site 2, Table 2; Fig. 2c, 2e), which suggest that it resides in two magnetic phases. Its direction, exhibited by the NRMs (Fig. 2a), suggests that it is a magnetization of Recent age. The reverse direction (C1), mainly found in unit P3, has $T_{UBS}$ and rcf(s) in the magnetite range (Fig. 2d, Table 2); but its direction appears to be significantly different from C2 and the present Earth's field direction (Table 2).

Magnetic components A and B are mainly uncovered after C (e.g. Fig. 4)(Table 3). They are differentiated somewhat on the contour plot of unit P3 (Fig. 2f), but are difficult to characterize and distinguish otherwise because of overlapping rcf and $T_{UB}$ spectra and the few results of A and B available from vector analysis (Table 3). Both are mainly

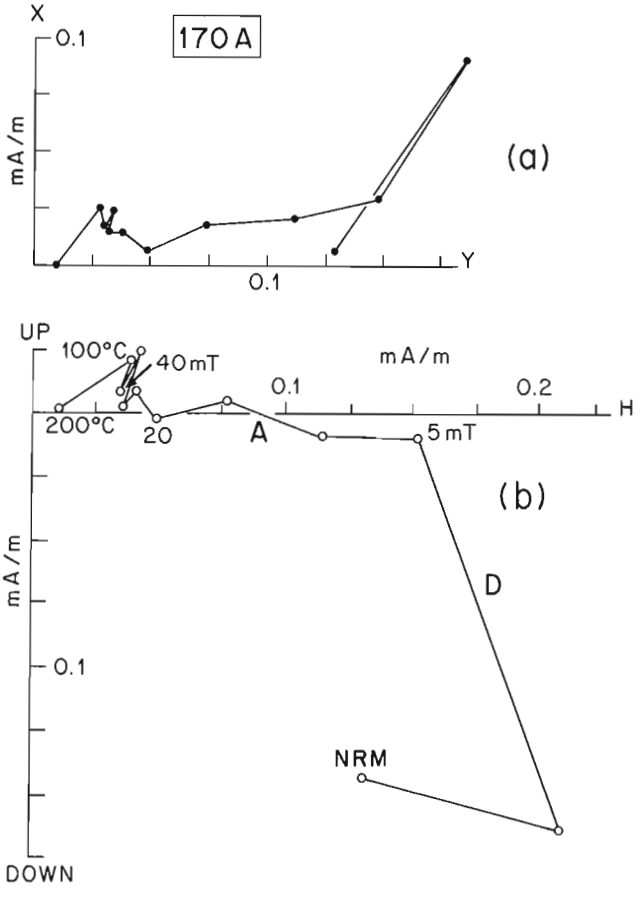


**Figure 3.** Vector diagram showing the combined alternating field and thermal demagnetization of a specimen from site 17 (unit P1). The remanent magnetization is plotted in the horizontal (**a**) and vertical (**b**) planes. $H = (X^2 + Y^2)^{1/2}$. Points on the horizontal plot are closed; those on the vertical plot, open. Magnetic Components (A and D) are opposite the ranges over which they are removed.

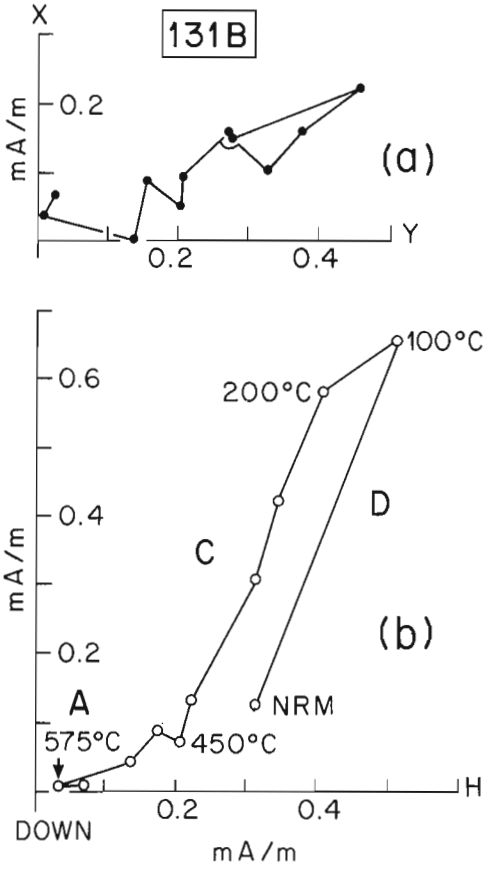


**Figure 4.** Vector diagram of the thermal demagnetization of a specimen from site 13 (unit P3). See Figure 3 for other explanations.

**Table 2.** Mean site directions of C1 and C2 components

| Sites | Treatment AF | Treatment TH/CH | *Sa* | *D°,I°* | *R* | *k* | $\alpha_{95}$° | pol. |
|---|---|---|---|---|---|---|---|---|
| **P1** | | | | | | | | |
| 17 | - | 200-400°C | 1 | 136,-84[1] | - | - | - | R |
| 18 | 5-015 mT | - | 1 | 138,-85[1] | - | - | - | R |
| **P2** | | | | | | | | |
| 2 | NRM-175 mT, | 100-550°C | 6 | 058,+82[2] | 5.96 | 122 | 6 | N |
| | 65-)270 mT, | 650-675°C | 5 | 052,+67[2] | 4.67 | 12 | 23 | N |
| **P3** | | | | | | | | |
| 4 | 5-035 mT, | 48-652 h | 3 | 331,+86[2] | 2.91 | 23 | 27 | N |
| | - | 100-575°C | 1 | 021,-75[1] | - | - | - | R |
| 11, 12 | no evidence for C components | | | | | | | |
| 13 | 5-060 mT, | 100-450°C | 4 | 091,-68[1] | 3.92 | 37 | 15 | R |
| 15 | NRM-045 mT, | 140-500°C | 5 | 125,-78[1] | 4.89 | 36 | 13 | R |
| *mean of C1 samples* | | | *12* | *101,-77[2]* | *11.66* | *32* | *8* | *R* |

NOTES: AF, alternating field; TH, thermal; CH, chemical (acid leaching); *Sa*, samples (results are the means of 1-3 specimens); *D°,I°* are the declination and inclination of the direction with respect to the paleohorizontal, unless otherwise indicated; *R* is the vector resultant; *k* is Fisher's (1953) parameter of precision; $\alpha_{95}$° is the half-angle of the circle of 95% confidence about the direction; pol. is the polarity: N, normal, R, reverse, M, mixed. Grand averages are in italics. [1] C2, with respect to paleohorizontal. [2] C1, with respect to present horizontal.

**Table 3.** Mean site directions of A and B components corrected for tilt

| Sites | Treatment AF/CH | Treatment TH/CH | *Sa* | *D°,I°* | *R* | *k* | $\alpha_{95}$° | comp. |
|---|---|---|---|---|---|---|---|---|
| **P1** | | | | | | | | |
| 17 | 5-)40 mT, | 100-340°C | 4 | 082,-15 | 3.72 | 11 | 29 | A |
| 18 | 5-045 mT, | 100-400°C | 4 | 099,-29 | 3.23 | 4 | 54 | A |
| **P2** | | | | | | | | |
| 2 | - | 575-650°C | 2 | 082,+05[1] | 1.76 | - | - | B |
| **P3** | | | | | | | | |
| 4 | 5-035 mT, | 535-)595°C | 2 | 264,+24 | 1.94 | - | - | A |
| | | 340-772 h | 1 | 084,+14 | - | - | - | B |
| 11 | >480 h, | 290-595°C | 2 | 055,-26 | 1.99 | - | - | A |
| | 5-020 mT, | 665-670°C | 2 | 060,+02 | 2.00 | - | - | B |
| | | 48-340 h | | | | | | |
| 12 | - | 340-405°C | 1 | 060,-28 | - | - | - | A |
| | - | 500-)640°C | 2 | 070,+05 | 1.90 | - | - | B |
| 13 | 5-075 mT, | 250-575°C | 5 | 080,-31 | | 66 | 10 | A |
| 16 | 15-050 mT, | 100-575°C | 4 | 126,-07 | 2.95 | 3 | 67 | A? |
| *mean of A samples, P3* | | | *10[2]* | *074,-28* | *9.69* | *29* | *9* | |
| *mean of B samples, P2 and P3* | | | *7* | *072,+06* | *6.55* | *13* | *17* | |

NOTES: see Table 2 for explanation of symbols. [1] Mixed components. [2] Excluding site 16, which has an unacceptably large error.

reversely directed to the east (Fig. 3, 4, 5) with moderate (A) to shallow (B) dips (Table 3). Unblocking temperature ranges suggest that A resides in both magnetite (Fig. 4, 5a) and hematite (Fig. 2f) and B in hematite (Fig. 5a, Table 3). Thermal treatment reveals both normal and reverse components in the hematite range of $T_{UBS}$ above 580°C in single specimens (Fig. 5a).

Comparison of CH and TH data helps to characterize more fully the nature of the A and B components. All chemical specimens (3 from site 4, 1 from site 11, 1 from site 13) reach endpoints during acid leaching (e.g. Fig. 5b), indicating that one or more magnetic phases are unaffected by the acid. This behaviour suggests either that the secondary quartz cement is preventing acid penetration to underlying magnetic phases (e.g. Park and Jefferson, 1991) or that the remaining phases are insoluble in acid, thus probably indicating the presence of magnetite (Henry, 1979). Thermal treatment following acid leaching reveals the endpoint remanence to have $T_{UBS}$ in the magnetite range, and to consist of either A (site 13 specimen) or A combined with D (sites 4, 13). Comparison of CH and TH specimens from site 11, which contain no evidence for C and little evidence for D, suggests that the insoluble phase (Fig. 5b) only consists of A with $T_{UBS}$ in the magnetite range (Fig. 5a).

Comparison of CH and TH specimens from site 11 also reveals the nature of the hematite phases. The reverse and normal components revealed thermally (Fig. 5a) are apparently not revealed by acid leaching (Fig. 5b). In view of the similar shapes of the CH and TH diagrams, it appears that the normal and reverse hematite components removed by 665°C (Fig. 5a) could reside in similar phases that are eliminated by acid leaching to 340 h (Fig. 5b). However, exactly where the removal of the normal phase is accommodated in the initial part of the vector diagram is not obvious. Thereafter, a third phase appears to be removed by both treatments (Fig. 5). Because hematite pigment is more soluble, is generally more accessible to the acid, and generally has lower $T_{UBS}$ than detrital hematite or martite, it is reasonable to ascribe the less stable phases to pigmental hematite and the most stable phase to detrital hematite or martite. The reverse hematite phase below 665°C is considered to harbour B and the normal phase above 665°C, to harbour A; but generally there are too few analyzed results available to distinguish these directions with complete

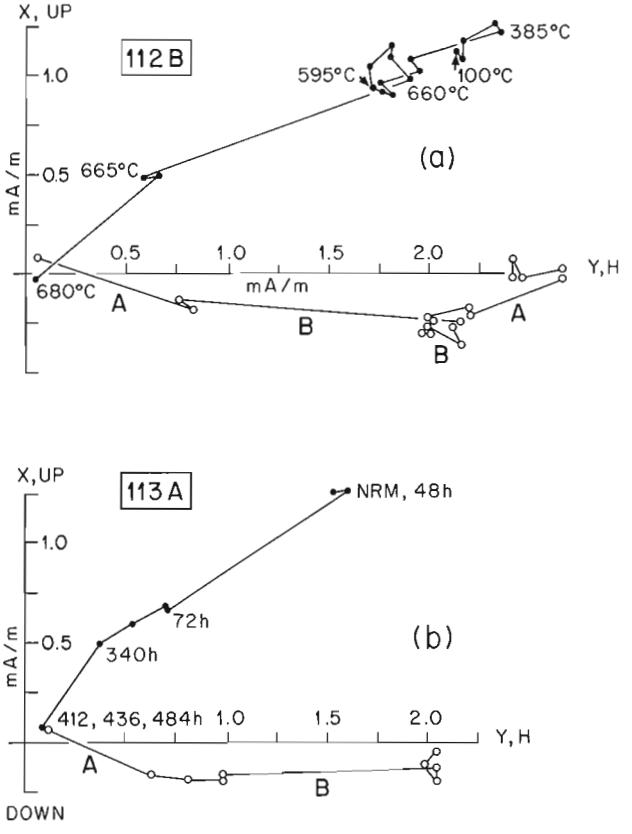


**Figure 5.** Vector diagrams of the thermal (**a**) and chemical (**b**) demagnetization of specimens from site 11 (unit P3). See Figure 3 for other explanations.

**Table 4.** Summary of poles

| Description | *Si(Sa)* | Pole (°W, °N) | $\delta p°, \delta m°$ | $\lambda$ (°N) |
|---|---|---|---|---|
| $P3_A$, from mean of Sa directions | 4(10) | 192, 09 | 5,10 | 15 |
| from contour plot[1] | - | 191, 12 | - | - |
| $P_B$, from mean of Sa directions | 4(7) | 196,-09 | 9,17 | -03 |
| from contour plot[2] | | 191,-12 | - | - |
| $P_{C1}$, from mean of Si directions | 5(12) | 180, 61 | 14,14 | 65 |

NOTES: *Si(Sa)*, sites (samples). $\delta p°, \delta m°$ are the semi-axes of the ellipse of confidence about the pole at the 95% probability level. $\lambda°$, paleolatitude. [1] Calculated from a cluster of directions that has a maximum concentration at 254°, +34° (total directions on plot 844). [2] Calculated from a cluster of directions that has a maximum concentration at 66°, +07° (total directions on plot 1509).

confidence. Contour plots (Fig. 2c-2f) yield similar directions to tabled values (Table 3), suggesting that A and B are distinct directions.

Vector diagrams tend to be quite noisy because specimens were often measured at the limit of magnetometer sensitivity. Some of the noise of AF specimens is due to the acquisition of a rotational remanent magnetization on tumbling (zig-zag behaviour, Fig. 3). Specimens were inverted in the tumbling device on alternate steps in order to detect and randomize this spurious component.

### *Opaque mineralogy*

The assemblage of opaque minerals is similar in all units. Detrital hematite (or martite after detrital magnetite) was only positively identified at sites 12, 13, and 18, but may be present at site 11. In site 12 it occurs as abraded particles up to 100 μm, confined in layers. Secondary hematite pigment ranges in abundance from rare (sites 4, 13, 17), to occasional (sites 12?, 18, 19), to pervasive (sites 2, 11), and may either predate (site 12, 18) or postdate (sites 4, 13) the secondary quartz. At site 19 patches of pigment occur with euhedral iron oxide grains (probably hematite) after magnetite. Many of the opaque minerals, including secondary hematite pigment, have been altered to rutile; it appears in close association with hematite pigment (site 11) and as alterations of detrital hematite (or martite)(site 15) and martite after secondary magnetite (site 19). Secondary sulphides may be numerous (pyrite at site 17) to occasional (sites 13, 16), and may also be associated with rutile.

## DISCUSSION

### *Correlations between paleomagnetic components and magnetic phases*

Evidence from the study of the paleomagnetism and the opaque mineralogy suggests some correlations of magnetic mineral phases with magnetic components and suggests a chronology of component acquisition. Sites 11 and 12, showing only evidence for components A and B, contain microscopically identified detrital hematite (martite?), and secondary hematite, which at site 12 is evidenced to predate the secondary quartz overgrowths. I associate B with the secondary hematite and A with detrital hematite (or martite) and probable unobserved magnetite. At sites 4 and 13, where their is definite evidence that the secondary hematite postdates the secondary quartz (although A is present), either C1 (e.g. Fig. 4) or C2 is present. Thus, B likely predates the secondary quartz overgrowths and C1 and C2 postdate them, with C2 being of Recent age. Therefore, the suggested chronology of component acquisition is: A, B, C1, C2.

### *Paleopoles*

Paleomagnetic poles of A ($P3_A$), B ($P_B$), and C1 ($P_{C1}$) are summarized in Table 4, and $P3_A$ and $P_B$ are plotted in Fig. 6. Insufficient A data are available from units P1 and P2 to calculate paleopoles. Pole $P3_A$ lies 20-25° east of poles $T_A/K_A$ from the geologically correlated Tsezotene Formation/Katherine Group of the Mackenzie Mountains (Fig. 6). The difference may be due to the limited data available from these studies and/or to bias caused by inadvertent mixing of A and B directions in the present study. Another possibility is that there has been a small relative rotation between the respective regions.

Pole $P_B$, closely agreeing with Franklin poles F(B) and F(W) (Fig. 6), is thought to record effects of the Franklin igneous episode. Site 2, which is only several metres above a diabase sill, contains component B rather than A. All other sites, showing evidence of A, are not demonstrably closer

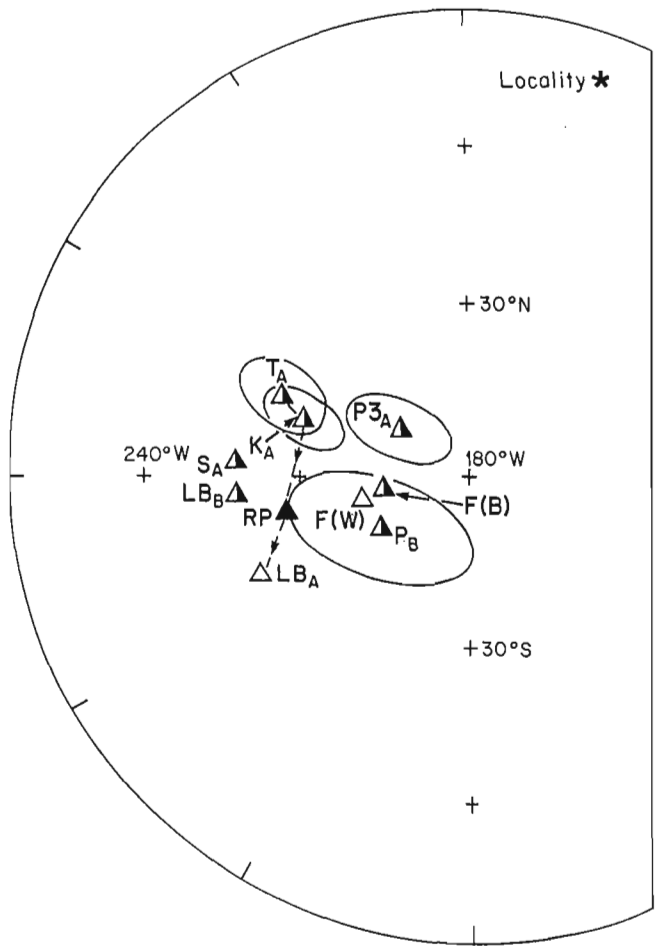


**Figure 6.** High-latitude poles derived from Late Proterozoic units of the Mackenzie Mountains and Brock Inlier: F(B), Franklin sills from the Brock Inlier (Park, 1981c); F(W), Franklin diabases and lavas from the western Arctic (Coronation sills, Victoria Island sills and lavas)(Fahrig et al., 1971; Palmer and Hayatsu, 1975; Robertson and Baragar, 1972), minus the Brock Inlier (Park, 1981c); $K_A$, Katherine Group (Park and Aitken, 1986a); $LB_B$, Little Dal Group, Basinal sequence (Park, 1981a); $P3_A$, unit P3 (this study); $P_B$, units P2, P3 (this study); RP, Reynolds Point Formation (Palmer et al., 1983); $S_A$, diabases of the Mackenzie Arc (Park, 1981b; Park et al., 1989); $T_A$, Tsezotene Fm. (Park and Aitken, 1986b). Open (closed) symbols indicate normal (reverse) poles; half-closed symbols, mixed poles. The dashed line represents a segment of the apparent polar wander path (Park and Aitken 1986 a, b).

than 40 m to a diabase intrusion. Evidently, in the sites sampled, the intrusion of the Franklin diabases mainly caused the chemical formation of hematite (Fig. 2e, 2f; Table 3), with some possible remagnetization of magnetite (Fig. 2c, 2d). The formation of secondary hematite in Shaler Group sediments may be analogous to the formation of hematite in Little Dal Group sediments of the Mackenzie Mountains at the time of diabase and Little Dal basalt emplacement at ca. 780 Ma. That event is represented by pole $LB_B$, which coincides with the diabase pole $S_A$.

Pole $P_{C1}$ (180°W, 61°N; $A_{95}$ = 14°), which postdates the secondary quartz overgrowths, agrees with a secondary pole $LB_C$ (190°W, 60°N; $A_{95}$ = 9°) from the Basinal sequence of the Lower Little Dal Group of the Mackenzie Mountains. This unit would be equivalent to part of unit P4 in the Brock Inlier (Table 1). $LB_C$ is the only definite prefolding high-latitude pole reported from the Mackenzie Mountains. It may slightly predate folding in post-Cretaceous times or relate to the Late Proterozoic (Park and Jefferson, 1991).

## CONCLUSIONS

1. The reasonably close agreement between paleopoles of the P3 unit of the Brock Inlier and Tsezotene/Katherine units of the Mackenzie Mountains is consistent with the proposed geological correlation.
2. Intrusion of the Franklin diabase variously caused remagnetization of existing magnetite and/or development of secondary hematite in units P1, P2, and P3.
3. A later secondary hematite component, acquired in P1 and P3 after quartz cementation, yields a pole $P_{C1}$ that agrees with a prefolding pole $LB_C$ from the Little Dal Group Basinal sequence of the Mackenzie Mountains.

## ACKNOWLEDGMENTS

This study would not have been possible without the logistical support and camping facilities of J.D. Aitken (now retired from the Geological Survey of Canada). I am grateful for the geological advice and sampling help he and D.G.F. Long (Laurentian University, Sudbury, Ontario) provided during the trip. D. Harris (Geological Survey of Canada) is thanked for information on the magnetic mineralogy. D. Champagne made some of the earlier measurements. R. Langridge facilitated the measurement and analysis of data by his numerous improvements to existing computer programs. K. Buchan and C.W. Jefferson are thanked for reviewing the manuscript, and R. Parrish for commenting upon it.

## REFERENCES

**Aitken, J.D., Long, D.G.F., and Semikhatov, M.A.**
1978: Correlation of Helikian strata, Mackenzie Mountains-Brock Inlier-Victoria Island; Note in Current Research, Part A; Geological Survey of Canada, Paper 78-1A, p. 485-486.

**Cook, D.G. and Aitken, J.D.**
1969: Erly Lake, District of Mackenzie (97A); Geological Survey of Canada, Map 5-1969.

**Fahrig, W.F., Irving, E., and Jackson, G.D.**
1971: Paleomagnetism of the Franklin diabases; Canadian Journal of Earth Sciences, v. 8, p. 455-467.

**Fisher, R.A.**
1953: Dispersion on a sphere; Proceedings of the Royal Society of London, Series A: Mathematical and Physical Sciences, v. 217, p. 295-305.

**Heaman, L.M., LeCheminant, A.N., and Rainbird, R.H.**
1990: A U-Pb baddeleyite study of Franklin igneous events, Canada; Geological Association of Canada, Program with Abstracts, v. 15, A55.

**Henry, S.G.**
1979: Chemical demagnetization: methods, procedures, and applications through vector analysis; Canadian Journal of Earth Sciences, v. 16, p. 1832-1841.

**Hoek, E. and Diederichs, M.**
1989: DIPS, version 2.2; Users Manual, advanced version, Rock Engineering Group, Department of Civil Engineering, University of Toronto, Toronto, Canada.

**Jefferson, C.W. and Jones, T.A.**
1991: Revised stratigraphy and structure of Proterozoic to Cretaceous strata in and around the Brock Inlier, NTS 97A and 97D: some implications for mineral and energy resource assessment of the proposed Bluenose Lake National Park, N.W.T.; in Part 2, Preliminary Reports on Geological work in the Northwest Territories; Mining, Exploration, and Geological Investigations; Northwest Territories Geology Division, Northern Affairs Program, Indian and Northern Affairs Canada.

**Jefferson, C.W. and Parrish, R.R.**
1989: Late Proterozoic stratigraphy, U-Pb zircon ages and rift tectonics, Mackenzie Mountains, northwestern Canada; Canadian Journal of Earth Sciences, v. 26, p. 1784-1801.

**Jefferson, C.W., and Young, G.M.**
1989: Late Proterozoic orange-weathering stromatolite biostrome, Mackenzie Mountains and western Arctic Canada; in Reefs, Canada and Adjacent Area, (ed.) H.H.J. Geldsetzer, N.P. James, and G.E. Tebbutt. Canadian Society of Petroleum Geologists, Memoir 13, p. 72-78.

**Kent, J.T., Briden, J.C., and Mardia, K.V.**
1983: Linear and planar structure in ordered multivariate data as applied to progressive demagnetization of paleomagnetic remanence; Geophysical Journal of the Royal Astronomical Society, v. 75, p. 593-621.

**Morris, W.A.**
1977: Paleolatitude of glaciogenic upper Precambrian Rapitan Group and the use of tillites as chronostratigraphic marker horizons; Geology, v. 5, p. 85-88.

**Morris, W.A. and Aitken, J.D.**
1982: Paleomagnetism of the Little Dal lavas, Mackenzie Mountains, Northwest Territories, Canada; Canadian Journal of Earth Sciences, v. 19, p. 2020-2027.

**Palmer, H.C. and Hayatsu, A.**
1975: Paleomagnetism and K-Ar dating of some Franklin lavas and diabases, Victoria Island; Canadian Journal of Earth Sciences, v. 12, p. 1439-1447.

**Palmer, H.C., Baragar, W.R.A., Fortier, M., and Foster, J.H.**
1983: Paleomagnetism of Late Proterozoic rocks, Victoria Island, Northwest Territories, Canada; Canadian Journal of Earth Sciences, v. 20, p. 1456-1469.

**Park, J.K.**
1970: Acid leaching of red beds and the relative stability of the red and black magnetic components; Canadian Journal of Earth Sciences, v. 7, p. 1086-1092.
1981a: Analysis of the multicomponent magnetization of the Little Dal Group, Mackenzie Mountains, Northwest Territories, Canada; Journal of Geophysical Research, v. 86, p. 5134-5146.
1981b: Paleomagnetism of the Late Proterozoic sills in the Tsezotene Formation, Mackenzie Mountains, Northwest Territories, Canada; Canadian Journal of Earth Sciences, v. 18, p. 1572-1580.
1981c: Paleomagnetism of basic intrusions from the Brock Inlier, Northwest Territories, Canada; Canadian Journal of Earth Sciences, v. 18, p. 1637-1641.

**Park, J.K. and Aitken, J.D.**
1986a: Paleomagnetism of the Katherine Group in the Mackenzie Mountains: implications for post-Grenville (Hadrynian) apparent polar wander; Canadian Journal of Earth Sciences, v. 23, p. 308-323.
1986b: Paleomagnetism of the Late Proterozoic Tsezotene Formation of northwestern Canada; Journal of Geophysical Research, v. 91, p. 4955-4970.

**Park, J.K. and Jefferson, C.W.**
1991: Magnetic and tectonic history of the Late Proterozoic upper Little Dal and Coates Lake Groups of northwestern Canada; Precambrian Research, v. 52, p. 1-35.

**Park, J.K., Norris, D.K., and Larochelle, A.**
1989: Paleomagnetism and the origin of the Mackenzie Arc of northwestern Canada; Canadian Journal of Earth Sciences, v. 26, p. 2194-2203.

**Robertson, W.A. and Baragar, W.R.A.**
1972: The petrology and paleomagnetism of the Coronation sills; Canadian Journal of Earth Sciences, v. 9, p. 123-140.

**Roy, J.L. and Park, J.K.**
1974: The magnetization process of certain red beds: vector analysis of chemical and thermal results; Canadian Journal of Earth Sciences, v. 11, p. 437-471.

**Roy, J.L., Reynolds, J., and Sanders, E.**
1973: An alternating field demagnetizer for rock magnetism studies; Publications of the Earth Physics Branch, Canada, no. 44 (3), p. 37-45.

**Roy, J.L., Sanders, E., and Reynolds, J.**
1972: Un four electrique pour l'etude des proprietes magnetiques des roches; Publication de la direction de la physique du globe, no. 42, p. 229-237.

**Thorsteinsson, R. and Tozer, E.T.**
1962: Banks, Victoria and Stefansson Islands, Arctic Archipelago; Geological Survey of Canada, Memoir 330, 85 p.

**Young, G.M.**
1977: Stratigraphic correlation of upper Proterozoic rocks of northwestern Canada; Canadian Journal of Earth Sciences, v. 14, p. 1771-1787.

**Young, G.M., Jefferson, C.W., Delany, G.D., and Yeo, G.M.**
1979: Middle and late Proterozoic evolution of the northern Canadian Cordillera and shield; Geology, v. 7, p. 125-128.

Geological Survey of Canada Project 820005

# Yttrium, rare-earths, and radioactive elements in selected mine tailings, Elliot Lake, Ontario

**N. Prasad and V. Ruzicka**
**Mineral Resources Division**

*Prasad, N. and Ruzicka, V., 1992: Yttrium, rare-earths, and radioactive elements in selected mine tailings, Elliot Lake, Ontario; in Current Research, Part C; Geological Survey of Canada, Paper 92-1C, p. 53-58.*

***Abstract***

*Uraninite, brannerite and monazite are the main minerals that contain U, Th, and REE in pyritic quartz-pebble conglomerate ores at Elliot Lake. A preliminary study of the chemistry of selected mill-heads and tailings indicates that at Rio Algom Mines more than 92% of U was recovered, but other ore constituents were disposed to tailings, which therefore contain elevated amounts of yttrium, other rare-earth elements, and Th. At Denison Mines, where Y is recovered from the leached solutions after U recovery, approximately 74% Y, 75% Yb and 70% Dy were also removed and the rest disposed in the tailings. The lighter REE are not recovered. Also 95% U and 82% Th are removed. Concentration of all other metals in tailings from both operations is too low to be of any economic interest.*

*Although only a fraction of U metal goes to tailings, they retain 60-90% of the initial radioactivity, because of the radioactive daughter products that are not extracted from the ores in the milling process.*

***Résumé***

*L'uraninite, la brannérite et la monazite sont les principaux minéraux contenant U, Th et des terres rares dans les minerais composés de conglomérats pyriteux à galets quartzeux, dans la région d'Elliot Lake. Une étude préliminaire de la chimie de minerais triés et de résidus miniers sélectionnés indiquent que dans les mines de la Rio Algom, on a récupéré plus de 92 % de U, mais que d'autres constituants du minerai ont été rejetés avec les résidus de triage, qui de ce fait contiennent des taux élevés d'yttrium, d'autres terres rares et de Th. Dans les mines Denison, où Y est récupéré dans les solutions de lixiviation après l'extraction de U, on a aussi retiré approximativement 74 % de Y, 75 % de Yb et 70 % de Dy, et l'on a rejeté le reste dans les résidus miniers. Les terres rares plus légères ne sont pas récupérées. On a aussi extrait 95 % de U et 82 % de Th. Dans les rebuts provenant de ces deux opérations, la concentration de tous les autres métaux est trop faible pour présenter le moindre intérêt commercial.*

*Bien que seulement une fraction de l'uranium (U) métallique se retrouve dans les résidus miniers, ceux-ci retiennent 60 à 90 % de la radioactivité initiale, en raison de la présence de produits de filiation radioactifs non extraits des minerais lors du broyage de ces minerais.*

## INTRODUCTION

The Elliot Lake mining camp, like other camps, has areas of mine-tailings disposal in the vicinity of producing as well as dormant mines. An estimate of the tailings in this area is in the order of 150 million tonnes. The scaling down of the production and imminent closure of uranium mines in Elliot Lake prompted the authors to examine selected mine tailings for contents of yttrium and rare-earth elements, and concentration of other metals.

The radioactive minerals of the pyritic quartz-pebble conglomerate and feldspathic quartzite ores are uraninite, brannerite, and monazite with minor amounts of uranothorite, thucolite, coffinite, and other minerals (Roscoe, 1969). Mineralogy of the Elliot Lake ores has been extensively studied in the past (see Theis, 1979 for an excellent summary of the previous work and reference list). Besides uranium, the Elliot Lake ores contain elevated amounts of yttrium, rare-earth elements, and thorium. This is well illustrated in the analyses given by Ruzicka (1988, Table II) of Denison Mines mill-head samples for each month of the year 1978. There are, however, inherent variations in the mineral proportions from one reef to the other and also within a reef along the paleoslope, as stated by the previous workers. Therefore, depending upon the stratigraphic position of the ore that is being mined, these in situ differences would cause variations in yttrium and other trace elements contents of the mill heads and the tailings.

Denison Mines added a leaching plant in 1966 to extract yttrium oxide from the ore after U is precipitated and before the disposal of mill tailings. Between 1967-69 and 1974-76 211.5 tonnes of yttrium oxide were recovered (Financial Post, 1979; Denison Mines, 1979; Ontario Division of Mines, 1975). Since then, although yttrium oxide has been produced intermittently, the amounts have not been published. Some thorium has been extracted by Rio Algom Mines, but the rare-earth elements remain in the tailings. The milling process at the two mills has been described in I.A.E.A.(1980, p. 124-127, 191, 196) and O.E.C.D. and I.A.E.A. (1983, p. 117, 172-174) reports. The latter report explains the rare-earth circuit at Denison mill as follows: "... lime was added to the barren solution from the uranium ion exchange step to raise the pH to about 8.5 to precipitate mixed oxides. Rare earths were then leached from this precipitate at pH 4.2. After clarification, a bulk precipitate containing about 30% total rare earth oxides was obtained using ammonia."

The tailings are in the form of fine grained sand, pale yellowish grey to light yellow with occasional yellow-rusty colored patches, which are due to limonitic weathering of sulphide-rich areas. The content of sulphur, which occurs mostly as pyrite, ranges from 0.26 to 4.79% (mean 2.4%) in the Quirke tailings and 2.96 to 8.60% (mean 4.36%) in the Denison Mines tailings. Mineralogically, the tailings consists of predominantly quartz with minor amounts of feldspar, pyrite, limonite, and dark colored heavy minerals. Some of the old mine tailings are mostly overgrown by vegetation. Rio Algom Mines are presently in the process of reclamation of their main tailings.

## SAMPLING METHOD AND ANALYSES

In order to compare the metal content of the ore prior to milling with that of the waste that goes to the tailings, composite samples of the mill-head (mill-feed) and the mill-tail (mill-waste) from the Denison Mines and Rio Algom Mines operations were analyzed (Tables 1 and 2). The Denison mill-head and mill-tail samples were collected for the month of July, 1990. The mill-head samples from Rio Algom Mines were from the period 28th March to 11th July, 1990; and one mill-tail sample was from 28th February to 4th July, the other for the week ending 15th July 1990. Since the sample periods do not coincide exactly some chemical variation would exist. Denison Mines subjected the leach solution to yttrium recovery as well. Additional minor amounts of U were also recovered in the Y recovery process.

Two tailing disposal areas - Rio Algom's Quirke and Denison Mines' main tailing areas (Fig. 1 and 2) - were chosen for the sampling of the tailings. A hand auger was used to collect samples up to a depth of about 1 m. The samples were homogenized and ground to -200 mesh size before being chemically analyzed. Thirteen samples from Denison tailings were collected along 3 lines each 80 m apart in east-west

**Figure 1.** A view of the Denison Mines' main tailings.

**Figure 2.** A view of the Rio Algom Mines' main Quirke tailings.

**Table 1.** Denison Mill samples July '90

| | Mill Head | Mill-Tail (leached residue) |
|---|---|---|
| (Percent) | | |
| $SiO_2$ | 83.3 | 82.4 |
| $TiO_2$ | .37 | .35 |
| $Al_2O_3$ | 6.9 | 6.6 |
| $Fe_2O_{3t}$ | 4.1 | 3.3 |
| MnO | <.01 | <.01 |
| MgO | .23 | .17 |
| CaO | .14 | .86 |
| $Na_2O$ | .10 | .10 |
| $K_2O$ | 2.38 | 2.35 |
| LOI | 2.55 | 2.57 |
| $P_2O_5$ | .11 | .10 |
| S | 2.77 | 2.84 |
| (ppm) | | |
| Ag | 1 | <1 |
| Ba | 330 | 370 |
| Be | 1.2 | .9 |
| Co | 38 | 29 |
| Cr | 32 | 23 |
| Cu | 69 | 52 |
| Ni | 31 | 21 |
| Pb | 290 | 270 |
| Ra | n.d. | n.d. |
| Rb | 100 | 87 |
| Sr | 11 | 12 |
| V | 13 | 11 |
| Zn | 40 | 0 |
| Zr | 120 | 120 |
| La | 460 | 380 |
| Ce | 850 | 690 |
| Nd | 310 | 240 |
| Sm | 54 | 38 |
| Eu | 2.7 | 1.7 |
| Gd | 35 | 18 |
| Dy | 23 | 6.9 |
| Yb | 5.7 | 1.4 |
| Y | 88 | 23 |
| U(icp) | 830 | 33 |
| Th(icp) | 540 | 270 |
| U(rad) | 610 | 561 |
| Th(rad) | 421 | 252 |

Note: n.d.-not detected. Detection limit of Ra 0.2 ppm, Nb <30 ppm.

**Table 2.** Quirke Mill samples

| | Mill-Head 28/3 to 11/7/90 | Total Mill-tail 28/2 to 4/7/90 | 9/7 to 15/7/90 |
|---|---|---|---|
| (Percent) | | | |
| $SiO_2$ | 82.9 | 79.7 | 80.5 |
| $TiO_2$ | .43 | .43 | .41 |
| $Al_2O_3$ | 6.3 | 6.5 | 5.9 |
| $Fe_2O_{3t}$ | 4.1 | 3.5 | 3.7 |
| MnO | <.01 | <.01 | <.01 |
| MgO | .19 | .2 | .19 |
| CaO | .14 | 1.66 | 1.53 |
| $Na_2O$ | .10 | .10 | .10 |
| $K_2O$ | 2.74 | 2.74 | 2.52 |
| LOI | 2.54 | 2.82 | 2.96 |
| $P_2O_5$ | .12 | .12 | .11 |
| S | 2.64 | 3.41 | 3.61 |
| (ppm) | | | |
| Ag | 1 | 1 | <1 |
| Ba | 1200 | 1200 | 1200 |
| Be | 1.0 | .9 | .8 |
| Co | 44 | 39 | 42 |
| Cr | 250 | 24 | 20 |
| Cu | 79 | 77 | 74 |
| Ni | 20 | 13 | 21 |
| Pb | 280 | 280 | 250 |
| Ra | n.d. | n.d. | n.d. |
| Rb | 110 | 100 | 91 |
| Sr | 23 | 28 | 31 |
| V | 13 | 11 | 10 |
| Zn | 8 | 12 | 11 |
| Zr | 130 | 110 | 120 |
| La | 520 | 510 | 490 |
| Ce | 960 | 940 | 890 |
| Nd | 340 | 340 | 320 |
| Sm | 57 | 58 | 55 |
| Eu | 3.3 | 3.3 | 3.0 |
| Gd | 35 | 35 | 34 |
| Dy | 18 | 20 | 20 |
| Yb | 3.1 | 4.6 | 5.7 |
| Y | 60 | 78 | 80 |
| U(icp) | 660 | 52 | 52 |
| Th(icp) | 530 | 550 | 540 |
| U(rad) | 643 | 582 | 464 |
| Th(rad) | 511 | 539 | 442 |

Note: n.d.-not detected. Detection limit of Ra 0.2 ppm, Nb <30 ppm.

**Table 3.** Denison Mine Tailings

| | Mean | Min. | Max. | Std. Dev. | Std. Error |
|---|---|---|---|---|---|
| (Percent) | | | | | |
| $SiO_2$ | 82.3 | 73.9 | 85.5 | 2.95 | .82 |
| $TiO_2$ | .02 | .33 | .41 | .02 | .01 |
| $Al_2O_3$ | 4.11 | 3.83 | 4.2 | .11 | .03 |
| $Fe_2O_{3t}$ | 5.51 | 3.5 | 10.8 | 1.84 | .51 |
| MnO | <.01 | | | | |
| MgO | .09 | <1 | .12 | .05 | .01 |
| CaO | .31 | .2 | .4 | .06 | .02 |
| $Na_2O$ | <0.1 | <0.1 | 0.1 | | |
| $K_2O$ | 1.42 | 1.27 | 1.48 | .05 | .02 |
| LOI | 4.86 | 4.00 | 7.4 | .92 | .26 |
| $P_2O_5$ | .08 | .06 | .12 | .02 | 0 |
| S | 4.36 | 2.96 | 8.6 | 1.43 | .4 |
| (ppm) | | | | | |
| Ag | <1 | <1 | 1 | | |
| Ba | 209 | 190 | 260 | 18.47 | 5.12 |
| Be | .64 | .6 | .7 | .05 | .01 |
| Co | 45.3 | 30 | 92 | 16 | 4.44 |
| Cr | 21.2 | 11 | 32 | 4.97 | 1.38 |
| Cu | 58.5 | 47 | 75 | 8.19 | 2.72 |
| Nb | 34.7 | 31 | 40 | 3.02 | .96 |
| Ni | 28.7 | 20 | 58 | 10.09 | 2.8 |
| Pb | 197 | 170 | 310 | 38.6 | 10.71 |
| Ra | n.d. | | | | |
| Rb | 52.7 | 47 | 57 | 3.4 | 1.08 |
| Sr | 8.77 | 6 | 13 | 2.49 | ,69 |
| V | 4.15 | 2 | 5 | 1.07 | .3 |
| Zn | 4.85 | 0 | 12 | 4.76 | 1.32 |
| Zr | 252 | 190 | 350 | 42.2 | 11.7 |
| La | 42.8 | 330 | 490 | 11.9 | 11.9 |
| Ce | 81.4 | 600 | 910 | 22.6 | 22.6 |
| Nd | 242 | 210 | 320 | 28.9 | 8 |
| Sm | 35.9 | 31 | 48 | 4.5 | 1.25 |
| Eu | 1.54 | 1.3 | 2 | .17 | .05 |
| Gd | 17.3 | 15 | 23 | 2.1 | .57 |
| Dy | 5.8 | 5 | 7.8 | .8 | .23 |
| Yb | 1.5 | 1.1 | 1.9 | .27 | .08 |
| Y | 20.2 | 17 | 26 | 3.3 | .93 |
| U(icp) | 40.7 | 15 | 63 | 14.9 | 6.18 |
| Th(icp) | 97.3 | 62 | 170 | 30.9 | 8.6 |
| U(rad) | 351 | 319 | 385 | 22.3 | 6.18 |
| Th(rad) | 135 | 107 | 180 | 22.9 | 6.35 |

Note: n.d.- not detected, Detection limit of Ra 0.2 ppm.

**Table 4.** Rio Algom Mines Tailings

| | Mean | Min. | Max. | Std. Dev. | Std. Error |
|---|---|---|---|---|---|
| (Percent) | | | | | |
| $SiO_2$ | 82.1 | 74.6 | 89.8 | 3.86 | 1.11 |
| $TiO_2$ | .39 | .31 | .49 | .06 | .02 |
| $Al_2O_3$ | 5.78 | 4.9 | 7.3 | .86 | .25 |
| $Fe_2O_{3t}$ | 2.78 | .5 | 6.2 | 1.7 | .49 |
| MnO | <.01 | | | | |
| MgO | .17 | .14 | .26 | .04 | .01 |
| CaO | 1. | <0.1 | 2.73 | .84 | .24 |
| Na2O | <0.1 | <1 | 0.2 | | |
| $K_2O$ | 2.42 | 1.93 | 2.95 | .32 | .09 |
| LOI | 3.17 | 1.20 | 5.20 | 1.15 | .33 |
| $P_2O_5$ | .1 | .07 | .15 | .02 | .01 |
| S | 2.4 | .26 | 4.79 | 1.42 | .41 |
| (ppm) | | | | | |
| Ag | <1 | <1 | 1. | | |
| Ba | 855 | 360 | 1300 | 269.7 | 77.9 |
| Be | .8 | .7 | 1.1 | .15 | .04 |
| Co | 28.7 | 1 | 69 | 22.9 | 6.6 |
| Cr | 19.1 | 14 | 23 | 2.23 | .6 |
| Cu | 53.4 | 28 | 85 | 19.79 | 5.7 |
| Nb | <30 | <30 | 39 | 15.02 | 4.34 |
| Ni | 15.6 | 1 | 29 | 10.4 | 3 |
| Pb | 290.8 | 200 | 470 | 81.3 | 23.5 |
| Ra | n.d. | | | | |
| Rb | 89.5 | 71 | 110 | 14.4 | 4.2 |
| Sr | 23.7 | 14 | 36 | 6.3 | 1.8 |
| V | 9.6 | 6 | 14 | 2.68 | .8 |
| Zn | 3.3 | 0 | 15 | 4.74 | 1.4 |
| Zr | 143.5 | 94 | 210 | 37.45 | 10.8 |
| La | 457.5 | 360 | 610 | 82.7 | 23.9 |
| Ce | 820.8 | 640 | 1100 | 153.5 | 44.3 |
| Nd | 287.5 | 210 | 380 | 54.3 | 15.7 |
| Sm | 42.7 | 28 | 66 | 12 | 3.5 |
| Eu | 2.2 | 1.2 | 3.7 | .7 | .2 |
| Gd | 22.3 | 13 | 42 | 8.7 | 2.5 |
| Dy | 9.4 | 3.6 | 27 | 7 | 2 |
| Yb | 2.3 | .4 | 7.9 | 2.3 | .7 |
| Y | 34.9 | 10 | 110 | 31 | 8.9 |
| U(icp) | 47.6 | 11 | 84 | 31.3 | 54.5 |
| Th(icp) | 267 | 60 | 880 | 251.5 | 40.2 |
| U(rad) | 541 | 311 | 1013 | 188.9 | 54.5 |
| Th(rad) | 291 | 123 | 635 | 139.1 | 40.2 |

Note: n.d. - not detected, Detection limit of Ra 0.02 ppm.

direction. From the Quirke Mine main tailings 12 samples were collected along 4 lines over a distance of 2800 m in an east-west direction. The results are given in Tables 3 and 4. Comparison of the analyses of the mill samples with those of the tailings provides a measure of the metals recovery and the contents of metals left over.

All analyses were done by Analytical Chemistry Section, Mineral Resources Division, Geological Survey of Canada. In addition U and Th, which were also analyzed spectrometrically in the laboratory of the Exploration Geophysics Subdivision, Geological Survey of Canada, and shown in the tables with (rad) suffix. Major oxides were analyzed by X-ray fluorescence, Pb and Ag were done by atomic absorption, trace elements were done by Induced Coupled Plasma Emission Spectroscopy (ICP-ES). Rare-earth elements, uranium, thorium and radium determined by ICP-Mass Spectroscopy (ICP-MS) method. Uranium and thorium analyzed by ICP method are shown with a suffix (icp). Sulphur was analyzed by rapid chemical methods. Total Fe is given as $Fe_2O_{3t}$.

## DISCUSSION

### *Yttrium and heavy REE*

A Quirke mill-head composite sample from 28th March to 11th July, 1990 contained 60 ppm Y. Two mill-tail samples were collected from 28th February to 4th July, 1990 and from

9th to 14th July, 1990. These mill-tail samples have 78 and 80 ppm Y. The higher Y content in tails as compared to the mill-head is probably due to the inherent higher concentration of Y in the ore that was mined at different periods. This variation is also apparent in the 12 mill-head samples of Denison Mines for the year 1978, which had Y values as follows (Ruzicka, 1988):

mean 104 ppm, std. dev. 22.47, range 45 to 130 ppm.

However, Y contents in the Quirke mill-tails (mean-79 ppm, Table 2) as well as in the tailings (mean-34.9 ppm, range-10 to 110 ppm, Table 4), are significantly higher than the 23 ppm Y in the Denison's leached residue (Table 1). Also the mean Y concentration of Rio Algom Mines' Quirke tailings (Table 4) is 34.9 ppm Y, as compared to the Denison Mines tailings, which is 20.2 ppm (Table 3). Similarly, higher contents of other heavy rare-earths – Gd, Dy, and Yb – in Rio Algom Mines tailings are noted as compared to the concentration of these elements in Denison Mines tailings (Tables 3 and 4). These differences in the Y and heavy REE would be expected because, as mentioned earlier, Denison Mines have extracted Y from their ore along with other rare-earth elements.

### *Light REE*

Elliot Lake ores are distinct with respect to the anomalously high content of Y in uraninite, reported as 1.5 to 4.5% by Theis (1979), and as 2.25 to 2.32% by Roscoe (1969, p. 134). Theis (1979, p. 33) reported that $Y_2O_3$ constitutes 40.6% of the total rare-earths in rare-earth concentrates of the Denison mill, whereas Ce and La oxides constitute only 3.7% and 1.3% respectively. He concluded that Y is extracted from the uraninite in the leaching process; whereas Ce, La, and other light REE are not extracted, because they reside in monazite, which is not attacked by the acid. Our data (Table 1) also show that the reduction of light REE - La by 17%, Ce by 19%, Nd by 23%, and Sm by 30% - by the leaching of the Denison mill-heads is significantly less than the removal of heavy REE - Gd by 49%, Dy by 70%, Yb by 75%, and Y by 74%. The Rio Algom mill samples show no significant removal of any rare-earth elements, and almost 100% of these are disposed in the tailings.

### *Uranium and thorium*

Uranium and thorium were analyzed by gamma-ray spectrometer, and also by ICP-MS. The two methods measure U and Th concentrations employing different principles. Gamma-ray spectrometry measures gamma-rays from Bismuth-214 and Thallium-208, the daughter nuclei produced by the radioactive decay of U and Th respectively, (Grasty et al., 1982); whereas ICP-MS method analyzes these elements on the basis of the atomic numbers and hence provides the elemental concentrations. The radiometric indications of U contents of the tailings are markedly higher than the U contents measured by ICP: 541 ppm (radiometric) versus 47.6 ppm (ICP) for Rio Algom Mines (Table 4); 351 ppm (radiometric) versus 40.7 ppm (ICP), for Denison Mines (Table 3). The differences in U contents as determined by spectrometric and ICP techniques are caused by the removal of U in the milling process, but most of the daughter radio-nuclei are not extracted and end up in the tailings, thus indicating higher values of U radiometrically. Similar, but much smaller discrepancies are found for Th that are also due to the accumulations of disequilibrium assemblages of daughter elements in the tailings. The analysis of mill-head and mill-tail samples for the two mines also illustrate this difference (Tables 1, 2).

There is a decrease in the Th content in case of Denison Mines, from mill-head content of 540 to 270 ppm after U is recovered. Presumably the ion exchange process employed to precipitate U and Y also removes part of Th from the solution in the form of very fine-grained solids in the slurry, which was not sampled. Therefore, a decrease in the Th content from mill-head to the leached residue from the Denison mill was observed (Table 1). However, it is interesting to note that there is no decrease in Th content of the mill-head and tails from the Quirke mill. Apparently more Th from Rio Algom mill goes to the tailings than in the case of Denison (Th(icp) 267 versus 97.3 ppm respectively).

The increase in CaO in the mill tails versus mill-heads is due to the addition of lime in the milling process to neutralize the excess sulphuric acid used for leaching the ore. The $CaSO_4$ residue goes to the tailings, which also accounts for the increase in S contents from mill-heads to tails. The concentration of other metals in the tailings corresponds to the initial trace amounts present in the ore or mill-heads as can be seen in the tables. Their concentration is too low to be of any importance.

## CONCLUSIONS

Our preliminary data on tailings suggest that the Rio Algom tailings contain elevated amounts of yttrium and heavy rare-earth elements. Denison Mines extracted yttrium, albeit intermittently, therefore it is possible that certain portions of their tailings that were produced when the yttrium circuit was not operative, may also contain elevated amounts of those elements. The tailings also contain significant amounts of thorium. Existing infra-structure, favourable location, the pulverized form amenable to dredging and proven chemical processing, may eventually allow classification of the tailings as resources for these commodities. Concentration of other metals is too low to be of any importance. However, in order to assess the economic potential of the Elliot Lake tailings, a comprehensive evaluation would be needed.

Comparison of the U and Th contents of the mill-heads and the mill-tails (Tables 1 and 2) shows that greater than 92% of U is removed (ICP values) by the milling processes, but about 60-90% of initial radioactivity due to U and 30 to 70% due to Th (radiometric values) end up in the tailings. Differences in the milling processes by the two mines probably account for more Th being extracted in the Denison mill than by the Quirke mill.

## ACKNOWLEDGMENTS

We are grateful to Denison Mines Ltd. and Rio Algom Mines Ltd. for providing their mill samples and permission to publish this data. Special thanks are due to David Armstrong of Rio Algom Mines Ltd. and Al MacEachern, Robert Webber, and Peter Townsend of Denison Mines Ltd. R.L. Grasty of Geological Survey of Canada kindly provided help and guidance in using the gamma-ray spectrometer laboratory. S.S. Gandhi and S.M. Roscoe reviewed the manuscript.

## REFERENCES

**Denison Mines Ltd.**
1979: Denison Mines Limited, Annual Report 1979.

**Financial Post**
1979: Financial Post Corporation Survey of Mines, Denison Mines Ltd. 11 May 1979.

**Grasty, R.L., Bristow, Q., Cameron, G.W., Dyck, W., Grant, J.A., and Killeen, P.G.**
1982: Calibration of a laboratory gamma-ray spectrometer for the measurement of potassium, uranium and thorium; in Proceedings of the Symposium on Uranium Exploration Methods, Paris, 1st-4th June 1982, Nuclear Agency, O.E.C.D. in collaboration with I.A.E.A.

**I.A.E.A.**
1980: Significance of mineralogy in the development of flowsheets for processing urnium ores; International Atomic Energy Agency, Technical Report Series no. 196, 265 p.

**O.E.C.D. and I.A.E.A.**
1983: Uranium Extraction Technology; A joint report by Organization for Economic Co-operation and Development (O.E.C.D.) and International Atomic Energy Agency (I.A.E.A.), 270 p.

**Ontario Division of Mines**
1975: Source Mineral Deposits Record, S.M.D.R. 000107; Ontario Division of Mines, (unpublished).

**Roscoe, S.M.**
1969: Huronian rocks and uraniferous conglomerates in the Canadian Shield; Geological Survey of Canada, Paper 68-40, 205 p.

**Ruzicka, V.**
1988: Geology and genesis of uranium deposits in the early Proterozoic: Blind River - Elliot Lake basin, Ontario, Canada; in Recognition of Uranium Provinces, Proceedings of the Technical Committee on recognition of uranium provinces; organized by I.A.E.A., London, 18-20th Sept. 1985, I.A.E.A. publication no. TC-450.5/5, p. 107-130.

**Theis, N.J.**
1979: Uranium-bearing and associated minerals in their geochemical and sedimentological context, Elliot Lake, Ontario; Geological Survey of Canada, Bulletin 304, 50 p.

Geological Survey of Canada Project 750010

# Preliminary report on the geology and structural evolution of the Komaktorvik Zone of the Early Proterozoic Torngat Orogen, Eclipse Harbour area, northern Labrador[1]

**Martin J. Van Kranendonk and David J. Scott[2]**
**Continental Geoscience Division**

*Van Kranendonk, M.J. and Scott, D.J., 1992: Preliminary report on the geology and structural evolution of the Komaktorvik Zone of the Early Proterozoic Torngat Orogen, Eclipse Harbour area, northern Labrador; in Current Research, Part C; Geological Survey of Canada, Paper 92-1C, p. 59-68.*

***Abstract***

*The Early Proterozoic Komaktorvik Zone of the Torngat Orogen is a north-south belt of deformed, amphibolite to granulite facies gneisses including two principal groups of rocks: 1) variably re-worked, Archean Nain Province gneisses and crosscutting, Early Proterozoic mafic dykes; intruded by 2) deformed, Early Proterozoic meta-igneous rocks that range in composition from oldest mafic diorite, through tonalite, to youngest granite and granitic pegmatite. Group 2 rocks may represent remnants of a more extensive continental arc to the west. The structural evolution of the Komaktorvik Zone involved oblique sinistral, east-side-up shearing with late folding of straightened to mylonitic fabrics. Intrusion of Group 2 magmas may have, in part, accompanied and facilitated deformation.*

***Résumé***

*La zone de Komaktorvik datant du Protérozoïque précoce et faisant partie de l'orogène de Torngat, est une zone à orientation nord-sud de gneiss déformés se situant entre le faciès des amphibolites et le faciès des granulites, et comprenant deux grands groupes de roches: 1) des gneiss archéens de la province de Nain diversement remaniés, et des dykes mafiques transversaux datés du Protérozoïque précoce; que pénètrent 2) des roches méta-ignées déformées, datées du Protérozoïque précoce, dont la composition couvre la gamme suivante: diorite mafique la plus ancienne, tonalite, puis granite et pegmatite granitique les plus récents. Les roches du groupe 2 représentent peut-être les restes d'un arc continental plus vaste à l'ouest. L'évolution structurale de la zone de Komaktorvik a inclus un cisaillement sénestre oblique, à compartiment supérieur du côté est, suivi du plissement tardif de fabriques redressées ou mylonitiques. Il est possible que l'intrusion des magmas du groupe 2 ait partiellement accompagné et facilité la déformation.*

[1] Contribution to the Canada-Newfoundland Cooperation Agreement on Mineral Development, 1990-94.
[2] GEOTOP, Université du Québec à Montréal, Case Postale 8888, Succursale A, Montréal, Québec, H3C 3P8.

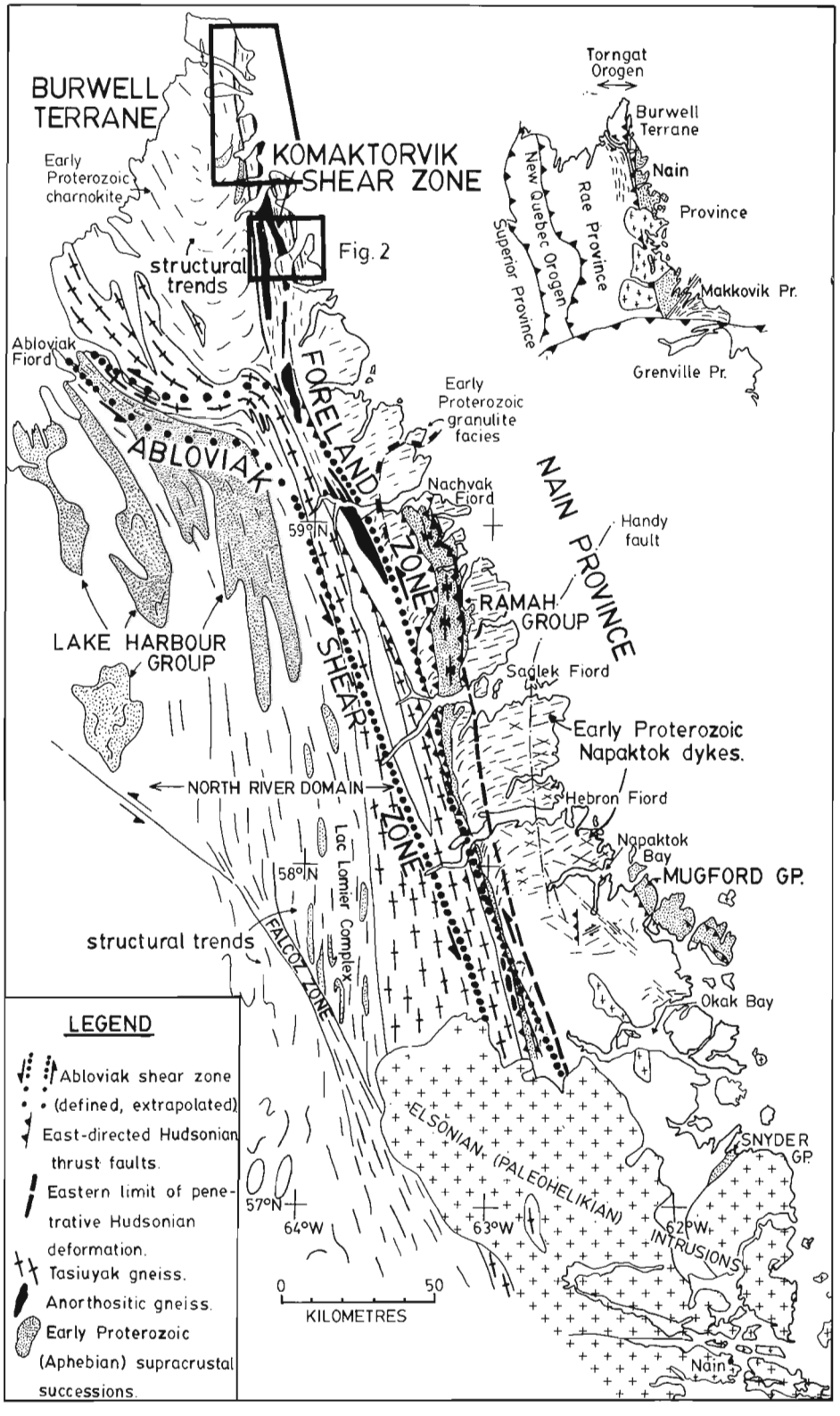


**Figure 1.** Generalized geological map of the Torngat Orogen in northern Labrador and northeastern Quebec. Map area discussed in this report outlined by small box labelled Fig. 2. Area covered by Wardle et al. (in prep.) outlined by larger box.

## INTRODUCTION

Geological mapping of the Eclipse Harbour area, northern Labrador (Fig. 1) was conducted at a scale of 1:50 000 during a 15-day period. Detailed study of this region compliments regional coverage of the Labrador coast immediately to the north, mapped during the balance of the summer together with R.J. Wardle (Newfoundland Department of Mines and Energy) and F. Mengel (U. of Copenhagen), as reported in Wardle et al. (in press) (see Fig. 1).

The map area is located within the Komaktorvik Zone of the Early Proterozoic Torngat Orogen (Korstgård et al., 1987; Bertrand et al., 1990), itself a part of the continental-scale Trans-Hudson Orogen. The Komaktorvik Zone is a north-south striking belt of deformed rocks with strong aeromagnetic grain (Korstgård et al., 1987) that splays from the 340°-striking Abloviak shear zone of the Torngat Orogen to the south (Fig. 1). The nature and kinematic history of the Komaktorvik Zone and its relationship with the Abloviak shear zone were unknown prior to this field season. In this report, we describe the rock types and kinematic history of the Komaktorvik Zone in the Eclipse Harbour area. A detailed evaluation of the relationship between the Komaktorvik Zone and the Abloviak shear zone will form the focus of subsequent reports following mapping in 1992 and 1993 to be conducted as a joint undertaking between the Geological Survey of Canada and the Newfoundland Department of Mines and Energy, under a Mineral Development Agreement.

## ROCK UNITS

Two principal groups of amphibolite to granulite facies rocks were identified in the region. Group 1) is composed of leucocratic tonalitic orthogneiss and migmatite, inclusions of supracrustal rocks of dominantly mafic and metapelitic compositions, metaanorthositic gneiss and remnants of layered mafic complexes, and local granitic gneiss. All these rocks were deformed and cut by a swarm of plagioclase-phyric mafic dykes. Group 2) is a suite of meta-igneous rocks that include foliated mafic diorite to amphibolite, foliated and gneissic, grey tonalite to granodiorite, grey to pink, foliated and gneissic, granodiorite to granite, and migmatitic gneiss composed predominantly of the latter two rock units with inclusions of Group 1 rocks (see legend of Fig. 2).

Groups 1 and 2 are interpreted as Archean and Early Proterozoic in age, respectively, based on the following observations. Group 1 rocks contain abundant leucosome veins and are characterized by several generations of folds and fabrics which indicate a polycyclic history. Mafic dykes cut these fabrics, and are themselves deformed by Early Proterozoic deformation in the Komaktorvik Zone. The mafic dykes are identical to the ca. 2400 Ma (e.g. Taylor, 1974) Napaktok dyke swarm found throughout the Archean gneisses of the Nain Province further to the south (e.g. Ermanovics et al., 1989: Fig. 1). This similarity and the polycyclic nature of Group 1 rocks is used to infer that this lithologic assemblage represents the northern extension of the Nain Province.

Group 2 rocks have a much less complex structural history than the polycyclic rocks of Group 1. The mafic dykes of Group 1 have not been observed cutting Group 2 rocks, whereas in several localities Group 2 rocks were observed to cut dykes and all other rocks of Group 1 (see Fig. 2 and 3e). Based on the Early Proterozoic age of the dykes, the rocks of Group 2 are interpreted as Early Proterozoic, or younger, in age. The voluminous, Early Proterozoic magmatism represented by Group 2 in the map area and along strike to the north (see Wardle et al., in press), does not occur further south in the Torngat Orogen (e.g. Bertrand et al., 1990) and therefore represents a unique feature of the Komaktorvik Zone.

### *Group 1: Archean Nain gneisses and Early Proterozoic mafic dykes*

#### Archean Nain gneisses

The Archean rocks of Group 1 are predominantly composed of leucocratic tonalitic orthogneiss and migmatite, and comprise ≤80% of the area underlain by Group 1 rocks. These gneisses contain abundant leucosome veins and thin (30 cm to 2 m) layers and inclusions of mafic gneiss and rusty, biotite-rich paragneiss. Some mafic layers, ≤50 cm wide, which are slightly discordant to migmatitic layering in the orthogneisses, contain ≤10%, centimetre-scale plagioclase phenocrysts and are cut by the Early Proterozoic mafic dykes (Fig. 3a). These porphyritic mafic layers closely resemble the Early Archean Saglek dykes described in the Saglek-Hebron area of the Nain Province (Collerson and Bridgwater, 1979).

Larger, more coherent units of interpreted supracrustal rocks (500 m wide by up to 3 km long) include compositionally-layered mafic gneiss (garnet-hornblende-plagioclase-clinopyroxene ± orthopyroxene), ultramafic gneiss (2 pyroxene-hornblende) and garnet-biotite ± sillimanite ± cordierite paragneiss. Locally, layered mafic gneisses grade into leucogabbro and anorthositic gneiss. At Murray Head (Fig. 2), a particularly large, continuous exposure of relatively undeformed, layered mafic and ultramafic rocks is preserved. It consists of predominantly coarse grained mafic gabbro on coastal exposures, and grades landward into leucogabbro and anorthosite. Relict igneous features include metre-scale compositional layering, crossbedding, cognate xenoliths of earlier, more mafic phases in some leucocratic phases, and in one 2 m thick, leucocratic layer, ≤5 cm long biotite aggregates that cut across the igneous layering at 90° (Fig. 3b). The exposure at Murray Head is thought to represent a fragment of a once larger, layered igneous body. Many of the smaller (tens to hundreds of metres) inclusions of layered mafic gneiss found throughout the tonalitic orthogneisses were probably derived from parental bodies such as that at Murray Head.

Two wide units of anorthositic gneiss are found in the western part of the map area (Fig. 2). These layers, up to 3 km wide, are composed predominantly of recrystallized,

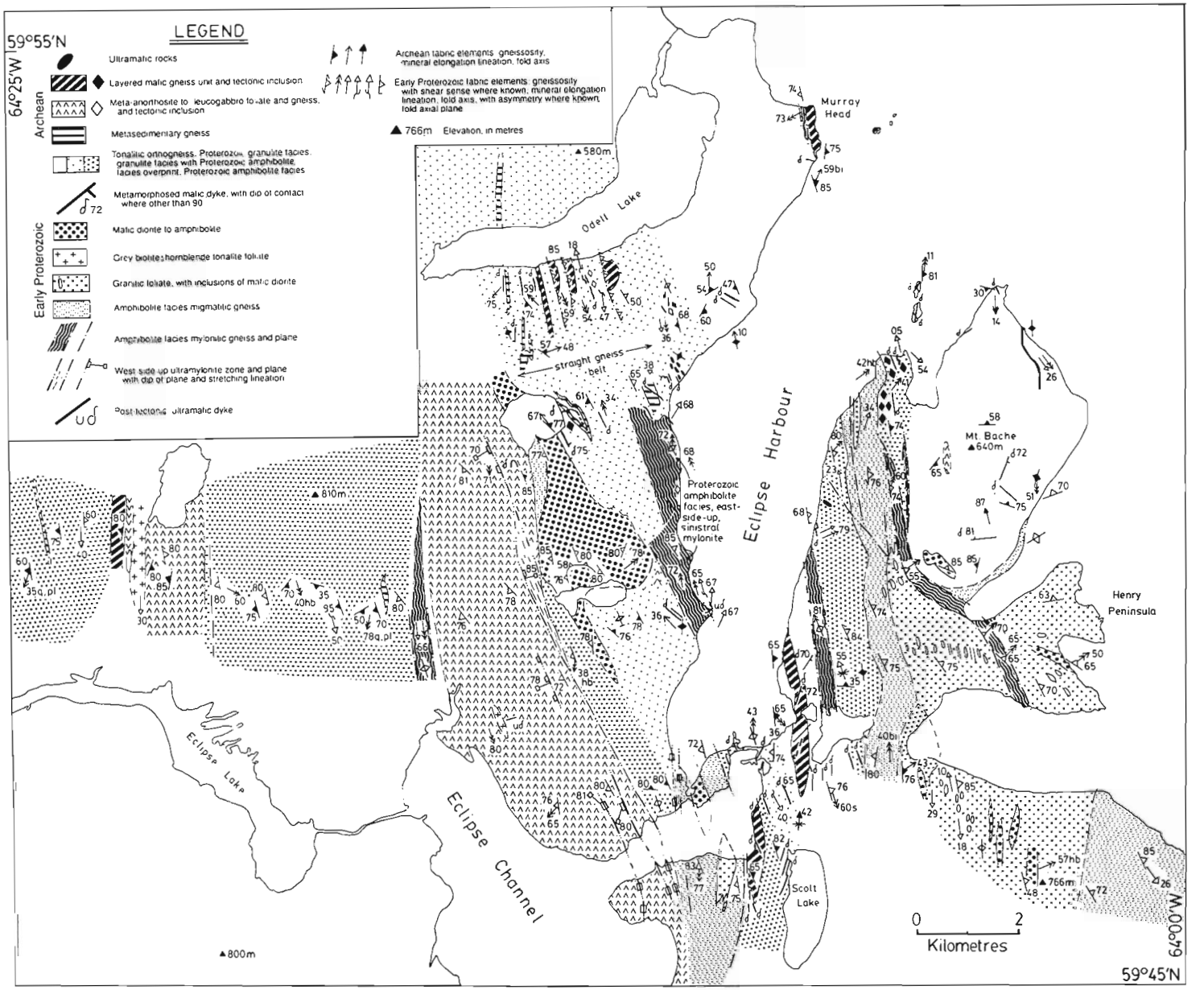


**Figure 2.** Geological map of the Eclipse Harbour area, northern Labrador. Archean gneisses and Early Proterozoic metamorphosed mafic dykes are referred to in the text as Group 1 and represent the reworked equivalents of the Nain Province. Those rocks labelled Early Proterozoic comprise the rocks of Group 2, that were emplaced within the Nain crust and are unique to the Komaktorvik Zone of the Torngat Orogen.

medium- to coarse-grained gabbroic anorthosite and leucogabbro that locally show irregular, 10 cm to 10 m scale layering (Fig. 3c) and extremely coarse grain size, with individual hypersthene crystals up to 60 cm in diameter. The anorthositic rocks are intruded by coarse grained, white granitoid veins and by plagioclase-phyric mafic dykes, which are taken to indicate an Archean age for the anorthositic rocks (see also Wardle, 1983, and Wilton and Wardle, 1990). The contacts between anorthositic gneiss and tonalitic orthogneisses are tectonic, and therefore preclude a relative chronology of these units. The anorthositic rocks are also intruded by thin sheets of foliated mafic diorite and hornblende tonalite interpreted as belonging to Group 2.

The anorthositic sheets in the map area represent the limbs of a large-scale, south-plunging fold (Fig. 1; Wardle et al., in press) and form part of a continuous series of exposures that stretches from just off the northernmost tip of Labrador, southward into the map area (Wardle et al., in prep.), and for several tens of kilometres further south (e.g. Taylor, 1979) (see Fig. 1).

Tonalitic orthogneisses and meta-anorthositic rocks are intruded by veins of coarse grained, leucocratic tonalite that locally form an interconnected network. These veins form an integral part of the tonalitic orthogneisses and are of unknown age except that they predate intrusion of the mafic dykes.

All rock units of Group 1, including the supracrustal rocks, are cut by white, biotite-allanite pegmatite sheets. These folded and foliated sheets, up to 3 m wide, are cut by the Early Proterozoic mafic dykes, and are therefore interpreted as Late Archean in age.

In the prominent bend on the west shore of Eclipse Harbour (Fig. 2), amphibolite-facies Archean gneisses are strongly deformed and contain numerous tectonic inclusions

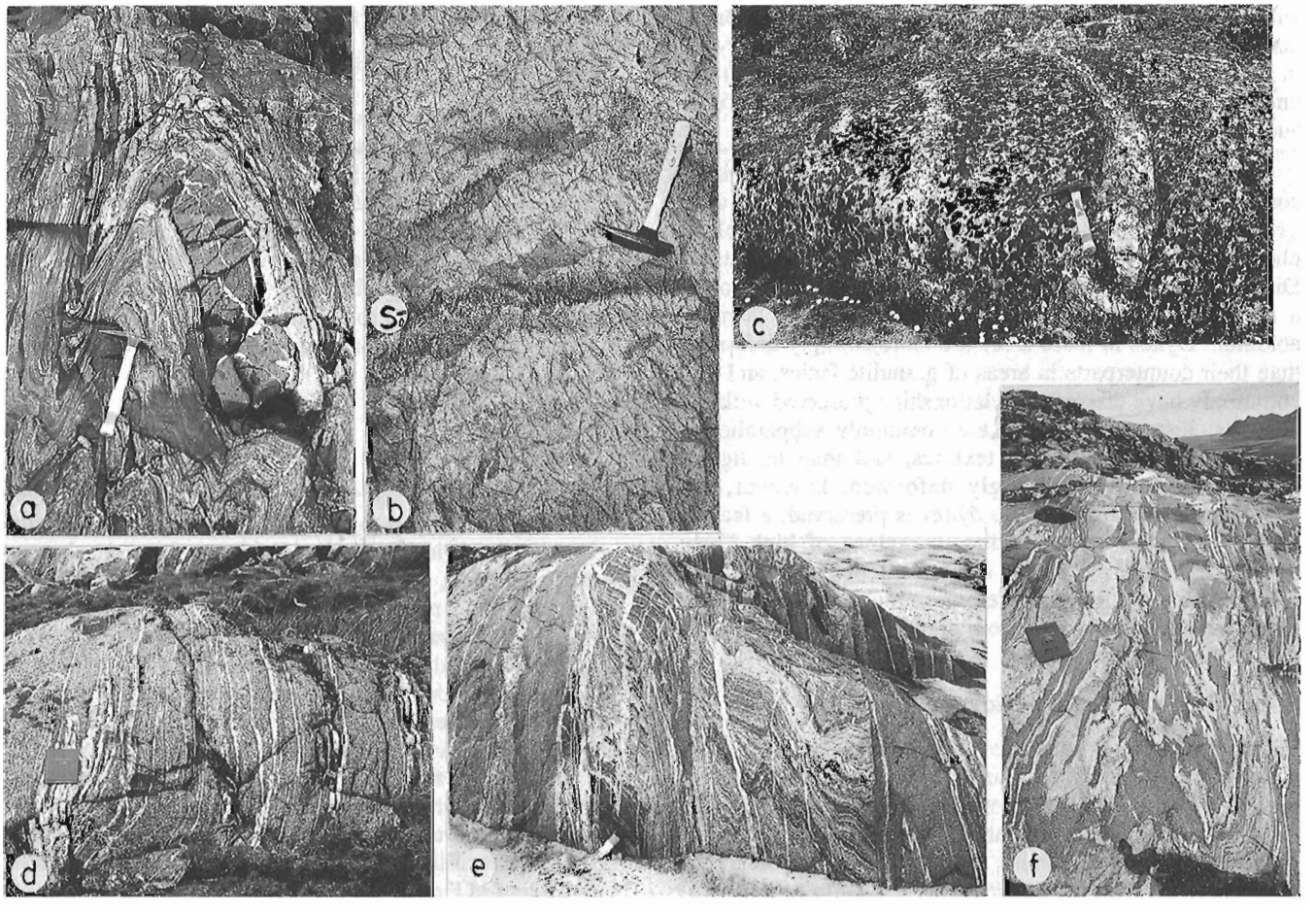


**Figure 3. a)** Folded and disrupted plagioclase-phyric amphibolite layer in Archean tonalitic orthogneiss, interpreted to represent a Saglek dyke: from the west shore of Eclipse Harbour. (GSC1991-573A) **b)** Leucocratic layer of the Murray Head layered igneous complex, showing relict igneous texture of finger-sized biotite aggregates perpendicular to primary layering ($S_0$). (GSC1991-573B) **c)** Coarse grained, layered leucogabbro: from the point on the east side of Eclipse Channel. (GSC1991-573C) **d)** Interlayered mafic diorite and granite veins of Group 2: from the island between Eclipse Channel and Eclipse Harbour. (GSC1991-573E) **e)** Grey, foliated tonalite sheets (dark) and granitic veins (light) of Group 2 intrusive into Archean Nain gneisses: from just west of Scolt Lake. (GSC1991-573H) **f)** Amphibolite facies migmatite, comprising grey and pink granitoid intrusive sheets of Group 2 and inclusions of Group 1 Archean gneiss: from northwest corner of the Mt. Bache peninsula. (GSC1991-573F) Hammer in a), b), c), and e) is 40 cm long, and notebook in d) and f) is 21 cm long.

of ultramafic rock. These rocks have a strong shear fabric and are intruded by sheets of granitic gneiss and pegmatite making up to 40% of individual outcrops. The granitic sheets and high-strain fabrics are cut by a mafic dyke interpreted to be of Early Proterozoic age, that is folded and sheared by subsequent deformation. These features suggest that the granite-rich gneisses at this locality may represent a zone of strong Late Archean deformation.

### Early Proterozoic mafic dykes

The colour, texture, and degree of deformation of the Early Proterozoic mafic dykes varies across the map area. In areas of granulite-facies gneisses (e.g. at Mount Bache; on the southeastern shore of Eclipse Harbour; and between Odell Lake and Murray Head: see Fig. 2), mafic dykes are brownish-green and massive, with equant, black to pale grey plagioclase phenocrysts in a medium grained, diabasic-textured matrix. These dykes commonly contain subeuhedral garnet porphyroblasts, either randomly distributed within the dyke matrix or along fractures. Dykes in these areas have clearly discordant relationships to the gneissosity in tonalitic orthogneisses and supracrustal rocks, and generally strike east.

In areas where granulite-facies, country rock gneisses contain an amphibolite facies overprint, mafic dykes are dark green, with ≤30% white, recrystallized plagioclase phenocrysts in a hornblende-plagioclase ± garnet matrix. Diabasic texture is locally preserved in the matrix, although a recrystallized, equigranular to foliated texture is more common. Dykes in these areas are more strongly deformed than their counterparts in areas of granulite facies, and less commonly have discordant relationships preserved with the gneisses. Instead, the dykes are commonly subparallel to gneissosity, have schistose textures, and may be tightly folded. Even where strongly deformed, however, the along-strike continuity of the dykes is preserved, a feature which aids their identification in regions of high Early Proterozoic strain. It is not clear from field observations whether the amphibolite facies assemblages in these dykes are prograde, or retrograde from granulite facies.

## *Group 2: Early Proterozoic igneous rocks*

The suite of Early Proterozoic igneous rocks that cuts Group 1 Archean gneisses and Early Proterozoic mafic dykes, ranges in composition from mafic diorite/amphibolite, through mafic and felsic tonalite and granodiorite, to coarse grained granodiorite, granite, and granitic pegmatite. These rocks have a relatively simple fabric related to deformation within the Komaktorvik Zone. Granulite facies mineral assemblages have only locally been observed in these rocks, suggesting that they were emplaced at higher crustal levels than the level at which their gneissic host rocks and mafic dykes were metamorphosed. Samples of all the major rock types described below were collected for U-Pb geochronology.

### Mafic diorite/amphibolite

This map unit is characterized by medium-grained, equigranular assemblages of hornblende-plagioclase ± quartz ± clinopyroxene and a variable color index in the range of 40-70%. Where it is found as inclusions within granitic rocks south of the Henry Peninsula and on the west shore of Eclipse Harbour (Fig. 2), it is weakly deformed, with <10% leucosome veins in a homogeneous matrix. On the small island that divides Eclipse Harbour from Eclipse Channel (Fig. 2), mafic diorite is composed of multiple, thin (5-40 cm wide) intrusive phases, each with a slightly different mafic mineral content (Fig. 3d). Such layering is considered to be of igneous origin, as it is generally weakly strained, except for a weak hornblende foliation that is axial planar to mesoscopic folds. In addition to map-scale bodies, this rock unit also occurs as several metres-wide sheets throughout the older gneisses (e.g. south of Mount Bache).

### Grey tonalite-granodiorite

Swarms of grey, biotite ± hornblende, tonalite-granodiorite (T-G) sheets, 30 cm to 5 m wide, are found across the map area. These fine- to medium-grained rocks locally contain up to 20% mafic minerals, including rare garnet, which define a foliation. A rare example, on the west shore of Eclipse Harbour, has 30% hornblende. These T-G sheets cut Archean gneissosity and the Early Proterozoic mafic dykes (Fig. 3e), and also crosscut the unit of mafic diorite/amphibolite. These sheets are particularly abundant within amphibolite-facies zones of strong, Early Proterozoic deformation and along the margins of the coarse grained, granodioritic to granitic bodies into which they grade.

### Migmatitic gneiss

Where the grey, T-G sheets form larger bodies, they commonly contain up to 20%, ≤10 cm wide, pink granitic veins with gradational margins. On the northeastern shore of Eclipse Harbour, these sheets and veins form a "swirly" migmatite with roughly equal proportions of i) Archean gneisses and supracrustal rocks, ii) grey T-G sheets, and iii) discontinuous and highly contorted veins of granite (Fig. 3f). This migmatite forms a distinct belt along the western side of the granite on Henry Peninsula (Fig. 2) in a zone of strong Early Proterozoic shear deformation at amphibolite facies. This close association of rock types, metamorphic grade, and intensity of shearing suggests that the granitic rocks were emplaced synchronously with the deformation, or that their contacts were utilized as planes of weakness during shearing (see Structural Evolution).

### Granitic rocks

Medium- to coarse-grained granitic rocks are found on Henry Peninsula and 1 km west of Scolt Lake (Fig. 2). The Henry Peninsula body is principally a mixture of foliated granite, with large inclusions of mafic diorite (up to 30%)

and Nain orthogneiss. On the peninsula itself, however, weakly- foliated, coarse grained and leucocratic granite forms >60% of the outcrops.

### Pegmatite veins

Biotite-bearing granitic pegmatite veins are found throughout the map area. They are up to 5 m wide, with grain size up to 10 cm. Some larger veins contain granophyric intergrowths

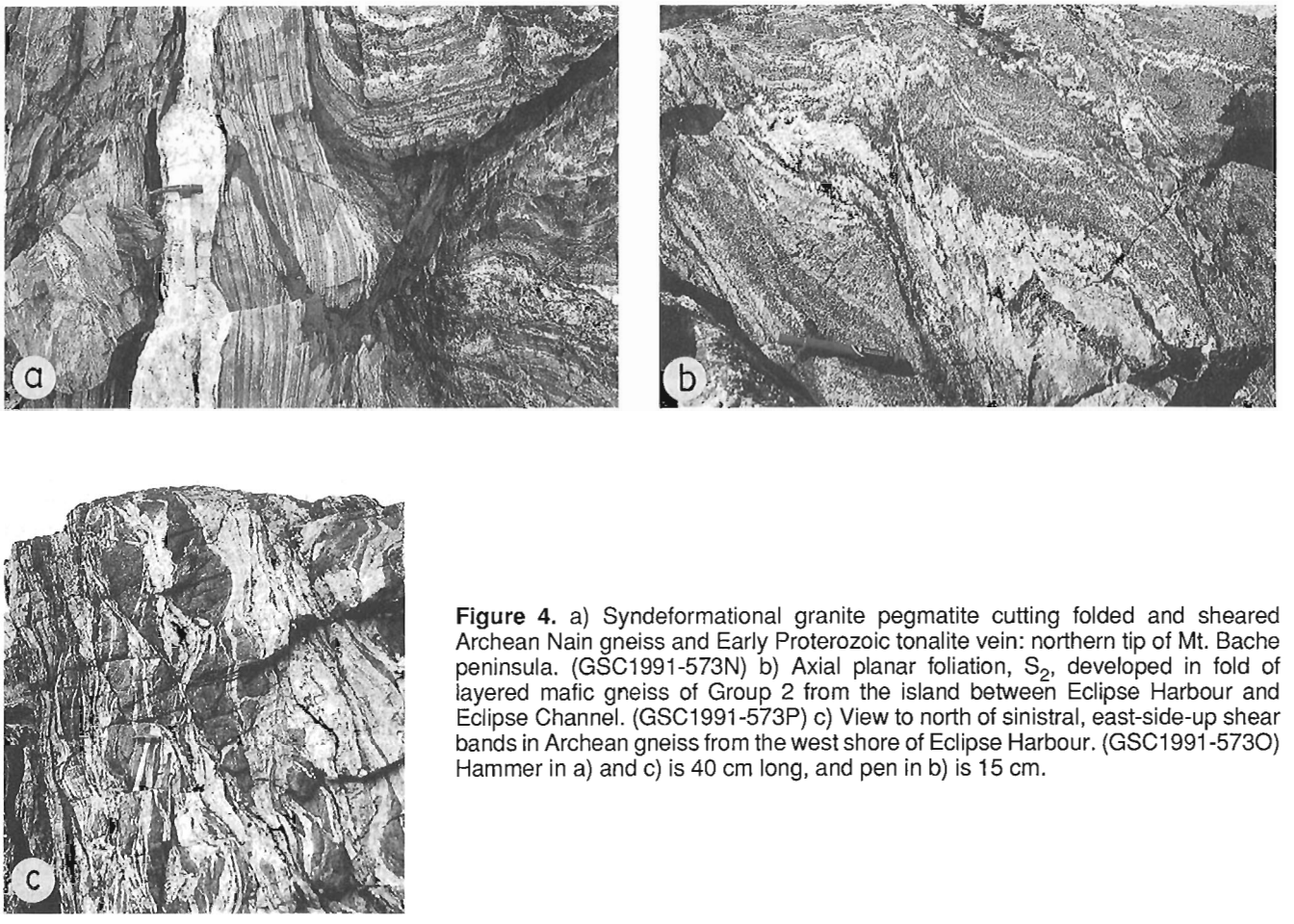


**Figure 4.** a) Syndeformational granite pegmatite cutting folded and sheared Archean Nain gneiss and Early Proterozoic tonalite vein: northern tip of Mt. Bache peninsula. (GSC1991-573N) b) Axial planar foliation, $S_2$, developed in fold of layered mafic gneiss of Group 2 from the island between Eclipse Harbour and Eclipse Channel. (GSC1991-573P) c) View to north of sinistral, east-side-up shear bands in Archean gneiss from the west shore of Eclipse Harbour. (GSC1991-573O) Hammer in a) and c) is 40 cm long, and pen in b) is 15 cm.

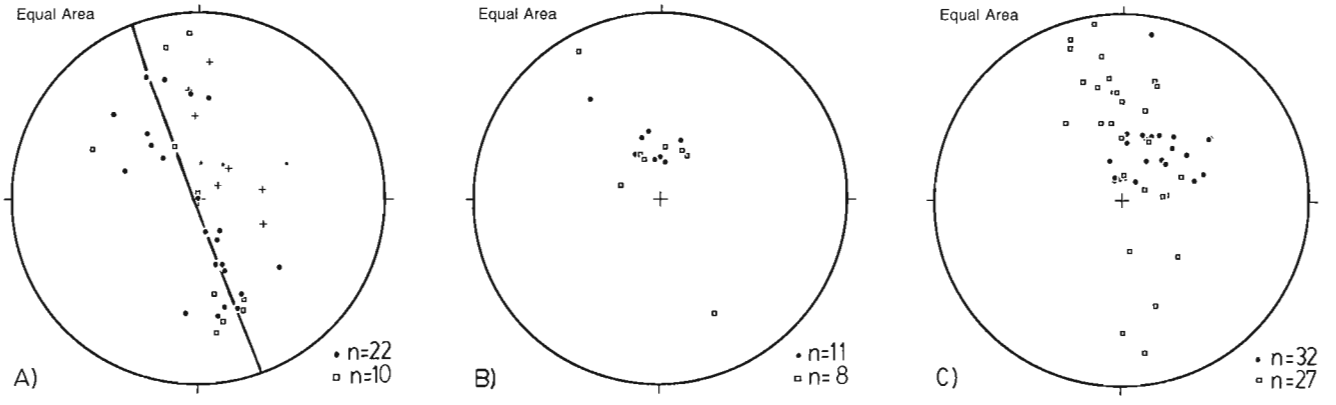


**Figure 5.** Equal area stereograms of Early Proterozoic fold axes (squares) and lineations (dots) from across the map area. a) Straight-gneiss belt located south of Odell Lake to Scolt Lake. Folds have "S" and "Z" asymmetry. + = relict Archean lineations; * = late biotite lineations in mylonitic zones. b) Amphibolite-facies mylonite zone on the west shore of Eclipse Harbour. Folds have "S" asymmetry. c) Amphibolite-facies migmatite and mylonite zone west of Mt. Bache. Folds have predominantly "Z" asymmetry.

of tourmaline-quartz and garnet-quartz as irregular patches up to 10 cm in diameter. Iron carbonate and coarse garnet are found in some veins. Undeformed, 060°-striking pegmatite veins have produced grey-blue retrogression halos where they intrude granulite-facies tonalitic gneisses. In amphibolite-facies shear zones, the pegmatite veins were emplaced along fold axial planes, have a strong foliation, and show pinch-and-swell structure (Fig. 4a). These features indicate that the pegmatite veins were synchronous with amphibolite-facies deformation in these zones.

## STRUCTURAL EVOLUTION

The Murray Head and Mount Bache blocks of granulite-facies tonalitic gneisses and east-west striking mafic dykes are interpreted as irregular-shaped, low-strain augen of relatively un-reworked Nain crust within 340°-striking belts of amphibolite- facies, Early Proterozoic shear deformation. The western margin of the Murray Head granulite block grades into a 3 km-wide belt of straightened gneisses in which relict granulite-facies mineralogy (Archean or Proterozoic?) is strongly overprinted by Proterozoic amphibolite facies. This belt, which extends southwards to Scolt Lake (Fig. 2), is characterized by penetrative development of protomylonitic textures which disrupt the pre-existing Archean gneissosity ($S_1$) and give the rocks a discontinuous, "shredded" appearance. Mafic dykes within this belt are subparallel to the gneissosity, and are locally tightly folded together with the gneisses. The dykes contain only amphibolite facies (garnet-hornblende) mineral assemblages and it is unclear whether these are prograde or retrograde.

Fold axes in the straight-gneiss belt plot on a stereonet about a north-northwest-trending great circle (Fig. 5a) and have both "S" and "Z" asymmetry. An axial planar foliation ($S_2$) in fold noses (Fig. 4b) strikes 340°, parallel to an $S_2$ schistosity in areas where Archean gneissosity is at an angle to the Proterozoic structural trend. The straight-gneiss belt is characterized by moderately south-southeast-plunging elongation lineations of Proterozoic amphibolite-facies minerals (Fig. 5a). Abundant sinistral shear bands are developed on fold limbs and in straightened gneisses, that indicate oblique sinistral, east-side-up displacement (Fig. 4c). Another set of north-northwest-plunging mineral lineations in this belt (Fig. 5a) are generally of biotite and quartz and are interpreted to reflect a later period of extension (see below). Relict Archean stretching lineations were locally observed (Fig. 2 and 5a).

Adjacent to the straight-gneiss belt along the west coast of Eclipse Harbour is a zone of amphibolite-facies mylonite in which Archean gneissosity and mafic dykes are transposed into the 340° trend of the Early Proterozoic deformation. Sheets of Group 2 grey tonalite are common in this zone, as are sheets of synkinematic granitic pegmatite. Mylonitic fabrics are characterized by steeply north-plunging stretching lineations that are parallel to tight folds of the mylonitic layering (Fig. 5b). The folds have a consistent "S" asymmetry. Shear band asymmetry and the rotation sense of feldspar porphyroclasts indicate east-side-up displacement in this zone (e.g. Fig. 4c).

The occurrence of folded mylonitic fabrics and thorough retrogression to amphibolite facies in this narrow zone of relatively strong deformation, suggests that it was superimposed on the more broadly distributed fabrics (characterized by south-southeast-plunging linear fabrics at granulite to amphibolite facies) within the straight-gneiss belt. North-northwest-plunging biotite and quartz elongation lineations in the straight-gneiss belt are parallel to the fold axes and lineations in the mylonite zone, and are therefore interpreted to be a reflection of this later deformation. A larger volume of Proterozoic igneous rocks within the mylonite belt suggests that its formation was aided by the synchronous emplacement of magmas or that magmatism concentrated the deformation.

The Mount Bache and Murray Head granulite-facies blocks are separated by a zone of deformed, migmatitic rocks at amphibolite facies, which outcrop along the northeastern shore of Eclipse Harbour (Fig. 2). The migmatitic rocks are a mixture of identifiable, but disrupted Archean tonalitic gneisses invaded by 20-50% by volume of Group 2 igneous rocks. This belt is characterized by swirly, irregular folds, discontinuous sheets of Group 2 tonalitic to granitic gneiss, and tectonic inclusions of Group 1 gneisses (Fig. 4f). Granulite-facies mineralogy is only rarely preserved in the Group 1 gneiss inclusions. Stretching lineations and fold axes within this zone plunge moderately to steeply to the north to north-northeast (Fig. 5c). Along the western margin of the Mount Bache granulite block and southwards within the Henry granite, a mylonite zone is characterized by a lineation at 045°/60° (Fig. 2 and 5c) and east-side-up displacement indicators. East-side-up (reverse) mylonite zones with northeast-plunging lineations are also found along the western contacts of wide mafic granulite layers within the straight belt south of Odell Lake (Fig. 2). These zones overprint all previous fabrics within the straight belt, and suggest that deformation zones with northeast- to east-plunging linear fabric elements are the latest in this period of east-side-up, sinistral shearing.

The change in the style of deformation through time, from a broad zone of straightening at granulite to amphibolite facies, to mylonitization and folding of earlier deformation fabrics at amphibolite facies, is considered to represent a continuum of shear deformation during uplift of the orogen. The observed increase in the volume of Proterozoic igneous rocks with belts of progressively higher strain suggests that the later periods of deformation were accompanied by the synchronous emplacement of largely granitic magmas.

Narrow zones (≤10 m) of steeply-dipping ultramylonite with down-dip mineral stretching lineations at amphibolite to greenschist facies were observed to cross cut the east-side-up, amphibolite facies shear fabrics described above (Fig. 2). Kinematic indicators, such as rotated feldspar porphyroclasts, shear bands, and C-S fabrics indicate west-side-up displacement in these zones. Along the eastern contact of the anorthosite body at Walker Lakes, up to 250

m of west-side-up, dip-lineated mylonite is developed within the anorthosite. This continuous belt splays into three branches further south, marked by black ultramylonite with hornblende blasts. Veins of pseudotachylyte are common within and adjacent to these zones, and suggest that this style of deformation continued to relatively shallow crustal levels. West-side-up mylonite zones are far less common in the present map area than along strike of the orogen south of Nachvak Fiord where they represent a volumetrically significant proportion of the Early Proterozoic deformation (e.g. Van Kranendonk, 1990).

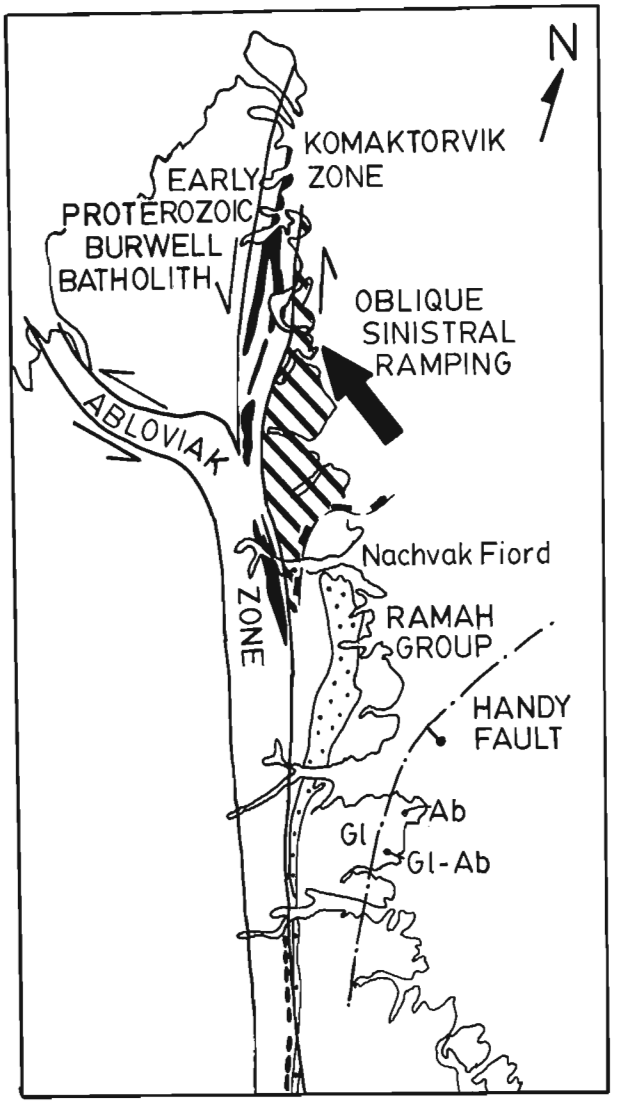


**Figure 6.** Schematic model for the development of some large-scale features of the Torngat Orogen, through oblique, sinistral, east-side-up ramping of the Nain crust over the Early Proterozoic Burwell batholith along the Komaktorvik Zone. This ramping produced an oblique section of the Nain crust and exposed Early Proterozoic granulite-facies rocks (striped pattern) across a curved isograd in the Nachvak Fiord region, and anorthositic rocks (black areas) along its base. The northward termination of the Ramah Group and the scissor-like movement on the Handy Fault may also be attributed to this style of deformation. Ab = Archean amphibolite facies; Gl = Archean granulite facies.

## DISCUSSION AND CONCLUSIONS

Two significant discoveries that pertain to the tectonic evolution of the Torngat Orogen were made this season in the Eclipse Harbour area of northern Labrador. First, a significant suite of Early Proterozoic igneous rocks that ranges in composition from mafic diorite through tonalite, granodiorite, and granite has been identified. These rocks were emplaced within the Nain crust, and the latest, granitic components of the suite may have been synchronous with Early Proterozoic, amphibolite-facies deformation. The compositional range and temporal development of this suite are similar to suites of rocks described from modern and ancient continental margins beneath which oceanic crust has been subducted. As such, this suite of rocks (Group 2) may represent eastern remnants of a continental magmatic arc developed within the Nain crust. The westward extent of this suite will be mapped in detail in the coming two field seasons.

Second, observed structural relations within the Komaktorvik Zone indicate that Nain gneisses and crosscutting mafic dykes have been progressively deformed by predominantly oblique sinistral, east-side-up shearing, under conditions which started at granulite facies, but continued through amphibolite facies. Subsequent, west-side-up deformation structures cut all previous fabrics and may represent a separate phase of deformation.

These observations are consistent with the regional picture developed for the Labrador coast to the north of the map area, as reported in Wardle et al. (in press). The style of Early Proterozoic, oblique, sinistral, east-side-up shear deformation suggests a possible mechanism to explain many of the broad-scale features of the northern part of the Torngat Orogen, as shown in Figure 6. In this model, oblique northwest-directed ramping of Nain Province over Early Proterozoic charnockitic rocks of the Burwell terrane is believed to have caused the exposure of an oblique crustal section of Nain crust. Archean crust metamorphosed to granulite facies in the Early Proterozoic was uplifted across a curved isograd in the Nachvak Fiord region (mapped by Taylor, 1979), and anorthositic rocks were exposed near the lower section of the crust now located within the Komaktorvik Zone of amphibolite-facies reworking. The northward termination of the Aphebian Ramah Group, and the scissor-like movement on the Handy fault may also be attributed to this style of deformation. The relationship between the tectonic evolution of the Komaktorvik Zone and that of the Abloviak shear zone at their junction will form the focus of mapping in 1992 and 1993.

## ACKNOWLEDGMENTS

We would like to thank Fred Alt and the crew of First Air for their excellent Twin Otter service this summer and the Canadian Coast Guard for their timely assistance. As well, it is with great pleasure that we acknowledge the assistance of

Hugh Jennings (Queen's University) in all matters geological, explorational, and quadrapedal. DJS gratefully acknowledges financial support from NSERC (PDF) and LITHOPROBE.

## REFERENCES

**Bertrand, J-M., Van Kranendonk, M.J., Hanmer, S., Roddick, J.C., and Ermanovics, I.F.**
1990: Structural and metamorphic geochronology of the Torngat Orogen in the North River-Nutak transect area, Labrador: Preliminary results of U-Pb dating; Geoscience Canada, v. 17, p. 297-301.

**Collerson, K.D. and Bridgwater, D.**
1979: Metamorphic development of Early Archean tonalitic and trondhjemitic gneisses: Saglek area, Labrador; in Trondhjemites, Dacites and Related Rocks, (ed.) F. Barker; Elsevier, Amsterdam, p. 205-273.

**Ermanovics, I.F., Van Kranendonk, M., Corriveau, L., Mengel, F., Bridgwater, D., and Sherlock, R.**
1989: The Boundary Zone of the Nain-Churchill provinces in the North River-Nutak map areas, Labrador; in Current Research, Part C; Geological Survey of Canada, Paper 89-1C, p. 385-394.

**Korstgård, J., Ryan, B., and Wardle, R.**
1987: The boundary between Archean and Proterozoic crustal blocks in central West Greenland and northern Labrador; in Evolution of the Lewisian and Comparable Precambrian High Grade Terrains, (ed.) R.G. Park and J. Tarney; Geological Society of London, Special Publication No. 27, p. 247-259.

**Taylor, F.C.**
1974: In Age determinations and geological studies, K-Ar isotopic ages, Report 12, (comp.) R.K. Wanless, R.D. Stevens, G.R. Lachance, and R.N.D. DeLabio; Geological Survey of Canada, Paper 74-2, p. 56.
1979: Reconnaissance geology of a part of the Precambrian Shield, northeastern Quebec, northern Labrador, and Northwest Territories; Geological Survey of Canada, Memoir 393, 99 p.

**Van Kranendonk, M.J.**
1990: Structural history and geotectonic evolution of the eastern Torngat Orogen in the North River map area, Labrador; in Current Research, Part C; Geological Survey of Canada, Paper 90-1C, p. 81-96.

**Wardle, R.J.**
1983: Nain-Churchill Province cross-section, Nachvak Fiord, northern Labrador; in Current Research, Newfoundland Department of Mines and Energy, Mineral Development Division, Report 83-1, p. 78-90.

**Wardle, R.J., Van Kranendonk, M.J., Mengel, F., and Scott, D.J.**
in press: Geological mapping in Torngat Orogen, northernmost Labrador. Newfoundland Department of Mines and Energy, Geological Survey Branch, Report of Activities for 1991.

**Wilton, D. and Wardle, R.J.**
1990: Geological Reconnaissance Survey of northernmost Labrador; Newfoundland Department of Mines and Energy, Geological Survey Branch, Report of Activities for 1990, p. 15-18.

Geological Survey of Canada Project 910034

# Vizien greenstone belt and adjacent high-grade domains of the Minto block, Ungava Peninsula, Quebec

**J.A. Percival and K.D. Card**
**Continental Geoscience Division**

*Percival, J.A., and Card, K.D., 1992: Vizien greenstone belt and adjacent high-grade domains of the Minto block, Ungava Peninsula, Quebec; in Current Research, Part C; Geological Survey of Canada, Paper 92-1C, p. 69-80.*

***Abstract***

*The Tikkerutuk, Lake Minto and Utsalik domains consist of plutonic and high-grade metamorphic rocks, whereas the Goudalie domain contains the well-preseved Vizien greenstone belt, enclosed by tonalitic gneisses. The west-northwest-stiking belt, about 40 x <10 km, consists of volcanic (mafic, intermediate, felsic), sedimentary (pelite, quartzite, conglomerate), and intrusive (peridotite, gabbro, tonalitic porphyry) units which form four discrete, fault-bound, steeply northeast-dipping lithotectonic panels. Mineral assemblages in volcanic rocks, including cordierite – anthophyllite – cummingtonite and garnet – cummingtonite – cordierite define mid- amphibolite-grade metamorphic conditions and suggest syngenetic alteration, possibly in a massive sulphide-forming environment. Tourmaline in mafic rocks and quartz veins could indicate gold potential.*

***Résumé***

*Les domaines de Tikkerutuk, de Lake Minto et d'Utsalik se composent de roches plutoniques et de roches fortement métamorphisées, tandis que le domaine de Goudalie renferme la zone bien conservée de roches vertes de Vizien, contenue dans des gneiss tonalitiques. La zone de direction ouest-nord-ouest, d'environ 40 sur <10 km, se compose d'unités volcaniques (mafiques, intermédiaires, felsiques), sédimentaires (pélite, quartzite, conglomérat), et intrusives (péridotite, gabbro, porphyre tonalitique), qui forment quatre panneaux lithotectoniques discrets, limités par des failles et à pendage nord-est prononcé. Les assemblages minéraux des roches volcaniques, en particulier les assemblages cordiérite-anthophyllite-cummingtonite et grenat-cummingtonite-cordiérite, définissent les conditions du métamorphisme correspondant au faciès intermédiaire des amphibolites, et laissent supposer une altération syngénétique, peut-être dans un milieu de formation de sulfures massifs. La présence de tourmaline dans des roches mafiques et dans des filons quartzeux pourrait indiquer un potentiel aurifère.*

## INTRODUCTION

The 1991 season concluded reconnaissance-level field investigations, begun in 1989 (Percival et al., 1990, 1991) in a 400-km long cross-strike transect of the Minto block of northeastern Superior Province at the latitude of Leaf River-Lake Minto. Major objectives of the project were to produce a 1:500 000-scale geological map and to decipher the geological history, through regional and detailed studies of the geochronology, geochemistry, petrology and paleomagnetism of major rock units. This year work focussed on the less accessible and more poorly exposed areas, with the resulting discovery of a relatively well-preserved greenstone belt in the Vizien River area. Several characteristics of the belt, including cordierite-anthophyllite and tourmaline-bearing alteration assemblages and garnet-grunerite-bearing iron-formations, indicate some potential for gold and massive sulphide mineralization.

Results of several detailed studies in progress are summarized within this report. J.K. Mortensen (G.S.C.) is responsible for U-Pb geochronological data. R.A. Stern (G.S.C.) produced geochemical and isotopic results. N.J. Bégin (Univ. of Calgary) is studying the petrology of high-grade metamorphic rocks. K.L. Buchan (G.S.C.) has determined preliminary paleomagnetic poles of Proterozoic dykes, and visited the field area, in conjunction with J.K. Mortensen, to carry out detailed sampling. N.L. Aleksejev (Institute of Precambrian Geology and Geochronology, Leningrad) visited for the 1991 season and will study the petrology and geochemistry of diverse mafic and ultramafic units.

## GEOLOGICAL FRAMEWORK

Northerly structural and aeromagnetic trends, first recognized by Stevenson (1968), distinguish the Minto block from east-trending structures and subprovinces of the southern Superior Province (Card and Ciesielski, 1986). The block can be divided into several north-trending domains (Fig. 1) on the basis of their distinct lithological, structural and aeromagnetic character (Percival et al., 1991, manuscript submitted). A suite of hornblende ± pyroxene-bearing granodiorites, dated at 2725-2721 Ma (Stern et al., 1991; Machado et al., 1989), and late granite occur within all domains. Variably-preserved older supracrustal and intrusive rocks provide the basis for lithological and isotopic distinction between domains.

From west to east the domains include (Fig. 1): 1) Inukjuak, made up of intrusive and supracrustal rocks including iron formation (Stevenson, 1968); 2) Tikkerutuk, consisting of hornblende granodiorite and granite; 3) Lake Minto, a heterogeneous high-grade domain made up of minor metasedimentary (greywacke, iron formation) and mafic metavolcanic supracrustal rocks, intruded by granodiorite

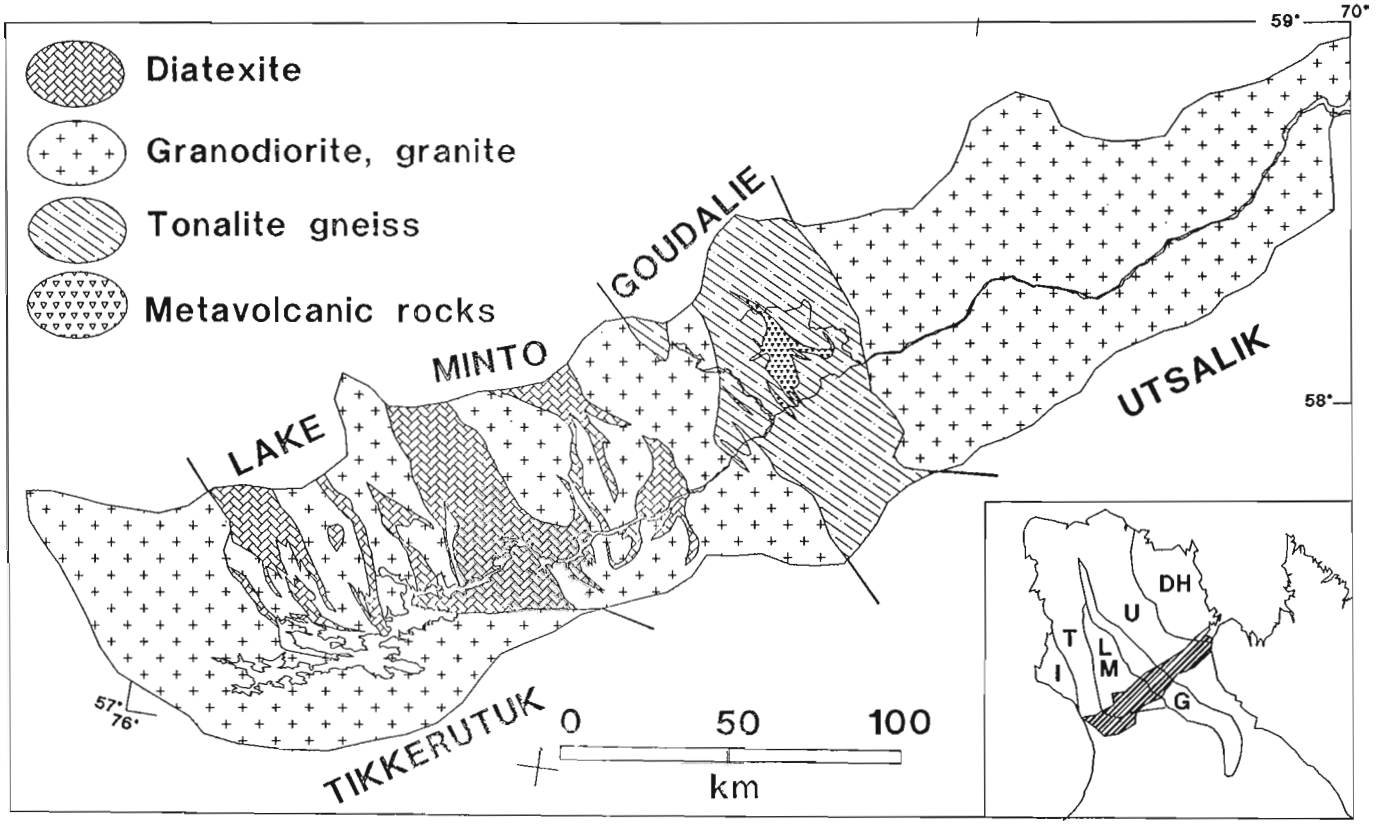


**Figure 1.** Simplified geological map of the Minto block showing lithotectonic domains in the Lake Minto-Leaf River area (after Percival et al., 1991). Inukjuak (I) domain is inferred to border the Tikkerutuk (T) domain to the west and Douglas Harbour (DH) domain to bound the Utsalik (U) domain on the northeast.

(2725 ± 3 Ma), diatexite (2712 ± 3 Ma), derived from crustal sources, and late granite (2693 ± 4 Ma); 4) Goudalie, mainly amphibolite-facies tonalitic rocks, but including the Vizien greenstone belt and its migmatitic extensions; 5) Utsalik, made up of hornblende and pyroxene-bearing granodiorite (2721, 2724 Ma) and granite, with minor mafic enclaves; and 6) Douglas Harbour, a domain of tonalitic rocks with ages in the 2880-2780 Ma range (Parrish, 1989; Machado et al., 1989). The Archean units are cut by at least three swarms of mafic dykes with distinct petrographic and paleomagnetic character.

## THE VIZIEN GREENSTONE BELT

Located within the eastern Goudalie domain (Fig. 1,2), the Vizien belt (Fig. 3) contains the largest area of preserved supracrustal rocks within the transect. Its geology, age and isotopic characteristics will serve as a useful basis for comparison with greenstone belts of the southern Superior Province. Preliminary isotopic results indicate at least two probable ages for rocks within the Goudalie domain. Tonalitic gneisses have Sm-Nd model ages in the range 2.8-3.1 Ga whereas a granodiorite has a U-Pb zircon age of 2.702 Ga.

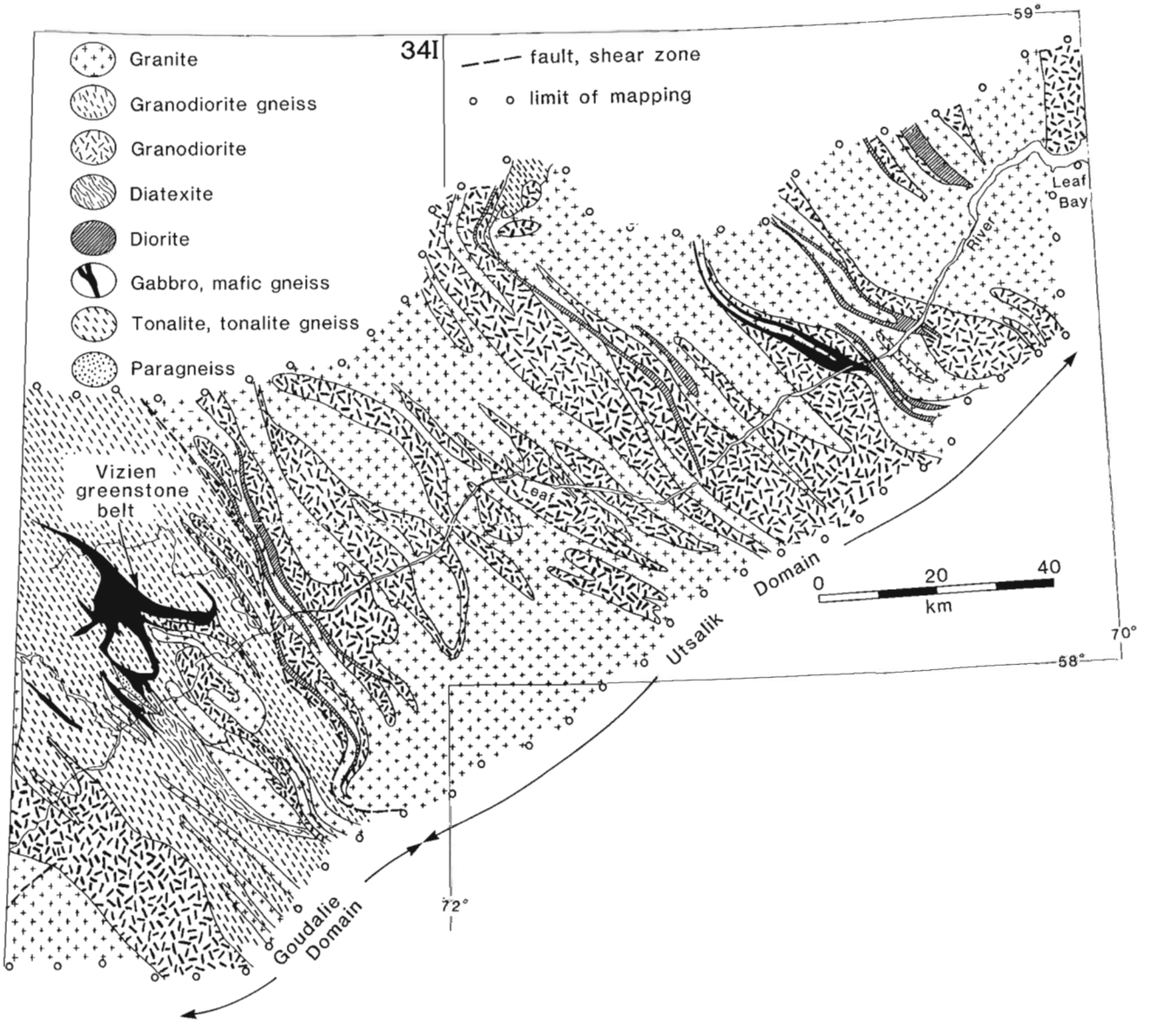


**Figure 2.** Generalized geological map showing lithological units of the Goudalie and Utsalik domains, based on 1990 and 1991 field investigations.

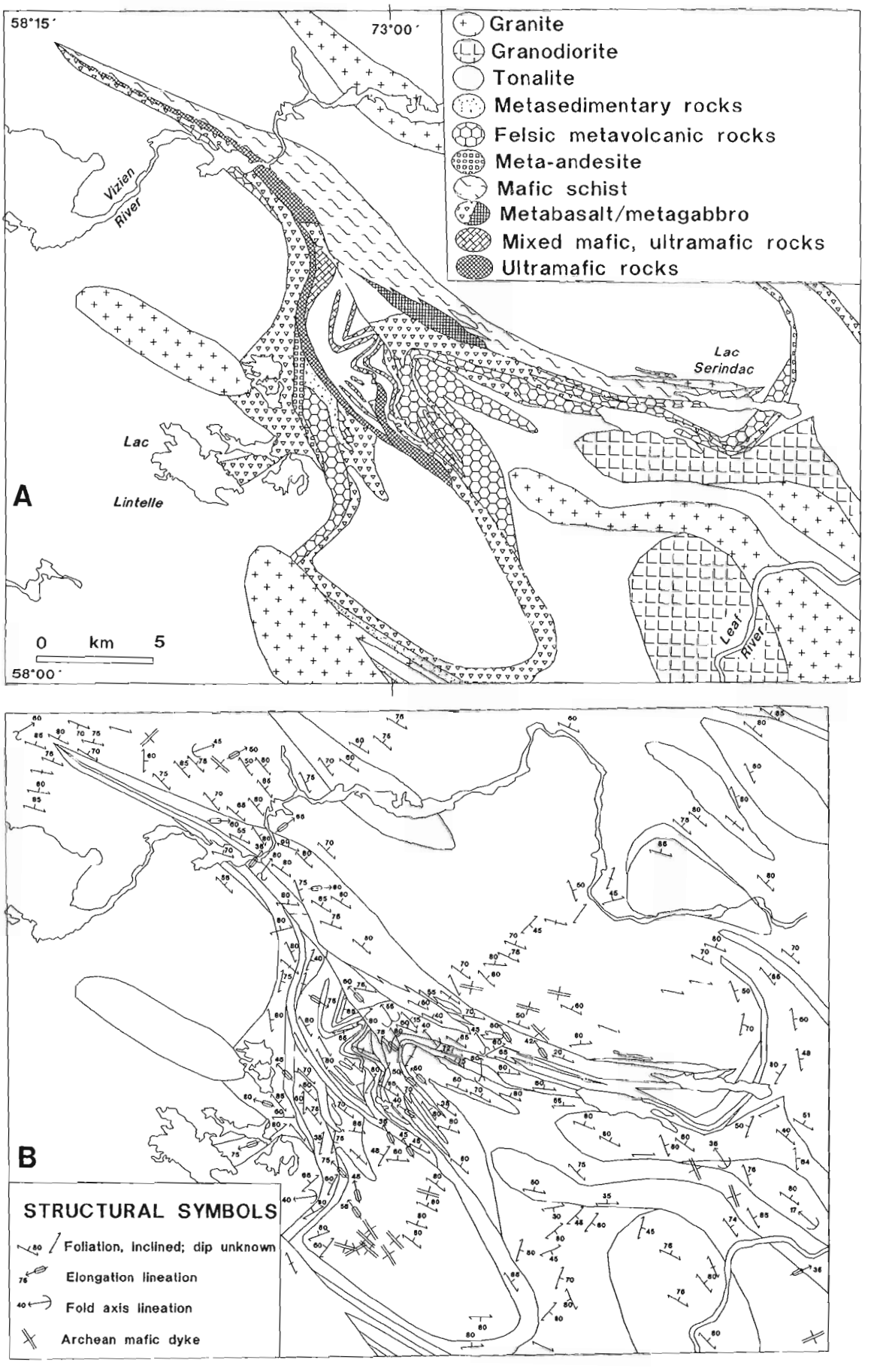
58°15'
73°00'
Granite
Granodiorite
Tonalite
Metasedimentary rocks
Felsic metavolcanic rocks
Meta-andesite
Mafic schist
Metabasalt/metagabbro
Mixed mafic, ultramafic rocks
Ultramafic rocks
Vizien River
Lac Serindac
Lac Lintelle
A
0 km 5
58°00'
Lear River
B
STRUCTURAL SYMBOLS
Foliation, inclined; dip unknown
Elongation lineation
Fold axis lineation
Archean mafic dyke

**Figure 3.**

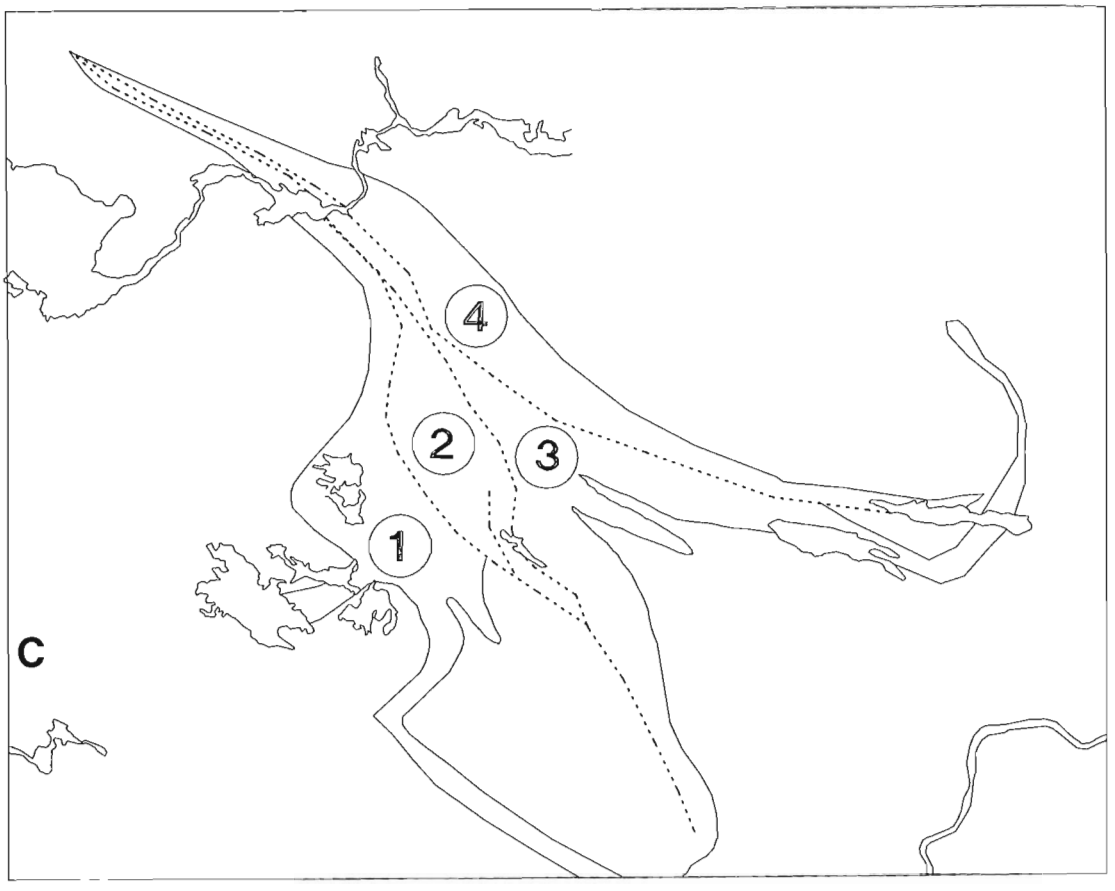


**Figure 3.** Geology of the Vizien greenstone belt: **A**) lithological map, shiwing distribution of rock types; **B**) structural map; and **C**) lithotectonic assemblage map showing location of coherent lithological panels (numbered 1 to 4) and major internal faults.

### *Lithology*

Primary features are preserved within both metavolcanic[1] and metasedimentary lithologies of the Vizien belt. Rocks of volcanic origin range in composition from basalt through andesite and dacite, to rhyolite. Basalt, generally aphanitic to fine grained, contains local carbonate- and quartz-filled amygdules (Fig. 4a) and rarely has preserved pillows and hyaloclastite breccia (Fig. 4b). Basalt is commonly associated with fine- to medium-grained gabbro and with ultramafic rocks of uncertain origin. Some of the associated ultramafic schists may be supracrustal in origin, whereas other, better-preserved occurrences have coarse primary textures and serpentine veins, possibly indicating an intrusive origin.

[1] All units are metamorphosed. The prefix "meta" is dropped from the subsequent descriptions for brevity.

Andesite forms a distinctive plagioclase-porphyritic unit (Fig. 4c) that occurs sporadically throughout the belt. It has a fine-grained, variably foliated matrix and 10-20% weakly to moderately aligned plagioclase phenocrysts on the 5-20 mm scale.

Dacites generally have a fine-grained to aphanitic matrix and may contain 5-10% plagioclase phenocrysts on the 1-5 mm scale. A common texture that occurs in well-foliated rocks consists of a fine-grained to aphanitic matrix with coarser-grained elliptical patches (Fig. 4d) up to 1 cm wide. Boundaries between the compositionally similar matrix and biotite-quartz-plagioclase patches are indistinct and two origins appear possible. The patches may be flattened and recrystallized primary features such as tuffaceous fragments, or they could be entirely secondary recrystallization features.

Rhyolites are recognized by their aphanitic grain size and pink weathered surface. They are generally homogeneous and may contain up to 10% phenocrysts of quartz and plagioclase. A heterolithic conglomerate or breccia with rounded clasts up to 30 cm in diameter forms a small unit locally within the otherwise fine-grained rhyolitic unit.

Several units of sedimentary origin occur locally within the Vizien belt. A muscovite schist unit occurs in association with felsic volcanic rocks. It consists of layers 1-10 cm thick of medium- to coarse-grained muscovite ± quartz ± garnet. Concordant centimetre-scale quartz veins locally contain

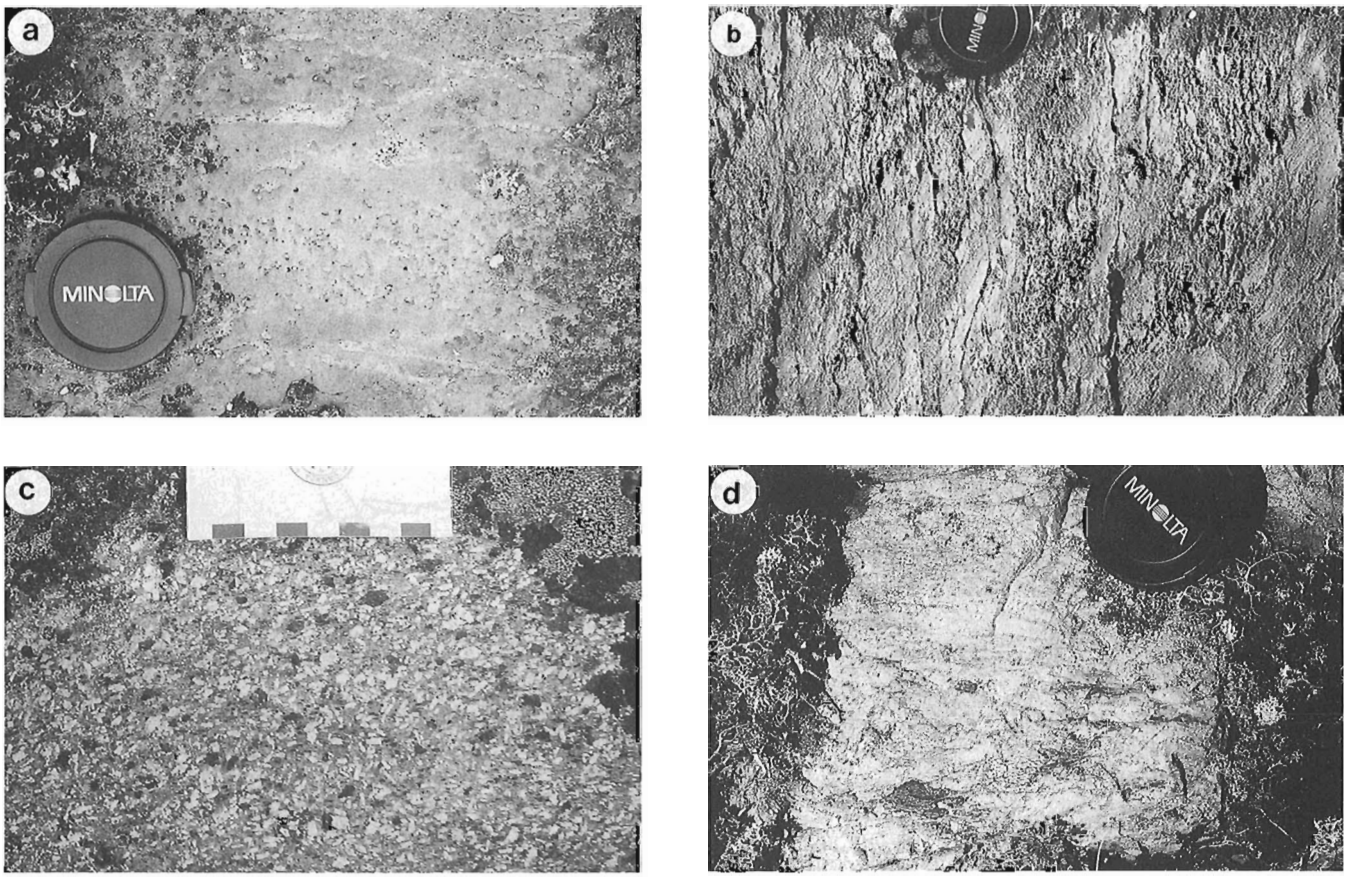


**Figure 4.** Outcrop photographs of representative volcanic rock types of the Vizien greenstone belt: **a**) fine-grained metabasalt with carbonate-filled amygdules, panel 1 (lens cap in this and subsequent photographs is 5 cm in diameter) (GSC 1991-576 A); **b**) hyaloclastite breccia in basalt, panel 2 (GSC 1991-576 K); **c**) plagioclase-porphyritic andesite, panel 1 (GSC 1991-576 J); **d**) dacitic metavolcanic rock with tuffaceous fragments, panel 3 (GSC 1991-576 I).

coarse andalusite and muscovite. Thinly-layered (millimetre-scale) arkosic siltstone (Fig. 5a) occurs locally within the unit.

A local lens of clast-supported conglomerate (Fig. 5a), a few hundred metres thick, occurs within the central part of the Vizien belt. Clasts are generally rounded, 10-50 cm in diameter, and include (in approximate order of abundance) tonalite, volcanic lithologies, and granite. Minor quartzite grit is associated with the unit and occurs locally elsewhere within the belt. Contacts between conglomerate and the surrounding mafic volcanic assemblage are not exposed.

Thin layers of iron-formation occur locally, mainly within altered mafic volcanic units. They are rusty-weathering pods and layers, up to several metres thick, composed of massive, medium-grained garnet, grunerite, quartz, pyrite and pyrrhotite. Associated mafic rocks show evidence of alteration including anthophyllite and tourmaline-bearing assemblages.

A wide compositional range of intrusive rock types makes up a significant proportion of the Vizien belt. The intrusive units have distinct forms and modes of occurrence. Ultramafic units range in composition from more common peridotites and serpentinites, to pyroxenite, hornblendite, and talc-actinolite schist. These rocks occur in concordant sill-like bodies within the belt, and as dyke-like bodies in the adjacent enclosing tonalites. Primary mineral assemblages, including olivine and pyroxene, are preserved in peridotite and pyroxenite in a few localities, however most assemblages are secondary. Veins of serpentine, possibly representing several generations of growth, are evident in most peridotite outcrops (Fig. 5c). A single 5m x 5m occurrence of chrysotile asbestos was noted. Ultramafic schists, consisting mainly of talc, chlorite, actinolite and serpentine, are commonly associated with mafic volcanic rocks. Although primary depositional textures were not observed, these occurrences could represent komatiitic flows, based on their association and extent of recrystallization.

Gabbroic rocks occur within mafic volcanic sequences and as discrete bodies on scales up to 2 x 5 km. They are homogeneous, variably foliated, medium- to fine-grained rocks that appear compositionally similar to basalt. Gabbroic rocks also occur as dykes within tonalite enclosing the Vizien

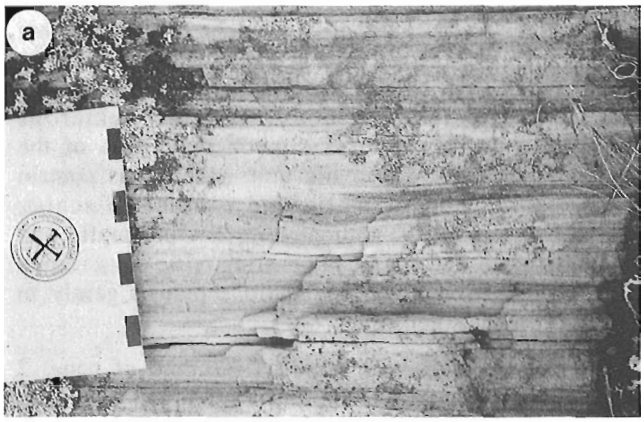


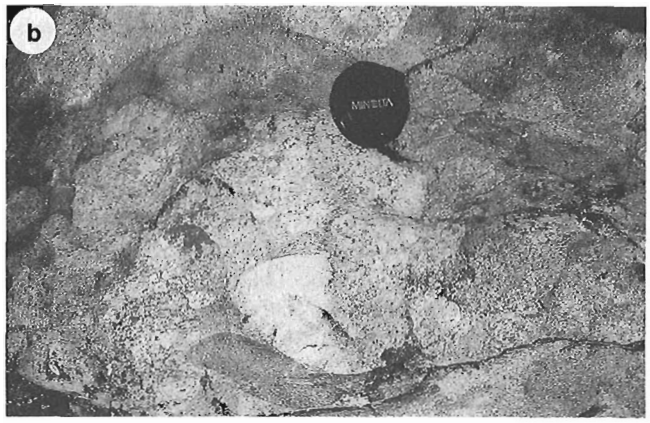


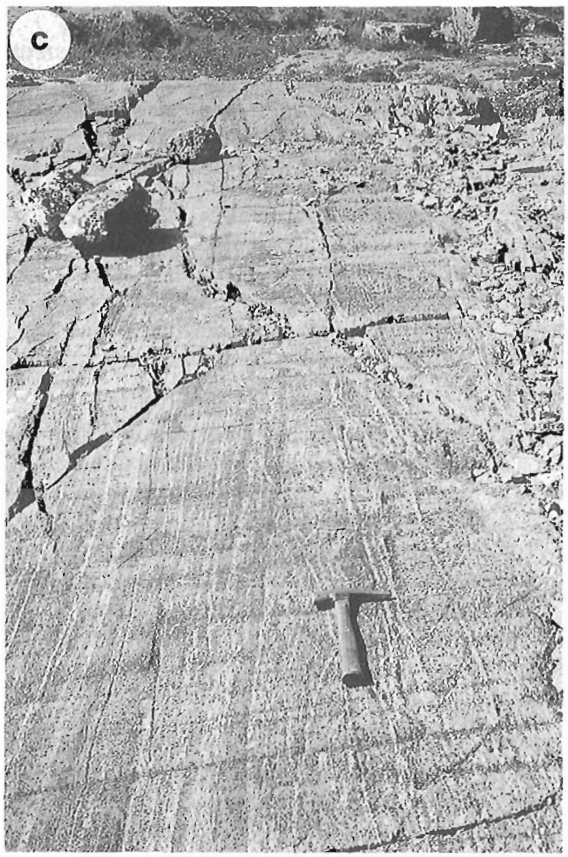



**Figure 5.** Outcrop photographs of representative sedimentary and intrusive rock types of the Vizien greenstone belt: **a**) thinly-layered arkosic siltstone from the sedimentary unit, panel 1 (GSC 1991-576 H); **b**) massive conglomerate consisting of subrounded clasts, up to 50 cm in size, of tonalite, metavolcanic rocks and some granite (panel 2) (GSC 1991-576 G); **c**) peridotite with serpentinite veins; relics of olivine are preserved locally (panel 2) (hammer handle in this and subsequent photographs is 30 cm long) (GSC 1991-576 F); **d**) boudinaged metagabbro dyke cutting foliated tonalite; the dykes are themselves cut by late granite (GSC 1991-576 E).

belt. The 1-10 metre-wide, variably foliated and boudinaged bodies cut foliated tonalite (Fig. 5d) but are themselves cut by later granites.

Tonalite also occurs within the Vizien belt, particularly within the central part. A body ~2 x 6 km in size contains numerous xenoliths of altered mafic-to-ultramafic rocks. The tonalite varies texturally from homogeneous and medium grained to quartz or plagioclase porphyritic (to 5 mm). The commonly strong foliation is defined by 5-10% aligned muscovite. Based on the porphyritic texture and muscovitic alteration, the body may be part of an intrusive complex, emplaced at high levels into the volcanic sequence.

Several varieties of tonalite border the Vizien belt. Most common, on the southern and eastern sides, is a homogeneous, medium-grained, strongly foliated biotite tonalite. It contains mafic enclaves that include both amphibolitic inclusions and metagabbroic dykes. The dykes constitute the northern part of a swarm of deformed mafic bodies recognized in the eastern Goudalie domain (Percival et al., 1991). Marginal tonalite has gneissic phases characterized by mafic layers, granitic leucosome on the millimetre to centimetre scale, and concordant granitic pegmatites. Although very poorly exposed, the area west of the belt appears to be partly underlain by a distinctive quartz-porphyritic biotite tonalite. Based on the few

reconnaissance observations, the weakly-foliated unit contains quartz phenocrysts to 1 cm in a medium-grained matrix and has sparse inclusions of possible volcanic origin.

A suite of distinctive peraluminous granitic pegmatites forms podiform bodies up to 10 m wide that cut the previously described units of the Vizien belt, particularly the mafic units. The white-weathering pegmatites contain abundant muscovite, as well as smaller quantities of tourmaline, garnet and amazonite feldspar. Parallel networks of pegmatite dykes and quartz veins of similar scale occur locally in zones of strong foliation. The spatial association suggests that the dykes and veins may be related.

### *Structure*

Several structural panels (Fig. 3B,C) make up the 10-km-wide central part of the 40-km long, northwest-trending Vizien belt. As the belt generally dips steeply to the northeast, the description will proceed up structural section, from southwest to northeast, although this may have no relationship to the stratigraphic order.

Panel 1, on the western edge of the belt (Fig. 3C), is obscured by glacial cover on the west; sparse exposure indicates that it is intruded on the west by quartz-porphyritic tonalite. The panel consists of a basal unit of basaltic rocks, including garnet-grunerite iron-formation and tourmaline-, cummingtonite- and anthophyllite-bearing alteration assemblages. Minor associated felsic volcanic rocks have garnet – cummingtonite – cordierite – quartz assemblages. The mafic rocks are structurally overlain by a unit of interlayered plagioclase-porphyritic and non-porphyritic andesite about 200 m thick, grading upward into a unit of felsic volcanic rocks. The unit of mixed dacite and quartz-porphyritic rhyolite also contains minor interlayered siltstone as well as some thin andesitic layers. The felsic layer is overlain structurally by a sedimentary unit made up mainly of muscovite schist, grading upward to thinly-layered quartz-rich siltstone. Units of panel 1 are truncated to the east by a fault carrying the concordant basal units of panel 2. Although younging indicators were not observed, in its present structural orientation, panel 1 appears to represent a steeply-dipping classical mafic through felsic volcanic cycle, capped by mature sedimentary rocks.

The fault separating panels 1 and 2 is marked by a valley, interpreted as coinciding with a fault, that truncates units within panel 1. The ultramafic basal unit of panel 2, which is concordant to the fault, extends the entire length of the panel, about 10 km, although its character varies along strike. In the north the unit is a prominent ridge of variably serpentinized peridotite, that changes along strike into talc schist associated with mafic volcanic rocks.

The basal unit grades to the east into a heterogeneous unit of interlayered, variably altered, ultramafic, mafic and felsic rocks. Alteration assemblages include widespread anthophyllite – biotite in mafic and ultramafic rocks, and muscovite ± sillimanite in felsic lithologies. Cordierite – anthophyllite – cummingtonite assemblages occur within both mafic and felsic units. The heterogeneous unit is cut on the east by a body of variably porphyritic, muscovitic foliated tonalite. The tonalite body contains numerous kilometre-scale, stratigraphically-coherent septa of the heterogeneous mafic-ultramafic unit. Inclusions contain some combination of mafic and ultramafic schist, metagabbro, chlorite – anthophyllite bearing mafic and ultramafic rocks, and sillimanite-bearing felsic units. Small folds, rodding and mineral lineations plunge gently to moderately to the southeast.

An internal fault near the southeast end of panel 2 truncates lithological layering at a low angle. The fault appears to repeat the basal unit of interlayered ultramafic and mafic schists, as well as the porphyritic tonalite.

Conglomerate units locally form the uppermost part of the panel, adjacent to the structurally overlying fault. Clasts appear to be derived from local tonalite and mafic volcanic sequences, except for rare graphic granite boulders.

The fault truncating panel 2 on the east is defined on the basis of a topographic lineament and a 20-m wide deformation zone within mafic schist. The chlorite schists within this zone contain several generations of quartz veins, the earlier of which are contorted into tight, rootless folds (Fig. 6a). Later quartz veins contain tourmaline and are semi-concordant to the strong, steeply-dipping penetrative schistosity.

On the regional scale, the fault truncates the southwestern limb of a northwest-plunging antiformal structure that makes up panel 3. In general, this tight fold structure has tonalitic rocks in its core, structurally overlain by felsic and then mafic volcanic rocks. Panel 3 forms a northwest-tapering wedge with arms of mafic and dacitic schist extending through migmatitic zones to the southeast and east. The axial zone of the fold, plunging ~50° northwest, has a strong axial planar foliation which appears to have localized pegmatite and quartz veins.

Panel 4, to the east of the regional fold, is a steeply northeast-dipping unit of deformed, schistose rocks with a sporadic, moderately northwest-plunging stretching lineation. Dominantly mafic in composition, the unit also contains fine-grained felsic schists of probable volcanic, tonalitic and granitic/pegmatitic origin as well as discordant pods of peridotite and pyroxenite. Based on grain size variations, the mafic components probably also represent rocks of extrusive and intrusive origin. The 3-km wide panel of intensely deformed, mixed rocks gives way to the northeast to gneissic and homogeneous tonalites with few mafic enclaves. Pods of ultramafic rock (serpentinite, pyroxenite) are common in tonalite within 300 m of the northeastern contact of the belt.

Panel 3 pinches out toward the north along bounding faults (Fig. 3C) and the others are highly attenuated north of the Vizien river. The basal ultramafic unit of panel 2 extends at least 5 km northeast of the river before becoming discontinuous and pervasively migmatitic.

The four panels comprising the Vizien belt have distinct internal stratigraphy and structural style, although there are some lithological similarities. The major faults bounding these panels, which truncate lithological layering at low angles, resemble thrust faults in cross section and it is possible that they represent early thrusts that have juxtaposed different parts of a single volcanic complex.

### *Metamorphism and alteration*

Assemblages in a variety of bulk compositions allow definition of metamorphic grade. Critical low-variance assemblages observed in the interior of the belt include: muscovite – quartz and andalusite – quartz (pelites), hornblende – plagioclase (metabasites), cordierite – anthophyllite - cummingtonite - chlorite (altered metabasites) (Fig. 6b), garnet – cummingtonite – cordierite (altered felsic volcanic rocks) and talc – serpentine – chlorite (ultramafic rocks). Preliminary assessment, based on field observations, suggests low-pressure, lower to middle amphibolite-facies conditions. Further work is underway by S. Schwarz as part of a B.Sc. thesis.

The metamorphic assemblages indicate significantly lower grade conditions for the Vizien belt than the typical regional granulite facies of supracrustal rocks elsewhere in the Minto block, consistent with previous recognition (Percival et al., 1991) that the Goudalie domain is dominantly in the amphibolite facies. Medium-grade metamorphic assemblages in pelitic rocks, including andalusite, staurolite and cordierite, were noted to the north of the Minto transect (Herd, 1978), suggesting that other relatively well-preserved supracrustal relicts may be present. Patches of granulite-facies metamorphic rock and orthopyroxene-bearing plutonic rocks occur within the Goudalie domain 20 and 45 km respectively, southeast of the Vizien belt.

Occurrences of cordierite – anthophyllite are characteristic of syngenetic alteration assemblages, metamorphosed under medium-grade conditions (e.g., James et al., 1978; Schneiderman and Tracy, 1991) and are commonly regarded as targets in massive sulphide exploration. Thin, stratiform, sulphide-bearing units occur in association with anthophyllite and tourmaline-bearing mafic rocks in panel 1, suggesting a link between alteration and sulphide mineralization. Detailed mapping is required to define alteration facies, as well as the spatial and stratigraphic extent of altered rock.

## UTSALIK DOMAIN

This 160-km-wide zone of north-northwest-striking plutonic units comprises a major magmatic complex virtually devoid of supracrustal remnants. U-Pb zircon dates from widely-separated samples of the major calc-alkaline granodiorite suite, 2721 (Machado et al., 1989) and 2724 Ma (J.K. Mortensen and R.A. Stern, unpublished), indicate similar crystallization ages across a wide region.

The oldest units within the Utsalik domain are rare tonalitic enclaves up to several kilometres in size, noted only in the north-central part of the domain. Tonalites are foliated to gneissic and are cut by hornblende-biotite granodiorite and later granite. The tonalites contain sporadic inclusions of garnet-biotite paragneiss, garnet-bearing mafic gneiss and fine-grained schist of possible felsic volcanic origin. These small remnants represent the only probable supracrustal component of the Utsalik domain. The affinity of the tonalitic rocks is unclear. The lithological assemblage resembles both that of the Goudalie domain to the east and Douglas Harbour domain to the northwest (Lucas and St-Onge, 1991).

Granodiorite and granite make up most of the Utsalik domain. Granodiorite has several mineralogical facies defined by mafic minerals including amphibole, pyroxenes and biotite. The end-member assemblages appear to be orthopyroxene - clinopyroxene – biotite, suggesting very low magmatic water contents (e.g., Naney, 1983), and hornblende – biotite, typical of calc-alkaline granodiorites. Although hornblende-bearing assemblages dominate, pyroxene-bearing units occur throughout the domain. Several observations indicate a primary igneous, rather than superimposed metamorphic, origin for these mineral assemblages. Both pyroxene- and amphibole-bearing rocks have coarse, hypidiomorphic textures and are generally only weakly foliated. Where transition zones between facies have been observed, hornblende occurs as overgrowths on pyroxene cores, demonstrating classic igneous reaction relationships.

Dyke-like mafic enclaves occur sporadically within granodiorite. The straight-walled, biotite - hornblende diorite to monzonite bodies vary in width from 2 to 100 cm and have length:width ratios from 2 to 200. A detailed study of an area with several dyke-like bodies concluded that the enclaves probably represent synplutonic dykes that may have been derived from a similar source as the host rock (Shore, 1991).

On the regional scale, mafic and dioritic bodies 5 to 50 m wide have apparent strike lengths of up to 50 km, although they are deformed, discontinuous, and probably boudinaged (Fig. 6c). Contact relations with enclosing granodiorite and granite are commonly equivocal, but the mafic bodies are cut by granite, in some locations in spectacular net-veined arrays. These large linear enclaves appear also to represent synplutonic mafic injections.

Several suites of granite occur as equant and linear north-northwest-trending plutons, dismembering the older granodiorite suite. The granites can be subdivided on the basis of their mafic mineral assemblages and probably represent different ages, based on cross-cutting relationships. The oldest granites are phases of the granodiorite suite, related through gradational contacts by changing proportions of commonly megacrystic K-feldspar. Similar mafic mineral assemblages and contents characterize related granite and granodiorite.

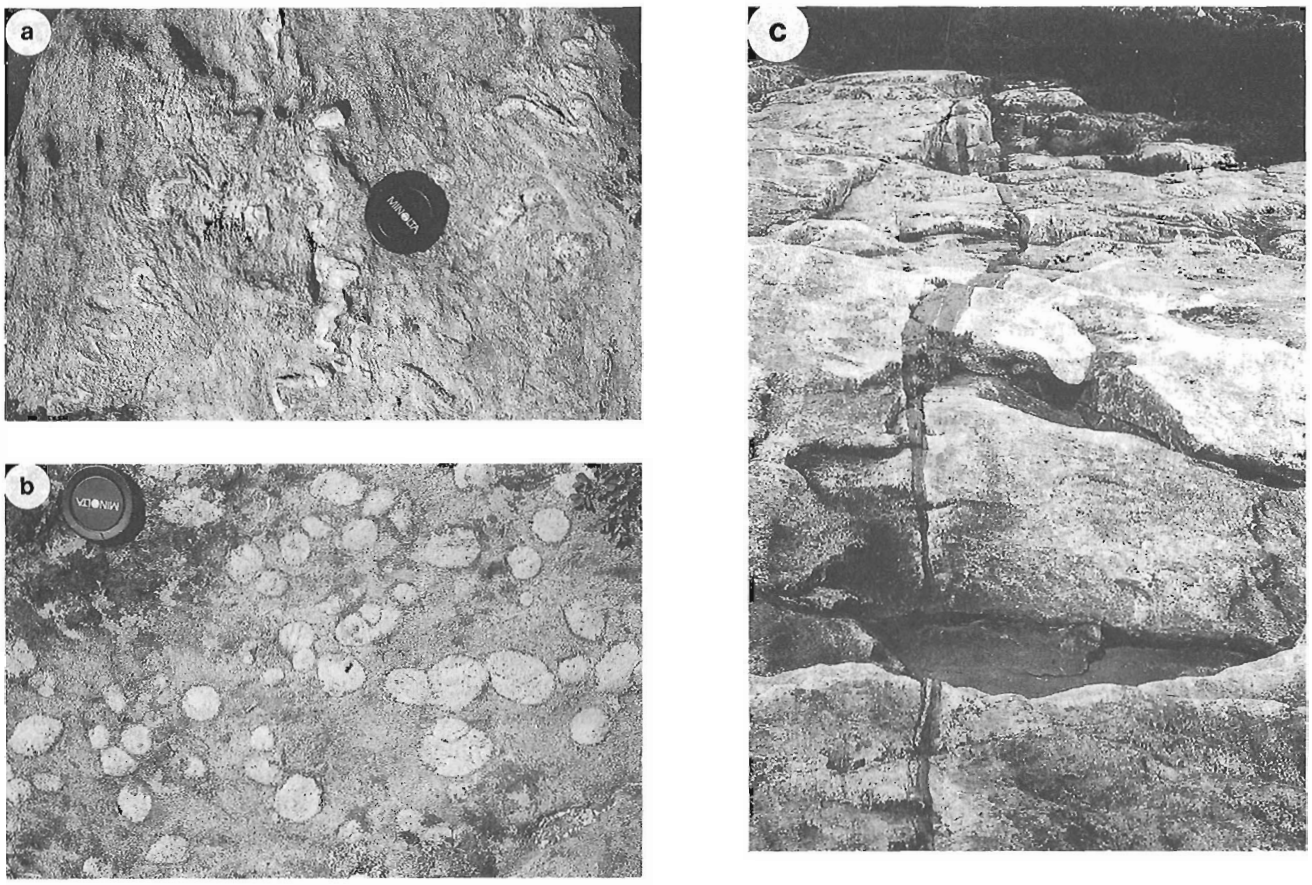


**Figure 6.** **a**) chloritic schist derived from mafic rocks, in a 20-m-wide fault zone (panel 2-3 boundary); tightly folded and dismembered quartz veins contain tourmaline (GSC 1991-576 D); **b**) altered metabasite containing felsic spherules, overgrown by cordierite-anthophyllite-cummingtonite assemblages. Panel 2, Vizien greenstone belt (GSC 1991-576 C); **c**) boudinaged metagabbro dyke cutting granodiorite, Utsalik domain. The dykes, locally traceable for ~50 km, are cut by late granites (GSC 1991-576 B).

A suite of clinopyroxene – biotite granites occurs in the central Utsalik domain. The granites cut and include granodiorite but are themselves variably foliated. In their least deformed and recrystallized state the granites are massive, coarse-grained rocks with megacrysts of grey K-feldspar to 1.5 cm and fresh clinopyroxene to 5 mm. With increasing foliation, megacrysts develop granular pink rims and clinopyroxene is rimmed by biotite. Locally-developed augen gneisses have granular K-feldspar augen in a biotite – plagioclase – quartz matrix. Granites of this suite are cut by later leucogranite. Clinopyroxene – biotite granite commonly contains dyke-like mafic enclaves. The discontinuous, 10- to 30-cm-wide, fine- to medium-grained biotite – hornblende dioritic bodies have length-to-width ratios >10. They are commonly discordant to mineral alignment in enclosing granite but are separated from on-strike dyke segments by tens-of-centimetres-wide areas of normal granite. The mafic bodies appear to have been intruded late in the crystallization history of the granite, before final solidification.

Biotite leucogranite is a ubiquitous phase that cuts all of the previously described units. It occurs as granite and pegmatite veins, sills and plutons that locally attain mappable dimension. These massive to weakly foliated rocks have a characteristic pink weathered surface and contain <5% mafic constituents, principally biotite. Accessory allanite and titanite are locally abundant.

All units of the Utsalik domain generally have a fresh appearance, with only minor alteration to epidote. On the regional scale, alteration is much more evident in the east. A zone approximately 25 km wide bordering the Labrador Trough is characterized by widespread east-trending cataclastic fabrics, associated with extensive epidote alteration. These features probably relate to effects on the basement of Early Proterozoic deformation in the New Quebec orogen.

### *Goudalie-Utsalik domain boundary*

The boundary between the Goudalie and Utsalik domains is defined lithologically on the basis of predominant foliated tonalitic units to the west and mainly granodiorite and granite

to the east (Fig. 2). Although generally not well exposed, the boundary is locally also expressed structurally as a discontinuity in foliation trends.

In the northern boundary zone of Figure 2 the western Utsalik domain consists of elongate, kilometre-scale units of hornblende – biotite granodiorite and granite with 100-m-scale septa of variably migmatitic, dyke-like hornblende – biotite diorite and gabbro. Granodiorite contains rare kilometre-scale inclusions of tonalitic gneiss. The lithological layering and parallel mineral-alignment foliation define a north-northwest-trending, steeply northeast-dipping structural panel. To the west, the Goudalie domain consists mainly of biotite ± hornblende tonalitic gneiss with sparse mafic gneiss inclusions and west-northwest structural orientations. The tonalites are cut by concordant, elongate plutons of granodiorite and later granite. Lithological units and foliation define a dextral reorientation into parallelism with the boundary within 5-10 km of the Goudalie-Utsalik boundary.

Based on contact relationships in both Goudalie and Utsalik domains, that show tonalites cut by granodiorites, it appears that the original boundary between the domains may have been an intrusive contact between Utsalik granodiorite and older Goudalie tonalites. Subsequent ductile dextral transcurrent movement along this contact zone left remnants of Goudalie tonalite within the western Utsalik domain.

In the vicinity of the Leaf River to the south (Fig. 2), the boundary separates pyroxene-bearing granodiorites to the east from tonalite with mafic enclaves to the west. Granulite-facies assemblages occur in tonalitic rocks in the vicinity of the boundary (Percival et al., 1991). The spatial association of pyroxene-bearing igneous rocks and granulite-facies gneisses is also suggestive of an intrusive relationship between Utsalik granodiorite and older Goudalie tonalite.

## PROTEROZOIC DYKES

Discordant mafic dykes ranging in width from about 1 to 30 m form several distinct petrographic and paleomagnetic swarms. The dykes cut and are chilled against the previously-described Archean rock units, are virtually undeformed but variably altered. The alteration comprises saussuritization of plagioclase, uralitization of pyroxene and serpentinization of olivine and is probably of deuteric origin.

In the Tikkerutuk and Lake Minto domains in the west, west-northwest-trending diabase dykes consist of calcic plagioclase, titaniferous augite, olivine, biotite, iron oxides and apatite. In the Goudalie and western Utsalik domains, dykes also trend generally west-northwest and consist of plagioclase and clinopyroxene, with some orthopyroxene, quartz and iron oxide. Dykes in the eastern Utsalik domain are mainly olivine diabase, with west-northwest and north-northeast trends. Zircon from a north-northeast-trending dyke gave an age of 2503 Ma.

Preliminary paleomagnetic investigations indicate at least three distinct poles (K. Buchan, pers. comm., 1991). The petrographically-defined swarms correspond to the paleomagnetic populations. Further work is underway to characterize the precise age and pole positions of each dyke swarm.

## ACKNOWLEDGMENTS

Capable and cheerful field assistance by S. Schwarz (Carleton University), G. DeSchutter (Concordia University) and J. Green is gratefully acknowledged. N. Alexsejev is thanked for his pertinent observations and refreshing perspective. Visits to the field, observations and discussions by J.K. Mortensen, K.L. Buchan and A.C. Colvine were greatly appreciated, as were comments on the manuscript by J.K. Mortensen. Field transportation by Johnny May's Air Charters (Kuujjuaq) and Capital City Helicopters (Ottawa) facilitated operations. Uncharacteristic co-operation by the Ungava weather was very thoroughly appreciated.

## REFERENCES

**Card, K.D.**
1990: A review of the Superior Province of the Canadian Shield, a product of Archean accretion; Precambrian Research, v. 48, p.99-156.

**Card, K.D. and Ciesielski, A.**
1986: Subdivisions of the Superior Province of the Canadian Shield; Geoscience Canada, v. 13, p.5-13.

**Herd, R.K.**
1978: Notes on metamorphism in new Quebec; in Metamorphism in the Canadian Shield; Geological Survey of Canada, Paper 78-10, p. 78-83.

**James, R.S., Grieve, R.A.F., and Pauk, L.**
1978: The petrology of cordierite-anthophyllite gneisses and associated mafic and pelitic gneisses at Manitouwadge, Ontario; American Journal of Science, v. 278, p.41-63.

**Lucas, S.B. and St-Onge, M.R.**
1991: Evolution of Archean and early Proterozoic magmatic arcs in northeastern Ungava Peninsula, Quebec; in Current Research Part C; Geological Survey of Canada Paper 91-1C, p.109-119.

**Machado, N., Goulet, N., and Gariépy, C.**
1989: U-Pb geochronology of reactivated Archean basement and of Hudsonian metamorphism in the northern Labrador Trough; Canadian Journal of Earth Sciences, v. 26, p.1-15.

**Naney, M.T.**
1983: Phase equilibria of rock-forming ferromagnesian silicates in granitic systems; American Journal of Science, v. 283, p. 993-1033.

**Parrish, R.R.**
1989: U-Pb geochronology of the Cape Smith belt and Sugluk block, northern Quebec; Geoscience Canada, v. 16, p.126-130.

**Percival, J.A., Mortensen, J.K., Stern, R.A., Card, K.D., and Bégin, N.J.**
in press:: Giant granulite terranes of northeastern Superior Province: the Ashuanipi complex and Minto block; Canadian Journal of Earth Sciences.

**Percival, J.A., Card, K.D., Stern, R.A., and Bégin, N.J.**
1990: A geological transect of northeastern Superior Province, Ungava Peninsula, Quebec: the Lake Minto area; in Current Research Part C; Geological Survey of Canada Paper 90-1C, p.133-141.
1991: A geological transect of the Leaf River area, northeastern Superior Province, Ungava Peninsula, Quebec; in Current Research Part C; Geological Survey of Canada Paper 91-1C, p.55-63.

**Schneiderman, J.S. and Tracy, R.J.**
1991: Petrology of orthoamphibole-cordierite gneisses from the Orijarvi area, southwest Finland; American Mineralogist, v. 76, p.942-955.

**Shore, G.T.**
1991: On the nature and origin of microgranitoid enclaves in the Leaf River area, Ungava Peninsula, Superior Province, Quebec; B.Sc. thesis, University of Toronto, Toronto.

**Stern, R.A., Percival, J.A., Card, K.D., and Mortensen, J.K.**
1991: Geochemistry and geochronology of the Minto subprovince, Quebec; Geological Association of Canada Program with Abstracts, v. 16, p.A118.

**Stevenson, I.M.**
1968: A geological reconnaissance of Leaf River map-area, new Quebec and Northwest Territories; Geological Survey of Canada, Memoir 356.

Geological Survey of Canada Project 890009

# Terrane characterization in the Central Metasedimentary Belt of the southern Grenville Orogen, Lac Nominingue map area, Quebec

**L. Corriveau and V. Jourdain**
**Quebec Geoscience Centre, Sainte-Foy**

*Corriveau, L. and Jourdain, V., 1992: Terrane characterization in the Central Metasedimentary Belt of the southern Grenville Orogen, Lac Nominingue map area, Quebec; in Current Research, Part C; Geological Survey of Canada, Paper 92-1C, p. 81-90.*

***Abstract***

*A domain postulated to be the northern extension of the Frontenac terrane in the Central Metasedimentary Belt of Québec was investigated in the Lac Nominingue area (31J/6). The western limit of this domain coincides with a sharp change in supracrustal sequence. Marble is prevalent to the west and quartzite is omnipresent in the domain. A north-trending high strain zone with late brittle deformation and quartz-carbonate-pyrite veins that show similarities with the gold-bearing Robertson Lake Mylonite Zone (CMB of Ontario) occurs near the eastern limit of the domain. This domain extends across the whole map area and its northern limit is not yet defined. The anorthositic rocks reported in this area occur in vertically layered mafic intrusions and are distinct from the massif-type anorthosites found in the Morin terrane. Porphyritic monzonite bodies, a K-rich alkaline pluton, dykes of lamprophyre, and a lamprophyric breccia pipe with ultramafic xenoliths are also present.*

***Résumé***

*Un domaine de la zone métasédimentaire centrale du Québec présumé être l'extension nord du terrane de Frontenac a fait l'objet d'études dans la région du lac Nominingue (31J/6). La limite ouest de ce domaine coïncide avec un changement abrupt de séquences supracrustales: marbre prédominant à l'ouest et quartzite omniprésente. À l'est, ce domaine est jalonné par une zone de déformation ductile caractérisée par une déformation cassante tardive et la présence de veines de quartz-carbonate-pyrite; elle présente des ressemblances avec la zone de cisaillement aurifère de Robertson Lake (ZMC, Ontario). Le domaine quartzitique s'étend jusqu'au nord de la carte et sa limite nord n'est pas encore définie. Les anorthosites rapportées dans cette région font partie d'intrusions mafiques verticalement litées et sont distinctes des anorthosites de type massif caractéristiques du terrane de Morin. Des monzonites porphyriques, un pluton alcalin potassique, des lamprophyres et une brèche ignée renferment des xénolites ultramafiques sont aussi présents.*

## INTRODUCTION

Parallels and differences between the supracrustal rocks and the plutonic suites of the Central Metasedimentary Belt (CMB) of Quebec and that of the neighboring Morin terrane were established in 1990 (Martignole and Corriveau, 1991). Questions arose concerning the possible extension of the Morin mangerite-anorthosite suite into the CMB, as anorthosite and mangerite have been reported in the CMB in the Lac Nominingue area (Wynne-Edwards et al., 1966). A major shear zone was also recognized in this area (Fig. 4c in Corriveau, 1991) along the northeastern boundary of a north-facing lobate domain devoid of 1089-1076 Ma K-rich alkaline plutons and postulated to be the northern extension of the Frontenac terrane (Corriveau, 1990b). Previous investigations of the Lac Nominingue area (NTS 31J/6; Fig. 1 and 2) include 1:63 360 scale mapping by Aubert de la Rue (1948) to the north and by Pollock (1956) to the south, and 1:250 000 scale mapping by Wynne-Edwards et al. (1966).

Here we report investigations of the apparent intra-CMB geological discontinuities that define the north-facing lobate domain; determine if the anorthosite-mangerite suite of the Morin terrane is present in the CMB, establish the extent and significance of the shear zone observed in 1990, and further characterize terranes in the CMB of Quebec and study their accretionary history. Targets for mineral exploration have been identified, and up-to-date geological maps and geoscientific data are being produced. The rock units, structure, and metamorphism of the Lac Nominingue area are described from a tectonic perspective.

## LITHOLOGIES

Paragneiss in the Lac Nominingue area consists mostly of quartzite and impure quartzite (32% of outcrops investigated) with metapelite and graphite-bearing rusty gneisses in the eastern and central part of the area, and marble and calc-silicate rocks in the west. Orthogneiss includes granitic to tonalitic gneisses and amphibolite. Plutonic rocks make up 10% of the map area. Four elongate, homogeneous porphyritic monzonite bodies (<20 km$^2$) occur along a north-trending corridor in the quartzite-rich domain. Subcircular to elongate, vertically layered mafic intrusions (<20 km$^2$) and other gabbroic bodies are sparsely distributed within the quartzite-rich domain. Isolated occurrences of layered metagabbro and anorthositic gabbro were also observed (UTM, NTS coordinate: 482900E, 5131200N). The 1081 Ma Lac Rouge K-rich alkaline syenitic pluton (23 km$^2$) occurs in the marble-rich domain (Fig. 2). Microdioritic dykes and net-veined dykes are spatially associated with the porphyritic monzonite and gabbro bodies. A clinopyroxene-bearing lamprophyre occurs in the vicinity of the Lac Rouge pluton. A few dykes of hornblende-bearing lamprophyre, an intrusion of phlogopite harzburgite, and a lamprophyric breccia pipe (Fig. 3c) were also encountered. Pegmatite veins and dykes crosscut all previous rock types.

### *Gneisses and marble*

#### Quartzite

On individual outcrops, decimetre- to-metre-scale layers of quartzite and impure quartzite (60% < qtz <90%; Fig. 3b, 4f) are intercalated with centimetre- to decimetre-scale layers of quartzofeldspathic gneiss, rusty-weathering graphitic gneiss, biotite gneiss, and metapelite (sillimanite-biotite). The quartzite layers, folded and boudinaged, form in general more than 60% of the outcrop. The quartzites are grey both in weathered and fresh surface, medium- to coarse-grained, and granoblastic. They locally have a weak biotite foliation and a well developed quartz stretching lineation. The impure quartzites are grey to rusty brown on weathered surfaces, fine- to medium-grained and granoblastic to foliated. Impurities consist of biotite, feldspar and garnet with local magnetite, muscovite, or orthopyroxene.

#### Aluminous paragneiss

Pelitic and semipelitic rocks (<5 m thick) and rare garnetite and Fe-rich metasediments (garnet-magnetite-quartz; <1 m thick) are intercalated with layers of quartzite, biotite gneiss, and rusty-weathering graphitic gneiss at the outcrop scale, and are commonly associated with zones rich in calcareous

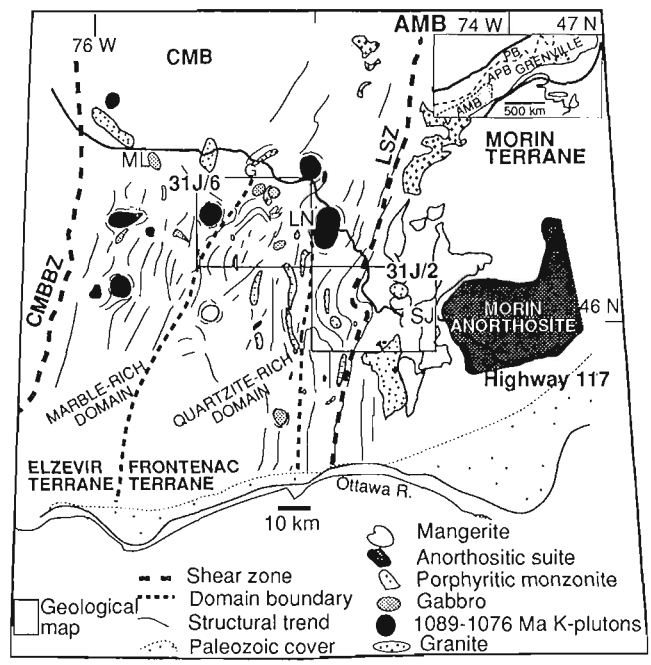


**Figure 1.** Divisions of the Grenville Province (inset; Rivers et al., 1989) and details of the Central Metasedimentary Belt (CMB) in Québec showing plutonic suites and preliminary terrane subdivisions. Abbreviations: AMB-Allochthonous Monocyclic Belt; APB-Allochthonous Polycyclic Belt; CMBBZ-Central Metasedimentary Belt boundary zone; LN-Lac Nominingue; LSZ-Labelle shear zone; ML-Mont-Laurier; PB-Parautochthonous Belt; SJ-Saint-Jovite.

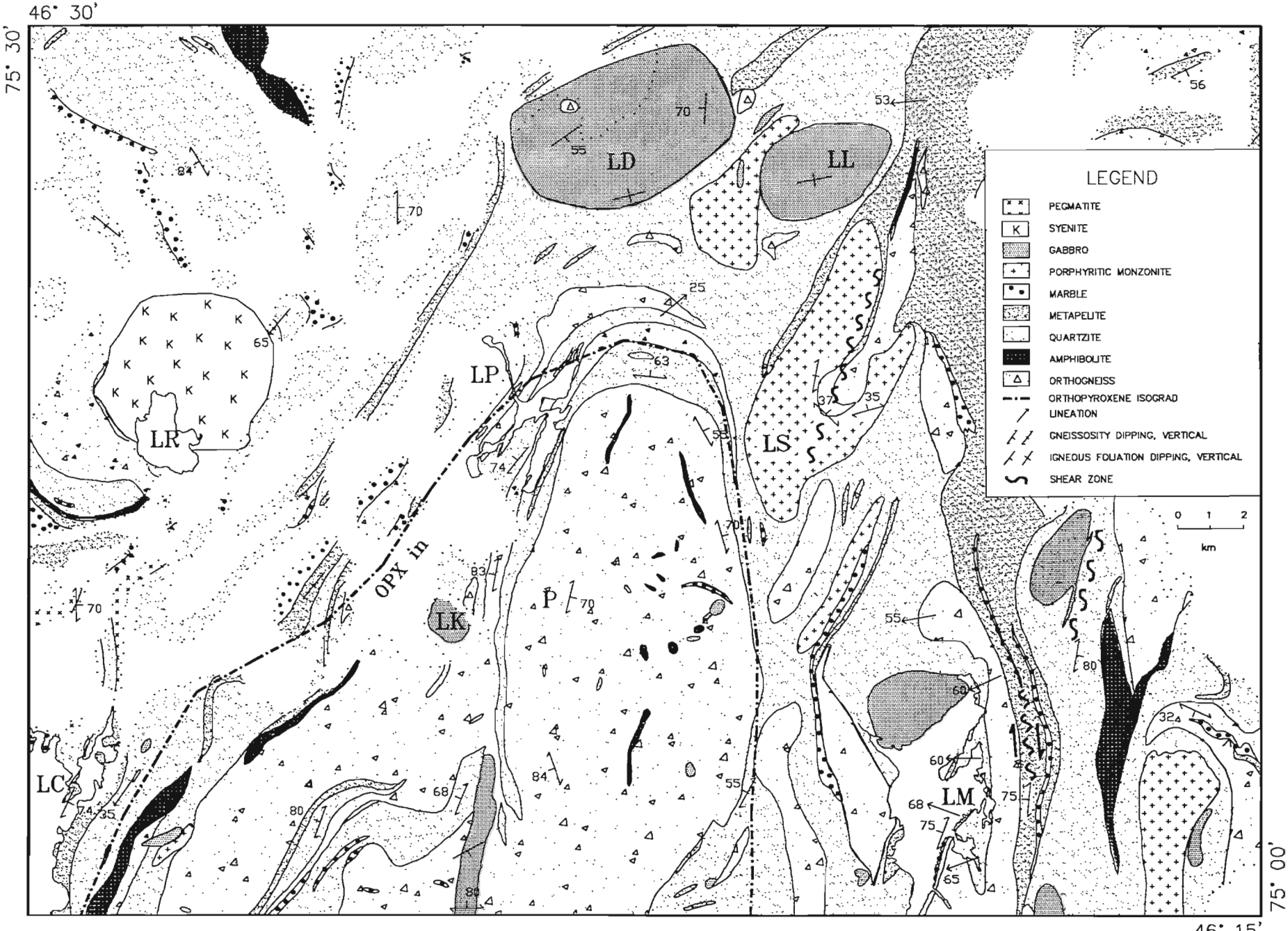


**Figure 2.** Geological map of the Lac Nominingue map area (31J/6). Abbreviations: LD-Lac du Diable ; LL-Lac Lacordaire; LK-Lac Kar-Ha-Kon; LM-Lac Montjoie; LR-Lac Rouge; LS-Lac Saint François; P-lamprophyric breccia pipe.

metasediments at the regional scale (Fig. 2). The aluminous paragneisses are grey, medium grained, foliated, and layered with a rusty weathering. The mineral assemblage biotite-garnet-feldspars-quartz with or without sillimanite is common. Orthopyroxene was found in only one metapelite. In this outcrop, garnet is surrounded by a fine corona of feldspar. Muscovite occurs mostly in an area east of Montjoie Lake and appears to be retrograde after sillimanite. Locally tourmaline, graphite, and Fe-sulphide are present. The orientation of biotite defines a foliation in all outcrops, and that of sillimanite locally defines a lineation. Granitic leucosomes locally carry garnet and occur as irregular veins (<10 cm thick) generally parallel to the foliation and only locally flanked by biotite-rich melanosomes.

### Graphitic gneiss

Graphite and sulphide-bearing quartzofeldspathic (rusty) gneisses are associated with supracrustal assemblages rich in aluminous or calcareous metasediments. Graphite generally forms less than 1% of these rocks.

### Marble

Marble and calc-silicate rocks, invariably invaded by white pegmatite, are poorly exposed but are interpreted to be the dominant unit in the northwestern part of the map area (Fig. 2). Straight layering in medium grained marble occurs southwest of Lac Rouge and may represent an annealed mylonitic fabric. Impurities consist mostly of diopside, graphite, phlogopite, and titanite. Layers of impure marble (<10 m thick) intercalated with quartzite and calc-silicate rocks (Fig. 3b) are scattered throughout the rest of the map area. Marble breccia occurs along Triplet Lake ("marble conglomerate"; Pollock, 1961) and north of Montjoie Lake. Diopsidite and other skarns (<1 m thick) occur mostly as isolated boudins. Hornblende gneiss, interpreted to be paragneiss, occurs north of Montjoie Lake. It is layered, rich in garnet, clinopyroxene or quartz, and intercalated with marble and calc-silicate rocks.

### Orthogneiss

Quartzofeldspathic orthogneisses with biotite, minor hornblende or orthopyroxene, and specks of garnet form heterogeneous units of granitic to tonalitic composition in the central part of the map area (Fig. 2). These orthogneisses weather white, beige, or occasionally pink. They are grey in fresh surface, medium- to fine-grained, and migmatized with granitic leucosomes (<10 cm) parallel to the foliation (Fig. 4e). Amphibolite occurs mostly as dykes (Fig. 3d, f) and transposed dykes (<1 m thick; Fig. 3e, f) in the paragneiss and orthogneiss units. The mineral assemblage hornblende-biotite-plagioclase prevails but garnet, clinopyroxene, and orthopyroxene are locally present (Fig. 4f). Thicker units (<10 m thick) were invaded by granitic veins and form agmatites. The leucosomes are white and hornblende- or orthopyroxene-bearing.

## *Plutonic rocks and dykes*

### Porphyritic monzonite

Porphyritic monzonite bodies are similar to those described in the Saint-Jovite area (Martignole and Corriveau, 1991) but more deformed. They consist of up to 40% K-feldspar augen in a fine- to medium-grained matrix of apatite, biotite, hornblende, K-feldspar, plagioclase, titanite, and zircon. The Lac Saint-François body forms an isoclinal fold and is sheared along one of its flanks (Fig. 2). Dykes of porphyritic monzodiorite, diorite, microdiorite, and net-veined microdioritic dykes (described in Corriveau, 1991) crosscut these plutons and are locally sheared.

### Mafic intrusions

Many of the gabbroic rocks in the map area occur in vertically layered mafic intrusions. A few subcircular or elongate bodies with massive to foliated ophitic gabbro are also present. Gabbros are in general ophitic, medium grained, grey, and mesocratic with an igneous foliation defined by the orientation of plagioclase laths. The grains of plagioclase vary from dark to pale grey but are little recrystallized. Clinopyroxene is the main mafic constituents; orthopyroxene and magnetite are subsidiary, and biotite is rare. Hornblende occurs mostly as thin discontinuous coronas on pyroxene. It is prevalent solely in the contact zones where the gabbros are fine- to medium-grained, recrystallized with a well- to poorly-preserved ophitic texture or a tectonic foliation displayed by the orientation of hornblende and biotite. Away from the contacts, faint- to well-developed modal layering was observed in three well exposed bodies. The layering is in general steeply dipping, discontinuous, and irregular in thickness. It is expressed by the alternation of decimetre- to metre-scale layers of mesocratic gabbro with decimetre-scale layers of anorthositic gabbro, melanocratic gabbro, and pyroxenite (Fig. 4a, c). Variations from outcrop to outcrop suggest that decametre-scale layering is also present. The clinopyroxenites have a few per cent Fe-sulphides and minor chalcopyrite. A xenolith (3 m across) of quartzite similar to quartzite in the country rock occur in the Lac du Diable body. Cognate xenoliths of anorthosite, pyroxenite, and gabbro are also present. Rhythmic layering observed in the Lac Kar-Ha-Kon body consists of magnetite-rich (60%) noritic melagabbro (<1 m thick) intercalated with layers of leucogabbro and mesocratic magnetite-bearing noritic gabbro (UTM: 474700E, 5130250N). In the Lac Lacordaire body, magmatic sedimentation structures include a "drop stone" of orthopyroxene-bearing anorthosite in a clinopyroxene-bearing mesocratic gabbro (Fig. 4b). A reaction rim rich in clinopyroxene formed around the inclusion and was later truncated by magmatic erosion with deposition of a mafic layer followed by the formation of trough bedding (Fig. 4c). Trough bedding was also observed in the Lac du Diable body. The igneous foliation in the latter body defines a concentric pattern parallel its contact. This pattern, the fining of grain size at the contacts of this body, and the presence of a decametre-scale inclusion of country-rock quartzite suggests that this gabbro crystallized in situ after the regional metamorphism, and that its layering

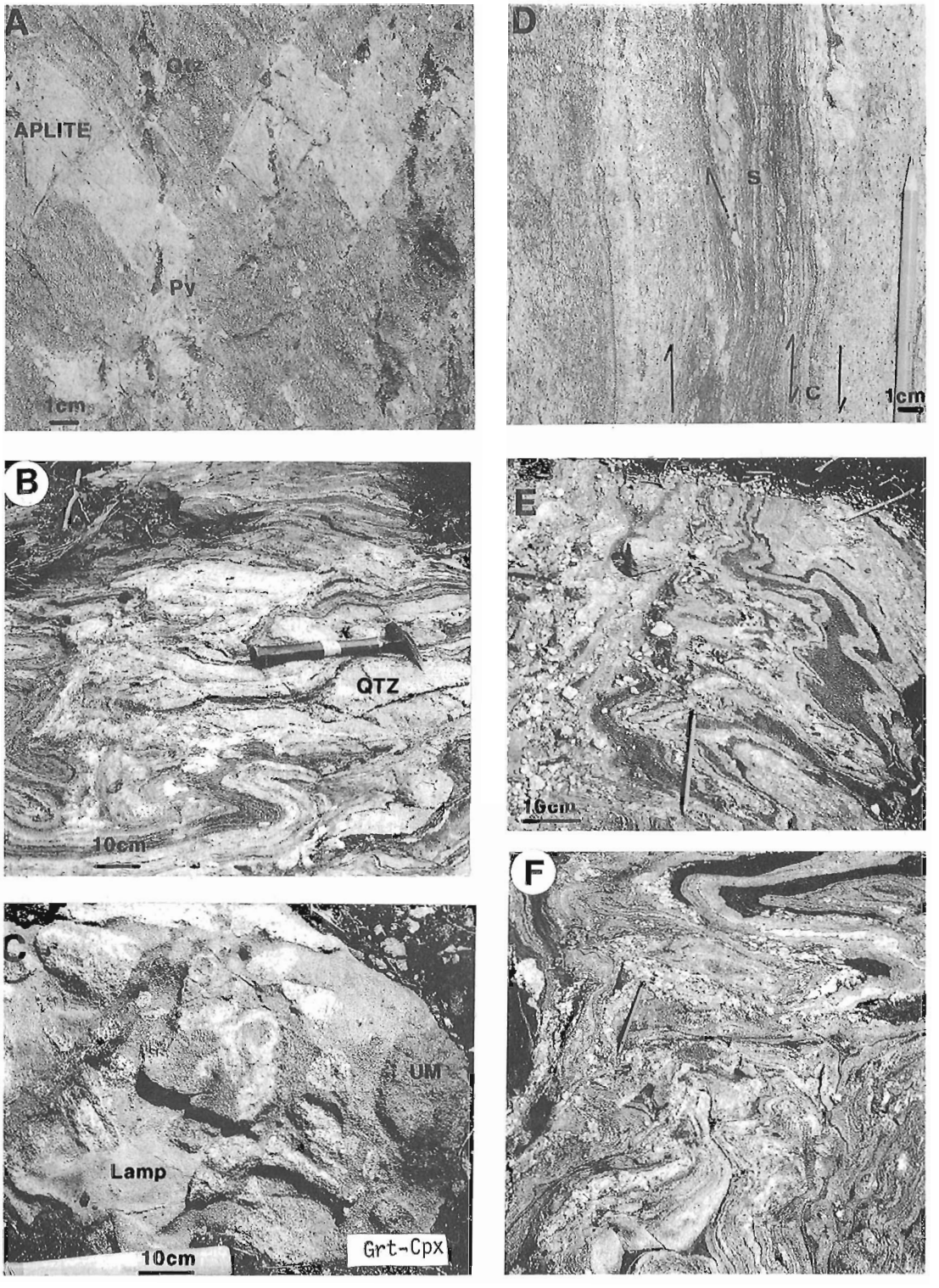


**Figure 3.** **A**) Quartz-pyrite-carbonate veins crosscutting late brittle sinistral faults in a ductile shear zone of the Lac Montjoie high strain zone (UTM: 495050E, 5130630N). **B**) Tightly folded quartzite layers intercalated with biotite-bearing quartzofeldspathic gneisses and calc-silicate rocks (UTM: 471480E, 5131200N). **C**) Lamprophyric breccia pipe with ultramafic xenoliths (UTM: 478440E, 5131570N). **D**) Dextral shear zone in metapelite of the Lac Montjoie high-strain zone; sillimanite lineation is horizontal and parallel to the pencil (UTM: 492980E, 5128670N). **E**), **F**) Disharmonic ptygmatitic folds and rare sheath folds in the Lac Montjoie high-strain zone. Hornblende lineation, quartz stretching lineation and most fold axis are subvertical. Pencils are parallel to the prevalent north-south gneissosity (UTM: 492170E, 5123510N).

was originally vertical. Other gabbroic masses do not show a fining of grain size toward their contact zones, instead coarse- to medium-grained gabbroic and anorthositic rocks are present. The igneous foliation in these bodies is oblique to their contacts. These bodies may be boudins dismembered from larger masses. The foliation of the country rocks is always deflected to concordance with the contacts of these bodies. Net-veined microdioritic dykes, dykes of homogeneous microdiorite, and pegmatites intruded these gabbros and their country rock. These dykes and their host gabbro were locally sheared at amphibolite facies.

### Alkaline rocks

The Lac Rouge pluton (Fig. 1, 2; 1081 ± 2 Ma, Corriveau et al., 1990) is a poorly exposed circular body of undeformed megacrystic potassic alkaline syenite, minor amounts of mica- and apatite-rich pyroxenite, and dykes of syenite and clinopyroxene-bearing lamprophyre (Corriveau, 1990a). Biotite, amphibole, apatite, baddeleyite, and zircon are the main accessory minerals in the syenite. The mica pyroxenite consists of clinopyroxene, biotite, apatite (up to 20%), and a few completely altered grains of nepheline (?). The contact zone consists of hybrid syenite rich in clinopyroxene that is locally injected lit-par-lit into the country rock. In the vicinity of the pluton, the strike of the foliation in the paragneissic country rocks is deflected into concordance with the contact of the pluton. Post-solidification deformation was not observed at the contact of the pluton, and this deflection of the country rock is imputed to diapiric emplacement of the syenite. This body is part of a 1089 to 1076 Ma K-rich alkaline plutonic suite (Corriveau et al., 1990).

An undeformed lamprophyric breccia pipe (>100 m x 1 m) is located in the core of the orthogneiss domain (Fig. 3c). It consists of a fine- to medium-grained hornblende- and biotite-bearing lamprophyre with a wide range of xenoliths. Biotite forms a feathery texture, and hornblende occurs as megacrysts. The xenoliths (<10 cm) are rounded to angular and form 60% of the dyke. The ultramafic xenoliths are rounded and include cpx-grt eclogite (?), medium grained equigranular dunite, clinopyroxenite, biotite-bearing pyroxenite, and websterite. The gabbroic xenoliths are subangular and include coarse massive ophitic gabbro, leucogabbro with an igneous foliation, heterogeneous fine- to coarse-grained gabbro, and recrystallized gabbro with garnet and hornblende. The country-rock xenoliths are angular, with ragged or straight boundaries. They include amphibolite, quartzite, and pegmatite. The shape of xenoliths is consistent with a longer transport for the ultramafic xenoliths which might be of mantle origin.

Phlogopite harzburgite (<1 km) occurs in an homogeneous, nondeformed intrusive (UTM: 481500E, 5132500N) of fresh, medium grained, euhedral olivine (very minor serpentine along fractures) with spinel inclusions, of subhedral orthopyroxene with exsolution lamellae and anhedral plagioclase, biotite, and brown amphibole. It is distinct from the 1089-1076 Ma K-rich alkaline rocks in having abundant olivine and brown amphibole.

Dykes of hornblende-bearing lamprophyre crosscut a gabbro body and a granitic orthogneiss (UTM: 491700E, 5122830N; 493300E, 5132300N).

### Pegmatites

White pegmatites are coarse- to medium-grained, leucocratic, granitic in composition massive to foliated, discontinuous in extent, irregular in thickness, and ubiquitous throughout the whole map sheet. A few pegmatite dykes (<10 cm) are straight and nondeformed. Muscovite- and tourmaline-bearing pegmatite veins are common throughout the Montjoie high-strain zone (see below) but rare in other areas of the map sheet.

## STRUCTURE

### *Regional structure*

The gneissosity ("S1" surface) is the dominant structure in the map area and is locally axial planar to isoclinal intrafolial F1 folds. It is generally oriented north to northeast and dips steeply to the east or west. The gneissosity is commonly tightly folded (F2 generation) without the development of an axial planar foliation. The F2 fold axial planes have a variable orientation from outcrop to outcrop and are locally refolded by an F3 generation (mostly divergent-convergent interference pattern) with an S3 foliation defined by the orientation of biotite along their axial plane. Microdioritic dykes crosscut the F2 folds; they are themselves tightly-to-openly folded (F3 generation) and have a strong mineral lineation parallel to the lineation of the country rock (Fig. 4d, f). In the central part of the map area, the S1 gneissosity defines an antiform of kilometre-scale amplitude with a fold axis plunging 30 to 35°N. The Lac Saint-François porphyritic monzonite forms a synform plunging at 40-45°N. A steeply-dipping shear zone traced over 6 km formed along the axial plane of this fold. Variations in the orientation and the type (S vs. Z) of the F2 folds along the same limb of the regional fold indicate that the latter is of the F3 generation. The regional foliation is deflected around the edges of the mafic intrusions. A circular foliation pattern a few kilometres in diameter is observed within the orthogneiss in the core of the antiform. Due west of this pattern, a lamprophyric breccia pipe has entrained xenoliths of a gabbro. The local concentric foliation pattern is attributed to the presence of a subsurface body of gabbro. As the axial plane of the regional F3 fold is subvertical, it is unlikely that this folding was induced by the emplacement of this or other mafic bodies. The major fold in the map area appears to result from a late period of regional deformation that postdates the emplacement of the monzonitic bodies.

Subvertical ductile shear zones (up to 1 m thick) have been observed in the central part of the map area along a set of norhwest-southeast lineaments; others have an east-west orientation.

### *The Lac Montjoie high-strain zone*

The Lac Montjoie high-strain zone (>10 km x 3 km) is a north trending structure that extends across the 31J/6 map sheet, east of Montjoie Lake (Fig. 2). It consists of discontinuous shear zones within a zone of pervasive high-strain ductile deformation. The western side is characterized by ubiquitous, tight to isoclinal M folds with subvertical axial plane, fold axis, mineral lineation (sillimanite in metapelite, hornblende in amphibolite), and quartz stretching lineation in pegmatitic veins. Vertical shear zones with C and S fabrics and a vertical lineation indicate a west side up sense of movement. Disharmonic ptygmatic folds and rare sheath folds occur in the center of the Lac Montjoie high-strain zone (Fig. 3e, f). The hornblende lineation, the quartz stretching lineation, and most fold axis are subvertical. This structural pattern suggests large-scale sheath folding in the area. To the east, the supracrustal rocks are strongly deformed with a steep foliation and well-developed subhorizontal mineral and stretching lineations. Shear-sense indicators suggest a dextral sense of movement along this shear zone (Fig. 2). A shear zone (Fig. 4 in Corriveau, 1991) with a gently, southeast dipping C foliation and a down-dip lineation outcrops at the northeastern edge of the deformation zone. It encloses blocks of ophitic to highly mylonitized metagabbro. Homogeneous and net-veined microdioritic dykes crosscut the shear fabrics and are themselves folded with the axial plane subparallel to the foliation in the shear zone and a hornblende lineation parallel to that of the shear zone.

The assemblages sillimanite-garnet-biotite-feldspars-quartz in metapelite with sillimanite lineation and of hornblende-biotite-plagioclase in amphibolite with hornblende lineation indicates that the ductile shearing took place at upper amphibolite facies. Retrogression of the maximum phase assemblages occurs locally with the appearance of muscovite in pelitic and semipelitic rocks.

Late brittle deformation is locally superimposed upon the ductile deformation on the eastern edge of the Lac Montjoie high-strain zone. Aplitic dykes are locally displaced along sinistral faults upon which are superposed tension gashes (Fig. 3a) filled with quartz-pyrite-carbonate. The veins are restricted to the aplite; their distribution is controlled by the competency of the rock. Centimetre-scale quartz-carbonate-pyrrhotite veins also occur farther east in an amphibolite.

## METAMORPHISM

Metamorphic grade ranges from upper amphibolite to granulite facies. In calcareous metasediments, the assemblage calcite-quartz is stable throughout the entire map area, and the prevalent assemblage is calcite-diopside-phlogopite-graphite with or without plagioclase. In metapelite, the assemblage biotite-garnet-sillimanite-K-feldspar-plagioclase-quartz occurs throughout the entire map area. Orthopyroxene was observed in a metapelite but does not appear to be in equilibrium with sillimanite, suggesting that pressure did not reached 800 MPa. The assemblages hornblende-plagioclase-biotite-quartz (amphibolite) and biotite-feldspars-quartz with or without garnet or hornblende (felsic orthogneisses) occur throughout the entire map area. In the south-central part of the map area, orthopyroxene was observed in felsic orthogneiss, transposed dykes of amphibolite, leucosomes parallels to the S1 gneissosity, and in dykes that crosscut the regional S1 foliation (Fig. 4f). Orthopyroxene was not observed in rocks of the marble-rich domain nor east of the Lac Montjoie high-strain zone. Based upon field observations, granulite facies rocks are thus restricted to the core of the regional antiform. The orthopyroxene isograd (Fig. 2) is folded and follows the eastern limit of the marble-rich domain, curves around the regional antiform with only a few occurrences of metamorphic orthopyroxene in the vicinity of the layered intrusions, then follows the western margin of the Lac Montjoie high-strain zone. Folding of this isograd is likely contemporaneous with the F3 folding in the area. The orthopyroxene isograd in the Labelle shear zone was also folded (Fig. 1 in Martignole and Corriveau, 1991). By tracing the orthopyroxene isograd throughout the CMB, the extent of the deformation contemporaneous with shearing along the Labelle shear zone could be established.

## GEOLOGICAL SETTINGS FAVORABLE FOR MINERAL DEPOSITS

The late episode of brittle deformation within the Lac Montjoie high-strain zone was a favorable setting for gold mineralization. It presents similarities with the Robertson Lake Mylonite Zone in the Ontario part of the CMB. The RLMZ is a major deformation zone traced over 70 km where ductile deformation was followed by brittle deformation. Several gold showings occur in this structure and the mineralization (filling open fractures in some places) is associated with the late brittle deformation (Jourdain et al., 1990).

The Lac Montjoie high-strain zone also contains an outcrop of sulphide-rich amphibolite (UTM: 496970E, 5129490N). The sulphides, pyrrhotite, and minor pyrite, occur in three different forms: as massive in a lens of 5 x 0.3 m parallel to the foliation of the amphibolite, disseminated in the amphibolite, and in quartz-carbonate veins perpendicular to the amphibolite body with decimetre spacing for about 40 m. The visible alteration zones associated with these veins (<2 cm) do not show any foliation suggesting that little movement was involved during the formation of the veins. Similar veins also occur locally in the adjacent quartzite and metapelite.

Two bands of metasediments include layers with more than 5% graphite. The first, located southeast of Pimodan Lake, is rich in metapelite and extends for 3 km with a width of 2-300 m (8-10% graphite in a Q-Fp gneiss 1 x 0.1 m; UTM 477070E, 5134120N). The second, located northeast of Lac du Cerf, contains some impure quartzites, calc-silicate rocks and metapelites, each unit may host significant amount of graphite (5% graphite, >5 m thick; UTM 469910E, 5134350N).

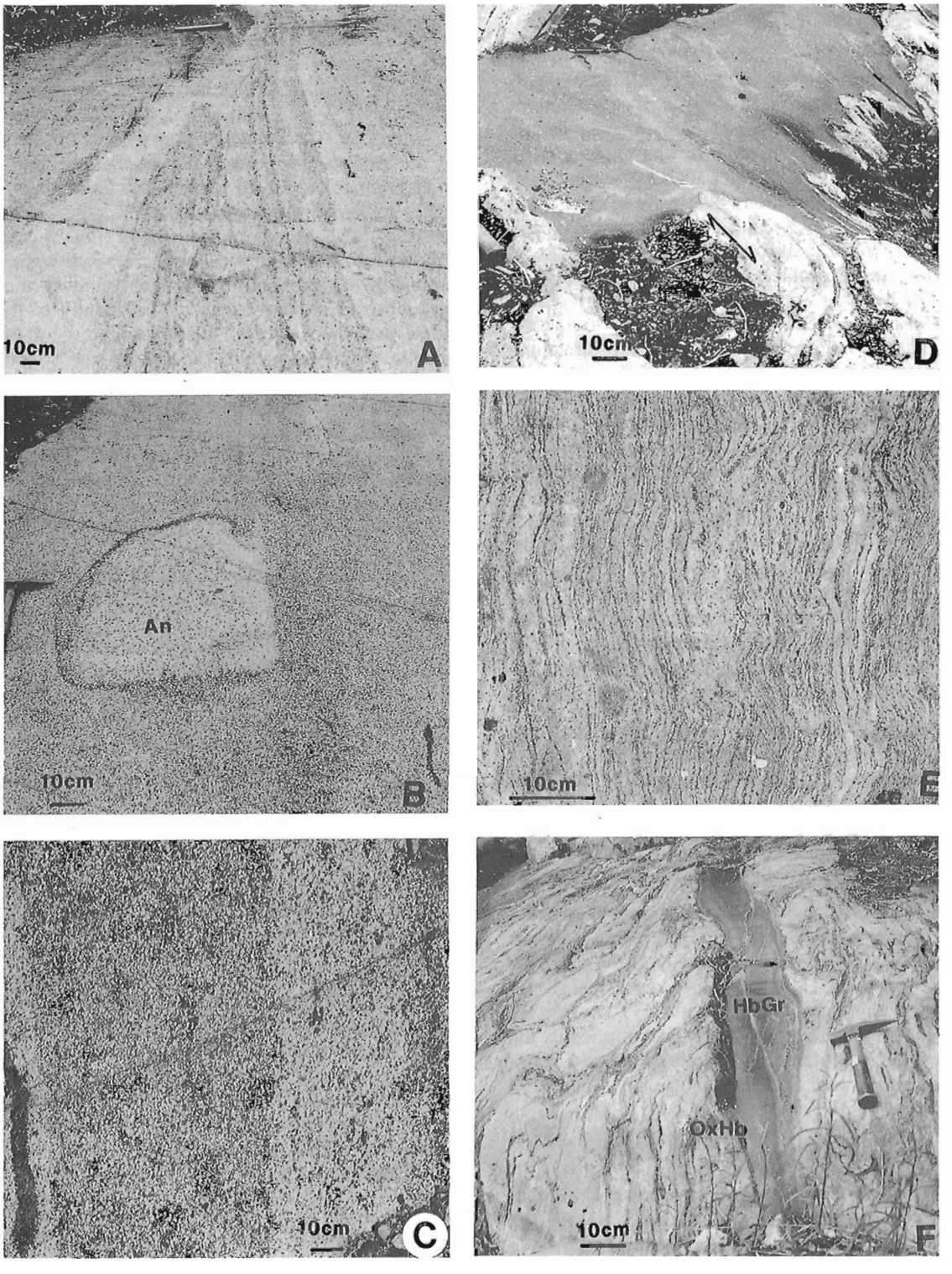


**Figure 4**. **A**), **B**) Vertical trough layering and anorthosite "drop stone" in the Lac Lacordaire mafic intrusion (UTM: 487360E, 5144880N). **C**) Rhythmic modal layering and pyroxenite schlieren in the Lac du Diable body (UTM: 477360E, 5146450N). **D**) Microdioritic dyke with a gabbroic enclave crosscutting the regional foliation in the quartzite and folded isoclinally. Hornblende lineation along the fold axis (UTM: 489590E, 5147130N). **E**) Migmatitic granitic orthogneiss with garnet and orthopyroxene (UTM: 470650E, 5125840N). **F**) Quartzite and metapelite, folded and boudinaged, crosscut by a folded amphibolite dyke (fold not shown in the photo). The dyke is zoned with hornblende and garnet at the center and a reaction rim of orthopyroxene and hornblende along the contact with quartzite (UTM: 476760E, 5138060N).

The vertically layered mafic intrusions offer some potential for Ni-Cu (PGE) mineralization. The poorly exposed mica pyroxenite in the Lac Rouge pluton includes up to 20% apatite.

## CONCLUDING REMARKS

### *Terrane characterization*

Two supracrustal domains have been documented in the Lac Nominingue area. Marble, subordinate quartzite, aluminous metasediments, and rusty graphitic gneiss characterize the western portion of the map area and the CMB in Quebec in general. In contrast, quartzite is omnipresent in the domain postulated to be an extension of the Frontenac terrane. The north-trending Lac Montjoie high strain zone occurs near the eastern limit of the quartzite-rich domain. At the formerly postulated north-facing lobate northern boundary of the domain, we found no break in the supracrustal sequence and no shear zone; further work is required to establish the northern extent of the quartzite-rich domain. The thick units of homogeneous fine- to medium-grained leucocratic orthogneiss, the amphibolite sills and the abundant rusty quartzofeldpathic graphitic gneiss along the eastern boundary of the CMB (31J/2 map area) are absent or rare in the quartzite-rich domain. The monzonitic plutons which were intercalated with metagabbro as sheet-like bodies along the regional structure of the Labelle shear zone (31J/2) form, in the quartzite-rich domain, individual homogeneous plutons that are locally isoclinally folded, whereas the gabbros occur as subcircular vertically layered intrusions. The lamprophyres and the phlogopite harzburgite in the quartzite-rich domain appear to have a composition distinct from that of the 1089-1076 Ma K-rich alkaline plutons found in the marble-rich domain.

Mapping has produced new evidence for the presence of distinct lithotectonic domains in the CMB. The quartzite-rich domain is likely an extension of the Frontenac terrane as both are characterized by abundant quartzite, irregular aeromagnetic anomalies, and granulite facies metamorphism. Anorthositic rocks reported in the Lac Nominingue area occur in the layered intrusions and are distinct from the massif-type anorthosites found in the Morin terrane. This confirms the marked differences of some of the plutonic suites between the Morin terrane and the CMB. There is, however, some continuity in structure across the Labelle shear zone.

### *Chronology of events*

A relative chronology of events is proposed for the quartzite-rich domain using the net-veined dykes as a regional marker. These dykes are spatially associated with the gabbroic intrusions; they crosscut the monzonitic and gabbroic rocks, the gneissosity and the F2 folds in the supracrustal rocks, and the gneissosity in the shear zones of the Montjoie high strain zone. These dykes are themselves openly to tightly folded (F3) with hornblende aligned parallel to the fold axis in the dyke and the mineral lineation in the host rocks. The mafic layered intrusions are not recrystallized except along some contact zones. Blocks of gabbro and mylonitized gabbro have been entrained in shear zones of the Lac Montjoie deformation zone. Thus the mafic intrusions postdate the regional metamorphism and penetrative "D1" and "D2" deformation at amphibolite to granulite facies but predate the ductile "D3" deformation at amphibolite facies. This deformation likely induced mantling of the foliation around the more competent gabbroic masses.

A partial chronology of events in the quartzite-rich domains is: supracrustal rocks were regionally deformed and metamorphosed to amphibolite to granulite facies, forming the S1 gneissosity and F2 folds. These supracrustal rocks were then intruded by monzonitic and gabbroic plutons and microdioritic net-veined dykes. The emplacement of gabbro as sheet-like bodies in the Labelle shear zone but as layered intrusions in the quartzite-rich domain suggests that deformation was in progress in the Labelle shear zone while the quartzite-rich domain was tectonically in extension or neutral. Following this magmatism, the rocks were subsequently deformed during a "D3" phase which refolded the supracrustal rocks, folded the orthopyroxene isograd and resulted in the kilometre-scale regional fold. Shearing along the Montjoie high strain zone at amphibolite facies may have been contemporaneous with the "D3" deformation. Shearing at amphibolite facies and folding of an orthopyroxene isograd were also observed in the Labelle shear zone. The "D3" deformation in the area was possibly contemporaneous with the sinistral shearing in the Labelle shear zone. Folding of the F3 axial plane suggests that the rocks were subsequently deformed by a "D4" deformation.

## ACKNOWLEDGMENTS

We thank Nalini Mohan and Glenna Gosselin for their assistance during the field season; Boyan Brodaric for his help with the Fieldlog computer program; Tony Davidson, Kathy Bethune, and Otto van Breemen for discussions in the field; and Graphicor for permission to publish our geological data located on their claims in the Rivard township. Tyson Birkett reviewed the manuscript.

## REFERENCES

**Aubert de la Rue, E.**

1948: Les régions de Nominingue et de Sicotte; Rapport géologique 23, Ministère des Mines, Québec, 74 p.

**Corriveau, L.**

1990a: Proterozoic potassium-rich alkaline plutonism in the southwestern Grenville Province; Ph.D. thesis, McGill University, Montréal, Canada, 263 p.

1990b: Proterozoic subduction and terrane amalgamation in the southwestern Grenville province, Canada: evidence from ultrapotassic to shoshonitic plutonism; Geology, v. 15, p. 614-617.

**Corriveau, L., Heaman, L.M., Marcantonio, F., and van Breemen, O.**

1990: 1.1 Ga K-rich alkaline plutonism in the southwestern Grenville Province – U-Pb constraints for the timing of subduction-related magmatism; Contributions to Mineralogy and Petrology, v. 105, p. 473-485.

1991: Lithotectonic studies in the Central Metasedimentary Belt of the southwestern Grenville Province: plutonic assemblages as indicators of tectonic setting; in Current Research, Part C; Geological Survey of Canada, Paper 91-1C, p. 89-98.

**Jourdain, V., Gauthier, M., and Guha, J.**
1990: Métallogénie de l'or dans le sud-ouest de la province de Grenville; Geological Survey of Canada, Open File 2287, 52 p.

**Martignole, J. and Corriveau, L.**
1991: Lithotectonic studies in the Central Metasedimentary Belt of the southern Grenville Province: lithology and structure of the Saint-Jovite map area, Québec; in Current Research, Part C; Geological Survey of Canada, Paper 91-1C, p. 77-88.

**Pollock, D.W.**
1961: Rapport préliminaire sur la région de Lesage-Rivard, comté Labelle; Ministère des Richesses naturelles, Québec, 12 p.

**Rivers, T, Martignole, J., Gower, C.F., and Davidson, A.**
1989: New tectonic divisions of the Grenville Province, southeast Canadian shield; Tectonics, v. 8, p. 63-84.

**Wynne-Edwards, H.R., Gregory, A.F., Hay, P.W., Giovanella, C.A., and Renhardt, E.W.**
1966: Mont-Laurier and Kempt lake map area, Quebec; Geological Survey of Canada, Paper 66-32, 32 p.

Geological Survey of Canada Project 900007

# The upper part of the Muskox Intrusion, Northwest Territories

**Jean H. Bédard and Mehmet F. Taner[1]**
**Quebec Geoscience Centre, Sainte-Foy**

*Bédard, J.H. and Taner, M.F., 1992: The upper part of the Muskox Intrusion, Northwest Territories; in Current Research, Part C; Geological Survey of Canada, Paper 92-1C, p. 91-101.*

***Abstract***

*The upper part of the Muskox layered intrusion is dominated by gabbro-norite, which becomes more differentiated upwards. Gabbro-norite evolution is periodically interrupted by peridotite layers. The appearance of peridotite is preceded by precursory changes in geochemical parameters, the re-appearance of pyroxenitic layers, and of coarse grained orthopyroxene in the interlayered gabbro-norite. Either the main replenishment was preceded by smaller pulses of primitive magma, or there was turbulent mixing near the head of the replenishing magma as it spread across the intrusion's floor. Peridotite is typically overlain by pyroxenite, and then by normal gabbro-norite. The pyroxenite that overlies peridotite may contain xenocrysts which suggest magma mixing or hybridization.*

***Résumé***

*La partie supérieure de l'intrusion litée du Muskox est dominée par des gabbro-norites qui sont plus différenciées vers le haut. L'évolution des gabbro-norites est périodiquement interrompue par d'épaisses couches de péridotite. L'apparition des péridotites est précédée par des changements géochimiques et minéralogiques précurseurs, ainsi que par la réapparition de lits de pyroxénite et des gabbro-norites à phénocristaux d'orthopyroxène. Soit que les afflux picritiques principaux ont été précédés par de petites injections, soit il y a eu des mélanges turbulents lorsque les afflux se sont répandus sur le plancher de l'intrusion. Les péridotites sont succédées par des pyroxénites et ensuite par des gabbro-norites normales. Certaines de ces pyroxénites contiennent des xénocristaux, signe que des processus d'hybridation ont joué un rôle dans leur genèse.*

[1] 3190 Édouard Monpetit, Apt. 510, Montreal, Quebec H3T 1K2

## INTRODUCTION

Magma chamber replenishment by primitive parental magmas is frequently invoked to explain cyclic alternations of peridotite and gabbro in layered intrusions (Wager and Brown, 1968). However, many cumulates from large layered intrusions are texturally re-equilibrated (Hunter, 1987). Imperfect textural preservation makes it difficult to demonstrate unambiguously that chamber replenishment has occurred (e.g., cf. Bédard et al., 1988; Lee and Butcher, 1990). In this paper we present new modal and petrographic data from the upper flank of the Muskox intrusion. The samples studied have orthocumulate textures, with euhedral, concentrically-zoned cumulus minerals and interstitial granophyre, mica, and oxides. The preservation of primary textures allows documentation of magma chamber replenishment.

In the Muskox, the relative order of liquidus minerals changes with time. The lower part of the complex is characterized by a lineage with early clinopyroxene and postcumulus orthopyroxene, while in the upper part orthopyroxene is an early, cumulus mineral (Irvine and Smith, 1967). Crustal contamination may account for the early appearance of liquidus orthopyroxene (Sparks, 1986) and the abundant interstitial granophyre. The studied section records deposition of cumulates belonging to these two lineages (early clinopyroxene versus orthopyroxene), and for local hybridization between them. This bears on the debate about the origin of cumulate orthopyroxenite to websterite layering sequences (Irvine, 1970).

We begin by describing the lithology and petrography of the section, followed by brief consideration of whole-rock and mineral-chemical profiles. A more complete study that integrates the mineral and whole-rock chemistry will be presented elsewhere.

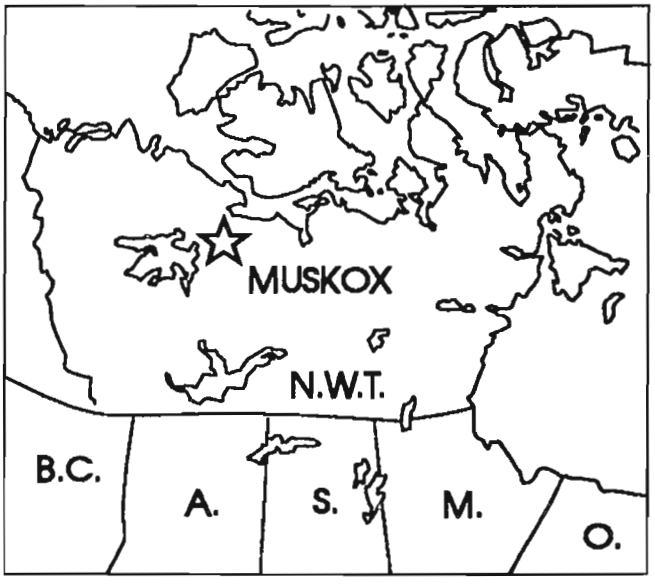


**Figure 1a.** Location map. A=Alberta, B.C.=British Columbia, S.=Saskatchewan, O.=Ontario, N.W.T.=Northwest Territories.

## BACKROUND AND METHODOLOGY

The Muskox is a funnel-shaped Proterozoic layered intrusion in the Northwest Territories (Fig. 1). It may be the southward extension of a larger body that also fed the Coppermine River Basalts (cf. Dostal et al., 1983).

This paper discusses composite sample Sections D and K (Figure 2). Section K is less than 100 m north of Section D, and is considered together with it. Stratigraphic height was measured in the field. Figure 8 (below) can be used as a lithological column for reference. For chemical analysis, altered rinds were removed with a saw prior to crushing in an agate shatterbox. Data was generated at the GSC in Ottawa. Mineral chemical analyses were done on a Cameca Camebax electron microprobe, either at the GSC or at McGill University. Analytical details will be presented elsewhere. Modal data was calculated by least-squares mixing of whole-rock and mineral analyses (Fig. 3, 4). Magnetite and ilmenite are idealized end-members. The granophyre component is a granophyric dyke (D35) collected from within the layered sequence. Where mineral chemical data was lacking, minerals from the nearest analogous sample were used. The weight % proportions were converted to volume modes using the conversion factors in Hutchison (1975). A constant Forsterite 82, Enstatite 82, Anorthite 60, Annite 25, pure magnetite, ilmenite, and Fe-chromite were used. Interstitial granophyre was assumed to be a 1:1:1 mix of albite, orthoclase and quartz. Rock names given are those of the traditional map units.

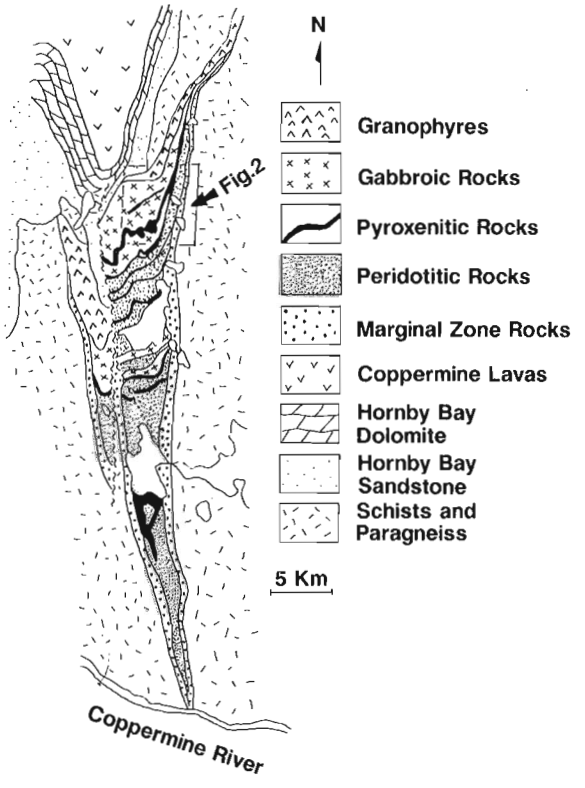


**Figure 1b.** Simplified map of the Muskox Intrusion, adapted from Irvine and Smith (1967).

## THE SECTION

Preservation of primary igneous mineralogy and textures is typical. Orthopyroxene commonly has fine, length-parallel exsolution lamellae of the Bushveld Type. In some units, it has random or oriented arrays of clinopyroxene blebs, referred to as vermicular in the text. It is uncertain whether these represent exsolution, symplectic recrystallization, or eutectoid intergrowth phenomena. Euhedral or ophitic clinopyroxene commonly has fine exsolution lamellae and turbidity. Commonly, clinopyroxene is partially to completely replaced by a sieve-textured aggregate of high-Ca clinopyroxene, mica, and magnetite. In some cases, a clear spatial association is observed between the development of sieved clinopyroxene and interstitial granophyre+ mica+oxides. This suggests that sieving results from a reaction between high-temperature clinopyroxene and K-Fe-rich interstitial melt. Partial serpentinization of olivine is common. Intense hydrothermal alteration is rare, with partial to complete sericitization of feldspar, chloritization of mica, and the development of turbidity in pyroxenes. Adjacent to granophyric dykes and quartz-calcite veins, chlorite and actinolite(?) replace pyroxenes, there is silicification or potassic(?) alteration of feldspars, and the local development of epidote and pumpellyite.

### *Unit 1, feldspathic heteradcumulate lherzolite, >40 metres*

The section is rooted in a feldspathic heteradcumulate peridotite, which may display indistinct 1-10 cm scale layering defined by variations in the mode of interstitial phases. Olivine is ovoid and generally about 1 mm in size. Tiny euhedral chromite (1-3%) is generally included in olivine. Olivine is embedded in oikocrysts (up to 2 cm) of plagioclase, orthopyroxene, clinopyroxene, and phlogopite. Trace sulphides (pyrite, chalcopyrite, pentlandite) are also present.

### *Unit 2, Fe-Ti-oxide gabbro-norite, 2 metres*

After a gap in the section, the first and only outcrop of Unit 2 is composed of foliated, medium grained, Fe-Ti-oxide-bearing gabbro-norite; the upper surface of which displays

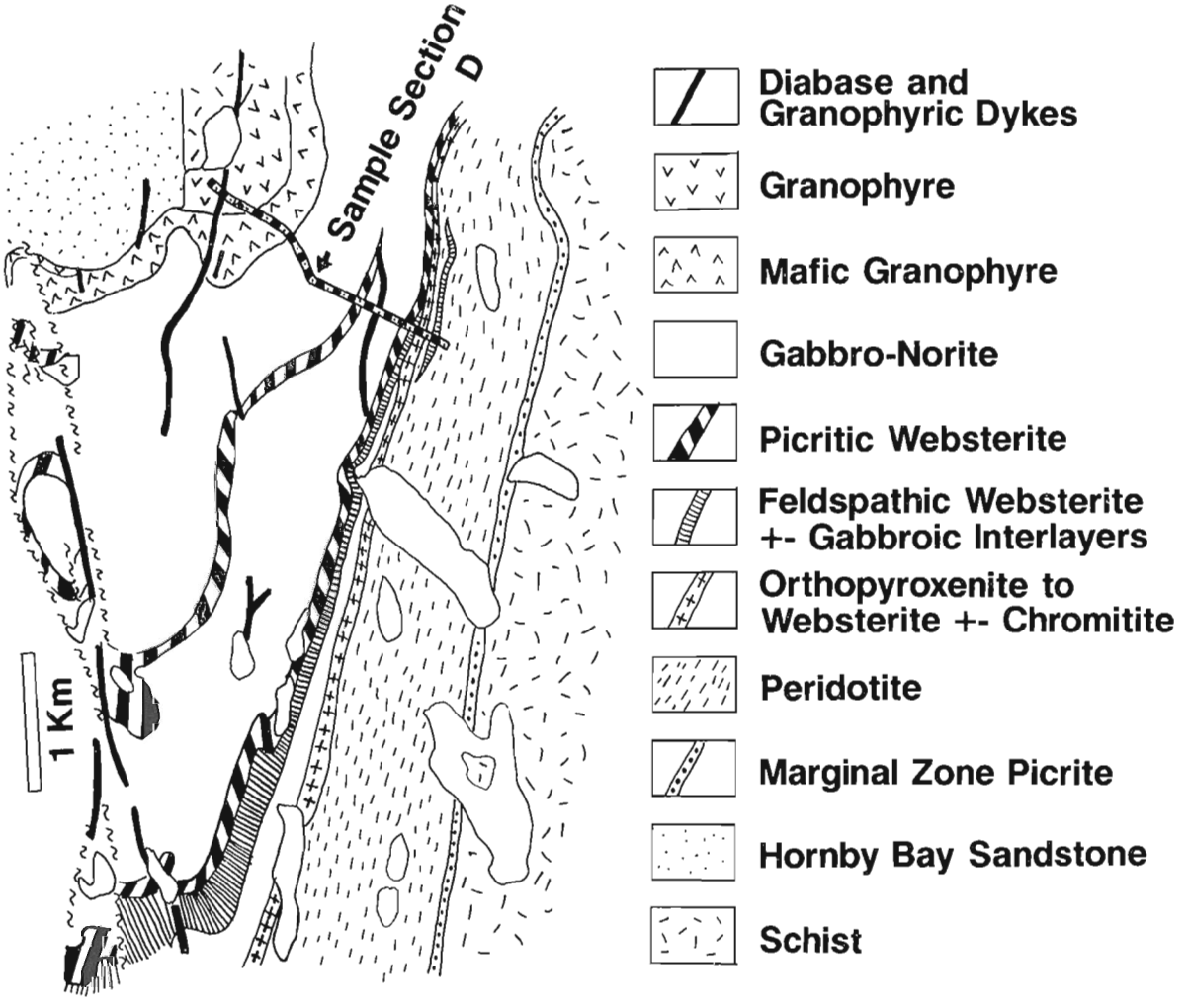


**Figure 2.** Simplified detail map adapted from Smith et al. (1963).

1 m of relief. Units 2 to 4 are laterally impersistent and occur nowhere else. The foliation is defined by the preferred orientation of orthopyroxene, plagioclase, and to a lesser extent clinopyroxene. Orthopyroxene is euhedral to subeuhedral, prismatic, has weak pink/green pleiochroism, is normally zoned, and may contain tiny, ovoid inclusions of plagioclase. Clinopyroxene is generally finer grained and less abundant than orthopyroxene; it is faintly greenish in thin section, and is generally anhedral. Plagioclase laths are almost completely sericitized. Magnetite and ilmenite occur as coarsely intergrown anhedral grains. Biotite, quartz, pyrite, and chalcopyrite occur in trace amounts.

### *Unit 3, inter-layered, olivine gabbro-norite and feldspathic olivine websterite, 4 metres*

Interlayered (223/22°N), foliated, olivine gabbro-norite, and feldspathic olivine websterite overlie Unit 2. Layers (2-5 cm) thin towards a culmination in Unit 2, and appear to drape over it. These features are consistent with a depositional origin, followed by a compaction event. The gabbro-norite layers are locally disrupted, forming convoluted lenses (Fig. 5). In places, the gabbro-norite lenses are discordant to the general layering orientation, and are penetrated by websterite fingers (Fig. 6), a texture which has been interpreted in terms of corrosion in other intrusions (cf. Robbins, 1982; Butcher et al., 1985; Bédard et al., 1988). In the example illustrated in Figure 6, anorthositic schlieren in the gabbro-norite lens are discordant to the internal foliation, but are parallel to the layering in the surrounding websterite. They may represent a late, postcumulate replacement event (cf. Figure 2b in McBirney, 1987).

The olivine gabbro-norite of Unit 3 differs from the underlying Unit 2 gabbro-norite by the presence of minor olivine, and a lower OPX/PX ratio. Olivine is anhedral, and includes small plagioclase laths. Plagioclase occurs as normally-zoned laths (average ~1 mm). The groundmass is dominated by plagioclase and fine grained clinopyroxene. Reddish mica is absent or rare.

In contrast, the interlayered feldspathic olivine websterite contains less plagioclase, and has more abundant pyroxene and olivine. The olivine is larger (0.5-2 mm) and may be

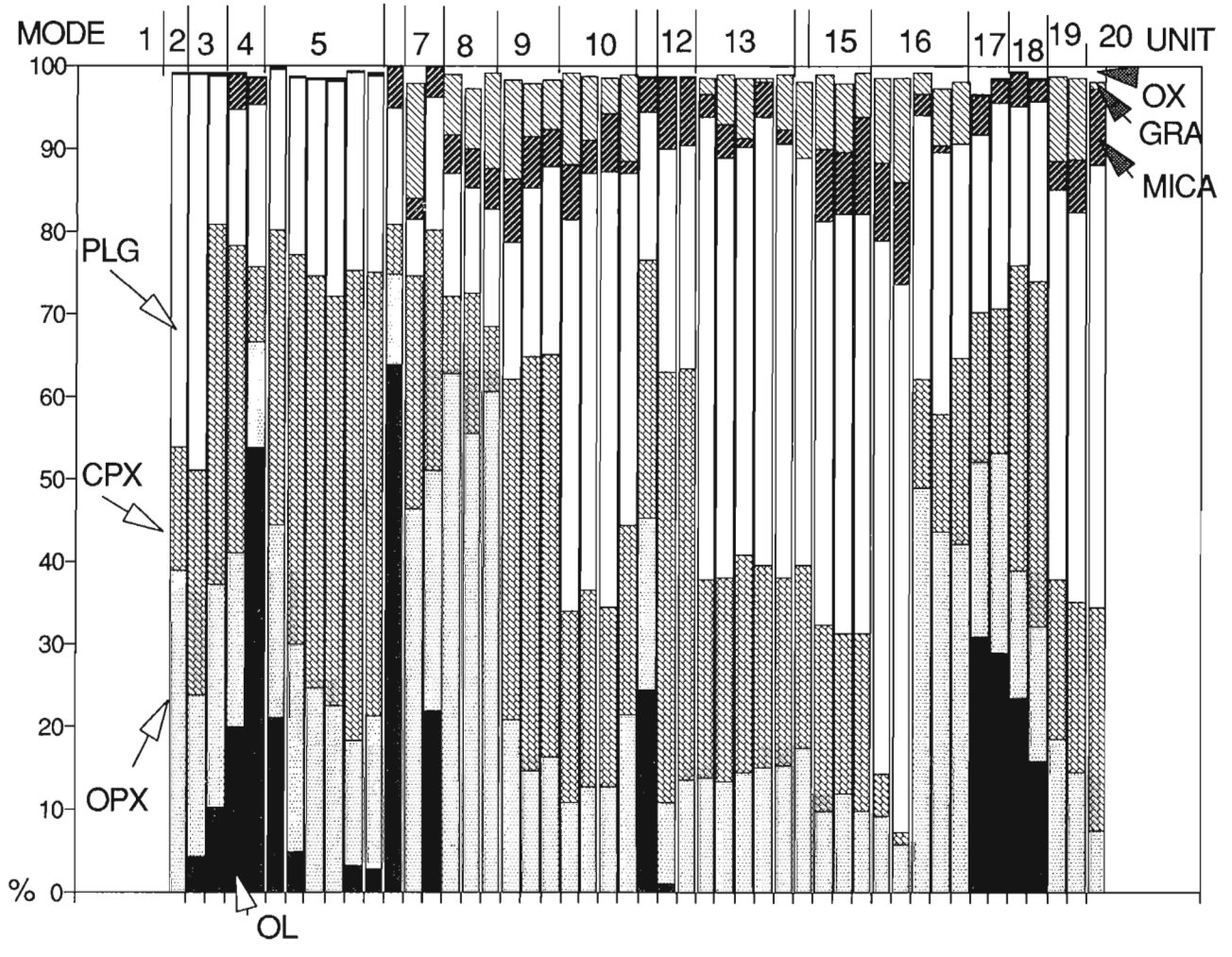


**Figure 3.** Modal stratigraphy of the complex. PLG=plagioclase, CPX=clinopyroxene, OPX=orthopyroxene, OL=olivine, GRA=granophyre, OX=oxides (ilmenite, magnetite, and spinel).

perfectly euhedral or subeuhedral. Orthopyroxene occurs as large (1-6 mm) euhedral to subeuhedral prisms that contain inclusions of olivine, clinopyroxene, plagioclase, and an Fe-oxide mineral. Textures suggest local replacement of olivine by orthopyroxene. Clinopyroxene is generally finer grained (0.2-0.8 mm). Some grains occur as well-shaped prisms, but most are anhedral to subeuhedral. Plagioclase forms large (up to 3 mm) anhedral oikocrysts, with 120° triple junctions. Some magnetite(?) grains contain coarse lamellar ilmenite(?) exsolutions. Red-brown mica is present in trace amounts. The pyroxenite interlayers and the replacive pyroxenite are texturally and modally similar. This suggests dissolution/precipitation, rather than metasomatic replacement.

### *Unit 4, interlayered feldspathic olivine websterite and feldspathic heteradcumulate lherzolite (same as Unit 1), 20 metres*

The Unit 3/4 boundary is defined as the last thick layer of gabbro-norite; only rare gabbroic schlieren occur in Unit 4. The section is dominated by thin (1-5 cm) layers of feldspathic olivine websterite (~30%) and feldspathic lherzolite (~70%). Layers are laterally continuous over at least 20 m, though some layers pinch out or thin laterally. No grain size or modal grading was observed. The lherzolite and pyroxenite are texturally almost identical to those of units 1 and 3, respectively, except for the greater abundance of olivine in the Unit 4 pyroxenite.

### *Unit 5, feldspathic olivine websterite and feldspathic websterite, 7.5 metres*

This unit is laterally continuous over at least 50m, and has sharp, conformable contacts. It is missing from sections taken to the south, but reappears towards the other margin of the intrusion, where its upper contact is lined by a thin chromitite seam. The lower half and uppermost contact are composed of feldspathic olivine websterite. It resembles the Unit 3 pyroxenite, save that: euhedral oxides also occur at grain boundaries; minor pyrite and pyrrhotite are found; and clinopyroxene is euhedral. The modal abundance of olivine and orthopyroxene decreases up-section, while clinopyroxene and plagioclase increase. Olivine disappears about 4 m from the base.

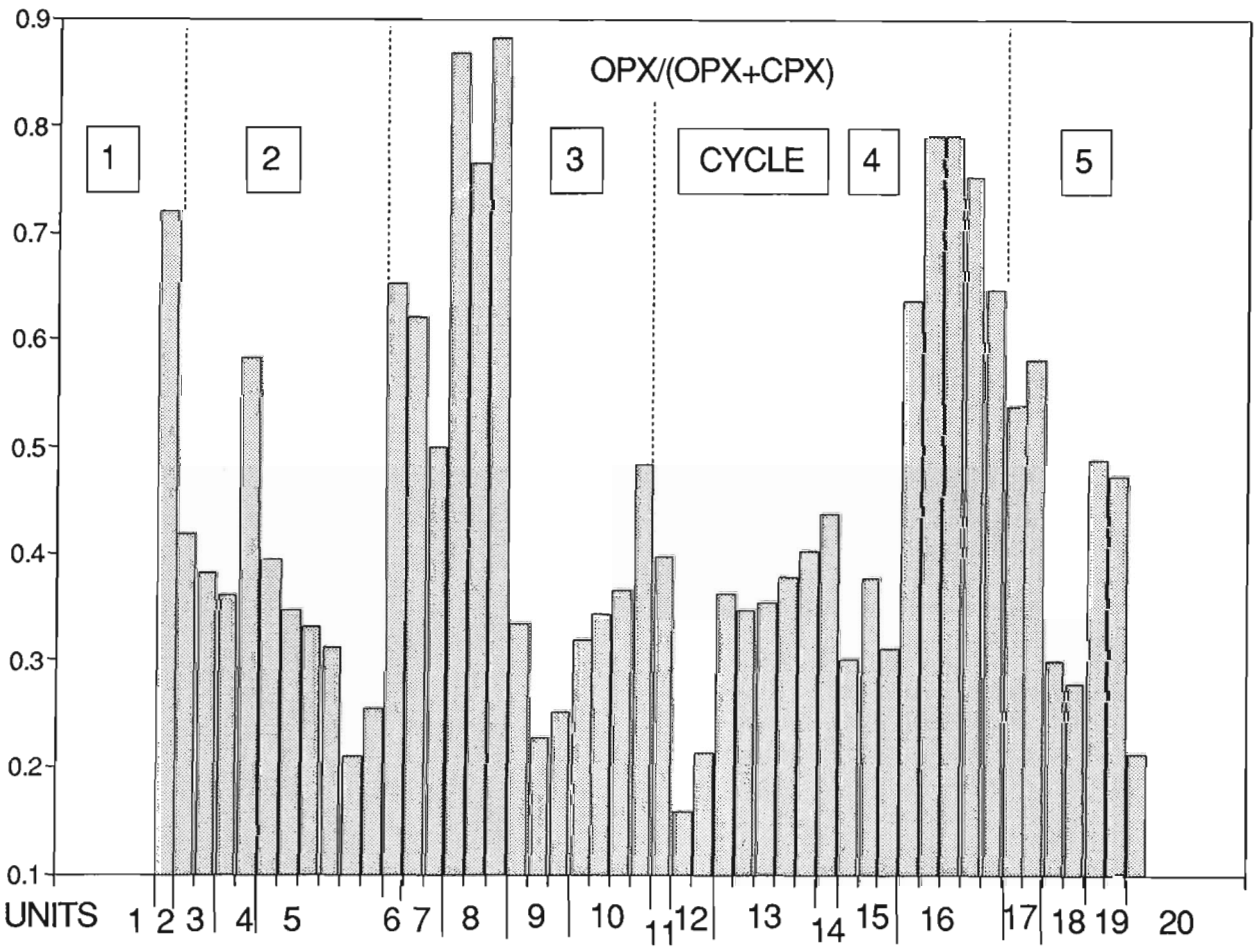


**Figure 4.** OPX/total pyroxene ratio.

### *Unit 6, massive, feldspathic, heteradcumulate lherzolite (same as units 1 and 4), ~30 metres*

This unit is composed of massive, unlayered feldspathic lherzolite similar to Unit 1.

### *Unit 7, layered, orthopyroxene-rich, granophyric, feldspathic websterite and olivine websterite, ~5 metres*

The contacts of Unit 7 are not exposed. An 8 m gap separates it from Unit 6. The only outcrop is composed of about 3 m of interlayered (3-5 cm scale) olivine-bearing and olivine-free feldspathic websterites. Olivine is texturally variable. Grains embedded in the interstitial to poikilitic plagioclase are euhedral; others are ragged, and appear to be partially replaced by orthopyroxene; still others seem to have a skeletal or poikilitic habit. Orthopyroxene is generally euhedral. Clinopyroxene is less abundant than orthopyroxene, and occurs either as small, anhedral interstitial grains; or as anhedral inclusions in orthopyroxene. The OPX/PX ratio (Fig. 4) is similar to that of Unit 6, suggesting a genetic link.

### *Unit 8, clinopyroxene-phyric, orthopyroxene-rich, feldspathic websterite, ~10 metres*

There is 2-3 m gap between units 7 and 8. Unit 8 is richer in orthopyroxene than Unit 7, yet it contains numerous, large (up to 7 mm), anhedral, partly to completely corroded clinopyroxene megacrysts. Interstitial granophyre and mica are more abundant than in the underlying units. Fe-Ti-oxide minerals occur both as euhedral grains and interstitially, they are coarsely-intergrown composites of 3 different oxide minerals. Pyrite and pyrrhotite are commonly present in trace amounts and are locally abundant, especially near the Unit 8/9 transition.

### *Unit 9, clinopyroxene-rich, feldspathic websterite, ~15 metres*

The base is poorly exposed, is hydrothermally altered, and is unusually rich in sulphides (up to 1 wt. % S, with 740 ppm Cu and 120 ppm Zn). The pyroxenites of this unit differ from those of Unit 8 by the euhedral form and great abundance of clinopyroxene. The OPX/PX ratio is similar to that of Unit 5, but interstitial granophyre and mica are much more abundant. Orthopyroxene is generally euhedral and smaller than clinopyroxene, though a few large grains are also present. Plagioclase forms an interstitial mosaic, and is slightly more abundant than in Unit 8. Rare subhedral plagioclase (<10%) in the uppermost part of the Unit foreshadows the transition to Unit 10.

### *Unit 10, interlayered websterite (same as Unit 9) and granophyric leuco-gabbro-norite, 12 metres*

The first appearance of cumulus plagioclase in foliated, equigranular, leuco-gabbro-norite interlayers (millimetre to centimetre scale layers) defines the base of this 12 m thick Unit. Layering is somewhat convolute (180/24°N; 216/26°N; 230/25°N). The OPX/PX ratio increases upwards along the trend established by Unit 9 (Fig. 4); and large, euhedral, orthopyroxene "phenocrysts" appear 2-3 m below the transition to Unit 11. The gabbro-norite of Unit 10 is more feldspathic than the gabbro-norites beneath.

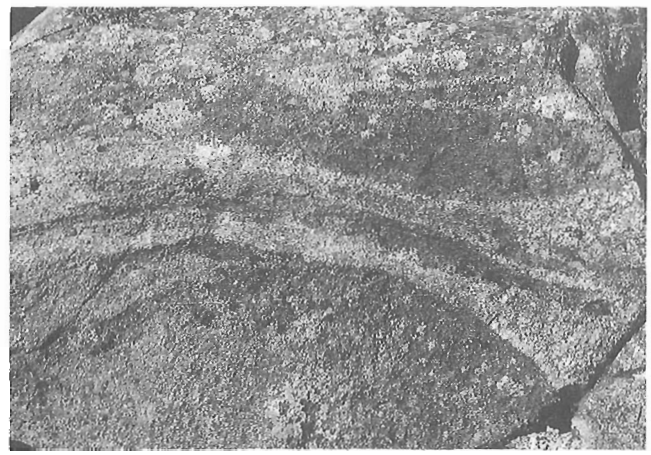

**Figure 5.** Convolute layers of gabbro-norite and pyroxenite, Unit 3. 1 metre field of view.

**Figure 6.** Pyroxenitic corrosion structure in gabbro-norite, Unit 3.

### *Unit 11, massive, red-weathering, picritic, feldspathic websterite, 10 metres*

The lower contact is sharp and conformable (216/26°N). The lowermost metre is texturally heterogeneous, locally containing angular (2-5 cm) xenoliths of gabbro-norite. To the south (Section P), the lower contact of this Unit exhibits metre-scale relief, the picritic websterite forming partially to completely detached lobes that deform the underlying layered rocks.

The picritic websterite is characterized by rare (<10%) medium grained (1-2 mm), faceted, euhedral olivine phenocrysts. These olivines may be partly replaced by postcumulus orthopyroxene. A second population of ovoid olivines is finer grained (<0.5 mm). They can occur as inclusions in orthopyroxene phenocrysts, where they may be intergrown with feldspar; but most are included in poikilitic plagioclase grains. Orthopyroxene typically forms normally-zoned, medium- to coarse-grained (4-8 mm), subhedral "phenocrysts". Olivine and clinopyroxene inclusions in orthopyroxene are common, plagioclase inclusions less so. In places, these rounded plagioclase inclusions themselves contain ovoid olivine inclusions. Clinopyroxene inclusions are typically ragged and sieved. The anhedral margins of the orthopyroxene seems to replace olivine and clinopyroxene with which they are in contact. They are interpreted to be postcumulus overgrowths on orthopyroxene phenocrysts. Clinopyroxene occurs as ragged anhedral inclusions in orthopyroxene and plagioclase, and as interstitial grains. The margins of included clinopyroxene may be sieved, even though the surrounding orthopyroxene phenocryst is free of alteration. Rarely, clinopyroxene occurs as larger (3-4 mm) anhedral grains which may represent relict phenocrysts. These too are sieved and seem to be partly resorbed. Plagioclase generally forms large (2-6 mm) anhedral oikocrysts which envelop most phases (except oxides and mica), but it also occurs as euhedral zoned laths included in orthopyroxene phenocrysts, or as anhedral inclusions intergrown with olivine in orthopyroxene phenocrysts. Euhedral Fe-oxides (millimetre-sized) and anhedral, reddish, interstitial Ti-phlogopite occur at grain boundaries.

### *Unit 12, massive, grey-weathering, feldspathic, granophyric, orthopyroxene-phyric websterite, 12 metres*

The contacts between units 11 and 12 appears gradational in the field (no interlayering or sharp contact). The transition is marked by the progressive disappearance of olivine and the increased abundance of plagioclase and clinopyroxene. Orthopyroxene phenocrysts similar to Unit 11 are present, some as glomeroporphyritic aggregates. However, most of the orthopyroxene occurs as smaller, euhedral, "groundmass" prisms. One grain contains a granophyric inclusion, which may represent infilling of an internal void created by skeletal growth. Elongated, zoned, prisms (up to 5 mm long, typically 0.5-1 mm wide) of clinopyroxene are included in orthopyroxene phenocrysts and in plagioclase oikocrysts, where they are free of sieving. Some clinopyroxene prisms are broken, perhaps due to compaction. Where clinopyroxene is in contact with interstitial mica, oxides, and granophyre, it is anhedral and is intensely sieved.

### *Unit 13, ophitic gabbro-norite (similar to Unit 10), 80 metres*

The Unit 12/13 contact also appears gradational. A strong foliation was not observed, and the rock appears massive. The OPX/PX ratio of Unit 13 differs markedly from that of Unit 12, but is similar to that of the Unit 10 gabbro-norites. At the base of Unit 13, orthopyroxene forms large (up to 1 cm) oikocrysts that are stuffed with plagioclase laths. The oikocrysts may be strongly zoned. Zoned, euhedral feldspar inclusions range in size from tiny laths, to dimensions typical of extra-oikocryst cumulus grains. Anhedral, corroded inclusions of clinopyroxene are uncommon. Large orthopyroxene grains decrease in abundance towards the top. Clinopyroxene is typically ophitic (1-2 mm) towards plagioclase laths. Cumulus plagioclase is euhedral, zoned, and generally inclusion-free. Oxide minerals, minor red mica, and granophyre occupy interstitial sites.

### *Unit 14, foliated, granophyric, gabbro-norite, ~20 metres*

This part of the intrusion (units 14 to 16) is characterized by small normal faults, and a slope that dips parallel to the regional layering, such that the stratigraphic thicknesses are only approximations.

The modal proportions of Unit 14 gabbro-norites are similar to those of Unit 13, but the macroscopic and microscopic textures are distinctive. Diffuse layering (198/18°N) and flattened anorthositic schlieren are observed. The rock is very strongly foliated, with all minerals sharing the same preferred orientation. Clinopyroxene generally occurs as subhedral prisms, although other grains have an ophitic habit, and one is oikocrystic, containing corroded plagioclase laths and polygonal internal domains of clinopyroxene that has a distinctly more turbid appearance. The internal domains may be the original cumulus grain, with the rest of the oikocryst representing a postcumulus overgrowth. Half of the orthopyroxene occurs as euhedral prisms, around which are draped plagioclase laths. Bushveld-type exsolution is well developed in some of these, but more common is a peculiar vermicular clinopyroxene intergrowth. The rest of the orthopyroxene occurs as ragged anhedral grains, that are sieved and veined by oxides, mica, and granophyre, and which are commonly included and corroded by clinopyroxene. Plagioclase forms euhedral, zoned laths. Interstitial granophyre, mica, and oxides are abundant.

The gabbro-norite is intruded by 5-10 cm thick branching dykes of Mackenzie-type diabase (186/82°W), and by a massive, 1 m-thick dyke of granophyre speckled with mafic clots.

### *Unit 15, foliated ophitic gabbro-norite, ~30 metres*

The dominant lithology is a foliated gabbro-norite. Near the base, local concentrations of anorthositic lenses and mafic schlieren define a weak layering (219/19°N). Orthopyroxene occurs as euhedral, inclusion-poor prisms. The vermicular texture that characterized Unit 14 is poorly developed. A few grains contain small plagioclase laths and ragged clinopyroxene inclusions. Orthopyroxene may be intergrown with clinopyroxene, with little evidence of a reaction relationship. Clinopyroxene is generally subophitic towards zoned laths of plagioclase, but also occurs as subhedral prisms that contain tiny plagioclase laths. Sieving is rare. Interstitial granophyre, mica, and oxides are abundant (up to 18%). Oxides are interstitial and form coarse intergrowths of magnetite and ilmenite. Very fine grained pyrite is rare. Groundmass granophyre locally replaces clinopyroxene.

There are anastomosing dykelets (2-6 cm) of granophyre, diabase, and hybrids of the two (059/57°E; 080/69°S; 086/83°S; 005/56°E; 004/66°E). In one place a granophyric dyke is surrounded by a 2 m-wide hydrothermal alteration halo and the development of quartz-calcite veins (018/73°E; 020/72°E; 020/70°E). The granophyre is strongly altered, but phenocrysts of quartz and feldspar in a graphic granophyre groundmass are easily recognized. The whole-rock geochemical analysis of one of these granophyres is used in the modal calculations. Globules of mafic material and crenulated contacts between diabasic and granophyric patches suggest liquid-liquid mixing of mafic and felsic magmas.

### *Unit 16, interlayered, granophyric, orthopyroxene-oikocrystic, leuco-gabbro-norite; and orthopyroxene-rich, feldspathic websterite, ~50 metres*

The base of the unit is defined by the first observed re-appearance of orthopyroxene oikocrysts and pyroxenite layers, a generally higher OPX/PX, and decreased modal granophyre. The closest analogue appers to be the Unit 2 gabbro-norite. Layers are generally sharply bounded and 5-10 cm thick. Modally graded rhythmic layers were observed locally, grading up from a basal mesocratic to an apical anorthositic gabbro-norite, topped (sharp contact) by

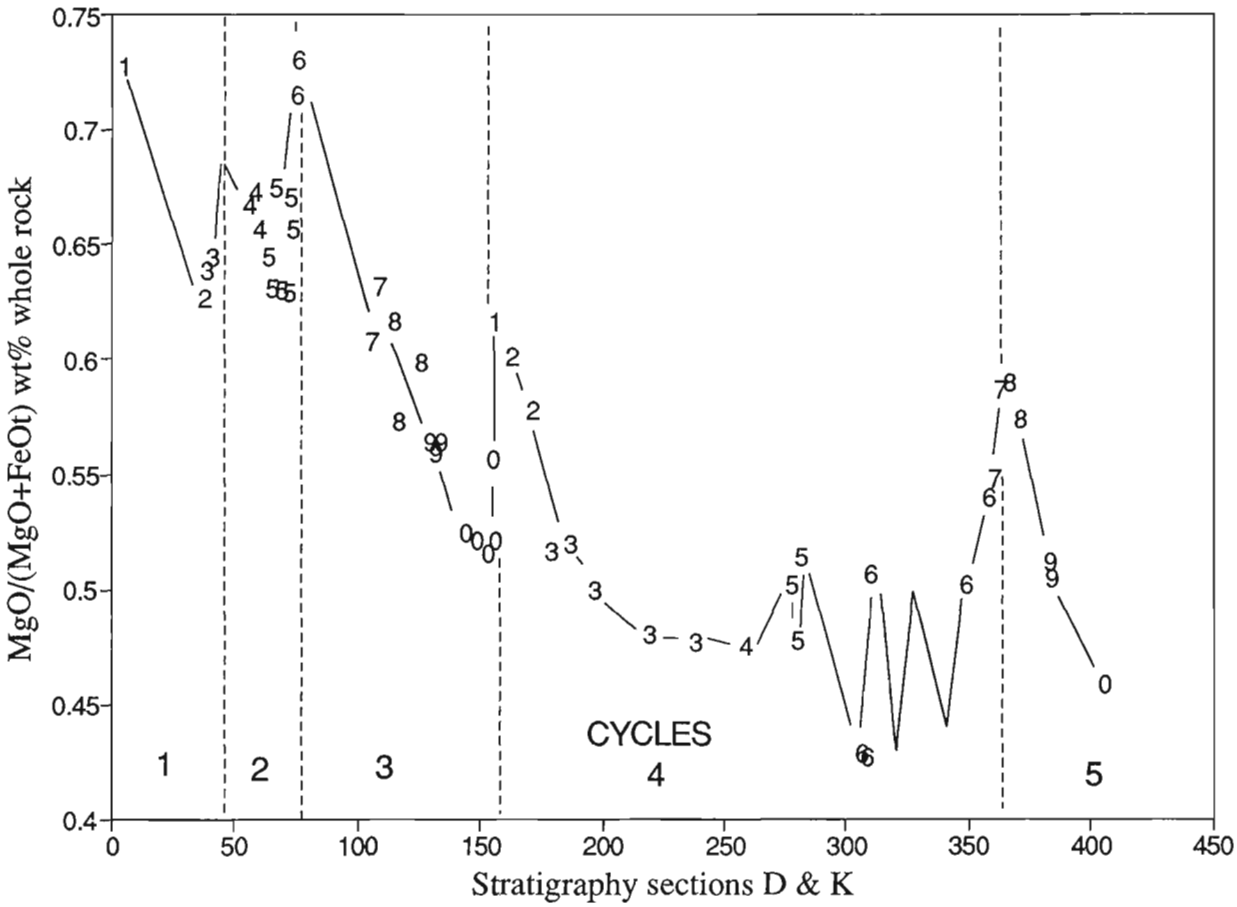


**Figure 7.** MgO/(MgO+FeO total) wt.%, whole rock, versus stratigraphy (in metres) for composite section D+K. Digits refer to units 1-10 and 11-20. The lowermost sample is from Section P.

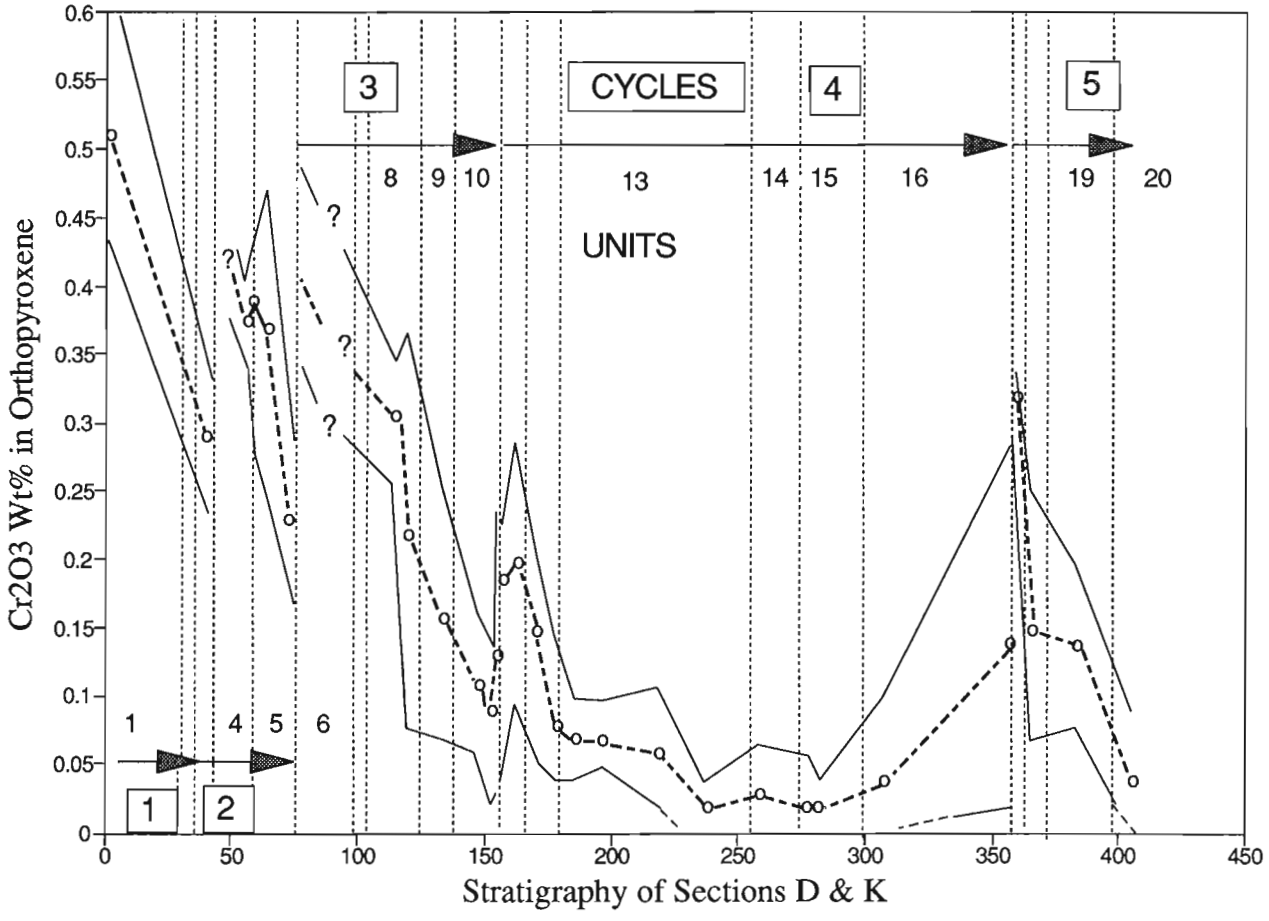


**Figure 8.** $Cr_2O_3$ wt.% in orthopyroxene versus stratigraphy. Circles represent average compositions, linked by a dashed line; the solid lines represent the compositional range.

a feldspathic websterite. Figure 3 illustrates the modal range. Layers are contorted in places. Melanocratic layers appear to increase in abundance upwards. This Unit is very heterogeneous and may contain unresolved subdivisions.

Only a single sample each of the mesocratic and leucocratic gabbro-norite are available. Both are more feldspathic than Unit 15 gabbro-norites, and have much higher OPX/PX ratios, similar to those of units 2 and 8. Zoned euhedral feldspar laths dominate. Most are sericitized. Orthopyroxene may form large (3-8 mm), subhedral grains with relatively clear cores and vermicular anhedral rims. Interstitial oxides are composed of intergrown magnetite and ilmenite. There is minor chalcopyrite and pyrite.

In the pyroxenite or mela gabbro-norite, some samples have euhedral, prismatic orthopyroxene, others have oikocrystic orthopyroxene. The latter contain numerous plagioclase laths and rarer, anhedral clinopyroxene. Clinopyroxene, granophyre, oxides, and mica are interstitial. Cumulus plagioclase laths have a seriate grain size distribution (0.5-5 mm). Mica is rare. Near the top of the unit, feldspathic olivine pyroxenite layers similar to those of the overlying unit appear.

### *Unit 17, massive, red-weathering, picritic, feldspathic websterite (similar to Unit 11), 10-12 metres*

In Section D the lower contact is exposed in only one place, where it appears sharp. To the south (Section G) it is the locus for the injection of coarse grained, gabbroic pegmatites and granophyric(?) dykes, but these were not observed in Section D. The picritic websterite is texturally very similar to the rocks of Unit 11, but differs in that: 1) the olivine grain size distribution is seriate rather than bimodal, and grains are generally faceted; 2) clinopyroxene is less intensely sieved and commonly contains inclusions of olivine; and 3) mica is generally coarser grained. Eutectoid intergrowth of orthopyroxene and plagioclase was also observed.

### *Unit 18, massive, grey-weathering, feldspathic websterite, ~12 metres*

The contact between units 17 and 18 is gradational in the field, with no observed interlayering. Textures are very similar to those of Unit 17. The transition is marked by a gradual decrease in modal olivine and orthopyroxene, and an increase in modal clinopyroxene.

### *Unit 19, foliated, layered, granophyric, gabbro-norite (similar to Unit 13), ~20 metres*

This unit is dominated by a gabbro-norite which closely resembles Unit 13 gabbro-norite, except that: it is better foliated, orthopyroxene is euhedral and prismatic (rather than oikocrystic), and the OPX/PX ratio is higher. In one place, fine grained (<0.5 mm) prismatic orthopyroxene is embedded in interstitial quartz. Mela-gabbro-norite schlieren are texturally similar.

### *Unit 20, clinopyroxene-rich, gabbro-norite (similar to Unit 15), >15 metres, <300 metres*

This unit consists of well foliated, wispily-layered gabbro-norite. The foliation wraps around small mafic schlieren. The contact with the underlying unit appears sharp. Unit 20 is well exposed for about 10-15 m. Outcrop then becomes very poor. The rocks closely resemble the Unit 15 gabbro-norite, though with a lower OPX/PX ratio. It contains abundant, principally ophitic clinopyroxene; though subhedral prisms are also present. Orthopyroxene is significantly less abundant than in the underlying unit, and ranges in habit from subhedral, vermicular prisms, to small subhedral inclusions in clinopyroxene. Plagioclase forms euhedral, zoned laths. Oxide minerals, granophyre, and mica are interstitial, and are more abundant than in the underlying unit. The amount of interstitial granophyre increases upwards.

### *Unit 21, granophyre, ~225 metres*

The first outcrop of granophyre is separated from the last gabbro outcrop by about 300 m (stratigraphic). About 75 m of red granophyre is succeeded by about 75 m of white granophyre, and then by about 75 m of a hybrid complex characterized by white granophyre that contains basaltic pods and hybrid facies. Alteration is pervasive, and pumpelleyite is commonly observed. In a few places, angular quartzite xenoliths are surrounded by dark rinds (now chlorite), and locally, the quartzite contain sulphide blebs. Although the granophyre exhibits considerable grain size and color heterogeneity (fine to coarse, white to red), it is mineralogically uniform, with 5-20% feldspar laths (variably altered), a few quartz phenocrysts, oikocrystic biotite, platy-to-skeletal Fe-Ti-oxides, sparse pyrite, and an abundant granophyric-textured groundmass.

## DISCUSSION

The interpretation of the petrographic data is supported by two preliminary geochemical profiles. Figure 7 shows whole-rock Mg# [MgO/($FeO_{total}$+MgO) wt.%], while Figure 8 shows $Cr_2O_3$ wt.% in orthopyroxene, versus stratigraphic height.

### *Replenishment events*

The stratigraphy is dominated by gabbro-norite, punctuated by thick peridotitic layers that were interpreted to represent replenishment events by Irvine and Smith (1967). The data presented above confirms and extends this interpretation. The peridotitic layers coincide with maxima in the Mg# and $Cr_2O_3$ in orthopyroxene. Textural evidence (Fig. 5 and 6) and the lateral impersistence of units 2 to 5 suggests that substantial floor erosion took place, and that this was more marked in the center of the intrusion. The loading structures found at the base of Unit 11 are interpreted to signify that the underlying cumulates were only partially consolidated, down to at least 3 m depth.

The peridotite layers are cumulates derived from large influxes of olivine-saturated magma, and correspond to replenishment events in the classical sense (e.g. Wager and Brown, 1968; Huppert and Sparks, 1980). These major replenishments are, however, foreshadowed by important precursory geochemical changes, such as increases in whole-rock Mg# (Fig. 7) and $Cr_2O_3$ in orthopyroxene (Fig. 8). The precursory changes may begin as much as 50 m below the main replenishment event, and coincide with the reappearance of pyroxenitic layers and of coarse grained orthopyroxene in the interlayered gabbro-norite. We propose that the main replenishment events were either a) preceded by smaller pulses of primitive magma which hybridized with resident, more evolved magmas; or b) there was turbulent mixing near the head of the replenishing magma as it spread across the floor of the intrusion.

Despite periodic resets (marked by peridotite and pyroxenite), the gabbro-norites show a systematic upward decrease in Mg#. This suggests that the picritic replenishments were insufficient to completely reset the chemistry of the intrusion, which was dominated by OPX-CPX-PLAG-saturated basalt. It may be that all the gabbro-norites crystallized from the same 3-phase basalt. This basalt would have remained as a resident magma, which was periodically separated from the crystallization interface by the ponding of dense, picritic replenishments (cf. Huppert and Sparks, 1980). The ponded picrite would have fractionated olivine, lowering the density of the residual magma to the point where mixing with the supernatant basalt could occur, allowing gabbro-norite to be deposited once again. The alternative possibility is that each gabbro-norite represents the fractionation residue of the picritic replenishment that preceded it. This second hypothesis is not favoured because the replenishing picrites have distinct mineral chemistries.

### *Mixture between contrasting liquid lines of descent*

The thick Unit 6 peridotite belongs to the lineage characterized by early liquidus orthopyroxene. It is overlain by layered orthopyroxene-rich pyroxenites (Unit 7) with similar textural characteristics that may represent precipitates from the fractionation residua of Unit 6 magmas. Athough they too are dominated by orthopyroxene, the rocks of Unit 8 also contain ragged, anhedral clinopyroxene megacrysts which appear to be partially resorbed xenocrysts. Unit 9, immediately above, is dominated by clinopyroxene. Irvine (1970) explained this cumulate stratigraphy in terms of a single liquid line of descent. We feel that the presence of xenocrystic clinopyroxene in Unit 8 suggests that that the

Unit 8 OPX-rich pyroxenites are hybrid rocks, and that units 8 and 9 belong to different lineages. Interestingly, this is the part of the intrusion where chromitites and sulphides are prominent.

## ACKNOWLEDGMENTS

International Platinum Corporation graciously allowed us to use their camp. Rod Stone expedited. Don Francis introduced J.B. to the Transition Lake Section. G. Sinclair, J. Stirling and G. Poirier assisted with the microprobes and supplied software. C. Tremblay and M. Laflèche provided comments. Geochemical analyses were executed under the direction of P. Bélanger. V. Desroches assisted in the field.

## REFERENCES

**Bédard, J.H., Sparks, R.S.J., Renner, R., Cheadle, M.J., and Hallworth, M.A.**
1988: Peridotite sills and metasomatic gabbros in the Eastern Layered Series of the Rhum complex; Journal of the Geological Society of London, v. 145, p. 207-224.

**Butcher, A.R., Young, I.M., and Faithfull, J.W.**
1985: Finger structures in the Rhum Complex; Geological magazine, v. 122, p. 491-502.

**Dostal, J., Baragar, W.R.A., and Dupey, C.**
1983: Geochemistry and petrogenesis of basaltic rocks from Coppermine River area, Northwest Territories; Canadian Journal of Earth Sciences, v. 20, p. 684-698.

**Hunter, R.H.**
1987: Textural equilibrium in layered igneous rocks; in Origins of Igneous Layering, (ed.) I. Parsons; NATO ASI series C, v. 196, p. 473-503.

**Huppert, H.E. and Sparks, R.S.J.**
1980: The fluid dynamics of a basaltic magma chamber replenished by influx of hot, dense, ultrabasic liquid; Contributions to Mineralogy and Petrology, v. 75, p. 279-289.

**Hutchison, C.S.**
1975: The Norm, its variations, their calculation and relationships; Schweizerische Mineralogische und Petrographische Mitteilungen, v. 55, p. 243-256.

**Irvine, T.N.**
1970: Crystallization sequences in the Muskox Intrusion and other layered intrusions. I. Olivine-pyroxene-plagioclase relations; in Symposium on the Bushveld Igneous Complex and Other Layered Intrusions, The Geological Society of South Africa, Special Publication no. 1, p. 441-476.

**Irvine, T.N. and Smith, C.H.**
1967: The ultramafic rocks of the Muskox intrusion, Northwest Territories, Canada; in Ultramafic and Related Rocks, (ed.) P.J. Wyllie; J. Wyllie and Sons, N.Y., p. 38-49.

**Lee, C.A. and Butcher, A.R.**
1990: Cyclicity in the Sr isotope stratigraphy through the Merensky and Bastard Reef Units, Atok Section, eastern Bushveld Complex; Economic Geology, v. 85, p. 877-883.

**McBirney, A.R.**
1987: Constitutional zone refining of layered intrusions; in Origins of Igneous Layering, (ed.) I. Parsons; NATO ASI series C, v. 196, p. 437-452.

**Robbins, B.**
1982: Finger structures in the Lille Kufjord layered intrusion, Northern Norway; Contributions to Mineralogy and Petrology, v. 81, p. 290-329.

**Smith C.H., Irvine, T.N., and Findlay, D.C.**
1963: Muskox Intrusion Geology, District of Mackenzie; Map 1213A, Geological Survey of Canada, scale 1:63 360.

**Sparks, R.S.J.**
1986: The role of crustal contamination in magma evolution through geological time; Earth and Planetary Science Letters, v. 78, p. 211-223.

**Wager, L.R. and Brown, G.M.**
1968: Layered Igneous Rocks; Oliver and Boyd, Edinburgh, Scotland.

Geological Survey of Canada Project 880011

# Lac Leclair carbonatitic ultramafic volcanic centre, Cape Smith Belt, Quebec

**W.R.A. Baragar[1], U. Mader[1], and G.M. LeCheminant[2]**

*Baragar, W.R.A., Mader, U., and LeCheminant, G.M., 1992: Lac Leclair carbonatitic ultramafic volcanic centre, Cape Smith Belt, Quebec; in Current Research, Part C; Geological Survey of Canada, Paper 92-1C, p. 103-109.*

***Abstract***

*The Lac Leclair volcanic centre comprising a 400 metre thick assemblage of lapilli tuffs and rare pillow lavas overlies banded cherty iron-formation that forms the basal unit resting unconformably on Archean basement at the south margin of the Cape Smith Belt. The lapilli tuffs are typically of centimetre size and commonly accretionary; bedding is rare and generally diffuse. Except for probable local inundations eruption was subaerial. The assemblage comprises carbonate-rich, ultramafics formed essentially of serpentine, chlorite, talc, carbonate (mainly dolomite), and magnetite, with minor ilmenite and chromite. Magnetite is especially conspicuous, in places forming blocky crystals up to 15 cm long. Highly fractionated, LREE enriched patterns and relatively high values of the high-field-strength elements Zr and Nb are suggestive of a carbonatitic affinity. Their compositon is closely similar to parts of the Lac Castignon carbonatite suite.*

***Résumé***

*Le centre volcanique du lac Leclair, comprenant un assemblage de 400 m d'épaisseur de tufs à lapilli et de rares laves en coussins, repose sur une formation ferrifère cherteuse rubanée qui constitue l'unité basale surmontant en discordance le socle archéen à la bordure sud de la zone de Cape Smith. Les tufs à lapilli de dimensions centimétriques sont dûs à l'accrétion; la stratification est rare et généralement diffuse. À l'exception d'inondations locales probables, l'éruption a été subaérienne. L'assemblage comporte des roches ultramafiques carbonatées comportées essentiellement de serpentinite, de chlorite, de talc, de carbonates (principalement dolomite) et de magnétite, avec un peu d'ilménite et de chromite. La magnétite est particulièrement évidente, formant par endroits des cristaux en blocs pouvant atteindre 15 cm de longueur. Les éléments des terres rares légers à température de fractionnement élevée et les concentrations elativement fortes en Zr et Nb à intensité de champ élevée indiquent une affinité carbonatitique. Leur composition est très semblable à certaines parties de la série de carbonatite du lac Castignon.*

[1] Continental Geoscience Division
[2] Mineral Resources Division

## INTRODUCTION

Some puzzling outcrops encountered near the southern margin of the Cape Smith Belt in the course of routine mapping in 1985 proved in subsequent laboratory investigations to have extraordinary mineralogical and chemical compositions. The rocks are obviously volcanic in texture but composed mainly of carbonate, serpentine, and magnetite. Moreover, they are much higher in some of the incompatible elements and the rare-earths are more highly fractionated than would normally be consistent with MgO-rich rocks. These characteristics were sufficiently suggestive of a carbonatitic magma that further field investigations seemed to be warrented. Accordingly, two weeks of this past summer were spent in detailed mapping of these outcrops and their environs. The following is an interim report that describes the field relationships and presents available petrochemical data.

The study area is about 60 km due east of the village of Akulivik on Hudson Bay and just to the east of Lac Leclair.

## GEOLOGY

The regional geology in the vicinity of Lac Leclair is shown in Figure 1 and detail of the volcanic centre and its surroundings, in Figure 2. Outcrop is commonly not abundant near the southern margin of the Cape Smith Belt so the nature and location of the boundary itself has been subject to some interpretation. Hoffman (1985) proposed that the Cape Smith Belt is a klippe bounded by thrust faults and this concept has constituted a model used and adapted by later investigators. Our detailed mapping in the Lac Leclair region shows that, although complicated by deformation, the boundary here is definitely an unconformity (Fig. 2). Figure 1 illustrates the degree to which the Archean basement is involved in Cape Smith deformation (see also Moorhead, 1988). Basement protrudes into sediments of the lower part of the Povungnituk Group in broad open folds and thrust slices. Foliation in the basement rocks immediately adjoining the Belt parallels the Belt itself but within as little as 0.5 km farther south (Fig. 1)

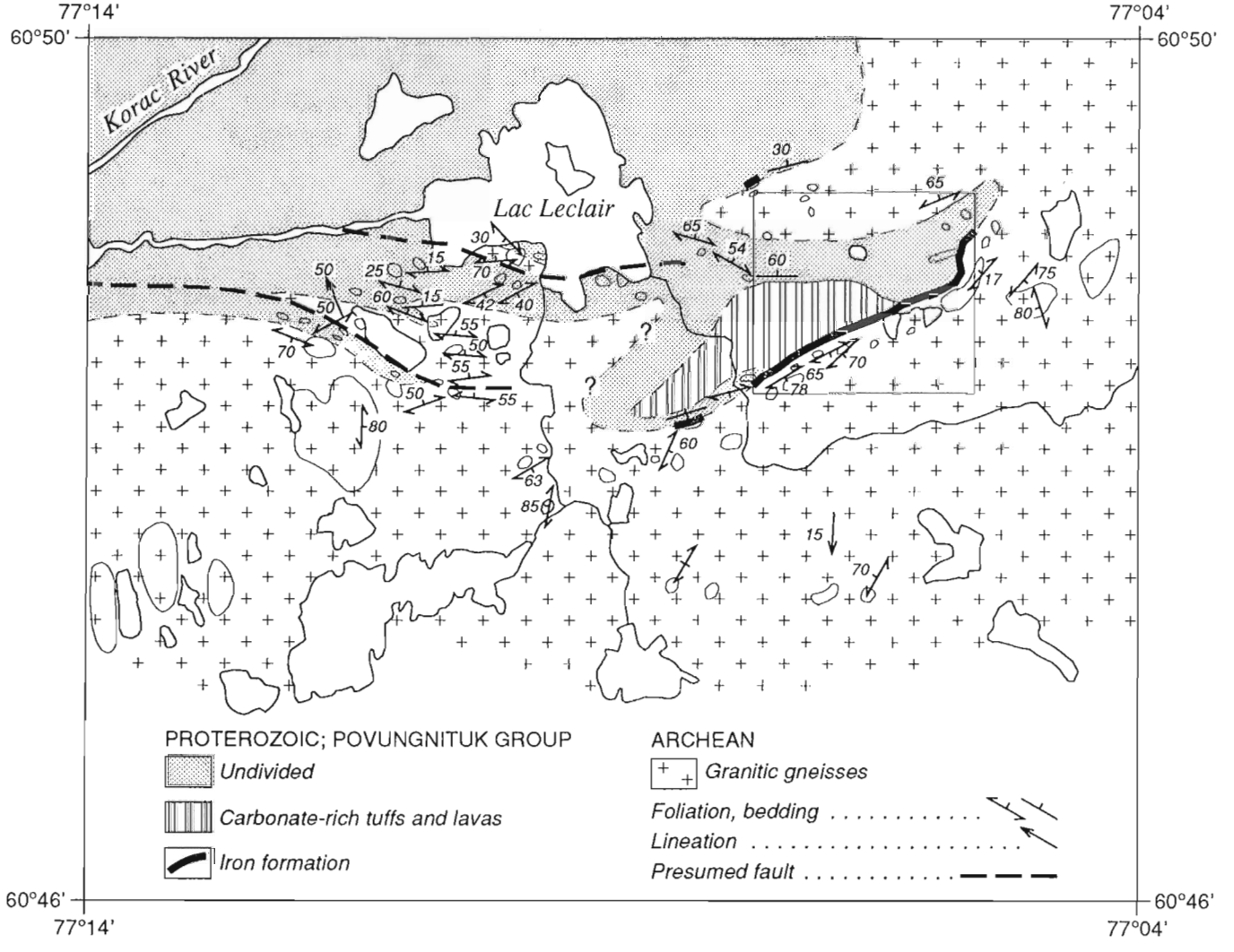


**Figure 1.** Regional map showing the setting of the Lac Leclair volcanic centre. Black outlined marks the locality of Figure 2.

passes into the north-south trend that characterizes the Archean of northern Quebec (Stevenson, 1968; Baragar, et al., 1986). At the base of the Povungnituk Group (Fig. 2) iron-formation rests directly on Archean basement but in one outcrop just to the west of the detailed map it is separated from basement by a few centimetres of quartz pebble conglomerate and grit. There can be no doubt, therefore, of the unconformable relationships at this contact.

The position in the stratigraphic sequence of the Lac Leclair volcanic rocks can be seen in the detailed map of Figure 2. They overlie the basal chert-carbonate iron-formation, which is here about 15 - 20 m thick, with apparant conformity. Both the iron-formation and volcanic rocks dip moderately (30 to 45 degrees) northward. At its maximum the volcanic unit is about 400 m thick but it thins rapidly eastward to zero within a distance of about a kilometre. Westward it disappears beneath overburden but since it does not reappear at the same stratigraphic level a few kilometres farther west, we have assumed it to have a conical profile as shown in Figure 1. Bedding trends within the volcanic pile which radiate from parallel to the base to oblique, upward in the sequence, are consistent with its interpretation as a volcanic cone. The volcanic rocks are succeeded in the stratigraphy by thin bedded black shales and cherts (which in the absence of the volcanic rocks lie directly on iron-formation) and, in turn, by orange-brown weathering dolomites. In contrast to the moderately-dipping iron-formation and volcanic rocks, these latter units, particularly the fissile shales, are severely deformed. It would seem likely from their position in the eastern half of the map of Figure 2 that the shales and carbonates, at least, have been squeezed between the limbs of a basement fold.

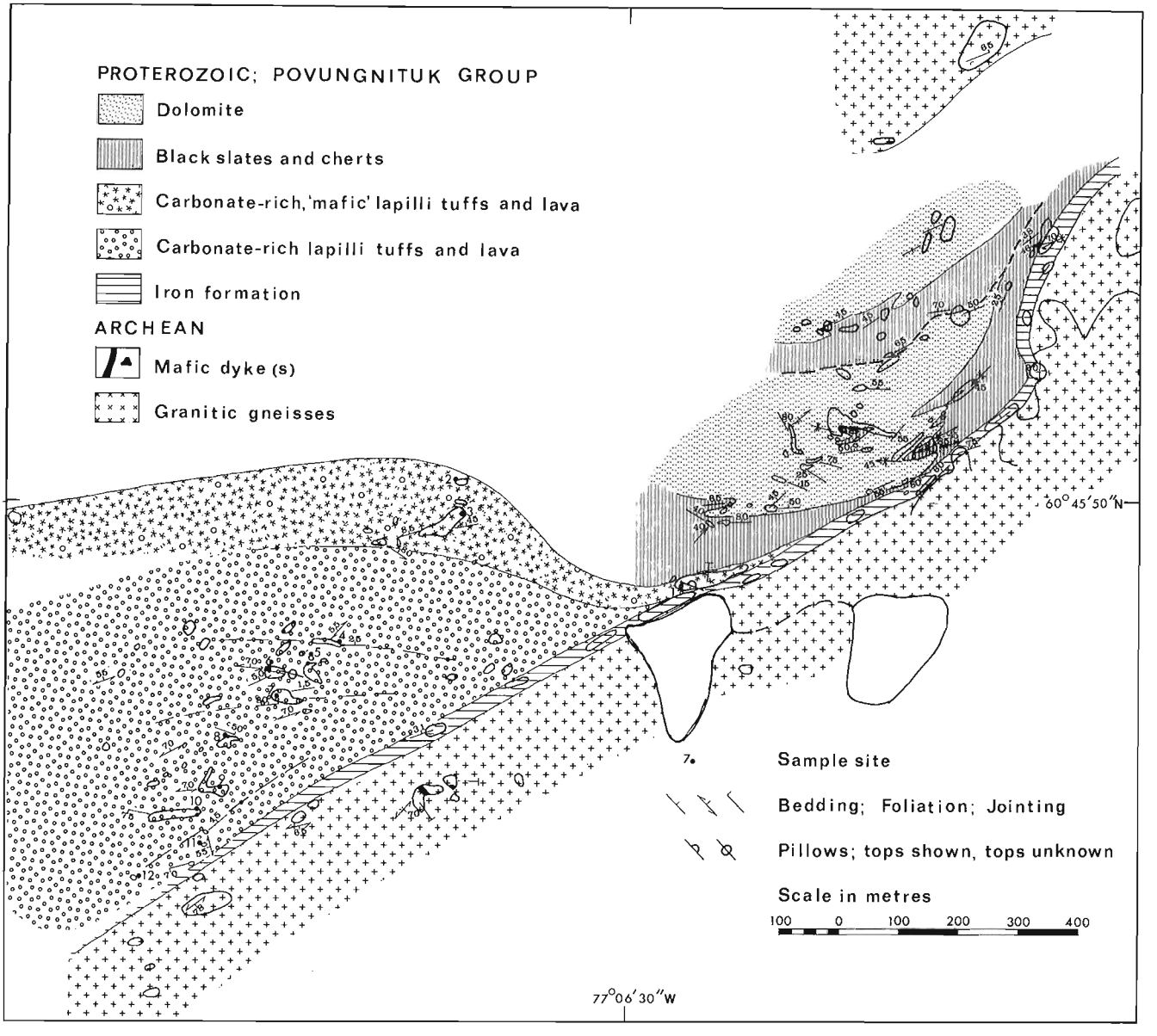


**Figure 2.** Detailed geological map of the Lac Leclair volcanic centre and its immediate surroundings.

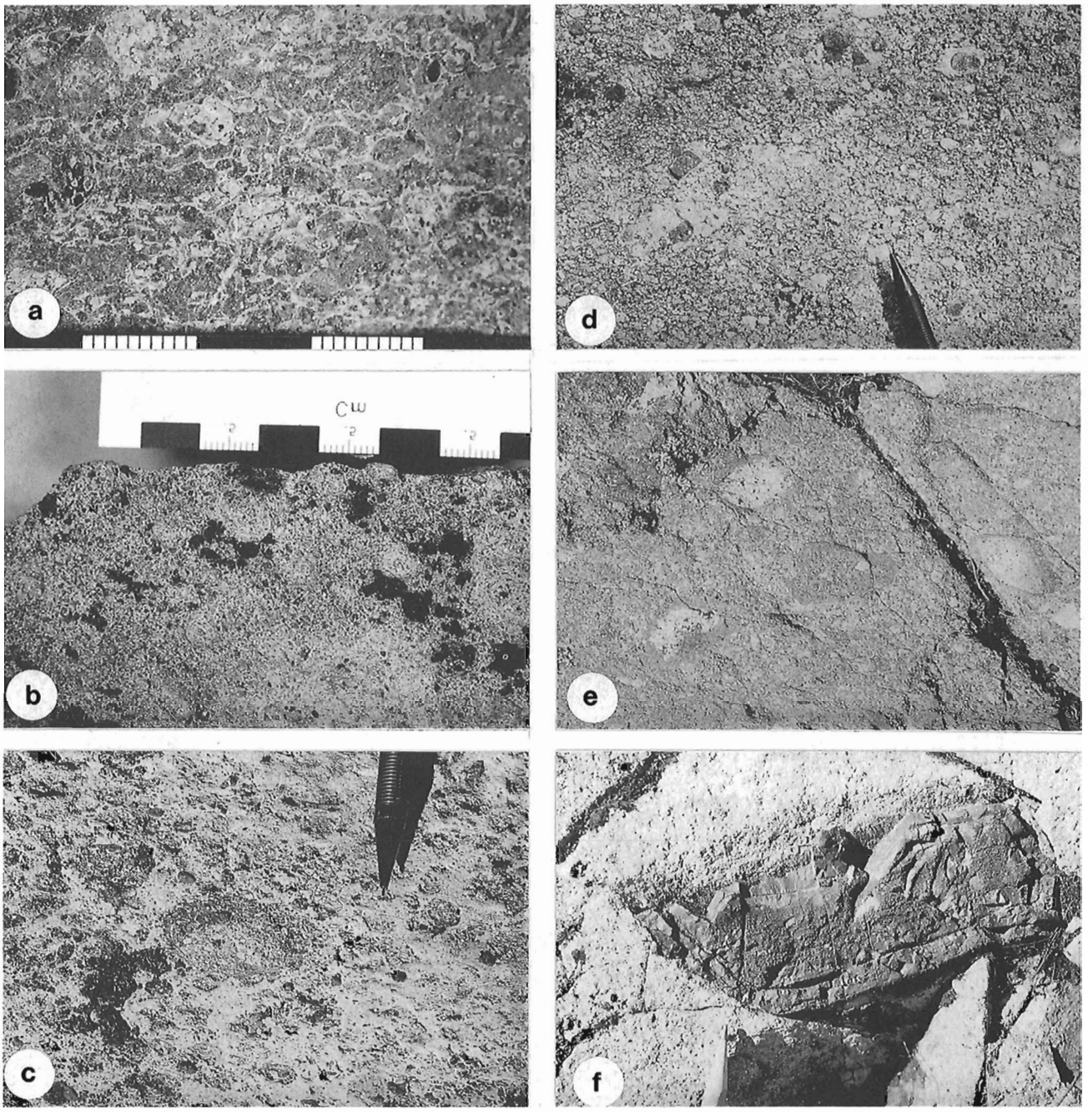


**Figure 3.** **a**) Texture of lapilli tuff of the lower unit showing the close-packing of the lapilli (centimetre scale). **b**) Accretionary lapilli accompanied by irregularly-shaped magnetite clots (dark). **c**) Large accretionary lapilli in tuffs showing fairly open packing. **d**) "Cored" lapilli with magnetite centres. **e**) Lapilli formed of lithic fragments enveloped by solidified magma (darker grey). Lapilli are 1-2 cm diameter. **f**) Magnetite megacrystal embedded in lapilli tuff. Note the thin recessive zone of silicate-carbonates that parallels the margin of the crystal. The crystal is about 10 cm long.

## PETROCHEMISTRY OF THE VOLCANIC ROCKS

### *Petrography*

The major part of the volcanic pile is composed of lapilli tuff with generally a particle size of about a centimetre or less. Except for the uppermost layer the rocks have a fairly uniform appearance; generally light grey weathering with a greenish grey interior and only rarely, diffuse bedding. Typically they comprise closely packed lapilli in a sparse groundmass (Fig. 3a). The upper layer (distinquished separately on the map) is distinctly darker in color and commonly less obviously tuffaceous. It is designated "mafic" in the legend of Figure 2 because of its darker color but both types are highly mafic and this may not be a very meaningful distinction. The lapilli are commonly accretionary (Fig. 3b, 3c) with a nucleous of a lithic fragment, carbonate crystal (or particle), or a grain of magnetite. Some are "cored" lapilli in that they are formed of a lithic or magnetite core enveloped by what is presumably solidified magma (Fig. 3d, 3e). Magnetite is a conspicuous component of the the lapilli tuffs, particularly in the lower unit. It generally composes 5-15% of the rock and appears as blocky or rounded particles or crystals ranging in size from <1 mm to 2-3 cm. At one place (near site 5, Fig. 2) several megacrystals are present (Fig. 3f) the largest of which measured 6x10x15 cm. A number of the blocky magnetite crystals are zoned, typically with one prominent zone of carbonate-silicate material, 1 - 2 mm thick, that parallels the margin a short distance into the crystal (Fig. 3f). The abundant presence of accretionary lapilli, the diffuse bedding, and the conical aspect of the volcanic mound are strong indications that the volcanism was essentially subaerial. Nevertheless, pillow lavas were observed at two stratigraphic levels; at about the middle of the lower unit and near the eastern termination of the upper unit. At the latter site the pillows are very thin rimmed and about a metre or less in average length (Fig. 4a). They are reminiscent of pillows that are characteristic of the high-magnesian flows of the Chukotat and equivalent rocks elsewhere in the Circum-Superior Belt (Baragar, 1984). Pillows of the lower unit are thick-rimmed and ill-formed (Fig. 4b), hence, pose some question as to whether or not they are truely pillows. Magnetite clots ranging from 1 cm to several centimetres across occur, in places, within the body of some of these thick-rimmed pillows.

As seen in thin section the textures of the volcanic rocks are not clearly defined due to extensive recrystallization. No primary silicate minerals were recognized. Generally the lapilli tuffs are composed of varying proportions of bladed antigorite, feathery-textured serpentine, carbonate, talc, chlorite, magnetite, ilmenite, and chromite. Lapilli particles are commonly formed of serpentine - particularly blades of antigorite set in a feathery serpentine-chlorite matrix - and clouded with finely crystalline carbonate and magnetite. The interparticle groundmass is typically a mosaic of intergrown coarser grained carbonate and feathery serpentine and chlorite but is rarely well distinguished from the particles. Many of the latter appear to have been replaced to varying degree by coarser carbonate grains similar to that of the groundmass. Commonly particles are outlined by a coating of very finely crystalline opaque mineral, probably magnetite or hematite. Some of the accretionary lapilli pellets seen in thin section comprise a core of fairly coarse grained carbonate, surrounded by successive rings of serpentine rimmed by a fine opaque dust. Magnetite, which is such a conspicuous constituent of the tuffs, occurs both as fine (<0.1 mm) subhedral crystals and as coarser (>0.25 mm) irregular masses. In places magnetite profusely veins the particles and appears to replace them to varying degree. The pillow lavas are more uniform in texture than the tuffs but are similarly composed of mainly serpentine, talc, carbonate, and magnetite. The only possible relict igneous texture identified is some millimetre-sized pellets of serpentine rimmed by finely crystalline magnetite which are reminiscent of olivine pseudomorphs. The principal distinctions in the petrography of the upper and lower units are a greater abundance of talc and chlorite in the upper unit and a paucity of coarse clots of magnetite. Carbonate is more abundant in the lower unit where, in places, it exceeds 50% of the rock.

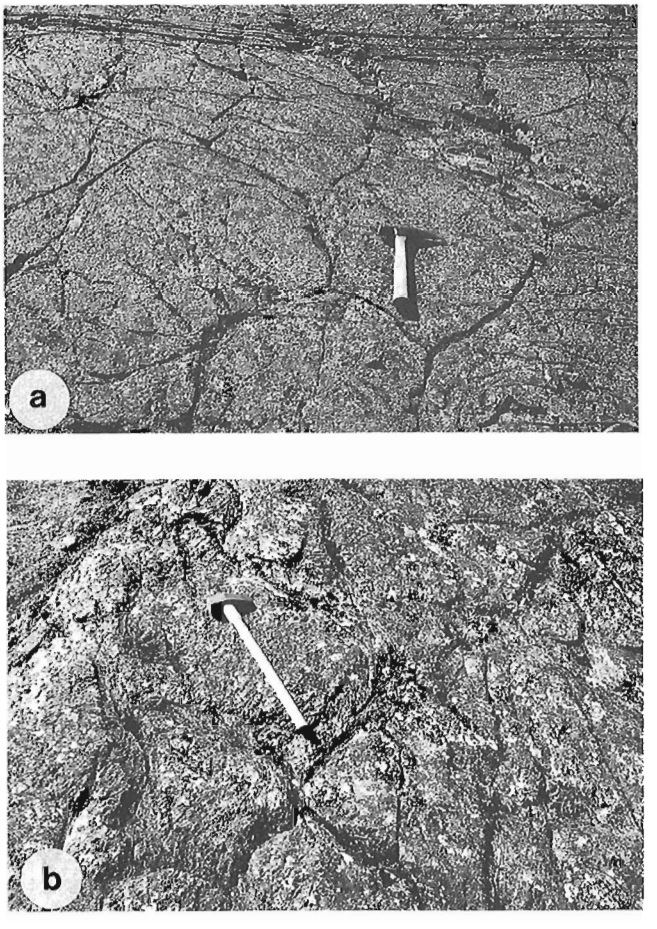


**Figure 4.** **a**) Thin-rimmed pillows in the upper unit of the Lac Leclair volcanic centre. Tops are to the right. The locality is immediately north of the western of the two lakes in Figure 2. **b**) Thick-rimmed pillow lavas (?) in the lower volcanic unit. Tops are to the right but this is not interpretable from the shapes of the pillows. The locality is sample site 6 shown in Figure 2.

### *Mineralogy*

Carbonates from the lower tuffs analyzed by electron microprobe are mainly dolomite but include some intergrowths of ankerite and magnesite. Two rare-earth element-bearing phases were detected and identified as monazite and an aeschynite-like mineral. Presumably these are the carriers of the rare-earth elements obtained in the whole rock analyses. Minor sulphides determined in the mineralogical examination of some of the rocks are pyrite, pyrrhotite(?), chalcopyrite, and nickel sulphide (heazlewoodite?).

### *Chemistry*

Two specimens from the lower lapilli tuffs have been analyzed to date for major and some trace elements, including the rare-earths (Table 1). Of particular interest are their high MgO (28.62-30.87%), Cr, and Ni contents coupled with relatively large values of the high-field strength, incompatible elements Nb (145-151 ppm) and Zr (239-253 ppm). Carbonate (assuming dolomite) forms about 30% and 20% respectively of the 2 samples. Their REE analyses show a highly fractionated pattern with very marked enrichment of the light end of the spectrum (Fig. 5).

These are extraordinary compositions for volcanic rocks if they can be assumed to be close to their original compositions. They are obviously recrystallized but otherwise are very little deformed. Mobility is evident in the replacement of some of the lapilli particles by magnetite and in the general blurring of boundaries between particles and matrix but this would seem to be local. There is a remarkable uniformity in the petrography throughout each of the units

**Table 1.**

| | Lac Leclair | | Lac Castignon | |
|---|---|---|---|---|
| | 1 | 2 | 3 | 4 |
| | BL85-153 | BL85-156 | P30-4 | 5B1 |
| SiO2 | 23.4 % | 28.5 % | 29.24 % | 34.18 % |
| TiO2 | 1.31 | 1.41 | 3.92 | 2.38 |
| Al2O3 | 1.3 | 1.2 | 3.93 | 2.20 |
| Fe2O3 | 9.8 | 9.3 | 2.31 | 8.79 |
| FeO | 4.5 | 4.4 | 14.55 | 7.43 |
| MnO | 0.26 | 0.27 | 0.23 | 0.29 |
| MgO | 28.62 | 30.87 | 16.38 | 21.39 |
| CaO | 9.62 | 6.85 | 10.22 | 8.99 |
| Na2O | 0.0 | 0.0 | 0.03 | 0.10 |
| K2O | 0.0 | 0.0 | 0.03 | 0.88 |
| H2O(T) | 6.4 | 7.0 | 4.66 | 5.59 |
| CO2 | 13.5 | 8.6 | 12.69 | 6.59 |
| P2O5 | 0.93 | 0.96 | 0.99 | 0.61 |
| S | 0.4 | 0.0 | 0.38 | 0.18 |
| Sr | 56 ppm | 67 ppm | 590 ppm | 340 ppm |
| Ba | 62 | 67 | 179 | 179 |
| Nb | 145 | 151 | 159 | 56 |
| Zr | 239 | 253 | | 259 |
| Ni | 930 | 910 | 470 | 1100 |
| Cr | 710 | 840 | 340 | 753 |
| Y | 28 | 31 | | |
| La | 150 | 160 | | |
| Ce | 280 | 300 | | |
| Nd | 130 | 130 | | |
| Sm | 15 | 16 | | |
| Eu | 6 | 5.4 | | |
| Gd | 14 | 14 | | |
| Dy | 7.6 | 7.8 | | |
| Yb | 1.5 | 1.7 | | |
| Total | 99.9 % | 100.4 % | | |

Notes: Columns 1 and 2 are analyses of lapilli tuffs from the lower unit of the Lac Leclair centre; columns 3 and 4 are from Dimroth (1970) and are analyses of carbonatized meimechite and a meimechite tuff respectively. Lac Leclair analyses were done at the Geological Survey Chemical Laboratories by the following methods: major elements XRF and rapid chemical methods; REE by ICP-ES after separation of majors by ion exchange; other trace elements by ICP-BS.

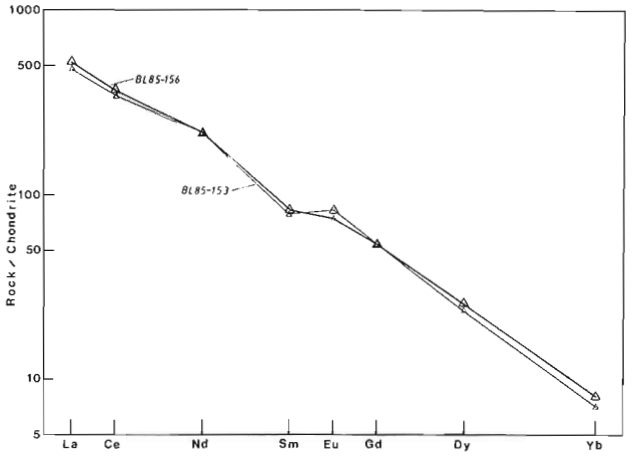


**Figure 5.** Patterns of rare-earth element analyses normalized to chondrite.

and in their chemistry, judging from the two analyses obtained to date. Note, for example, the nearly identical RRE patterns for the two widely separated tuffs of the lower unit. This would tend to support the view that the compositions may be close to those of the original volcanic deposit although not necessarily to that of the pre-eruption magma. Deuteric alteration may have imposed its own modification.

## DISCUSSION

The Lac Leclair volcanics are essentially carbonated ultramafic rocks. Without the carbonate content they would approach the composition of peridotites but their enrichment in some of the incompatible elements and light rare-earths gives them an alkaline affinity. In this regard their lack of the mobile alkalis K and Na can probably be attributed to deuteric alteration rather than primary depletion. If these rocks can be linked to a carbonatite suite it should probably be that of the magnesiocarbonatites (Woolley and Kempe, 1989).

The Lac Leclair volcanics are similar in some respects to parts of the Lac Castignon carbonatite suite of the Labrador Trough (Dimroth, 1970; Dressler, 1975). Analyses of two of the more mafic members of the Lac Castignon suite are given in Table 1 for comparison. Although the latter suite ranges in composition from an olivine-rich end member (now talc-serpentine), termed meimechite by Dimroth (1970) and lamprophyre by Dressler (1975), to carbonatites with over 50% carbonate, none are as mafic as the Lac Leclair rocks analyzed. Nevertheless the amounts and distributions of compositions at its mafic end are generally similar to those of the Lac Leclair suite and would require little projection to encompass them. Note the very similar enrichment in both suites of the high-field-strength, incompatible elements Nb and Zr and compatible elements Cr and Ni. The two suites also occupy a similar poition in the foreland of their respective segments of the Trans-Hudson Orogen where they are contemporaneous with parts of its platformal facies (cf. Dressler, 1975; Cheve and Machado, 1988).

Carbonatites are normally associated with an alkaline silicate counterpart, commonly nephelinites (Le Bas, 1989). The recently reported occurrence of an alkaline suite comprising basinite/nephelintes and phonolites (Gaonac'h et al., 1989) within the Povungnituk Group about 100-150 km to the east is, therefore, of special interest in its possible relationship to the Lac Leclair occurrence.

## ACKNOWLEDGMENTS

Logistic support for our field work was provided by Marc St.-Onge and Stephen Lucas to whom we owe a very sincere and grateful thanks which extends as well to the kind hospitality given to us at their camp. We would also like to acknowledge the cooperation and friendliness shown us by the community of Akulivik during our brief visits there.

## REFERENCES

**Baragar, W.R.A.**
1984: Pillow formation and layered flows in the Circum-Superior Belt of eastern Hudson Bay; Canadian Journal of Earth Science, v. 21, p. 781-792.

**Baragar, W.R.A., Hervet, M., and Charland, M.**
1986: Structual character and plutonic setting at the western end of the Ungava Trough, in Exploration en Ungava; Quebec Ministere de l' Energie et des Ressources, DV86-16, p. 41-43.

**Cheve, S.R. and Machado, N.**
1988: Reinvestigation of the Castignon Lake carbonatite complex, Labrador Trough, New Quebec; Geological Association of Canada/ Mineralogical Association of Canada, Program with Abstracts, v. 13, p. A20.

**Dimroth, E.**
1970: Meimechites and carbonatites of the Castignon Lake complex, New Quebec; Neues Jahrbuch fur Mineralogie Abhandlung, v. 112, p. 239-278.

**Dressler, B.**
1975: Lamprophyres of the north-central Labrador Trough, Quebec, Canada: Neues Jahrbuch fur Mineralogie Monathefte, jg. 1975, p. 268-280.

**Gaonac'h, H., Picard, C., Ludden, J.N., and Francis, D.M.**
1989: Alkaline rocks from a Proterozoic island in the Cape Smith thrust belt, New Quebec; Geoscience Canada, v. 16, p. 137-139.

**Hoffman, P.H.**
1985: Is the Cape Smith Belt (northern Quebec) a klippe?; Canadian Journal of Earth Sciences, v. 22, p. 1361-1369.

**Le Bas, M.J.**
1989: Diversification of carbonatite, in Carbonatites Genesis and Evolution, (ed.) Keith Bell; Unwin Hyman, London, p. 428-447.

**Moorhead, J.**
1988: Geologie de la region du Lac Vigneau, Nouveau Quebec; Ministere de l' Energie et des Ressouces, DP 88-05.

**Stevenson, I.M.**
1968: A geological reconnaissance of Leaf River map-area, New Quebec and Northwest Territories; Geological Survey of Canada, Memoir 356, 112 p.

**Woolley, A.R. and Kempe, D.R.C.**
1989: Carbonatites: nomenclature, average chemical compositions, and element distribution, in Carbonatites Genesis and Evolution, (ed.) Keith Bell; Unwin Hyman, London, p. 1-14.

Geological Survey of Canada Project 780012

# Preliminary stratigraphy and sedimentology of the Glenelg Formation, lower Shaler Group and correlatives in the Amundsen Basin, Northwest Territories: relevance to sediment-hosted copper[1]

**R.H. Rainbird[2], W. Darch[3], C.W. Jefferson[4], R. Lustwerk[3], M. Rees[3], K. Telmer[5], and T.A. Jones[6]**

*Rainbird, R.H., Darch, W., Jefferson, C.W., Lustwerk, R., Rees, M., Telmer, K., and Jones, T.A., 1992: Preliminary stratigraphy and sedimentology of the Glenelg Formation, lower Shaler Group and correlatives in the Amundsen Basin, Northwest Territories: relevance to sediment-hosted copper; in Current Research, Part C; Geological Survey of Canada, Paper 92-1C, p. 111-119.*

***Abstract***

*Disseminated chalcopyrite has been discovered in quartzarenite from the lower Shaler Group in the Minto Inlier of Victoria Island and in correlative strata from the Rae Group. The style of mineralization suggests that metals were introduced along aquifers during diagenesis of the sandstone. Regional mapping in conjunction with paleocurrent and isopach studies will be employed to delineate the geometry and paleogeography of these prospects as it pertains to localization of ore-bearing fluids. Preliminary work in the Minto Inlier confirms a three-fold subdivision of the Glenelg Formation, and correlation with the Rae Group near Coppermine and with units in the Brock Inlier. The Lower Clastic Member consists of very poorly exposed deep-water mudstones and rare turbiditic sandstone intercalations. It is overlain by shallow water limestones and cherty stromatolitic dolostones of the Cherty Carbonate Member. A sporadic karstic topography underlies the Upper Clastic Member: a coarsening-upward succession of siliciclastic rocks interpreted as a prograding fluvio-deltaic complex. Marine inundation reworked the uppermost quartzarenites and deposited a distinctive, regionally extensive stromatolite biostrome which caps the formation.*

***Résumé***

*De la chalcopyrite disséminée a été découverte dans une quartzarénite de la partie inférieure du groupe de Shaler dans la boutonnière de Minto de l'île Victoria et dans des couches équivalentes de la boutonnière de Brock. Le style de minéralisation semble indiquer que les métaux se sont introduits le long des aquifères durant la diagenèse du grès. Pour délimiter la géométrie et la paléogéographie de ces zones d'intérêt et ainsi localiser les fluides minéralisés, il est prévu de cartographier la région et de réaliser des études des paléocourants et des isopaques. Les travaux préliminaires dans la boutonnière de Minto confirment la subdivision en trois parties de la formation de Glenelg ainsi que sa corrélation avec le groupe de Rae près de Coppermine et avec les unités contenues dans la boutonnière de Brock. Le membre clastique inférieur est composé de mudstones d'eau profonde très mal exposés et de rares intercalations de grès turbiditique. Il est surmonté de calcaires et de roches dolomitiques stromatolitiques cherteuses d'eau peu profonde du membre carbonaté cherteux. Au-dessous du membre clastique supérieur, on observe une topographie karstique sporadique : une succession à granoclassement inverse de roches silicoclastiques interprétée comme un complexe fluvio-deltaïque en progression. Une inondation marine a remanié les quartzarénites sommitales et déposé un biostrome à stromatolites distinct d'échelle régionale sur la formation.*

[1] Contribution to the Canada-Northwest Territories Economic Development Agreement Minerals Initiative 1991-96

[2] Continental Geoscience Division

[3] Noranda Exploration Co. Ltd., Winnipeg

[4] Mineral Resources Division

[5] Geology Dept., University of Ottawa

[6] Geology Dept., Cambrian College, Sudbury

## INTRODUCTION

Paleogeographic reconstructions of Late Proterozoic rocks in the Minto Inlier, Brock Inlier, Coppermine Homocline, and Mackenzie Mountains (Fig. 1) are important in evaluating their potential as hosts to copper deposits. Furthermore, detailed analysis of these sequences in outcrop can constrain interpretations of subsurface data, and so aid in the exploration for hydrocarbons in Paleozoic cover rocks. In this paper, we present the preliminary results of field work in Minto and Brock inliers that help revise the lithostratigraphic correlations of Jefferson and Young (1989; Fig. 1) and introduce refinements to existing paleogeographic models. This study also presents preliminary descriptions of sediment-hosted stratiform copper prospects in the two areas.

Data from Minto Inlier represent the first field season of a Canada-N.W.T. Minerals Initiative study designed to focus on basin analysis and 1:50 000 scale mapping of potential ore-hosting stratigraphic units, supported by detailed geological mapping and diamond drilling by Noranda Exploration. The work in Brock Inlier results from a resource assessment that will provide information for public consultations on a proposed national park (Jones et al., in prep.).

## MINTO INLIER

Minto Inlier, exposed on Victoria Island (Fig. 1), has not been mapped since 1:1 000 000 scale preliminary geological surveys in 1959 (Thorsteinsson and Tozer, 1962), yet it has continued to be an active area for mineral exploration (Jefferson et al., 1985). The age of the strata, presence of evaporites and cupriferous volcanic rocks make it a prime target for sediment-hosted stratiform copper (Kirkham, 1989).

### *Regional geology*

The Minto Inlier includes gently dipping late Proterozoic sedimentary rocks of the Shaler Group (Fig. 1) which comprises the Glenelg, Reynolds Point, Minto Inlet, Wynniatt, and Kilian formations (Thorsteinsson and Tozer, 1962; Fig. 1). The Kilian Formation was subsequently subdivided, and a new name (Kuujjua Formation) was informally proposed for the lithologically distinct unit of quartzarenite which caps the sedimentary sequence in the Southwest Domain (Jefferson et al., 1985; Rainbird, 1991).

The Shaler Group is unconformably to conformably overlain by flood basalts of the Natkusiak Formation. The flood basalts are fed by 723 Ma Franklin diabase dykes and

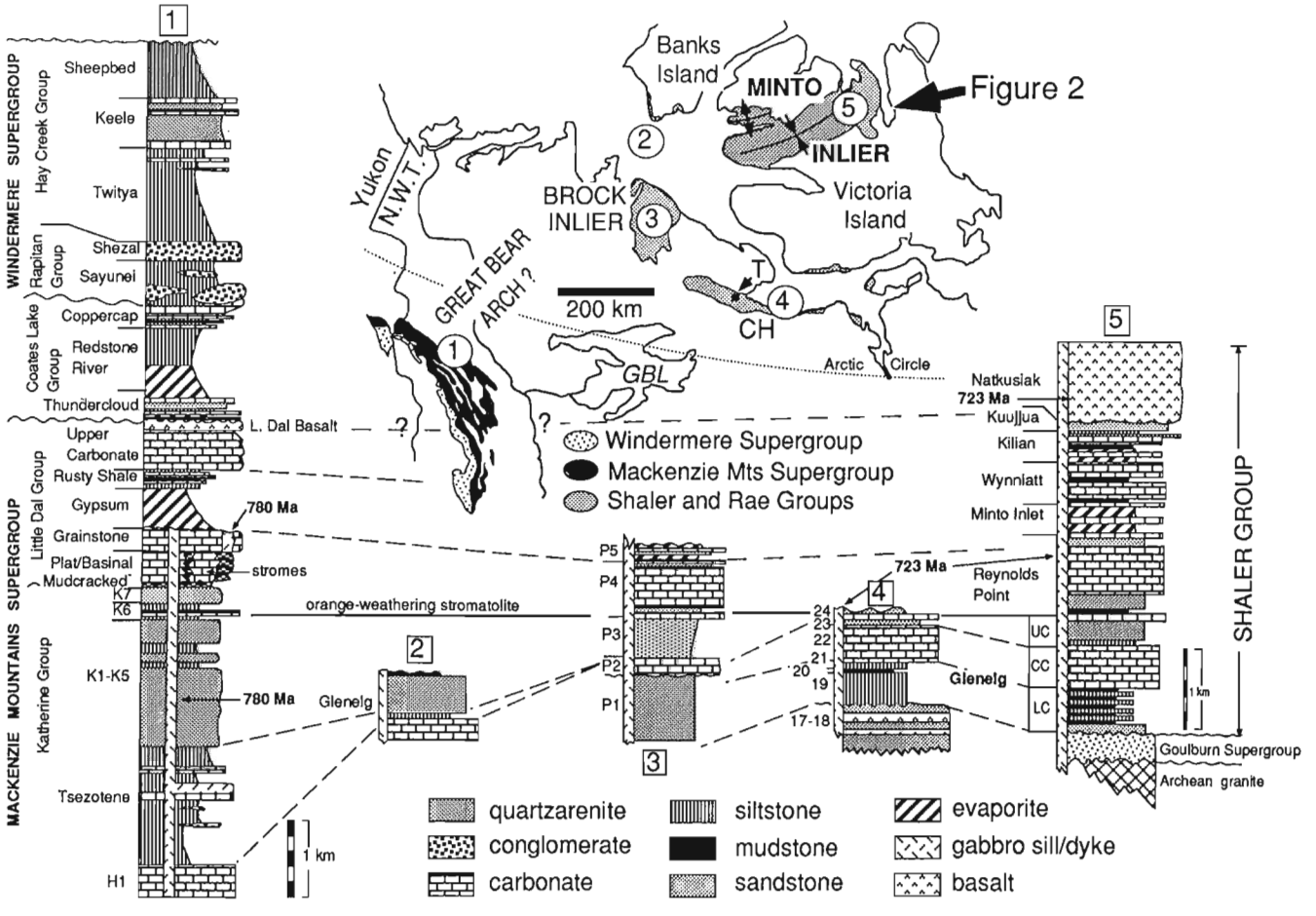


**Figure 1.** Regional correlation of late Proterozoic strata from northwestern Canada (after Jefferson and Young, 1989). CH, Coppermine Homocline (Rae Group); T, Turner Showing.

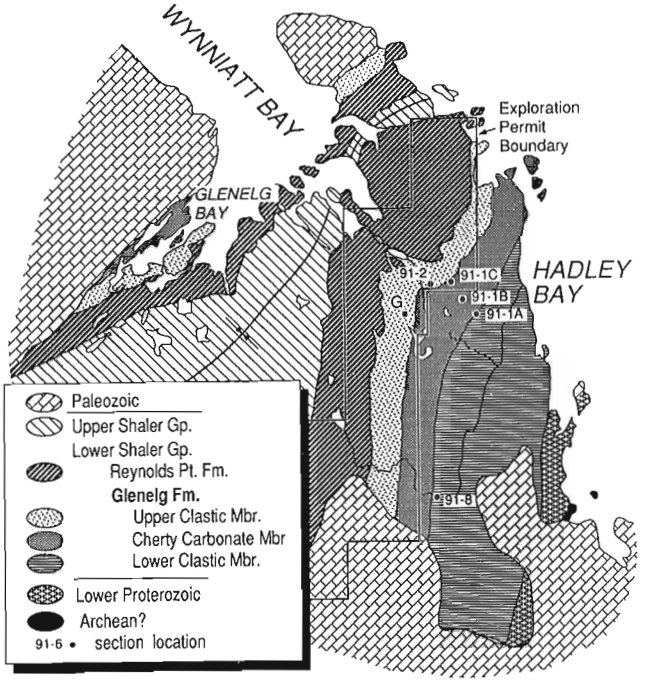


**Figure 2.** General geology of the Northeast Domain of the Minto Inlier emphasizing approximate distribution of the members of the Glenelg Formation and stratigraphic section locations (after Thorsteinsson and Tozer, 1962). G = Greenhills Showing.

sills (Heaman et al., 1992) that intrude the sedimentary strata preferentially along faults and bedding planes. A lower age limit for the Shaler Group of 1.11 Ga has been established by U-Pb dating of detrital zircons from the lower Reynolds Point Formation (Rainbird, 1991).

The Shaler Group unconformably overlies a small inlier of steeply dipping quartzose arenites and minor carbonate rocks on the southwest side of Hadley Bay (Fig. 2). These strata have been correlated with the Goulburn Supergroup in the Kilohigok Basin of the Bathurst Inlet area (Campbell and Cecile, 1981), and are underlain by granodiorite dated by K-Ar at 2.4 Ga but thought to be late Archean (Thorsteinsson and Tozer, 1962).

The Glenelg Formation is the principal unit of investigation because it is host to disseminated copper sulphides. Previous descriptions of the Glenelg Formation indicate that it is divisible into three members: the Lower Clastic Member, Cherty Carbonate Member, and Upper Clastic Member (Dixon, 1979; Thorsteinsson and Tozer, 1962; Young, 1981).

## *Glenelg Formation*

### Lower Clastic Member

The Lower Clastic Member is a recessive unit composed primarily of mudstone and siltstone. We examined only the upper part of the Member at a creek gully draining the coastal plain on the west side of Hadley Bay (Section 91-8; Fig. 3). The lower contact of the member with the Goulburn Supergroup is not exposed; an angular unconformity is assumed on the basis of steep dips in subjacent Goulburn that contrast with the very shallow dips of the Glenelg Formation.

The base of section 91-8 is composed of fine, rhythmically laminated green-grey mudstone and siltstone interbedded with thin beds of pinkish grey fine sandstone exhibiting both parallel and ripple cross-lamination. Ball-and-pillow structures are common at the base of sandstone layers. Gutters also are common and indicate an east-west sense of transport. Rare sandstone lenses are up to 2 m thick and several tens of metres wide. Lamination parallels the broad undulose lower bounding surfaces of these lenses. Further upsection the Lower Clastic Member comprises a 50-60 m thick sequence of very thinly laminated, fissile black mudstone. Carbonaceous films and flakes are common on bedding planes. Up to 20 cm elongate carbonate concretions are common in the upper 20 metres of this sequence. They are aligned within bedding and display aspect ratios of up to 10. Near the top of the member a distinctive 3 m-thick unit of red rudite is composed of rounded hematitic limestone pebbles and granules in a sandy matrix containing abundant glauconite. This unit is interbedded with 10-20 cm thick layers of variegated red mudstone and green siltstone.

The Lower Clastic Member is interpreted as a relatively deep water (below wave base) deposit based on the predominance of thick units of thinly laminated mudstone, lack of desiccation features and presence of intercalated sandstone interbeds displaying evidence for rapid deposition such as load structures and gutters. Such lithofacies sequences are typical of distal suspended sediment deposition (muds) punctuated by density current deposition triggered by failures on continental slopes (Pickering et al., 1989).

### Cherty Carbonate Member

A flat to broadly undulatory contact between the Cherty Carbonate and the Lower Clastic members of the Glenelg Formation is well exposed at section 91-8 (Fig. 3), where carbonates lie abruptly over thinly laminated black mudstone. Basal Cherty Carbonate Member strata comprise parallel to wavy laminated pink to red calcisiltite with thin interlaminations of maroon to red mudstone. Red mudstone interlayers and red coloration in the carbonate grade into uniform grey dolostone about 40 m above the basal contact. Lenticular to tabular flat chip rudite interbeds 5 to 20 cm thick compose up to half of the basal 50 m of the Cherty Carbonate Member. Some of the rudite layers exhibit normal grading.

The basal strata are overlain by a horizon containing numerous isolated carbonate mounds several metres wide and up to 2 m thick (Section 91-1A, Fig. 4). The mounds appear to be intercalated with and draped by the adjacent strata but have no preserved internal morphology. Overlying the mound horizon is a relatively thick succession of poorly preserved rhythmically bedded cream-colored dolosiltite cut by several diabase sills. Above the sills is a sequence of alternating dolosiltite, dolarenite, and intercalated flat chip rudite layers and pods. Some of the arenite beds display variably preserved planar crossbedding and hummocky

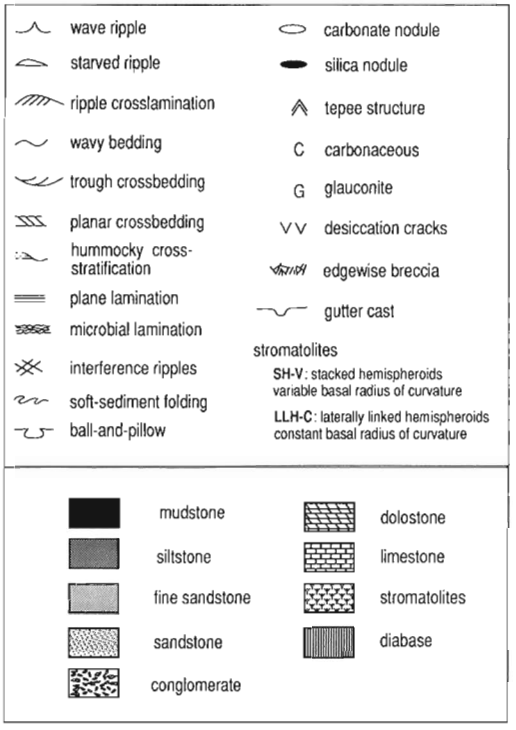


Key to sedimentary structure symbols and lithologic patterns used to describe stratigraphic columns (Figures 3 to 6, 8)

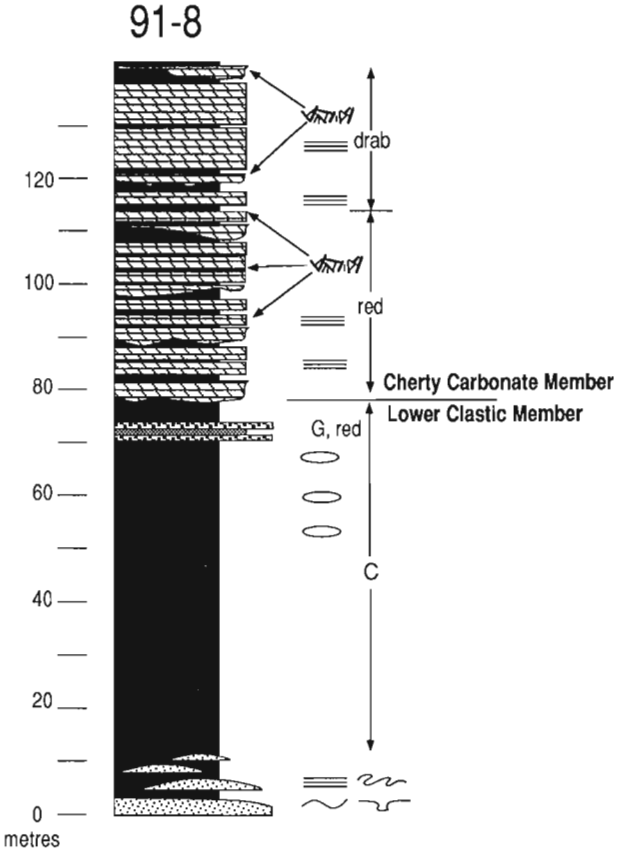


**Figure 3**. Section 91-8.

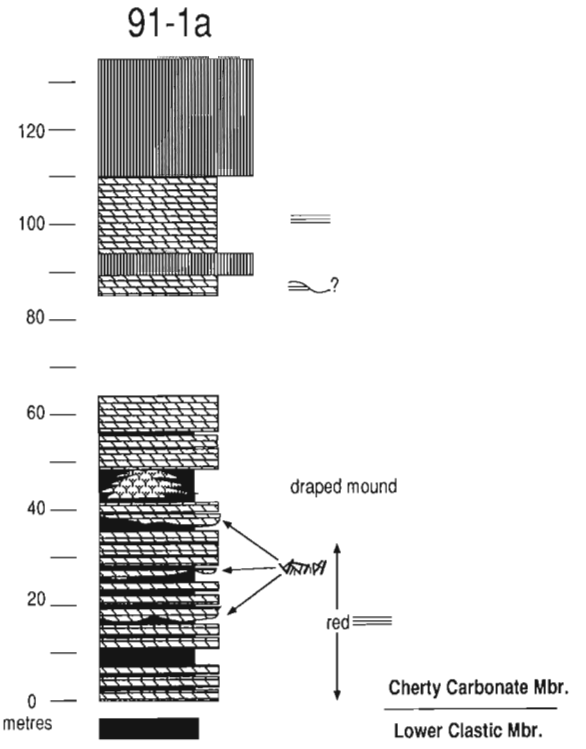


**Figure 4**. Section 91-1A.

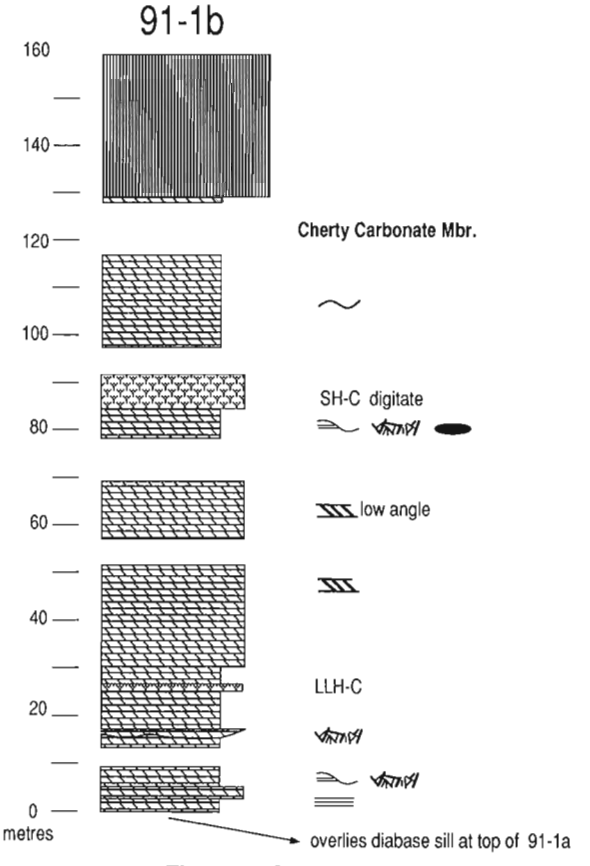


**Figure 5**. Section 91-1B.

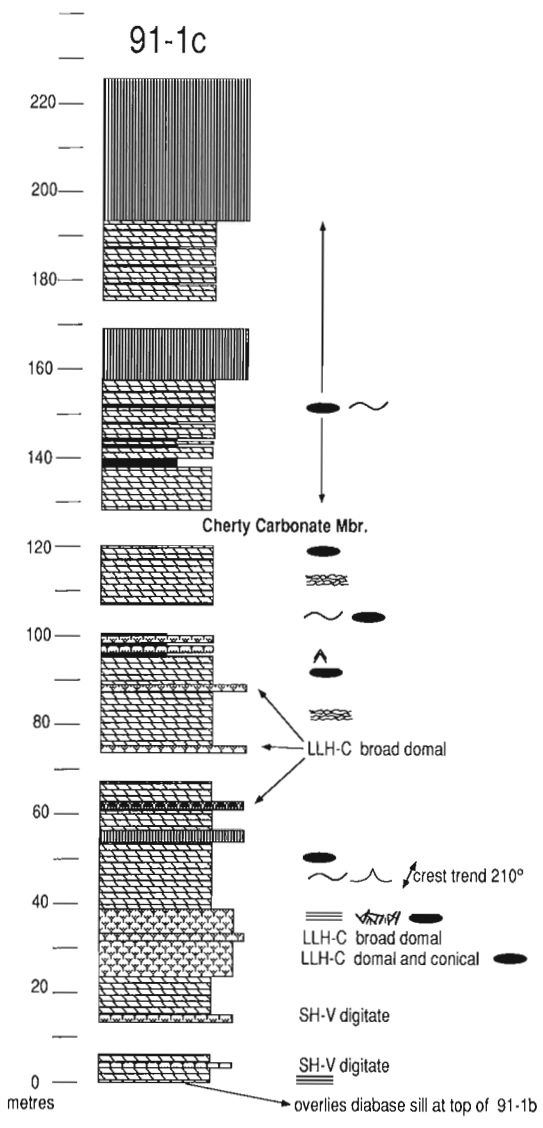


**Figure 6.** Section 91-1C.

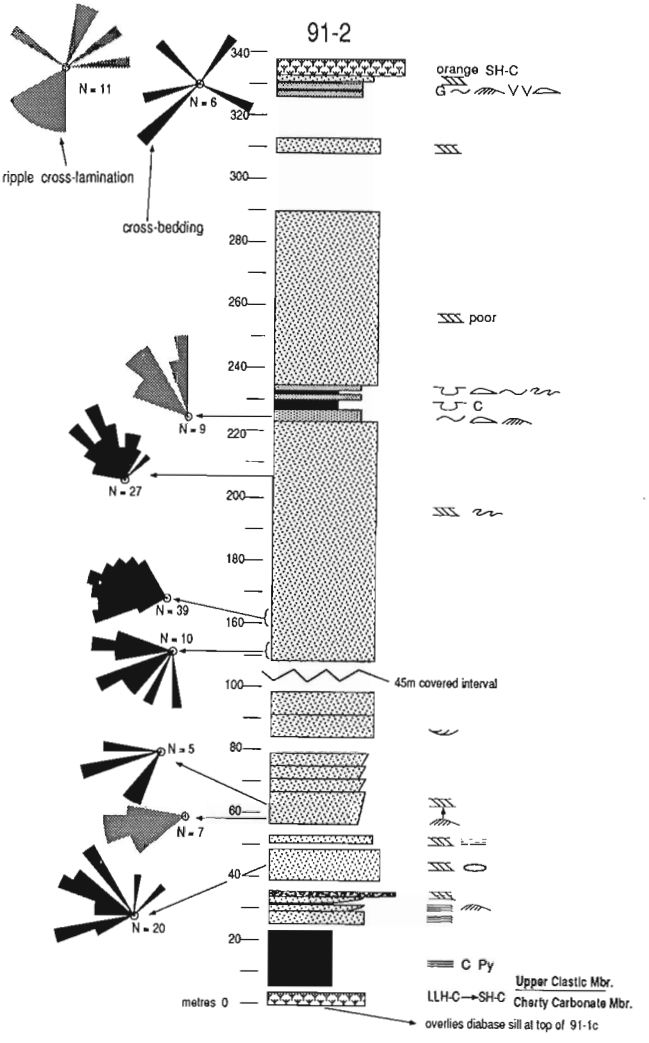


**Figure 8.** Section 91-2.

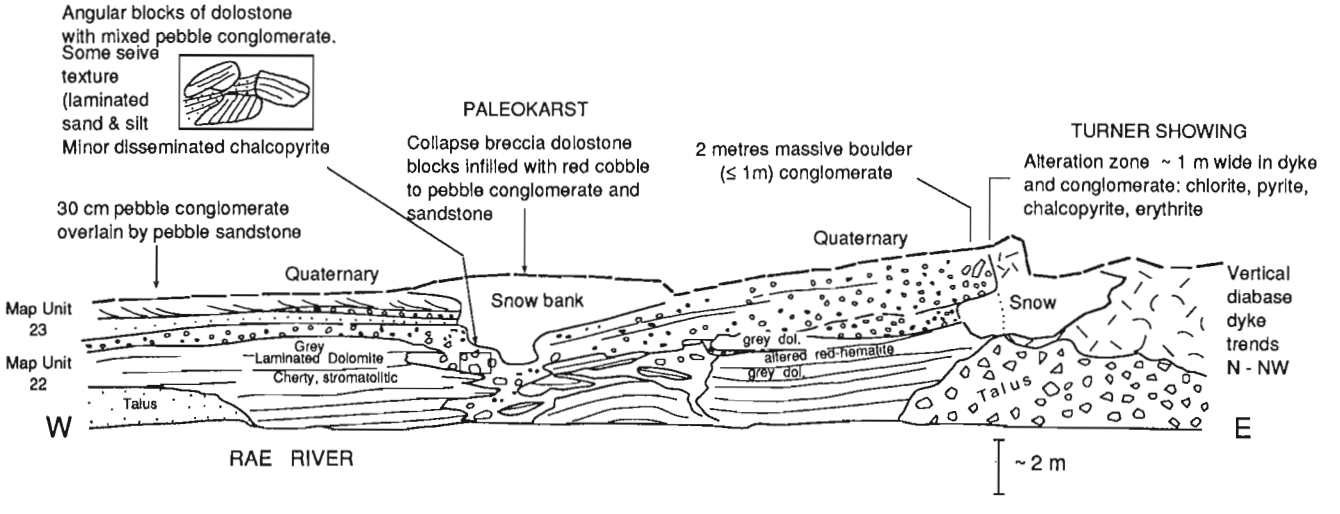


**Figure 7.** Sketch from photograph of paleokarst developed at the contact between equivalents of the Cherty Carbonate Member (Map Unit 22) and the Upper Clastic Member (Map Unit 23) at the Turner showing in the Rae Group, lower Rae River (Located on Figure 1).

cross-stratification (HCS) (see Section 91-1B, Fig. 5). Some of the interbedded siltstones exhibit possible microbial (crinkly) lamination and at least one stratum comprises laterally linked domal stromatolites.

Overlying the coarse clastic-textured carbonates are a series of stromatolitic layers of both laterally linked (LLH-C) and columnar digitate (SH-C, SH-V) forms interbedded with microbial laminites (see Section 91-1B and 91-1C, Fig. 5 and 6). Digitate forms are more common at the base and include a 7 m thick biostrome of 2-4 cm wide branching columns (Section 91-1B) and several thinner layers composed of larger non-branching club-like forms with variable basal radius of curvature (SH-V, Section 91-1C). Domal and rarer conical, laterally linked forms characterize the upper part of the stromatolitic subunit. Black and grey to frothy white chert patches and more continuous layers are ubiquitous within the upper half of the Cherty Carbonate Member particularly within the stromatolitic horizons where they constitute up to 40% of the rock. Microbial laminae are particularly well preserved by the silicification which has allowed recognition of a variety of filimentous and coccoid microfossils (Jefferson, 1977). The uppermost Cherty Carbonate Member strata are poorly preserved due to thermal alteration by diabase sills but stromatolites appear to predominate. Green and maroon mudstone interlayers are common in the upper 50-60 m.

Initial deposition of the Cherty Carbonate Member represents an abrupt switch from deep water clastic deposition to deposition of carbonates, presumably in shallower water, above the carbonate compensation depth. Also a change from drab to red coloration suggests oxidizing conditions which typically would be more common in shallower water. Reddening is considered to be early diagenetic or primary because it is present in the isolated rudite layer near the top of the Lower Clastic Member which is interpreted as resedimented detritus from a shallower water carbonate source. Likewise the edgewise rudite layers in the basal Cherty Carbonate Member are interpreted as outer shelf debris flow lobes and sheets derived from brecciation of early cemented inner shelf carbonates. Gradual shallowing is indicated by the upsection appearance of HCS and planar cross-bedding produced by storm waves on the inner shelf (e.g. Duke et al., 1991). The stromatolitic subunit at the top of the cherty carbonate member likely represents even shallower water deposition. The thick digitate stromatolite biostrome at the top of Section 91-1B could be the fringing reef of a carbonate bank which produced much of the resedimented detritus described above. Laterally linked stromatolites would have thrived in a lower energy back-reef setting. Smaller scale shallowing-upward cycles from an equivalent stratigraphic interval on Banks Island were described by Young and Jefferson (1975), however they have yet to be recognized in this study.

### Upper Clastic Member

At Section 91-2, and in several diamond drill cores, the stromatolitic Cherty Carbonate Member is draped by thin laminated mudstones of the Upper Clastic Member. Basal conglomeratic units were, however, observed locally. Typically, the basal strata rest on a rusty weathering stromatolite biostrome composed of 20-30 cm wide laterally linked domes with up to 15 cm of synoptic relief and elongation parallel to 030°. In a few other areas the substrate is flat, possibly microbial-laminated dolostone. At several field localities and in drill core the contact is marked by bleached and brecciated fragments of locally derived carbonate and chert. The breccia is overlain by a conglomerate composed of subrounded pebbles of chert and carbonate in a matrix of quartzarenite. Pyrite alteration is very common within the conglomerate and extends through fractures and veinlets into the underlying carbonate. These features and isopachs from diamond drill sections through the Upper Clastic Member (not provided) suggest paleotopography on the Upper Cherty Carbonate Member was on the order of tens of metres.

Vuggy alteration and sulphide mineralization along with in situ brecciation are features common to karst topography or exposure surfaces developed on emergent carbonate platforms (James and Choquette, 1988). This interpretation for the upper contact of the Cherty Carbonate Member is consistent with the overall emergent trend observed and with apparent paleotopography inferred from drill log isopachs. A similar and better developed paleokarst, with evidence of faulting, is preserved at the same stratigraphic horizon in Rae Group strata outcropping in the Coppermine Homocline (see discussion below and Fig. 7).

As noted above, the basal rock type of the Upper Clastic Member of the Glenelg Formation differs depending on locality, however in most areas it is a thinly laminated black carbonaceous to pyritic mudstone which drapes the stromatolitic unit at the top of the Cherty Carbonate Member. Grain size and lamination thickness increase and colour changes to grey-green up-section. Further up-section red siltstone interbeds and fine sand starved ripples are common. The total thickness of the fine grained interval varies from 0-25 m in sections examined to date. In the Brock Inlier this unit is 0-10 m thick; in the Mackenzie Mountains the equivalent Tzesotene Formation is about 1300 m thick (Fig. 1).

In the Minto Inlier, this fine grained unit is gradationally overlain by fine-grained pink to grey quartzarenite with thin wavy siltstone interlaminations. At section 91-2 (Fig. 8) this interval is characterized by two 2-4 m thick coarsening-up cycles capped by plane bedded quartzarenite. The second cycle is overlain by an 80 cm-thick bed of planar crossbedded white to grey chert-pebble conglomerate. Crossbeds indicate transport to the northwest. A similar but thinner conglomerate also was observed in several drill cores taken through this interval. Overlying the conglomerate is a sequence of alternating ripple crosslaminated to thin planar-crossbedded fine sandstone and parallel-laminated to lenticular-bedded siltstone. Gradual coarsening upward and disappearance of the siltstone units was noted. The siltstone units were seen only in drill core and probably are represented by the recessive covered intervals in the lower part of section 91-2 (Fig. 8). Ripple crosslamination and small-scale crossbeds in the quartzarenite units indicate mainly westerly paleocurrents (Fig. 8).

Above is an approximately 80 m thick unit of fine- to medium-grained white to light pink quartzarenite interbedded with thin (m) intercalations of red ripple crosslaminated to parallel-bedded siltstone and very fine quartzarenite. Small- to moderate-scale planar-tabular crossbedding characterizes the coarser grained quartzarenites, recording strongly unimodal westerly paleocurrents in the lower part of the unit and northwesterly transport in the upper part (Fig. 8). Recumbently folded crossbedding and water escape structures have been described from this unit by (Young, 1974) and also occur in the Brock Inlier and Coppermine Homocline. The fine red units may form the tops of several-metre-thick fining upward cycles; rip-ups were observed at the base of sandstone units in drill core. Coarsening up cycles, similar in scale to the one at the base of section 91-2, were observed in reconnaissance examination of cliff sections in Glenelg Bay (Fig. 2).

Overlying the thick sandstone unit at section 91-2 is a wavy to lenticular bedded fine buff sandstone and green siltstone horizon with well preserved ripple crosslamination yielding north to northwesterly paleocurrents. This fines upward to a distinctive 3-4 m thick black carbonaceous mudstone and fine sandstone horizon containing spectacular ball-and-pillow structures with sand balls up to 3 m long and 1 m thick. This in turn coarsens upward through another unit of wavy to lenticular bedded sandstone and siltstone into a 50-60 m thick massive to faintly crossbedded, conchoidally fractured white quartzarenite.

Above a thick covered interval is a unique variegated unit of parallel bedded to planar crossbedded fine grained pink to green quartzarenite interbedded with wavy- to lenticular-bedded fine sandstone and green siltstone. Glauconite is present throughout accounting for the local dark green hue of the quartzarenite. Both wave and current ripples are present and show polymodal paleocurrents (Fig. 8). Desiccation cracks are preserved on bedding plane surfaces exposed on talus blocks below the outcrop.

The Glenelg Formation is capped by an orange-weathering dolostone biostrome composed of relatively large, straight and branching columnar stromatolites which have been described in detail by Jefferson (1977) and Jefferson and Young (1989). The biostrome is up to 160 m thick, although it is generally less than 35 m thick in the present study area, and forms one or two prominent markers which have been traced to the Brock Inlier, Coppermine Homocline, and southward as far as the Mackenzie Mountains (Jefferson and Young, 1989).

The coarsening upward cycle at the base of the Upper Clastic Member of the Glenelg Formation was first described by (Young, 1974), who interpreted it as the deposit of a prograding delta. Our data strongly support this interpretation. We consider that the multiple coarsening upward cycles represent overlapping delta lobe sands, and the intervening fine grained sediments are interdistributary, delta slope and prodelta deposits. The large scale of the coarsening upward sequences, and features indicative of rapid deposition on a slope (slumps and ball-and pillow structures) are typical of river-dominated delta deposits (Coleman and Prior, 1980). Smaller scale fining-upward cycles within the thick sandstone units at the tops of the larger cycles are typical of stacked braided stream channel deposition and bar top aggradation (Miall, 1984). A braided stream interpretation is consistent with the unimodal paleocurrents which indicate that the rivers built deltas which prograded to the northwest. The uppermost sandstone and siltstone unit offers the first indication, within the Upper Clastic Member, of shallow marine influence with the presence of glauconite and with crossbeds and ripples indicating polymodal paleocurrents. Tides and waves probably reworked the delta top as river current influence waned. Continued marine influence and cessation of clastic influx is recorded by deposition of the regionally extensive orange-weathering stromatolite marker at the top of the Glenelg Formation (Jefferson and Young, 1989).

## BROCK INLIER AND RAE GROUP: NEW INSIGHTS ON MINTO INLIER-BROCK INLIER-COPPERMINE HOMOCLINE-MACKENZIE MOUNTAINS CORRELATION

Equivalents of the Glenelg Formation are shown in Figure 1 (references in Jefferson and Young 1989). Contrary to earlier interpretations, Jefferson and Jones, (1991) suggested that Proterozoic sedimentation in Brock Inlier was more basinal (but still platformal), in comparison to proximal shoreline deposition elsewhere in Amundsen Basin[1]. The following observations relate stratigraphic observations in the Brock Inlier and the Rae Group to those of the Glenelg Formation.

The Brock Inlier exposes an unmetamorphosed late Proterozoic sedimentary sequence which is gently dipping with local steep dips and faults. The oldest map-unit, P1, is an estimated 900 m of drab grey mudstone and siltstone containing carbonate concretions, some of which preserve HCS. P1 is a more basinal equivalent of the Lower Clastic Member of the Glenelg Formation on Victoria Island, and map-units 19 to 21 in the Rae Group (Fig. 1). Its equivalent is not exposed in Mackenzie Mountains. In the Rae Group, map-unit 21 is a red and green crossbedded sandstone that may correspond to the red rudite unit at the top of the Lower ClasticMember of the Glenelg Formation.

P2 in the Brock Inlier gradationally overlies map-unit P1, comprising up to 240 m of grey cherty dolostone with stacked flat-chip intraformational breccia and stratiform, bulbous, and columnar stromatolites. The stromatolites form biostromes with little growth relief. P2 records flat sabkha-like shoreline sedimentation. The P2 cherty carbonate facies and stromatolites correspond very closely to the Cherty

[1]Amundsen Basin (also referred to as Amundsen Embayment) is an inferred contiguous late Proterozoic depository of which the Minto Inlier, southern Banks Island Inlier, Duke of York Inlier, Brock Inlier (Shaler Gp.), and Coppermine Homocline (Rae Gp.) are remanent components.

Carbonate Member of Glenelg Formation, to map-unit H1 of Mackenzie Mountains Supergroup, and to unit 22 of the Rae Group (Fig. 1). The base of unit 22 is interdigitated with unit 21, which contains zones of 1 to 3 m stromatolite bioherms initiated on intraformational breccia. Concretions preserve HCS and breccia. Siltstones above the bioherms are deep green and glauconitic.

Map-Unit P3 is a coarsening-upward quartzarenite sequence, estimated to be 450 m thick and interpreted as a northwest-prograding fluvio-deltaic braidplain. In southern Brock Inlier the cherty dolostones (P2) are abruptly overlain by 2 to 10 m of deep red flaggy fine sandstone and siltstone with shale interbeds and local glauconite. These grade upward to pale red quartzarenites that form the bulk of P3. North of the Brock River canyon, however, several metres of black, green, and red shales between the dolostone and sandstone suggest a more basinal setting. Correlative Shaler Group strata are the Upper Clastic Member of Glenelg Formation. P3 correlatives to the southeast are thinner (Rae Group Unit 23 = 90 m), but to the southwest are >2.5 km (Tsezotene mudstones >1200 m + Katherine quartzarenites K1 to K5 >1300 m). The base of the quartzarenite sequence in the Rae Group (Unit 23) is characterized by spectacular karst paleotopography, paleokarst breccias, and wedges of locally derived orthoconglomerate.

The paleokarst zones in the Rae Group trend northerly, as do thin lenses of pyritic conglomerate which fine upward to grey trough-cross-bedded sandstones. These are blanketed by red hematitic trough-cross-bedded arenites recording easterly paleocurrents. G.M Young (pers. comm., 1991) reports that white quartzarenites of Unit 21 contain overturned tabular crossbeds, northwest-paleocurrents (mean 309°, n=30) and large cylindrical dewatering structures. The coarsening-upward paleodelta blanket model applies to map-unit 23, above the basal coarse clastics.

Previous paleogeographic models have shown that the Brock Inlier occupies the east flank of the Great Bear Arch (see Young, 1981, Fig. 12-2), suggesting proximity to a northwesterly-trending paleo-shoreline. The above thickness and paleocurrent data are more compatible with a northeasterly trending paleo-shoreline. We therefore interpret the depositional setting of the Brock Inlier as deeper platform compared to the Coppermine Homocline and Minto Inlier where thinner arenites abruptly overlie paleokarsted dolostones and local basal conglomerates. The Great Bear "Arch" appears to have been more of a shoulder facing northwesterly into the Amundsen Basin and southwesterly into the Cordilleran basin (Fig. 1), rather than an active arch separating the two basins during P3 sedimentation.

A key stratigraphic element in the history of the Amundsen Embayment and its mineral potential is recognition of the unconformity between the Cherty Carbonate and Upper Clastic Members of the Glenelg Formation and their equivalents. In deeper platformal sections (e.g. Wynniatt Bay, northern Brock Inlier, and Mackenzie Mountains; Fig. 1 and 2) this hiatus is represented only by the abrupt contact between carbonates and mudstones. Only in marginal areas, such as Hadley Bay (Minto Inlier) and and Coppermine Homocline, is the sedimentary record of uplift, local faulting, weathering, and alluvial reworking of the carbonates evident. The tectonic implications of this unconformity and its link to the prograding delta deposits of the Upper Clastic Member require further investigations.

## COPPER PROSPECTS

### *Upper Clastic Member, Glenelg Formation, Minto Inlier*

Three styles of copper mineralization with variable cobalt, silver, and nickel have been recognized within the Glenelg Formation: 1) disseminated stratiform sulphides, widespread within quartzarenites of the Upper Clastic Member; 2) sulphides from contact metamorphism along the lower margin of a diabase sill that intrudes portions of the Upper Clastic Member-Cherty Carbonate Member contact; and 3) extensive zones of massive sulphide replacement associated with karsting of the Cherty Carbonate Member.

Stratiform copper has been discovered within several stratigraphic levels of the Upper Clastic Member. The highest concentrations are hosted by the lowermost quartzarenite and the irregularly developed chert-pebble conglomerate. Chalcopyrite and pyrite with subordinate tennanite and enargite form disseminations and massive matrix/cement replacements. Malachite and erythrite are developed locally along fractures and on weathered outcrop surfaces. The basal quartzarenite unit is mineralized over an extensive area and exhibits crude, large-scale mineral zonation. The easternmost exposures of the quartzarenite contain sparsely disseminated pyrite with rare chalcopyrite grains and minor malachite. Pyrite and chalcopyrite increase toward the recently discovered Green Hills showing on the extreme western edge of the exposed lower quartzarenite horizon. Silver, cobalt, and nickel generally increase with increased copper grade but the irregular distribution of element values suggests that there may be a vertical as well as lateral zonation. As indicated by diamond drilling, Upper Clastic Member strata thin toward what is interpreted to represent a northeast-trending paleo-ridge. An apparent concentration of disseminated pyrobitumen along the ridge trend is considered to have been important in localizing sulphide mineralization.

A carbonate replacement style of mineralization occurs over the karst-altered upper surface of the Cherty Carbonate Member. An Input airborne electromagnetic survey has defined the limits of this highly conductive sulphide accumulation which is confined to a 15 by 30 km area, centered on the interpreted paleotopographic ridge. Limited diamond drilling has intersected up to 20 metres of massive pyrite and subordinate chalcopyrite, tennanite and enargite.

Contact metamorphic sulphide concentrations have been noted at the partly altered and serpentinized contact between the uppermost Cherty Carbonate Member and an overlying diabase sill. Semi-massive chalcopyrite with malachite and erythrite forms narrow pods within the altered carbonate and is interpreted as remobilized karst-hosted mineralization. High quality specimens of specularite have also been observed filling vugs in contact zone carbonates.

### *Unit P3-Brock Inlier*

Unit P3 in Brock Inlier was investigated as a possible host for disseminated copper sulphides because it correlates with the Upper Clastic Member of the Glenelg Formation. Unit P3 contains minor pyrite and gossans at its base in Brock River Canyon, and its thick red-bed sequence is characteristic of the stratabound sediment-hosted copper deposit model. Examination and trace element analysis of hand samples, stream silts and soil samples from the P2-P3 contact at nearly a dozen localities has located minor copper (up to 180 ppm) at one site in the Brock River canyon. Details of these surveys are given by Jones et al. (in prep.).

The re-interpretation of Proterozoic rocks in Brock Inlier representing a more basinal setting than equivalent units leads us to tentatively conclude that the sequence in Brock Inlier is less prospective for copper.

### *Turner Showing-Upper Rae Group, Coppermine Homocline*

The Turner Showing was previously described by Thorpe (1970, p. 143; see Fig. 1 and 7) based on oral communication from Mr. Turner. The element associations noted by Thorpe are very similar to those in the Glenelg Formation.

At the Turner Showing a diabase dyke occupies a precursor fault inferred from the combination of a 2-metre thick westward-tapering conglomerate abutting its western contact, versus trough crossbedded sandstone on the east. Chalcopyrite (with erythrite) is disseminated in the orthoconglomerate, the paleokarst collapse breccia, and a one metre alteration zone on the west side of the dyke.

## ACKNOWLEDGMENTS

This contribution is jointly funded by DIAND, GSC, Canadian Parks Service (A-Base) and Canada-Government of Northwest Territories Mineral Development Agreement 1991-96. Polar Continental Shelf Project supplied helicopter support in the Brock Inlier, through the excellent piloting of Bruce Swain and the capable engineering of Kevin Bond. We also thank Noranda Exploration company, Aber Resources Ltd. and Nanisivik Mines Ltd. for support and permission to describe the mineral showings in the Glenelg Formation. We thank Larry Aspler for considerable improvements to an earlier version of the manuscript.

## REFERENCES

**Campbell, F.H.A. and Cecile, M.P.**
1981: Evolution of the early Proterozoic Kilohigok Basin, Bathurst Inlet-Victoria Island, N.W.T.; in Proterozoic Basins of Canada, (ed.) F.H.A. Campbell; Geological Survey of Canada, Paper 81-10, p. 103-131.

**Coleman, J.M. and Prior, D.B.**
1980: Deltaic sand bodies; American Association of Petroleum Geologists, Education Course Note Series No. 15, 171 p.

**Dixon, J.**
1979: Comments on the Proterozoic stratigraphy of Victoria Island and the Coppermine area, Northwest Territories; in Current Research, Part B; Geological Survey of Canada, Paper 79-1B, p. 263-267.

**Duke, W.L., Arnott, R.W.C., and Cheel, R.J.**
1991: Shelf sandstones and hummocky cross-stratification: New insights on a stormy debate; Geology, v. 19, p. 625-628.

**Heaman, L.M., LeCheminant, A.N., and Rainbird, R.H.**
in press: Nature and timing of Franklin igneous events, Canada: Implications for a late Proterozoic mantle plume and the break-up of Laurentia; Earth and Planetary Science Letters.

**James, N.P. and Choquette, P.W.**
1988: Introduction, in Paleokarst, (ed.) N.P. James and P.W. Choquette; New York, Springer-Verlag, p. 1-21.

**Jefferson, C.W.**
1977: Stromatolites stratigraphy and sedimentology of parts of the Amundsen Basin, N.W.T.; unpublished MSc. thesis, University of Western Ontario, London, Ontario, 260 p.

**Jefferson, C.W. and Jones, T.A.**
1991: Revised Stratigraphy and Structure of Proterozoic to Cretaceous Strata in and around the Brock Inlier, NTS 97A and 97D: Some Implications for Mineral and Energy Resource Assessment of the Proposed Bluenose Lake National Park, N.W.T; in Exploration Overview: Mining, Exploration and Geological Investigations, Northwest Territories 1991; Geology Division, Northern Affairs Program, Yellowknife, N.W.T.

**Jefferson, C.W. and Young, G.M.**
1989: Late Proterozoic orange-weathering stromatolite biostrome, Mackenzie Mountains and western Arctic Canada; in Reefs, Canada and adjacent areas, (ed.) H.H.J. Geldsetzer, N.P. James, and G.E. Tebbutt; Canadian Society of Petroleum Geologists, Memoir 13, p. 72-80.

**Jefferson, C.W., Nelson, W.E., Kirkham, R.V., Reedman, J.H., and Scoates, R.F.J.**
1985: Geology and copper occurrences of the Natkusiak basalts, Victoria Island, District of Franklin: in Current Research, Part A; Geological Survey of Canada, Paper 85-1A, p. 203-214.

**Jones, T.A., Jefferson, C.W., and Morrell, G.**
in prep.: Evaluation of the mineral and energy resource potential of the Brock Inlier - Bluenose Lake Area; Geological Survey of Canada, Open File 2434.

**Kirkham, R.V.**
1989: Distribution, settings and genesis of sediment-hosted copper deposits, in Sediment-hosted Stratiform Copper Deposits, (ed.) R.W. Boyle, A.C. Brown, C.W. Jefferson, E.C. Jowett, and R.V. Kirkham; Geological Association of Canada, Special Paper 36, p. 3-38.

**Miall, A.D.**
1984: Sandy fluvial systems, in Facies Models, (ed.) R.G. Walker; Geological Association of Canada, Geoscience Canada Reprint Series No. 1, p. 71-90.

**Pickering, K.T., Hiscott, R.N., and Hein, F.J.**
1989: Deep Marine Environments: Clastic sedimentation and tectonics: London, Unwin and Hyman, 416 p.

**Rainbird, R.H.**
1991: Stratigraphy, sedimentology and tectonic setting of the upper Shaler Group, Victoria Island, Northwest Territories; PhD. thesis, University of Western Ontario, London, Ontario, 257 p.

**Thorpe, R.I.**
1970: Geological exploration in the Coppermine River area, Northwest Territories, 1966-1968; Geological Survey of Canada, Paper 70-47, 150 p.

**Thorsteinsson, R. and Tozer, E.T.**
1962: Banks, Victoria and Stefansson Islands, Arctic Archipelago; Geological Survey of Canada, Memoir 330, 83 p.

**Young, G.M.**
1974: Stratigraphy paleocurrents and stromatolites of the Hadrynian (upper Precambrian) rocks of Victoria Island, Arctic Archipelago, Canada; Precambrian Research, v. 1, p. 13-41.
1981: The Amundsen Embayment, Northwest Territories; relevance to the upper Proterozoic evolution of North America, in Proterozoic Basins of Canada, (ed.) F.H.A. Campbell; Geological Survey of Canada, Paper 81-10, p. 203-211.

**Young, G.M. and Jefferson, C.W.**
1975: Late Precambrian shallow water deposits, Banks and Victoria Islands, Arctic Archipelago; Canadian Journal of Earth Sciences, v. 12, p. 1734-1748.

**Young, G.M. and Long, D.G.F.**
1977: A tide-influenced delta complex in the upper Proterozoic Shaler Group, Victoria Island, Canada; Canadian Journal of Earth Sciences, v. 14, p. 2246-2261.

Geological Survey of Canada Project 890011

# Relationship between faults in the Southern Province and the Grenville Front southeast of Sudbury, Ontario

**A. Davidson**
**Continental Geoscience Division**

*Davidson, A., 1992: Relationship between faults in the Southern Province and the Grenville Front southeast of Sudbury, Ontario; in Current Research, Part C; Geological Survey of Canada, Paper 92-1C, p. 121-127.*

***Abstract***

*Just south of Coniston, Ontario, the east-northeast continuation of the Murray fault, a major, steep fault in the Southern Province truncates the southeast-dipping, thrust-sense mylonite zone that constitutes the Grenville Front to the southwest. East of Coniston, this fault, known as the Wanapitei fault, is geometrically constrained to having downward displacement of Grenville Province high-grade gneisses with respect to low-grade Huronian rocks in the adjacent Southern Province. West of the mylonite zone truncation, the Murray fault shows net displacement of the opposite sense, as documented by recognition that formations on the south side are lower in the Huronian succession than those on the north. The opposing senses of displacement can be reconciled by allowing reactivation of the Murray/Wanapitei fault after formation and uplift of the Grenville Front mylonite zone, possibly related to development of the St. Lawrence rift system during the late Proterozoic.*

***Résumé***

*Juste au sud de Coniston (Ontario), le prolongement est-nord-est de la faille Murray, une grande faille abrupte dans la province du Sud, tronque la zone mylonitique suivant le sens du chevauchement et plongeant vers le sud-est, qui constitue le front de Grenville au sud-ouest. À l'est de Coniston, cette faille, appelée faille de Wanapitei, est géométriquement limitée, caractérisée par un déplacement vers le bas des gneiss de la province de Grenville fortement métamorphisée comparativement aux roches huroniennes à faible degré de métamorphisme situées dans la province du Sud adjacente. À l'ouest de la troncature de la zone mylonitique, la faille Murray présente un déplacement net à direction opposée, documenté par le fait que les formations dans le compartiment sud sont plus basses dans la succession huronienne que celles dans le compartiment nord. Les directions opposées du déplacement peuvent s'expliquer par une réactivation de la faille Murray/Wanapitei après la formation et le soulèvement de la zone mylonitique du front de Grenville, peut-être liés à la mise en place du système d'effondrement du Saint-Laurent au cours du Protérozoïque tardif.*

## INTRODUCTION

The boundary between the Grenville and Southern provinces southeast of Sudbury has long been known to have two distinct manifestations (Phemister, 1961; Grant et al., 1962; Dalziel et al., 1969). Southwest of Coniston (Fig. 1) it is represented by a moderately southeast-dipping zone of intense mylonitization involving Southern Province rocks and overlying gneisses of uncertain correlation. East-northeast of Coniston it is the locus of a major, steep, brittle fault, the Wanapitei fault, which truncates the Grenville Front mylonite zone and passes westward into the Southern Province, where it is continuous with the well-known Murray fault.

Southwest of Coniston, the Grenville Front was interpreted as a metamorphic transition by Phemister (1961; Grant et al., 1962), whereby the Huronian sedimentary rocks and Nipissing gabbro of the Southern Province were abruptly metamorphosed and granitized to make gneissic and migmatitic rocks in the Grenville Province. Kwak (1968) documented an abnormally high metamorphic gradient across this zone. Dalziel et al. (1969) recognized that mylonitization was an important factor in the transition and that metamorphism preceded the earliest recorded folds; however, they did not favour the concept of large-scale tectonic transport by thrusting to explain the telescoping of older isograds, even though they expressed some doubt about the equivalence of rocks on either side of the front. More recently, the advent of kinematic analysis of fabrics in mylonitic rocks has allowed recognition that the sense of displacement recorded in these southeast-dipping rocks is one of thrusting to the northwest. The potential magnitude of displacement hinges on the still unanswered question whether or not the Grenville Province gneisses are highly metamorphosed and deformed equivalents of Southern Province rocks.

Concerning the faulted segment of the front east to Coniston, Phemister (1961, p. 61) stated: "One of the features that makes this region of special interest is that here the Wanapitei fault is seen to cut across the "front" of metamorphism leaving no doubt therefore that it marks a younger event in the structural history of the region.... Thus ... the boundary in the western section is a metamorphic "front" while in the eastern part it is a fault." Dalziel et al. (1969, p. 211) described the Wanapitei fault as a brittle fracture, being a later effect which obscures "... the fundamental tectonic character of the front ...". An alternative interpretation was given by Lumbers (1975), who combined the front mylonite zone and the Wanapitei fault east of Coniston as a single feature, the "Grenville Front Boundary Fault"; his map shows the Murray fault (Wanapitei fault of earlier workers) passing northeastward from Daisy Lake (Fig. 1, 2) and remaining within the Southern Province rather than continuing along the front. This interpretation has been reproduced on subsequent geological compilations (Card and Lumbers, 1977; Dressler, 1984a).

There is concurrence of interpretation that the Wanapitei/Murray fault southwest of Coniston is a steep reverse fault, south-side-up, with a horizontal component of dextral displacement (Cooke, 1946; Phemister, 1961; Grant et al., 1962). Estimates of the amount of displacement, however, remained conjectural, as no marker units had been recognized by which to gauge the amount of offset. Phemister (1961, p. 43) suggested that, if the dextral component is displacement is great, the Grenville Province schists and gneisses should reappear north of the fault

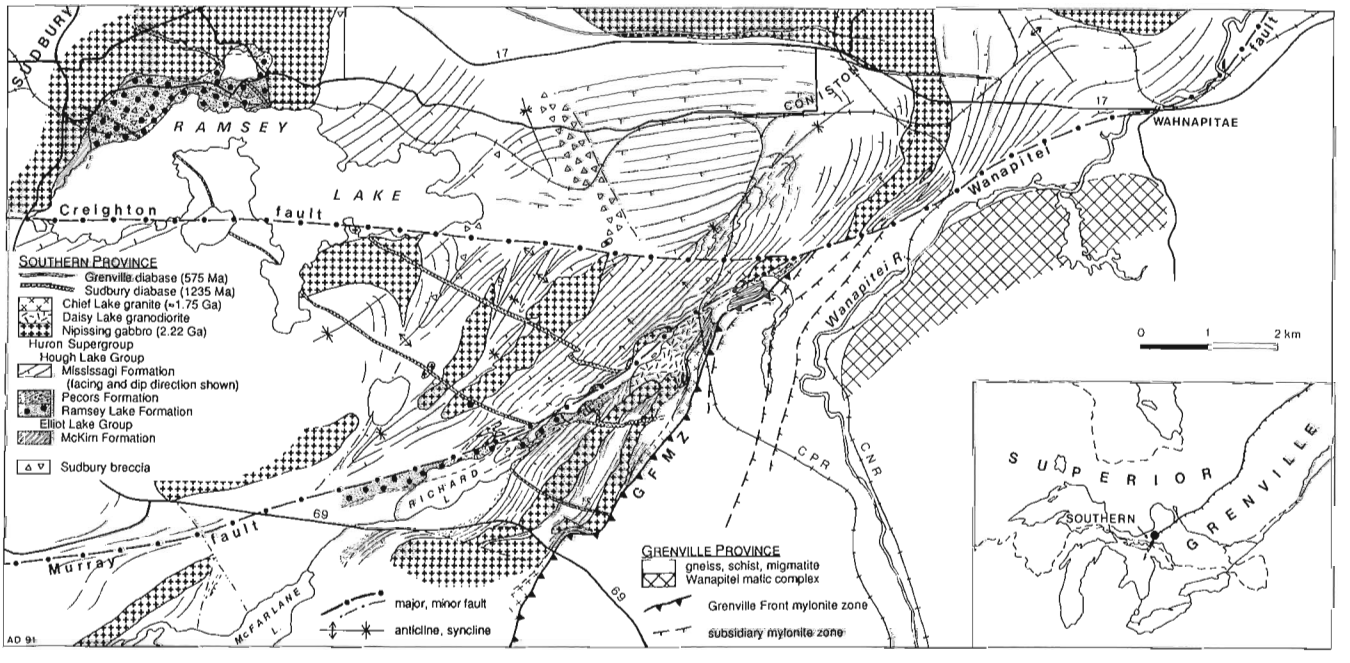


**Figure 1.** Geology and structure in the Southern Province next to the Grenville Front southeast of Sudbury. Geology, in part revised, from Thomson (1962) and Innes (1978).

"... somewhere to the east." According to the map compiled by Thomson (1962), the predicted reappearance does not occur for at least 14 km to the east; this amount of dextral displacement is an order of magnitude greater than recorded on the Worthington sector of the Murray fault to the west (≈1500 m; Yates, 1948).

Ignoring the regional context, it would seem logical to ascribe a south-side-up displacement across the Wanapitei fault east of Coniston, if for no other reason than the fact that high-grade gneissic rocks on the south side are juxtaposed against low-grade Huronian rocks to the north; this would be in keeping with observations along most parts of the Grenville Front that the Grenville is uplifted with respect to its foreland. However, if the Wanapitei fault displaces the Grenville Front mylonite zone, and if the dextral displacement is not great, simple geometry dictates that the dominant sense of displacement east of Coniston must be south-side-*down*. This would imply that the adjacent Southern Province rocks were once underneath the Grenville Front mylonite zone, now eroded north of the fault. A possible complicating factor in the displacement history may be that there has been some complementary offset along the Creighton fault (Fig. 1), which converges with the Wanapitei fault where the mylonite zone is cut out. Farther west, Yates (1948) estimated a dextral displacement component of ≈700 m on the Creighton fault.

In order to resolve questions concerning displacements on faults near the Grenville Front, it is necessary that the stratigraphy and structure of the Huronian rocks adjacent to the front be properly understood. Unfortunately, the stratigraphic succession in the area from Coniston to the southwest has been the subject of controversy ever since the region was first mapped (Coleman, 1914). The Mississagi Formation had at first been named the Wanapitei quartzite, assigned to the Sudbury series, and considered to be pre-Huronian (Coleman, 1914). Collins (1936) was the first to correlate formations in the Sudbury area with those of the type area far to the west. He traced the basal conglomerate eastward and found it to correlate with conglomerate stratigraphically beneath the Wanapitei quartzite in the vicinity of Ramsey Lake. Since the Ramsey Lake conglomerate itself does not lie unconformably on Archean rocks, but conformably on older sedimentary (McKim greywacke) and volcanic rocks, he restricted the older strata to the pre-Huronian Sudbury series, correlated the Mississagi and Wanapitei units, and assigned the Ramsey Lake and Mississagi to the Huronian Bruce Group. At the same time

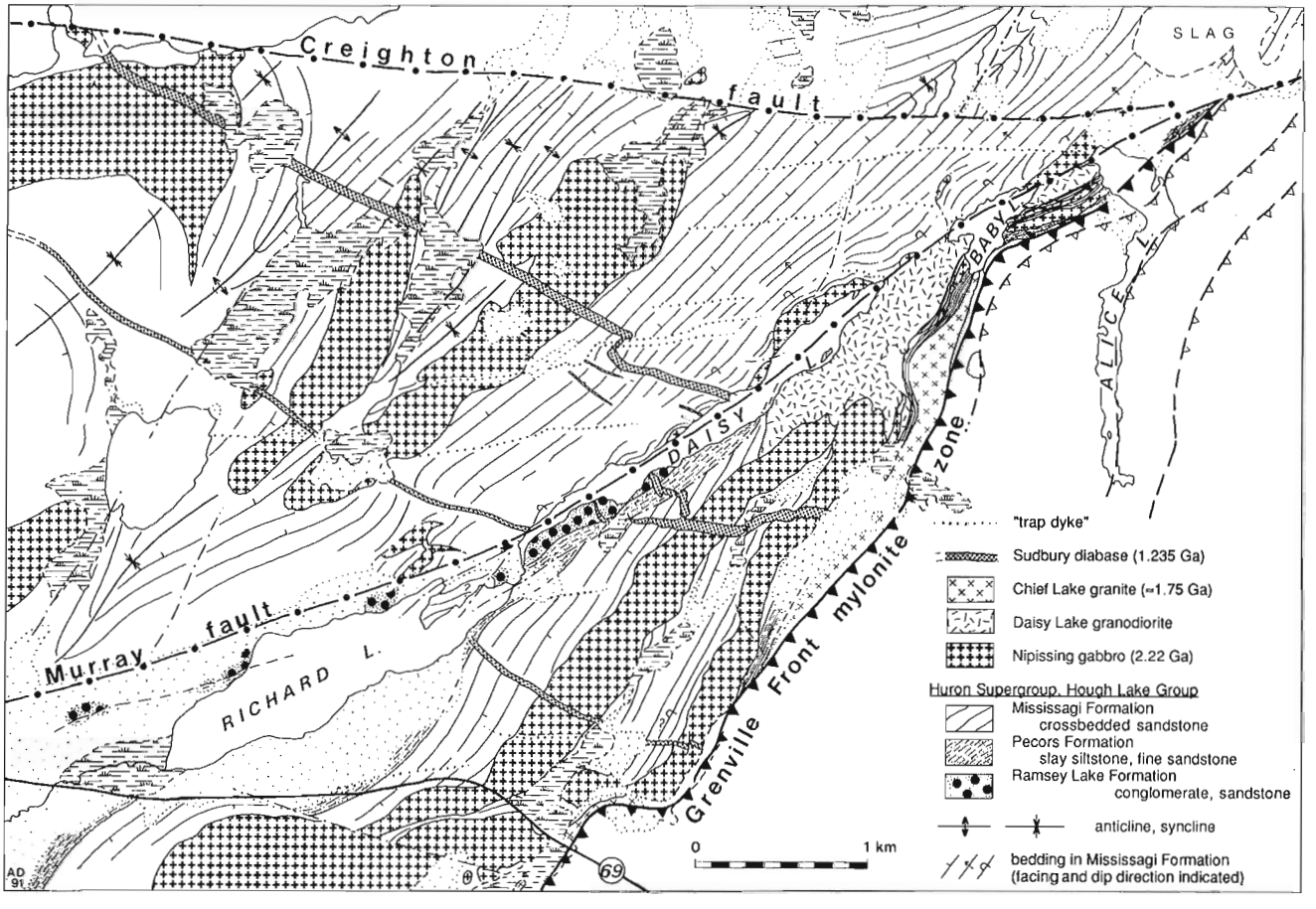


**Figure 2.** Detail of the area northeast of Richard Lake.

he recognized conglomerate of identical type to the south, in a strip along Daisy, Richard, McFarlane and Long lakes (Fig. 2). He postulated the two conglomerate occurrences to outline a major syncline, cored by the Mississagi "quartzite", and assigned the strata southeast of the Daisy-Long lakes strip to the Sudbury series. Cooke (1946) extended the Huronian succession to include the formations unconformably beneath the Ramsey Lake conglomerate in the Sudbury area, but could not resolve the fact that these formations apparently do not occur on the southeast side of Collins' syncline. He coined the name Coniston group for the mylonitic and schistose metasedimentary rocks that are now known to be associated with the Grenville Front, and considered them to be pre-Huronian.

Detailed mapping of the townships southeast of Sudbury in the late 1950s resulted in a compilation by Thomson (1962) in which he did not assign formation names; apparently unconvinced by the preceding interpretations, he exercised caution and produced a lithologic map. Lumbers (1975) and Card (1978), however, at a time when the Huronian stratigraphy had become much better understood (e.g. Robertson et al., 1969; Young, 1973), assigned formation names in the Sudbury area. They interpreted the occurrences of conglomerate and greywacke in the Daisy-Long lakes area as intraformational members of the Mississagi Formation, refuting Collins' identification of Ramsey Lake conglomerate and getting rid of Cooke's Coniston group.

The most recent geological map of the Sudbury region (Dressler, 1984a) follows this interpretation. It shows the Huronian rocks immediately adjacent to the front to belong entirely to the Mississagi Formation, a thick unit of well bedded, cross-stratified, feldspathic quartz sandstone with thin, silty interbeds. This unit is cut by several intrusions of Nipissing gabbro (2.22 Ga; Corfu and Andrews, 1986). Southwest-trending folding of the Mississagi strata in part predated Nipissing gabbro emplacement. Metamorphic grade in both units is in the greenschist facies, locally reaching lower amphibolite facies south of the Murray fault. Also south of the fault, both are intruded near the Grenville Front by ≈1.7 Ga granitoid rocks (Krogh and Davis, 1970), which may be in part responsible for the somewhat higher grade in that area. Present throughout the region are lamprophyre dykes of unknown age, southeast-trending olivine diabase dykes of the 1235-Ma Sudbury swarm (Krogh et al., 1987; F.Ö. Dudàs, pers. comm., 1990), and east-trending diabase dykes of the 575-Ma Grenville swarm (S. Kumarapelli, 1990, pers. comm.), to which may be related some of the "trap dykes" in the Sudbury region (Grant et al., 1962).

## EVALUATION OF FAULT DISPLACEMENTS

Field work undertaken in late September, 1991, was aimed at evaluating the apparent truncation of the front mylonite zone and the sense and timing of displacement on the various converging faults. Collins' (1936) identification of Ramsey Lake conglomerate in the Daisy-Long lakes area was reassessed. Particular attention was paid to structure within the different fault blocks in the Southern Province with a view to determining what changes occur from block to block as the Grenville Front is approached. Field work was restricted to within a few kilometres of the front between Richard Lake and the village of Wahnapitae (Fig. 1).

### *Creighton fault*

Geological maps covering the southeastern part of the Sudbury region (e.g. Dressler, 1984a) show a homoclinal succession comprising the Elliot Lake and Hough Lake groups dipping and facing southeast from the south range of the Sudbury irruptive to the north shore of Ramsey Lake (Fig. 1). Here the highest unit of the Hough Lake Group, the Mississagi Formation, overlies the poorly exposed Pecors Formation of slate and siltstone with fine sandstone interbeds, itself conformable on conglomerate of the Ramsey Lake Formation. East of Ramsey Lake, bedding trend in the Mississagi Formation swings from northeast to east, maintaining a southerly dip averaging about 50°. The axial trace of this open fold trends southeast and is occupied by a broad zone of "Sudbury breccia", considered by many to be related to the impact of the bolide responsible for the Sudbury structure, and to have formed in diatreme-like fashion (Dressler, 1984b).

East of the breccia zone the Mississagi Formation maintains a steady easterly strike in a section with estimated true thickness exceeding 2200 m (Grant et al., 1962). To the east, a large syncline, more important than the minor status accorded to it by Phemister (1961, p. 38), passes southwest through Coniston, east of which bedding strikes southwest and faces northwest. Dips on the southeast limb vary from 60° NW through vertical to slightly overturned, and remain relatively steep around the hinge; the fold axial plane is thus inclined steeply northwest and the axis plunges moderately to steeply southwest. Several closely spaced folds in the hinge area are accommodated southwestward by tightening between the main limbs. Tightening is accompanied by brecciation of the thicker, more resistant sandstone beds in the fold hinges, within a cleaved matrix derived from silty interbeds. Large blocks of sandstone maintain their bedding orientation with respect to the folds, and commonly display oversteepened foresets in crossbedded units. Slaty and fracture cleavage are developed in the silty and sandy beds respectively, show a refraction relationship, and are related directly to fold geometry.

A large sill-like intrusion of massive Nipissing gabbro follows the course of bedding around this fold, but in detail cuts across bedding and, apparently, fold-related cleavage in its sedimentary host. Exposed contacts, however, are the loci of narrow zones of Sudbury breccia with fragments of both sandstone and gabbro. Sudbury breccia is also locally developed in the hinge zone of folds within the Mississagi Formation, where it includes blocks of previously cleaved rock. Between the Nipissing gabbro intrusion and Wahnapitae village, the Mississagi Formation faces consistently northwest, except where reversed in a minor fold pair close to the southeast contact of the gabbro body (Fig. 1). Nipissing gabbro apparently intruded folded Mississagi

Formation. The arcuate form of Nipissing gabbro bodies may reflect later, open folding; alternatively, the shapes of the gabbro intrusions may have been controlled by pre-existing structure.

The northeast-trending fault shown by Lumbers (1975) as the continuation of the Murray fault passing just east of Coniston does not seem to be the locus of major displacement; it lies within the northwest-facing limb of the "Coniston syncline" and is associated with only minor discordance of bedding attitude and of the west contact of the Nipissing gabbro body. The significance of this observation will be apparent after evaluation of displacement on the Murray fault to the southwest. A fault of similar attitude, with little apparent displacement, passes close to the northwest side of the "Coniston syncline".

The Creighton fault east of Ramsey Lake seems to have been misplaced on the published geological maps; there is no significant break of any kind where it is shown to cross the "Coniston syncline". Discordant bedding attitudes reported by Grant et al. (1962) are within a zone of Sudbury brecciation. A significant topographic lineament, occupied locally by a "trap dyke", occurs about 500 m south of the fault position shown by Thomson (1962), converging westward with the mapped position at Ramsey Lake. South of this fault the Mississagi Formation is thrown into a number of southwest-trending folds with moderate southwest plunges, open in the area south of Ramsey Lake and becoming tighter eastward. Nipissing gabbro intrusions appear to cut across axial traces of folds. The axial trace of the "Coniston syncline" north of the fault, however, is juxtaposed against a uniformly northwest-facing succession of Mississagi sandstone beds south of it, clearly showing a mismatch of structure across the fault. The fault itself is not exposed, but 1300 m from the northwest end of Alice Lake it occupies a gully only a few metres wide between outcrops of heavily fractured Mississagi sandstone. The straight course of the fault lineament across topography points to a near-vertical attitude. If the several folds south of the Creighton fault represent a higher level of the "Coniston syncline" as it opens upward, then there is a net horizontal displacement of dextral sense, amounting to 1 km or more, and a net vertical, south-side-down displacement of unknown magnitude.

Southeast of Ramsey Lake, two southeast-trending dykes of Sudbury diabase have characteristic widths - the southwestern dyke is ≈35 m wide, the northeastern one, ≈65 m. Two dykes of similar widths and spacing mapped on the north shore of Ramsey Lake (Innes, 1978) are directly on strike with the dykes to the southeast. As these dykes are not offset, lateral displacement on the Creighton fault occurred before ≈1235 Ma. However, if the trap dyke within this fault belongs to the Grenville swarm, fracturing, veining, and low-grade alteration of the dyke attest to some later activity along this fault.

### *Murray fault*

The northwest-facing succession southeast of the folds outlined above flanks the northwest side of the Murray fault at least as far as the west end of Richard Lake (Fig. 2). Approaching the fault, bedding steepens to vertical and becomes overturned within a few hundred metres of the fault, with dips as low as 60°SE. In the same interval the average bed thickness decreases; accompanying decrease in the discordant angle of foresets and between bedding and cleavage attests to this being an effect of deformation. Resistant sandstone beds are pulled into elongate, tabular lenses with tapering necks, and a strong cleavage is developed in the finer grained interbeds. Exposures along the northwest shore of Daisy Lake exhibit considerable open buckling, especially adjacent to the occurrences of Nipissing gabbro which probably belong to a single body partly cut out along the fault. Nipissing gabbro closest to the fault is highly altered to a pale aggregate of albite, zoisite, and actinolite; Mississagi sandstone is indurated with recrystallized feldspar and laced with irregular quartz veinlets. This deformation zone next to the fault is cut by the two large dykes of Sudbury diabase, as well as a few metre-wide dykes of the same swarm, which are unaltered and structurally intact, even at the shore of Daisy Lake. The irregularity in the course of the thick dyke northwest of Daisy Lake is an original intrusive phenomenon; a narrow dyke connects the two segments and is itself cut by a branching, east-trending pair of "trap dykes".

The geology southeast of the Murray fault contrasts strongly with that to the northwest. Thomson's (1962) compilation distinguishes units of "gritty greywacke" and "interbedded quartzite and greywacke" from the crossbedded sandstones typical of the Mississagi Formation. Low hills along the north shore of Richard Lake are underlain primarily by dark, compact, locally foliated conglomeratic sandstone characterized by scattered, clear quartz grains up to 1 cm across and widely separated pebbles and boulders of grey, rarely pink, granitoid rock; one boulder is nearly 2 m in diameter. This is Collins' Ramsey Lake conglomerate. The south sides of the outcrops west of Richard Lake expose dark grey, slaty siltstones with fine, pale grey sandy interbeds. South of Richard Lake at least 10 m of grey slaty siltstone lie stratigraphically beneath crossbedded sandstones typical of the Mississagi Formation. Despite the fact that conglomerate and siltstone lenses do occur as local variants within the Mississagi Formation, the intraformational conglomerates are not of the type described above, and the silty beds are rarely this thick (K.D. Card, pers. comm., 1991). The conglomerate-siltstone succession beneath unequivocal Mississagi Formation is therefore correlated with the Ramsey Lake and Pecors formations which underlie the Mississagi north and west of Ramsey Lake, some 6 km to the northwest. The same units are well-exposed along the south shore of Daisy Lake, where the Pecors Formation siltstones are interbedded with thin-bedded sandstones that rarely show cross-stratification. A subsidiary fault separates this assemblages from typical Mississagi sandstones to the south, with mild discordance of bedding. Facing direction is southeast, opposed to that north of the Murray fault. Similar sub-Mississagi rocks occur around McFarlane and Long lakes to the southwest in a complex anticlinal culmination. It is noted that the Pecors Formation between the Ramsey Lake and Mississagi had not been recognized when Collins made

his correlation. He therefore considered the greywacke-siltstone unit to be McKim, implying northwest facing compatible with his syncline hypothesis.

The sedimentary rocks close to the southeast shore of Daisy Lake become more thoroughly cleaved eastward toward the Grenville Front mylonite zone, and unlike those on the opposite shore, carry a dip-parallel lineation. At the northeast end of the lake, grey granodiorite intrudes Mississagi sandstone and Nipissing gabbro and is cut off by the fault. Most of this small pluton has a protomylonitic foliation that dips moderately southeast and is discordant with the fault trace. Between Daisy and Baby lakes a narrow layer of brecciated mylonite derived from Mississagi sandstone is exposed at the base of a cliff of the granodiorite. This, and attitudes in general along both sides of Daisy Lake, suggest that the Murray fault dips moderately to steeply southeast. The two Sudbury dykes mentioned earlier were located southeast of the fault by Kwak (1968), although they do not appear on subsequent geological compilations. They are offset dextrally across the fault by somewhat less than one kilometre. The thicker dyke shows considerable irregularity near Daisy Lake, with many narrow offshoots between its two main arms; in contrast, the thinner dyke to the southwest is 'well-behaved'. More importantly, both dykes are pervasively hydrated to actinolite-plagioclase assemblages, a metamorphic effect not seen northwest of the Murray fault. It is important to note that neither dyke continues southeast of the Grenville Front mylonite zone. However, disrupted remnants of Sudbury dykes occur within Grenville Province gneisses some 4 km to the east, where they are metamorphosed to coronitic metadiabase containing orthopyroxene, clinopyroxene and garnet.

It is clear from the above that pre-Sudbury-dyke geology cannot be matched across the Murray fault, and it is likely that major activity occurred along the fault before dyke intrusion at 1235 Ma. Apart from the fact that the Huronian sedimentary rocks face in opposite directions on either side of the fault, the presence of probable Ramsey Lake and Pecors formations on the hangingwall suggests considerable south-side-up displacement. In addition, if the metamorphism of the Sudbury dykes is due to heating by the formerly overlying Grenville block, a later normal displacement is indicated.

### *Wanapitei fault*

The boundary between the Southern and Grenville provinces from Coniston east-northeast beyond Wahnapitae is evidently the locus, not exposed, of a narrow brittle fault. Immediately northeast of Alice Lake and again near Wahnapitae, compositional layering and planar leucosomes in high-grade, nonmylonitic gneisses are discordant with the fault trace. The same is true of the Grenville Front mylonite zone at the northeast shore of Alice Lake. In contrast, the Mississagi Formation north of the fault shows neither mylonitization, fault-parallel cleavage, nor increase in metamorphism. Primary sedimentary structures are just as well preserved close to the fault as they are well north of it; for example, superb examples of trough-crossbedded sandstone are exposed where the Canadian National Railway crosses the fault trace (Fig. 1), a stone's throw from garnet amphibolite south of the fault. However, farther east (Fig. 3), the Mississagi Formation closest to the fault near Wahnapitae shows thinned and buckled bedding, and about 8 km farther along the Wanapitei fault, Mississagi Formation exposed on the southeast side of the Wanapitei River is mylonitized. At Timmins Creek, 20 km along the fault from Wahnapitae, the same marked contrast that occurs near Coniston is again present on either side of a 300 m covered interval. A further 5 km east at Crerar, fault breccia involving earlier mylonite has been reported (Fairbairn, 1939; Dalziel and Bailey, 1968).

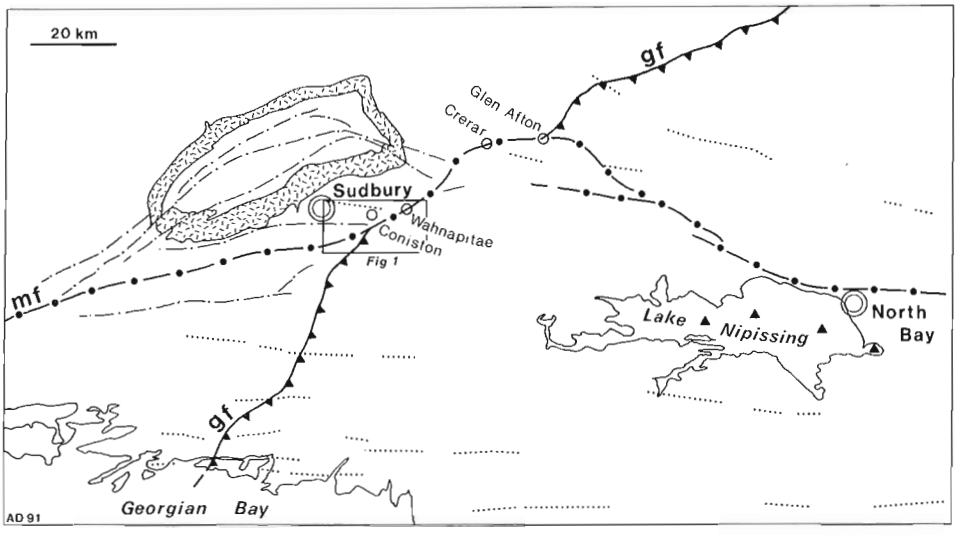


**Figure 3.** Normal faulting of the Grenville Front east of Sudbury. Principal fault locations taken from Card and Lumbers (1977). Dotted lines are diabase dykes of the 575-Ma Grenville swarm; triangles in Lake Nipissing are alkaline intrusions of similar age. **gf** - Grenville Front, **mf** - Murray fault.

It is not until near Glen Afton, some 50 km along the boundary from Coniston, that the full spectrum of mylonite development associated with thrust tectonics once again characterizes the Grenville Front (Davidson, 1986). Here the major lineament than marks the boundary fault to the west cuts east-southeast into the Grenville Province (Card and Lumbers, 1977), where it trends in the same direction as major rift faults mapped in the North Bay area (Lumbers, 1971); Lumbers suggested a connection farther east with the Ottawa-Bonnechere graben, part of the St. Lawrence rift system that initiated in the late Precambrian.

## CONCLUSIONS

The observations outlined above confirm that i), the Murray fault in the Southern Province near the Grenville Front has greater displacement and a longer history than the Creighton fault; ii) it extends eastward as the Wanapitei fault and not as the northeast fault just east of Coniston (although this may be a splay); iii), it was the locus of considerable south-side-down displacement, with less than a 1 km dextral component, after formation of the Grenville Front mylonite zone. Alternation of mylonitic and nonmylonitic Mississagi sandstone just north of the Wanapitei fault between Coniston and Glen Afton indicates that the overriding Grenville Front mylonite zone now eroded from the north side was not very far above the present surface. West of Coniston, at least some of the south-side-up displacement occurred after Sudbury diabase emplacement. Post-Grenvillian normal displacement on this sector of the fault must have reduced the former amount of reverse displacement. Post-Grenvillian movement that offset the Grenville Front may have been related to faulting associated with the St. Lawrence rift system to the east.

## REFERENCES


**Card, K.D.**
1978: Sudbury-Manitoulin; Ontario Geological Survey Map 2360, scale 1:126 720.

**Card, K.D. and Lumbers, S.B.**
1977: Sudbury-Cobalt; Ontario Geological Survey Map 2361, Geological Compilation Series, scale 1:253 440.

**Coleman, A.P.**
1914: The pre-Cambrian rocks north of Lake Huron, with special reference to the Sudbury Series; Ontario Bureau of Mines, v. 23, p. 204-236.

**Collins, W.H.**
1936: Sudbury Series; Geological Society of America Bulletin, v. 47, p. 1675-1679.

**Cooke, H.C.**
1946: Problems of Sudbury Geology, Ontario; Geological Survey of Canada Bulletin 3, 77 p.

**Corfu, F. and Andrews, J.A.**
1986: A U-Pb age for mineralized Nipissing diabase, Gowganda, Ontario; Canadian Journal of Earth Sciences, v. 23, p. 107-109.

**Dalziel, I.W.D. and Bailey, S.W.**
1968: Deformed garnets in a mylonitic rock from the Grenville Front and their tectonic significance; American Journal of Science, v. 266, p. 542-562.

**Dalziel, I.W.D., Brown, J.M., and Warren, T.E.**
1969: The structural and metamorphic history of the rocks adjacent to the Grenville Front near Sudbury, Ontario, and Mount Wright, Quebec; in Age Relations in High-grade Metamorphic Terrains, (ed.) H.R. Wynne-Edwards; Geological Association of Canada Special Paper 5, p. 207-224.

**Davidson, A.**
1986: A New Look at the Grenville Front; Geological Association of Canada, Field Trip 15, Guidebook, 31 p.

**Dressler, B.O.**
1984a: Sudbury Geological Compilation; Ontario Geological Survey Map 2491, Precambrian Geology Series, scale 1:50 000.
1984b: The effects of the Sudbury event and the intrusion of the Sudbury igneous complex on the footwall rocks of the Sudbury structure; in The Geology and Ore Deposits of the Sudbury Structure, (ed.) E.G. Pye, A.J. Naldrett, and P.E. Giblin; Ontario Geological Survey Special Volume 1, p. 97-136.

**Fairbairn, H.W.**
1939: Geology of the Ashigami Lake area; Ontario Department of Mines, Annual Report, v. 48, p. 1-15.

**Grant, J.A., Pearson, W.J., Phemister, T.C., and Thomson, J.E.**
1962: Geology of Broder, Dill, Neelon, and Dryden Townships, District of Sudbury; Ontario Department of Mines Geological Report 9, p. 1-24.

**Innes, D.G.**
1978: McKim Township, District of Sudbury; Ontario Geological Survey Preliminary Map P.1978, Geological Series, scale 1:15 840.

**Krogh, T.E. and Davis, G.L.**
1970: Isotopic ages along the Grenville Front in Ontario; Carnegie Institution of Washington Yearbook 68, p. 309-313.

**Krogh, T.E., Corfu, F., Davis, D.W., Dunning, G.R., Heaman, L.M., Kamo, S.L., Machado, N., Greenough, J.D., and Nakamura, E.**
1987: Precise U-Pb isotopic ages of diabase dykes and mafic to ultramafic rocks using trace amounts of baddeleyite and zircon; in Mafic Dykes Swarms, (ed.) H.C. Halls and W.F. Fahrig; Geological Association of Canada, Special Paper 34, p. 147-152.

**Kwak, T.A.P.**
1968: Metamorphic Petrology and Geochemistry Across the Grenville Province, Southern Province Boundary, Dill Township, Sudbury, Ontario; Ph.D. thesis, McMaster University, Hamilton, Ontario.

**Lumbers, S.B.**
1971: Geology of the North Bay Area, Districts of Nipissing and Parry Sound; Ontario Department of Mines and Northern Affairs, Geological Report 94, 104 p.
1975: Geology of the Burwash Area, Districts of Nipissing, Sudbury, and Parry Sound; Ontario Division of Mines Geological Report 116, 158 p.

**Phemister, T.C.**
1961: The boundary between the Timiskaming and Grenville subprovinces in the townships of Neelon, Dryden, Dill and Broder, District of Sudbury; Ontario Department of Mines, Preliminary Report 1961-5, 61 p.

**Robertson, J.A., Frarey, M.J., and Card, K.D.**
1969: The Federal–Provincial Committee on Huronian stratigraphy; Canadian Journal of Earth Sciences, v. 6, p. 335-336.

**Thomson, J.E., (comp.)**
1962: Broder, Dill, Neelon, and Dryden Townships, District of Sudbury; Ontario Department of Mines Map 2017, scale 1:31 680.

**Yates, A.B.**
1948: Properties of International Nickel Company of Canada; in Structural Geology of Ore Deposits, Canadian Institute of Mining and Metallurgy, Jubilee Volume, p. 596-617.

**Young, G.M. (ed.)**
1973: Huronian Stratigraphy and Sedimentation; Geological Association of Canada, Special Paper 12, 271 p.


Geological Survey of Canada Project 760061

# A proposed revision of Early Proterozoic stratigraphy of the Thelon and Baker Lake basins, Northwest Territories

**Q. Gall[1], T.D. Peterson, and J.A. Donaldson[1]**
**Continental Geoscience Division**

*Gall, Q., Peterson, T.D., and Donaldson, J.A., 1992: A proposed revision of Early Proterozoic stratigraphy of the Thelon and Baker Lake basins, Northwest Territories; in Current Research, Part C; Geological Survey of Canada, Paper 92-1 C, p. 129-137.*

***Abstract***

*Since the Dubawnt Group and its formations were first described during regional mapping projects of the Geological Survey of Canada, detailed mapping, petrologic studies, and new geochronological data, have shown that some of the rock units are lithologically and temporally more distinct than originally considered. For this reason, revision of the stratigraphic nomenclature for the Dubawnt Group (as originally defined) is herein proposed. The revised stratigraphy, from oldest to youngest rock unit, is as follows: Baker Lake Group (South Channel Formation [sedimentary], Kazan Formation [sedimentary], Christopher Island Formation [ca. 1.85 Ga, volcanic-sedimentary], Kunwak Formation [sedimentary]); Wharton Group (Pitz Formation [1.76 Ga, volcanic-sedimentary] and anorogenic granite); Barrensland Group (Thelon Formation [ca. 1.72 Ga, sedimentary], Kuungmi Formation [volcanic], Lookout Point Formation [sedimentary]). All three groups constitute the Dubawnt Supergroup.*

***Résumé***

*Depuis que le groupe de Dubawnt et ses formations ont été pour la première fois décrits dans le cadre de projets de cartographie régionale de la CGC, on a dressé des cartes détaillées, réalisé des études pétrologiques et recueilli des données géochronologiques montrant que certaines unités rocheuses sont lithologiquement et temporellement plus différentes que ce que l'on avait prévu à l'origine. Pour cette raison, une révision de la nomenclature du groupe de Dubawnt (selon sa définition originelle) est proposée dans le présent document. La stratigraphie révisée, de l'unité la plus ancienne à la plus récente, est la suivante : le groupe de Baker Lake (formation de South Channel [sédimentaire], la formation de Kazan [sédimentaire], la formation de Christopher Island [vers 1,85 Ga, volcanique et sédimentaire], la formation de Kunwak [sédimentaire]); le groupe de Wharton (la formation de Pitz [1,76 Ga, volcanique et sédimentaire] et un granite anorogénique); le groupe de Barrensland (la formation de Thelon [vers 1,72 Ga, sédimentaire], la formation de Kuungmi [volcanique], la formation de Lookout Point [sédimentaire]). Ces trois groupes font tous partie du supergroupe de Dubawnt.*

[1] Derry/Rust Research Group, Ottawa-Carleton Geoscience Centre, Dept. of Earth Sciences, Carleton University, Ottawa, Ontario. K1S 5B6

## INTRODUCTION

In the 130 Ma after the end of the Trans-Hudson orogeny (ca. 1.85 Ga), epicontinental sedimentary and volcanic rocks were deposited throughout the central Churchill Province in an area about 450 x 350 km (Fig 1). Two basin systems are recognized. The older Baker Lake basin, extending from the northeast shore of Baker Lake to south of Dubawnt Lake, contains tilted redbed successions (mainly conglomerate and arkose), potassic to ultrapotassic volcanic rocks and their intrusive equivalents, and epiclastic derivatives of the alkalic suite (mainly conglomerate and lithic arenite). The Thelon basin, straddling the border between the districts of Keewatin and Mackenzie, contains mainly flat-lying conglomerate and sandstone, and is thought to have once been continuous with outliers of Thelon Formation to the east.

The rocks in these basins, plus an intervening sequence of rhyolites and aeolian sandstones, were assigned to the Dubawnt Group by Wright (1955). However, later mapping (Donaldson, 1965; LeCheminant et al., 1979a; Blake, 1980) and geochronological data (Tella et al., 1985; Loveridge et al., 1987; Miller et al., 1989) have shown that some formations within these sequences are separated by major unconformities, and age differences among them can exceed 130 Ma. Strong contrasts in igneous associations and sedimentology indicate that these Early Proterozoic rocks were deposited in different tectonic regimes (Hoffman and Peterson, 1991). We consider that a revision of the stratigraphy of the Dubawnt Group could better reflect the post-Hudsonian history of the Churchill Province. In this paper, we present a revised stratigraphy, summarize the lithological characteristics of each formation, and offer tectonic interpretations for these Early Proterozoic units.

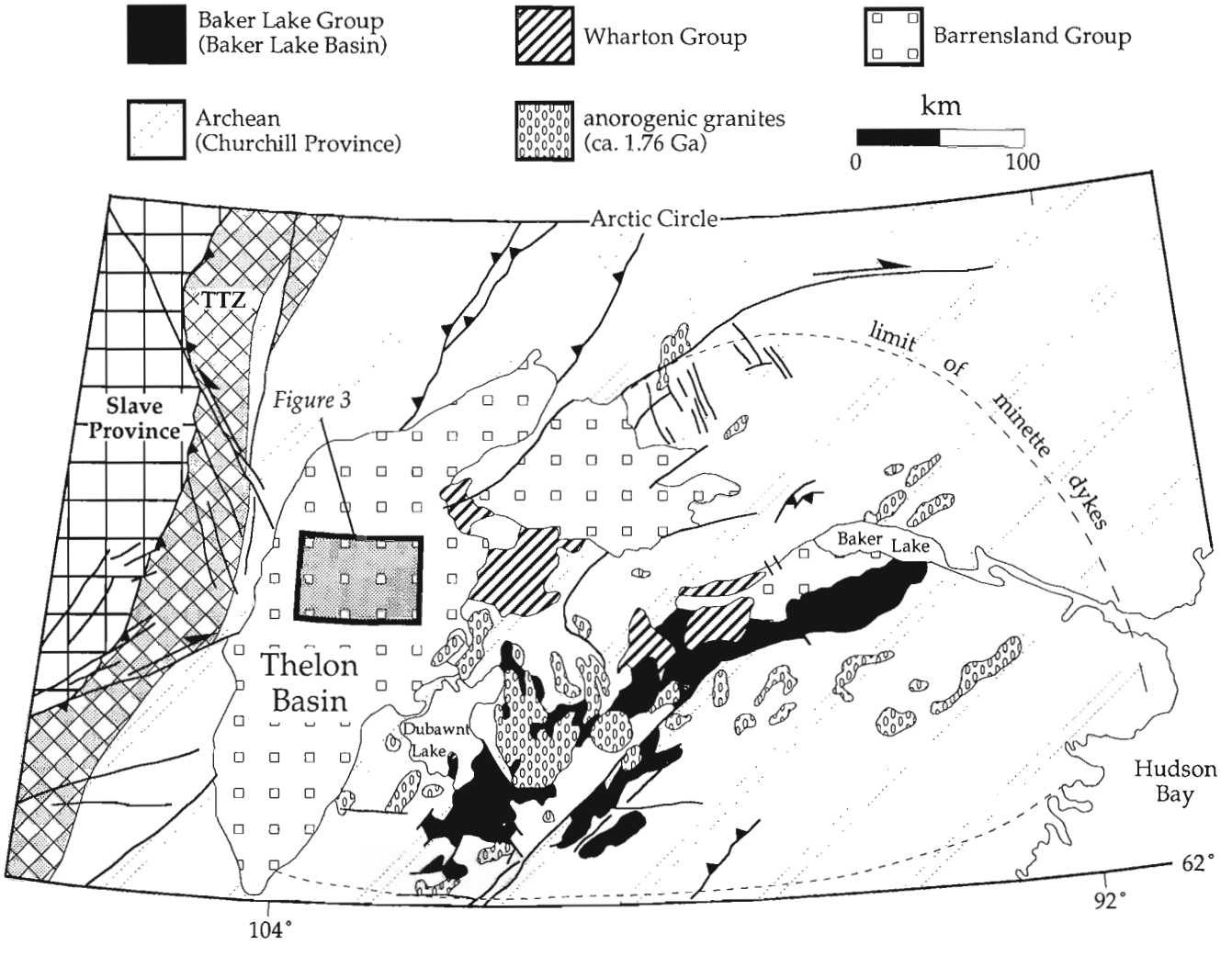


**Figure 1.** Geologic map showing the distribution of the Early Proterozoic Baker Lake, Wharton and Barrensland groups and ca. 1.76 Ga anorogenic granites, within and adjacent to the Baker Lake and Thelon basins. TTZ=Thelon Tectonic Zone.

## PREVIOUS AND REVISED STRATIGRAPHY

The existing stratigraphy, as amended by Blake (1980), is compared to our revision in Figure 2. No formation names have been changed. However, the Angikuni Formation defined by Blake has been deleted, since the type section is lithologically very similar to the Kazan Formation, and its stratigraphic position is uncertain. The former Dubawnt Group has been divided into three new groups: the Baker Lake Group, which is restricted to rocks of the Baker Lake basin; the Wharton Group (rhyolite and sandstone); and the Barrensland Group which comprises all strata within the Thelon basin and its outliers. The Dubawnt Group of Wright (1955) is raised in rank to the Dubawnt Supergroup.

### *Baker Lake Group*

The Baker Lake Group may be conveniently divided into lower (Kazan and South Channel fms.), middle (Christopher Island Fm.) and upper (Kunwak Fm.) portions. All formations in the Baker Lake Group are subaerial or subaqueous, terrestrial deposits. In the following descriptions, estimated maximum thicknesses of formations are indicated, but thicknesses vary widely. Lower Baker Lake Group rocks are mainly absent from the west end of the Baker Lake basin.

#### South Channel Formation (1800 m)

The moderately to steeply dipping South Channel Formation (Donaldson, 1965), named after the channel leading into the east end of Baker Lake, is separated from Archean and older Proterozoic basement rocks by a major unconformity. According to Blake (1980), it consists of massive, poorly sorted, polymictic conglomerate with up to boulder-size, rounded to angular clasts. Clasts and matrix are mainly derived from local basement rocks; the matrix is locally calcareous. Fine-grained lenses consist of sandstone and mudstone. The South Channel Formation has been interpreted as an alluvial fan/braided stream deposit (Donaldson, 1965; Macey, 1973).

#### Kazan Formation (1000 m)

The Kazan Formation (Donaldson, 1965), named for sections exposed along the lower Kazan River, locally overlies the South Channel Formation both conformably and disconformably. It consists mainly of flaggy, pink to reddish- brown weathering arkosic sandstone, locally pebbly. Cross-bedding, channel scours, and intraformational slumps are common. Although predominantly fluvial, mudstones with desiccation cracks and arkoses with large-scale cross-beds, which may indicate a locally developed aeolian facies (Blake, 1980), are observed. Although clearly underlying the Christopher Island Formation, a conglomeratic marker bed with pebbles of volcanic rocks containing phenocrysts of

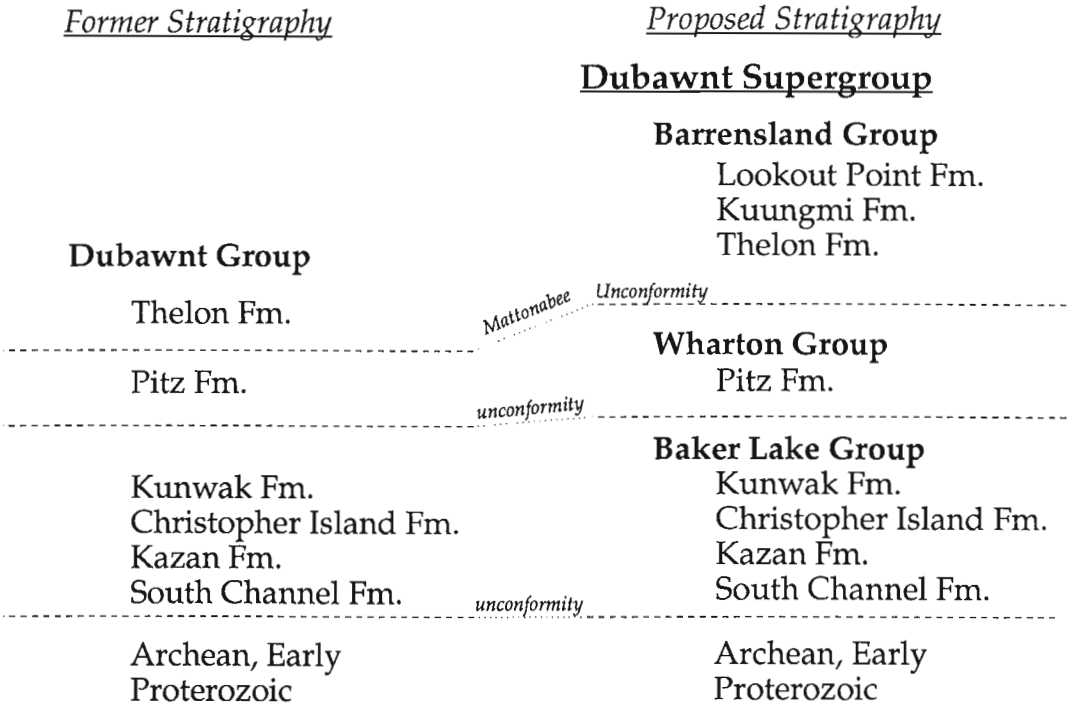


**Figure 2.** Comparison of the previous and proposed stratigraphic nomenclature.

potassium feldspar, biotite and clinopyroxene indicates that some minor volcanic activity occurred during deposition of the Kazan Formation.

### Christopher Island Formation (2500 m)

The Christopher Island Formation (Donaldson, 1965) was named after an island in Baker Lake where a flat-lying volcanic centre is exposed. The following description is drawn mainly from observations made during studies in the Dubawnt Lake area (Peterson et al., 1989; Rainbird and Peterson, 1990). At Dubawnt Lake, the Christopher Island Formation (CIF) rests unconformably on Archean basement rocks, but it has been observed conformably to overlie the Kazan Formation in the Baker Lake area (Blake, 1980). Except for a thin basal member of angular pebble conglomerate, the CIF at Dubawnt Lake consists entirely of subaqueous and subaerial volcanic flows and derived epiclastic rocks. Intrusive equivalents of the flows occur as plutonic bodies composed mainly of biotite and alkali feldspar (the Martell syenite) and lamprophyre dykes which occur throughout a large area in the central Churchill Province (Fig. 1).

Previous workers (e.g., Blake, 1980; LeCheminant et al., 1987a) described the volcanic rocks of the CIF as mafic to felsic trachytes. However, as noted by Peterson and Rainbird (1990) they are geochemically and petrographically intermediate between minette and lamproite. All of the CIF flows and dikes are potassic to ultrapotassic, with high K/Na and K/Al.

A typical section, 2.1 km thick, has been described by Peterson and Rainbird (1990). The basal member (0-200 m thick) is overlain by a sequence of thin (ca. 2 m) flows of purplish, vesicular mafic minette (ca. 10% MgO) containing abundant phenocrysts of phlogopite and clinopyroxene, with rare olivine and abundant potassium feldspar in the groundmass. The mafic minettes are generally subaqueous and some are interbedded with hyaloclastic flow breccia; however, subaerial lapilli tuffs and welded agglomerate occur locally.

The mafic minettes are overlain by a thick (up to 800 m) sequence of turbiditic debris flows consisting of well-rounded minette boulders and pebbles in a minette sand matrix. The debris flows grade into laminated, grey to cream-weathering siltstones interpreted as lacustrine deposits, interbedded with thin (1-2 m) flows of grey intermediate minette (ca. 5% MgO) which are generally aphanitic with highly vesicular flow tops. A subaerial facies of this member contains oxidized flow breccias. Lacustrine or fluvial sediments overlying the grey minettes, coarsen upwards and grade into Kunwak Formation with the appearance of increasing amounts of locally derived basement clasts. The transition to Kunwak Formation can be abrupt (<1 m) or gradual (>500 m).

### Kunwak Formation (2 km)

The Kunwak Formation (LeCheminant et al., 1979b) was named after the Kunwak River, which flows south from Princess Mary Lake, where the unit was first recognized. It is a coarse redbed sequence with no clearly defined vertical stratigraphy; however, at Dubawnt Lake rapid lateral facies variations are readily correlated with proximity to basin margins (Peterson et al., 1989; Rainbird and Peterson, 1990). It is conformable with the Christopher Island Formation, but locally rests unconformably on basement rocks.

Coarse massive debris flows and crudely bedded conglomerate containing moderately rounded clasts, up to 1 m in diameter, are exposed near the margins of the Baker Lake basin, along the western shore of Dubawnt Lake. Clast imbrication data (Gall, unpublished data) indicate sediment transport away from the basin margin. Except immediately above the CIF, clasts consist almost entirely of Archean source rocks. Carbonate cement occurs locally in the coarse conglomerates. At localities distal (>2 km) from the basin margins, cross-bedded sandstones, siltstones with fluid escape structures, and mudstones with desiccation cracks are interbedded with planar-bedded and trough cross-bedded pebbly conglomerate. The sedimentology of the Kunwak Formation is similar to the South Channel Formation. However, most Kunwak and South Channel conglomerates can be readily distinguished, because detritus from the CIF minette volcanics is restricted to the Kunwak Formation, giving this formation a distinct brick-red colour. The Kunwak Formation is also inferred to comprise alluvial fan/braided stream deposits.

The maximum thickness of the Kunwak Formation is difficult to estimate due to post- and syn-depositional faulting. Exceptionally thick (>5 km) sequences may have formed by "conveyor-belt" stacking along an active strike-slip fault at Dubawnt Lake (Rainbird and Peterson 1990).

### Tectonic interpretation

A precise U-Pb age has not yet been obtained for the Baker Lake Group. Tella et al. (1985) report a zircon age of 1850 +30/-10 Ma for a syenite, which is consistent with cross-cutting relationships between the Christopher Island Formation and earlier granites and later fault systems. The possible age range of the CIF coincides with the indentation of the Slave Province through the Thelon Tectonic Zone, which likely occurred in response to a continent-continent collision on the western margin of the Slave Province (Hoffman, 1980). More importantly, it immediately postdates the Trans-Hudson orogeny. Volcanic rocks within the CIF (minettes and closely related rocks) are characteristic of post-orogenic igneous suites, and are typically associated with strike-slip basins, such as the Karakorum Fault Zone near the Tibetan Plateau (Pognante, 1990). We consider that the Baker Lake basin is a complex of extensional, and probably strike-slip, basins which developed over thickened lithosphere in the hinterlands of the Trans-Hudson orogen and the older (2.0-1.9 Ga) Thelon orogen. This scenario is consistent with the structure and sedimentology of the Baker Lake basin, which strongly indicate syndepositional faulting, erosion of escarpments, and substantial local variations in basin thickness.

### *Wharton Group*

Separated from the Baker Lake Group and from Early Proterozoic and Archean basement rocks by an angular unconformity, are up to 200 m of intercalated grey, maroon and red rhyolite to dacite flows, pyroclastic rocks, and subordinate sedimentary rocks. Granite and granodiorite, which locally display rapikivi textures and contain fluorite, intrude the Baker Lake Group (Fig. 1). All these lithologies are unconformably overlain by the Barrensland Group. We propose that this sequence of volcanic and sedimentary rocks and granitic intrusions be assigned to the Wharton Group, named after a lake permitting access to the largest exposed area of volcanic rocks.

The grey- and red-coloured, quartz- and feldspar-phyric volcanic flows are named the Pitz Formation by Donaldson (1965), after their type locality immediately west of Pitz Lake. LeCheminant et al. (1987b) have reported a U-Pb radiometric age of 1760 Ma for the volcanic flows. A U-Pb radiometric age of 1748 Ma has recently been obtained for one of the rapikivi granite plutons (C. Roddick, unpublished data), and other plutons have ages up to 1.76 Ga (LeCheminant et al., 1987a). The granites typically have phenocryst assemblages identical to local extrusive rocks, and LeCheminant et al. (1979a) and Booth (1983) have demonstrated that the Pamiutuq Granite is coeval and cogenetic with the Pitz Formation volcanic rocks in the Pamiutuq Lake area. Thus, the anorogenic granites are considered to be shallow intrusive equivalents of the Pitz Formation.

Detailed mapping within the central and western Baker Lake basin has shown that the siliceous volcanic rocks, which locally occur as rhyolite domes, are associated with hydrothermal deposits such as travertine and carbonate-cemented conglomerate. The volcanic rocks are underlain by, and interbedded with, a variety of conglomerates and sandstones. These sedimentary units include red alluvial fan orthoconglomerates and quartz arenites (LeCheminant et al., 1979a, 1979b, 1981) and more mature quartz arenite of possible aeolian origin (LeCheminant et al., 1983). These units are, for now, simply ranked as informal sedimentary members of the Pitz Formation, which is the only formation recognized in the Wharton Group.

#### Tectonic interpretation

Model Nd ages for the anorogenic granites demonstrate that their source region was in Archean lithosphere (Dudás et al., 1991). Evidence for contemporary basaltic volcanism is scant, but basaltic magma was mingled with granitic magma in the Pamiutuq Granite (Booth, 1983). The anorogenic granites are geologically similar to, but at least 100 million years older than, the mid-continent anorogenic suite extending from Labrador to the central United States. Hoffman and Peterson (1991) suggested that after deposition of the Baker Lake Group, a thickened mantle keel formed during the Thelon and Trans-Hudson orogenies cooled and detached, resulting in upwelling of asthenosphere, injection of basalt into the lower crust, and partial melting of crustal rocks to produce the anorogenic granites. In this model, rhyolites and aeolian sands were deposited in basins produced by extensional collapse over thinned and uplifted lithosphere.

### *Barrensland Group*

The Barrensland Group is a new stratigraphic unit erected to include the undeformed and unmetamorphosed tripartite sequence of the basal siliciclastic Thelon Formation (Donaldson, 1965), the middle volcanic Kuungmi Formation (new name), and the upper dolomitic Lookout Point Formation (new name). Of these units, only the Thelon Formation directly overlies the widespread Matonabbee unconformity (Gall, unpublished data). The unconformity includes a thin (few metres) to thick (ca. 50 m) paleoweathering zone, the Thelon paleosol, containing possible silcretes (Ross and Chiarenzelli, 1985), which developed on most of the older Early Proterozoic and Archean lithologies.

#### Thelon Formation (1920 m)

The Thelon Formation was named by Donaldson (1965) for the flat-lying, quartz-rich conglomerate, sandstone and minor siltstone which underlies most of the Thelon game sanctuary north and west of Dubawnt Lake. It is characteristically white to grey to red, with medium- to thick-bedded and cross-stratified conglomerate and quartz arenite at its base, and carbonate-cemented cross-bedded sandstone dominant at the top of the formation. This is inferred to reflect an ascending change from alluvial fan – fluvial sedimentation to shallow marine sedimentation (Donaldson, 1965; Cecile, 1973). An aeolian facies has also been identified by Jackson et al. (1984) within the fluvial sequence. The maximum thickness of the Thelon Formation is based on seismic data from the centre of the Thelon basin (Overton, 1971). Phosphate cement within the basal Thelon Formation has a maximum U-Pb radiometric age of 1720 +/- 6 Ma (Miller et al., 1989).

#### Kuungmi Formation (10 m)

During regional mapping of the central Thelon Plain, Donaldson (1969) identified an aphanitic, green- to maroon-coloured "basalt" which overlies the Thelon Formation. It is best exposed immediately northwest of an unnamed lake situated approximately 18 km southwest of Lookout Point on the Thelon River (Fig. 3). The authors revisited these exposures during the summer of 1991, and discovered contorted Thelon Formation sandstones, interpreted as soft sediment deformation structures, underlying thin (<1 m) amygdaloidal flows. Sandstones were also observed overlying the flows, limiting their total thickness to a few (<10) metres. Strong flow-top oxidation, abundant chalcedony in the vesicles, and a high content of hematite and oxidized "basalt" sand grains in the overlying sandstones indicate significant subaerial exposure. Similar mafic flows of uncertain stratigraphic position occur at the south end of Dubawnt Lake. We propose that this stratiform, mappable volcanic unit be called the Kuungmi Formation, a

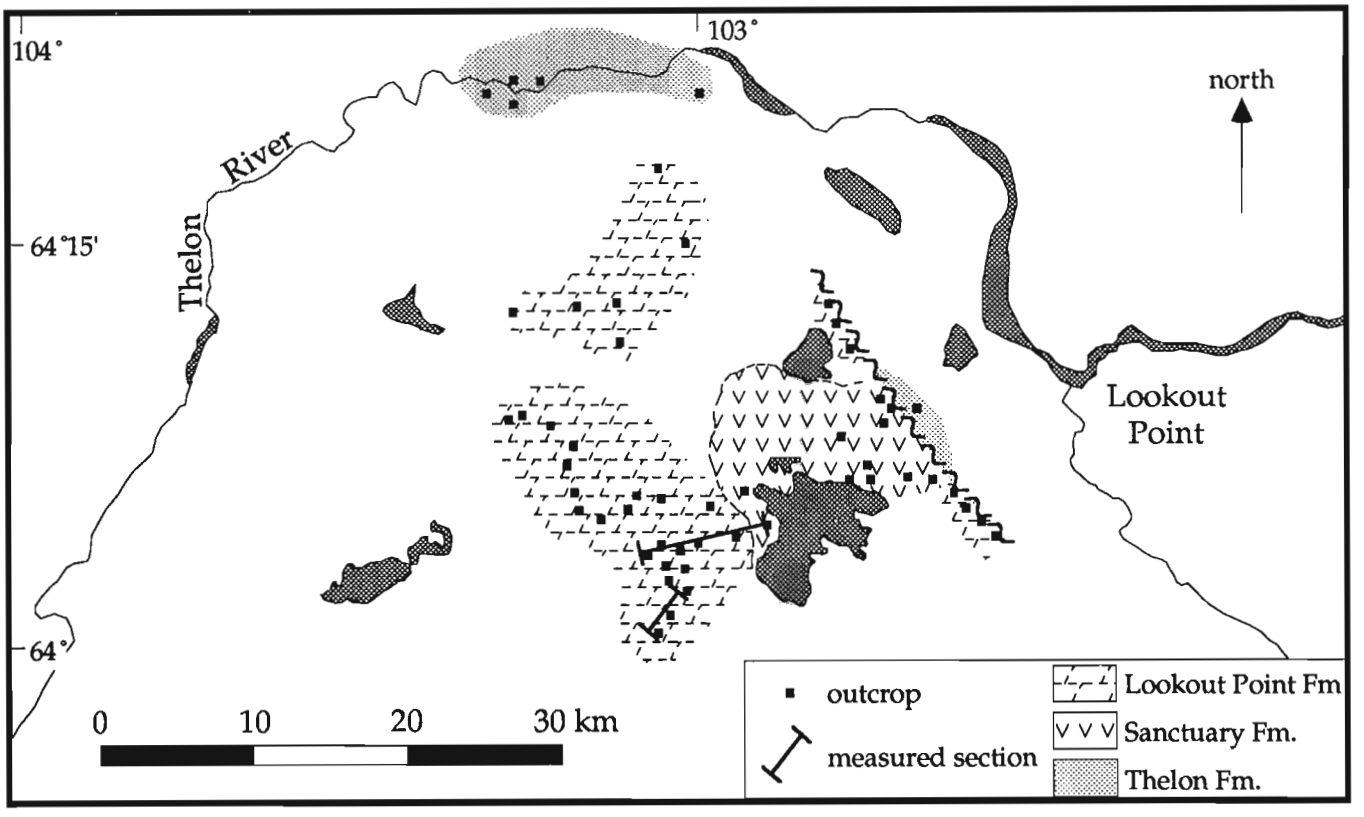


**Figure 3.** Distribution of the Thelon, Kuungmi, and Lookout Point formations in the central Thelon Plain, and locality of measured section for the Lookout Point Formation.

name which reflects the area of most extensive exposure in the centre of the Thelon Game Sanctuary. "Kuungmi Ujaqat Qanuittuuninga" is the Inuktituk term for "Thelon Game Sanctuary" (Inuit Cultural Institute, 1987).

### Lookout Point Formation (40 m)

Donaldson (1969) also identified a siliceous stromatolitic dolostone south of the Thelon River. It is best exposed in an area of raised beaches immediately west of, and at higher elevation than, exposures of the Kuungmi Formation (Fig. 3). A stratigraphic section was measured (Fig. 4) from discontinuous outcrop in the area of raised beaches. We propose that these dolostones, which conformably overlie the Kuungmi Formation and Thelon Formation, be named the Lookout Point Formation after the closest named geographic feature, approximately 20 km to the northeast on the Thelon River.

The measured section for the Lookout Point Formation (Fig. 4) consists of silicified and finely- crystalline cryptalgal dolostone and thin bedded, medium grained siliceous arenites, gradationally overlain by a thicker section of silicified stromatolitic dolostone with minor arenite interbeds. The basal contact of the Lookout Point Formation is not exposed, but to the west and east of the unnamed lake it consistently occurs at higher topographic elevations than the Kuungmi Formation, and is interpreted to overlie this formation. The top of the measured section occurs at the highest regional elevations, and has been extensively brecciated by faulting. Low-angle fault surfaces were locally observed at the top of the section, but only high-angle fault traces have so far been mapped regionally.

Throughout the measured section, the Lookout Point Formation is generally cream to pale grey to buff, thin to medium bedded microcrystalline dolostone. It has been pervasively silicified diagenetically, so that it is now extremely well indurated. Silica replacement has accentuated stromatolite laminae. At the base of the section, the dolostone contains thin to medium beds of fine-grained quartzose sandstone interbedded on a metre scale. Stromatolites at the base are both discrete and laterally linked domal forms, commonly with a synoptic relief of five to ten centimetres, and rarely 30 centimetres. Some beds are dominated by well-laminated low-relief hummocky ("egg carton") stromatolites. The upper half of the section contains fewer quartzose sandstone interbeds and more laminar cryptalgal dolostone. Both discrete, and laterally-linked domal stromatolites persist through to the top of the section, and are more abundant than near the base of the section. Near the top of the section the laterally-linked domal stromatolites increase in size, with the largest domes being approximately 40 centimetres in diameter, with 15 centimetres of synoptic relief. Teepee structures, oncolites, edgewise conglomerates, desiccation cracks and hopper crystal casts are common within the upper parts of the section.

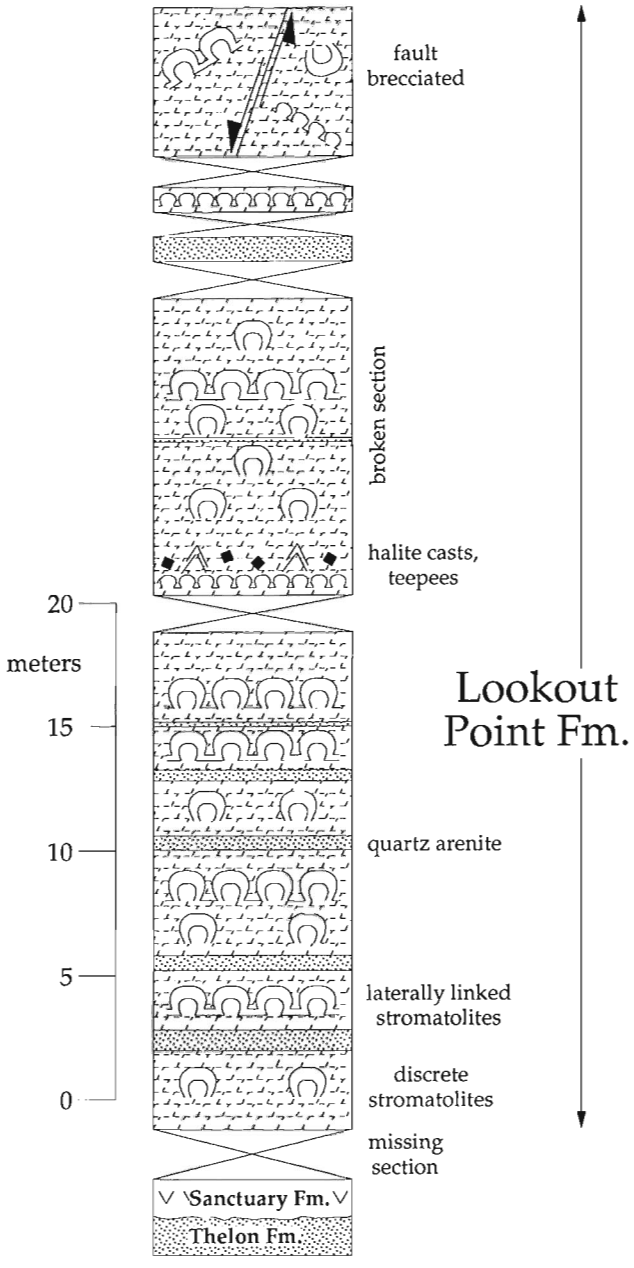


**Figure 4.** Stratigraphic section for Lookout Point Formation (locality of the measured section shown in Fig. 2).

### Tectonic interpretation

The presence of outliers of Thelon Formation as far east as Baker Lake (Fig. 1) indicates that the depositional basin of the Barrensland Group was much more extensive than the present limit of exposures, and that substantial Proterozoic cover within the Churchill Province has been stripped during subsequent uplift. The Thelon basin can be interpreted as an intracontinental or interior cratonic basin (sensu Dickinson, 1974; Klein, 1987), or more specifically a continental interior sag or fracture basin (Kingston et al., 1983). Typical of the basal Thelon Formation are coarse, quartz-rich conglomerates and sandstones deposited in continental alluvial fan and fluvial environments. Most of the rest of the Thelon Formation has been interpreted as marine by Cecile (1973), and probably reflects shallow continental platform deposition. The characteristics of the Kuungmi Formation are consistent with a shallow fluvial, terrestrial environment. The Lookout Point Formation is interpreted as having developed on a stable continental platform, probably in a peritidal environment.

Correlation between the Thelon basin strata and similar successions in the Athabasca basin, Hornby basin, and Elu basin, has been suggested by Donaldson (1967) and by Fraser et al. (1970), based on gross stratigraphy, persistent west - southwesterly paleocurrents, and some geochronology. More recently, correlation between these basins has been bolstered using the Matonabbee unconformity as a datum for correlation, new geochronologic data, similarity in basal paleosol character, and diagenetic paragenesis within the basal siliciclastic rocks (Gall and Donaldson, 1990; Gall, unpublished data). Our examination of the Lookout Point Formation suggests that it is similar to Unit 15 of the Dismal Lakes Group (Kerans et al., 1981), or Sulky Formation (Ross and Kerans, 1989), as well as the Carswell Formation (Ramaekers, 1981).

## SUMMARY

The Baker Lake and Thelon basins in the central Northwest Territories are composed of thick sequences of Early Proterozoic sedimentary rocks, volcanic rocks and intrusive equivalents of the volcanic rocks. Since the early geological reconnaissance mapping of Wright (1955) and Donaldson (1965, 1969), subsequent detailed mapping of the basins supported by petrological, geochemical, and geochronological analyses, has highlighted the peculiarities of each lithologic unit, demonstrating the need to revise the initial stratigraphic nomenclature.

The revised stratigraphic nomenclature, from the oldest to the youngest unit, is as follows. The Baker Lake Group comprises the basal rudaceous South Channel Formation, the arenaceous Kazan Formation, the Christopher Island Formation potassic to ultrapotassic volcanic suite and subordinate rudaceous sedimentary rocks, and the rudaceous Kunwak Formation. The younger Wharton Group comprises the ca. 1.76 Ga Pitz Formation felsic volcanic and subordinate arenaceous sedimentary rocks, and coeval and cogenetic anorogenic granites. The overlying Barrensland Group comprises the basal siliciclastic Thelon Formation (ca. 1720 Ma), the volcanic Kuungmi Formation, and the upper carbonate Lookout Point Formation.

Redbed sedimentation and minette volcanism of the Baker Lake Group appears to have been confined to coalesced and fault-bounded sub-basins of the Baker Lake basin, formed by brittle faulting in an orogenic hinterland. The felsic volcanic rocks, intercalated continental sedimentary rocks, and associated intrusions of the Wharton Group do not fill clearly delineated basins and are considered to represent regional heating of the lower crust. The Barrensland Group was deposited within the larger Thelon basin, formed on continental crust after significant uplift and

erosion, in response to fracturing and/or sagging of the crust. Similarity of the petrology, petrography and age of continental to marine sedimentary rocks in the Thelon basin, to that of sedimentary successions in the Athabasca, Hornby Bay and Elu basins, suggests that these basin successions can be correlated.

Note added in proof: Chemical analyses at Kuungmi Fm. flows from the south end of Dubawnt Lake show that these flows are potassic, low-Ca extrusives similar to those at the CIF, indicating that alkaline volcanism was temporally extensive throughout the central Churchill Province.

## ACKNOWLEDGMENTS

We would like to thank A. LeCheminant for a thorough and constructive review. Discussions with S. Tella, R. Rainbird, R. Bell, M. Schau, and P. Hoffman provided the impetus for this work.

## REFERENCES

**Blake, D.H.**
1980: Volcanic rocks of the Paleohelikian Dubawnt Group in the Baker Lake-Angikuni Lake area, District of Keewatin, N.W.T.; Geological Survey of Canada, Bulletin 309, 39 p.

**Booth, G.W.**
1983: The petrology and geochemistry of the Pamiutuq Lake Batholith, Northwest Territories; M.Sc. thesis, University of Toronto, Toronto, 168 p.

**Cecile, M.P.**
1973: Lithofacies analysis of the Proterozoic Thelon Formation, Northwest Territories (including computer analysis of field data); M.Sc. thesis, Carleton University, Ottawa, 119 p.

**Dickinson, W.R.**
1974: Plate tectonics and sedimentation; in Tectonics and sedimentation, W.R. Dickinson; (ed.), Society of Economic Paleontologists and Mineralogists, Special Publication 22, p. 1-27.

**Donaldson, J.A.**
1965: The Dubawnt Group, District of Keewatin and Mackenzie; Geological Survey of Canada, Paper 64-20, 11 p.
1967: Two Proterozoic clastic sequences: a sedimentological comparison; Geological Association of Canada, Proceedings, v. 18, p. 33-54.
1969: Descriptive notes (with particular reference to the Late Proterozoic Dubawnt Group) to accompany a geological map of central Thelon Plain, Districts of Keewatin and Mackenzie; Geological Survey of Canada, Paper 68-49, 4 p.

**Dudás, F.Ö., LeCheminant, A.N., and Sullivan, R.W.**
1991: Reconnaissance Nd isotopic study of granitoid rocks from the Baker Lake region, District of Keewatin, N.W.T., and observations on analytical procedures; in Radiogenic Age and Isotopic Studies: Report 4, Geological Survey of Canada, Paper 90-2, p. 101-112.

**Fraser, J.A., Donaldson, J.A., Fahrig, W.F., and Tremblay, L.P.**
1970: Helikian basins and geosynclines of the northwestern Canadian Shield; Geological Survey of Canada, Paper 70-40, p. 213-238.

**Gall, Q.**
1991: Precambrian paleosols in Canada: an overview; Geological Association of Canada, Mineralogical Association of Canada joint annual meeting with Society of Economic Geologists, Program with Abstracts, v. 16, p. A41.

**Gall, Q. and Donaldson, J.A.**
1990: The sub-Thelon Formation paleosol, and its correlation with similar paleosols in the northwestern part of the Canadian Shield; Geological Association of Canada and Mineralogical Association of Canada, Program with Abstracts, v. 15, p. A43.

**Hoffman, P.F.**
1980: Wopmay orogen: a Wilson cycle of early Proterozoic age in the northwest of the Canadian Shield; in The continental crust and its mineral deposits, D.W. Strangway (ed.); Geological Association of Canada, Special Publication 20, p. 523-549.

**Hoffman, P.F. and Peterson, T.D.**
1991: Tectonic evolution of the Keewatin hinterland during the consolidation of Laurentia (1.8-1.6 Ga); Geological Association of Canada, Mineralogical Association of Canada joint annual meeting with Society of Economic Geologists, Program with Abstracts, v. 16, p. A57.

**Inuit Cultural Institute**
1987: ICI Inuktituk Glossary, Inuit Cultural Institute, Arviat, N.W.T.

**Jackson, M.J., Pianosi, J.G., and Donaldson, J.A.**
1984: Aeolian dunes in Early Proterozoic Thelon Formation near Schultz Lake, central Keewatin; Geological Survey of Canada, Paper 84-1B, p. 53-63.

**Kerans, C., Ross, G.M., Donaldson, J.A., and Geldsetzer, H.J.**
1981: Tectonism and depositional history of the Helikian Hornby Bay and Dismal Lakes Groups, District of Mackenzie; Geological Survey of Canada, Paper 81-10, p. 157-182.

**Kingston, D.R., Dishroom, C.P., and Williams, P.A.**
1983: Global basin classification system; The American Association of Petroleum Geologists, Bulletin, v. 67, p. 2175-2193.

**Klein, G. deV.**
1987: Current aspects of basin analysis; Sedimentary Geology, v. 50, p. 95-118.

**LeCheminant, A.N., Lambert, M.B., Miller, A.R. and Booth, G.W.**
1979a: Geological studies: Tebesjuak Lake map area, District of Keewatin; Geological Survey of Canada, Paper 79-1A, p. 179-186.

**LeCheminant, A.N., Leatherbarrow, R.W., and Miller, A.R.**
1979b: Thirty Mile Lake map area, District of Keewatin; Geological Survey of Canada, Paper 79-1B, p. 319- 327.

**LeCheminant, A.N., Iannelli, T.R., Zaitlin, B., and Miller, A.R.**
1981: Geology of Tebesjuak Lake map area, District of Keewatin: a progress report; Geological Survey of Canada, Paper 81-1B, p. 113-128.

**LeCheminant, A.N., Ashton, K.E., Chiarenzelli, J., Donaldson, J.A., Best, M.A., Tella, S., and Thompson, D.L.**
1983: Geology of Aberdeen Lake map area, District of Keewatin: preliminary report; Geological Survey of Canada, Paper 83-1A, p. 437-448.

**LeCheminant, A.N., Miller, A.R., and LeCheminant, G.M.**
1987a: Early Proterozoic alkaline igneous rocks, District of Keewatin, Canada: petrogenesis and mineralization; in Geochemistry and mineralization of Proterozoic volcanic suites, Ed. T.C. Pharaoh, R.D. Beckinsale and D. Richard; Geological Society of London, Special Publication 33, p. 219-240.

**LeCheminant, A.N., Roddick, J.C., and Henderson, J.R.**
1987b: Geochronology of Archean and Early Proterozoic magmatism in the Baker Lake - Wager Bay region, N.W.T.; Geological Association of Canada and Mineralogical Association of Canada, Program with Abstracts, v. 12, p. 66.

**Loveridge, W.D., Eade, K.E., and Roddick, J.C.**
1987: A U-Pb age on zircon from a granite pluton, Kamilikuak area, District of Keewatin, establishes a lower limit for the age of the Christopher Island Formation, Dubawnt Group; Geological Survey of Canada, Paper 87-2, p. 67-71.

**Macey, G.**
1973: A sedimentological comparison of two Proterozoic red bed successions (the South Channel and Kazan formations of Baker Lake, N.W.T. and the Martin Formation at Uranium City, Saskatchewan); M.Sc thesis, Carleton University, Ottawa.

**Miller, A.R., Cumming, G.L., and Krstic, D.**
1989: U-Pb, Pb-Pb, and K-Ar isotopic study and petrography of uraniferous phosphate-bearing rocks in the Thelon Formation, Dubawnt Group, Northwest Territories, Canada; Canadian Journal of Earth Sciences, v. 26, p. 867-880.

**Overton, A.**
1971: Seismic survey of the Dubawnt Group; Geological Survey of Canada, Paper 71-1A, p. 58.

**Peterson, T.D., LeCheminant, and Rainbird, R.H.**
1989: Preliminary report on the geology of northwestern Dubawnt Lake area, District of Keewatin, N.W.T.; Geological Survey of Canada, Paper 89-1C, p. 173-183.

**Peterson, T.D. and Rainbird, R.H.**
1990: Tectonic and petrological significance of regional lamproite-minette volcanism in the Thelon and Trans-Hudson hinterlands, Northwest Territories; Geological Survey of Canada, Paper 90-1C, p. 69-79.

**Pognante, U.**
1990: Shoshonitic and ultrapotassic post-collisional dykes from northern Karakorum (Sinkiang, China); Lithos, v. 26, p. 305-316.

**Rainbird, R.H. and Peterson, T.D.**
1990: Physical volcanology and sedimentology of lower Dubawnt Group strata, Dubawnt Lake, District of Keewatin, N.W.T.; Geological Survey of Canada, Paper 90-1C, p. 207-217.

**Ramaekers, P.**
1981: Hudsonian and Helikian basins of the Athabasca region, northern Saskatchewan; Geological Survey of Canada, Paper 81-10, p. 219-233.

**Ross, G.M. and Chiarenzelli, J.R.**
1985: Paleoclimatic significance of widespread Proterozoic silcretes in the Bear and Churchill Provinces of the northwestern Canadian Shield; Journal of Sedimentary Petrology, v. 55, p. 196-204.

**Ross, G.M. and Kerans, C.**
1989: Geology, Hornby Bay and Dismal Lakes groups, Coppermine Homocline, District of Mackenzie, Northwest Territories; Geological Survey of Canada, Map 1663A, scale 1:250 000.

**Tella, S., Heywood, W.W., and Loveridge, W.D.**
1985: A U-Pb age on zircon from a quartz syenite intrusion, Amer Lake, District of Keewatin, NWT; Geological Survey of Canada, Paper 85-1B, p. 367-370.

**Wright, G.M.**
1955: Geological notes on central District of Keewatin, Northwest Territories; Geological Survey of Canada, Paper 55-17.

Geological Survey of Canada Project 880012

# Geology and structural relationships along the east margin of the St. Maurice tectonic zone, north of Montauban, Grenville Orogen, Quebec[1]

**L. Nadeau, P. Brouillette, and C. Hébert[2]**
**Quebec Geoscience Centre, Sainte-Foy**

*Nadeau, L., Brouillette, P., and Hébert, C., 1992: Geology and structural relationships along the east margin of the St. Maurice tectonic zone, north of Montauban, Grenville Orogen, Quebec; in Current Research, Part C; Geological Survey of Canada, Paper 92-1C, p. 139-146.*

***Abstract***

*In the Talbot area (31P/01), the eastern margin of the St. Maurice tectonic zone includes meta-plutonic rocks of La Bostonnais complex and a steep one kilometre-wide belt of high-grade supracrustal rocks tentatively correlated with the volcano-sedimentary rocks of the Montauban group, outcropping 10 kilometres to the south. The Laurentides Park plutonic complex to the east includes several contrasting lithologic units.*

*The boundary between the St. Maurice tectonic zone and the Laurentides Park plutonic complex is denoted by major changes in regional structural style and lithologic assemblages. Although locally marked by mylonites, much of the boundary is unexposed and its nature remains uncertain elsewhere.*

***Résumé***

*Dans la région de Talbot (31P/01), la marge orientale de la zone tectonique du Saint-Maurice comprend des roches méta-plutoniques appartenant au complexe de La Bostonnais et une zone de roches supracrustales redressée d'un kilomètre d'épaisseur possiblement corrélatives avec les roches volcano-sédimentaires du groupe de Montauban, affleurant dix kilomètres plus au sud. A l'est, le complexe plutonique du parc des Laurentides compte plusieurs unités lithologiques distinctes.*

*La bordure entre la zone tectonique du Saint-Maurice et le complexe plutonique du parc des Laurentides est le siège de changements importants dans le style de la déformation régionale ainsi que dans les assemblages lithologiques. Quoique marquée par endroits par la présence de mylonites, la plus grande partie de la zone de bordure n'est pas exposée et sa nature demeure incertaine.*

[1] Joint mapping project, Geological Survey of Canada-Ministère de l'Énergie et des Ressources du Québec (MERQ), nature and structural setting of La Bostonnais plutonic complex, MERQ contribution no. 91-5110-31.

[2] Ministère de l'Énergie et des Ressources du Québec, 5700 4e avenue ouest, Charlesbourg, Québec G1H 6R1

## INTRODUCTION

Three contrasting lithotectonic domains have been delineated in the Portneuf-St. Maurice region of the Grenville orogen (Fig. 1 and 2; Nadeau and Corrigan, 1991). The Laurentides Park plutonic complex (a segment of the Allochthonous Polycyclic Belt (Rivers et al., 1989); Fig. 1) is separated from the Mékinac domain (Nadeau and Corrigan, 1991) to the west (an extension of the Allochthonous Monocyclic Belt ?) by a third lithotectonic domain over 30 kilometres wide known as the St. Maurice tectonic zone (Nadeau and Corrigan 1991). This lithotectonic domain is an easterly-dipping, homoclinal belt underlain by amphibolite and granulite facies plutonic and subordinate supracrustal rocks. The latter includes migmatitic paragneiss and related mafic gneiss, as well as lower- to middle-amphibolite facies metasedimentary and metavolcanic rocks of the Montauban group (Rondot, 1978). Meta-plutonic rocks comprise granitic orthogneisses, metagabbro, and the contrasting dioritic to granodioritic rocks of La Bostonnais complex (Rondot, 1978).

The nature and tectonic significance of the Laurentides Park and of the La Bostonnais plutonic complexes, as well as the St. Maurice tectonic zone are not fully established, nor are the relationships between the high-grade supracrustal gneisses and the lower grade metasedimentary and associated metavolcanic rocks of the Montauban area. This progress report focuses on the results of mapping (Hébert et Nadeau, 1990; Nadeau et Hébert, 1990) at a scale of 1:50 000 in the Talbot map sheet (NTS 31P/01), a previously unmapped area to the north of Montauban (Fig. 2). We briefly describe the major rock units and their structural and metamorphic overprint prior to discussing: 1) the composite nature of the Laurentides Park plutonic complex; 2) the possible correlation between the high-grade supracrustal rocks in the area and the lower grade volcano-sedimentary rocks at Montauban; and 3) the tectonic significance of the eastern boundary of the St. Maurice tectonic zone.

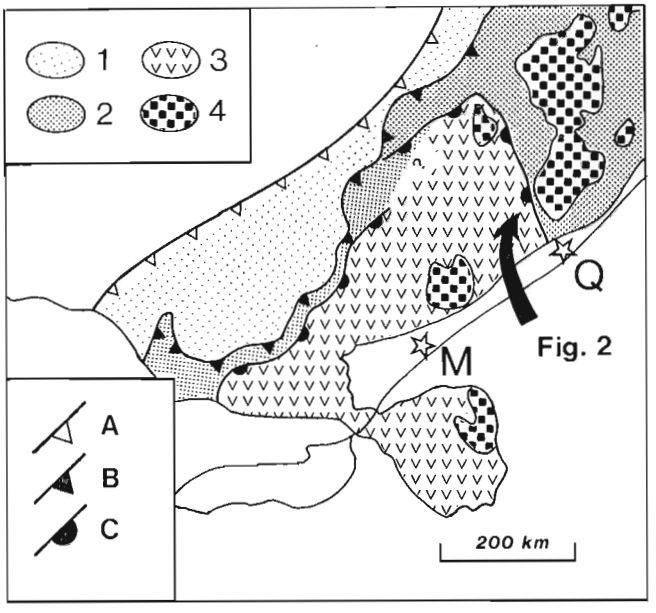


**Figure 1.** Location sketch map and tectonic subdivisions of the Grenville orogen after Rivers et al. (1989). (1) Parautochthonous Belt; (2) Allochthonous Polycyclic Belt; (3) Allochthonous Monocyclic Belt; (4) Anorthosite-mangerite-charnockite-granite suite; [A] Grenville Front; [B] Allochthon boundary thrust; [C] Monocyclic belt boundary thrust.

## DESCRIPTION OF THE MAJOR ROCK UNITS

### *Supracrustal rocks*

Supracrustal rocks outcrop in three settings (Fig. 3, 4): 1) the metasedimentary rocks of the Montauban group outcrop in the Lac Hackett area (units 3, 6, and 7); 2) they compose a steep north-northwest- to northwest-striking belt, one km wide, which transects the central part of the map area (units 1 and 2); this belt is hereafter referred to as the "central belt" for convenience; and, 3) they occur as small screens scattered in the Laurentides Park plutonic complex.

#### Central belt

Supracrustal rocks of the central belt compose two map units (Fig. 3). Unit 1 consists of migmatitic paragneisses with ubiquitous decimetre-wide discontinuous layers and boudins of calc-silicates and of a variety of mafic rocks. Unit 2 is made up of interlayered high-grade mafic gneiss, paragneiss, and mesocratic biotite-hornblende-garnet gneiss.

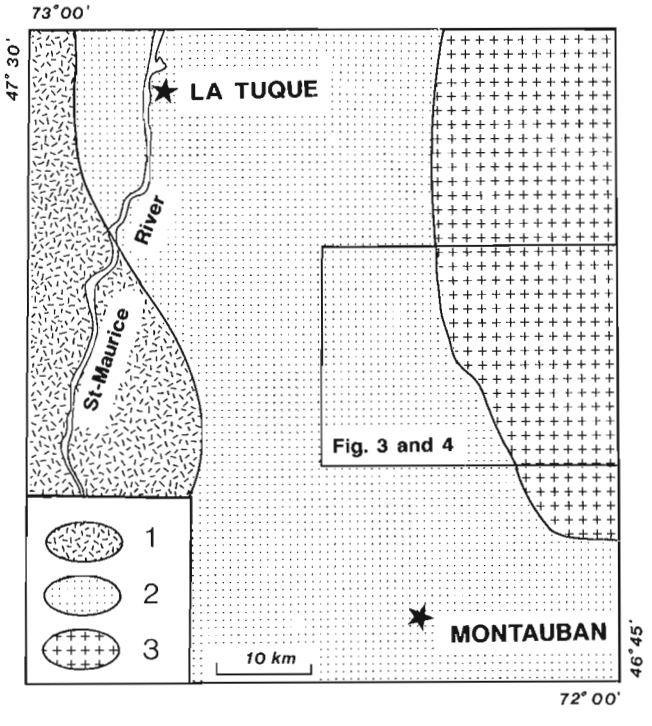


**Figure 2.** Sketch map outlying lithotectonic domains within the Grenville orogen in the Portneuf-St. Maurice region and the location of the Talbot map area (31P/01). (1) Mékinac domain; (2) St. Maurice tectonic zone; (3) Laurentides Park plutonic complex.

Paragneisses are fine- to medium-grained garnet-biotite-plagioclase-orthoclase-quartz-sillimanite rocks with up to 20% white granitic leucosome. Garnet plus biotite content ranges from 15 to 25%. Centimetre-thick layering, expressed by variations in granoblastic grain size and mafic mineral proportion, is pervasively developed. Layers are typically irregular and discontinuous with gradational contacts. Although this layering partly reflects primary compositional variations, the following observations indicate that bedding has been extensively disrupted and transposed, and that the present layering is the result of the combined effects of intense ductile deformation and high-grade metamorphism. Layering is expressed by variations in the granoblastic grain size and in the proportion of porphyroblastic garnet, and is locally enhanced by the development of concordant granitic migmatitic segregations (Fig. 5a). Parallel composite $S_0$-$S_1$ surfaces have been tightly to isoclinally folded, and subsequently boudinaged during the development of the dominant $S_2$ foliation (Fig. 5b). Ubiquitous boudinage of mafic and calc-silicate (diopside-grossularite-calcite) layers attests to the destruction of the initial lithologic succession. Stretching lineation parallel to detached fold closures indicates considerable extension.

Mafic rocks, typically in metre-thick discontinuous layers and boudins within paragneisses, compose up to 30% of unit 1 (Fig. 5c). They include at least three types with distinct mineralogical assemblages: hornblende-plagioclase, clinopyroxene-hornblende-plagioclase, and garnet porphyroblastic hornblende-plagioclase-clinopyroxene.

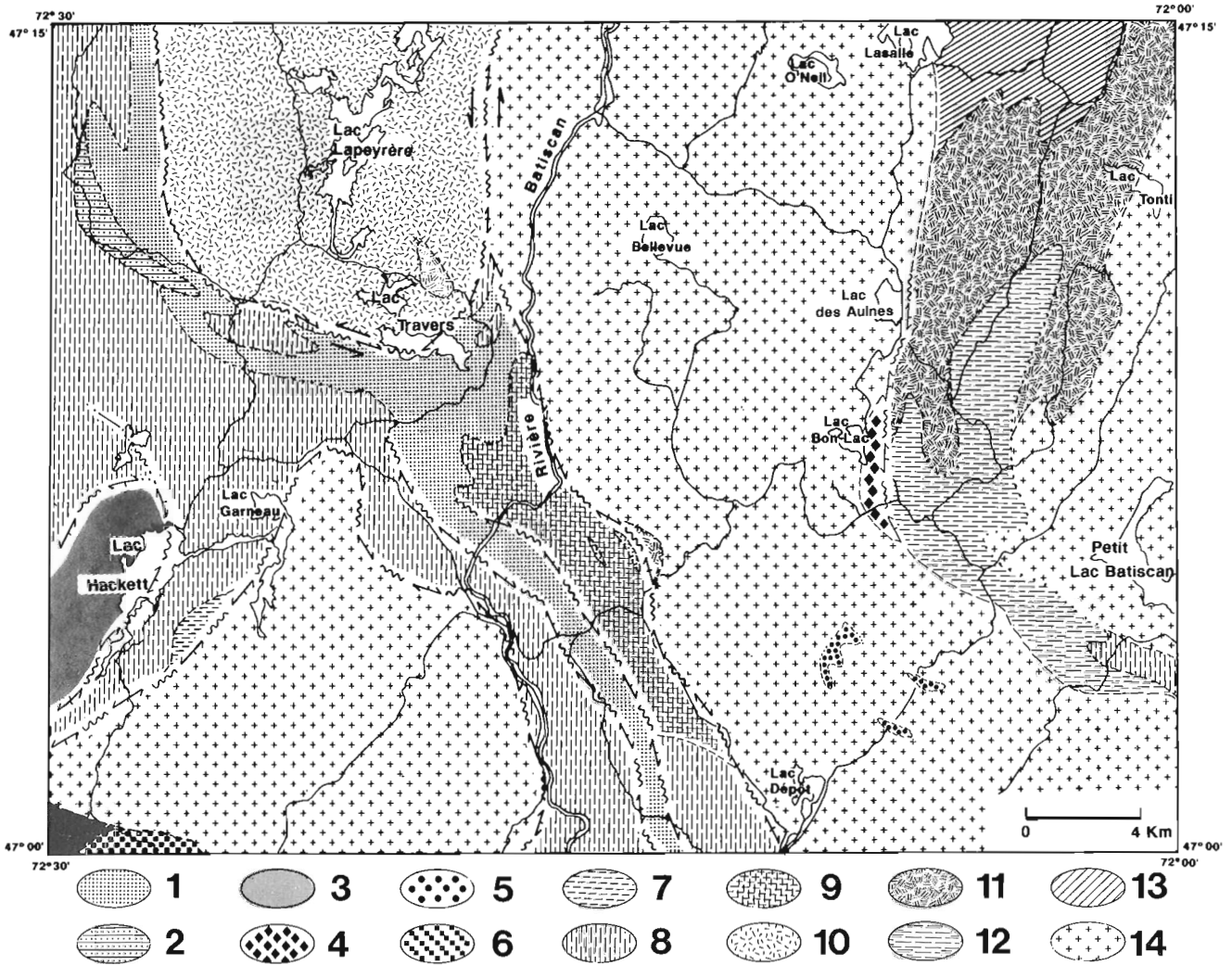


**Figure 3.** Geological sketch map of the Talbot area (31 P/01). Major rock units includes: (1) aluminous paragneiss with subordinate mafic layers and boudins; (2) mafic gneiss with subordinate paragneiss; (3) biotite-muscovite-garnet-sillimanite quartzofeldspathic paragneiss; (4) metaquartzite; (5) brecciated calc-silicate rock; (6) metaconglomerate; (7) diatexitic biotite-hornblende paragneiss; (8) undivided diorite, quartz-diorite and granodiorite, ranging from massive to migmatitique and mylonitique; (9) same as 8 with up to 20% paragneisses associated; (10) Lac Lapeyrère metagabbro; (11) migmatitic charnockitic orthogneiss; (12) alaskitic granulite; (13) migmatitic biotite granite gneiss; (14) porphyritic biotite-hornblende granite and monzonite

All of these mafic rock types are commonly present in outcrops together with calc-silicate boudins. The mafic rocks are invariably fine- to medium-grained, generally granoblastic, foliated, and heterogeneous. They locally preserve a centimetre-scale relict layering expressed by variations in grain-size and garnet amount which could be interpreted as volcanic features. The variable nature of the mafic rocks and their constant association with calc-silicate layers and paragneiss lead to their interpretation as a volcano-sedimentary sequence.

Mafic rocks of the types described above, together with heterogeneous, mesocratic biotite-hornblende-plagioclase-garnet gneiss, are the major constituents of unit 2. These rocks are fine- to medium-grained, variably migmatitic, well-foliated and form concordant layers up to tens of metres thick. The greater proportion and thickness of mafic gneisses with respect to paragneisses distinguish unit 1 from unit 2.

**Lac Hackett area**

Unit 3, part of the Montauban group, consists of light gray, rusty weathering, fine- to medium-grained, thinly layered, biotite-muscovite quartzofeldspathic gneiss with minor garnet and sillimanite. This gneiss is locally interlayered with fine grained biotite-hornblende gneiss.

Other supracrustal rocks include minor granoblastic quartzite (unit 4); calc-silicate breccia (unit 5); metaconglomerate (?) (unit 6); and fine grained, light to medium grey, thinly layered, diatexitic biotite-hornblende gneiss (unit 7; Fig. 5d).

### *La Bostonnais plutonic complex*

In the Talbot area, the La Bostonnais plutonic complex is composed of rocks ranging from two pyroxene-hornblende diorite to hornblende-biotite granodiorite with 40 to 15% mafic minerals. Unit 8 is composed mainly of massive to gneissic, and migmatitic orthogneiss, whereas unit 9,

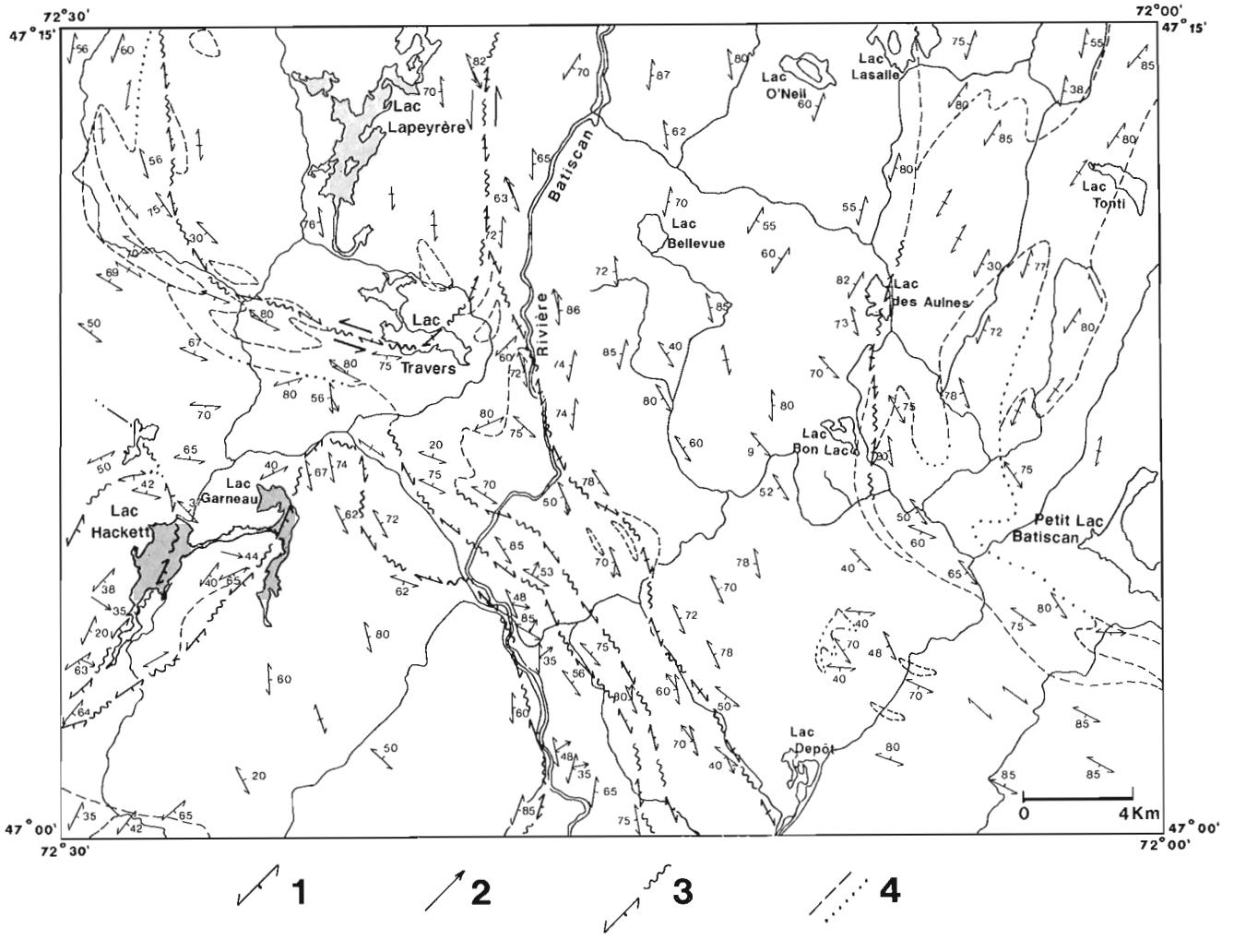


**Figure 4.** Generalized structural map: (1) foliation and layering; (2) mineral and stretching lineation; (3) sheared geological contact; (4) geological contact, assumed, interpreted

although dominated by metaplutonic rocks, includes ubiquitous metre to outcrop-scale supracrustal xenoliths. The main lithologic attributes of the rocks of this plutonic complex are summarized in Nadeau and Corrigan (1991).

### *Laurentides Park plutonic complex*

The Laurentides Park plutonic complex (Rondot, 1978) underlies the east half of the map area (Fig. 2 and 3) and a large segment of the Allocthhonous Polycyclic Belt (Fig. 1). It is essentially made up of granitic plutonic and high-grade metaplutonic rocks with local screens of supracrustal gneisses. Five contrasting units are present in the map area and appear to have the following intrusive order: 1) migmatitic charnockitic orthogneiss; 2) alaskitic granulite; 3(?) migmatitic biotite granitic gneiss; 4(?) hornblende-biotite granodioritic gneiss; and 5) porphyritic quartz-monzonite and granite.

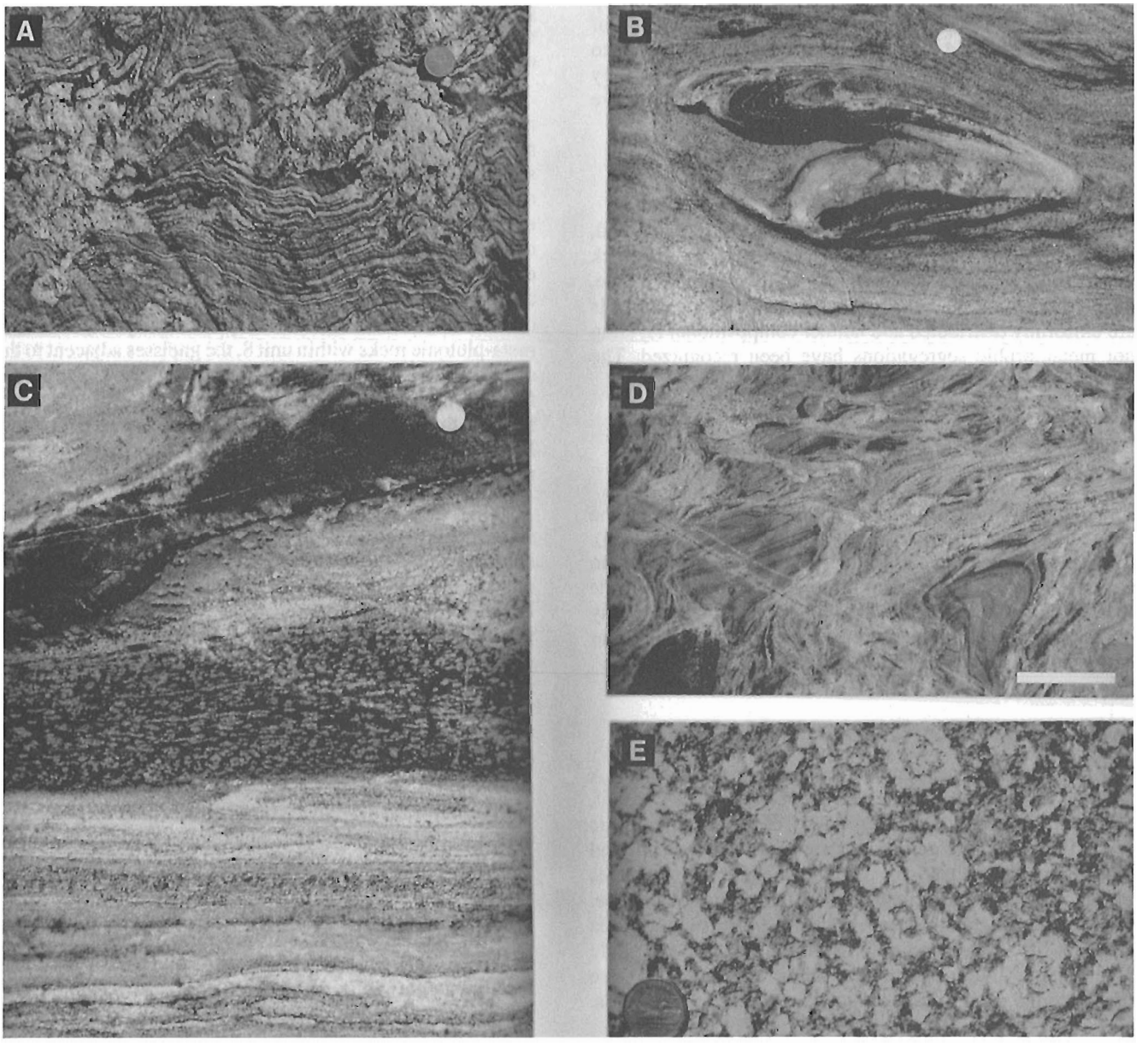


**Figure 5.** Characteristic structures of high-grade supracrustal rocks and porphyritic granite. **A.** Typical appearance of migmatitic, high strain, aluminous migmatitic paragneiss (garnet-biotite-sillimanite-feldspar-quartz), scale = 2.5 cm. **B.** Isoclinal folding and boudinage of competent layer in fine-grained, granoblastic aluminous paragneiss, scale = 2.5 cm. **C.** Contrasting types of mafic rock in sheared and migmatitic aluminous paragneiss; mineral assemblage is hornblende-plagioclase in the upper layer and garnet-hornblende-plagioclase in the lower layer. **D.** Thinly layered, diatexitic biotite-hornblende gneiss. **E.** Porphyritic biotite-hornblende granite exhibiting zoned feldspar with plagioclase cores and K-feldspar rims, scale = 15 cm.

### Migmatitic charnockitic orthogneiss (unit 11; Fig. 3)

This unit outcrops in the northeast quadrant of the map area and consists of buff-brown weathering, olive green, equigranular, fine- to medium-grained, mesoperthitic granite with 5 to 10% orthopyroxene-clinopyroxene- hornblende-biotite and accessory magnetite-apatite-zircon. This orthogneiss is granoblastic, invariably well foliated, and contains up to 15% coarser grained, centimetre-scale and uniformly distributed stromatic granitic segregations, locally with millimetre-scale melanocratic selvages. The rock show no primary layering and although migmatitic at an outcrop scale, appear homogeneous at larger scale. Orientations of both hypersthene and the stromatic segregations contribute to the planar fabric. These rocks are locally cut by centimetre-thick deformed aplitic dykes which have petrographic similarities with the alaskitic granulites.

### Alaskitic granulite (unit 12; Fig. 3)

This unit is a cream weathering, pinkish, fine grained, equigranular, granoblastic, quartz-mesoperthite granitic rock with 5 to 20% oligoclase and accessory hornblende, biotite, magnetite, zircon, and relic orthopyroxene. Mafic minerals are uniformly distributed and neither compositional layering nor metamorphic segregations have been recognized. The well developed foliation is defined by platy quartz.

### Porphyritic quartz-monzonite and granite (unit 14; Fig. 3)

The rocks of unit 14 is the dominant lithology of the Laurentides Park plutonic complex in the Talbot area (Fig. 3). The rocks are medium grained, with K-feldspar crystals up to 2 cm, light grey, and contain up to 10% biotite-hornblende locally with orthopyroxene. The feldspar phenocrysts locally exhibit an anti-rapakivi texture where mantles of K-feldspar completely enclose plagioclase grains (Fig. 5e).

## DEFORMATION AND METAMORPHISM

The foliation and lineation data are summarized in Fig. 4. A close correspondence is observed between the lithologic unit, the strain intensity and the extent of the metamorphic overprint. Granulite facies rocks are limited to units 11 and 12, of the Laurentides Park plutonic complex. Paragneisses of the central belt (units 1 and 2) are muscovite free, migmatitic to various extents and exhibit uppermost amphibolite facies mineral assemblages. Lower grade assemblages including muscovite-sillimanite-garnet are limited to the paragneisses of unit 3, in the Lac Hackett area.

The Laurentides Park plutonic complex is characterized by vertical or steeply-dipping, northwesterly to northeasterly-trending foliations (Fig. 4). The lineation is generally indistinct. The porphyritic granites (unit 14) are either massive or exhibit a faint foliation. An increase in strain is locally observed toward the contacts. By contrast, the other units in the complex are well foliated and metamorphosed to high grade. The porphyritic granite appears to be in fault contact with the Lac Lapeyrère metagabbro. An abrupt strain gradient with local development of centimetre-thick ultramylonite is observed in the outcrops of porphyritic granite nearest the contact. Here mylonitic granite several metres thick contains centimetre-thick ultramylonites. The mylonites are steeply-dipping and contain a subhorizontal lineation. Shear-sense indicators such as S-C fabrics and rotated porphyroclasts indicate sinistral shearing. Further south, along the Batiscan River, the contact of the porphyritic granite is locally marked by a zone of mylonite several metres thick. This zone has been traced over one kilometre; elsewhere the contact is not exposed.

The central belt is dominated by north-northwest- to northwest-striking and moderately to steeply, east- to northeast-dipping gneisses. These orientations conform to the structural pattern of the St. Maurice tectonic zone (Nadeau and Corrigan, 1991). Southwest dips are limited to gneisses adjacent to the Laurentides Park plutonic complex. The trend of the stretching lineation shifts from northwest-southeast to east-northeast away from the Lac Lapeyrère metagabbro and the Laurentides Park plutonic complex. With the exception of a few small masses of well preserved, partly massive, meta-plutonic rocks within unit 8, the gneisses adjacent to the central belt are commonly migmatitic and show ubiquitous features indicative of intense ductile flow. The dominant fabric in the high-grade paragneisses is a transposed foliation. Mesoscopic-scale overprinting structures in highly strained migmatitic orthogneiss also indicate polyphase deformation.

The Lac Hackett area features a series of southeast-dipping sheets. The lowermost sheet (unit 3) is composed of well foliated, shallow- to moderately-dipping, structurally concordant paragneiss with an easterly-plunging lineation. It is overlain by concordant, mesocratic, migmatitic biotite-hornblende gneisses (unit 8) which include lenses of granodioritic orthogneiss and screens of garnet porphyroblastic-biotite-sillimanite gneiss and diatexitic biotite-hornblende paragneisses. The structurally uppermost sheet is composed of porphyritic granite (unit 14). Its contact relationships are as follows. 1) The northwest contact of the sheet and its marginal foliation are structurally concordant with the fabric in the underlying gneisses. 2) In the southwest corner of the map area, the contact dips shallowly to the east and is structurally discordant with respect to the northeast-trending fabric of the underlying gneiss. The latter conforms to the fabric observed along the northwest contact. 3) Intrusive apophyses of porphyritic granite in the underlying unit 6, and xenoliths of paragneisses (unit 3) are locally present along the contact. Moreover, a porphyritic granite dyke crosscuts concordant migmatitic gneisses at the contact at Lac Garneau. 4) The northeast contact is also structurally concordant and dips moderately to steeply to the east. Although largely massive, the interior of this granite sheet is locally well foliated. This granite may represent a late-syntectonic intrusion possibly linked to the emplacement of the Laurentide Park complex to the east.

## DISCUSSION

### *Nature of the Laurentides Park complex*

The geology of the Laurentides Park plutonic complex is poorly known; much of the complex has only been mapped at reconnaissance level (Laurin and Sharma, 1975). It is generally considered to be underlain by genetically linked, monotonous and largely massive charnockitic and mangeritic rocks widely assumed to be part of the anorthosite-mangerite-charnockite-granite suite (McLelland, 1989; Emslie and Hunt, 1990). This interpretation hinges on the spatial association of the complex with the Lac St. Jean anorthosite massif, and is supported by the clustering, in the 1.1-1.0 Ga range, of Rb-Sr ages from late-tectonic, crosscutting intrusions (Frith and Doig, 1973). Although initially interpreted as igneous crystallization ages, the Rb-Sr data may partly reflect closure of the Rb-Sr whole rock system during regional cooling. Moreover, it is stressed that all the ages have been obtained from the late intrusions and that no attempts have been made to date earlier phases of the complex.

Our mapping, although limited in extent, shows that the Laurentides Park plutonic complex is composed of several distinct rock units with contrasting deformational and metamorphic overprints. While charnockitic migmatitic orthogneiss (unit 11) and alaskitic granulite (unit 12) have experienced penetrative granulite facies deformation, the porphyritic quartz-monzonite and granite (unit 14) are largely massive, the amphibolite facies deformation fabric being limited to the margin of the bodies. The hypothesis that the bulk of the complex is made up of mangeritic-charnockitic-granitic intrusions genetically linked to the Lac St. Jean anorthosite complex cannot be ruled out from the existing data. The possibility that a significant portion of the complex comprises unrelated intrusive bodies of widely differing ages is, however, raised.

### *Correlation of the supracrustal rocks*

The following observations and views provide a basis for a tentative correlation of the high-grade migmatitic supracrustal rocks of the central belt and the lower grade volcano-sedimentary rocks of the Montauban Group. 1) A gradational passage from a metagreywacke(?) typical of the metasediment at Montauban to a high-grade migmatitic paragneiss, identical to that dominating unit 1, is observed across continuous outcrop 15 kilometres northwest of Montauban, near the Lac des Américains. Fine grained, light colored and rusty weathering, muscovite-biotite quartzofeldspathic rocks grade progressively to coarser grained, light grey, migmatitic, sillimanite-garnet porphyroblastic-biotite paragneiss containing up to 20% granitic stromatic veins. 2) The local preservation of relict layering and the possible volcano-sedimentary nature of the high-grade supracrustal rocks support their correlation with the lower grade rocks at Montauban. 3) Crosscutting relationships indicate that both the high-grade supracrustal rocks and the lower grade rocks of the Montauban Group are older than the plutonic rocks of La Bostonnais complex and appear to be at the base of the geological succession.

### *Tectonic significance of the eastern boundary of the St. Maurice tectonic zone*

The eastern boundary of the St. Maurice tectonic zone was described as 1) a "ductile shear zone with a sinistral strike-slip component", across which 2) "major changes in regional structural style and rock assemblages occur" (Nadeau and Corrigan, 1991).

No mesoscopic-scale intrusive structures have been recognized in the boundary zone. A zone of mylonite several metres thick has been traced for one kilometre along the Batiscan River. This group of outcrops represents the best-exposed segment of the boundary zone in the Talbot area; elsewhere the boundary zone is not exposed and its nature remains uncertain. These mylonites may indicate minor structural readjustments and have a limited regional significance. It could be argued that the sheet of porphyritic granite outcropping in the southwest corner of the map area represents a satellite intrusion from the Laurentides Park plutonic complex. This, in itself, does not exclude the possibility that tectonically significant displacement may have taken place along the boundary.

The second assertion that "major changes in regional structural style and rock assemblages occur" across the boundary zone is supported by the results of regional reconnaissance studies and the more detailed mapping of the Talbot area reported here. That the Laurentides Park plutonic complex and the lithotectonic domain recognized to the west (the St. Maurice tectonic zone) have evolved in distinct paleo-tectonic settings is undeniable. The question remains whether these two domains developed in proximity or have been juxtaposed.

## CONCLUSIONS

1) The Laurentides Park plutonic complex is composed of several contrasting metaplutonic rock units. A significant portion of the complex may include unrelated intrusive bodies of widely differing ages.

2) Further west, a one kilometre-wide belt of high-grade supracrustal rocks is recognized, and tentatively correlated with volcano-sedimentary rocks of the Montauban Group.

3) A close correspondence is observed across the map area between the rock units, the strain intensity, and the extent of the metamorphic overprint; some units are poly-deformed whereas others have recorded evidence for only one deformational event.

4) The eastern boundary of the St. Maurice tectonic zone is marked by major changes in regional structural style and rock assemblages. Although locally marked by mylonites, elsewhere the boundary is unexposed and its nature remains uncertain.

## ACKNOWLEDGMENTS

Renald Gervais, Eric Lemieux, David Corrigan, Sylvie Lévesque, and Michel Dion are gratefully acknowledged for their support during mapping. The original manuscript was much improved by the critical and careful review of G. Lynch (CGQ), L. Corriveau (CGQ) and T. Birkett (CGQ).

## REFERENCES

**Emslie, R.F. and Hunt, P.A.**
1990: Ages and petrogenetic significance of igneous mangerite-charnockite suites associated with massif anorthosites, Grenville Province; Journal of Geology, v. 98, p. 213-231.

**Frith, A. and Doig, R.**
1973: Rb-Sr isotopic ages and petrologic studies of the rocks in the Lac. St. Jean area, Quebec; Canadian Journal of Earth Sciences, v. 10, p. 881-899.

**Hébert, C. and Nadeau, L.**
1990: Géologie du feuillet SNRC 31 P/1 (Talbot): implications tectoniques et économiques; in Rapport d'activités 1990, Ministère de l'Énergie et des Ressources du Québec, DV 90-10, p. 15-17.

**Laurin, A.F. and Sharma, K.N.M.**
1975: Région des Rivières Mistassini-Péribonka-Saguenay; Rapport Géologique 161, Ministère des Richesses Naturelles du Québec, 89 p.

**McLelland, J.M.**
1989: Crustal growth associated with anorogenic, mid-Proterozoic anorthosite massifs in northeastern north America; Tectonophysics, v. 161, p. 331-341.

**Nadeau, L. and Corrigan, D.**
1991: Preliminary notes on the geology of the St. Maurice tectonic zone, Grenville orogen, Quebec; in Current Research, Part E; Geological Survey of Canada, Paper 91-1E, p. 245-255.

**Nadeau, L. and Hébert, C.**
1990: Déformation et extension de l'assemblage métasédimentaire de Montauban dans la réserve de Portneuf; dans Nouveaux horizons pour l'exploration 1990, Ministère de l'Energie et des Ressources du Québec, DV 90-40, p. 11-14.

**Rivers, T., Martignole, J., Gower, C.F., and Davidson, A.**
1989: New tectonic divisions of the Grenville Province, southeast canadian shield; Tectonics, v. 8, p. 63-84.

**Rondot, J.**
1978: Région du Saint-Maurice; Ministère des Richesses Naturelles de Québec, DPV-594,85 p.

Geological Survey of Canada Project 900010

# Geological controls on the 1989 Ungava surface rupture: a preliminary interpretation

**John Adams[1], J.A. Percival[2], R.J. Wetmiller[1], J.A. Drysdale[1], and P.B. Robertson[1]**

*Adams, J., Percival, J.A., Wetmiller, R.J., Drysdale, J.A., and Robertson, P.B., 1992: Geological controls on the 1989 Ungava surface rupture: a preliminary interpretation; in Current Research, Part C; Geological Survey of Canada, Paper 92-1C, p. 147-155.*

***Abstract***

*The December 25, 1989 Ungava earthquake (magnitude 6.3) in northern Quebec produced the first known surface faulting from an historical earthquake in the stable continental interior of North America. The 1991 field study, a continuation of work started in 1990, revealed the faulting was controlled by geology at all scales from regional to outcrop. The rupture appears to have been controlled by compositional layering and foliation within a steeply-dipping sequence of paragneiss and granite containing concordant ductile high-strain zones. The rupture occurred along a ductile Archean fault, but there is no evidence of subsequent reactivation as a brittle fault in the Phanerozoic prior to 1989.*

***Résumé***

*Le tremblement de terre de l'Ungava dans le nord du Québec survenu le 25 décembre 1989 (magnitude 6,3) a occasionné la première rupture de surface dans l'histoire des séismes enregistrés dans la région continentale stable de l'intérieur de l'Amérique du Nord. Le levé de terrain de 1991, qui fait suite aux travaux de 1990, indique que la structure géologique de la région épicentrale exerçait un contrôle sur la rupture aussi bien à l'échelle locale qu'au niveau de l'affleurement. La stratification et la foliation à l'intérieur d'une séquence de paragneiss et granite à fort pendage et ayant des zones de concordance ductiles très déformées ont contrôlé la rupture. Cette rupture a suivi une faille ductile archéenne, et il n'y a aucune indication avant 1989 de reprise d'activité le long de la faille au cours du Phanérozoïque.*

[1] Geophysics Division, Geological Survey of Canada
[2] Continental Geoscience Division, Geological Survey of Canada

## INTRODUCTION

The first known surface faulting from an historical earthquake in the stable continental interior of North America – and one of only 10 such documented from stable continental regions worldwide (Johnston and Bullard, 1990) – resulted from the magnitude ($M_S$) 6.3 Ungava earthquake of 25 December 1989 in northern Quebec. The 10-km rupture (of average strike 030° and centred at 60.12°N, 73.60°W) represents thrust faulting on a near-surface, steeply-dipping, curved fault plane with a maximum throw of 1.8 m (Adams et al., 1991a,b).

The Ungava rupture lies north of the treeline in an area of continuous permafrost. The gneissic bedrock is typical of the glaciated 2.7-Ga-old Superior Province of the Canadian Shield. Local relief is only 70 m, and about half the region is covered by water, with Lac Bécard surrounding the epicentre on three sides. December temperatures of -35°C, snow cover, short daylight (<3 h/day), and remoteness precluded an immediate visit, but surface faulting was discovered in July 1990 during an aftershock field survey. The 1990 survey was based in Kangirsuk, 200 km to the east, with daily access by chartered helicopter. The majority of the helicopter time had been used before the discovery, so the field crew had only 17 hours on the ground to map the rupture. Accordingly, a second field survey was organized for the summer of 1991, and additional remote sensing was flown in the fall of 1990.

## REMOTE SENSING

Vertical air photograph (black and white) coverage exists at a scale of 1:42 000 (EMR, flown in July 1955) and 1:32 000 (Province of Quebec flown in August 1957). A 1:50 000 topographic map (sheet 35A/4) has been constructed from the first set of photographs. Oblique photographs (Tri-mets) flown in July 1948 are also available (Fig. 1). The small-scale photographs are useful in outlining topographic and structural regional patterns. For example, Figure 2 shows clear bedrock control of the topography, especially along the shores of Lac Turquoise and Lac Sorcier. [Lac Turquoise and Lac Sorcier are informal geographic names. Lac Turquoise was coloured by suspended silt after the earthquake and Lac Sorcier ('Wizard') has a triangular shape, controlled by structure, that resembles a wizard's hat.]

As a result of discovering the surface rupture, the Geological Survey of Canada contracted low-level (1:3 000) colour air photography of the fault rupture in September 1990. Additional information for regional interpretation was provided by airborne synthetic aperture C-band radar (SAR), flown in August 1990 by the Canada Centre for Remote Sensing. The SAR was flown with a 64-km swath width and incidence angles from 45° to 85°. Three lines were flown, one looking southeast, one looking southwest, and the third looking northwest; slant-corrected images were produced. Because of the varied look directions, all three images contain complementary information on linear features (faults, layering, dykes, etc.). The second image is reproduced here (Fig. 3) because it illustrates the north-northeast-trending structures parallel to the fault reasonably well and does the best overall job of illuminating the regional structures.

## 1991 FIELD OPERATIONS

The 1991 field survey was conducted July 8-22 from a field camp on Lac Bécard adjacent to the fault scarp. Access to the campsite was by float-plane from Kuujjuaq, Quebec, and transportation around the field area (approximately 12 by 4 km) was by inflatable "Zodiac" boats and on foot. Participants included the authors (except Robertson), W.W. Shilts of Terrain Sciences Division, and students J. Boily and S. McCuaig. The 1991 objectives included detailed mapping of the surface rupture and its secondary dislocational features, documenting relative shoreline (lakeshore) elevation changes, monitoring ongoing seismic activity, retrieving three strong-motion recorders deployed in the fall of 1990, investigating possible disturbances of lake-bottom sediments using a subbottom acoustic profiling system, sampling soft-sediment deformational features, determining what if any local pre-existing geological features might control the surface faulting, and investigating a possible impact crater revealed by the SAR imagery.

A full account of the results will be published elsewhere; here, we note merely that a) continuing seismic activity along the fault scarp was minimal and no seismic events large enough to trigger the strong-motion recorders deployed in the fall of 1990 had occurred and b) approximately 80 km of profiling of the lake bottoms of Bécard, Turquoise, and Sorcier showed generally thin sediment cover (except in Lac Turquoise), and revealed isolated pockets of disturbed sediments in all three lakes. A thin layer of recently-deposited sediment was found in the southern end of Lac Sorcier, confirming the conclusion of Adams et al. (1991b) that the lake discolouration was due to silt washed into the lake because of earthquake-induced partial drainage of Lac Turquoise.

The main surface rupture was found to extend 2 km farther north than reported earlier, and many previously undocumented secondary ruptures were identified, including tensional and strike-slip dislocations. Matching of torn peat across the secondary faults showed evidence for a consistent left-lateral strike-slip component, reaching half of the total slip at the northern end of the rupture. The strike-slip component was missed in the 1990 survey because the irregular ground surface provides few large-scale reference lines to demonstrate horizontal offset on the main fault trace (by contrast vertical displacements were easily seen from displaced lake shorelines, Adams et al., 1991a), and because the strike-slip component is most evident at the northern end of the rupture, not visited in 1990. The average slip direction on the fault is inferred to be 355 ± 15° based on resolving the slip across secondary faults, thrust ridge orientation, and individual thrust boulders. This slip is resolved onto a curved fault plane that strikes 050° at Lac Turquoise and 020° north of Lac Sorcier (Fig. 2).

As noted during the 1990 survey (Adams et al., 1991b), the surface rupture appears to follow the shorelines of Lac Turquoise and Lac Sorcier quite closely, at places deviating through angles of up to 25° from a smooth curve to do so. It was inferred from this that the rupture was "controlled by a pre-existing fault .... that also controlled the glacial erosion which produced the present topography and hence lake shores." As we describe below, both the topography and the location of the surface rupture are strongly dependent on the local lithology, and while there is evidence for ductile Archean faulting, there is no evidence of subsequent reactivation prior to 1989.

## REGIONAL GEOLOGY

The bedrock of the epicentral region is within the Minto subprovince of the northeastern Superior Province (Card and Ciesielski, 1986). A regional reconnaissance geological map covering the Archean rocks of the Ungava Peninsula at a scale of 1:1 000 000 (Stevenson, 1968) is based on wide-spaced helicopter traverses and has limited reliability for the purposes of this study. For example, the study area is underlain by pyroxene-bearing granodiorite according to Stevenson (1968), whereas our observations indicate an interlayered sequence of north-trending amphibolite-facies

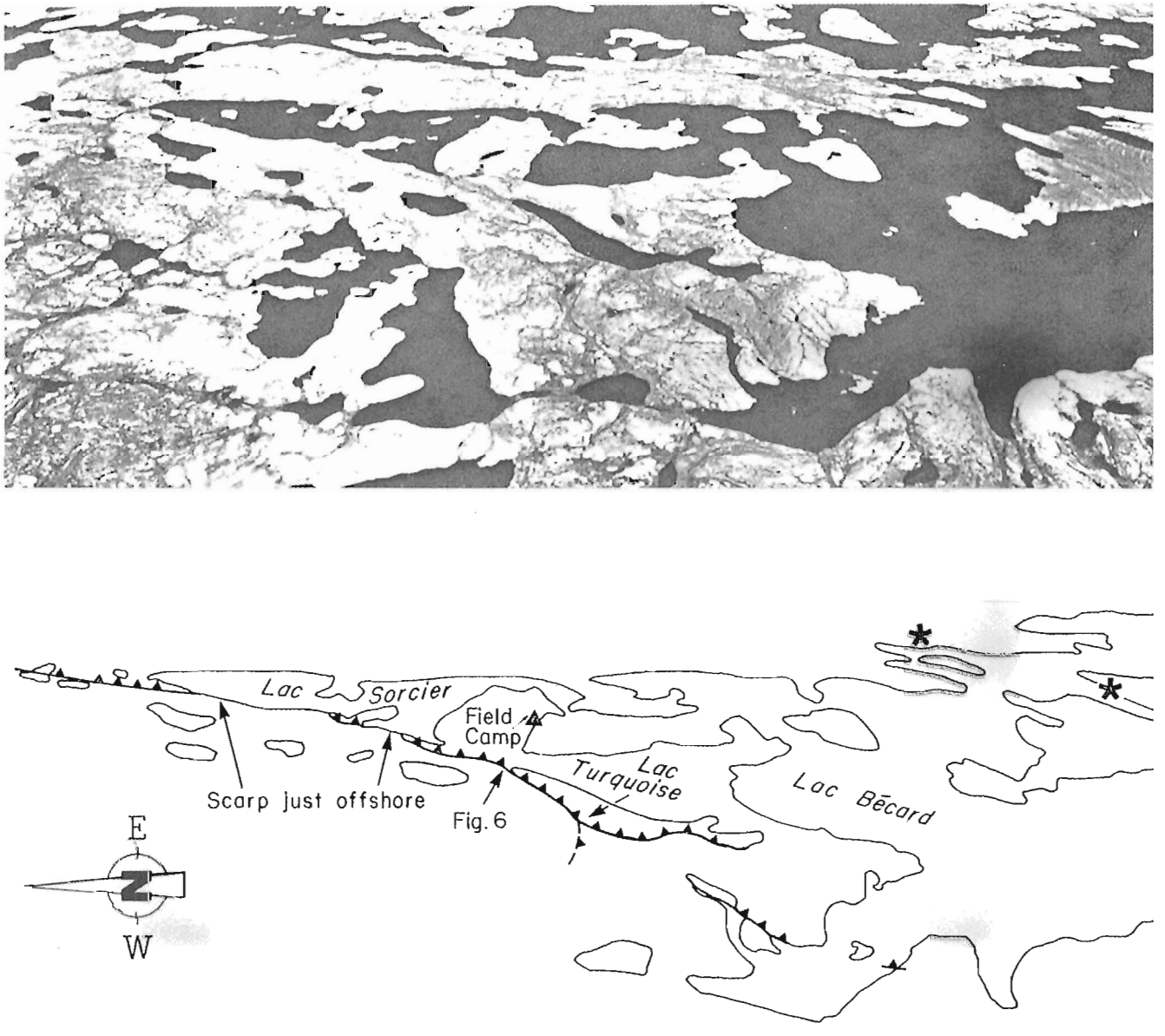


**Figure 1.** Portion of oblique air photograph T193R-153 showing the region of the surface faulting viewed from the west. The sketch diagram below locates the rupture and Figure 6 and adds geographic names. Stars at the upper right locate rocks sampled for possible shock metamorphism.

paragneiss and biotite granite. At the regional scale, metasedimentary remnants are a common component of Stevenson's granodiorite unit (Percival et al., 1990).

The southern extension of the Ungava rupture disappears at the northern shoreline of Lac Bécard. The Lac Bécard area comprises an interconnected network of bays, islands, peninsulas, and arcuate shorelines that define an indistinct circular feature 15 km in diameter (Fig. 3). In a terrain characterized by rectilinear structural patterns and scattered small lakes, the curvilinear trends and the large, interconnected, water-filled basins of the Lac Bécard feature are unusual. They may result, for example, from a fold closure within softer paragneiss or, more speculatively, from an ancient impact structure. Whatever the cause, the structural control from this feature might have influenced the southern termination of the rupture.

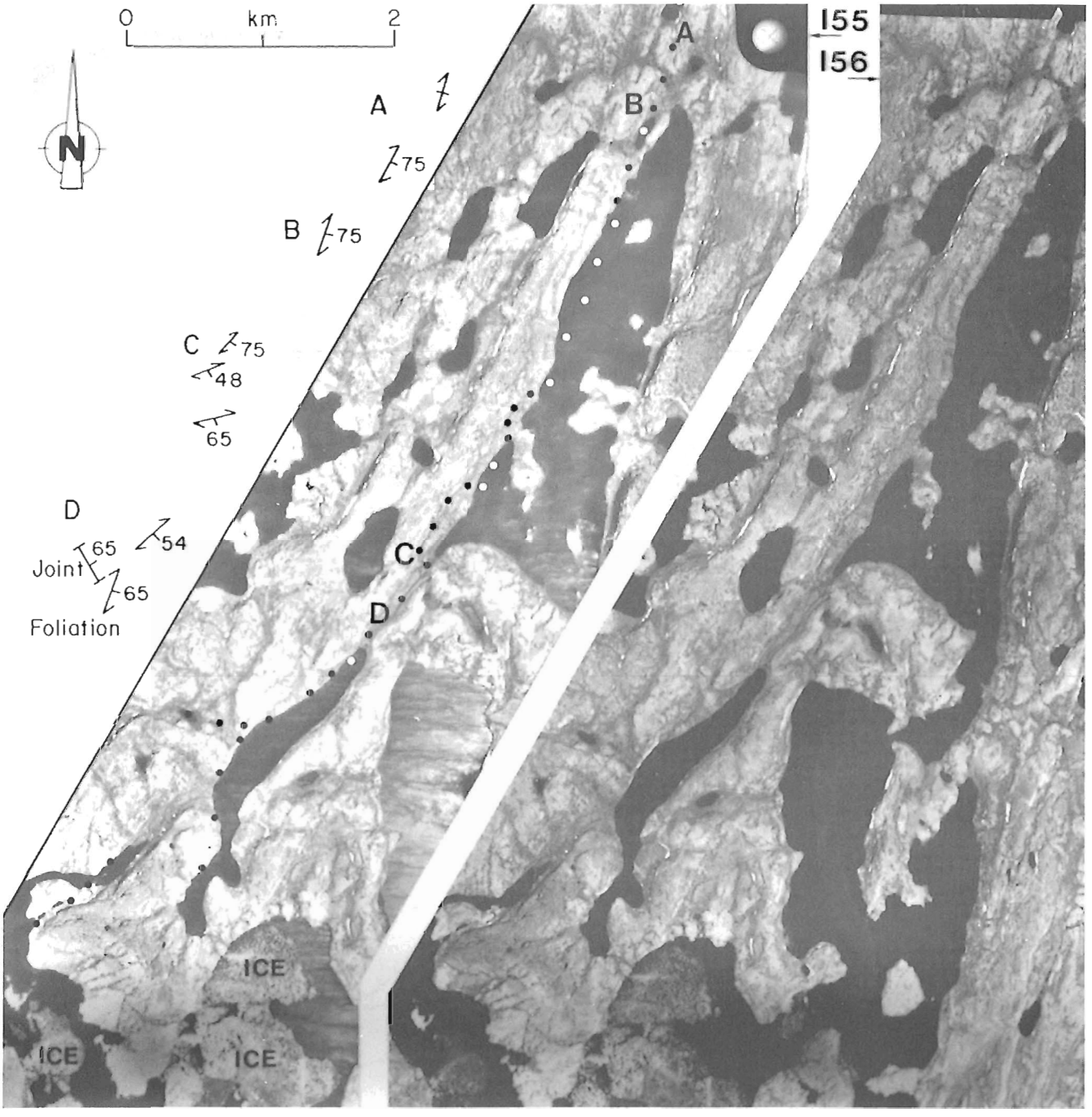


**Figure 2.** Stereo pair of photographs A-14692-155 and -156 revealing the topography and its structural control. The position of the rupture is indicated by black dots on land and white dots in the lakes. Structural geology observations made in 1991 are keyed to sites A-D on the left image.

If the structure is an ancient impact site, it would be comparable to the Lac Couture impact structure, located in Archean gneiss 110 km to the west. Lac Couture is smaller (8 km in diameter), yet less eroded than Lac Bécard and, therefore, at roughly 400-450 Ma (Grieve and Robertson, 1987) appears to be a distinctly younger feature. A number of rather distinct craters with ages to 600 Ma have been identified in shield areas of the world (Grieve and Robertson, 1987), and retention of deep-seated crater remnants for much longer periods in stable cratons with low erosion rates seems probable. A major west-northwest-striking dyke crossing the south-centre of Lac Bécard is not disrupted (Fig. 3), so it must postdate the structure. A minimum age for the feature – impact structure or otherwise – therefore awaits paleomagnetic and geochronological dating of samples collected from the dyke in 1991, but it is almost certainly Proterozoic like most of the other dykes of Ungava (K. Buchan, pers. comm., 1991).

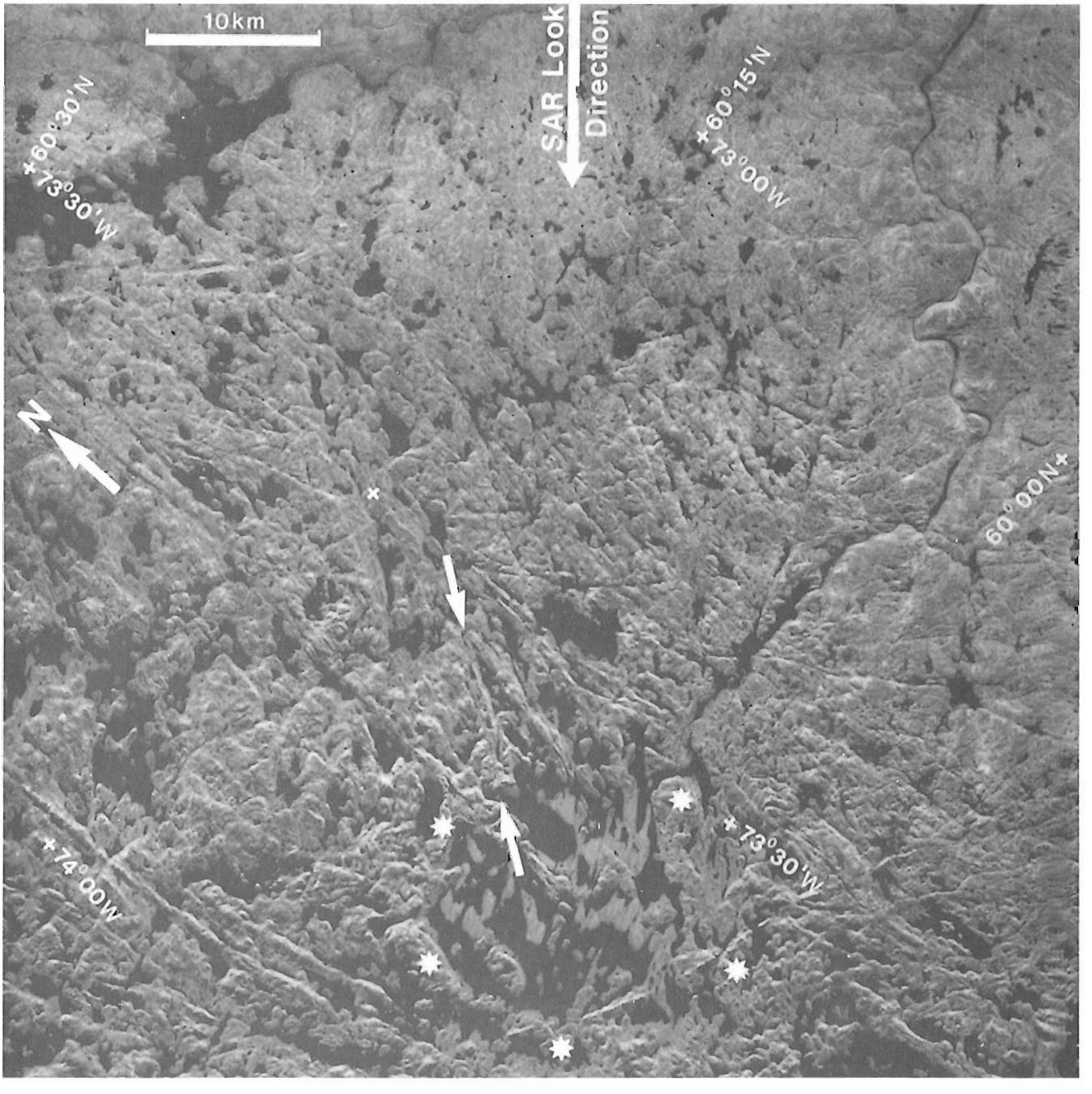


**Figure 3.** Synthetic aperture radar image of the region surrounding the surface rupture. The topography was illuminated from the top (northeast) of the image. The ends of the rupture are marked by white arrows. A circle of white stars lies just outside the circular topographic feature that contains much of Lac Bécard. A prominent dyke passes obliquely across the southern part of the feature.

If Lac Bécard is an ancient impact feature, at a diameter of 15 km its islands and peninsulas would be the remnants of a deeply eroded central uplift where evidence of shock deformation could be retained. Such evidence has been detected down to depths exceeding 1 km in the central uplift of the 22-km-diameter East Clearwater Lake crater (P.B. Robertson, unpub. data, 1983), and these weak levels of shock metamorphism are also preserved in very old impact structures (1800 Ma; Grieve and Robertson, 1987). Circumstances prevented the 1991 field party from sampling near the centre of the circular feature, however, and thin section examination of samples collected from two localities near its northern margin (Fig. 1) revealed no evidence of shock metamorphism. This negative observation does not exclude an impact origin, however, since definitive shock features are not developed beyond roughly half the radius from the crater centre, due to rapid shock wave attenuation (Robertson, 1975).

## FIELD INVESTIGATIONS OF THE BEDROCK GEOLOGY

For most of its length, the surface rupture follows a 200-metre-wide valley between north-northeast-trending ridges of paragneiss. From south to north the valley is occupied by an arm of Lac Bécard, contains the northwestern two-thirds of Lac Turquoise, forms the western shore of Lac Sorcier, and contains three small ponds at the north end. The paragneisses consist of a medium grained schistose paleosome (70-90%) of biotite – plagioclase – quartz ± garnet ± cordierite and concordant veins of coarse grained biotite ± garnet granitic leucosome (10-30%) on a scale of centimetres to metres. Quartz-rich layers occur locally within the paleosome. Foliation and leucosome layering in ridges both east and west of the rupture strike northeasterly (010-075°) and dip moderately to steeply to the southeast (50-75°) (observations are located on Fig. 2). Gentle swings of up to 30° in foliation azimuth occur over 100-metre-scale distances. A prominent joint set is oriented 325/65 NE (Fig. 4).

Bedrock exposure in the intervening valley is limited to a few outcrops near the northern end of the rupture. A few metres to the west of the projected surface rupture is a coarse grained, homogeneous, foliated biotite ± garnet granite with abundant garnet – biotite paragneiss enclaves. The inclusions are oriented parallel to a steeply-dipping, north-northeast-striking fabric defined by biotite alignment and concordant granitic pegmatite veins. K-feldspar is equant in both granite and pegmatite. A few metres east of the projected rupture is an exposure of strongly foliated to gneissic (010/73 SE) granodiorite consisting of a fine grained matrix enclosing augen porphyroclasts of K-feldspar up to 8 mm in size. Textural evidence of brittle deformation was not observed, despite detailed field examination. About 30 m farther east, coarse grained, K-feldspar megacrystic, biotite – magnetite granodiorite probably represents the relatively unstrained equivalent of the augen gneiss just east of the rupture.

Based on the inferred gradient in intensity of ductile deformation fabrics within the eastern granodiorite unit, its juxtaposition with the biotite ± garnet granite to the west probably occurred along a ductile shear zone. The age of faulting is probably late Archean as no subsequent high-temperature orogenic events are recorded from the region. The sense and extent of movement are unconstrained; however, based on the similarity of composition and structural orientations within paragneisses east and west of the fault, major displacement is unlikely.

From our limited observations, the lack of evidence for brittle deformation and iron-stained rock precludes Phanerozoic reactivation of the ductile shear zone as a brittle fault, prior to its movement in 1989. This is despite evidence for extensive Cretaceous faulting, presumably reactivating pre-existing structures, in Hudson Strait and Ungava Bay (Sanford and Grant, 1990), some 250 km to the north.

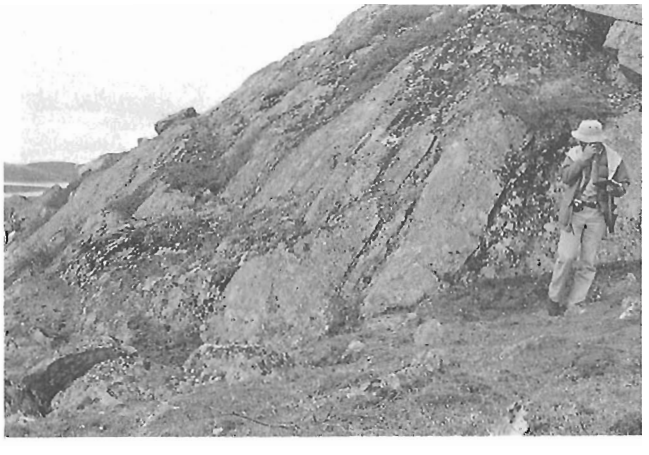

**Figure 4.** Outcrop of paragneiss between Lac Turquoise and Lac Sorcier, dipping into the valley and truncated, behind the geologist, by the prominent 325° joint set.

**Figure 5.** Photograph of a pressure ridge representing the typical surface expression of the Ungava fault rupture. The ridges are evident because of their height, the cracked peat, and especially the clean, light-coloured boulders exposed.

## GEOLOGICAL CONTROL OF THE SURFACE RUPTURE

The rugged terrain with its surface roughness of about 1 m approaching the amount of offset, made direct observation of the sense of movement difficult. In many places the surface trace of the rupture was evident as an uplifted ridge of boulders, distinctive because they were clean and light-coloured (Fig. 5), and not grey and lichen-covered like the undisturbed boulders. The general trend of the rupture was easily seen, and appeared to have geological control at four scales: the $10^4$ m scale, the $10^3$ m scale, the $10^2$ m scale, and the 10 m scale.

### Control at $10^4$ m scale

From the synthetic aperture radar image (Fig. 3), the terrain around the the rupture is characterized by rectilinear structural patterns with scattered small lakes. Linear topographic features, accentuated by aligned lakes or occupied by incised rivers in the eastern half of the image are evident over most of the image. Linear features more than a few kilometres long are spaced less than a kilometre apart. The dominant trends appear to be 000°, 060°, and 100°; northeast to north-northeast trends, parallel to the surface rupture, are by no means absent but are not very common. Curvilinear trends, with the exception of the large basin of Lac Bécard (discussed above), are unusual. They may be indicative of an older structural control, for example resulting from a fold closure within paragneiss units and explaining the A-shaped structure of Lac Sorcier.

### Control at $10^3$ m scale

Geological control at this scale is by the trend of kilometre-long ridges of paragneiss, notably the long ridge extending along the western shores of Lac Sorcier and Lac Turquoise (Fig. 2). Based on the kilometre scale of the ridges, we expect that the structure seen at the surface does extend to the depths of 2 km found for the aftershocks and ≈3 km determined for the mainshock (Adams et al., 1991b).

The surface rupture is associated with the eastern side of the long ridge over 70% of its length. The southern 3 km of the rupture, from the middle of Lac Turquoise south, is complex and splits into three or more branches (Fig. 1). The complexity was not evident during the brief 1990 survey and was not documented in Adams et al. (1991b). It occurs where the long ridge loses its character and may be offset 300 m dextrally, perhaps on a west-northwest-trending fault. This region of the rupture had the greatest aftershock activity during the 1990 seismicity survey, directly reflecting the structural complexity. Averaged foliation and leucosome layering strike northeasterly (010-075°), parallel to the ridge, and dip moderately to steeply to the southeast (50-75°). Adams et al. (1991a) deduced a 70° dip for the rupture plane, based on the lakeshore deformation pattern. Hence, both the surface strike of the rupture and its inferred dip are fully consistent, the rupture being confined to a single layer within the sequence.

### Control at $10^2$ m scale

For most of the distance between Lac Turquoise and Lac Sorcier the rupture lies in the middle of the shallow valley; however, at the southwest corner of Lac Sorcier, the compressional expression of the rupture dies out to the north and compressional deformation appears at the foot of the bedrock ridge 100 m to the west (near letter 'C' on Fig. 2). The motion is transferred by 2 or 3 left-lateral faults that trend 325°. These transfer faults show clear evidence of dominant left-lateral offset, but appear as a shallow groove in the terrain, suggesting a small additional component of extension. The sense of displacement is consistent with our understanding of the slip direction on the rupture (355 ± 15°), which is fairly constant from north to south despite the curvature of the rupture.

The left step occurs at a topographic offset in the flanking bedrock ridge, which also steps to the left 100 m. We infer that bedrock structure, perhaps an ancient fault offsetting the northeast-striking layering, controls both the offset topography and the offset of the rupture.

Two right steps occur on the southern half of the western shore of Lac Sorcier, one north and one south of the large peninsula. In each place, the rupture leaves the foot of the bedrock ridge and trends easterly to the lake shore. As predicted by the overall slip direction on the fault, these surface expressions have a compressional character.

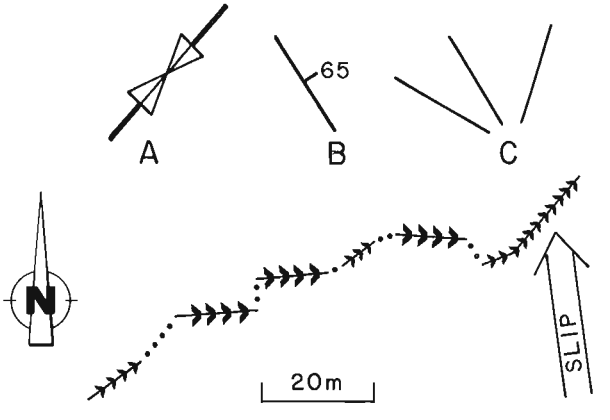


**Figure 6.** Sketch map of pressure ridges just north of the north end of Lac Turquoise (see Fig. 1 for location). Size of chevrons indicates relative height of the ridge. Ridges normal to the inferred slip direction are the highest. Above the sketch map are: A: mean strike and range of foliation in the adjacent bedrock; B: strike and dip of a prominent joint set; and C: strike of bedrock lineaments observed from low level photography.

### Control at 10 m scale

At the 10 m scale, the trend of the rupture was often accommodated by a series of linear ridges arranged in a zig-zag. Thus a rupture with a general trend of 070°, perhaps making a right step in the generally north-northeast-trending rupture, comprised a series of ridges with trends of 060° and 100° (Fig. 6). We interpret these zig-zag ridges, for which there were commonly pairs of ridge orientations intersecting at a high angle, as reflecting near-surface structural control from bedrock layering, joints or foliation, propagated through a thin layer of frozen surficial material. As we remark elsewhere, the general trend of the rupture appears to be controlled by macroscopic layering and foliation; at the detailed level both foliation and fractures (Fig. 6, top) exert control.

## COMPARISON WITH GEOLOGICAL CONTROL OF SURFACE FAULTING IN SWEDEN AND AUSTRALIA

One of us has recently participated in a field review of late-glacial neotectonic fault scarps in northern Sweden (Adams, 1991). These faults are remarkable for their length (up to 120 km), their large single-event throw (typically 3-7 m, but exceptionally 20 m) and the fact that they all occurred in a brief period following the deglaciation of the Fennoscandian Shield (Bäckblom and Stanfors, 1989; Muir Wood, 1989). Although the evidence is not yet complete, it appears that none of the faults has had more than one neotectonic rupture, certainly not in the last $10^4$ a, and perhaps not in the last $10^5$ a. Excavation of the Lansjärv Fault at Molberget showed the postglacial rupture (with slip and length about twice that for Ungava) to have been a single slip event about 9000 a ago on a Proterozoic shear zone. The shear zone is now composed of a 10 m wide, highly crushed zone with intense iron-staining, reflecting hydrothermal alteration and weathering (Eliasson et al., 1991). Observations of bedrock exposures within 2 m of the Ungava rupture at its northern end did not indicate evidence of comparable iron-staining, low grade alteration or cataclastic structures that could have formed during fault reactivation in Phanerozoic times. Instead, only ductile movement is inferred, of presumed Archean age.

Analogies with the Australian surface ruptures – a second suitable analog – are more difficult because the Australian terrain is far more deeply weathered. Bowman et al. (1990) have noted that parts of the 1988 Tennant Creek surface rupture are adjacent to quartz detritus ridges in other places in the Australian outback represent silicified fault zones. Hence, reactivation of an ancient fault is likely. The lack of pre-existing topography across the recent scarps, however, suggests that the fault had not been reactivated for at least 2.5 x $10^4$ a in this region of very slow erosion (Bowman et al., 1990, p. 95).

## CONCLUSIONS

Geological control on the Ungava rupture is evident at all scales, from the regional to the outcrop. The rupture appears to have been controlled by compositional layering and foliation within a steeply-dipping sequence of paragneiss and granite containing concordant ductile high-strain zones. There is no evidence to support the notion that the rupture occurred on a major fault that underwent reactivation in the Phanerozoic. Furthermore, the active structure follows only one of many equally-dominant fault-and-fold trends visible on the regional scale, and we have no insight as to why this particular feature was reactivated. Analogies with Sweden and Australia suggest that in stable continental interiors surface ruptures will follow pre-existing structures, but that the recurrence rate on any single structure is very low. Hence, although the geological controls on the Ungava rupture appear to be well-constrained, it seems unlikely that we will be able to predict which of the many other structures visible on the SAR image will be the locus of the next large earthquake. Therefore, until we identify and study prehistoric ruptures or until future ruptures that might yield further insight occur, the best approach is to compute hazard probabilities based on the random occurrence of Ungava-type earthquakes within the Canadian Shield.

## ACKNOWLEDGMENTS

We thank W.W. Shilts of Terrain Sciences Division, J. Boily and S. McCuaig for assistance in the field, and A. Bent and K. Card for constructive reviews.

## REFERENCES

**Adams, J.**
1991: Field visit to sites of postglacial faulting in Sweden, June 1991; Geophysics Division Internal Report 91-2, 11 p.

**Adams, J., Wetmiller, R.J., Hasegawa, H.S., and Drysdale, J.**
1991a: The first surface faulting from a historical intraplate earthquake in North America; Nature, v. 352, p. 617-619.

**Adams, J., Wetmiller, R.J., Drysdale, J., and Hasegawa, H.S.**
1991b: The first surface rupture from an earthquake in eastern North America; in Current Research, Part C; Geological Survey of Canada, Paper 91-1C, p. 9-15.

**Bäckblom, G. and Stanfors, R. (ed.)**
1989: Interdisciplinary study of post-glacial faulting in the Lansjärv area northern Sweden 1986-1988; Svensk Kärnbränslehantering (SKB), Stockholm, Sweden, Technical Report 89-31, 179 p.

**Bowman, J.R., Gibson, G., and Jones, T.**
1990: Aftershocks of the 1988 January 22 Tennant Creek, Australia intraplate earthquakes; evidence for a complex thrust-fault geometry; Geophysical Journal International, v. 100, p. 87-97.

**Card, K.D. and Ciesielski, A.**
1986: Subdivisions of the Superior Province of the Canadian Shield; Geoscience Canada, v. 13, p. 5-13.

**Eliasson, T., Smellie, J., and Tullborg, E-L.**
1991: Mineralogical studies of the "post-glacial" fault exposed at Molberget, Lansjärv area, northern Sweden; Svensk Kärnbränslehantering (SKB), Stockholm, Sweden, Technical Report 91-14, 21 p.

**Grieve, R.A.F. and Robertson, P.B.**
1987: Terrestrial impact structures; Geological Survey of Canada, Map 1658A, scale 1:63 000 000.

**Johnston, A.C. and Bullard, T.**
1990: The Ungava, Quebec, earthquake: Eastern North America's first modern surface rupture; Seismological Research Letters, v. 61, p. 152-153.

**Muir Wood, R.**
1989: Extraordinary deglacial reverse faulting in northern Fennoscandia; in Earthquakes at North Atlantic Passive Margins: Neotectonics and Postglacial Rebound, (ed.) S. Gregersen and P.W. Basham; Kluwer Academic Publishers, Dordrecht, p. 141-173.

**Percival, J.A., Card, K.D., Stern, R.A., and Bégin, N.J.**
1990: A geological transect of northeastern Superior Province, Ungava Peninsula, Quebec: the Lake Minto area; in Current Research, Part C; Geological Survey of Canada, Paper 90-1C, p. 133-141.

**Robertson, P.B.**
1975: Zones of shock metamorphism at the Charlevoix impact structure, Quebec; Bulletin of the Geological Society of America, v. 86, p. 1630-1638.

**Sanford, B.V. and Grant, A.C.**
1990: New findings relating to the stratigraphy and structure of the Hudson Platform; in Current Research, Part D; Geological Survey of Canada, Paper 90-1D, p. 17-30.

**Stevenson, I.M.**
1968: A geological reconnaissance of Leaf River map-area, new Quebec and Northwest Territories; Geological Survey of Canada, Memoir 356, 112 p.

Geological Survey of Canada Project 860046

# Geology of the Henik, Montgomery Lake, and Hurwitz groups in the Bray-Montgomery-Ameto lakes area, southern District of Keewatin, Northwest Territories[1]

**Lawrence B. Aspler[2], Terry L. Bursey[3], and A.N. LeCheminant[4]**

*Aspler, L.B., Bursey, T.L., and LeCheminant, A.N., 1992: Geology of the Henik, Montgomery Lake, and Hurwitz groups in the Bray-Montgomery-Ameto lakes area, southern District of Keewatin, Northwest Territories; in Current Research, Part C, Geological Survey of Canada, Paper 92-1C, p. 157-170.*

***Abstract***

*The Henik Group (Archean) consists of (ascending order): felsic volcaniclastic and siliciclastic rocks; magnetite-chert BIF; a mafic volcanic/gabbro complex; and turbidites. Montgomery Group siliciclastic rocks mantle tilted Henik Group, and record a westward-draining fluvial plain. An angular unconformity separates the Montgomery and Hurwitz groups; rocks formerly considered "Montgomery Group" in the northeast are reassigned to the basal Hurwitz Group. The Hurwitz Group was deposited in an intracratonic basin unrelated to Trans-Hudson orogen. Terrestrial to marine onlap (Padlei and Kinga formations) signifies progressive basin broadening. Immature siliciclastic rocks (Ameto Formation) represent drowning of the Kinga shelf. The basin narrowed and deepened during uplift along a northeast-trending arch between Bates and Griffin lakes (Ameto to Tavani formations offlap away from arch). Proterozoic north- and northwest-vergent thrusts and northwest-trending oblique-slip faults cut Archean structures and structures in the Montgomery Group. Gossans with elevated gold were mapped in all three groups.*

***Résumé***

*Le Groupe de Henik (Archéen) est composé (par ordre ascendant) : de roches volcanoclastiques et silicoclastiques felsiques; d'une formation ferrifère rubanée à magnétite et chert; d'un complexe de roches volcaniques et gabbro mafiques; et de turbidites. Les roches slilicoclastiques du groupe de Montgomery recouvrent le groupe de Henik incliné et témoignent de la présence antérieure d'une plaine fluviale se drainant à l'ouest. Une discordance angulaire sépare les groupes de Montgomery et de Hurwitz; les roches autrefois considérées comme faisant partie du «groupe de Montgomery» dans le nord-est ont été redésignées comme appartenant à la partie basale du groupe de Hurwitz. La sédimentation du groupe de Hurwitz a eu lieu dans un bassin intracratonique n'ayant pas de liens avec l'orogène transhudsonien. Le biseau d'aggradation, dont la nature varie de terrestre à marine (formations de Padlei et de Kinga), indique un élargissement progressif du bassin. Les roches silicoclastiques immatures (formation d'Ameto) représentent l'inondation de la plate-forme de Kinga. Le bassin a rétréci et s'est approfondi durant le soulèvement qui s'est produit le long d'une arche à direction nord-est entre les lacs Bates et Griffin (recouvrement en retrait des formations d'Ameto à Tavani en s'éloignant de l'arche). Les chevauchements protérozoïques à vergence nord et nord-ouest et les failles d'effrondrement obliques à direction nord-ouest recoupent les structures archéennes et les structures du groupe de Montgomery. Des chapeaux ferrugineux à haute teneur en or ont été cartographiés dans les trois groupes.*

[1] Contribution to the Canada-Northwest Territories Economic Development Agreement Minerals Initiative 1991-96

[2] 23 Newton Street, Ottawa, K1S 2S6

[3] Department of Earth Sciences, Carleton University, Ottawa K1S 5B6

[4] Continental Geoscience Division

## INTRODUCTION

Although Archean and Proterozoic supracrustal rocks in the southern District of Keewatin have long been the focus of gold and base metal exploration, mapping over much of the region has remained at a reconnaissance-level. This report presents preliminary results of 1:50 000 scale mapping carried out in the Bray-Montgomery-Ameto lakes area during the first field season of a Canada-NWT Minerals Initiative project. Three unconformity-bounded supracrustal packages are exposed: the Henik Group (Archean, part of the Ennadai-Rankin greenstone belt), the Montgomery Lake Group (age uncertain), and the Hurwitz Group (Early Proterozoic). Principal goals of the study are to: 1) establish the local stratigraphy of the Henik Group; 2) define the boundary relationships, stratigraphy, and depositional significance of the Montgomery Lake Group and, in particular, address the controversy regarding the nature of the Montgomery Lake Group-Hurwitz Group transition; 3) refine the stratigraphic and facies relationships of the Hurwitz Group in order to establish the original configuration, subsidence mechanisms, and tectonic significance of Hurwitz Basin; 4) undertake structural analysis, emphasizing the degree to which Proterozoic strain has affected Archean rocks and the degree to which Archean structures have controlled Proterozoic sedimentation and deformation; and 5) map and sample gossans, to help determine the geological setting of mineral occurrences and define exploration targets. The maps presented herein are also available at 1:50 000 scale (Aspler, 1991).

## STRATIGRAPHY AND SEDIMENTOLOGY

Descriptions and preliminary interpretations of the map units are summarized in Table 1; stratigraphic relationships are emphasized below.

### *Henik Group*

Low metamorphic grade, low strain, and good outcrop in the Montgomery Lake area permit resolution of the local Archean stratigraphy. Units A1 to A4 are within the type area of the Henik Group (Eade, 1974), near the middle of the Ennadai-Rankin greenstone belt (Fig. 1). The Henik Group is assumed to be Archean on the basis of U-Pb zircon ages to the northeast: Tavani (2630 Ma, Tella et al., 1991); Kaminak Lake (2697 ± 14, 2692 ±1 Ma, Mortensen and Thorpe, 1987; 2681 ±3 Ma, Patterson and Heaman, 1990); and to the southwest: Saskatchewan (2682 ± 5.9 Ma, Chiarenzelli and Macdonald, 1986; 2708 +3/-2 Ma, Delaney et al., 1990).

At Montgomery Lake, the Henik Group forms a northeast-dipping homocline; younging data are predominantly tops-northeast and evidence for thrust repetition is lacking. A minimum thickness of 11 km is indicated. Despite this, metamorphism is at or below biotite-grade. The base of the Henik Group is not exposed in the map area; it is not known if units A1 to A4 were deposited directly on older gneissic basement (e.g. Loveridge et al., 1988) or if they represent parts of a thicker volcano-sedimentary pile.

### *Montgomery Lake Group*

The principal exposures of the Montgomery Lake Group (Eade, 1974) are in a northeast-trending outlier, eastern Montgomery Lake, and in a discontinuous belt to the north (Fig. 1). An angular unconformity at the base of the group is inferred because: 1) Henik Group stratigraphy is continuous on either side of the outlier but is truncated at both northwest and southeast contacts, where moderately northeast-dipping Henik Group is overlain by gently south- and west-dipping Montgomery Lake Group; and 2) the east-northeast-trending Henik Group stratigraphy north of Montgomery Lake is truncated by the east-trending belt of Montgomery Lake Group rocks. Clasts in basal Montgomery Lake Group reflect adjacent basement rock types (e.g. Fig. 3).

Cross beds from the entire Montgomery Lake Group indicate west, south-southwest, and north-northwest paleoflow (Fig. 1). A tentative depositional model is that of a low-relief sub-Montgomery paleotopography with local fluvial channels (implied by the limited thickness and distribution of basal conglomerate) that drained westward across a fluvial plain (M3 sandstone) with local paleoridges (M1b breccia) and ponds (M2 sandstone/ siltstone).

### *The Montgomery Lake Group-Hurwitz Group transition*

Contact relationships between the Montgomery Lake Group and the Hurwitz Group have been controversial. Bell (1970a, b), Eade (1974), and Wanless and Eade (1975a, b) considered that an unconformity separated the two units, whereas Young (1973, 1975) argued for a conformable transition. Our mapping suggests an angular unconformity is present at Montgomery Lake, and immediately west of the abandoned settlement of Padlei. However, in the Noomut River area, units previously mapped as "Montgomery Lake Group" (Bell, 1970b) are conformable with the overlying section, and we consider these units basal Maguse Member, Hurwitz Group (see also Heywood and Roscoe, 1967; cf. Roscoe, 1981).

Interpretation of an unconformity at Montgomery Lake is based on: 1) outcrops northeast of the lake, where south-striking bedding and carbonate veins in Montgomery Lake Group sandstones are truncated by east-striking breccias containing clasts of subjacent Montgomery Group (Fig. 4); and 2) map relationships in which Montgomery Lake Group outliers are oblique to, and appear to be truncated by, the Hurwitz Group (Fig. 1). West of Padlei, quartz-rich sandstones that are probably Montgomery Lake Group are cut by centimetre- to decimetre-scale quartz veins that form a breccia-stockwork system (30-50% quartz veins). These sandstones are overlain by Padlei Formation polymictic conglomerates that lack such quartz veins. Although the contact between the two units is not exposed, these observations are consistent with Bell's (1970b) suggestion of a Montgomery Lake Group-Hurwitz Group unconformity in this, the Padlei Formation type area.

In the Noomut River area (Fig. 2) rocks originally mapped as "Montgomery Lake Group" differ markedly from type-area Montgomery Lake Group, and are lithologically similar to, or indistinguishable from, rocks of the Maguse Member. At the measured section north of Noomut River (Fig. 2), a 100 m covered interval separates Henik Group iron-formation-bearing sandstone to mudstone turbidites and felsic tuffs from grey, green, and red subarkoses with decimetre- to metre-scale quartz pebble conglomerate layers. The conglomerates contain pyrite, and are historical gold-uranium targets (Bell, 1970b). They differ from "type" Maguse conglomerates only in having a greater proportion of quartz clasts. Sandstones interbedded with the conglomerates differ from typical Maguse sandstones only in being slightly less mature. Furthermore, above the 135 m level, conglomerates disappear and the compositional maturity of the sandstones increase such that they are indistinguishable from Maguse sandstones. In contrast, quartz pebble conglomerates are not known from the Montgomery Lake Group in the type area, and the Montgomery sandstones contain ubiquitous disseminated pyrite and lack redbeds. At about the 350 m level is a 25 m thick unit of mudstone with layers and lenticles of subarkose to quartz arenite (Fig. 2; unit HKm4). Bell (1970b) mapped this interval as part of the Padlei Formation, separating the "Montgomery Lake Group" from the Maguse Member. However, it lacks the varve-like rhythmite character typical of the Padlei Formation, and the sandstones below, above, and interbedded with, the mudstones are indistinguishable from Maguse Member rocks. Hence we interpret this interval as a locally-developed facies within the Maguse Member, similar to rocks near the Maguse-Whiterock Member transition east of Bray Lake (Table 1, unit HKm5p).

Pebbly beds above the unconformity east of the measured section contain a more diverse clast suite than the quartz pebble conglomerates (unit HKm1; Table 1). Yet interbedded sandstones are identical to those interbedded with the quartz pebble conglomerate (and are commonly red), and the unit grades upsection to sandstones with quartz pebble beds. Hence we conclude that this unit (and the lithologically identical lens above the unconformity on the northwest side of the map area; Fig. 2) are a less mature basal facies of the Maguse Member.

Mapping in the remainder of the Padlei belt to the northeast (planned for 1992) and an M.Sc. thesis study (Bursey, Carleton University) will further examine the regional distribution of the Montgomery Lake Group.

### *Hurwitz Group*

Conglomerate and sandstone of the Padlei Formation are distributed as discontinuous lenses that are interpreted as paleovalley deposits (Young and Mclennan, 1981; Aspler and Bursey, 1990). The upper contact of the Padlei Formation is conformable with the Maguse Member: polymictic conglomerates and arkoses grade over an interval of less than 10 m to quartz-jasper-chert pebble conglomerates. Where the Maguse Member is overlapped by the Whiterock Member, the upper contact of the Padlei Formation is also conformable, with interbeds of white quartz arenite appearing at the very top of the Padlei Formation section.

Bell (1970a, b) recognized that rocks of the Maguse Member make up a map unit distinct from the remainder of the Kinga Formation. The Maguse Member provides a useful marker in mapping Hurwitz Group structure; we have traced a 320-400 m section west to Bray Lake (cf. Eade, 1974). Farther west the unit pinches out beneath the Whiterock Member (Fig. 1) or appears as local slivers conformably overlain by the Whiterock Member (Aspler and Bursey, 1990). Typically, metre-scale interbeds of Whiterock-like quartz arenite are in the upper 20 m of the unit, but south of Bray Lake, the transition is marked by 25 m of probable eolianites (Fig. 5) and 34 m of interbedded subarkose and pelite (Table 1, units HKm5e, HKm5p).

The Whiterock Member is a regionally persistent marker (the "backbone" of the Hurwitz Group, Bell, 1970a), that extends from Rankin Inlet (Tella et al., 1986) to Windy River (Aspler et al., 1989). It is remarkably homogeneous, consisting of supermature quartz arenite exclusively. Also remarkable is the abundance of wave ripple marks in the upper 200 m (spaced at decimetre-scale stratigraphic intervals). Trends of symmetric and asymmetric ripples in the Bray Lake area are northwest-southeast; asymmetric ripples indicate both northeast and southwest (onshore-offshore?) paleoflow (Fig. 1). On a regional level, ripple trends are predominantly northeast-southwest (Bell, 1970a; Eade, 1974; Tella et al., 1986); departure from the regional trend in the Bray Lake area may reflect an embayment in the paleoshoreline.

The upper contact of the Whiterock Member is abrupt; bedded cherts of the Hawk Hill Member, previously interpreted as unconformity-related silcretes, are re-interpreted as conformable sinter deposits (see Aspler,1990, in press). New exposures of the Hawk Hill Member were mapped southeast of Bray Lake, northwest of Montgomery Lake, and northeast of Ameto Lake. Southeast of Bray Lake, steeply dipping centimetre- to metre-scale breccia zones cut gently dipping uppermost Whiterock Member quartz arenites. The breccias consist of Whiterock Member clasts and rare concentrically coated chert clasts in an iron oxide-rich maroon chert matrix identical to the conformably layered chert. Wall rock to breccia zone transitions include: 1) in situ wall rock with maroon chert-filled hairline fractures; 2) breccia with jig-saw fit to host rock; 3) imbricated tabular slabs of wall rock in maroon chert; and 4) subrounded to rounded wall rock floating in maroon chert. The discordant breccias are interpreted to mark feeder pipes that channeled waters to the surface. They likely formed through a process of repeated hydraulic fracturing; fluidized ascending waters caused clast-clast attrition and rounding (pseudoconglomerates of Paris et al., 1985). The upper contact of the Hawk Hill Member is abrupt but conformable, with the lowermost few metres of Ameto Formation slates bearing a hematitic quartz cement.

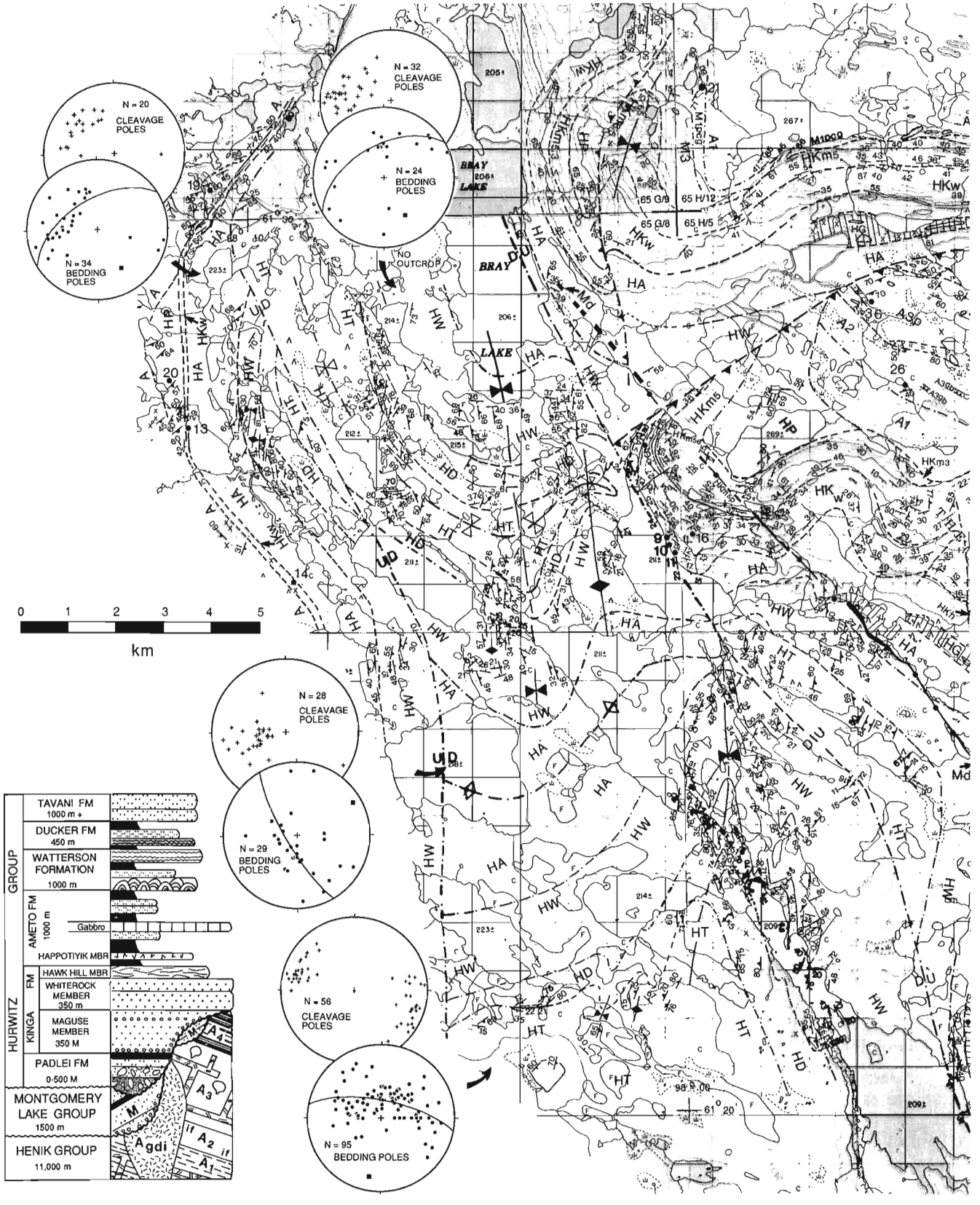


**Figure 1.** Geological map, Bray-Montgomery Lake area. Map units as in Table 1. Stereonets are equal angle, lower hemisphere projections (square denotes pole to cylindrical best-fit great circle).

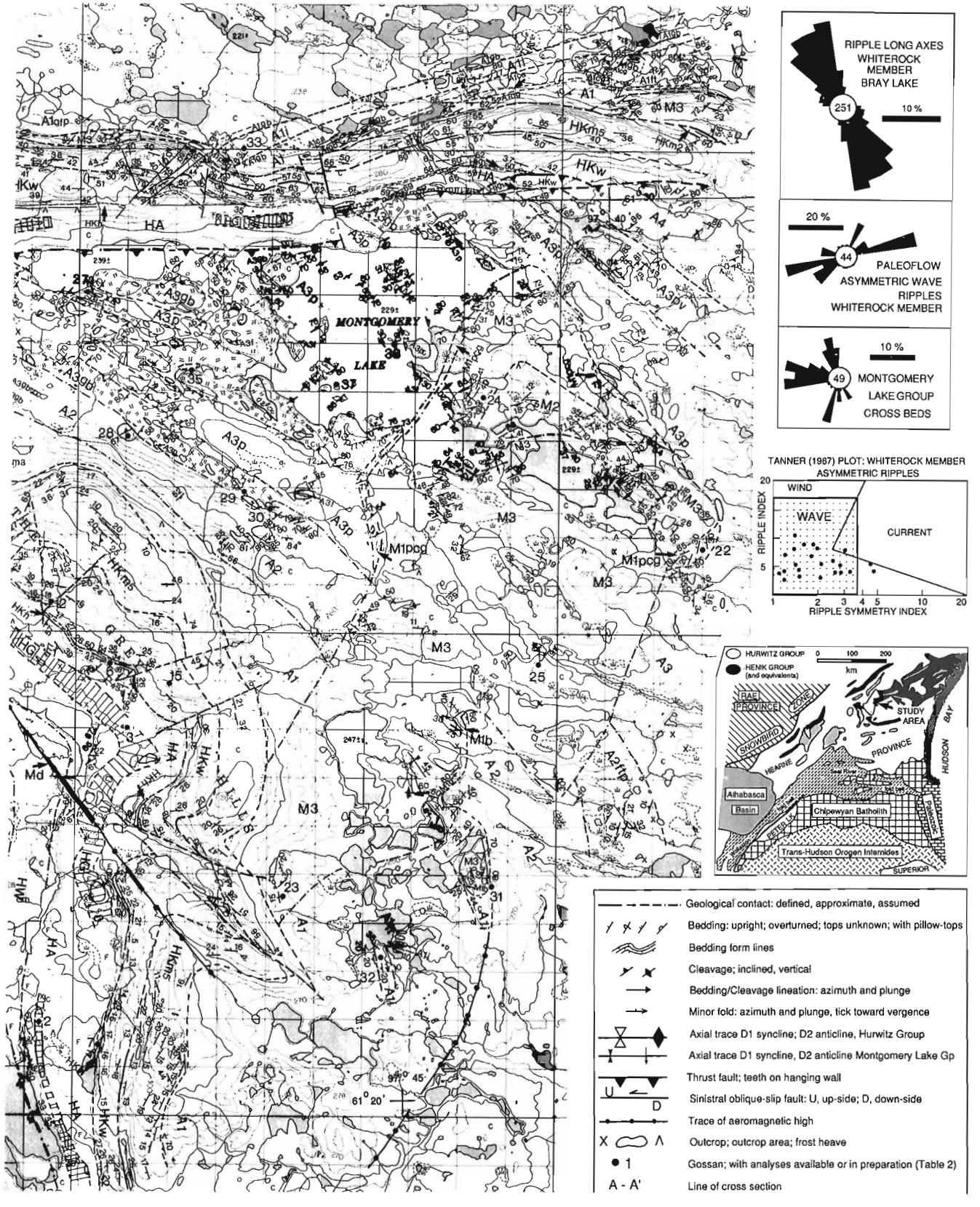


**Figure 1** (cont.)

**Table 1**. Description and preliminary interpretation of map units, Bray-Montgomery and northeastern Ameto (Noomut River) lakes area.

| UNIT | | | | DESCRIPTION | COMMENT/INTERPRETATION |
|---|---|---|---|---|---|
| Mackenzie Diabase | | | | Coarse-grained, non-foliated, unmetamorphosed, northwest-trending | 1267+/- 2 ma baddeleyite: LeCheminant & Heaman, 1989 |
| HURWITZ GROUP | GABBRO HG | | | Discontinuous gabbro sills emplaced at different levels within Ameto Fm. Green weathering, coarse-grained, poikilitic. Locally well-foliated; chloritic shear zones common. Local fine-grained sills (with chilled margins) within coarse-grained sills | Post Ducker Fm, pre-Hurwitz Gp folding. 2094 baddeleyite (Patterson and Heaman, 1990). Relationship to Tavani Fm and to Happotiyik Member uncertain (Aspler & Bursey 1990). |
| | TAVANI FM HT | | | Tan and grey weathering subarkose, local parallel and cross-stratified heavy mineral bands; rare interbeds of green shale and mudchip breccia. | Shallow subaqueous to subaerial coastal plain. |
| | DUCKER FM HD | | | Discontinuous unit with cm to dm-scale fining-upward cycles of grey and tan arkose to blue argillite; discrete beds of arkose with parallel-stratification. Dm-m-scale interbeds of orange cryptalgal laminate at base. Developed only west of Bray Lake; to east Tavani Fm directly overlies Watterson Fm. | Local lagoons between Tavani coastal plain and Watterson carbonate ramp. Below wave-base mass flows alternating with arkose sheetfloods and algal mounds. |
| | WATTERSON FM HW | | | Siliciclastic-free intervals of rose, flesh and orange stromatolitic and cryptalgal dolostone; local intraclastic breccia. Stromatolites close, laterally-linked, bulbous to nodular hemispheroids. Mixed carbonate and siliciclastic intervals of grey arkose with angular carbonate intraclasts grading to orange cryptalgal laminate; arkose to slate fining-upward sequences interbedded with orange cryptalgal laminate. | Intertidal to supratidal stromatolite ramp; tidal channel breccias; Punctuated (storm?) and facies mixing of arkose (see Mount, 1984); below wave base mass flows alternating with shallow subtidal to intertidal carbonate flats. |
| | AMETO FM HA | | | At base: red, blue, green slate with mm-cm-scale parallel-stratified arkose. Up-section: cm-dm-scale arkose to slate fining-upward cycles. At top: 0.1-2m cryptalgal laminates. Fine-grained, locally feldspar-phyric, 20 m thick, concordant mafic unit 80 m above base at Ameto type section. | Below wave-base sedimentation interrupted by turbidity currents; shoaling-upward to Watterson carbonate ramp. Mafic unit possibly volcanic (Happotiyik Member, Bell ,1970 b) or sill (Eade, 1974). |
| | KINGA FORMATION | Hawk Hill Mbr HKh | | Discontinuous unit of bedded white chert, maroon chert and chert breccia conformable between the Whiterock Mbr and Ameto Fm. Discordant hematitic breccias at top of Whiterock Mbr | Previously considered silcretes; re-interpreted as sinters formed by surface discharge of hot springs (Aspler, 1990 in press). |
| | | Whiterock Mbr HKw | | Fine-coarse-grained supermature quartz arenite. Lower part of section commonly massive; upper 200 m with ubiquitous symmetric and asymmetric wave ripples: tuning-fork bifurcations; straight crest-lines; within wave field on ripple index/ripple symmetry index plot (Fig. 1). Common interference ripples. Locally crests flattened or rounded due to emergence. Local parallel stratification. | Wave-dominated shallow marine; locally near-emergent. Transgressive reworking of underlying units. |
| | | Maguse Member HKm | HKm 5 | Maroon, pink, grey subarkose to quartz arenite; interbeds of white quartz arenite at top. Local black parallel and cross-stratified heavy mineral bands. Near top of section south of Bray Lake **HKm5e**: 25 m of large-scale (3-8m) high-angle cross beds with asymptotic toes, multiple bounding surfaces, adhesion structures (Fig. 5) overlain by **HKm5p:** 34m of interbedded m-scale coarse subarkose (+/- mud partings; mudchip breccia) and dm-m intervals with cm-scale graded subarkose to slate | Fluvial/eolian plain. South of Bray Lake: coastal eolian complex with superposed lower portions of north and NE-migrating barchan dunes; ephemeral ponds. |
| | | | HKm 4 | 25 m thick discontinuous unit at transition between HKm3 and HKm5 in Ameto Lake area. Dm-m-scale pink, grey subarkose to quartz arenite with local mudcurls and mudchips, rare interference ripples; interbedded with dm-m-scale mudstone with 10-50% cm-scale, non-graded subarkose to quartz arenite lenses. | Ephemeral pond within fluvial/eolian plain. Previously mapped as Padlei Fm (Bell, 1970 b; see text). |
| | | | HKm 3 | Subarkose to quartz arenite with discontinuous dm-m-scale interbeds of framework-intact conglomerate. Very well rounded, spherical white quartz, jasper, blue and grey chert in coarse-grained subarkose to quartz arenite matrix (primarily at base). In Ameto Lk area: grey subarkose with red-green variegation; pebble beds almost entirely quartz. | Pebble lags from intensive fluvial/eolian reworking. In the Ameto Lake area, previously mapped as Montgomery Group (Bell, 1970 b,see text). Only locally mappable as separate unit. |
| | | | HKm 2 | Breccia (3 m thick) with self-supporting clasts (to 1 m) of Montgomery Gp sandstone (Fig. 4) with rare rounded mafic volcanic, carbonate, and granitic pebbles; above *in situ* Montgomery Gp NE of Montgomery Lake (UTM 65H/12; 730204). Carbonate veins in Montgomery Gp truncated at contact. Overlain by 10 m of pebbly sandstone with rounded sandstone, milky quartz, jasper and mafic volcanic clasts. | Talus breccia above unconformity with Montgomery Gp. Minor contribution from nearby Henik Gp. Evidence of sub-Maguse chemical paleosol is lacking. Abrupt transition to HKm 3 from reworking of breccia. |
| | | | HKm 1 | Pebbly sandstone and grit with clasts of rhyolite,granite, milky quartz, chert, interbedded with grey, green and red arkose at unconformity with Henik Gp rhyolite agglomerate NW Noomut R. (UTM 65H/11; 028445). One metre zone of hematite-altered agglomerate at contact. Pebbly sandstone with clasts of felsic tuff, milky quartz, chert, granite, interbedded with grey, green and red sandstone at unconformity with Henik Gp well-foliated crystal tuff SE Noomut R. (UTM 65H/10; 093393). | Probably fluvial; incipient sub-Maguse hematitic paleosol or non- paleosol alteration zone along unconformity. On west, previously mapped as Padlei Fm (?); on east previously mapped as Montgomery Group (Bell, 1970b; see text). |
| | PADLEI FM HP | | | Lenses of massive and stratified cobble-boulder polymictic conglomerate; rare coarse sandstone interbeds. Framework-intact to disrupted; both mixtite and coarse sandstone matrix. Clasts well-rounded: granitic; felsic and mafic volcanic; quartz; jasper; BIF. Upsection: interbedded pebbly mixtite and well-sorted stratified grits; mm-cm-scale very fine sandstone, siltstone, mudstone rhythmites with local micro cross-lamination, graded bedding, coarse sand lonestones (with rucking structures) and pebble lonestones (Plate 1 D in Young, 1973). At unconformity with Henik Gp in Ameto Lk area (UTM 65H/15; 099495; originally discovered by Bell, 1970 b): sharp contact between Henik Gp rhyolite, rhyolite agglomerate and cobble-boulder conglomerate with very well rounded granodiorite and rhyolite clasts. | Both mass flow (mixtite matrix-supported conglomerate) and fluvial (clast-supported, sand matrix conglomerate; stratified sandstone). Rhythmites probably lacustrine; lonestones probably ice-transported. Glacigenic (Bell 1970a; Young 1973; 1988; Young and McLennan, 1981) or alluvial fan-lacustrine (cold climate). |

**Table 1** (cont.)

| GP | | | | |
|---|---|---|---|---|
| MONTGOMERY | M3 | Sandstone | Thinly-bedded, light grey to tan subarkose, common cross-stratification; heavy mineral bands; local chaotic soft sediment folds. Predominantly westward paleocurrents (Fig. 1). Ubiquitous disseminated pyrite. | Fluvial plain on low-relief sub-Montgomery topography. |
| | M2 | Sandstone - Siltstone | Lens of interbedded grey subarkose, dark grey very fine sandstone (with local ripples, mudcurls, mudchips) and cm-layers of black mudstone (with local flame structures; ball and pillow structures). Cm-scale disseminated euhedral pyrite. | Local ponds within fluvial plain. |
| | M1 | M1 pcg Polymictic Conglomerate | Polymictic, granule to boulder (to 1.2m) conglomerate. 50-80% clasts of angular and tabular-shaped mafic volcanic and subrounded to rounded granite, quartz, jasper, chert and sandstone in coarse arkose matrix. Local dm-m-scale pebbly arkose interbeds. Two 15 m wide, 2 m deep channels (paleoflow to west) on easternmost exposure. Ubiquitous disseminated pyrite. Unique exposure east of Bray Lk with pebbles-cobbles of pyrite and pyrite-quartz mixed with volcanic and granitic clasts. (UTM 65H/12 537212). | Fluvial channel deposits from local streams that drained sub-Montgomery paleotopography. |
| | | M1 b Breccia | Massive, framework-intact breccia of BIF clasts (to 1 m) in coarse sandstone matrix; at base of section, breccias in contact with *in situ* BIF. Internal breccia zones, quartz veins are truncated at sharp clast boundaries (Fig. 3). | Talus breccia rimming BIF paleoridge in sub-Montgomery topography. |
| HENIK | Agdi | Granodiorite | Well-foliated granodiorite (2512+/- 112 ma; Rb/Sr whole rock; Wanless and Eade, 1975) | Intrusive into Henik Gp (Eade, 1974). |
| | GROUP A4 | Turbidite | Dm-m scale fining-upward sequences; sharp-based, graded sandstone to mudstone, local ripple-drift cross stratification. | Below wave base mass flows. |
| | A3 | Pillow Volcanic Gabbro sill/dyke Complex | **A3p**: fine-grained mafic volcanic with well-developed pillows (to 1m diameter); local pillow shelves; budding structures; flow-top breccia; rare interflow slate. Stratigraphic position of mafic rocks west of Bray Lake is unknown. **A3pv**: with variolitic flows. Cut by **A3gb** : up to 200 m wide gabbro sills and dykes and **A3t**: 2 to 20 m wide fine-medium grained feldspar-hornblende-quartz porphyry dykes. Apparent decrease of gabbro to top of volcanic pile. | Flows and mafic sills are probably co-magmatic. Sulphides common between pillows and along selvages; also at gabbro-flow contacts. |
| | A2 | Magnetite-Chert Banded Iron Formation | Mm-cm-dm scale rhythmites of jasper, grey chert, white chert and black magnetite. Intraformational jig-saw breccia of chert fragments in magnetite-rich matrix; chaotic soft sediment folds. Interbedded with 2-15 m thick quartz-eye micaceous tuffs. At top southwest of Montgomery Lake: discontinuous zone of BIF cut by gabbro; local breccia of BIF xenoliths (to 0.5 m) floating in gabbro matrix. At top southeast of Montgomery Lake: **A2 ftp** : pebbly crystal tuff like A1ftp. | Starved chemical sedimentation undiluted by clastic input except for local felsic pyroclastic (epiclastic?) rocks. Common sulphide-bearing quartz veins. |
| | A1 | Mixed Sedimentary/ Volcanic Assemblage | **A1i**: Dm-scale graded sandstone to mudstone; mm and cm-scale sandstone to magnetite iron formation rhythmites, locally graded. **A1ft**: feldspar-quartz crystal tuff. **A1ftp**: pebbly crystal tuff with 10-20% angular to subrounded felsic clasts in feldspar- quartz crystal matrix. **A1cg**: m-scale interbeds of coarse sandstone and framework-intact granule to cobble conglomerate with subrounded to angular clasts of milky quartz and jasper. **A1ca**: laminated and massive dolostone. **A1mv**: local mafic flows; tuffs. **A1gb**: 1m to 125 m wide medium to coarse gabbro sills, with chill margins. **A1qfp**: medium to coarse feldspar-quartz sills (flows?). **A1r**: feldspar-phyric rhyolite. **A1 ra**: rhyolite agglomerate, with30-80% ameboid-shaped clasts of rhyolite in coarse feldspar-quartz matrix (north of Ameto Lk). | Below wave-base chemical sedimentation between mass flow pulses. Periodically interrupted by felsic pyroclastic and/or epiclastic sedimentation; mafic volcanism. Local emergence and sedimentary reworking. Stratigraphic position of Ar; Ara: unknown. |

The conformable fine grained mafic unit 80 m above the base of the Ameto Formation at the type section (Table 1) was mapped by Bell (1970b) as a flow (Happotiyik Member) and by Eade (1974) as a sill. This feldspar-phyric unit differs markedly from typical Hurwitz gabbro, but features diagnostic of either interpretation are lacking.

The Ameto Formation grades conformably upsection to the Watterson Formation, with the appearance of 0.1-2 m scale interbeds of cryptalgal laminates in uppermost Ameto Formation slates and arkoses. Three informal map units of the Watterson Formation recognized at Watterson Lake (Eade and Chandler, 1975) and Hawk Hill-Griffin lakes (Aspler and Bursey, 1990) were not distinguishable in the present study area. The upper contact of the Watterson Formation is conformable, as indicated by local cryptalgal laminates interbedded with basal Ducker Formation arkoses and slates. The lateral impersistence of the Ducker Formation is characteristic of the unit (Eade and Chandler, 1975; Aspler and Bursey, 1990). West of the study area, basal units of the Tavani Formation, consisting of arkose with interbeds of cryptalgal laminate and intraformational conglomerate mark a conformable Watterson to Tavani transition (Aspler et al., 1989; Aspler and Bursey, 1990). Farther west, the Tavani Formation is unconformable on basement (Bate Lake, Eade and Chandler, 1975) and to the east, on Pork Peninsula, Bell (1970a) has documented sub-Tavani cover to basement stripping. In the present area, the basal units recognized to the west are not developed and the transition to the Tavani Formation is abrupt. Evidence for a sub-Tavani unconformity is lacking and a conformable contact is assumed.

### *Sedimentation and tectonics*

Interpretation of the tectonic significance of the Henik Group must await further mapping in the Ennadai-Rankin greenstone belt. The Montgomery Lake Group could be Archean and represent a molassoid sequence developed late in the evolution of the greenstone terrane (analogous to the Jackson Lake Formation in the Yellowknife greenstone belt, or the Timiskaming Group in the Abitibi greenstone belt). Alternatively, it could represent an Early Proterozoic precursor to Hurwitz Group sedimentation. The original extent and nature of the Montgomery Lake Group is unknown. As preserved, the unit is predominantly arkose, with only local conglomerates, unlike typical rift deposits. Examination of possible

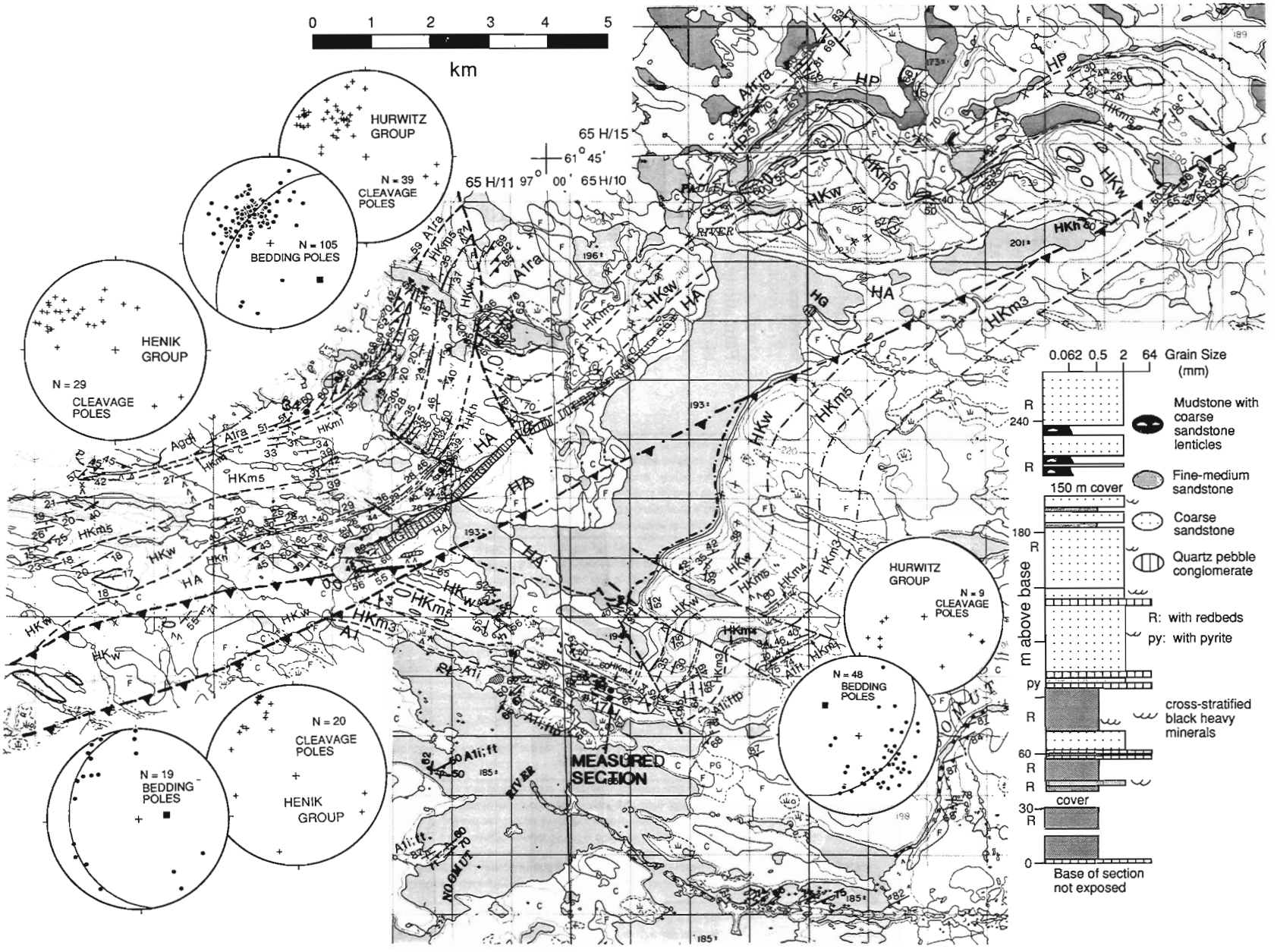


**Figure 2.** Geological map, northeastern Ameto Lake (Noomut River) area. Legend and map units as in Figure 1 and Table1.

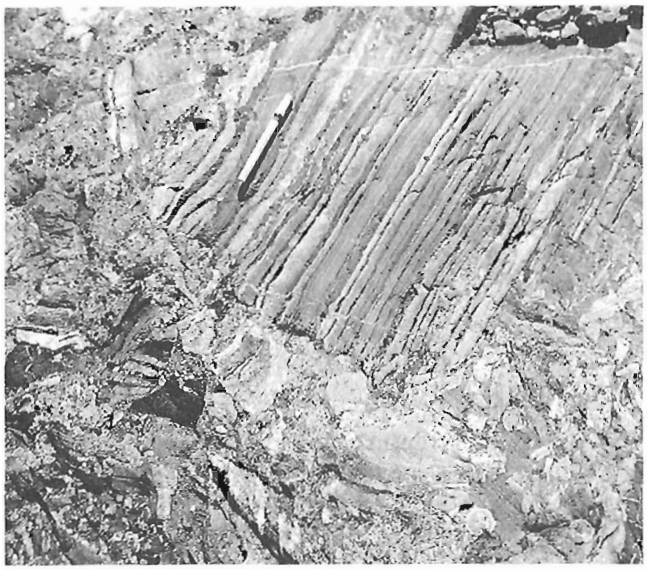

**Figure 3.** Basal Montgomery Lake Group breccia containing BIF clasts, Henik Group-Montgomery Lake Group unconformity (unit M1b).

Montgomery Lake Group clasts in lower Hurwitz Group units and detrital zircon geochronology will address these problems.

Previously, Young (1988) and Aspler et al. (1989) interpreted lower Hurwitz Group stratigraphy in terms of a rift-cratonic basin model, with subsequent cycles of sedimentation attributed to forebulge/foredeep migration caused by ca. 1.91-1.87 Ga collisions in Trans-Hudson orogen. However, stratigraphic arguments (Young, 1975; Aspler and Bursey, 1990) and a preliminary U-Pb age of ca. 2.09 Ga from Hurwitz gabbros (Patterson and Heaman, 1990) indicate that the Hurwitz Group is older than any known collisional event in Trans-Hudson orogen. Furthermore, units above the Kinga Formation do not display the asymmetry demanded of the foredeep model (do not thicken toward the presumed thrust load) and, although thrusting is locally significant the predominant structural style appears to be that of basement-cover infolding.

Characteristics of the Hurwitz Group are more consistent with an intracratonic basin model. Accordingly, basin initiation was by regional subsidence of a moderate relief topography, preserving Padlei Formation valley fills, rather than by rifting. Broadening of the basin by continued subsidence is recorded by progressive onlap of lower Hurwitz Group units in a terrestrial to marine transition (Padlei Formation to Whiterock Member). The progressive increase in textural and compositional maturity upsection denotes transgressive reworking. Symmetric thickness variation (Bell, 1970a; Aspler, 1990, in press) and absence of rocks that could represent a shelf-slope-rise sequence argue against a passive margin setting. Although most modern geothermal areas form near active plate boundaries and are associated with magmatic processes, scope exists for the generation of hot spring deposits (Hawk Hill Member) in intracratonic basins without concurrent magmatism (e.g. Cull and Conley, 1983; Bethke, 1986).

The end of sinter deposition and the abrupt appearance of immature siliciclastic debris are attributed to drowning of the Kinga shelf concurrent with uplift along a northeast-trending arch between Bate and Griffin lakes (Aspler, 1990, in press). The basin narrowed and deepened in an offlap sequence prograding away from the arch. Accordingly, Ameto

**Figure 4.** Basal Maguse Member breccia containing Montgomery Lake Group clasts; Montgomery Lake Group-Hurwitz Group unconformity (unit HKm2).

**Figure 5.** Large-scale high-angle crossbeds near top of Maguse Member south of Bray Lake (unit HKme).

Formation pelites represent a distal ramp, Watterson Formation carbonates indicate an inner ramp, lenses of Ducker Formation semi-pelite (± carbonate) suggest lagoons, and Tavani Formation immature siliciclastic rocks signify a coastal sand plain. The interpreted coincidence of basin narrowing with basin deepening denotes tectonic rather than eustatic control. Similar relationships elsewhere have been attributed to effects of intraplate stress in intracratonic and passive margin basins (Karner, 1986; Cloetingh, 1988).

Mechanisms of intracratonic basin subsidence are problematic; both extensional and compressional processes have been advocated (e.g. Quinlan, 1987). For Hurwitz Basin, regional relationships are permissive for either possibility. Geochronologic data in Tremblay et al. (1981), Bell (1985), Bickford et al. (1990) and Bostock et al. (1991) point to 2.4-2.1 Ga thermotectonic processes that affected both the Rae and Hearne provinces (Hoffman, 1990). Coincidence between distribution of the Hurwitz Group (as preserved) and rocks of the Ennadai-Rankin greenstone belt, noted by Wanless and Eade (1975b) and Hoffman (1990), may imply a causal link. Was formation of Hurwitz Basin due to high density rocks of the Ennadai-Rankin greenstone belt serving as excess mass in the upper crust that, upon application of intraplate compressive stress, induced basin subsidence? (see DeRito et al., 1983; Howell and van der Pluijm, 1990). Alternatively, extensional processes between ca. 2.2-2.1 Ga are also indicated, in the form of rift assemblages, and mafic sills and dyke swarms in both the Churchill and Superior provinces (Fahrig, 1987; Chandler and Parrish, 1989; Hoffman, 1989).

## STRUCTURAL GEOLOGY

### *Bray-Montgomery Lakes area*

The principal structural elements that affect the Hurwitz Group are: 1) a northeast and east-trending, north-vergent thrust north of Montgomery Lake, that juxtaposes Henik Group and lower Hurwitz Group above upper Hurwitz Group (recognized by Eade, 1974); 2) the gently soutwest-plunging Grey Hills synclinorium in the hanging wall of the thrust, with minor folds and oblique-slip faults distributed in a box-like array; 3) a gently southwest-plunging anticlinorium in the footwall of the thrust, with a south-vergent back-thrust; and 4) two northwest-trending oblique-slip faults that bound a block of upper Hurwitz Group strata west of Bray Lake, in which a Type II interference pattern has resulted from cleavage-bearing north- and northeast-trending folds refolding earlier folds that lack an associated cleavage (Fig. 1, 6a).

In the Montgomery Lake Group, a variably penetrative, northeast-trending cleavage, associated with open folds, is concordant with cleavage in the Hurwitz Group (Fig. 1, 6b). Older northwest-trending folds lack a related cleavage and are cut by the northeast-trending cleavage. Axial surfaces of the northwest-trending folds are concordant with bedding trends in subjacent Henik Group.

Archean rocks in the hanging wall of the east-trending Proterozoic thrust define a moderately to steeply northeast-dipping homocline (Fig. 1, 6b). Northwest-trending folds and cleavage are rare; northeast-trending cleavage is predominant and appears to intensify toward the Proterozoic thrust. The homocline appears to follow the outline of the Grey Hills synclinorium south of the map area (Eade, 1974; Geological Survey of Canada, 1965). In the footwall of the thrust, Archean rocks are folded about northeast-trending axial surfaces and are steeply (50-90°) plunging.

### *Northeastern Ameto Lake (Noomut River) area*

The principal structure north of Ameto Lake is a northeast-trending, northwest-vergent imbricated thrust (Fig. 2). In the footwall, the Hurwitz Group and basement are folded in a Type I interference relationship defined by folds with steeply dipping northwest-trending and northeast-trending axial surfaces. The northwest-trending folds lack an associated cleavage. In the hanging wall, the Hurwitz Group and the basement-cover contact are folded in a northwest-plunging syncline and cut by northwest-trending cross faults. However, cleavage trends are predominantly northeast. Archean rocks in the footwall are folded about a northeast-trending cleavage; the folds are steeply plunging (>70°; commonly downward-facing). Although Archean rocks are deformed together with the Hurwitz Group, an earlier strain history is indicated by the contrast in plunge and orientation of folds in the two units, by the presence of foliated Archean clasts in basal Hurwitz Group, and by a contrast in apparent strain at the Henik Group-Hurwitz Group unconformity.

## ECONOMIC GEOLOGY

Mineral occurrences mapped and sampled are plotted on Figures 1 and 2; UTM locations and available analytical results are given in Table 2.

Gossans in the Henik Group are abundant and include: 1) chalcopyrite-pyrite-bearing quartz veins cutting rhyolite agglomerates northwest of Noomut River; 2) pyrite-bearing quartz veins cutting banded iron-formation west of Montgomery Lake; 3) sulphide disseminations along pillow selvages and inter-pillow zones, Montgomery Lake; and 4) pyrite-bearing quartz veins at pillow volcanic-gabbro contacts, Montgomery Lake.

Gossans from disseminated pyrite are ubiquitous in the Montgomery Lake Group. East of Bray Lake, basal polymictic conglomerates contain gold-bearing, pebble to cobble-sized pyritic chert clasts (Gossan 21; to 1600 ppb). Basement rocks that could have been the source of the clasts have not yet been mapped.

Background gold values in the Hurwitz Group are typically below 1 ppb Au (Aspler, 1990, and references therein). Above background gold values were recorded from the Padlei Formation west of Bray Lake; from the Whiterock Member west of Bray Lake, and from a Hurwitz gabbro sill near the upper contact of the Ameto Formation and close to

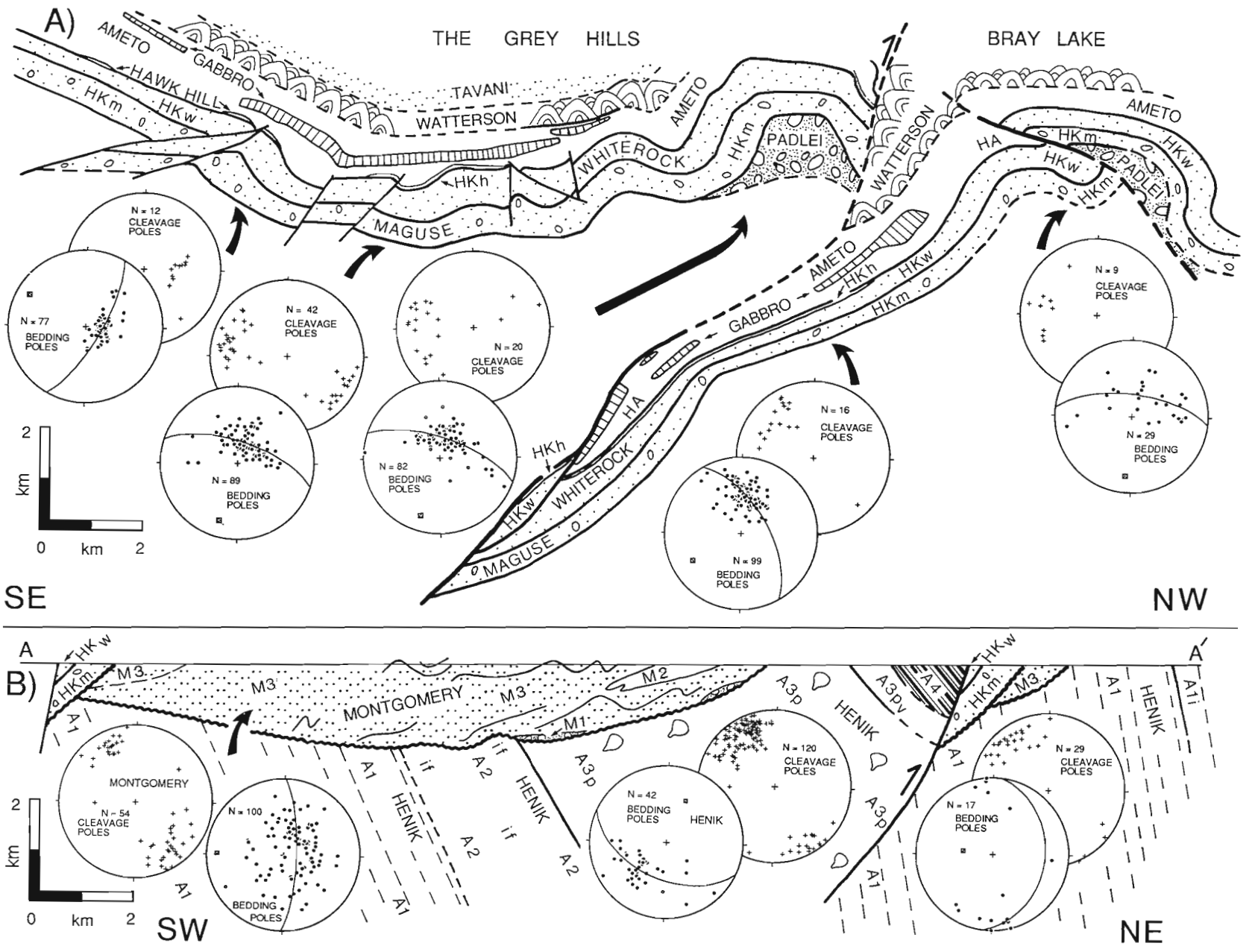


**Figure 6. A**) Downplunge projection; view to the southwest from northeast of Montgomery Lake to southwest of The Grey Hills. The gap on the southeast side results from structures that are close to the plane of the projection. **B**) Cross-section illustrating Henik Group-Montgomery Lake Group-Hurwitz Group relationships, Montgomery Lake area (see Fig. 1 for section line). Legend and map units as in Figure 1 and Table 1.

**Table 2.** Geochemistry of grab samples. Gossan numbers are plotted on Figures 1 and 2. Geochemistry of gossans with no reported values is in progress. All analyses by X-Ray Assay Laboratories, Don Mills, Ontario.

| | | | ELEMENT | Au | Co | Ni | Cu | Zn | As | Mo | Ag | Cd | Sb | W | Pb |
|---|---|---|---|---|---|---|---|---|---|---|---|---|---|---|---|
| | | | METHOD | NA | DCP | DCP | DCP | DCP | NA | DCP | DCP | DCP | NA | NA | DCP |
| | | | DETECTION LIMIT | 5 | 1 | 1 | 0.5 | 0.5 | 2 | 1 | 0.5 | 1 | 0.5 | 2 | 2 |
| | | | | ppb | ppm | ppm | ppm | ppm | ppm | ppm | ppm | ppm | ppm | ppm | ppm |
| GOSSAN | SAMPLE | UTM | LITHOLOGY | | | | | | | | | | | | |
| 1 | 91-9-25A | 65H/5; 565107 | Disseminated sulphides | <5 | 8 | 5 | 22.9 | 23.5 | 7 | 5 | .9 | 2 | .7 | 2 | <2 |
| 1 | 91-9-25B | " | in Hurwitz gabbro and | 11 | 17 | 15 | 37.9 | 20.5 | 8 | 5 | <.5 | <1 | 1.1 | <2 | <2 |
| 1 | 91-9-25C | " | Ameto Formation near | 6 | 66 | 39 | 151 | 44.4 | 28 | 4 | <.5 | 2 | 1.4 | 2 | <2 |
| 1 | 91-9-25D | " | Mackenzie db contact | <5 | 12 | 27 | 26.1 | 31.6 | 17 | 3 | <.5 | <1 | 1.1 | <2 | <2 |
| 2 | 91-20-36 | 65H/5; 595015 | Sulphides in quartz | <5 | 20 | 27 | 289 | 9.7 | 5 | 11 | <.5 | <1 | 1.9 | <2 | <2 |
| 3 | 91-16-3 | 65H/5; 611080 | veins cutting Hurwitz | <5 | 3 | 10 | 15.4 | 4.9 | <2 | 12 | 1.5 | <1 | <.5 | <2 | 4 |
| 4 | 91-54-20C | 65H/11;038426 | gabbro | | | | | | | | | | | | |
| 5 | 91-6-3A | 65G/8; 505196 | Oxides in concordant | | | | | | | | | | | | |
| 6 | 91-15-34 | 65H/5; 606095 | layered chert and chert | | | | | | | | | | | | |
| 7 | 91-28-71 | 65H/5; 605015 | breccia; Hawk Hill | | | | | | | | | | | | |
| 8 | 91-54-30 | 65H/11;036425 | Member | | | | | | | | | | | | |
| 9 | 91-13-6 | 65G/8; 530119 | | <5 | 2 | 6 | 5.6 | 5.0 | 3 | 14 | <.5 | <1 | 8.9 | 13 | <2 |
| 10 | 91-25-1 | 65G/8; 531118 | | <5 | 2 | 2 | 3.0 | 2.8 | 5 | 9 | <.5 | <1 | 3.1 | 8 | 12 |
| 10 | 91-25-2 | " | Oxides in discordant | <5 | 1 | 3 | 3.6 | 3.3 | 12 | 9 | <.5 | <1 | 7.4 | 15 | <2 |
| 10 | 91-25-3 | " | chert breccia; Hawk | <5 | 2 | 6 | 106 | 5.3 | 10 | 8 | <.5 | <1 | 8.6 | 51 | <2 |
| 11 | 91-1-1 | 65G/8; 534117 | Hill Member | <5 | <1 | 4 | 3.1 | 4.6 | 2 | 12 | <.5 | <1 | 3.9 | 30 | 2 |
| 11 | 91-1-2 | " | | <5 | 2 | 7 | 4.6 | 7.1 | 5 | 15 | <.5 | <1 | 44.0 | 59 | 2 |
| 11 | 91-1-3 | " | | <5 | 2 | 7 | 3.8 | 5.0 | 11 | 15 | <.5 | <1 | 13.0 | 77 | 2 |
| 12 | 91-7-20 | 65H/5; 595106 | | 6 | 1 | 5 | 3.1 | 4.8 | <2 | 10 | <.5 | <1 | 1.7 | 3 | <2 |
| 13 | 91-19-9 | 65G/8; 431144 | Sulphides/oxides in | <5 | 1 | 3 | 2.1 | 1.9 | <2 | 8 | <.5 | <1 | .5 | <2 | <2 |
| 14 | 91-23-3B | 65G/8; 453111 | quartz arenites; | <5 | <1 | 3 | 3.2 | 1.3 | <2 | 13 | <.5 | <1 | <.5 | 2 | <2 |
| 15 | 91-15-22 | 65H/5; 619089 | Whiterock Member | <5 | 10 | 9 | 3.5 | 2.6 | <2 | 8 | <.5 | <1 | <.5 | <2 | <2 |
| 16 | 91-12-1 | 65H/5; 536121 | | <5 | 2 | 5 | 2.6 | 4.2 | 10 | 8 | <.5 | <1 | 4.7 | 67 | <2 |
| 17 | MS3-1 | 65H/10;065387 | Maguse Mbr qtz-pebble | | | | | | | | | | | | |
| 18 | MS3-2 | 65H/10;066388 | conglomerate, with py | | | | | | | | | | | | |
| 19 | 91-29-10 | 65G/9; 435193 | Sulphides in Padlei Fm | 190 | 4 | 6 | 14.2 | 8.8 | 11 | 9 | <.5 | <1 | 1.5 | <2 | <2 |
| 20 | 91-19-15 | 65G/8; 426151 | mixtite conglomerate | 14 | 12 | 24 | 78.0 | 27.1 | 2 | 7 | <.5 | <1 | 1.0 | <2 | <2 |
| 21 | 91-26-14A | 65H/12;537212 | Pebble-cobble, py-qtz | 480 | 59 | 72 | 69.7 | 30.8 | 54 | 5 | <.5 | <1 | 4.3 | <2 | 10 |
| 21 | 91-26-14B | " | clasts in Montgomery | 120 | 56 | 50 | 135 | 12.8 | 760 | 7 | .8 | <1 | 3.4 | <2 | 12 |
| 21 | 91-26-14C | " | Lake Gp conglomerate | 1600 | 120 | 140 | 151 | 14.7 | 120 | 9 | .8 | <1 | 7.0 | <2 | 28 |
| 22 | 91-39-18C | 65H/5; 727116 | Disseminated | | | | | | | | | | | | |
| 23 | 91-28-40 | 65H/5; 606005 | sulphides; Montgomery | 6 | 5 | 8 | 7.5 | 9.7 | 13 | 9 | <.5 | <1 | <.5 | 2 | <2 |
| 24 | 91-32-6A | 65H/5; 683150 | Lake Gp sandstone and | | | | | | | | | | | | |
| 25 | 91-50-4 | 65H/5; 697096 | conglomerate | | | | | | | | | | | | |
| 26 | 91-44-42 | 65H/5; 580150 | | <5 | 2 | 2 | 13.9 | 20.6 | 15 | <1 | <.5 | <1 | <.5 | 2 | <2 |
| 27 | 91-44-15 | 65H/5; 602169 | | 7 | 4 | 7 | 13.9 | 20.5 | 3 | <1 | <.5 | <1 | <.5 | <2 | 2 |
| 28 | 91-47-9 | 65H/5; 611141 | Disseminated pyrite in | 31 | 4 | 10 | 89.8 | 8.0 | <2 | 3 | <.5 | <1 | 5 | <2 | <2 |
| 29 | 91-47-28A | 65H/5; 634129 | quartz veins; Henik | <5 | 6 | 8 | 26.7 | 10.3 | 10 | <1 | <.5 | <1 | 1.5 | <2 | <2 |
| 29 | 91-47-28B | " | Group BIF (unit A2) | 310 | 87 | 96 | 61.8 | 10.3 | 46 | 6 | 1.6 | <1 | 6.8 | <2 | 32 |
| 30 | 91-42-9 | 65H/5; 640127 | | 170 | 122 | 136 | 783 | 64.1 | 7 | 3 | <.5 | <1 | 1.5 | <2 | 4 |
| 31 | 91-52-16A | 65H/5; 686049 | | | | | | | | | | | | | |
| 32 | 91-52-2 | 65H/5; 664033 | Py in qtz veins; A1 IF | | | | | | | | | | | | |
| 33 | 91-38-5 | 65H/12;635190 | mudstone-mag. A1 IF | <5 | 9 | 19 | 46.1 | 39.5 | 9 | 1 | <.5 | <1 | 3.4 | <2 | <2 |
| 34 | 91-60-25 | 65H/11;016434 | Cpy-py qtz vein Henik Gp rhyolite agglomerate | 1600 | 139 | 499 | 1280 | 3.2 | 3 | <1 | 2.3 | <1 | <.5 | <2 | <2 |
| 35 | 91-LAA-T37 | 65H/5; 624155 | Sulphides at volcanic/ | 80 | 73 | 74 | 217 | 94.7 | 17 | 6 | 3.5 | <1 | 9.7 | <2 | 64 |
| 36 | 91-44-33 | 65H/5; 572169 | gabbro contacts | 11 | 51 | 183 | 40.2 | 96.4 | 10 | 3 | <.5 | <1 | <.5 | <2 | <2 |
| 37 | 91-LAA-T42 | 65H/5; 654151 | Sulphides along pillow | 28 | 97 | 51 | 1390 | 17.2 | 5 | 4 | .9 | 1 | 1.1 | <2 | <2 |
| 37 | 91-41-14 | " | selvages and inter- | <5 | 20 | 13 | 708 | 23.8 | 36 | 3 | 1.0 | <1 | 1.0 | <2 | <2 |
| 38 | 91-LAA-T45 | 65H/5; 666161 | pillow zones | 34 | 34 | 46 | 6540 | 67.5 | 3 | 3 | 3.9 | <1 | .8 | 33 | <2 |

the contact with a Mackenzie diabase dyke. Although discordant hematitic breccias that are interpreted as feeder pipes to layered cherts of the Hawk Hill Member are not anomalous in Au, Ag, or As, they are elevated in the epithermal pathfinder elements W, Sb, and Mo (Table 2; see Nelson, 1988).

## ACKNOWLEDGMENTS

This project is funded by: the Canada-NWT Minerals Initiative 1991-1996; NWT Geology Division (DIAND Yellowknife); NSERC Operating Grant A5536 (Bursey, to J.A. Donaldson); and the Northern Scientific Training Program (Bursey; DIAND, Ottawa). We appreciate the continued support and encouragement given by C.W. Jefferson and W.A. Padgham. L.H. Heaman contributed perceptive questioning during a field visit; a visit by M. Stubley enabled reconnaissance work near Padlei. Logistical support was from Treeline Lodge (Nueltin Lake); we thank Gary Gurke, Ingrid Brooks, and Boyd Jackson for expediting and radio contact, and Cessna pilot Ron Last for efficient camp moves and set outs. Sample preparation and technical assistance by R. Lancaster and R. Burke is greatly appreciated. John Broome provided aeromagnetic data. R. Herd arranged for the loan of archival air photos. The stereonets were prepared using the Allmendinger program.

Discussions and critical comments by R.T. Bell, C.W. Jefferson, and G.M. Young helped to improve the manuscript.

## REFERENCES

**Aspler, L.B.**
1990: Economic significance of hot spring cherts: the Hawk Hill Member (Early Proterozoic Hurwitz Group), District of Keewatin; NWT Geology Division Yellowknife, Open File, EGS 1990-22, 67 p.
1991: Geological maps of the Bray Lake-Montgomery Lake and northeastern Ameto Lake (Noomut River) areas, District of Keewatin, NWT; Geological Survey of Canada, Open File 2428.
in press: Early Proterozoic hot spring deposition of bedded cherts: the Hawk Hill Member (Hurwitz Group), District of Keewatin, NWT; Canadian Journal of Earth Sciences.

**Aspler, L.B. and Bursey, T.L.**
1990: Stratigraphy, sedimentation, dome and basin basement-cover infolding and implications for gold in the Hurwitz Group, Hawk Hill-Griffin-Mountain Lakes area, District of Keewatin; in Current Research, Part C; Geological Survey of Canada, Paper 90-1C, p. 219-230.

**Aspler, L.B., Bursey, T.L., and Miller, A.R.**
1989: Sedimentology, structure and economic geology of the Poorfish-Windy thrust-fold belt, Ennadai Lake area, District of Keewatin, and the shelf to foreland transition in the foreland of Trans Hudson Orogen; in Current Research, Part C; Geological Survey of Canada, Paper 89-1C, p. 143-155.

**Bell, K.**
1985: Geochronology of the Carswell area, northern Saskatchewan; in The Carswell Structure Uranium Deposits, Saskatchewan, (ed.) R. Lainé, D. Alonso, and M. Svab; Geological Association of Canada, Special Publication 29, p. 33-46.

**Bell, R.T.**
1970a: The Hurwitz Group-a prototype for deposition on metastable cratons; in Symposium on basin and geosynclines of the Canadian Shield, (ed.) A.J. Baer; Geological Survey of Canada, Paper 70-40, p. 159-169.
1970b: Preliminary notes on the Hurwitz Group, Padlei map area, Northwest Territories; Geological Survey of Canada, Paper 69-52,13p.

**Bethke, C.M.**
1986: Hydrologic constraints on the genesis of the Upper Mississippi Valley Mineral District from Illinois Basin brines; Economic Geology, v. 81, p. 233-249.

**Bickford, M.E., Collerson, K.D., Lewry J.F., Van Schmus, W.R., and Chiarenzelli, J.R.**
1990: Proterozoic collisional tectonism in the Trans-Hudson orogen, Saskatchewan; Geology, v. 18, p. 14-18.

**Bostock, H.H., van Breeman, O., and Loveridge, W.D.**
1991: Further geochronology of plutonic rocks in northern Taltson Magmatic Zone, District of Mackenzie, N.W.T.; in Radiogenic Age and Isotopic Studies, Report 4, Geological Survey of Canada, Paper 90-2, p. 67-78.

**Chandler, F.W. and Parrish, R.R.**
1989: Age of the Richmond Gulf Group and implications for rifting in the Trans-Hudson orogen, Canada; Precambrian Research, v. 44, p. 277-288.

**Chiarenzelli, J.R. and Macdonald, R.**
1986: A U-Pb zircon date for the Ennadai Group; in Saskatchewan Geological Survey, Miscellaneous Report 86-4, p. 112-113.

**Cloetingh, S.**
1988: Intraplate stress: a new element in basin analysis; in New perspectives in basin analysis, (ed.) K. Kleinspehn and C. Paola; Springer-Verlag, New York, p. 204-230.

**Cull, J.P. and Conley, D.**
1983: Geothermal gradients and heat flow in Australian sedimentary basins; Bureau of Mineral Resources, Journal of Australian Geology and Geophysics, v. 8, p. 330-337.

**Delaney, G.D., Heaman, L.M., Kamo, S., Parrish, R.R., Slimmon, W.L., and Reilly, B.A.**
1990: U-Pb sphene/zircon geochronological investigations; in Saskatchewan Geological Survey, Miscellaneous Report 90-4, p. 54-57.

**DeRito, R., Cozzarelli, F.A., and Hodge, D.S.**
1983: Mechanism of subsidence of ancient cratonic rift basins; Tectonophysics, v. 94, p. 141-168.

**Eade, K.E.**
1974: Geology of Kognak River area, District of Keewatin, Northwest Territories; Geological Survey of Canada, Memoir 377, 66 p.

**Eade, K.E. and Chandler, F.**
1975: Geology of Watterson Lake (west half) map area, District of Keewatin; Geological Survey of Canada, Paper 74-64, 10 p.

**Fahrig, W.F.**
1987: The tectonic settings of continental mafic dyke swarms: failed arm and early passive margin, in Mafic Dyke Swarms, (ed.) H.C. Halls and W.F. Fahrig; Geological Association of Canada, Special Publication 34, p. 331-348.

**Geological Survey of Canada**
1965: Aeromagnetic series map, NTS 65 H/5; 3218 G.

**Heywood, W.W. and Roscoe, S.M.**
1967: Pyritic quartz pebble conglomerate in the Hurwitz Group, District of Keewatin; in Report of Activities Part A, Geological Survey of Canada, Paper 67-1A, p. 21-22.

**Hoffman, P.F.**
1989: Precambrian geology and tectonic history of North America; in The Geology of North America- An Overview, (ed.) A.W. Bally and A.R. Palmer; Geological Society of America, Boulder, p. 447-512.
1990: Subdivision of the Churchill Province and extent of the Trans-Hudson orogen; in The Early Proterozoic Trans-Hudson Orogen of North America; (ed.) J.F. Lewry and M.R. Stauffer; Geological Association of Canada, Special Paper 37, p. 15-39.

**Howell, P.D. and van der Pluijm, B.A.**
1990: Early history of the Michigan Basin: subsidence and Appalachian tectonics; Geology, v. 18, p. 1195-1198.

**Karner, G.D.**
1986: Effects of lithospheric in-plane stress on sedimentary basin stratigraphy: Tectonics, v. 5, p. 573-588.

**LeCheminant, A.N. and Heaman, L.M.**
1989: Mackenzie igneous events, Canada: Middle Proterozoic hotspot magmatism associated with ocean opening; Earth and Planetary Science Letters, v. 96, p. 38-48.

**Loveridge, W.D., Eade, K.E., and Sullivan, R.W.**
1988: Geochronological studies from Precambrian rocks from the southern District of Keewatin; Geological Survey of Canada, Paper 88-18, 36 p.

**Mortensen, J.K. and Thorpe, R.I.**
1987: U-Pb zircon ages of felsic volcanic rocks in the Kaminak Lake area, District of Keewatin; in Radiogenic Age and Isotopic Studies: Report 1, Geological Survey of Canada, Paper 87-2, p. 123-128.

**Mount, J.F.**
1984: Mixing of siliciclastic and carbonate sediments in shallow shelf environments; Geology, v. 12, p. 432-435.

**Nelson, C.E.**
1988: Gold deposits in their hot spring environment; in Bulk Mineable Precious Metal Deposits of the Western United States, (ed.) R.W. Schafer, J.J. Cooper, and P.G. Vikre; The Geological Society of Nevada, Reno, p. 417-431.

**Paris, I., Stanistreet, I.G., and Hughes, M.J.**
1985: Cherts of the Barberton greenstone belt interpreted as products of submarine exhalative activity; Journal of Geology, v. 93, p. 111-129.

**Patterson, J.G. and Heaman, L.M.**
1990: Geochronological contraints on the depositional age of the Hurwitz Group, N.W.T; Geological Association of Canada, Program With Abstracts, v. 5, p. A102.

**Quinlan, G.**
1987: Models of subsidence mechanisms in intracratonic basins, and their applicability to North American examples; in Sedimentary Basins and Basin-Forming Mechanisms, (ed.) C. Beaumont and A.J. Tankard; Canadian Society of Petroleum Geologists, Memoir 12, p. 463-481.

**Roscoe, S.M.**
1981: Temporal and other factors affecting deposition of uraniferous conglomerates; in Genesis of Uranium- and Gold-bearing conglomerates, (ed.) F.C. Armstrong; United States Geological Survey, Professional Paper 1161-A-BB, p. W1-W17.

**Tanner, W.F.**
1967: Ripple mark indices and their uses; Sedimentology, v. 9, p. 89-104.

**Tella, S., Annesley, I.R., Borradaile, G.J., and Henderson, J.R.**
1986: Precambrian geology of parts of Tavani, Marble Island and Chesterfield Inlet map areas, District of Keewatin: a progress report; Geological Survey of Canada, Paper 86-13, 20 p.

**Tella, S., Roddick, J.C., Park, A.F., and Ralser, S.**
1991: Geochronological constraints on the tectonic history of the Archean and lower Proterozoic rocks in the Tavani, Rankin Inlet, and Chesterfield inlet regions, Churchill Structural Province, N.W.T.; in Program With Abstracts, Geological Survey of Canada, Current Activities Forum, p. 15.

**Tremblay, L.P., Loveridge, W.D., and Sullivan, R.W.**
1981: U-Pb ages of zircons from the Foot Bay gneiss and the Donaldson Lake gneiss, Beaverlodge area, northern Saskatchewan, in Current Research, Part C; Geological Survey of Canada, Paper 81-1C, p.123-126.

**Wanless, R.K. and Eade, K.E.**
1975a: Geochronology of Archean and Proterozoic rocks in the southern District of Keewatin; Canadian Journal of Earth Sciences, v. 12, p. 95-114.
1975b: Geochronology of Archean and Proterozoic rocks in the southern District of Keewatin: Reply; Canadian Journal of Earth Sciences, v. 2, p. 1254-1255.

**Young, G.M.**
1973: Tillites and aluminous quartzites as possible time markers for Middle Precambrian (Aphebian) rocks of North America; in Huronian stratigraphy and sedimentation, (ed.) G.M. Young; Geological Association of Canada Special Publication 12, p. 97-127.
1975: Geochronology of Archean and Proterozoic rocks in the southern District of Keewatin: Discussion; Canadian Journal of Earth Sciences, v. 12, p. 1250-1254.
1988: Proterozoic plate tectonics, glaciation and iron formations; Sedimentary Geology, v. 58, p. 127-144.

**Young, G.M. and Mclennan, S.M.**
1981: Early Proterozoic Padlei Formation, Northwest Territories, Canada; in Earth's Pre-Pleistocene glacial record; (ed.) M.J. Hambrey and W.B. Harland; Cambridge University Press, Cambridge, England, p. 790-794.

Geological Survey of Canada Project 780008

# Lower Paleozoic and Proterozoic stratigraphy in the Colville Hills-Tweed Lake area, Northwest Territories: implications for regional seismic stratigraphic correlations

**Frederick A. Cook**[1]

*Cook, F.A., 1992: Lower Paleozoic and Proterozoic stratigraphy in the Colville Hills-Tweed Lake area, Northwest Territories: implications for regional seismic stratigraphic correlations; in Current Research, Part C; Geological Survey of Canada, Paper 92-1C, p. 171-178.*

***Abstract***

*Correlations of stratigraphic horizons in recently drilled wells to seismic reflections in the Colville Hills-Tweed Lake region of the Northwest Territories suggest that Proterozoic basalts are unconformably overlain by Proterozoic clastics and carbonates that may be equivalent to Mackenzie Mountains Supergroup strata.*

***Résumé***

*Selon les corrélations d'horizons stratigraphiques traversés par des sondages récents de sismique réflexion dans la région des collines Colville et du lac Tweed dans les Territoires du Nord-Ouest, les basaltes protérozoïques sont surmontés en discordance par des roches clastiques et des roches carbonatées protérozoïques qui pourraient être équivalentes aux couches du supergroupe de Mackenzie Mountains.*

[1] Department of Geology and Geophysics, University of Calgary, Calgary, Alberta T2N 1N4

## INTRODUCTION

Interpretations of seismic reflection data are enhanced when reflections can be correlated with known stratigraphy. In northwestern Canada, a large quantity of industry reflection data and deep crustal reflection data have imaged outstanding sub-Paleozoic structures that have little, if any, surface expression (Cook, 1988a, b). Accordingly, it is difficult to provide detailed analyses of stratigraphic variations and timing of deformation for these features. In this article, wells that have been drilled in the Colville Hills-Tweed Lake region and that have penetrated to rocks below the basal Cambrian clastics are examined to aid the interpretation of the reflection data.

The analysis presented here incorporates wells that were drilled in the vicinity of the PCI Canterra Tweed Lake M-47, as this well penetrated into basalts that are almost certainly Proterozoic and are likely equivalent to the ca. 1.27 Ga Coppermine lavas that are exposed some 250-300 km to the east (Sevigny et al., 1991). Additional drillholes, most of which were drilled after the M-47, have penetrated to basalt that may or may not be the same as the M-47 basalt. Others in the vicinity drilled into carbonates and/or clastics that have been interpreted as stratigraphically equivalent to lower formations (H1 carbonate and underlying clastics) of the Proterozoic Mackenzie Mountains Supergroup (Pugh, 1983; Aitken and Pugh, 1984). Cook (1988b), Cook and Coflin (1990) and Sevigny et al. (1991) have interpreted a section of clastics and carbonates that overlie the M-47 basalts and that underlie the identifiable Cambrian Mount Clark formation as equivalent to Aitken and Pugh's (1984) Mackenzie Mountains Supergroup strata. Here, these interpretations are evaluated and their implications for the regional setting of the Proterozoic are discussed.

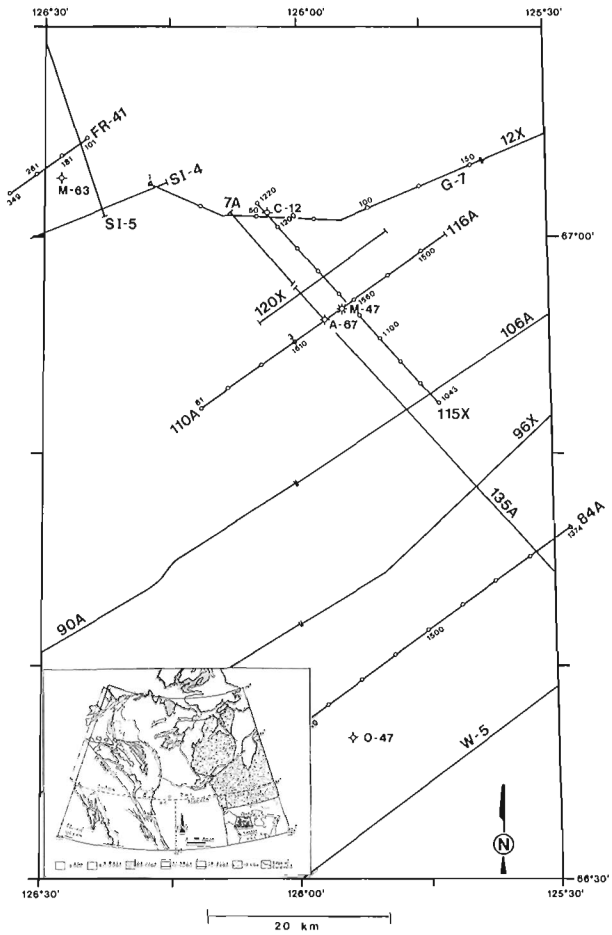


**Figure 1.** Map of seismic profile locations and drill hole locations in the Tweed lake region. Additional seismic line locations of data not yet released are not shown. Inset shows general location in northwest Canada (arrow).

## DRILL HOLES

Locations of drill holes in the vicinity of the M-47 (Fig. 1), and a summary of the lithologies that are visible below the top of the Saline River salt (Fig. 2a) and the Mount Clark formation (Fig. 2b), illustrate the importance of stratigraphic correlations in the area. For example, the interval between the Saline River salt and the Proterozoic (Fig. 2a) is different from well to well. Pugh (1983) has suggested that the Mount Cap-Proterozoic interval may vary as a result of topography on the Proterozoic. Although this is likely the case in some areas to the west (Pugh, 1983), it is unlikely to be the cause for variations of this interval within this local area as the topography on the Proterozoic during deposition of the Mount Clark clastics (Fig. 2b) was minimal.

Two drill holes (M-63 and C-12) penetrated 13-21 m of Mount Clark and entered a carbonate that was interpreted (for the M-63 drill hole) by Pugh (1983) and Aitken and Pugh (1984) as the H1. The M-63 then drilled into a clastic unit at about 1173 m that is interpreted as the lower sand/shale unit of the Mackenzie Moutains Supergroup (Aitken and Pugh, 1984).

Three drill holes penetrated from the Mount Clark directly into basalt (M-47, A-67, and O-35), and one well (O-47) may have penetrated 2 m of red shale above the basalt. In all of these drill holes, the Lower Cambrian Mount Clark clastic sequence is between 13 and 30 m thick (Fig. 2b). The A-67 drill hole penetrated the volcanics between about 1300 and 1325 m and then drilled about 22 m of clastics.

The M-47 drill hole (Fig. 2) intersected Proterozoic volcanics at about 1234 m and, according to the well cuttings, drilled through a section of volcanics, gray/green pyritic shales, and occasional carbonate to a depth of about 1310 m. Between 1310 m and about 1340 m, the lithology appears to be dominated by gray/green pyritic shale, and below 1340 m, the lithology is again dominated by volcanics with minor carbonate and shale. Core between 1400 and 1409 m recovered about 8 m of basalt (Sevigny et al., 1991).

Geochemical analyses of the cored volcanics at 1400-1409 m in the M-47 suggest this basalt is correlative with the Coppermine basalt that is exposed to the east (Sevigny et al., 1991). Because this material is overlain in the well by rocks that include significant quantities of shale and occasional carbonates, we interpreted the sequence between the cored volcanics and the base of the Cambrian Mount Clark formation to be correlative with Mackenzie Mountains Supergroup strata that were suggested by Aitken and Pugh

(1984) to be present in this area. This was the basis for our statement that the M-47 drill hole penetrated "stratigraphically below layers interpreted by Aitken and Pugh (1984) as the H1 and sand-shale units" of the Mackenzie Mountains Supergroup (Sevigny et al., 1991, p. 185; see also Cook, 1988b; Cook and Coflin, 1990).

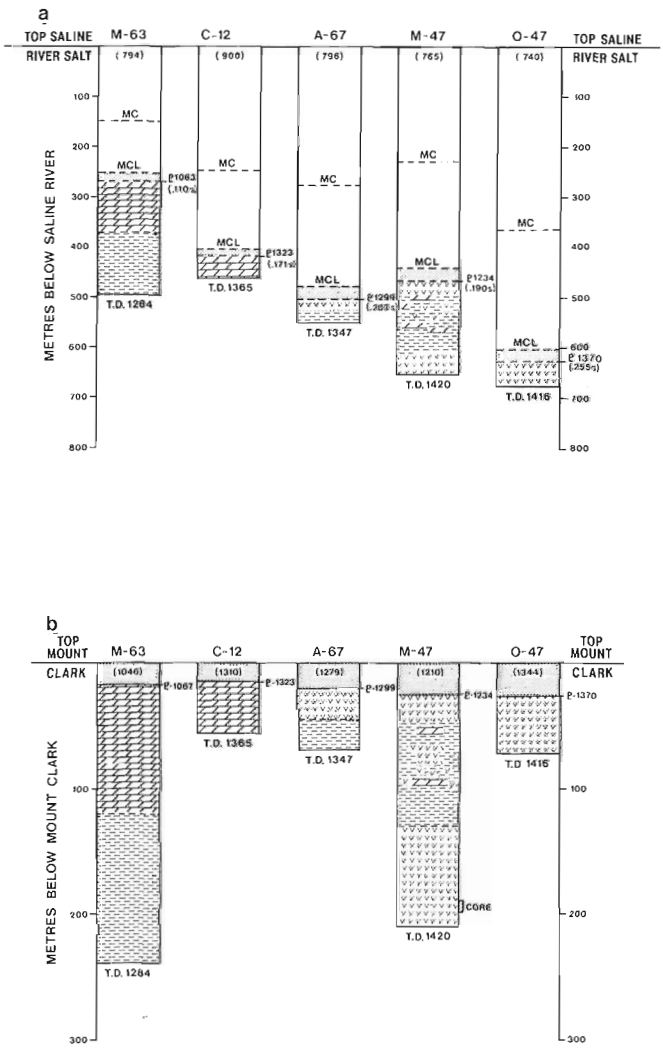


**Figure 2.** Summary of the lower Paleozoic and Proterozoic stratigraphy in the Tweed Lake region. a) Stratigraphic cross section with the top of the Saline River (Cambrian) salt as a datum with important stratigraphic tops indicated and lithologies for basal Cambrian clastics (Mount Clark - MCL) and Proterozoic indicated. Numbers in parentheses below the well identifications are depths to the salt. Numbers adjacent to the Proterozoic symbol (P) are depths to Proterozoic and numbers in parentheses below Proterozoic depths are the two-way travel time between the salt and the Proterozoic. Note that the two-way time at the location of the M-63 drill hole is only .110 s. Labels used are: MC = Mount Cap formation. b) Stratigraphic cross section from the M-63 to the O-47 summarizing thicknesses and lithologies below the Mount Clark formation. Note that the top of Proterozoic is at a nearly constant level (20-30 m) below the top of Mount Clark. This indicates that there was little topography on the Proterozoic during Mount Clark deposition.

The nature and stratigraphic relationship of the volcanic rocks that are present between 1250 m and about 1300 m in the M-47 are unknown. They may be Coppermine basalts above the 1400 m Coppermine, in which case the interpretation of the Proterozoic clastics and carbonates that occur between these volcanics and the cored basalts at 1400 m as equivalent to the Mackenzie Mountains supergroup sedimentary rocks would be unlikely. They may be correlative with the Little Dal volcanics of the Mackenzie Mountains Supergroup in the Cordillera, in which case the interrpetation of the carbonates and shales between 1310 m and 1400 m as part of the Mackenzie Mountains Supergroup (Cook, 1988b; Sevigny et al., 1991) is highly likely.

Although geochemical analyses of these shallow volcanics might prove valuable for regional correlations, we have chosen not to examine the geochemistry because the sample quantity available from well cuttings is insufficient for reliable trace element and rare-earth element analyses such as those carried out by Sevigny et al. (1991) for the cored basalts. Hence although volcanics are present between the Paleozoic and the cored basalts, the regional correlation of these higher volcanics is somewhat ambiguous.

The correlation of stratigraphic horizons from the M-47 drill hole to the A-67 drill hole about 2 km to the west (Fig. 2) is important for a complete understanding of the Proterozoic stratigraphy and its relationship to the seismic data. Both wells penetrated volcanics below the Cambrian, and both wells appeared to penetrate clastics below these shallow volcanics. However, because the M-47 drilled more than 170 m below the Mount Clark formation, it intersected basalts at greater depth as well. Figure 3 illustrates one possible correlation of the rocks in these wells. Here, the A-67 basalt and the shallow M-47 volcanics are considered to be the same, the clastics beneath the A-67 basalt may correlate with the M-47 clastics, and the A-67 well did not drill deep enough to intersect the deep basalt of the M-47.

An alternative interpretation is that the A-67 basalt correlates with the deep cored basalt of the M-47 at 1400-1409 m. In this case the Proterozoic section that overlies the M-47 deep basalt would be younger, and may or may not correlate with the Mackenzie Mountains Supergroup strata. The implications of these possible correlations are discussed below after we examine the relationship of the drill hole stratigraphy to the seismic reflection data.

## CORRELATION TO THE SEISMIC DATA

The correlation of the drill hole information to adjacent seismic reflection data has been addressed in Cook and Coflin (1990) and Sevigny et al. (1991). Here, these correlations and their stratigraphic implications are discussed with the additional well control in greater detail.

Drill holes M-47 and A-67 are both located on seismic reflection profile 110a-116a (Sevigny et al., 1991; Fig. 1). The first 1.50 s of this profile is enlarged here in a coherency filtered version at 5:1 vertical exaggeration (Fig. 4a, b).The coherency filter attenuates much of the background random

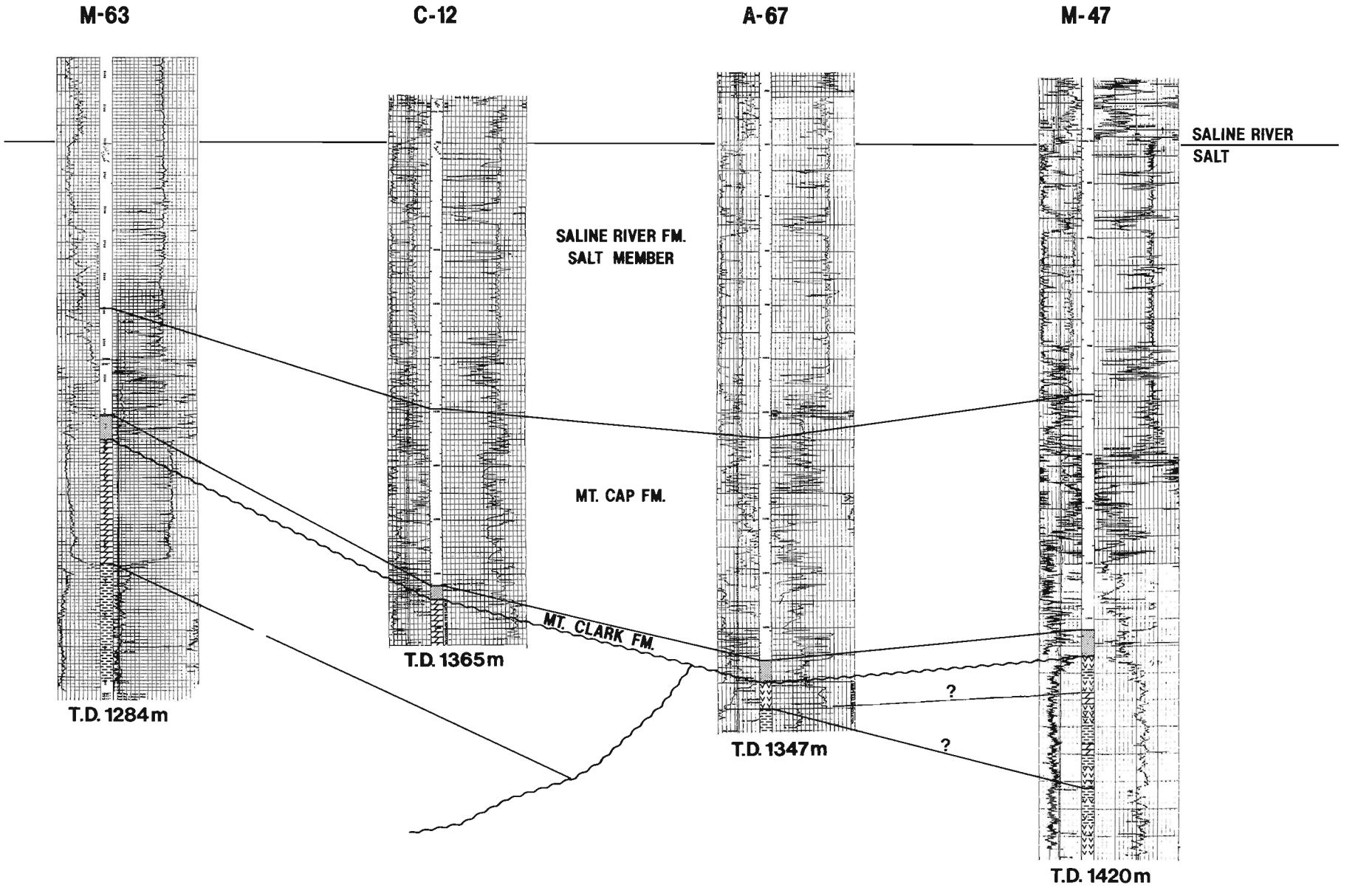


**Figure 3.** Correlations of well logs from the Tweed Lake area as discussed in the text. The nature of the correlation from the A-67 volcanic to the M-47 is uncertain; it is shown here with the volcanic of the A-67 correlating with the higher volcanics of the M-47. Other possibilities are discussed in the text.

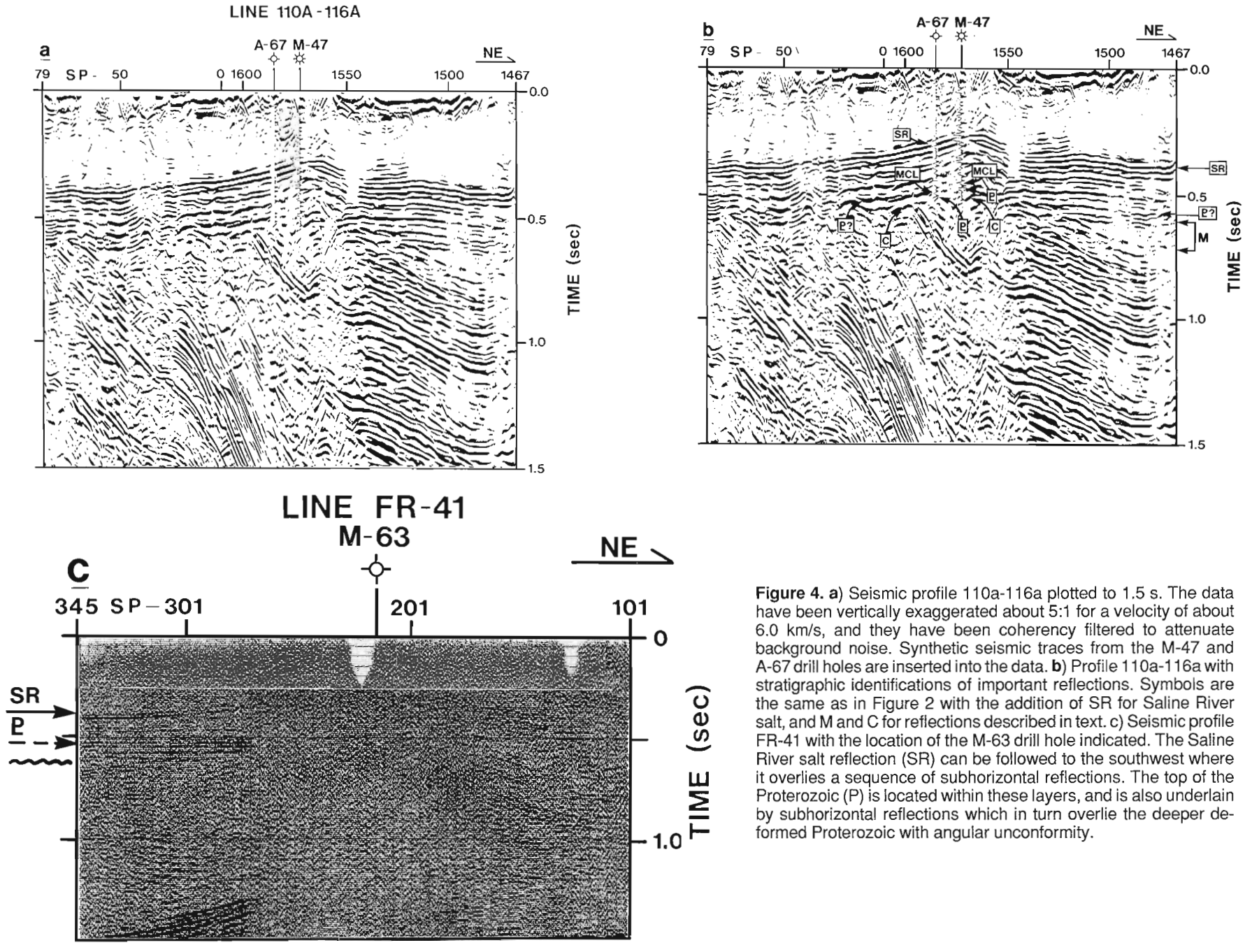


**Figure 4. a**) Seismic profile 110a-116a plotted to 1.5 s. The data have been vertically exaggerated about 5:1 for a velocity of about 6.0 km/s, and they have been coherency filtered to attenuate background noise. Synthetic seismic traces from the M-47 and A-67 drill holes are inserted into the data. **b**) Profile 110a-116a with stratigraphic identifications of important reflections. Symbols are the same as in Figure 2 with the addition of SR for Saline River salt, and M and C for reflections described in text. c) Seismic profile FR-41 with the location of the M-63 drill hole indicated. The Saline River salt reflection (SR) can be followed to the southwest where it overlies a sequence of subhorizontal reflections. The top of the Proterozoic (P) is located within these layers, and is also underlain by subhorizontal reflections which in turn overlie the deeper deformed Proterozoic with angular unconformity.

noise thus aiding in correlation of the synthetic seismic traces determined from the drill hole logs to the seismic data. The vertical exaggeration accentuates dip.

The M-47 drill hole is located near S. P. 1570, and the A-67 is located near S. P. 1585 (Fig. 1). Synthetic seismic traces calculated from the sonic logs are shown at these locations on the profile (Fig. 4a, b). In both cases, the Cambrian Saline River formation reflection is the most obvious event in the first .300 s (Fig. 4b), and thus represents a good marker horizon to relate to the other events. The Cambrian Mount Clark is represented by a trough, and the top of the Proterozoic is represented by a peak. The M-47 well drilled to a depth corresponding to about .060 s below the top of the Proterozoic.

The position of the Saline River and Proterozoic can be followed to the east and west of the uplift upon which these wells were drilled. To the west, the Proterozoic reflection appears to be located at the top of a thin (about .050 s) subhorizontal reflection zone that in turn overlies the eastward dipping Proterozoic (Fig. 4b). To the east, the Proterozoic top appears to overlie an eastward thickening zone of reflections (labeled M on Fig. 4b) that in turn onlap the underlying deformed layers. Thus there is evidence both to the east and to the west of the wells that the stratigraphic section thickens between the Mount Clark sandstones and the top of the deformed Proterozoic. Whether this thickening on the east occurs entirely within the Paleozoic, or whether it occurs by the addition of thin Proterozoic layers unconformably overlying the deformed Proterozoic is an unresolved, but significant, question.

At the location of the M-47 well, the top of the Proterozoic correlates to a reflection that is subhorizontal and that appears to be the same as a subhorizontal reflection to the west (P on Fig. 4b). This reflection is underlain by a reflection trough and then another peak (C on Fig. 4b) about .050 s lower. The volcanic layer that is cored at about 1400-1409 m in the M-47 and that may have its top a few tens of meters shallower appears to be represented by the lowest reflection peak on the M-47 synthetic trace (Fig. 4b) about .050 s below P. When correlated to the seismic data, this peak falls at or below C. This correlation was the basis for our previous interpretation that the 1400 m basalt of the M-47 well is located within the deformed Proterozoic and is overlain by younger Proterozoic with angular unconformity (Cook, 1988b; Cook and Coflin, 1990; Sevigny et al., 1991).

The A-67 synthetic appears to confirm the interpretation of reflection P as the top of the Proterozoic, as this reflection corresponds to the reflection for the top of the volcanics in this well. As the A-67 only drilled about 47 m below the top of the Proterozoic, it apparently did not reach reflection C (Fig. 4b). Accordingly, it appears that the most appropriate interpretation at this time is that the 1400 m volcanics of the M-47 are part of the deformed Proterozoic below reflection C and that these volcanics are unconformably overlain by younger Proterozoic rocks that include volcanics, clastics (primarily shale), and some carbonate. An alternative interpretation, as discussed below, is that the 1400 m basalt in the M-47 well is represented by the subhorizontal reflection C and is not within the deformed zone below.

To the east of the M-47 location, the seismic data indicate a greatly expanded stratigraphic section above the deformed, east dipping Proterozoic (reflections M in Fig. 4). From the Saline River reflection to the dipping Proterozoic the travel time is more than .300 s near S. P. 1467, whereas at the M-47, this interval is only about .200 s. This increase of about .100 s represents a thickness of about 250 m for a velocity of 5000 m/s. Furthermore, the expanded section in this region consists of a series of layers that onlap the east-dipping Proterozoic below (reflections M in Fig. 4). Thus, this expansion is caused by either lower Cambrian thickening and onlapping onto topographic highs in Proterozoic rocks, or by post-deformation Proterozoic rocks onlapping the horizons below. As no increase of this magnitude is observed for the Cambrian below the Mount Clark in this area (Pugh, 1983), it is likely that the expanded section consists of Proterozoic strata.

To the west and northwest of the M-47 and A-67 locations, the M-63 and C-12 drill holes penetrated into Proterozoic carbonate beneath the Cambrian (Fig. 2). The travel times for the interval between the Saline River salt and the Proterozoic are about .110 and .171 s, respectively (Fig. 2a). At the location of the C-12 drill hole, our examination of seismic data (line 115x, approximately S. P. 1210) indicates that the prominent angular unconformity occurs about .240 -.250 s below the Saline River salt reflection. Thus, it appears that nearly .070 -.080 s of Proterozoic is paraconformable with the overlying Paleozoic, and overlies deeper Proterozoic with angular unconformity at this location.

A similar situation exists near the M-63 drill hole. Here, Proterozoic dolomite was drilled about 269 m (about .110 s two-way time) below the top of the Saline River salt (Pugh, 1983; Fig. 2a). Profile FR-41 shows that in the vicinity of this drill hole, the prominent angular unconformity occurs about .200 s below the Saline River reflection (Fig. 4c). It thus appears that there is a zone of Proterozoic strata that has a time thickness of about .090 s (about 225 m) below the Cambrian and above the deformed Proterozoic. I believe a reasonable interpretation is that these subhorizontal Proterozoic include Mackenzie Mountains Supergroup sedimentary rocks as suggested by Pugh (1983) and Aitken and Pugh (1984).

## REGIONAL CONSIDERATIONS

The nature of the stratigraphic correlation between the A-67 and M-47 volcanics and clastics, their relationship to other drill holes such as the C-12 and M-63 that apparently penetrated Proterozoic sediments, and their implications for the interpretation of the seismic reflection data are summarized in Figure 5. Four possibilities include:

1) The A-67 volcanics and M-47 volcanics are all part of the same Proterozoic sequence that is a thin layer unconformably overlying the deformed older Proterozoic (Fig. 5a).

2) The A-67 volcanics correlate with the shallow (1250-1300 m) volcanics of the M-47, but unconformably overlie the deeper (1350-1420) volcanics of the M-47 (Fig. 5b).

3) The A-67 and M-47 volcanics are part of the same sequence, but both lie below the unconformity (Fig. 5c), and

4) The A-67 and deep (1400 m) M-47 volcanics are the same and are located below the unconformity, but the shallower sedimentary and volcanic rocks of the M-47 are part of the onlapping layers (Fig. 5d).

Models 2 and 4 (Fig. 5b and d) are similar to that presented in Cook (1988b), Cook and Coflin (1990), and Sevigny et al. (1991) in that they suggest the deformation responsible for the dipping Proterozoic layers occurred following extrusion of the M-47 1400 m basalts, and prior to deposition of the Mackenzie Mountains Supergroup. Observations from the C-12 and M-63 drillholes that indicate a thin layer of Proterozoic sedimentary rocks unconformably overlies the deformed layers are also consistent with these models.

Model 3 (Fig. 5c) is the least likely because correlation of the synthetic seismic trace to the data at the location of the M-47 indicates that the top of the Proterozoic occurs at the top of a thin layer that unconformably overlies the dipping Proterozoic (Fig. 4b). Model 1 (Fig. 5a) could be consistent with the reflection data if the deep (1400 m) basalt of the M-47 is not located below the unconformity. In this case the deformation would have taken place prior to extrusion of the Coppermine basalts, and the onlapping layers (M in Fig. 4b) would likely be Proterozoic that is pre-Coppermine. This model is not preferred because comparison of the M-47 and A-67 synthetic traces to the seismic data away from the complexity of the uplift indicates the 1400 m basalts are located below the unconformity (Sevigny et al., 1991).

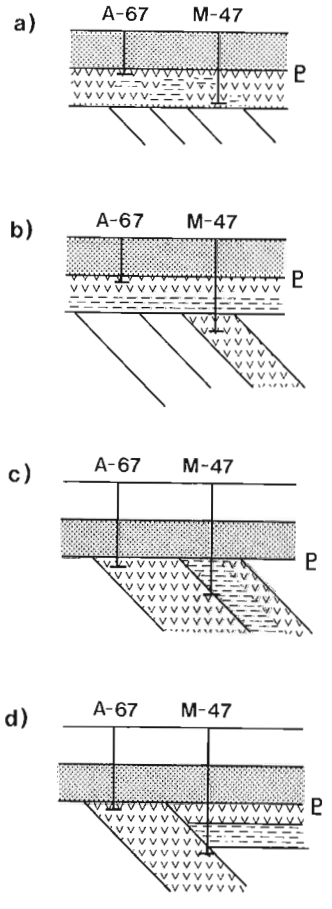


**Figure 5.** Four possible correlations of Proterozoic stratigraphy from the A-67 to the M-47 drill holes. Implications are discussed in the text.

## CONCLUSIONS

Detailed correlation of lithologic information from some drill holes in the Tweed Lake-Colville Hills region suggests that:

1) Deformed Proterozoic layers are unconformably overlain by Proterozoic sediments, including horizontally layered carbonates and clastics, that may be correlative with the Mackenzie Mountains Supergroup (Pugh, 1983; Aitken and Pugh, 1984; Sevigny et al., 1991).

2) The deep basalts of the M-47 are overlain by volcanics, clastics, and minor carbonate of uncertain significance, but that could be either part of the Mackenzie Mountains Supergroup (Cook, 1988b; Sevigny et al., 1991), or part of the deeper, deformed Proterozoic (Fig. 4).

3) The deep (1400 m) basalts of the M-47 drill hole are likely Coppermine lavas (Sevigny et al., 1991) and are probably part of the deformed Proterozoic.

If the basalts cored at 1400 m in the M-47 well are indeed Coppermine (Sevigny et al., 1991), it is clear that a significant amount of deformation occurred prior to the extrusion of these lavas at about 1.27 Ga following deposition of the Dismal Lakes and Hornby Bay sedimentary rocks (Cook, 1988b; Sevigny et al., 1991). If the lavas are also part of the deformed Proterozoic layers, a second phase of deformation also occurred after extrusion (Sevigny et al., 1991).

## ACKNOWLEDGMENTS

This research was supported by a research agreement (no. 016-4-91) from the Department of Energy Mines and Resources, Canada.

## REFERENCES

**Aitken, J. and Pugh, D.**
1984: The Fort Norman and Leith Ridge structures: major, buried Precambrian features underlying Franklin Mountains and Great Bear and Mackenzie plains; Canadian Petroleum Geology, Bulletin, v. 32, p. 255-268.

**Cook, F.**
1988a: Proterozoic thin-skinned thrust and fold belt beneath the interior platform in northwest Canada; Geological Society of America, Bulletin, v. 100, p. 877-890.
1988b: Middle Proterozoic compressional orogen in northwest Canada; Journal of Geophysical Research, v. 93, p. 8985-9005.

**Cook, F. and Coflin, K.**
1990: Reactivation tectonics in northwest Canada; Marine Geology, v. 93, p. 303-316.

**Pugh, D.**
1983: Pre-Mesozoic geology in the subsurface of Peel River map area, Yukon Territory and District of Mackenzie; Geological Survey of Canada, Memoir 401, 61 p.

**Sevigny, J., Cook, F., and Clark, E.**
1991: Geochemical signature and seismic stratigraphic setting of Coppermine basalts drilled beneath the Anderson Plains in northwest Canada; Canadian Journal of Earth Sciences, v. 28, p. 184-194.

Geological Survey of Canada Project 870045

# Structural studies in Southern Province, south of Sudbury, Ontario

**Frank Fueten[1] and Dan Redmond[1]**

*Fueten, F. and Redmond, D., 1992: Structural studies in Southern Province, south of Sudbury, Ontario; in Current Research, Part C; Geological Survey of Canada, Paper 92-1C, p. 179-187.*

***Abstract***

*A structural mapping project was undertaken to study the Huronian sedimentary rocks along a corridor between the south range of the Sudbury Structure and the Grenville Front. The map area is cut by two major faults, the Murray fault zone and the Long Lake fault. Both faults show evidence for early ductile thrusting with southeast side up, as well as for later motion with at least a dextral component. Changes in structural style are very pronounced across Long Lake fault, which suggests that it is the more structurally significant fault in this area. Deformed Sudbury breccia is evidence of deformation postdating the Sudbury event (1850 Ma) and disruption of 1238-Ma dykes may indicate that at least some deformation is younger. Several conglomerates have been identified in the area which are of enigmatic origin and warrant further study.*

***Résumé***

*Un projet de cartographie structurale a été entrepris pour étudier les roches sédimentaires huroniennes longeant un corridor séparant la chaîne méridionale de la structure de Sudbury et le front de Grenville. La région cartographique est découpée par deux grandes failles, la faille Murray et la faille Long Lake. Les deux failles témoignent d'un chevauchement ductile précoce accompagné d'un soulèvement du compartiment sud-est et un déplacement ultérieur caractérisé par au moins une composante dextre. Les changements très prononcés du style structural à travers la faille Long Lake en font la faille la plus significative sur le plan structural de cette région. Les brèches déformées de Sudbury révèlent une déformation postérieure à l'événement de Sudbury (1850 Ma) et les dykes disloqués de 1238 Ma pourraient indiquer qu'une certaine composante de la déformation aurait eu lieu plus récemment. Plusieurs conglomérats d'origine incertaine localisés dans la région justifient la réalisation d'autres recherches.*

[1] Department of Geological Sciences, Brock University, St. Catharines, Ontario L2S 3A1

## INTRODUCTION

During the summer of 1991 a structural mapping project was undertaken in a section of the Huronian Supergroup south of the Sudbury Structure. These metasedimentary rocks occur between the Proterozoic granitoid suite of the Grenville Front Tectonic Zone and mafic rocks that define the Sudbury Igneous Complex. The map area encompasses approximately 170 km$^2$.

The objectives of the project were to understand the deformation history in the area and to assign different aspects of the deformation to the separate events that have affected the region. The research will provide a better understanding of the role of reverse shear in the eastern Southern Province and of the northern limits of Grenvillian deformation.

The follow-up research will use structural petrology to focus on microstructural kinematic indicators (including quartz c-axis fabrics and deformed grain shape analysis) to quantify the intensity and style of deformation along the major faults in the area. It is hoped that the field data summarized here will be useful to constrain the seismic reflection data developed from the recent Lithoprobe transect.

## REGIONAL SETTING

Rocks of the eastern Southern Province form a linear easterly trending belt that separates the high grade granites and gneisses of the Grenville Province from the intrusives that form the Sudbury Igneous Complex.

The rocks have undergone several deformation events including the Penokean Orogeny (Brocoum and Dalziel, 1974; Van Schmus, 1976; Card et al., 1984), the 1850 Ma Sudbury Event (Krogh et al., 1982), post-Sudbury event deformation (1600 to 1300 Ma) (Shanks and Schwerdtner, 1989), and the 1000-1200 Ma Grenvillian orogeny (Davidson, 1986). In the map area (Figure 1), the Huronian metasedimentary rocks are more intensely deformed than their equivalents in both the Espanola region to the southwest

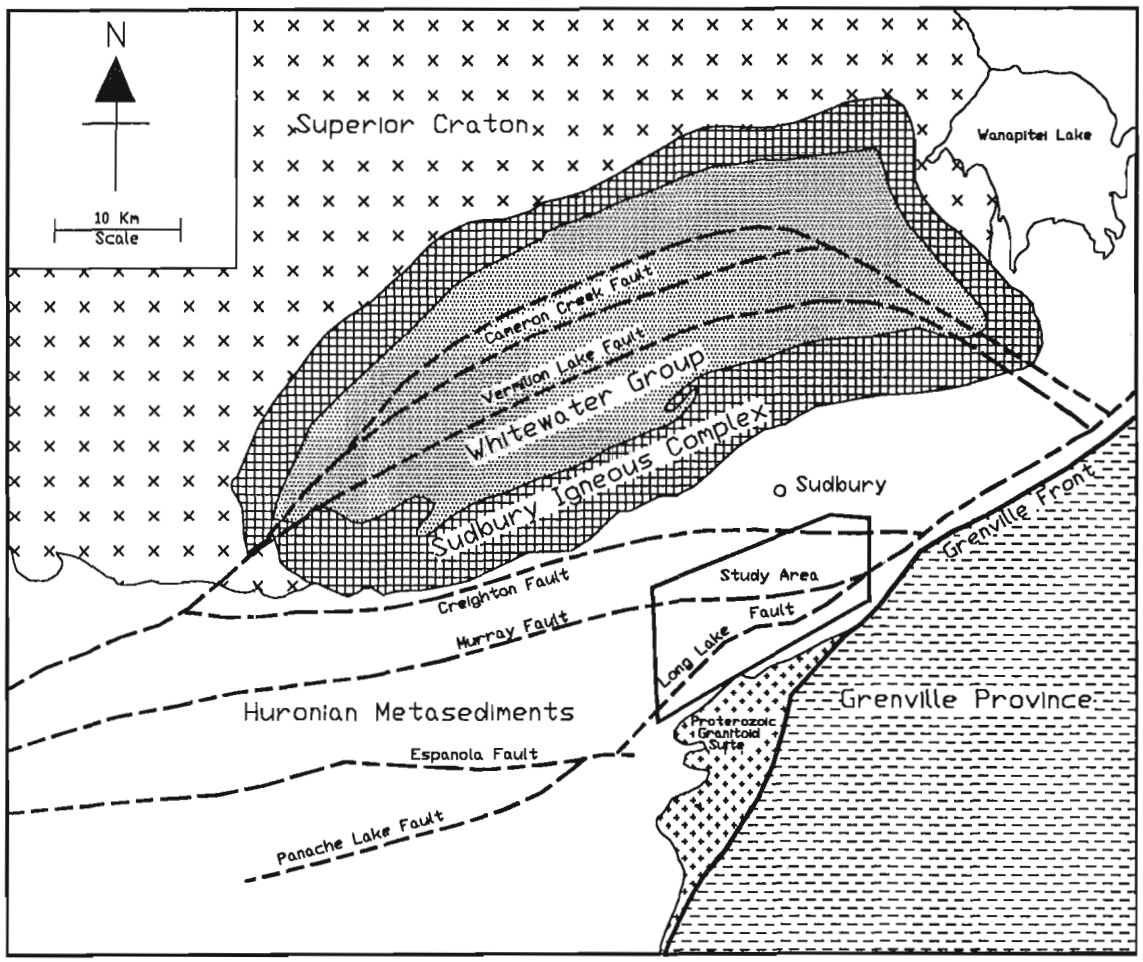


**Figure 1.** Location of study area. The figure also illustrates the orientations of major faults on the regional scale.

and the Coniston area to the northeast. The map area is transected by two major tectonic features: the Murray fault system and the Long Lake fault system.

## MAP UNITS

Rocks of the Huronian Supergroup form an early Proterozoic assemblage of volcanics and dominantly clastic sediments. Deposition of the supergroup occurred between 2500 Ma and 2219 Ma (Corfu and Andrews, 1986; Card et al., 1977). Sedimentary rocks of the Huronian Supergroup are characterized by a cyclical repetition of conglomerate, mudstone, and quartz-feldspar arenite. Based on the cyclical nature of the sediments, the Huronian Supergroup has been subdivided into four groups, namely the Elliot Lake, Hough Lake, Quirke Lake, and Cobalt groups. Rocks in the study area have been correlated with the Hough Lake Group and the lower Quirke Lake Group.

### *Ramsey Lake Formation*

Conglomerates of the Ramsey Lake Formation outcrop in several locations along the northwestern perimeter of the study area (Fig. 2). They are matrix supported polymictic conglomerates and include clast types of white quartz, white granites, and mafic rocks. The conglomerate is bimodal with 5 to 50 cm clasts forming the large fraction within a matrix containing quartz microclasts. The matrix is composed of

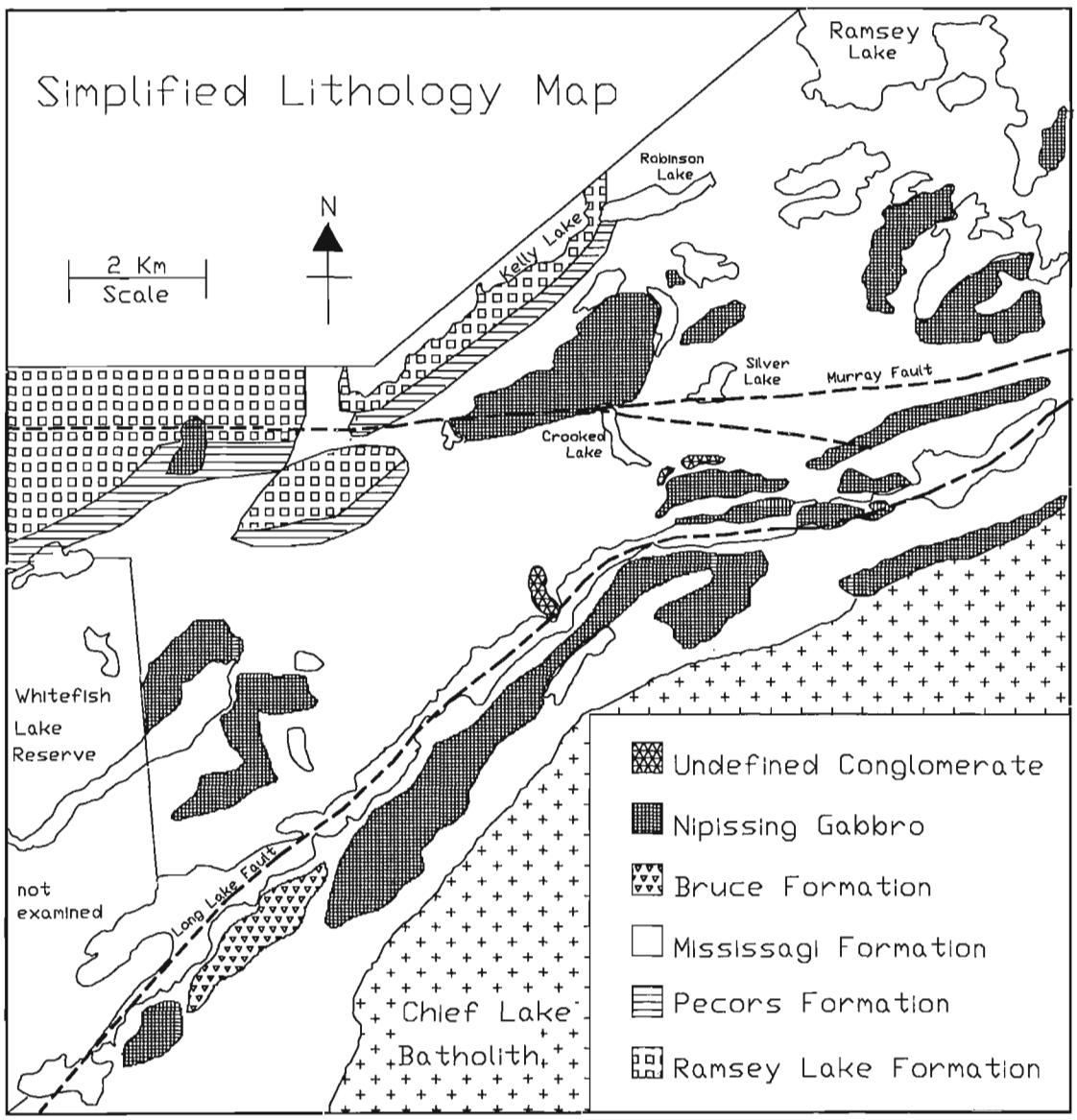


**Figure 2.** Simplified lithology map. Exposure west of Kelly Lake is poor; contacts are inferred and may be due to faulting. Note the location of the Bruce Formation and the undefined conglomerate.

muscovite and fine grained quartz with minor amounts of biotite and chlorite. The unit displays no apparent sorting and bedding is rare.

North of Robinson Lake, the conglomerate has been intensely brecciated. In this area, the Ramsey Lake Formation is up to 500 m thick.

### *Pecors Formation*

Quartz-rich pelites of the Pecors Formation conformably overlie the Ramsey Lake conglomerate. Mineralogically, rocks of the Pecors Formation consist dominantly of muscovite and/or biotite, fine grained quartz, chlorite, and minor amounts of plagioclase feldspar. The unit displays a well developed slaty cleavage and small scale sedimentary structures, including climbing ripples and small scale trough cross strata.

The contact with the overlying Mississagi Formation is gradational with the transition from pelite to sandstone occurring over 75 m in some locations. In the map area, the Pecors Formation ranges in thickness from 3 m to 100 m.

### *Mississagi Formation*

Sandstone of the Mississagi Formation is the dominant rock type in the map area and comprises approximately 80% of the total exposure. The Mississagi sandstones consist of 50 to 60% quartz, 20 to 30% feldspar, and 5 to 10% biotite and/or muscovite. Average grain size varies greatly depending on the extent of deformation and recrystallization. Fresh surfaces range in colour from dull grey to pale green. Bedding is well developed with bed thickness ranging from a few centimetres up to one metre. In most instances, quartzite beds are separated by thin (1 to 5 cm) pelitic interbeds.

Primary sedimentary structures are generally preserved in the sandstones, although many have been deformed. Planar crossbedding is the dominant sedimentary structure with lesser amounts of small scale trough-crossbedding. Due to the structural complexities, the total thickness of the formation cannot be determined in the map area. Estimates of the total thickness of the unit vary considerably from less than 425 m to 3000 m (Dressler, 1984b).

### *Bruce Formation*

Conglomerate forms a large outcrop in the southwestern corner of the map area and has been identified as belonging to the Bruce Formation by several workers (Card et al., 1977; Henderson, 1967; Collins, 1938). The Bruce conglomerate in the map area can be described as a matrix supported, polymictic conglomerate with clast sizes ranging from 1 to 10 cm on average with a few as large as 30 cm in diameter. The unit is not bedded and displays no apparent sorting of clast size or type. Clast types include both white and yellow quartzites, coarse grained white granite and minor amounts of greenstone. Clast shapes range from well rounded to angular depending on size. The larger clasts, dominantly the white granite, are quite angular whereas the smaller quartzite clasts are generally well rounded.

The matrix is composed of equal proportions of fine grained quartz and muscovite with lesser amounts of biotite. Fresh surfaces are blueish grey but weathered surfaces are rusty red. The matrix contains abundant well rounded micro-clasts (dominantly quartzite). This outcrop is surrounded by southerly-dipping Mississagi quartzites. The southern limit of the conglomerate is delineated by a large shear zone. The southwestern edge of the Bruce Formation outcrop has been intruded by Nipissing gabbro (2219 Ma; Corfu and Andrews, 1986). At the northeastern edge of the outcrop, the conglomerate is intruded by a pink granite believed to be part of the Chief Lake batholith (Henderson, 1967) dated ca. 1750 Ma (Krogh, 1967).

### *Conglomerate of undefined origin*

Conglomerates of undefined origin crop out north of Long Lake in several locations. The conglomerates closely resemble those of the Bruce Formation described south of Long Lake, with a few notable exceptions. North of Long Lake, pink granite clasts from 10 cm to 2 m in diameter are dispersed throughout the conglomerate outcrops. These granites may be loosely categorized as coarse grained or fine grained varieties and are unfoliated to poorly foliated. Pink granites have rarely been reported in the lower formations of the Huronian Supergroup, with the notable exception documented by Long (1977). The conglomerate also contains quartzite clasts (possibly Mississagi Formation) as large as 15 m in diameter (Fig. 3). The matrix of these conglomerates is gritty and contains less muscovite and more quartz than the matrix of Huronian conglomerates to the southwest. Syntectonic biotite defines the foliation. The conglomerates unconformably overlie Mississagi sandstone, but the nature of the unconformity is uncertain. Late olivine diabase dykes (1238 Ma; Krogh et al., 1987) intrude the conglomerate outcrop. Several explanations for the occurrence of these conglomerates can be advanced:

1) In the eastern part of the Southern Province, the Bruce-Mississagi contact has been described as conformable to unconformable and pink granite clasts have been described in the Bruce Formation (Long, 1977). However no pink granite clasts were identified in the Bruce Formation outcropping out south of Long Lake. If these conglomerates are part of the Bruce Formation, an explanation for the pink granite clasts may be that the northern and southern outcrops of the Bruce Formation have different source regions, or else the deformation has resulted in nearly juxtaposing very different horizons of the Bruce Formation.

2) Ramsey Lake conglomerate has been reported by Collins (1936) and Davidson (1992) near the shore of Richard Lake. These outcrops are roughly on strike with our undefined conglomerates. While quartz pebbles are commonly reported within the Ramsey Lake Formation,

large quartzite clasts have not been reported. The large clast present in our undefined conglomerate would have to be of some unit other than Mississagi Formation, as the Mississagi Formation is younger than the Ramsey Lake Formation. However if these conglomerates are Ramsey Lake Formation, one might also question the identification of the outcrops to the southeast as Bruce Formation.

3) Another explanation for these conglomerates is that they represent a post-Huronian sedimentation event. The source of the pink granites may be the Chief Lake batholith which is located less than a kilometre south of the conglomerate. Several pink granite clasts were sampled from one outcrop in the centre of Long Lake and are currently being dated at the Royal Ontario Museum. An early Proterozoic date for the pink granites would confirm this hypothesis. Clearly these conglomerates deserve further study.

### *Unconformable conglomerate*

A small outcrop of conglomerate was found 500 m north of McFarlane Lake. The total area of the outcrop is less than 100 $m^2$. This subhorizontal conglomerate unconformably overlies vertical Mississagi sandstone (Fig. 4). The unit can be described as a monomictic, unimodal, matrix supported conglomerate. The single clast type present is white quartz that may be either vein quartz or very clean quartzite. Clast size ranges from less than 1 to 3 cm in diameter. These quartz clasts are generally angular in shape. The matrix consists of quartz, plagioclase, and lesser amounts of biotite and muscovite; quartz and plagioclase have undergone some recrystallization. The unit displays no bedding or sorting of clasts. The contact with the Mississagi is erosional and the conglomerate is no more than 0.5 m thick, giving it the appearance of a thin blanket. The conglomerate is foliated but is less deformed than the underlying Mississagi sandstone.

This conglomerate appears to have formed during a post-Huronian sedimentary event. Based on the monomictic nature and limited occurrence this was a locally limited event. No similar conglomerates have been reported in the region and no other outcrops of this conglomerate were found in the map area.

### *Nipissing gabbro*

Nipissing gabbroic rocks (2219 Ma; Corfu and Andrews, 1986) have intruded Huronian metasedimentary rocks in many locations and are the second most dominant lithology in the area. Nipissing gabbroic rocks can range in appearance from large intrusive masses to narrow dykes. In most cases, gabbro outcrops trend in a southwest-northeasterly direction. This trend is most notable south of Long Lake. The gabbroic rocks are more resistant to erosion than the surrounding metasediments.

Nipissing gabbro is dull green on fresh surfaces and weathers black. In an unaltered state, Nipissing gabbro consists of fine grained plagioclase, clinopyroxene, hornblende, magnetite, and pyrite. In several locations the gabbro has been brecciated.

### *Late olivine diabase dykes*

Olivine diabase dykes (1238 Ma; Krogh et al., 1987) cut all rock types in the area. The dykes trend in a northwest direction and range in width from 30 cm to 5 m. Several of these dykes outcrop along Long Lake road, near Long Lake. They consist of euhedral grains of olivine, plagioclase, and minor clinopyroxene. Phenocrysts of plagioclase are as large as 3 cm in length. It has not been possible to trace any of these dykes across either the Murray or the Long Lake fault.

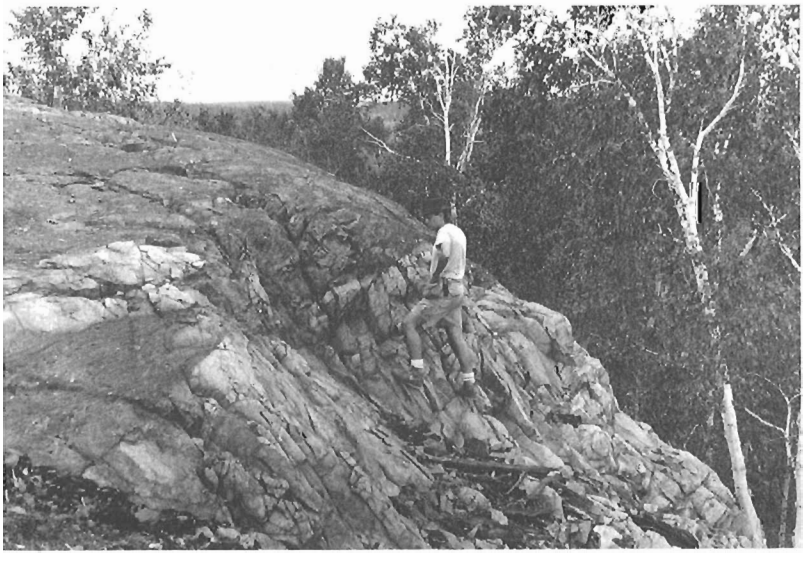

**Figure 3.** Photo of large sandstone clasts within the undefined conglomerate. The clasts are believed to be part of the Mississagi Formation. The person is standing near the contact of a 15 m long clast. Note the smaller clast at left.

### *Late rhyolitic felsic dykes*

In several locations, felsic dykes with a rhyolitic composition cut the Mississagi Formation. The most notable outcrop is located in a road cut on Long Lake Road near Silver Lake. The dyke trends in a southwesterly direction and is approximately 1 m wide. Similar outcrops of felsic dykes were found on the south shore of Crooked Lake and the north shore of Long Lake. It appears from the outcrop locations that this is a single dyke. The dyke is composed of phenocrysts of quartz, zoned plagioclase, and orthoclase in a fine grained matrix of quartz, biotite, and muscovite.

### *Structural geology*

Two major structural features cross the map area, the Murray fault and the Long Lake-McFarlane Lake fault. The faults are major structural breaks in the area and the deformation of the area will be discussed with reference to the faults.

**Figure 4.** Contact of the unconformable conglomerate with the Mississagi Formation. A fine grained tongue of the unconformable unit cuts across vertical Mississagi quartzite. The unconformable unit is less deformed than the underlying sandstone. Note that this is not a sandstone dyke but a thin layer on top of the sandstone.

### *Murray fault zone*

The Murray fault zone (MFZ) has long been considered to be an important deformation zone. Card and Hutchinson (1972) found evidence that the MFZ system originated prior to Huronian sedimentation and was initially part of a graben system forming depositional basins for Huronian sediments. During later deformation the MFZ became a southerly dipping thrust fault (Cooke, 1946; Zolnai et al., 1984) with considerable right lateral displacement (Cooke, 1946; Yates, 1948; Card, 1968; Zolnai et al., 1984). Zolnai et al. (1984) concluded 10-15 km of structural relief exists across the MFZ and attributed late brittle right-lateral movement on the Murray Fault to be due to northwest-southeast compression during the Grenvillian Orogeny.

In outcrops of Huronian sediments near or on the MFZ, bedding is invariably steeply south-dipping to vertical (Fig. 5). Angular discordances between beds are common, as is intense fracturing. No shear sense indicators were found in the field to indicate a movement direction and no markers have been found that could be traced across the MFZ. No difference in metamorphic grade is apparent across the fault; biotite occurs both north and south of it. Hence in this area there is no direct evidence for the 10-15 km of structural relief, suggested by Zolnai et al. (1984). In several localities rocks of the Mississagi Formation are cut by a network of anastomosing fractures and narrow shear zones, which outline lozenges ranging in size from metres to several millimetres. The shear zones may be several centimetres to less than a millimetre in width. The long dimensions of the lozenges lie within local bedding which controls the formation of the lozenges. The long axes of the lozenges as measured on several outcrops along the Murray fault, using the method outlined by Gapais et al. (1987), plunge between 45° to the southeast and 45° to the northwest. This technique was developed to determine the bulk kinematics in homogenous rocks. It is expected that in the layered rocks of the Mississagi formation the kinematic XZ plane will be constrained to lie in the bedding plane. However the orientation of the X and Y axis and any variation in the X/Y ratios will provide valuable information related to the larger scale kinematics of the MFZ.

In some localities a weak dip-parallel stretching lineation is developed in the Mississagi sandstones. In some areas of intense brecciation, clasts contain a stretching lineation which varies in orientation, suggesting that the brittle deformation overprinted ductilely deformed rocks. In outcrops which contain Sudbury breccia, the long axes of breccia fragments show a strong preferred orientation parallel to the foliation, when measured on a near horizontal outcrop surface. This indicates that a significant amount of deformation postdates the Sudbury event. Late sinistral and dextral minor folds with subvertical fold axes are present, indicating that there has been some late movement with a strike slip component.

As stated above, several Sudbury dykes have been found both north and south of the Murray fault. Unfortunately there is nothing distinctive about the dykes which would allow us to correlate them across the Murray fault. Davidson (1992)

reports a distinctive pair of Sudbury dykes which have dextral offset across the Murray fault. If one considers the two dykes in our area to be the same dyke, disrupted across the fault, the sense and approximate magnitude of offset would be the same as reported by Davidson (1992) and would further support a late movement with a dextral component.

### *Deformation north and south of the Murray fault*

The Huronian rocks to the north and the south of the Murray fault zone display relatively little deformation. Bedding orientations vary with both northerly and southerly dips common, however no complete folds can be traced out (Fig. 5). The rocks display little fracturing and sedimentary structures are preserved. To the north of the Murray fault, Sudbury breccia clasts display a random orientation when measured on a near horizontal outcrop surface. To the south of the Murray fault, Sudbury breccia clasts show either a weak alignment parallel to foliation or nearly random orientations. This may indicate that the area south of the Murray fault is slightly more deformed than the area to the north.

### *Long Lake fault*

The Long Lake – McFarlane Lake fault joins the Murray fault near Richard Lake in the northeast, and the Lake Panache and Espanola faults in the southwest. It can therefore be considered to be part of the Murray fault system.

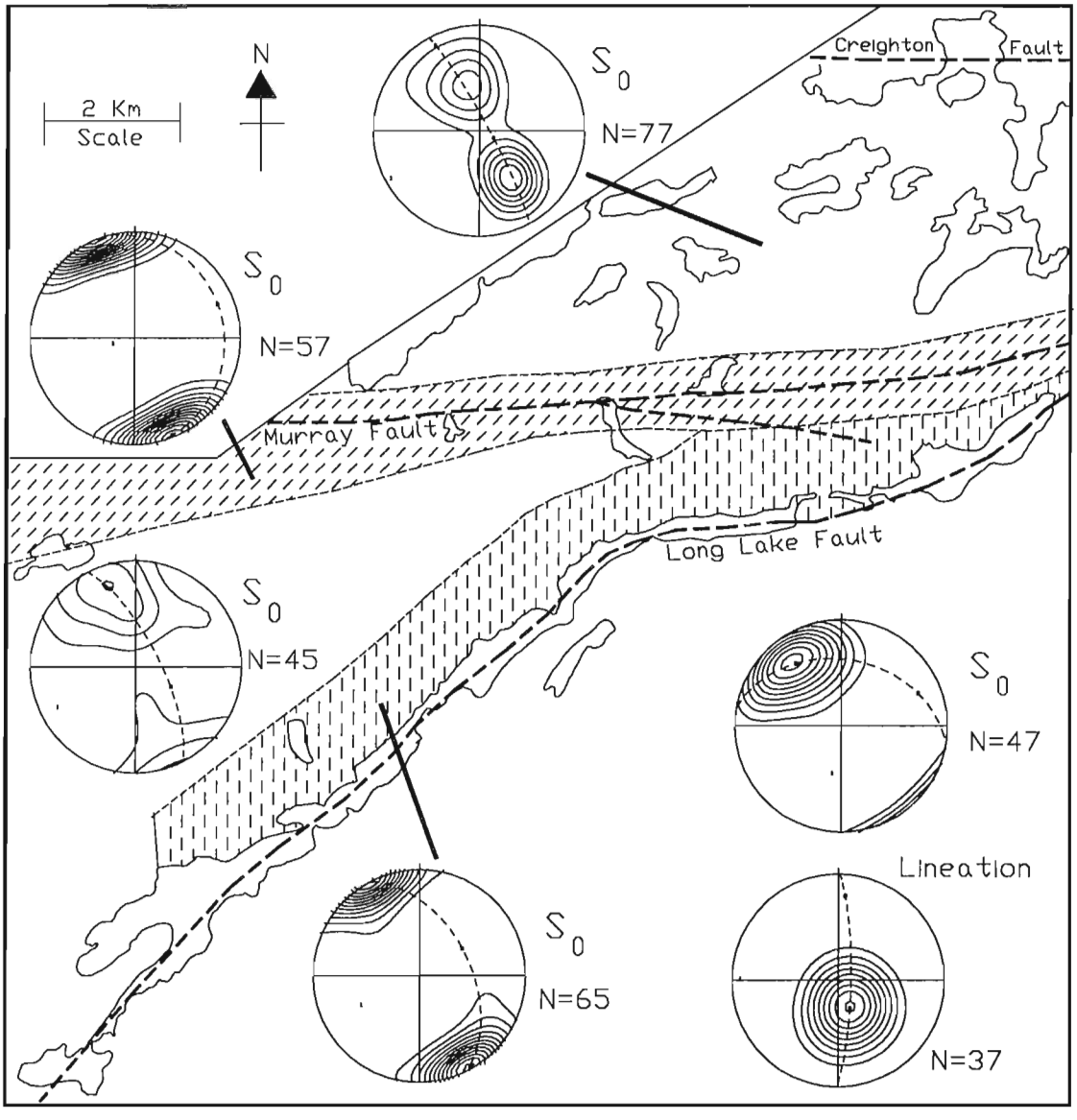


**Figure 5.** Preliminary map of bedding orientations of the different structural domains within the map area. Bedding orientations are shown for 1) the area north of the Murray fault, 2) rocks affected by the deformation in the Murray fault, 3) rocks in the triangular zone between the Murray and the Long Lake fault, 4) rocks immediately north of the Long Lake fault and 5) the area south of Long Lake. Stretching lineations are shown for the region south of Long Lake.

The Long Lake fault is a system of numerous steep southerly dipping shear zones. Individual shear zones tend to be on the order of one metre wide and may cut across bedding, separating lenses of less deformed rock. Within quartz rich bands in the shear zones a dip-parallel stretching lineation is well developed. This lineation trends between 110° and 140° and plunges between 60° and 80° (Fig. 5).

The sandstones of the Mississagi Formation do not readily produce shear sense indicators and hence the sense of movement on the fault cannot be directly deduced in the field. However, evidence argues for a south over north reverse displacement. Virtually all Huronian rocks south of Long Lake display evidence of ductile deformation. Bedding south of Long Lake consistently dips steeply to the south. A down-dip stretching lineation can be found on most outcrops south of Long Lake (Fig. 5). The outcrop of Bruce Formation south of Long Lake is surrounded by southerly dipping Mississagi Formation, and is best explained as resulting from a series of thrust imbricates.

Some outcrops of pelitic rocks south of Long Lake display retrogressed staurolite and andalusite. The staurolite has grown in the southerly dipping foliation and is therefore posttectonic or late syntectonic. The outcrops are close to the Chief Lake granite (Henderson, 1972) and it is not certain whether the staurolite and andalusite were produced during a period of regional or contact metamorphism. If they were produced during a period of regional metamorphism this may indicate significant uplift.

Immediately north of Long Lake, rocks of the Mississagi Formation display both ductile and brittle deformation features. A dip-parallel lineation is present and the rocks are intensely fractured. Where Sudbury breccia is found, the long axes of clasts display a strong preferred orientation.

As on the MFZ, evidence for a dextral component of displacement has been found on the Long Lake fault. Minor folds with vertical fold axes fold the quartz-rich layers containing the stretching lineation. The asymmetry of the folds indicates dextral motion. On one conglomerate outcrop within Long Lake, granite clasts are rotated in a dextral sense. It is unknown whether this represents a separate late dextral deformation event or if the late stage of reverse motion was oblique with a dextral component.

### *Folding*

Large regional folds are present within the Huronian Supergroup to the west of the study area and smaller folds are observed to the east of the area (Davidson, 1992). Several fold axes are indicated on the published maps of the study area (Grant et al., 1962; Card et al., 1977; Dressler, 1984a). The axial traces of an anticline syncline pair of folds have been previously mapped as cutting across Crooked Lake and the axis of a major anticline has been placed through the centre of Long Lake. No evidence was found to support the existence of these fold axes. The angular discordances of bedding near Crooked Lake which led to their interpretation as folds are due to faulting which has juxtaposed shallow dipping brittly deformed rocks of the Mississagi Formation and steeply dipping ductilely deformed Mississagi Formation. Long Lake is the site of a major fault discussed above. This fault may have started as a thrust through the limb or hinge of a major fold but there is no direct evidence remaining for folding.

Bedding orientations north of the Murray fault (Fig. 5) and in the area between the Murray fault and Long Lake fault have both northerly and southerly dips. While it was impossible to map out complete fold closures in these relatively undeformed areas, folds may be present. Davidson (1992) reports a major syncline east of Ramsey Lake in the relatively undeformed area north of the Murray fault.

### *Summary of deformation*

Both the MFZ and the Long Lake fault record ductile as well as brittle deformation. The deformation of the Sudbury breccia indicates that some ductile deformation postdates the Sudbury event (Shanks and Schwerdtner, 1989). Based on the change in deformational style across the Long Lake fault, it can be considered to be structurally more significant than the Murray fault in this area. The large regional folds which exist to the southeast and northwest of this area cannot be documented here and several previously interpreted fold axes are the result of faulting. Rocks north and south of the Murray fault are relatively undeformed with attitudes which are likely the result of folding in the Southern Province, i.e. northerly as well as southerly dips exist. Evidence for late movement with at least a dextral component is present on both faults. While the timing of the dextral motion is uncertain, there is evidence that this motion took place after 1238 Ma. One may be tempted to speculate that a dextral transpressive event is associated with the Grenvillian orogeny as suggested by Zolnai et al. (1984).

The overall deformation in the area appears to be much more intense than to the southwest or northeast of the area. The Murray and Long Lake faults converge to form a 'triangle zone' and it may well be that a room problem, created during motion on these faults, is responsible for the greater amount of deformation where these two faults are in close proximity with each other and join. Alternatively, intrusion of the Chief Lake granite to the south, or the close proximity of the area to the Grenville Front and associated Grenvillian deformation may be responsible.

## CONCLUSION

The objectives of the project are to understand the complex deformation of the Southern Province and to assign different aspects of the deformation to the separate deformation events which have influenced the region. To date the following preliminary conclusions can be made:

1) The overall intensity of the deformation increases southward. The rocks south of Long Lake are, on average, the most intensely deformed rocks in the area.

2) No large regional folds can be documented in the area. Several previously mapped fold axes are angular discordances of bedding produced by faulting.

3) Two major faults cut across the area. There is evidence for ductile thrusting as well as for later displacement with at least a dextral component on both the Murray fault zone and the Long Lake fault.

4) Deformed Sudbury breccia is evidence that deformation postdates the 1850-Ma Sudbury event. There is also some evidence that deformation postdates 1238 Ma and is therefore likely associated with the Grenvillian Orogeny.

5) Conglomerates of undefined origin have been identified and warrant further study.

Follow-up research will focus on microstructural analysis. Quartz c-axis fabrics should provide some shear sense indicators in the plastically deformed sandstones, and structural and metamorphic petrology will address the question of timing of separately identified deformation events. Dating of the conglomerate clasts will establish the maximum age of deposition.

## ACKNOWLEDGMENTS

The manuscript was greatly improved by reviews from A. Davidson, J.R. Henderson, and P. MacKinnon. (Funding primarly by EMR Research Agreement 130-4-91) Additional funding for this study was provided by Lithoprobe and NSERC operating grants to FF.

## REFERENCES

**Brocoum, S.T. and Dalziel, I.W.D.**
1974: The Sudbury Basin, the Southern Province, the Grenville Front and the Penokean Orogeny; Geological Society of America Bulletin, v. 85, p. 1571-1580.

**Card, K.D.**
1968: Geology of Denison-Waters area; Ontario Deptartment of Mines, Geological Report 60, 63 p.

**Card, K.D. and Hutchinson, R.W.**
1972: The Sudbury Structure: its regional geologic setting; in New Developments in Sudbury Geology, (ed.) J.V. Guy-bray; Geological Association of Canada, Special Paper 10, p. 67-78.

**Card, K.D., Gupta, V.K., McGrath, P.H., and Grant F.S.**
1984: The Sudbury Structure: its regional geological and geophysical Setting; in The Geology and Ore Deposits of the Sudbury Structure, (ed.) E.G. Pye, A.J. Naldrett, and P.E. Giblin; Ontario Geological Survey, Special Volume 1, p. 25-45.

**Card, K.D., Innes, D.G., and Deblicki, R.L.**
1977: Stratigraphy, Sedimentology and Petrology of the Huronian Supergroup in the Sudbury - Espanola Area; Ontario Division of Mines, Geoscience Study 16, 99 p.

**Collins, W.H.**
1936: Sudbury Series; Geological Society of America Bulletin, v. 47, p. 1675-1679.
1938: Copper Cliff sheet; Geological Survey of Canada, Map No. 292A.

**Cooke, H.C.**
1946: Problems of Sudbury Geology, Ontario; Geological Survey of Canada, Bulletin 3, 77 p.

**Corfu, F. and Andrews, J.A.**
1986: A U-Pb age for the mineralized Nipissing diabase, Gowganda, Ontario; Canadian Journal of Earth Sciences, v. 23, p. 107-109.

**Davidson, A.**
1986: A New Look at the Grenville Front in Ontario; Geological Association of Canada, Field Trip 15, Guidebook, 31 p.
1992: Relationship between faults in the Southern Province and the Grenville Front southeast of Sudbury, Ontario; in Current Research, Part C; Geological Survey of Canada, Paper 92-1C, p.

**Dressler, B.O.**
1984a: Sudbury Geological Compilation; Ontario Geological Survey, Map 2491, Precambrian Geology Series, scale 1:50 000.
1984b: The effects of the Sudbury event and the intrusion of the Sudbury Igneous Complex on the footwall rocks of the Sudbury structure; in The Geology and Ore Deposits of the Sudbury Structure, (ed.) E.G. Pye, A.J. Naldrett, and P.E. Giblin; Ontario Geological Survey, Special Volume 1, p. 97-136.

**Gapais, D., Bale, P., Choukroune, P., Cobbold, P.R., Mahjoub, Y., and Marquer, D.**
1987: Bulk kinematics from shear zone patterns: some field examples; Journal of Structural Geology, v. 9, p. 635-646.

**Grant, J.A., Pearson, W.J., Phemister, T.C., and Thomson, J.E.**
1962: Geology of Broder, Dill, Neelon, and Dryden Townships, District of Sudbury; Ontario Department of Mines, Geological Report 9, p. 1-24.

**Henderson, J.R.**
1967: Structural and Petrologic relations across the Grenville province - Southern Province Boundary, Sudbury District, Ontario; Ph.D. thesis, McMaster University, 119 p.
1972: Deformation of the Killarney Granite, Ontario, Canada; 24th IGC-Section 3, p. 505-515.

**Krogh, T.E.**
1967: Rb/Sr chronology of the granitic rocks southeast of Sudbury, Ontario; in Geochronology, (ed.) G.L. Davis, S.R. Hart, L.T. Aldrich, T.E. Krogh, and F. Munizaga; Carnegie Institution of Washington. Yearbook 65, p. 1965-1966.

**Krogh, T.E., Corfu, F., Davis, D.W., Dunning, G.R., Heaman, L.M., Kamo, S.L., Machado, N., Greenough, J.D., and Nakamura, E.**
1987: Precise U-Pb isotopic ages of diabase dykes and mafic to ultramafic rocks using trace amounts of baddeleyite and zircon; in Mafic Dyke Swarms, (ed.) H.C. Halls and W.F. Fahrig; Geological Association of Canada, Special Paper 34, p. 147-152.

**Krogh, T.E., McNutt, R.H., and Davis, G.L.**
1982: Two high precision U-Pb zircon ages for the Sudbury Nickel Irruptive; Canadian Journal of Earth Sciences. v. 19, p. 723-728.

**Long, D.G.F.**
1977: Resedimented conglomerates of Huronian (lower Aphebian age), from the north shore of lake Huron, Ontario, Canada; Canadian Journal of Earth Sciences, v. 14, p. 2495-2509.

**Shanks, W.S. and Schwerdtner, W.M.**
1989: Deformation of the Sudbury Structure and its Footwall; in Geoscience Research Grant Program, Summary of Research 1988-1989, (ed.) V.G. Milne; Ontario Geological Survey, Miscellaneous Paper 144, p. 4-17
1976: Early and Middle Proterozoic history of the Great Lakes area, North America; Royal Society of London, Philosophical Transactions, v. 12, p. 1175-1189.

**Yates, A.B.**
1948: Properties of the International Nickel Company of Canada; in Structural Geology of Canadian Ore deposits, Canadian Institute of Mining and Metallurgy, Jubile Volume, pt. 7, p. 596-617.

**Zolnai, A.I., Price, R.A., and Helmstaedt, H.**
1984: Regional cross section of the Southern Province adjacent to Lake Huron, Ontario: implications for the tectonic significance of the Murray Fault Zone; Canadian Journal of Earth Sciences, v. 21, p. 447-456.

# Structure and stratigraphic succession of an Archean stratovolcano, Slave Province, Northwest Territories

**M.B. Lambert, C. Beaumont-Smith[1], and D. Paul**
**Continental Geoscience Division**

*Lambert, M.B., Beaumont-Smith, C. and Paul, D., 1992: Structure and stratigraphic succession of an Archean stratovolcano, Slave Province, Northwest Territories; in Current Research, Part C; Geological Survey of Canada, Paper 92-1C, p. 189-200.*

***Abstract***

*Four volcano-sedimentary sequences define the stratigraphy and major episodes of volcanism, construction, and erosion of this stratovolcano. The Innerring sequence represents the upper part of an ancestral volcano. The Thlewycho sequence, documenting the main constructional phase of the stratovolcano, varies from 5 cycles of lava effusion followed by deposition of volcaniclastic debris on the north side, to effusion of 30 subaerial, dominantly-andesitic lava flows on the eastern side. The northern Boucher-Regan sequence, records effusion of basaltic pillow lava followed by andesitic lavas and late stage felsic lava domes. The Keish sequence is a clastic fan recording erosion of the volcanic pile. Sulphidic iron-rich mudstone/siltstones and iron-formations mark the close of each major volcanic cycle.*

*The form of the volcanic complex defines a regional scale, northwest oriented, refolded, doubly plunging, second generation structure. During deformation the complex behaved as a large competent mass within a ductile sedimentary matrix.*

***Résumé***

*La stratigraphie et les principaux épisodes de volcanisme, de construction et d'érosion de ce stratovolcan sont définis par quatre séquences volcano-sédimentaires. La séquence d'Innerring représente la partie supérieure d'un volcan ancien. La séquence de Thlewycho, documentant la principale phase de construction du stratovolcan, varie de cinq cycles d'effusion de laves à un dépôt de débris volcanoclastiques sur le flanc nord, à l'effusion de 30 coulées de laves andésitiques subaériennes sur le flanc est. La séquence septentrionale de Boucher-Regan, fait était d'une effusion de laves en coussins basaltiques suivies de laves andésitiques et de dômes de lave felsique de stade tardif. La séquence de Keish est un cône clastique témoignant de l'érosion de l'amas volcanique. Des mudstones et siltstones ferrifères sulfurés et des formations ferrifères marquent la fin de chaque cycle volcanique important.*

*La forme du complexe volcanique définit une structure de seconde génération à plongement double, replissée , orientée au nord-ouest et d'échelle régionale. Durant la déformation, le complexe s'est comporté comme une vaste masse compétente au sein d'une matrice sédimentaire ductile.*

[1] Department of Geology, University of New Brunswick, Fredericton, New Brunswick E3B 5A3

## INTRODUCTION

The Back River volcanic complex (of the Back Group, Yellowknife Supergroup; Henderson, 1970) is a ca. 2.7 Ga (van Breemen et al., 1987) stratovolcano which lies about 480 km northeast of Yellowknife, N.W.T. Previous publications (Lambert, 1976, 1977, 1978, 1982a, b; Moore, 1977; Frith, 1987; Lambert et al., 1990) provide generalized descriptions of rock units and outline preliminary stratigraphy of the complex, which is exposed in a structural dome. This paper presents new data that: (1) records detailed stratigraphy of large, previously undivided volcanic units, (2) provides a basis for subdivision of the complex and (3) documents deformational events in the volcanic formations that were identified previously (Lambert et al., 1990) in metaturbidites of the overlying Beechy Lake Group.

Three new stromatolite localities were found in addition to the 6 localities discovered in 1989 (Lambert, et al., 1990).

## STRATIGRAPHY

Stratigraphy of the volcanic complex is presented in terms of four volcano-sedimentary sequences that reflect stages of growth and destruction of this complex Archean stratovolcano. These informal sequences are referred to herein as the Innerring sequence, Thlewycho sequence, Boucher-Regan sequence, and the Keish sequence (Fig. 1). The Innerring and Thlewycho sequences comprise the main part of the stratovolcano. The Boucher-Regan sequence represents a dominantly subaqueous succession deposited in the northern parts of the complex and may include units related to both of the major constructional episodes to the south. The Keish sequence documents erosion from the western flanks of the volcanic pile.

### *Innerring sequence*

The Innerring sequence includes lavas and tuffs exposed in an 8 x 12 km elliptical area near the south-central part of the complex. Because of their position at the crest of a structural dome, the units are gently dipping to almost flat lying and only the uppermost part of this sequence is exposed. All units have features consistent with subaerial deposition.

The exposed succession comprises massive porphyritic andesite lava units overlain by dacite lavas (one flow is more than 35 m thick) and massive volcaniclastic units interpreted as ash-flow tuffs. A rhyolite lava dome along the eastern side of the sequence has a carapace of monomictic megabreccia and an apron of landslide debris. The monomictic megabreccias commonly contain rhyolite blocks up to 1 m, and in one place up to 20 m across, enclosed in an intact framework of cobble- to pebble-sized clasts.The top of this sequence is defined by mudstone units exposed intermittently along the east central side of the sequence and on the north and northwestern sides near Innerring Lake.

On the eastern side, (locality 1, Fig. 1) the sedimentary sequence overlies a rhyolite/dacite lava dome. Here, a coarse clastic margin of the lava dome grades upwards from closely packed carapace breccia to rhyolite fragment breccia and pebble conglomerate. These clastic rocks have a poorly-sorted, carbonate-cemented, felsic granule matrix with no distinct bedding. Conformably overlying this rhyolitic debris apron is a 35 metre succession consisting upward of laminated siltstone, black slates and shale, black siltstone and green volcanic siltstone. The shale/siltstone units contain abundant disseminated pyrite and pyrite- rich layers that weather as prominent gossans. Although this pyrite-rich succession may be considered as a sulphide iron-formation, no banded chert-magnetite or chert-hematite iron-formation is exposed. Pyrite also occurs as nodules up to 20 cm across in underlying rhyolite. Neither the upper part of this sedimentary succession nor the contact with the Thlewycho sequence are exposed at this locality.

This sedimentary sequence is equivalent to the sulphide-rich black mudstones that occur beneath rhyolite lava flows of the Thlewycho sequence at Innerring Lake. At this locality the lower parts of the black mudstone succession are cut off by an arcuate rhyolite body that has intruded between the Innerring and Thlewycho sequences. This body was previously interpreted as a ring fracture intrusion (Lambert, 1978) and may be the roots of domes that effused at the surface.

Along its southern side, the Innerring sequence appears to be overlain conformably by andesitic lavas of the Thlewycho sequence: the shale/siltstone units are absent.

### *Thlewycho sequence*

The Thlewycho sequence describes an annulus around the Innerring sequence that extends eastward to the Back River, westward to Thlewycho Lake, and northward almost to Boucher Lake. It is essentially a homoclinal succession that dips radially outward from the centre of the dome. Attitudes of units are 25-30° on the eastern side, 35-50° on the northern side, and steep (60-80°) along the western side.

Stratigraphy within this sequence changes dramatically around the volcano. Figure 2 illustrates the stratigraphic variation in two sections, one near Rusty Lake (north) and the other at Gold Lake (east).

The base of this sequence is defined at the first lava effusions above the mudstones that marks the end of the Innerring sequence. The top of the sequence is at the mudstones, iron-formation, or turbidites of the Beechy Lake Group.

#### Gold Lake section

This section, exposed on the west side of Gold Lake, comprises dominantly subaerial andesitic lavas and few intermittent pyroclastic and epi-volcaniclastic units totalling about 2500 m thick, plus felsic domes to north and south of section amounting to another 300-500 m. The section (Fig. 2) documents the following eruptive sequence.

1. Eruption of three 5-10 m felsic lavas each separated by bedded felsic volcaniclastic siltstones or tuff. These interflow volcaniclastic rocks contain abundant pyrite and form prominent gossans in the lower part of the sequence. Sulphidic alteration spread along interflow sediments for as much as 1700 m and locally has completely altered parts of several lava flow units. Alteration stops abruptly at the base of one lava flow unit which makes a baked contact with the underlying pyrite-rich volcanic sand. This area of intense alteration that has sulphidized and bleached part of the lava sequence may mark a fossil vent.
2. Continuous eruption of 1100 m of andesitic lavas (12 flows) ranging from 7-110 m thick. These flows, characterized by massive interiors and thick flow breccias at tops, and by an absence of pillowed units, are typical subaerial lava flows.
3. Explosive eruptions produced about 300 m of pyroclastic flows interrupted by 1 or 2 thin lavas. The uppermost 15 m of this unit comprises four air-fall pyroclastic cycles each comprising crudely layered agglomerate overlain by fine-ash tuffs (see inset, Fig. 2). The agglomerates contain scoriaceous bombs and blocks 1-15 cm across in fine ash to lapilli tuff matrix. These cycles document four explosions that occurred before the effusion of the next lava series.
4. Deposition of 170 m of breccias, air fall tuffs, and agglomerates.
5. Effusion of 8 andesitic lava flows (totalling 425 m thickness) topped by two 50-60 m thick dacite lavas.
6. Effusion of a large rhyolite dome/flow complex (1500 x 7300 m) south of Gold Lake (see Lambert et al., 1990, for detailed description of this dome).

Avalanches locally spread across and filled valleys in the latter lavas and dome effusions.

### Rusty Lake section

The Rusty Lake section, totals close to 5 km thick. It may in part form an onlapping succession and thus was never a single pile of that thickness. The thick units shown in this section are lenticular and taper out or change facies around the eastern and western sides of the complex.

Compared to the Gold Lake section, the Rusty Lake section has a high proportion of volcaniclastic units, fewer but much thicker flow units, a higher proportion of felsic lavas, and shows a change in depositional environment from subaqueous in the lower half to subaerial in the upper parts.

This section illustrates 5 cycles of lava effusion followed by volcaniclastic sedimentation and the following sequence of events.

1. Effusion of two rhyolite lava flows.
2. Deposition of a thick succession of volcaniclastic rocks comprising:
   a) 20+ m well bedded succession containing laminated to crossbedded sand and silt, volcanic turbidites (30 cm to 2 m and rarely 5 m thick), and small (ca. 2 m thick) subaqueous debris flows (Fig. 3). Many thin (1-2 cm) layers of fine water-laid ash dispersed throughout the succession (Fig. 4) indicate numerous minor explosive events that were harbingers of the major eruptions to follow.
   b) 600-700 m of bedded volcaniclastic units.
   c) About 1000 m of thick massive volcaniclastic units that include debris flows and possibly pyroclastic flows. These volcaniclastic units typically contain abundant felsic clasts. Thin-bedded ash horizons, in some cases are only 20 cm thick, mark boundaries of depositional units.
3. Subaqueous eruption of dacitic then andesitic pillow lavas. Blocks of vesicular dacite in cores of some andesite pillows, indicate that the andesite erupted through the dacite pillowed pile.
4. Eruption of massive plagioclase phyric andesite lava flows forming units 150 to 300 m thick.
5. A monogenetic rhyolite dome 700 m across protruded these lavas.
6. Continued eruption of porphyritic andesite lava and related breccias overlain by, and interbedded with, massive volcaniclastic rocks; possibly pyroclastic flows and debris flows.
7. Effusion of a thick andesitic lava and volaniclastic rocks.
8. Deposition of a thick succession of volcaniclastic units including pyroclastic flows and debris flows and turbidite-like units. They were interrupted twice by eruption of local small columnar jointed rhyolite lava flows (Fig. 5).
9. Major eruption of 7 rhyolite and dacite lava flows of total thickness about 1400 m.

### *Boucher-Regan sequence*

This sequence is loosely defined as including most of the volcanic units between Outterring Lake (3 km north of Rusty Lake) and Regan Lake. It may include flows and tuffs of the Thlewycho sequence to the south.

The only major volume of basaltic pillow lavas in the volcanic complex occurs near the apparent base of the sequence in the northwestern part of the map area and about 12 km west of the main complex. West of Regan Lake the basalts are overlain by a diverse unit of andesitic pillow lavas, breccias, and massive flows that form extensive units to the southeast. Along the western margin of the complex the basalts are overlain directly by turbidites of the Beechy Lake Group. Dacitic lavas, tuffs, and lava domes locally overlie the andesitic units. The youngest part of this sequence is a large rhyolite lava dome and a series of smaller rhyolite domes that occur along the northwestern and western sides of the volcanic complex. Some of these lavas overlie or

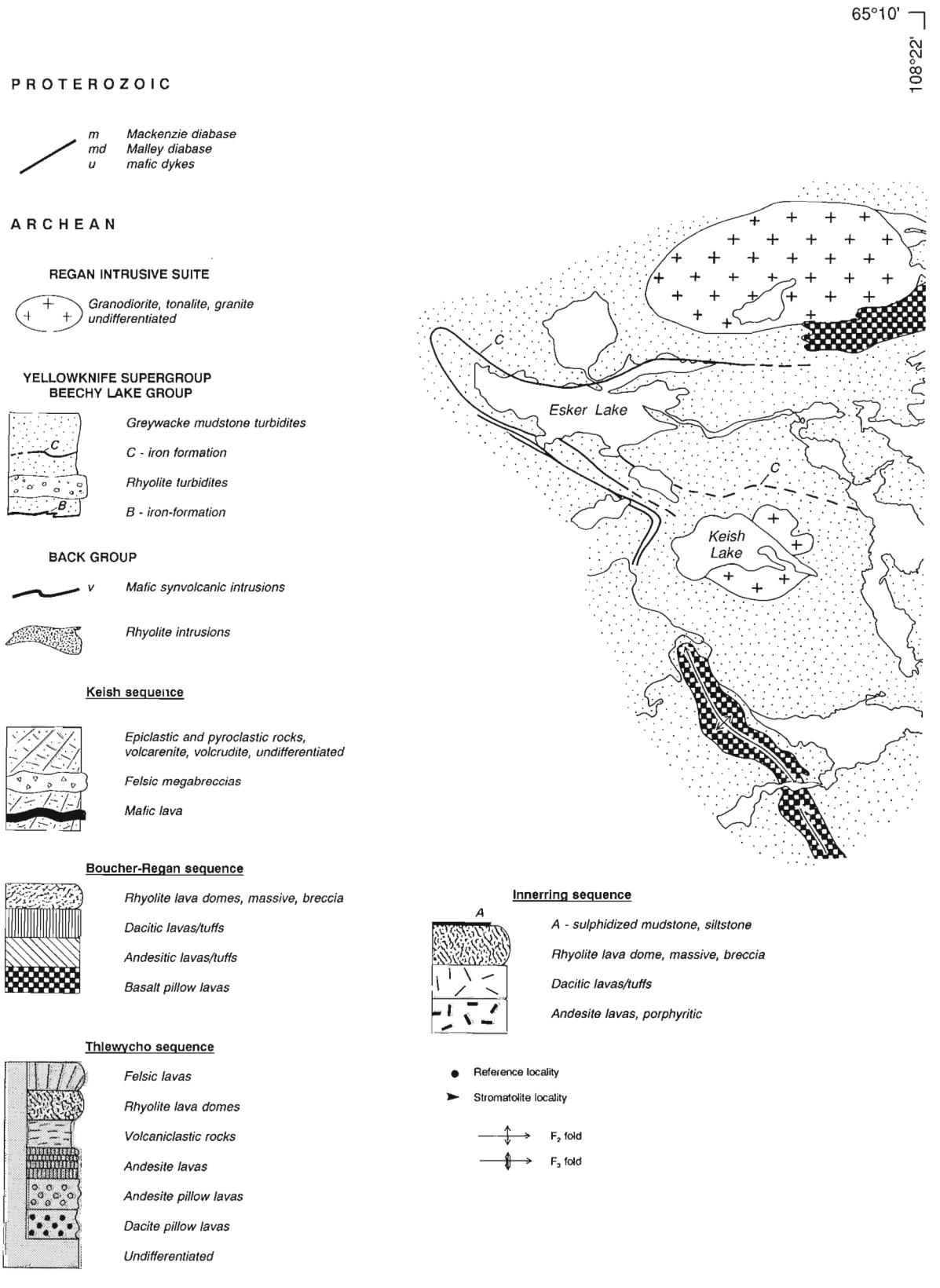


**Figure 1.** Generalized geology of the Back River volcanic complex.

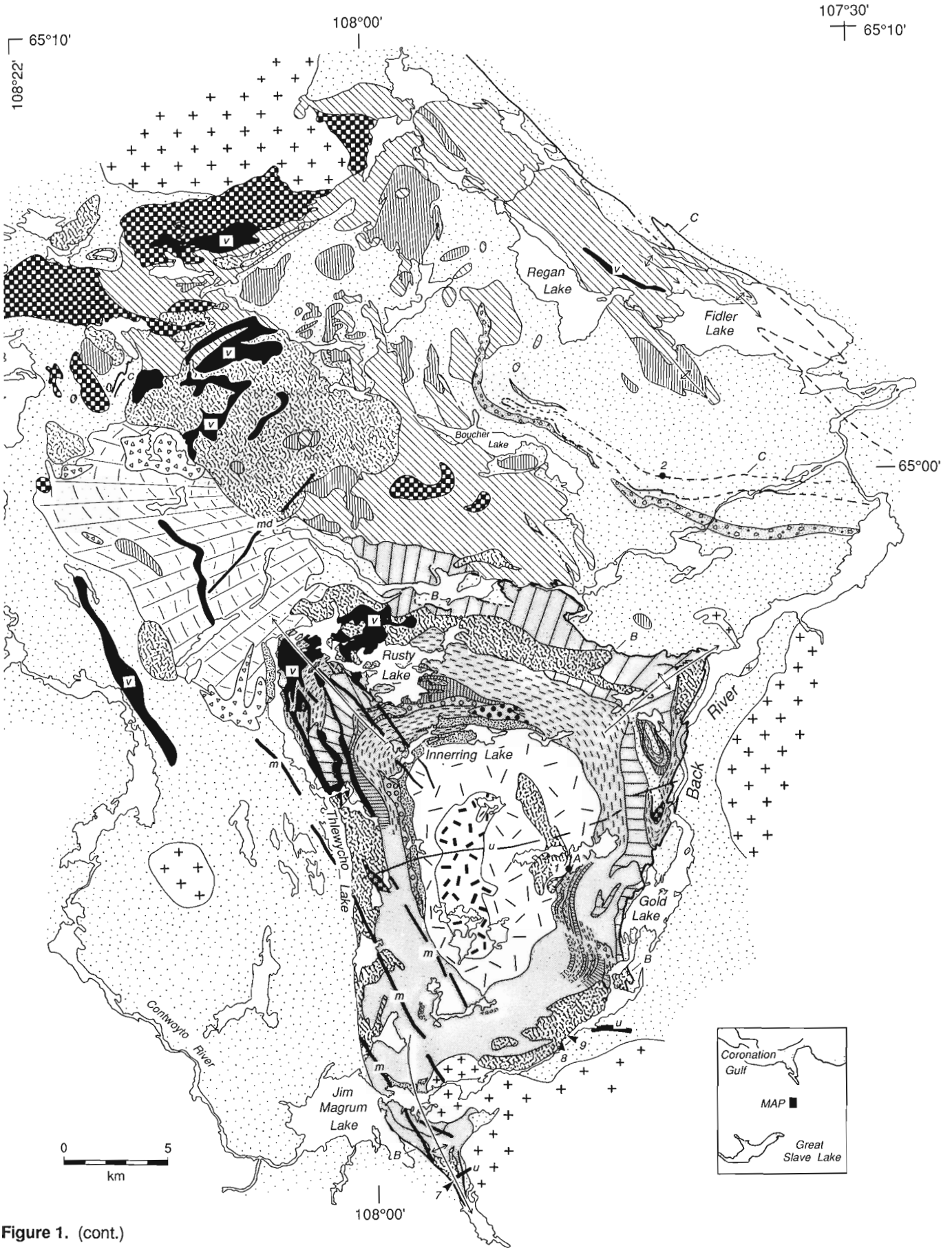


**Figure 1.** (cont.)

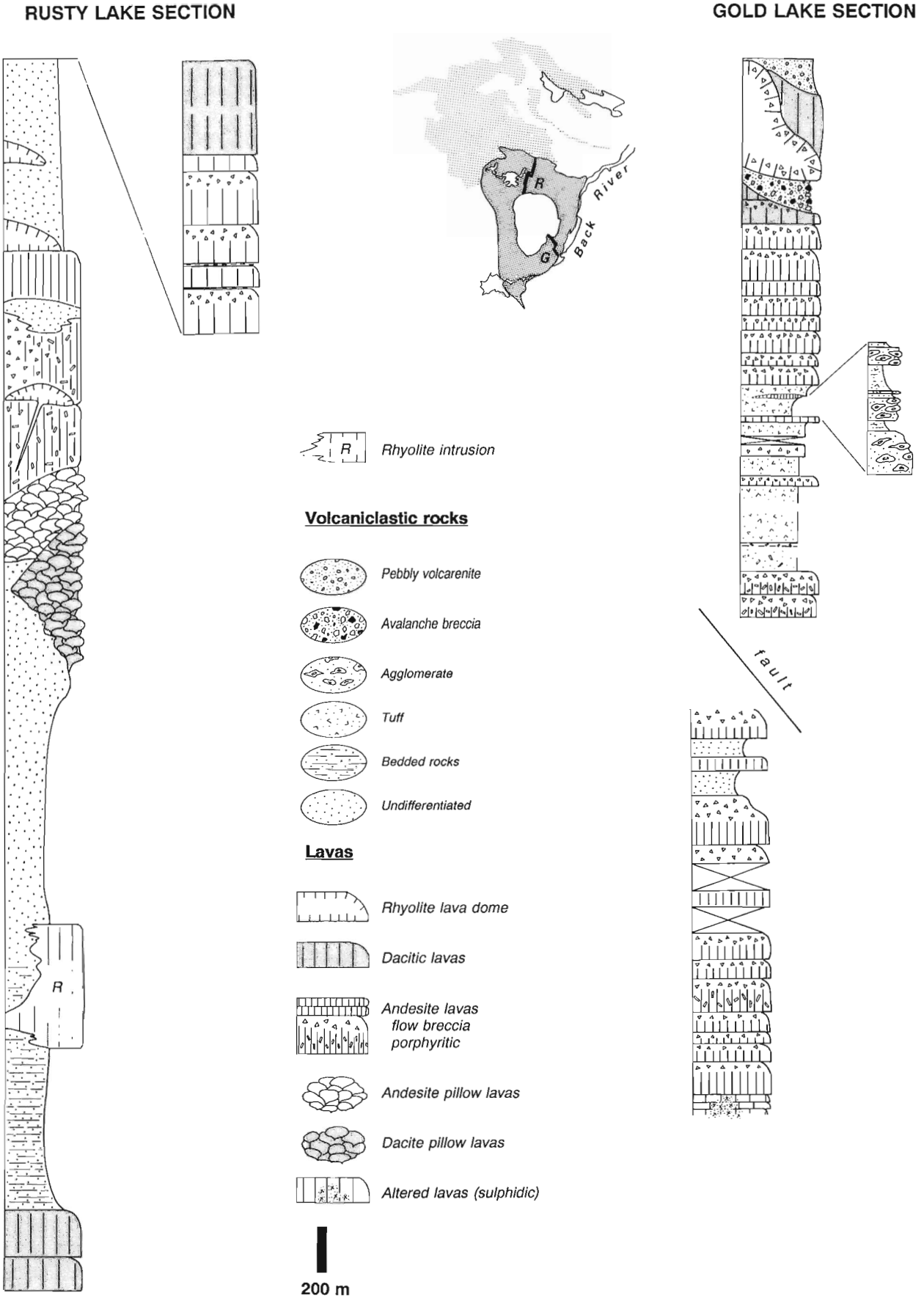


**Figure 2.** Stratigraphic sections through the Thlewycho sequence (dark grey in index map) near Rusty Lake and west of Gold Lake (R and G respectively in index map).

interfinger with Beechy Lake Group turbidites. Although most of the Boucher-Regan sequence was deposited in a subaqueous environment, some of the felsic lavas/domes may have emerged.

### *Keish sequence*

This sequence forms a broad apron chiefly of volcaniclastic sediments centred about 7 km southeast of Keish Lake in the western part of the map area. The diverse sequence contains epiclastic volcarenite, monomictic rhyolite to dacite block breccias (of debris flow, scree or landslide origin) adjacent lava domes, polymictic breccias and conglomerates containing andesite and dacite/rhyolite clasts, andesitic tuffs, and a single unit of mafic pillowed to massive lava.

**Figure 3.** Debris flow 10 m above base of lowest volcanclastic succession of Rusty Lake section (Fig. 2), Thlewycho sequence. This 2 m thick unit has inversely graded base, intact framework of large clasts in centre and massive, poorly sorted pebbly sand to coarse sand in upper half. The flow rests on thin bedded coarse sandstone. Scale bar is 50 cm. GSC 1991-579B.

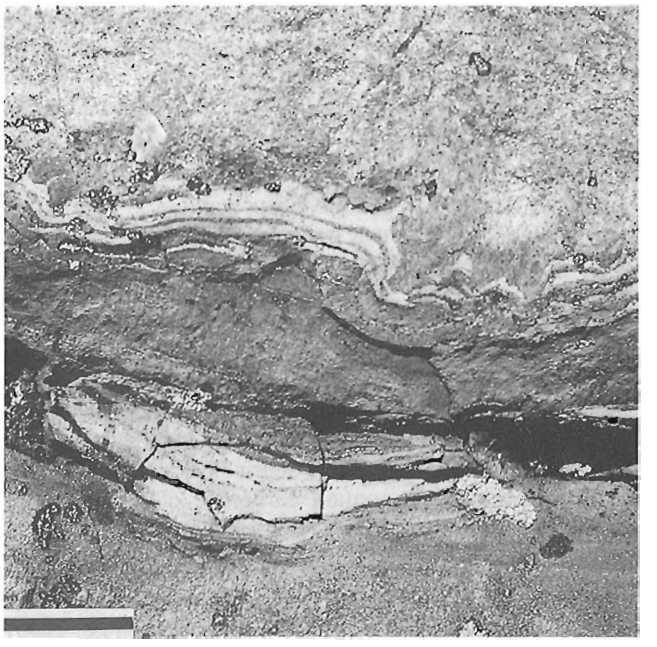

**Figure 4.** Load and flame structures in white volcanic ash layers at the base of a 20 cm thick turbidite unit in thin bedded rocks, 4 m above base of lowest volcaniclastic succession of the Rusty Lake section (Fig. 2), Thlewycho sequence. Scale bar is 2 cm. GSC 1999-579E.

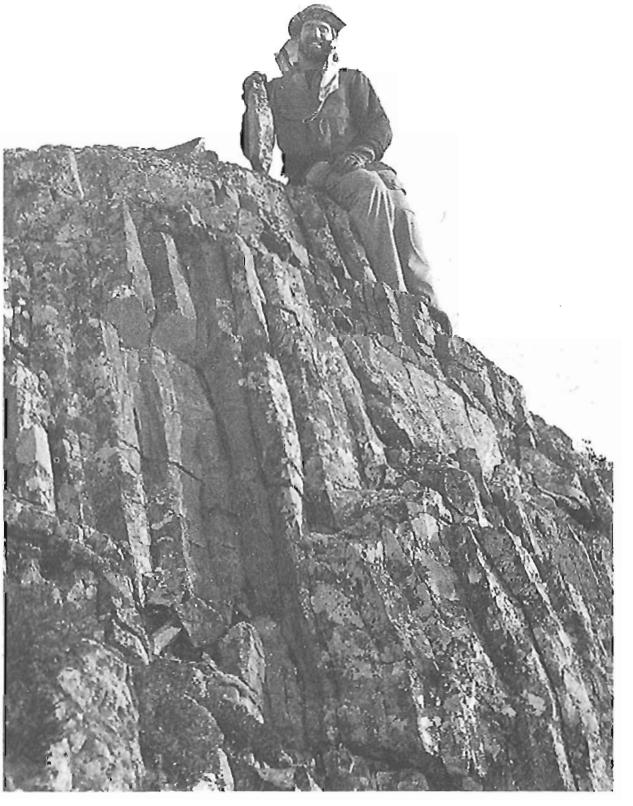

**Figure 5.** Columnar jointed rhyolite lava flow on island near the east side of Rusty Lake. Near vertical columns attest to the shallow attitude of flows in this area.

This sequence is interpreted as a submarine clastic fan derived by degradation of the volcanic pile on its northwest side.

## CARBONATE UNITS

Carbonate occurs throughout the volcanic complex but is most abundant as cement or fracture fillings in felsic breccias of rhyolite domes, pods and lenses in faults and shear zones, breccia zones around arcuate ring fracture intrusions, and rhyolite flow breccias at the top of the Thlewycho sequence (Lambert, 1978; Lambert et al., 1990). At the top of the Thlewycho sequence carbonate is less common as a primary chemical sediment in the form of interlayers in cherty iron-formations and stratified carbonate locally containing oolites and stromatolites. Some debris flows associated with rhyolite lava domes, contain carbonate clasts indicating presence of primary carbonate strata.

Stromatolites were found at 3 new localities (localities 7, 8, and 9, Fig. 1) in addition to the 6 localities where they were first discovered in 1989 (see Fig. 1 in Lambert et al., 1990). Like the previous finds, the new localities are at the boundary between late stage rhyolite/dacite domes of the Thlewycho sequence and the overlying turbiditic sedimentary rocks of the Beechy Lake Group.

Co-ordinates of new localities are:

| Locality | Latitude | Longitude |
|---|---|---|
| 7 | 64°42′05″N | 107°55′40″W |
| 8 | 64°45′33″N | 107°48′55″W |
| 9 | 64°45′35″N | 107°48′42″W |

At Locality 7 (southeast of Jim Magrum Lake) stromatolites occur in an area about 2 m across within carbonate impregnated, dacite breccia associated with a felsic dome complex where they are best preserved within 2 m of the southern contact of an east trending gabbroic dyke. They form a 10-15 cm thick horizon between brown weathering, massive, carbonate-cemented sand and underlying breccia containing blocks 2-20 cm across. The stromatolites have grown around larger blocks in the breccia. In plan view they form concentric laminations (3-5 mm thick) 15 to 25 cm across.

Locality 8 is about 110 m north of locality 2 on the west shore of the Back River. Here stromatolites have overgrown vesicular rhyolite blocks that are part of a carbonate cemented coarse breccia apron at the margin of a large rhyolite dome. Stromatolites form small laminated mounds 5-12 cm high (Fig. 6) and 10 to 25 cm apart. The stromatolite horizon is generally less than 15 cm thick. Well bedded, poorly sorted, coarse sand has filled troughs between the stromatolite mounds. This locality records short lived biological activity that has been abruptly terminated by high-energy influx of coarse clastic material.

At Locality 9, stromatolite laminae that accumulated to a thickness less than 5 cm, have grown over blocks of black scoreaceous basalt. The growth mounds are about 3 cm high. The blocks are part of a nonlayered and poorly sorted breccia deposit, exposed for about 75 m along the shoreline, comprising angular to subangular blocks (ranging from 5 to 200 cm across) of scoreaceous basalt and minor clasts of vesicular rhyolite in a dark grey arenaceous matrix. The nature of this deposit, its restricted distribution and the lack of any basaltic lava in the general area suggests that this rudite was transported to a shoreline possibly by landslide or debris

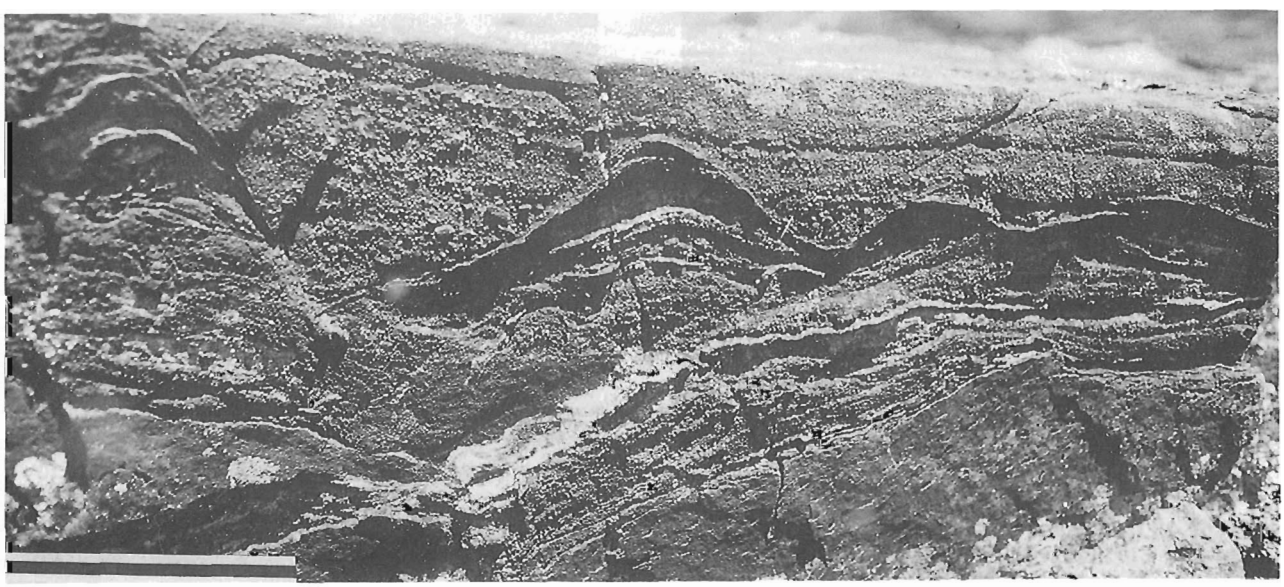

**Figure 6.** Stromatolites at Locality 8. Coarse sand detritus has filled troughs between laminated stromatolite mounds. Scale bar is 10 cm. GSC 1991-579I.

flow. The blocks are clasts derived from a scoreaceous lava flow and do not have the internal structure nor external form of bombs.

## IRON-FORMATIONS

Three iron-rich sedimentary sequences (labelled A, B, and C, in Fig. 1) were described previously (Lambert et al., 1990; Jefferson et al., 1989) in volcanic and sedimentary strata near this complex. Sequence A occurs at the boundary between the Innerring and Thlewycho volcanic sequences. Sequences B and C both lie above the volcanic complex and are considered part of the Beechy Lake Group.

Sequence C, north of Boucher Lake, was previously interpreted, on the basis of a strong aeromagnetic anomaly, as a single unit. Further mapping of this unit in 1991 revealed that it traces the crest of a overturned anticline. On the north limb of the fold (locality 2) an iron-rich sequence comprises 6 units of banded iron-formation, ranging from 30 cm to 7.5 m thick, separated by turbidite units and fine laminated siltstone (Fig. 7, 8). Cumulative thickness of iron-formation is 20 m. The group of iron-formation strata is overlain and underlain by 10-15 m of finely laminated siltstone forming a package about 50 m thick within thin- to thick-bedded turbidites. Weakly magnetic, magnetite-bearing green-grey siltstones, occurring 4 km northwest of the nose of the folded iron-formation, also contribute to the strong magnetic anomaly in this area.

The stratigraphic distance of this iron-formation above major units of the volcanic complex (or from the rhyolite turbidite unit or bedded volcaniclastic units related to the volcanic complex) ranges from 200 to 500 m.

## STRUCTURAL GEOLOGY

The Back River volcanic complex has undergone three deformational events easily observable within metaturbidites of the Beechy Lake Group (Lambert et al., 1990). Work in 1991 extended the structural geology from metaturbiditic rocks into the volcanic rocks.

### *Structures in metaturbidites*

The first deformation ($D_1$) produced isoclinal to tight folds occurring at scales from kilometre amplitude to centimetre scale intrafolial folds (Fig. 9). Due to the lack of marker horizons within metaturbidites the folds are rarely observed and most commonly recognized by reversals in facing direction. The development of foliation associated with this generation is heterogeneous, but it usually forms a bedding-parallel slaty cleavage ($S_1$).

The dominant structural event in this area, the second deformation ($D_2$), formed tight to isoclinal folds and regional $S_2$ foliation. $F_2$ structures are moderately to steeply plunging similar folds with steep axial planes. Local attenuation of the limbs has produced small shear offsets along the foliation. Bedding/cleavage relationships involving $S_2$ are the most useful features for the structural interpretation. The morphology of the $S_2$ foliation is a function of heterogeneous development of $S_1$. $S_2$ forms crenulation cleavage and crenulation lineation in areas where $S_1$ is developed, and a domainal slaty cleavage in areas where $S_1$ is not developed. Thus, $D_1$ and $D_2$ show considerable overlap in the style of

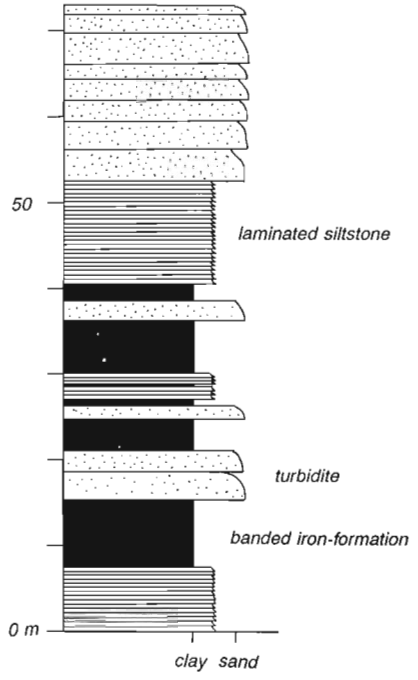


**Figure 7.** Stratigraphy of banded iron-formation north of Boucher Lake. Locality 2.

**Figure 8.** Banded iron-formation north of Boucher Lake (Locality 2), from section in Figure 7. GSC 1999-579A. Scale bar is 2 cm.

both folds and foliation. Although $F_2$ folds may be common, the lack of markers makes their identification difficult and overprinting relationships are rare.

These two deformation events appear to have occurred before the peak of metamorphism. In the southern part of the map area, metamorphic conditions reach lower amphibolite grade with development of cordierite-staurolite-biotite and andalusite-cordierite-biotite assemblages. Coarse, helicitic cordierite porphyroblasts include $S_2$ foliation, therefore the porphyroblasts grew after the second deformational event. $S_1$ has not been identified within cordierite.

The youngest penetrative deformation ($D_3$) forms rare northwest- and northeast-orientated open folds and kink bands. These structures locally form conjugate pairs but generally occur in domains of one orientation. Northwest orientation is the most prevalent along the western and southern margins of the complex. The $F_3$ folds are open, weakly asymmetrical, and they plunge moderately to the north. They appear to be the product of flexural slip and plunge down earlier structures. The most common feature of this event is a differentiated crenulation cleavage ($S_2$) and crenulation lineation. In compositionally graded semipelite-pelite beds $S_2$ and $S_3$ form a "herring-bone" cleavage in which $S_2$ is well preserved in the semipelite layers and $S_3$ is preferentially developed within the pelitic horizons. The two foliations are at an angle of about 60 degrees to each other. This deformational event took place after peak metamorphic conditions, rotating the helicitic porphyroblasts with $S_3$ wrapping around them.

### *Structure in volcanic rocks*

Due to the contrast in competency between the metaturbidites and rocks of the volcanic pile, deformation has been partitioned along the southern boundary of the volcanic complex. This partitioning is expressed by highly strained and locally mylonitic rocks along much of the southeastern and southwestern boundary of the complex, especially in the carbonate-impregnated breccias. The high strain zones involve a 1 km width of the southwestern boundary but they are restricted to the carbonate cemented breccias along the southeastern side. The interior of the complex is relatively unstrained.

$S_2$ foliation parallels the boundary of the complex. Although $F_2$ has steep axial planes in the turbidites, $S_2$ becomes shallower as the complex is approached, suggesting that $F_2$ folds become reclined near the complex. Immediately adjacent to the complex, $F_2$ folds become noncylindrical with highly variable plunges. Near the contact, development of shear fabrics within metavolcanic rocks that have the same orientation as $S_2$ suggests that the boundary of the complex became the locus of deformation during $D_2$.

$D_2$ deformation forms large folds of the volcanic boundary that plunge both northeasterly (10 km north of Gold Lake) and southeasterly (near Jim Magrum Lake). Mylonitic rocks are best seen along the western boundary of the complex south of Thlewycho Lake. In this area, intense $S_2$ development in metaturbidites can be traced into the

**Figure 9.** Intrafolial $F_1$ fold transected by $S_2$ in turbidite near Gold Lake. $S_2$ is parallel to pen (13 cm long).

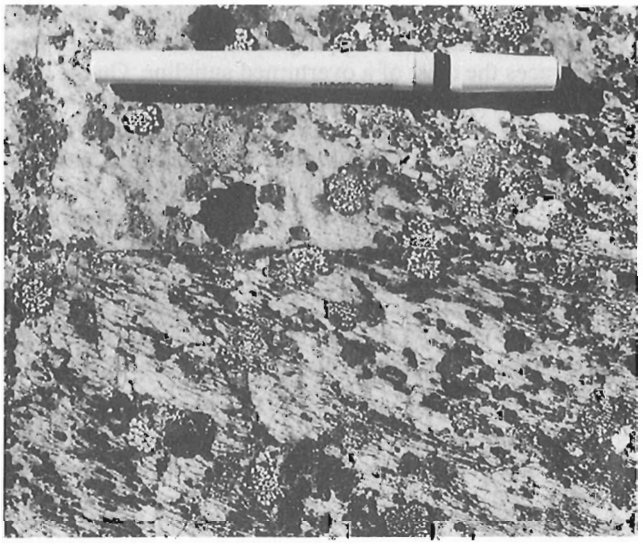

**Figure 10.** Mylonitized rhyolite with well developed shape fabric, on southwestern side of the complex, 1.5 km north of Jim Magrum Lake. Pen is 13 cm long.

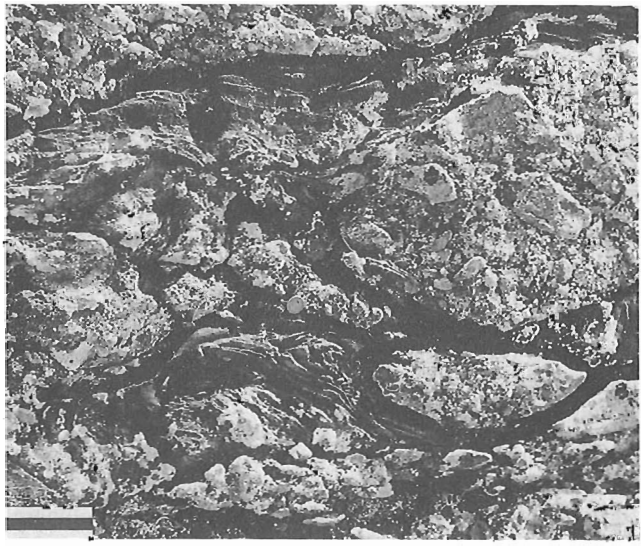

**Figure 11.** Tectonically brecciated primary volcanic breccia containing sheath fold in carbonate matrix. 2.5 km southwest of Jim Magrum Lake. Scale bar is 100 cm.

complex through strongly lineated and foliated carbonate-impregnated rhyolite breccia with well developed shape fabric, into aphanitic or brecciated rhyolite containing mylonitic fabrics (Fig. 10). The fabrics have sinistral S-C relationships with the S-surface shallower than the C-plane. The C-plane has the same orientation as $S_2$ in the metaturbidites, where $F_2$ folds are reclined. Stretching lineation plunges moderately to the northwest and coincides with S-C intersection lineation. This anomolous situation is not understood, and is currently being studied (P. Williams, pers. comm., 1991). Orientation of stretching lineation and the S-C relationships suggest that the metaturbidites have moved down and northward relative to the volcanic complex.

Along the southern and southeastern margins of the complex, strain partitioning takes place within carbonate-cemented rhyolitic to dacitic breccias. These rocks commonly are tectonically brecciated depositional breccias (Fig. 11), highly strained, lineated, and locally have mylonitic carbonate matrix (Fig. 12) containing sheath folds (Fig. 13, 14). Matrix carbonate has deformed ductilely whereas felsic clasts have deformed brittly. Because these rocks recrystallized during metamorphism they do not yield kinematic information.

The final deformational event ($D_3$) has refolded the large $F_2$ folds about a northwest axis distorting the shape of the southern part of the complex. The western periphery of the complex has sinistral bedding/cleavage relationships inconsistent with the northwest corner of the Thlewycho sequence being an $F_2$ fold hinge. This corner of the complex has been interpreted as an $F_3$ fold, as it folds the regional cleavage and has a weak, axial planar northwest oriented cleavage.

## SUMMARY AND INTERPRETATION

Four volcano-sedimentary sequences define the gross stratigraphy and represent the major episodes of volcanism, construction, and erosion of this Archean stratovolcano. Dacitic to andesitic flows of the Innerring sequence represent the upper part of an ancestral volcano.

The Thlewycho sequence documents the main constructional phase of the stratovolcano. The eruptive sequence varied from 5 cycles of voluminous submarine to subaerial, lava effusions interrupted by extensive volcaniclastic deposits on the present northern flanks, to rapid effusion of about 30 subaerial lava flows on the eastern side. The volcaniclastic debris (containing abundant rhyolite clasts) near the base of the northern succession suggests erosion from felsic parts of the ancestral volcano.

The Boucher-Regan sequence, in the northern and northwestern parts of the area, record the only major effusion of basaltic pillow lava. Andesitic effusions (probably from subaqueous fissures) followed the basaltic eruptions and eventually coalesced to central eruptions forming overlapping piles topped by intermediate to felsic tuffs and late stage emergent felsic lava domes.

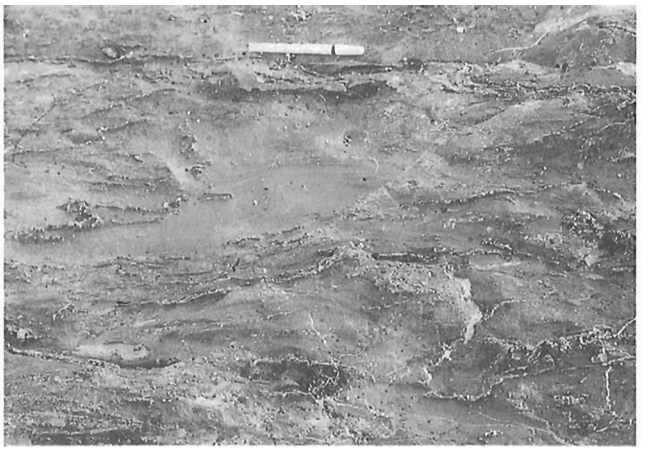

**Figure 12.** Carbonate mylonite along the Back River, near stromatolite locality 8. Pen is 13 cm long.

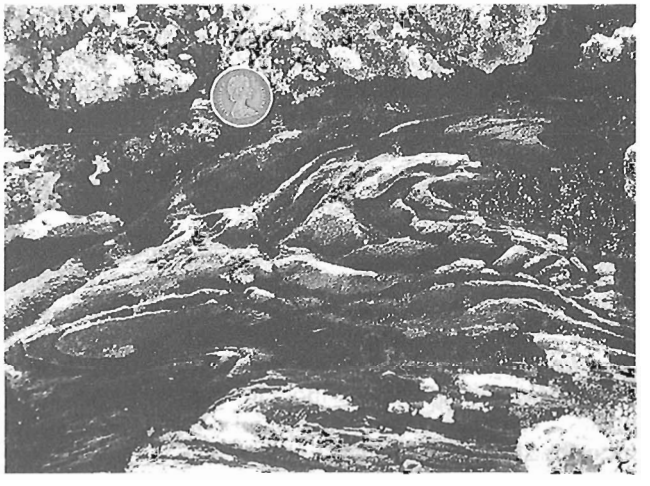

**Figure 13.** Close up of sheath fold in Figure 11. Coin is 18 mm across.

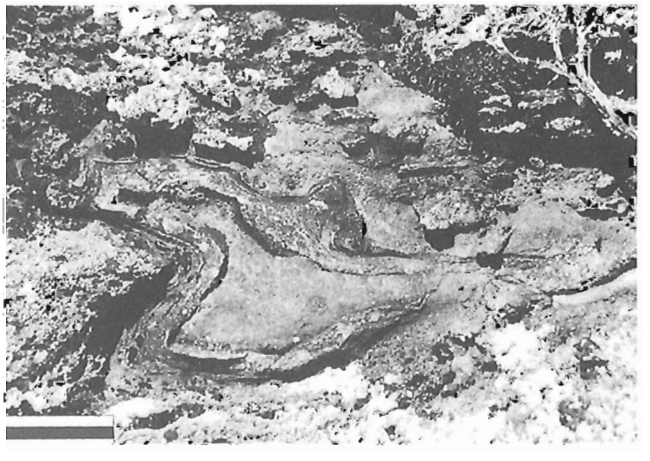

**Figure 14.** Sheath fold within carbonate matrix of rhyolite breccia, northeast side of Jim Magrum Lake. Scale bar is 3 cm.

The Keish sequence is a clastic fan recording erosion of the volcanic pile on its western side.Tuffs, rhyolite turbidites, and debris flows within metasediments of the Beechy Lake Group indicate that the eroding volcano was still emergent and active while turbidites were being deposited in the immediately adjacent sea.

Sulphidic iron-rich mudstone/siltstone sequences and banded chert-, magnetite-, sulphide-, siderite iron-formations mark the close of each major volcanic cycle. Stromatolites preserved in carbonate along the shallow margins of the volcano record that life flourished for brief instances during the waning stages of this Archean stratovolcano.

The domal form of the southern part of the volcanic complex appears to represent a regional scale, northwest oriented, refolded second-generation structure. During $D_2$ regional shortening, shear strain partitioned along the boundary of the complex. The mylonitic fabrics suggest that the southern half of the volcanic complex has behaved as a large competent mass within a ductile matrix (Beechy Lake turbidites): the original form of the stratovolcano may have influenced the present geometry. The metaturbidites, therefore, may be para-authochtonous with respect to the volcanic complex.

## ACKNOWLEDGMENTS

Cathy Langill and Mark Smith provided enthusiastic and competent assistance during field work. We thank Dr. Hans Hofmann (University of Montreal) for sharing his expertise in the investigation and interpretation of stromatolite localities, and Dr. Paul Williams (University of New Brunswick) for his participation in monitoring structural studies. We thank Peter H. Thompson and J. E. King for critical reading of the manuscript.

## REFERENCES

**Frith, R.A.**
1987: Precambrian geology of the Hackett River area, District of Mackenzie, N.W.T.; Geological Survey of Canada, Memoir 417, 61 p.

**Henderson, J.B.**
1970: Stratigraphy of the Archean Yellowknife Supergroup, Yellowknife Bay-Prosperous Lake area, District of Mackenzie; Geological Survey of Canada, Paper 70-26, 12 p.

**Jefferson, C.W., Beaumont-Smith, C.J., and Lustwerk, R.L.**
1989: Stratigraphy and structural setting of iron-formations and gold in the Back River area, District of Mackenzie, N.W.T.; in Current Research, Part C; Geological Survey of Canada, Paper 89-1C, p. 293-304.

**Lambert, M.B.**
1976: The Back River Volcanic Complex, District of Mackenzie; in Report of Activities, Part A, Geological Survey of Canada, Paper 76-1A, p. 363-367.
1977: The southwestern margin of the Back River Volcanic Complex; in Report of Activities, Part A, Geological Survey of Canada, Paper 77-1A, p. 153-158.
1978: The Back River Complex - a cauldron subsidence structure of Archean age; in Report of Activities, Part A, Geological Survey of Canada, Paper 78-1A, p. 153-158.
1982a: Felsic domes and flank deposits of the Back River volcanic complex, District of Mackenzie; in Current Research, Part A; Geological Survey of Canada, Paper 82-1A, p. 159-164.
1982b: The Back River Volcanic Complex, District of Mackenzie, N.W.T.; Geological Survey of Canada, Open File 848, 1:50 000 scale map.

**Lambert, M.B., Burbidge, G., Jefferson, C.W., Beaumont-Smith, C.J., and Lustwerk, R.**
1990: Stratigraphy, facies and structure in volcanic and sedimentary rocks of the Archean Back River volcanic complex, N.W.T.; in Current Research, Part C; Geological Survey of Canada, Paper 90-1C, p. 151-165.

**Moore, D.W.**
1977: Geology and geochemistry of a gold-bearing iron-formation and associated rocks, Back River, Northwest Territories; MSc. thesis, University of Toronto, Toronto, Ontario, 186 p.

**van Breemen, O., Henderson, J.B., Sullivan, R.W., and Thompson, P.H.**
1987: U-Pb, zircon and monazite ages from the eastern Slave Province, Healey Lake area, N.W.T.; in Radiogenic Age and Isotopic Studies: Report 1, Geological Survey of Canada, Paper 87-2, p. 101-110.

Geological Survey of Canada Project 740019

# Reconnaissance studies in the Hepburn Island map area, northern Slave Province, Northwest Territories

**C. Relf[1], V.A. Jackson[2], M.B. Lambert, M. Stubley[3], M. Villeneuve, and J.E. King**
**Continental Geoscience Division**

*Relf, C., Jackson, V.A., Lambert, M.B., Stubley, M., Villeneuve, M., and King, J.E., 1992: Reconnaissance studies in the Hepburn Island map area, northern Slave Province, Northwest Territories; in Current Research, Part C; Geological Survey of Canada, Paper 92-1C, p. 201-208.*

***Abstract***

*Reconnaissance in the Hepburn Island map area of the northern Slave Province identified important new stratigraphic-structural-metamorphic relations. A distinctive orthogneiss near Arcadia Bay has yielded a lower intercept of 1988 ± 16 Ma and an upper intercept of 4044 ± 90 Ma (U-Pb zircon). The ca. 2.69 Ga Anialik River igneous complex (spatially associated with Au mineralization) has locally intrusive contacts with the Anialik River volcanic belt. This contact subsequently underwent severe deformation, the nature and timing of which is not constrained. A regionally dominant planar fabric in the Anialik River volcanic belt can be resolved into three sets of foliations and folds, but the relationship of these to the deformed margin of the igneous complex is not yet known.*

***Résumé***

*Les travaux de reconnaissance réalisés dans la région cartographique de l'île Hepburn dans le nord de la province des Esclaves ont permis d'établir de nouveaux liens stratigraphiques, structuraux et métamorphiques. Un orthogneiss distinctif près de la baie d'Arcadia a donné une interception inférieure de 1988 ± 16 Ma et une interception supérieure de 4044 ± 90 Ma (U-Pb sur zircon) avec la courbe Concordia. Le complexe igné d'Anialik River datant d'environ 2,69 Ga (spatialement associé à la minéralisation aurifère) comporte par endroits des contacts intrusifs avec la zone volcanique d'Anialik River. Ce contact a par la suite subi une importante déformation dont la nature et la chronologie n'ont pas été précisées. La fabrique planaire d'échelle régionale observée dans la zone volcanique d'Anialik River peut s'expliquer par la présence de trois séries de foliations et de plis, mais le lien qui existe entre ceux-ci et la marge déformée du complexe ignée n'a pas encore été établi.*

[1] Department of Geological Sciences, Queen's University, Kingston, Ontario K7L 3N6
[2] Department of Indian Affairs and Northern Development, Northwest Territories Geology Division, Box 1500 Yellowknife, N.W.T. X1A 2R3
[3] Energy, Mines and Petroleum Resources, Mineral Initiatives Office, Government of the Northwest Territories, Box 1320, Yellowknife, Northwest Territories X1A 2L9

## INTRODUCTION

Geologists from the Geological Survey of Canada, the Department of Indian Affairs and Northern Development, and the Government of the Northwest Territories' Geoscience Initiatives Office investigated selected parts of the Hepburn Island map area (NTS 76M) as part of the National Mapping Program's (GSC NATMAP Committee, 1990) Slave Province project. The purpose of this year's work was to evaluate scientific objectives, priorities and logistics for the three participating agencies in order that coordinated studies can be carried out over the next four years. Detailed studies, funded by the Canada – N.W.T. Mineral Initiatives Program, will be conducted in the Anialik River and High Lake volcanic belts (delivered by the Mineral Initiatives Office of the GNWT and the GSC, respectively) concomitantly with a reassessment of regional geological problems in the area as part of a GSC project. This paper presents observations made during the reconnaissance and reports significant new geochronological data.

## PREVIOUS WORK

Fraser (1964) mapped the Hepburn Island map sheet (Fig. 1) at a scale of 1:500 000, during "Operation Bathurst Inlet". Between 1974 and 1985, DIAND and the GSC carried out 1:30 000 to 1:50 000 scale mapping of parts of the Hepburn Island sheet: Padgham et al. (1973) mapped part of the High Lake volcanic belt near High Lake, Tirrul and Bell (1980) mapped part of the Anialik River volcanic belt and Anialik River igneous complex, and Easton et al. (1982), Yeo et al. (1983), and Jackson et al. (1985, 1986) covered the remaining areas. Jackson (1989) synthesized and compiled these studies in a 1:125 000 map which will serve as a solid basis for the planned studies. Abraham (1987, 1989) mapped the western part of the Anialik River igneous complex and the adjacent volcanic rocks in the Arcadia Bay area at a scale of 1:15 000, focusing on gold mineralization in shear zones within the complex.

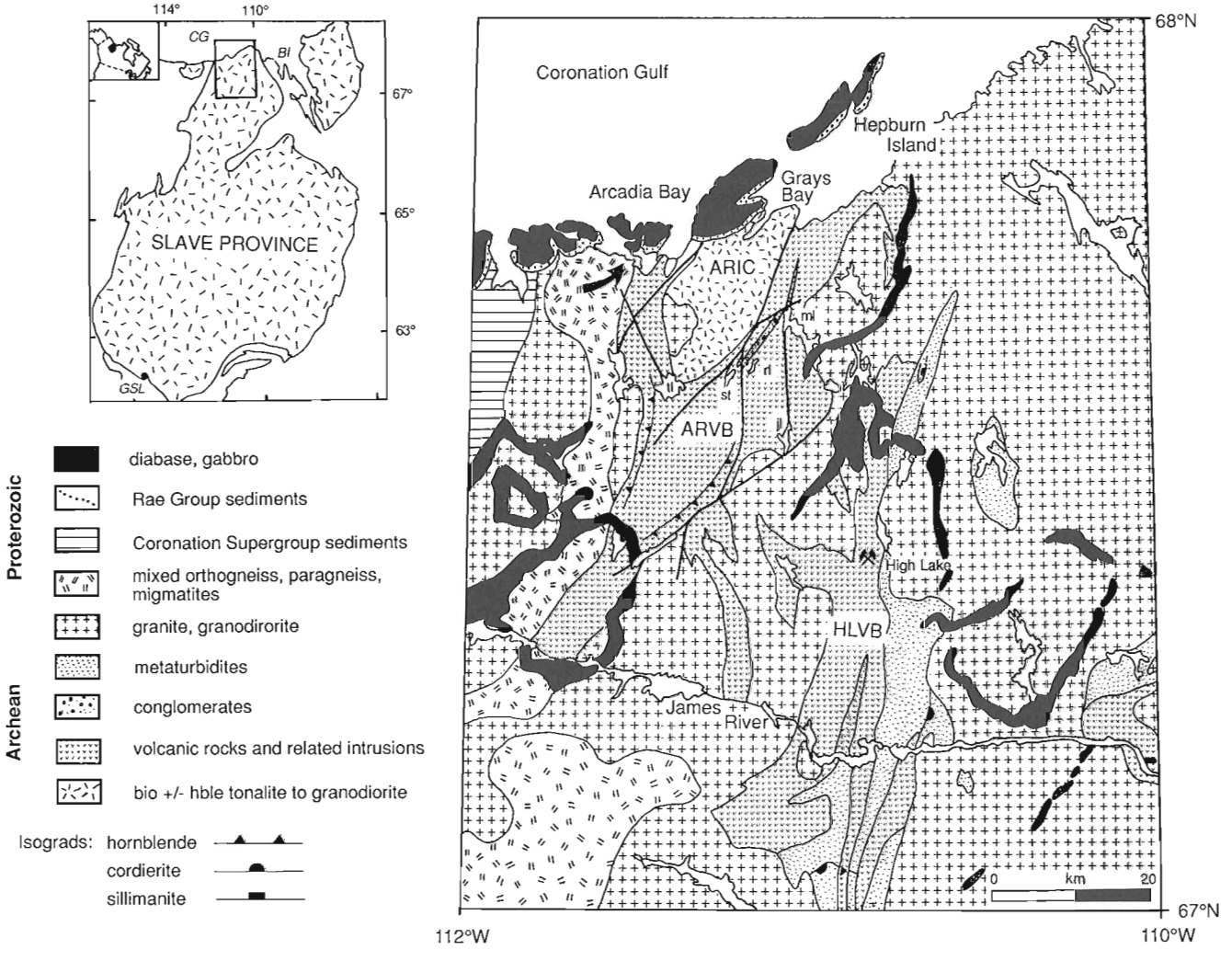


**Figure 1.** Simplified geological compilation of the Hepburn Island map area from Jackson (1989). Arrow indicates location of the orthogneiss at Arcadia Bay; location of High Lake massive sulphide deposit shown by crossed hammers; Abbreviations: ARIC - Anialik River igneous complex; ARVB - Anialik River volcanic belt; HLVB - High Lake volcanic belt; jl -Joy lake; ml - Mistake lake; rl - Run lake; sl - String lake; tl - Turtle lake. Location of the map area in the Slave Province and in Canada shown on left.

## GRANITOID ROCKS

### *Tonalitic gneiss at Arcadia Bay*

A distinctive tonalitic gneiss at the north end of an extensive belt of mixed gneisses and migmatites along the western side of the Hepburn Island map area (Easton et al.,1982; Jackson, 1989), was examined at Arcadia Bay (Fig. 1, 2). At this locality, the tonalitic gneiss comprises two main phases, the older a strongly foliated and recrystallized, medium-grained biotite tonalitic gneiss, and the younger a medium- to coarse-grained biotite monzogranite. In addition to these leucocratic phases, chloritic pods up to 1m in length occur locally. Their origin is uncertain. At least two fold generations have deformed all phases of the orthogneiss. Although these orthogneisses were previously correlated with the ca. 2690 Ma Anialik River igneous complex (Jackson, 1989), they are more pervasively deformed and recrystallized, and hence, appear to be distinct from that complex. Contact relations between this orthogneiss and the rest of the gneiss unit and with the adjacent Anialik River volcanic belt (shown as gradational and fault contacts, respectively on Jackson, 1989) were not observed. Both phases of the orthogneisses were sampled for U-Pb zircon geochronology. Zircons separated from the tonalite have a prismatic and euhedral morphology typical of crystals formed from a melt. These zircons were separated into three groups (Table 1, Fig. 3): "A"-series grains are clear, crack-free crystals, "B"-series grains are less clear, and are visibly zoned, and C-grains contain cores. Zoned B-series grains are difficult to distinguish from "C"-series grains. "C"-series grains were abraded to remove overgrowths in order to determine the age of inherited zircons. The "A" grains and B-2 plot along a chord (Fig. 3) that has a lower intercept of 1988 ± 16 Ma and an upper intercept of 4044 ± 90 Ma (modified York, 1969; cf. Parrish et al., 1987). The high U content of the "C" grains, coupled with their metamict state, could be responsible for the different Pb-loss trajectory followed by these grains.

**Figure 2.** Strongly deformed and recrystallized tonalite gneiss west of Arcadia Bay. Arrows point to monzogranite veins that cross-cut gneissic layering, but are involved in folding. Hammer is 36 cm. GSC 1991-566G

**Table 1.** U-Pb analytical data for the tonalite gneiss near Arcadia Bay (sample #R-38-91)

| Fraction[a] | Wt.[b] | U | Pb[c] | $^{206}Pb$/$^{204}Pb$[d] | Pb[c] | $^{208}Pb$[f] | Radiogenic ratios (±1σ, %)[g] | | | Ages (Ma, ±2σ)[h] | | |
|---|---|---|---|---|---|---|---|---|---|---|---|---|
| | | | | | | | $^{206}Pb$/$^{238}U$ | $^{207}Pb$/$^{235}U$ | $^{207}Pb$/$^{206}Pb$ | $^{206}Pb$/$^{238}U$ | $^{207}Pb$/$^{235}U$ | $^{207}Pb$/$^{206}Pb$ |
| | mg | ppm | ppm | | pg | % | | | | | | |
| A-1 | 0.005 | 1360 | 570 | 159 | 915 | 6.3 | 0.3908±0.17 | 8.975±0.62 | 0.16655±0.52 | 2127±6 | 2325±11 | 2523±17 |
| A-2 | 0.007 | 882 | 403 | 265 | 516 | 6.9 | 0.4151±0.12 | 10.956±0.32 | 0.19144±0.26 | 2238±4 | 2519±6 | 2754±9 |
| A-3 | 0.003 | 195 | 96 | 225 | 64 | 12.6 | 0.4195±0.19 | 11.553±0.35 | 0.19976±0.27 | 2258±7 | 2569±6 | 2824±9 |
| A-4 | 0.002 | 660 | 307 | 252 | 127 | 8.0 | 0.4168±0.15 | 11.005±0.34 | 0.19147±0.27 | 2246±6 | 2523±6 | 2755±9 |
| B-1 | 0.002 | 2591 | 811 | 159 | 688 | 5.4 | 0.2986±0.18 | 6.319±0.64 | 0.15349±0.54 | 1684±5 | 2021±11 | 2385±18 |
| B-2 | 0.001 | 2755 | 1024 | 5173 | 12 | 3.9 | 0.3674±0.09 | 6.629±0.10 | 0.13085±0.04 | 2017.2 | 2063±2 | 2109±1 |
| C-1 | 0.011 | 875 | 292 | 223 | 751 | 8.1 | 0.3011±0.14 | 7.639±0.41 | 0.18401±0.33 | 1697±4 | 2189±7 | 2689±11 |
| C-2 | 0.008 | 912 | 265 | 146 | 784 | 7.9 | 0.2704±0.19 | 5.734±0.71 | 0.15380±0.60 | 1543±5 | 1937±12 | 2389±20 |
| C-3 | 0.008 | 1311 | 361 | 146 | 1101 | 8.4 | 0.2537±0.20 | 5.418±0.73 | 0.15487±0.61 | 1458±5 | 1888±13 | 2400±21 |
| C-4 | 0.008 | 672 | 241 | 170 | 612 | 8.6 | 0.3244±0.16 | 7.753±0.56 | 0.17334±0.47 | 1811±5 | 2203±10 | 2590±1 |

[a]All fractions are single grain and abraded except A-1 and A-2, each of which is comprised of 4 abraded crystals
[b]Error on weight =±0.001 mg
[c]Radiogenic Pb
[d]Measured ratio corrected for spike and Pb fractionation of 0.09±0.03%/AMU
[e]Total common Pb on analysis corrected for fractionation and spike
[f]Radiogenic Pb
[g]Corrected for blank Pb and U and common Pb (Stacey-Kramers model Pb composition equivalent to the $^{207}Pb/^{206}Pb$ age)
[h]Corrected for blank and common Pb

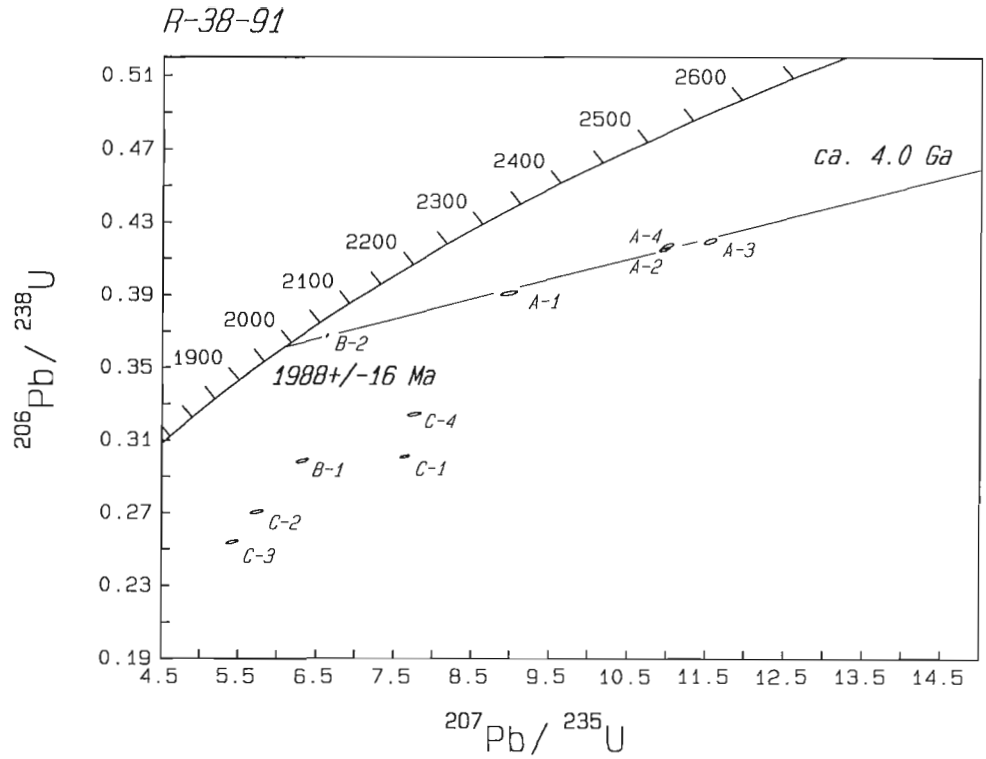


**Figure 3.** Concordia diagram of zircon data from tonalite gneiss near Arcadia Bay (sample #R-38-91).

The lower intercept of ca. 1.99 Ga could represent a metamorphic event that caused extreme lead loss in early Archean zircons, or it could represent a primary crystallization age with minor, single-age, early Archean inheritance. Further geologic mapping should provide evidence to descriminate between these interpretations. At present, the lower intercept is tentatively interpreted as a crystallization age because (1) multi-grain and single-grain analyses both plot along this chord, (2) the U-Pb systematics of low-U crystals (A-3, A-4) are indistinguishable from the high-U fractions, and (3) the grains have morphology of igneous grains.

### *The Anialik River igneous complex*

The ca. 2703 - 2682 Ma Anialik River igneous complex is one of the few granitoid complexes in the area that has been studied in detail (Padgham et al., 1983; Abraham et al., 1991). The complex comprises mainly tonalite with minor diorite and monzogranite and is cut by granitic bodies of unknown age (Jackson, 1989; Abraham et al., 1991). It is surrounded and structurally overlain by volcanic rocks of the Anialik River volcanic belt (Tirrul and Bell, 1980; Jackson et al., 1985). Although no age has yet been determined for the volcanic belt, Abraham et al. (1991) suggested that older phases of the igneous complex may be basement to the volcanic rocks. However, our observations of granitoid sills that are compositionally and texturally similar to phases of the Anialik River igneous complex within volcanic rocks east of the complex, suggests that at least some plutonism may have overlapped in time with volcanism.

The eastern and western margins of the Anialik River igneous complex are characterized by steeply- to shallowly-outward-dipping zones of mixed volcanic and granitic rocks, and the interpreted sheared equivalents of both (Jackson, 1985; Abraham, 1989). We examined the eastern contact where mylonitic granitoid rocks (related to the igneous complex), felsic dykes, and chlorite schist (possibly volcanic in origin) are involved in shallowly east-dipping, overturned to recumbent folds. The timing and kinematics of the shear zones and the relationship to the recumbent folds is unknown. On the west side of the complex, Abraham (1987) reported that granitoid veins, interpreted to be young phases of the Anialik River igneous complex cut across high-strain zones.

### *Other plutonic rocks*

Previous mapping in the Hepburn Island area concentrated largely on the supracrustal rocks, which host numerous base and precious metal showings. The plutonic rocks, which comprise more than half of the map area, remain largely unsubdivided, and are poorly understood. Field observations and regional magnetic data (Geological Survey of Canada, 1979), indicate that a wide range of compositions, textures, and deformation states are represented by the plutonic rocks. Further mapping and radiometric dating of these units should

define distinct plutonic suites, and distinguish their temporal relationship with other rock units, different structure sets, and mineralization.

## VOLCANIC BELTS

The High Lake and Anialik River volcanic belts form two of the largest greenstone belts in the Slave Province. Both contain a high proportion of felsic volcanic rocks similar to the Hackett River volcanic belt (Padgham, 1985), and numerous base and precious metal showings. Exploration has revealed alteration zones commonly associated with volcanogenic massive sulphide deposits (e.g. O'Sullivan, 1989), although the stratigraphic and/or structural controls on the distribution and grade of the ore are not well understood. Preliminary observations were made in eight selected localities in these belts to determine suitability for detailed structural, stratigraphic and volcanological studies and to collect samples to obtain the first radiometric dates from these belts.

In the Anialik River volcanic belt, felsic volcanic rocks were examined at a locality 5 km north of Joy lake, and at Gray's Bay (Fig. 1). Near Joy lake an extensive area of rhyolitic breccia lies on the west side of a 15 km long, north-northwesterly trending fault (Easton et al., 1982). Here, the rhyolite body is so highly strained that no primary features are recognizable and any attempt to define stratigraphy would be futile. At Gray's Bay, however, large rhyolite bodies are not highly strained and contain primary textures. This unit comprises at least two phases of massive, buff- to orange-weathering quartz-feldspar-phyric rhyolite, one more coarsely and abundantly porphyritic than the other. Both have brecciated margins, and are cut by granitic and mafic dykes. These bodies are interpreted as remnants of large lavadome complexes. The coarsely porphyritic phase was collected for radiometric dating.

Felsic volcanic rocks were also examined in the core of a large anticline at the southern margin of the Anialik igneous complex (Fig. 1). Here, amid a complicated series of granitoid sills and volcanic rocks, we identified bedded felsic volcanic rocks, containing well preserved primary volcanic textures suggesting that they may be felsic ash-tuffs.

In an area of 'dominantly mafic volcanics' at the northeastern tip of the Anialik belt at Gray's Bay (Easton et al., 1982), a succession of dark grey to green, thin-to thick-bedded shales and volcanic siltstones, minor banded iron-formation, and magnetite-bearing carbonate were observed. These rocks suggest that there may be a larger amount of sediment within the volcanic belts than are shown on present maps.

A variety of felsic volcanic rocks were observed near High Lake and at three localities along the James River. The High Lake massive sulphide deposit is marked by a spectacular gossan in sheared ?rhyolite cut by mafic dykes.

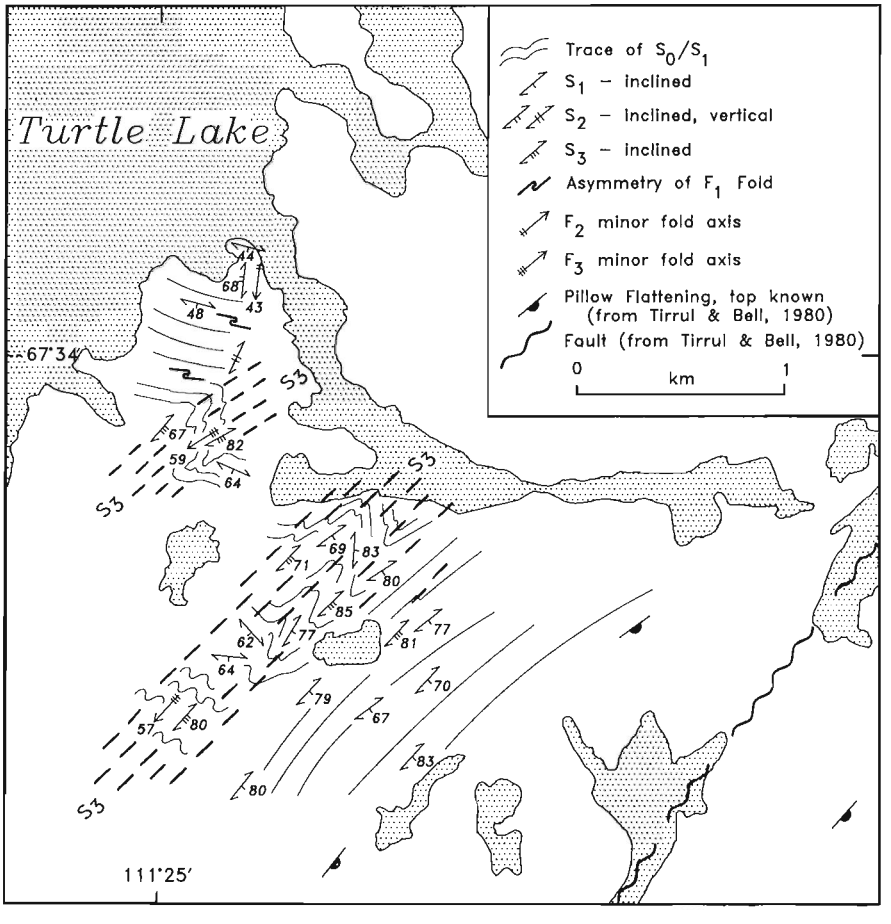


**Figure 4**

Main structural elements in mixed volcanic and mafic intrusive rocks, south of Turtle lake.

Both units contain sulphide mineralization. A breccia having a highly schistose matrix and clasts flattened parallel to the schistosity was observed on the west shore of High Lake east of the deposit. Although it was not clearly established whether this is a fault breccia or a deformed primary breccia, the zone has the same trend as northerly trending faults shown by Pagham et al. (1973). At the James River localities, rhyolite domes and breccias are not highly strained and a variety of thick- to thin-bedded epiclastic volcarenites and volcrudites, as well as bedded tuffs, preserve identifiable primary textures and structures. A massive porphyritic rhyolite unit from this area was sampled for radiometric dating.

In summary, our preliminary investigations suggest that the volcanic rocks locally preserve primary features and offer potential for conducting interpretive volcanic studies and for establishing a volcanic stratigraphy. However, the presence of numerous high-strain zones implies that the stratigraphic sequence may be disrupted by faults. Careful stratigraphic and structural mapping should lead to a better understanding of the volcanic environment and constraints on genetic models for mineralization in the volcanic belts.

## STRUCTURE

### *Structures in the Anialik River volcanic belt*

Throughout most of the Anialik River volcanic belt, the dominant planar fabric is defined by compositional layering (interpreted as bedding) and a well-developed layer-parallel foliation. These fabrics parallel foliations in the Anialik River igneous complex near its east and west margins. At the south end of the complex (Turtle lake area, Fig. 1, 4), however, the foliation in the volcanic rocks can be resolved into at least four planar fabrics (bedding, $S_1$, $S_2$, $S_3$), and three sets of folds ($F_1$, $F_2$, $F_3$). Correlations between these various planar elements and folds, both within the volcanic belt and between the volcanic belt and the igneous complex, have not yet been established. Furthermore, the relationship between the shear zones at the margins of the complex and the foliations is not clear. The structure sets resolved in the Turtle lake area are described below.

The earliest structures in the volcanic rocks, observed south of Turtle lake (Fig. 4), are tight to isoclinal, Z-shaped folds of bedding (plunge unknown) about a penetrative chlorite foliation. These features are designated $F_1$ and $S_1$, respectively. $F_1$ folds were only observed in two outcrops; elsewhere, $S_1$ is parallel to bedding.

The second set of structures includes rare, metre-scale folds ($F_2$) and locally-developed crenulations and incipient crenulation cleavage ($S_2$) that deform bedding and $S_1$ (Fig. 4). Lithological contacts, bedding, and $S_1$ in the volcanic rocks wrap concordantly around and dip moderately away from the south end of the Anialik River igneous complex (Fig. 5a) (Tirrul and Bell, 1980). Foliation in the igneous complex also appears to parallel this curve. This regional warping of fabrics is attributed to a first-order, south-southwest-plunging antiform which exposes the structurally underlying igneous complex, and is designated as an $F_2$ fold. The small-scale structures described above parallel the axial trace of the first-order antiform.

The third set of structures in the Turtle lake area is characterized by outcrop-scale warps and intensely developed, chevron-style folds of bedding and $S_1$ about a steep northeast-striking crenulation cleavage (Fig. 4). These folds and crenulations occur west of the axial trace of the

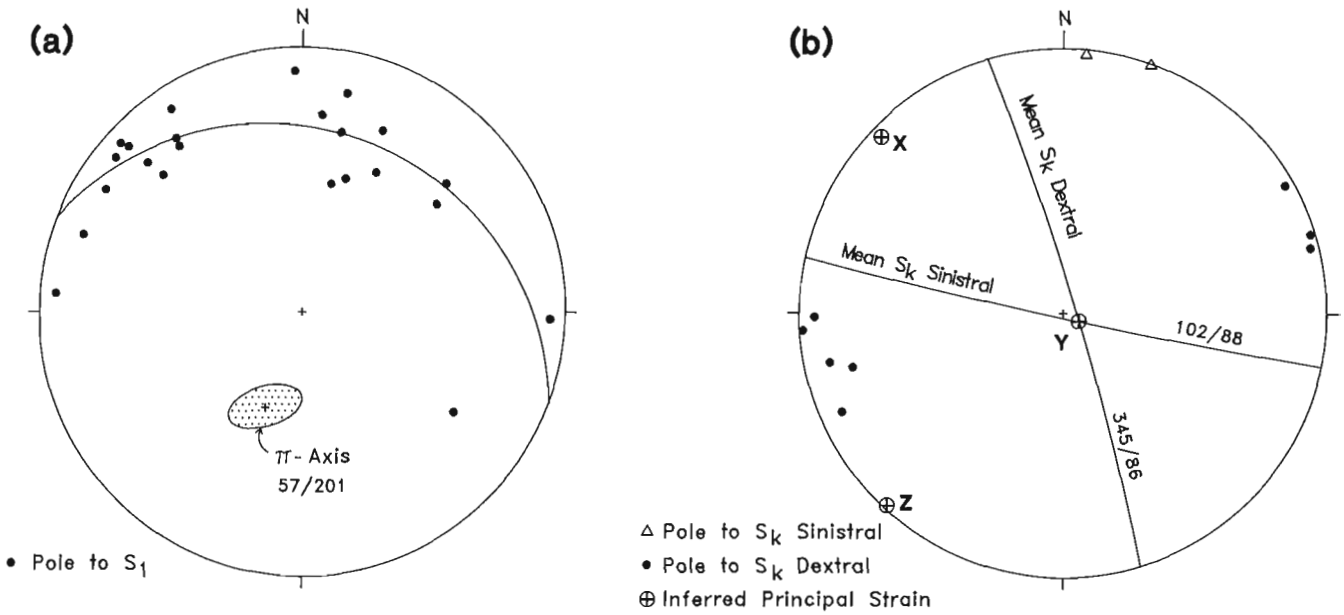


**Figure 5.** Stereoplots of preliminary structural data from the Anialik River volcanic belt; lower-hemisphere equal-area projections. **a**) Poles to $S_1$ and Pi axis for $S_1$ distribution (95% confidence) in the Turtle lake area; **b**) conjugate kink bands and crenulations from the Run Lake area and inferred principal axes of strain ellipsoid (X>Y>Z).

major $F_2$ anticline cored by the Anialik River igneous complex. East of the major $F_2$ axial trace, bedding and $S_1$ strike northeast, and therefore these folds were not recognized. Although clear overprinting relationships between these folds and outcrop-scale $F_2$ folds have not been observed, the apparent confinement of these folds to the west limb of the $F_2$ anticline implies that they postdate $F_2$: shortening on the east limb would not produce folds or a foliation that is easily distinguished from $S_1$. The folds and related cleavage are therefore designated $F_3$ and $S_3$.

In addition to the structures described above, conjugate kink bands and a set of overturned folds, both of unknown age, were recognized. Conjugate kink bands and spaced crenulations ($S_k$) were observed locally in the supracrustal rocks near Run and String lakes (Fig. 1), and probably correspond to $S_3$ of Tirrul and Bell (1980). Kink bands with axial surfaces striking approximately 345° have dextral asymmetry and are more abundant than sinistral kink bands that strike ~100° (Fig. 5b). The inferred shortening direction from the conjugate orientation and asymmetry of the conjugate pairs is northeast-southwest and subhorizontal (Z in Fig. 5b). An apparent increase in density of $S_k$ towards the north-south fault between Run and String lakes (Fig. 1) suggests a possible genetic relationship, and the inferred shortening direction is compatible with dextral strike slip displacement along the fault, in accord with the sense of offset of the faulted conglomerate mapped by Tirrul and Bell (1980). Jackson (1985) found kink bands spatially associated with northeast- and northwest-striking faults, which Tirrul and Bell (1980) interpreted to be younger than the north-south fault set (see below). The distribution of kink bands and the relationship between kink band formation and different generations of faults in the study area requires further examination. The kink bands could prove to be useful shear-sense indicators in the evaluation of the kinematic history of the faults.

Outcrop-scale overturned folds of bedding and $S_1$ were documented by Jackson (1989) on the hanging wall of a shallowly to moderately east-dipping north-south fault between Mistake and Joy lakes (Fig. 1). These folds have a westward structural vergence. Based on the spatial association of the folds with the fault, displacement was interpreted as east-side-up reverse slip (ibid.). The relative ages of these folds and the overturned folds near the margin of the Anialik River igneous complex are not presently known.

The youngest structures in the Hepburn Island map area are northeast- and northwest-striking brittle faults (Fig. 1), which were interpreted by Tirrul and Bell (1980) as conjugate dextral and sinistral transcurrent faults, respectively. These faults cross-cut all map units, and truncate the north-south fault set described above (Tirrul and Bell, 1980). They are similar in their relative timing, orientation and kinematic framework to Proterozoic faults in the Wopmay orogen about 15 km to the west (Hoffman, 1984), and therefore are interpreted to be part of the same Proterozoic fault system.

### *Structures in metasedimentary rocks near the High Lake volcanic belt*

In biotite-grade metaturbidites east of the High Lake volcanic belt (Fig. 1), at least one fold set and two foliations were recognized. The orientation and the number of generations of folds were not determined, although in places outcrop is sufficiently abundant and well-exposed that careful structural analysis could determine the folding history. Both foliations are penetrative, slaty cleavages, but one is oriented 10-30° clockwise from bedding, and the other is 10-30° counterclockwise. Although the two foliations were not observed together, and their relative ages are therefore unknown, they are interpreted as two different fabrics (rather than a single foliation in folded beds) because both are present in east-striking, south-facing beds. Farther west, adjacent to the High Lake volcanic belt, bedding and foliation in the metaturbidites are subvertical and strike north, parallel to the volcanic contact.

Within the volcanic belt, only one north-south foliation, parallel to compositional layering, is evident. Whether the metaturbidites have a different, more protracted structural history than the volcanic rocks, or whether they simply preserve structures better, is a question that arises here as it has in other supracrustal belts in the Slave Province (e.g. the Yellowknife basin (Henderson, 1985), Point Lake (Jackson, 1984), Contwoyto Lake (Relf, in prep.)).

## METAMORPHISM

Metamorphic grade in the Hepburn Island map area ranges from lower greenschist to upper amphibolite facies (Tirrul and Bell, 1980; Easton et al., 1982; Jackson, 1989). Jackson et al. (1986) mapped the cordierite isograd in metaturbidites east of the High Lake volcanic belt in the James River area, and Easton et al. (1982) delineated the sillimanite isograd farther north along the same belt (Fig. 1). Mineral assemblages observed in supracrustal rocks indicated that there is potential to conduct pressure-temperature studies in a variety of bulk compositions (mafic volcanic and intrusive rocks, volcaniclastic rocks and pelites) in order to constrain the thermal evolution of the area.

In the Anialik River volcanic belt metamorphic grade increases from greenschist facies adjacent to the Anialik River igneous complex to amphibolite facies towards the margins of the belt (Tirrul and Bell, 1980; Jackson, 1989) (Fig. 1). As the complex sits structurally below the volcanic belt, it therefore cores the *lowest* grade part of the belt, with metamorphic grade increasing towards *higher* structural levels. Around other structural domes in the Slave Province metamorphic grade either increases downwards (e.g. Hackett River dome (Percival, 1978; Frith, 1987); Wishbone monzogranite (King et al., 1988; Relf, in prep.)), or transects the dome, showing no obvious spatial relationship (e.g. Brislane tonalite (Heywood and Davidson, 1969)). The metamorphic configuration in the Anialik River volcanic belt may be unique in the Slave Province, and warrants further study.

## CONCLUSIONS

Previous mapping in the Hepburn Island map area established regional geological relationships, and provided a focus for more specific geological questions to be addressed. Reconnaissance, directed by study of previous maps, has identified several important questions, such as the extent of possible 1.99 Ga gneisses at Arcadia Bay, structural and stratigraphic complications in the supracrustal belts, subdivision of the plutonic units, and the history of metamorphism. These studies will be the focus of GSC NATMAP and Canada-NWT Geoscience Initiative bedrock mapping projects that will be conducted in the Hepburn Island map area over the next four years.

## ACKNOWLEDGMENTS

We thank H. Helmstaedt, M. van Kranendonk, W.A. Padgham and S. Hanmer for reviewing the original manuscript. Special thanks are due to Marc Hutcheson and Scott Dinsmore for flight and kitchen support and to Covello, Bryan and Associates for use of their comfortable camp during field work. Polar Continental Shelf provided helicopter support.

## REFERENCES

**Abraham, A.P.G.**
1987: Preliminary report on the geology of the Arcadia Bay Property, Coronation Gulf, N.W.T.: A granitoid-hosted gold deposit; NWT Geology Division, Northern Affairs Program, Yellowknife, Open File report EGS 1987-8, 26 p. (with map).
1989: Tonalite-hosted Au-quartz vein/shear zone mineralization in the Arcadia Bay area, Slave province, N.W.T.; NWT Geology Division, Northern Affairs Program, Yellowknife, Open File report EGS 1989-6, 70 p.

**Abraham, A.P.G., Kamo, S.L., Davis, D.W., and Spooner, E.T.C.**
1991: Geochronological constraints on magmatic evolution and gold mineralization in the Anialik River area, Slave province; in Geological Association of Canada-Mineralogical Association of Canada-Society of Economic Geologists Joint Annual Meeting, v. 16, p. A1.

**Easton, R.M., Ellis, C.E., Dean, M., and Bailey, G.**
1982: Geology of the Typhoon Point map area, High Lake greenstone belt (76M/10 and 76M/15 south-half); Indian and Northern Affairs Canada, Northern Affairs Program, Geology Division, Yellowknife, EGS-1982-6 (with marginal notes).

**Fraser, J.A.**
1964: Geological notes on northeastern District of Mackenzie; Geological Survey of Canada, Paper 63-40 (with map 45-1963).

**Frith, R.A.**
1987: Precambrian geology of the Hackett River area, District of Mackenzie, N.WT.; Geological Survey of Canada Memoir 417, 61 p.

**Geological Survey of Canada**
1979: Hepburn Island, Northwest Territories; Geological Survey of Canada Aeromagnetic Map 7917G, scale 1:250,000.

**Geological Survey of Canada NATMAP Committee**
1990: NATMAP - Canada's National Geoscience Mapping Program; Geological Survey of Canada, Open File 2256, 83 p.

**Henderson, J.B.**
1985: Geology of the Yellowknife-Hearne Lake area, District of Mackenzie: a segment across an Archean basin; Geological Survey of Canada, Memoir 414.

**Heywood, W.W., and Davidson, A.**
1969: Geology of Benjamin Lake map-area, District of Mackenzie (75 M/2); Geological Survey of Canada, Memoir 361, 35 p. (with Map 1198A).

**Hoffman, P.F.**
1984: Geology, northern internides of Wopmay Orogen, District of Mackenzie, Northwest Territories; Geological Survey of Canada, Map 1576A, scale 1:250,000.

**Jackson, V.A.**
1984: Structure and metamorphism of the Keskarrah Bay area, Point Lake, N.W.T., Second Preliminary Report; Contributions to the Geology of the Northwest Territories, Volume 1, Indian and Northern Affairs Canada, EGS 1984-6, p. 47-54.
1985: Geology of the eastern Hepburn Island area (76M); in Exploration Overview, Indian and Northern Affairs Canada, Northern Affairs Program, Geology Division, Yellowknife, p. 20-21.
1989: Preliminary geological compilation of Hepburn Island map area (76M); Indian and Northern Affairs Canada, Northern Affairs Program, Geology Division, Yellowknife, EGS-1989-11 (with marginal notes).

**Jackson, V.A., Crux, J., Ellis, C.E., Howson, S., Padgham, W.A., and Relf, C.**
1985: Geology of the Mistake Lake area, Anialik River greenstone belt, N.W.T., 76M/11; Indian and Northern Affairs Canada, Northern Affairs Program, Geology Division, Yellowknife, EGS-1985-5 (with marginal notes).

**Jackson, V.A., Bell, R., Bishop, S., Daniels, A., Howson, S., Kerr, D.E., and Tregenza, M.**
1986: Preliminary geology of the eastern Hepburn Island area (76M/1, M/2, M/8, M/9, M/15 north half, M/16); Indian and Northern Affairs Canada, Northern Affairs Program, Geology Division, Yellowknife, EGS-1986-6 (with marginal notes).

**King, J.E., Davis, W.J., Relf, C., and Avery, R.W.**
1988: Deformation and plutonism in the western Contwoyto Lake map area, central Slave Province, District of Mackenzie, N.W.T.; in Current Research, Part C; Geological Survey of Canada, Paper 88-1C, p. 161-176.

**O'Sullivan, C.N.**
1989: Continental Pacific Resources Inc. Semi-Annual Report, December 31, 1989, Report on the Anialik River/High Lake volcanic belts, 9 p.

**Padgham, W.A.**
1985: Observations and speculations on supracrustal successions in the Slave Structural Province; in Evolution of Archean Supracrustal Sequences, (ed.) L.D. Ayres, P.C. Thurston, K.D. Card, and W. Weber; Geological Association of Canada, Special Paper 28, p. 133-151.

**Padgham, W.A., Jefferson, C.W., Hughes, D.R., and Shegelski, R.J.**
1973: Geology of the High Lake area, N.W.T. (NTS 76M/7); Indian and Northern Affairs Canada, Northern Affairs Program, Geology Division, Yellowknife, Open File 208 (with marginal notes).

**Padgham, W.A., Roscoe, S.M., van Schmus, W.R., and Bowring, S.A.**
1983: Anialik Gneiss: 2.7 Ga-old anatectic, Slave Province, N.W.T.; Geological Association of Canada - Mineralogical Association of Canada, Program with Abstracts, v. 8, p. 52.

**Parrish, R.R., Roddick, J.C., Loveridge, W.D., and Sullivan, R.W.**
1987: Uranium-lead analytical techniques at the geochronology laboratory, Geological Survey of Canada; in Radiogenic Age and Isotopic Studies: Report 1, Geological Survey of Canada, Paper 87-2, p. 3-7.

**Percival, J.A.**
1978: Stratigraphy, structure and metamorphism of the Hackett River Gneiss Dome, District of Mackenzie, N.W.T.; M.Sc. thesis, Queen's University, Kingston, Ont., 129 p.

**Tirrul, R., and Bell, I.**
1980: Geology of the Anialik River Greenstone Belt, Hepburn Island map area, District of Mackenzie; in Current Research, Part A; Geological Survey of Canada, Paper 80-1A, p. 157-164.

**Yeo, G.M., Bailey, G., Crux, J., Fischer, B., Jackson, V., Relf, C., and Walroth, J.**
1983: Preliminary geology of western Hepburn Island map area, N.W.T. (NTS 76M/3, M/4, M/5, M/6, M/11, M/12, M/13, M/14); Indian and Northern Affairs Canada, Northern Affairs Program, Geology Division, Yellowknife, EGS-1983-8.

**York, D.**
1969: Least squares fitting of a straight line with correlated errors; Earth and Planetary Science Letters, v. 5, p. 320-324.

Geological Survey of Canada Project 870008

# Geological reconnaissance of the southeast corner of Snowdrift area, District of Mackenzie, Northwest Territories

**H.H. Bostock**
**Continental Geoscience Division**

*Bostock, H.H., 1992: Geological reconnaissance of the southeast corner of Snowdrift area, District of Mackenzie, Northwest Territories; in Current Research, Part C; Geological Survey of Canada, Paper 92-1C, p. 209-215.*

***Abstract***

*The southeast corner of the Snowdrift area encompasses the confluence of two major shear zones: the Great Slave Lake shear zone (GSLsz) separating Slave Province from Churchill Province; and a second fault zone marginal to northeastern Taltson Magmatic Zone (TMZ) which separates most of this part of TMZ on the west from Rae Province on the east. Before intersecting GSLsz, the TMZ-marginal zone splays northeastward into three dextral mylonite belts.*

*Map-units involved in the four fault blocks southeast from GSLsz are: 1) mixed gneiss, and granite-diatexite (1.96 Ga) intruded by megacrystic granite (1.94 Ga.); 2) more highly deformed granite-diatexite; 3) strongly foliated megacrystic granite; 4) equigranular granite (1.88 Ga.). Block 1) has a central zone of trace fluorite mineralization. Moderately southwest plunging mineral lineations affect the central two blocks. These rocks are cut by diabase dykes likely correlative with the Sparrow dyke swarm (1.83 Ga).*

***Résumé***

*Le coin sud-est de la région de Snowdrift s'étend sur la confluence de deux zones de cisaillement importantes : la zone de cisaillement de Great Slave Lake (zcGSL) séparant la province des Esclaves de la province de Churchill; et une deuxième zone faillée en bordure du nord-est de la zone magmatique de Taltson (ZMT) qui sépare presque toute cette partie de la ZMT, à l'ouest, de la province de Rae, à l'est. Avant de recouper la zcGSL, la zone en bordure de la ZMT déborde vers le nord-est pour former trois zones mylonitiques dextres.*

*Les unités cartographiées dans les quatre blocs faillés au sud-est de la zcGSL sont : 1) un gneiss mélangé et un granite-diatexite (1,96 Ga) lesquels ont été pénétrés par un granite mégacristallin (1,94 Ga); 2) un granite-diatexite plus déformé; 3) un granite mégacristallin fortement feuilleté; 4) un granite isogranulaire (1,88 Ga). Le bloc 1) comporte une zone centrale de minéralisation de fluorite à l'état de traces. Des linéations minérales plongeant modérément vers le sud-ouest touchent les deux blocs centraux. Ces roches sont recoupées par des dykes de diabase probablement équivalents à l'essaim de dykes de Sparrow (1,83 Ga).*

## INTRODUCTION

The current project area in the southeast corner of Snowdrift sheet (75L), is roughly triangular with its south and east boundaries at 62° N. lat., and 110°W. long. respectively (Fig. 1). Geologically, it lies in the western part of Churchill Province at the confluence of Great Slave Lake shear zone (GSLsz) and the northeast margin of Taltson Magmatic Zone (TMZ). The GSLsz is a continental scale shear zone superimposed upon early high grade paragneisses engulfed in a granitic complex of batholithic dimensions (Hanmer,1988b; Hanmer et al., in press). It is bordered on the southeast by a less severely sheared contact zone within which adjacent wall rock units are in places predominant, whereas elsewhere the granitic rocks of the complex are more abundant. The western part of Churchill Province (ie. TMZ) consists predominantly of similar high grade paragneisses engulfed within garnet cordierite-bearing, megacrystic and equigranular granites (Bostock, 1988). In the east (ie. western Rae Province) somewhat older sphene-bearing gneisses of predominantly granitic composition contain remnants of mafic rocks.

Previous reconnaissance of the area was made by G.M. Wright of the Geological Survey who published a preliminary map (Wright, 1951) at 1 inch to 2 miles. The same data are shown on a coloured compilation map (Geological Survey of Canada, 1968) at 1 inch to 4 miles. A modern map of GSLsz covers most of the country immediately to the northwest (Hanmer, 1988a). A preliminary report, (Bostock, 1988) describes the geology of the north half of the Taltson Lake sheet (75E) immediately south of the map area.


### *Acknowledgment*

Ronald Scott ably assisted the writer during the current work.


## GENERAL GEOLOGY

### *Paragneiss*

The oldest rocks in the Snowdrift area (Fig. 2) are believed to be remnants of paragneiss and metabasite engulfed in quartz monzonite of the Slave granite. For the most part these remnants are intermixed so intimately with the Slave granite that they have not been mapped separately from it, and the mixture is termed Slave granite-diatexite. Three bodies of gneiss, which occur along the shores of Gagnon Lake, are larger and more coherent than such remnants elsewhere and have been mapped separately (Fig. 2). These bodies are approximately collinear and may be connected beneath the waters of the lake. An extensive additional area of paragneiss more intimately intermixed with granite occurs along the northern projection of this locus, but is not differentiated from Slave granite at the current scale of mapping.

The paragneiss consists of commonly rusty, banded to foliated, biotite and/or chlorite gneiss with scattered, interleaved bands or lenses of quartz-rich gneiss, calc-silicate gneiss and mafic rocks of possible igneous origin. Most of the paragneiss has been variably altered by greenschist facies metamorphism. Nevertheless, remnants of garnet, and locally of sillimanite, indicate that the paragneiss has reached at least middle amphibolite facies. Metabasites also, are so extensively chloritized that primary mafic minerals are no longer recognizable in the field. By analogy with similar rocks in the Taltson Lake area immediately to the south (Bostock, 1988), it seems likely that the maximum metamorphic grade attained was upper amphibolite or granulite facies.

The paragneiss is engulfed within the Slave granite (U/Pb monazite 1955-1960 Ma, Bostock et al., 1987; Hanmer et al., in press) and is therefore older than this. It is possible

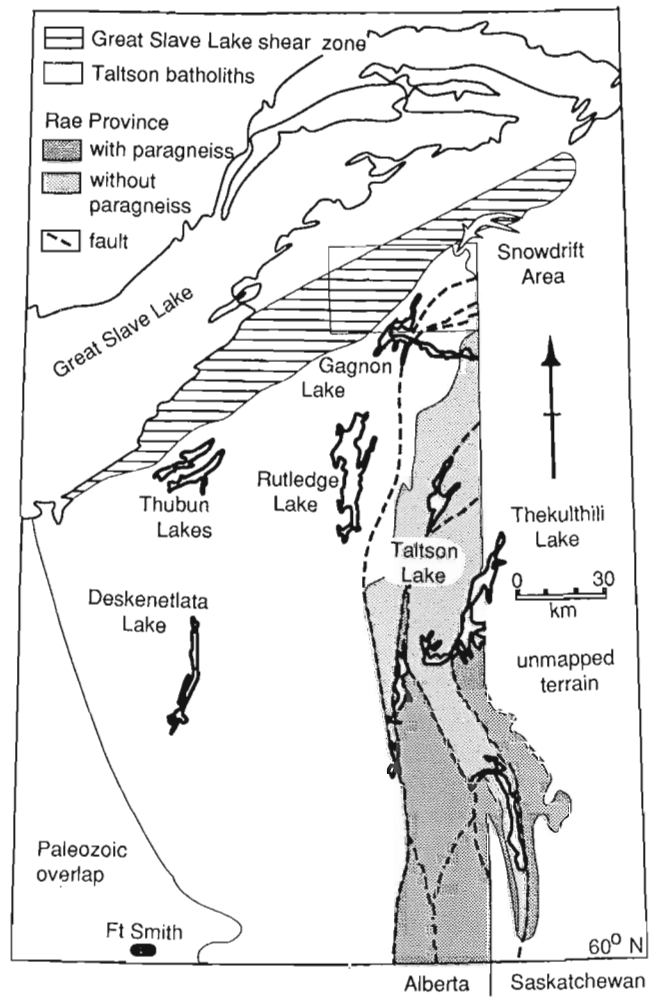


**Figure 1.** Index Map showing the location of the Snowdrift Area.

however, that more than one unit of sedimentary rocks has been engulfed in the granite over this extensive terrain, and that the rocks concerned here may be of more than one pre-1955-60 Ma age.

### *Slave granite-diatexite*

The Slave granite-diatexite forms a northeasterly striking belt across the central part of the map area. Together with the eastern mixed gneiss unit, which has probably been derived from the same protolith by further deformation, it is the predominant lithology within the area.

The Slave granite-diatexite, in its least altered state, consists of buff to white, medium- to fine-grained, massive to foliated, mostly equigranular biotite quartz monzonite. It is widely, and commonly intimately, contaminated with metasediment which mostly persists as diffuse bands or lenses of mafic-, quartz-, or garnet-rich material. South of the map area cordierite is a widespread local constituent (Bostock, 1988), but in the Snowdrift area it is recognized only locally as chloritized pseudomorphs. Garnet is typically heavily altered to chlorite. Locally the Slave granite has white to pinkish potash feldspar megacrysts up to 2 cm in length. These are most common in the vicinity of Konth megacrystic granite, and contacts appear to be locally gradational.

No definitive contacts between Slave and Konth granites were found in the Snowdrift area. U/Pb dating of the two granites south and west of Snowdrift area indicate that the Konth granite (1935 Ma., Bostock and Loveridge, 1988) is younger than Slave granite (1955-60 Ma., Bostock et al.,1987; Hanmer et al., in press).

### *Eastern mixed gneiss*

The eastern mixed gneiss unit is substantially similar to the Slave granite-diatexite (monzogranite with high grade paragneiss remnants) from which it differs mainly in greater deformation and finer grain size. It forms a large lenticular fault block east of Gagnon Lake stretching northeast from the central south boundary of the present map area to its central east boundary. Within the map area, the block is entirely bounded by mylonite (Fig. 2). Its presence is made apparent on air photos by the distinctive blocky surface which it displays.

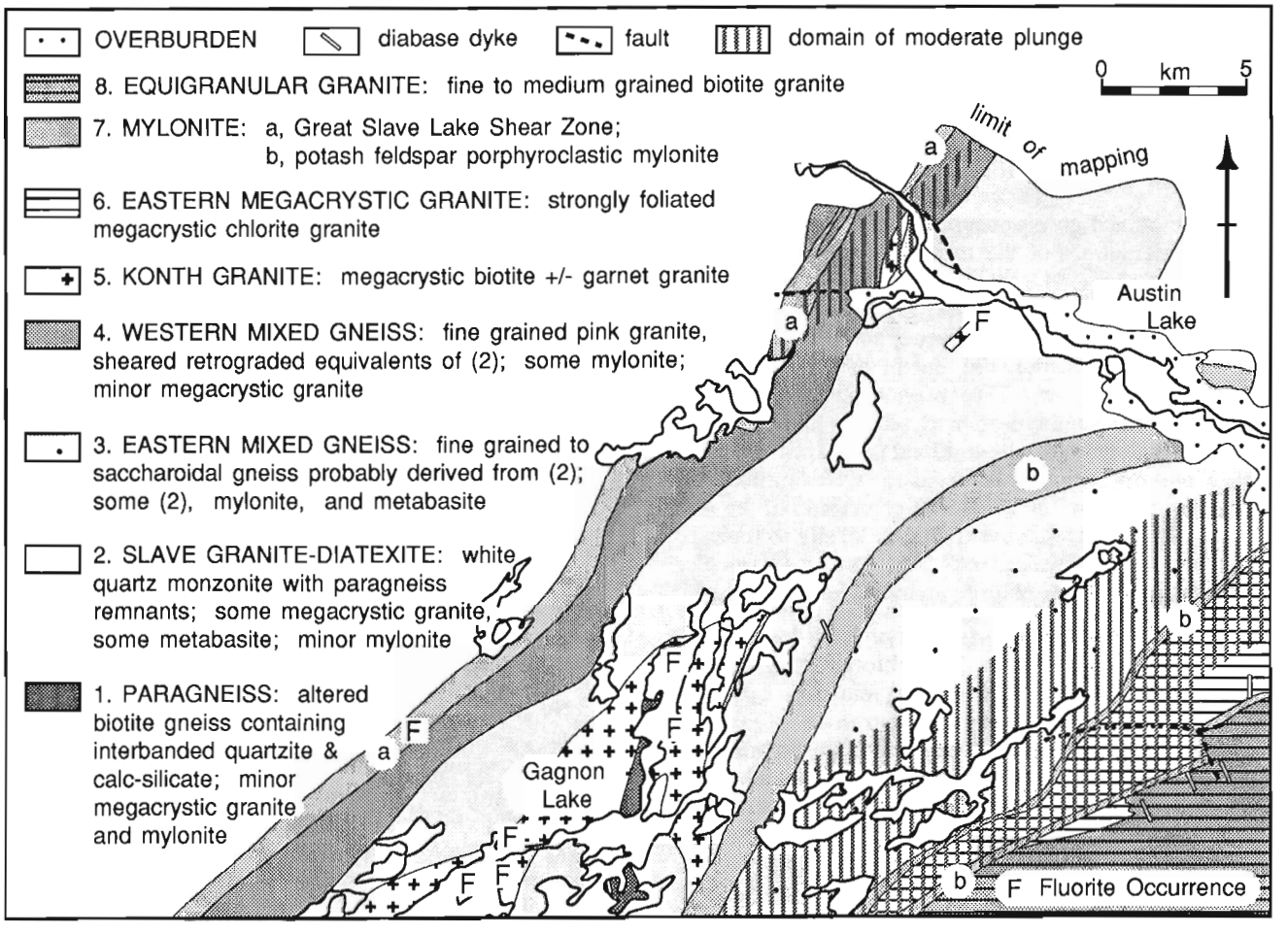


**Figure 2.** Geological map of the Snowdrift Area.

Rocks within the eastern mixed gneiss unit are mostly foliated, and fine grained to saccharoidal, but, in some northern parts of the unit, they are more commonly fine to medium grained. White to buff felsic bands and lenses are commonly interleaved with amphibolite and biotite- to chlorite-rich bands and lenses. Along the south and southeastern margins of the block the rocks are locally exceptionally fine grained and pass into coarsely porphyroclastic mylonites from which they differ mainly in their content of mafic bands and absence of porphyroclasts. Foliation tends to be straight rather than wavy. Similar very fine-grained rocks are present locally along the northwest margin of the block but appear to be much less extensive. In the northern part of the block, southwest of Austin Lake, (Fig. 2) garnetiferous gneiss is locally included within a white, medium-grained, less foliated monzogranite, and fine-grained paragneisses locally have an olive green colour suggestive of granulite facies metamorphism.

The eastern mixed gneisses contain lithologies that are comparable to those found in the Slave granite-diatexite unit. The more deformed southern part of the eastern mixed gneisses resemble gneisses found locally east of northern Rutledge lake (Fig. 1, Bostock, 1988). This similarity, and the fact that they are enclosed by bands of dextral mylonite, suggest that they may once have been continuous with gneisses east of Rutledge lake. The granitic component of the eastern mixed gneiss is therefore probably the same age as the Slave granite (1.96 Ga., Bostock et al., 1987; Hanmer et al., in press).

### *Western mixed gneiss*

The western mixed gneiss occupies a continuous belt along the northwest margin of the map area where it separates mylonites of the GSLsz on the northwest from Slave granite-diatexite to the southeast (Fig. 2). The unit is a particularly heterogeneous one, being composed mostly of fine-grained, pink leucogranite, but including fine-grained gneissic rocks that may have been derived from Slave granite-diatexite, medium-grained biotite-chlorite granite and megacrystic granite, mylonite, and migmatitic rocks that display a more ptygmatic style of deformation and recrystallization than that evident in other parts of the unit. The fine-grained leucogranite is at least locally tectonically interbanded with gneissic rocks, but some equigranular, medium-grained, biotite-chlorite granite is intrusive.

The pink leucogranite component of the western mixed gneiss typically has 5% or less chlorite in a fine- to medium-grained matrix of quartz and feldspar. Locally it grades to medium-grained leucogranite of similar composition. Commonly the fine-grained leucogranite is foliated, but in places it is more massive and foliations are difficult to discern. Rarely samples from such massive localities have a weak, steeply plunging lineation. Elsewhere the leucogranite includes bands of more chlorite-rich, fine-grained rocks up to several feet in thickness that may represent deformed mafic dykes. Locally fine grained white granite may have been derived from the Slave granite-diatexite, but no indications of the aluminous minerals commonly evident in that unit persist. Three kilometres north of Gagnon Lake an isolated area of medium-grained migmatite comprising large remnants of ptygmatically folded biotite gneiss within buff weathering, weakly foliated granite occurs within the unit. No remnants of quartz-rich gneiss like those found in the Slave granite-diatexite were seen within the migmatite. In the mixed gneiss west of Austin Lake, fine-grained foliated granite typical of this unit is cut by irregular lenses of a coarser more weakly foliated granite, possibly a distinct later unit. A belt of sheared megacrystic granite occurs along the southeast contact of the unit southwest of Snowdrift River (Fig. 2), and a thin band of coarsely porphyroclastic mylonite (not shown) occurs at this contact north of the river. Minor belts of mylonite are present elsewhere within the unit.

Reconnaissance of the western mixed gneiss unit suggests that it is a complex tectonic mix related spatially, and therefore perhaps temporally, to GSLsz. Textural variation in the granites which make up its bulk suggests that the western gneiss complex comprises remnants of the southeastern margin of GSLsz incorporated in plutonic material that was emplaced and deformed during more than one period in the development of the GSLsz.

### *Konth granite*

The greater part of the Konth granite in the map area occurs within a large roughly triangular area (some 50 sq km) with its base along the southern map boundary (Fig. 1). Minor bodies of similar megacrystic granite occur within the Slave granite-diatexite farther to the northeast. Regionally the granite is part of a major batholith extending far to the south into Alberta (Godfrey and Langenberg, 1978).

The Konth granite is typically a syenogranite characterized by 1 to 3 cm potash feldspar megacrysts in a fine- to medium-fine-grained matrix of quartz, plagioclase and biotite-chlorite. Garnet, and cordierite are common constituents south of the present map area but only garnet persists through the greenschist facies alteration within the present map area. Prominent ridges of Konth granite in which the megacrysts are relatively elongate are common in the western part of the pluton whereas less abundant more equidimensional megacrysts are common in the eastern parts of the pluton. Brecciation and greenschist facies alteration, though evident over most of the pluton, are particularly prominent in the northern parts.

No contacts between Konth and Slave granites were seen in the present map area, though textural variation in the eastern parts suggest that contacts may be gradational there. South of the map area exposed contacts are few but intrusive contacts of Konth into Slave granite have been seen (Bostock, 1987). Uranium/Lead monazite dating in the Fort Smith area suggests that the Konth granite was emplaced about 1935 Ma (Bostock and Loveridge, 1988).

### *Eastern megacrystic granite*

The eastern megacrystic granite lies between two thin but prominent, continuous mylonite belts that cut across the southeast part of the map area. In the southwest it pinches out between these belts, but its extent to the northeast is unknown.

The eastern megacrystic granite consists of abundant potash feldspar megacrysts one to three cm in length, in a strongly sheared matrix of quartz, feldspar, chlorite and epidote. Much of the pluton might have been classified as protomylonite, but the matrix is significantly coarser than that found in the adjacent mylonites, and unmappable zones within it are significantly less strongly foliated.

The eastern megacrystic granite does not intrude either of the mylonite belts that border it. It is therefore probably older than both of these mylonites. The eastern megacrystic granite is lithologically similar to the megacrystic phase in a complex area of megacrystic and equigranular granite that intersects the southeast arm of Gagnon Lake immediately south of the present map area (Fig. 1 and Bostock, 1988). This southern megacrystic granite has an age of emplacement of 1.940 +/- 8 Ma (van Breemen et al., 1991).

### *Equigranular granite*

Equigranular granite occupies some 40 sq. km in the southeast corner of the map area (Fig. 1). It is contiguous with the equigranular phase in a larger area of equigranular and megacrystic rocks that straddles the southeast arm of Gagnon Lake farther south (van Breemen et al., 1991).

The equigranular granite is typically a medium- to fine-grained, and unfoliated monzogranite with 5 to 10 percent of biotite. A few scattered megacrysts of potash feldspar are present locally. It tends to be finer grained near its margins, and late, medium- to coarse-grained segregations occur within it. Some parts are red stained and chloritized. Mafic inclusions within the equigranular granite are rare.

The northwest contact of the equigranular granite is mostly followed by a narrow, poorly exposed zone in which the granite either grades into a chloritic gneiss-migmatite, or is intercalated with thin bands of megacrystic granite; contacts with the larger lens of eastern megacrystic granite south of the mylonite belt (Fig. 2) are not exposed. This zone is followed, immediately to the northwest, by a mylonite belt (the southern lesser mylonite belt described under the heading, mylonite belts). No dykes of equigranular granite were found to cut any part of the contact zone. Although the equigranular granite is probably younger than the gneiss-migmatite into which it grades and the eastern megacrystic granite whose trend it crosses, age relations with the mylonite have not been established in the field. Initial U/Pb zircon dating for similar equigranular granite near the east arm of Gagnon Lake south of the map area has suggested an age of 1882 +7/-6 Ma. (van Breemen et al., 1991).

The equigranular granite as a whole occurs in the northern part of a complex granite area formerly called the Gagnon granite south of the present mapping (Bostock, 1988). The southern part of this area is occupied by largely unfoliated megacrystic granite that is apparently distinctly older than the equigranular granite (van Breemen et al., 1991). This complex granite area is further peculiar in that it is the only extensive body of largely unfoliated granitic rocks that lies immediately east of the northern part of the main fault margin of TMZ, yet whose geochronology suggests a temporal relationship with TMZ.

### *Mylonite belts*

Northeasterly trending mylonite belts form a major component of the current map area (Fig. 2). The extensive GSLsz (Hanmer, 1988b) follows the entire northwestern boundary of mapping (Fig. 1) but the current study has only examined it to a width of one or two hundred metres. A second major belt of mylonite, 1.5 to 2.5 km in width, here called the central mylonite belt, extends northeasterly to easterly across the central part of the map area. Two lesser mylonite belts, generally less than one kilometre in width, extend northeasterly across the southeast corner of the map area. Minor mylonite belts up to several hundred metres across are present within or along the margins of most of the plutonic map-units, but have not been found to be traceable from one traverse intersection to the next. Kinematic indicators found along all the larger mylonite belts and some of the minor ones have suggested dextral strike slip movements.

The three continuous mylonite belts of the central and southeastern parts of the map area merge at their intersection with the southeast arm of Gagnon Lake immediately south of the map area (Fig. 1 and Bostock, 1988). This single belt may be continuous southward for at least 100 km into the central part of the Fort Smith sheet (75D) (Bostock,.1988; Bostock and Loveridge, 1988).

The mylonite belts comprise rocks varying from protomylonite to ultramylonite and some strongly foliated megacrystic granite, but the predominant lithology is coarsely porphyroclastic mylonite. Rounded porphyroclasts of pink to white or rarely grey potash feldspar up to 2-3 cm in length are common. Chlorite and epidote are the predominant mafic minerals in the southern lesser mylonite belt, in the central mylonite belt, and in the southwestern, mapped part of GSLsz. Biotite is the predominant mafic in the northeastern part of this zone, and in the northern of the lesser mylonite belts.

The GSLsz, which flanks the northwestern edge of the map area, is distinct from the other continuous mylonite belts that merge at the southeast arm of Gagnon Lake (south of the map area). At least some of the shearing associated with GSLsz is older than an unfoliated (undated) granite phase which forms a component of the western mixed gneiss unit of the present map area. Hanmer (1988b) considers that this major shear zone was active primarily within the period 1.9-2.0 Ga.

The other mylonite belts mapped are not known to be intruded by any granitic dykes and are therefore probably younger than the plutonic rocks which directly border them,

but no sharply defined contacts were seen. A possible exception to this generalization is the southern lesser mylonite belt which may be completely separated from the equigranular granite by a thin contact zone of gneiss and megacrystic granite. Nevertheless these mylonites are probably younger than the main phase of Taltson magmatism (Konth granite 1935 Ma., Bostock and Loveridge, 1988). They could also be younger than the 1882 Ma age of the equigranular granite because no definitive contact relations were found between these two lithologies. All of the mylonite belts are probably older than the diabase dykes (1.83 Ga., van Breemen et al., 1991), one of which intrudes the central mylonite belt (Fig. 2).

Some further absolute age constraint is applicable to the dextral, north-south TMZ-marginal fault zone of which the central and lesser mylonite belts form a part (Fig. 1). Near the southern extremity of this zone the maximum age of local movement is later than the 1906 Ma age of the Benna Thy Granite (Bostock and Loveridge, 1988).

### *Diabase dykes*

North to northwesterly trending diabase dykes up to about 2 m in thickness have been found in the central eastern and southeastern parts of the map area. They appear to be most common within the equigranular granite. The dykes are massive, fine grained, dark grey, and display chilled margins against their hosts. Contacts are typically not continuous for more than a few metres due to minor offsets along joints and pinch-outs.

The dykes are probably part of the northwest to north trending Sparrow dyke swarm abundantly intruded about Nonacho basin farther south. They are most common in the northern part of the equigranular granite. One dyke was found to cut the central mylonite belt. A preliminary U/Pb baddeleyite age of 1.83 Ga has been obtained for the Sparrow dykes (van Breemen et al., 1991).

## STRUCTURAL GEOLOGY

### *Foliations*

Foliations throughout the map area tend to be steeply dipping and northeasterly trending, but there is divergence to more easterly and more northwesterly trends north of the central mylonite belt about Austin Lake. The boundary between the domains of diverging foliation extends approximately north-northeastward from the northern tip of Gagnon Lake and the rocks along this boundary appear to have undergone the most severe greenschist facies alteration. Furthermore, this boundary, projected southward, coincides with a diffuse zone along which 6 out of the 7 fluorite veins and minor fluorite occurrences in the map area have been found (Fig. 2). It is possible, therefore, that the north-northeasterly trending valley of Gagnon Lake represents a zone of brittle faulting and late low grade alteration accompanied by fluorite mineralization. In the area along this trend south of the present map area, fluorite appears to be associated with a swarm of felsitic dykes (Bostock, 1988), but no dykes of this type have been found during work for the current project.

### *Lineations*

Mineral lineations within the map area vary from sub horizontal (0 to 25 degrees plunge) to moderately plunging (25 to 52 degrees plunge). Two extensive domains of moderate plunge (Fig. 2) are located: 1) near the south border of the map area where an ubiquitous lineation is present in the two lesser mylonite belts, in the eastern megacrystic granite, and in the southern part of the eastern mixed gneiss; and 2) in the western mixed gneiss, adjacent Slave granite-diatexite and minor Konth granite on either side of Snowdrift River, and possibly in some mylonite of GSLsz. A minor discordant domain of subhorizontal lineations is present within eastern megacrystic granite and the southern lesser mylonite belt adjacent to the east boundary of the map area (Fig. 2). In the southern domain the lineations plunge south to southwest, whereas in the northern one about Snowdrift River they plunge mostly northerly.

Expression of southwest plunging lineations within both of the lesser mylonite belts where dextral kinematic indicators have been found, and in the eastern mixed gneisses and megacrystic granite, suggests that the lineations in these three different lithologies developed during the same strain regime. The domain of southwest plunging lineations therefore probably indicates relative uplift of rocks to the northwest of the domain with respect to those on the southeast. This conclusion is consistent with dextral convergence of TMZ and Slave Province west of the TMZ-marginal fault zone.

## CONCLUSION

Reconnaissance of the southeast corner of the Snowdrift area is of particular interest because it includes the predicted confluence of two major mylonite belts: the GSLsz, (Hanmer and Lucas, 1985; Hoffman, 1987; Hanmer, 1988b); and a northerly trending fault zone which marks the contact between most of northern TMZ and the gneisses of western Rae Province (Fig. 1). Mapping covered by the present report shows that these two shear zones do not actually intersect, but rather, the TMZ marginal shear zone splays abruptly northeastward before reaching GSLsz. It also indicates that at least a part of the movement along the northern TMZ-marginal fault zone (that involved in the central mylonite belt) is older than the 1.83 Ga. age of the Sparrow Dykes.

## REFERENCES

**Bostock, H.H.**
1987: Geology of the south half of the Taltson Lake map area, District of Mackenzie; in Current Research, Part A, Geological Survey of Canada, Paper 87-1A, p. 443-450.

**Bostock, H.H.**
1988: Geology of the north half of the Taltson Lake map-area, District of Mackenzie; in Current Research, Part C, Geological Survey of Canada Paper 88-1C, p. 189-198.
**Bostock, H.H., van Breemen, O., and Loveridge, W.D.**
1987: Proterozoic geochronology in the Taltson Magmatic Zone, N.W.T.; in Radiogenic Age and Isotopic Studies: Report 1, Geological Survey of Canada Paper 87-2, p. 73-80.
**Bostock, H.H. and Loveridge, W.D.**
1988: Geochronology of the Taltson Magmatic Zone and its eastern Cratonic Margin, District of Mackenzie; in Radiogenic Age and Isotopic Studies: Report 2, Geological Survey of Canada Paper 88-2, p. 59-65.
**Geological Survey of Canada**
1968: Christie Bay; Geological Survey of Canada, Map 1122A with marginal notes.
**Godfrey, J.D. and Langenberg, C.W.**
1978: Metamorphism in the Canadian Shield of Northeastern Alberta; in Metamorphism in the Canadian Shield, Geological Survey of Canada, Paper 78-10, p. 129-138.
**Hanmer, S.**
1988a: Geology, Great Slave Lake Shear Zone: northwest Territories; Geological Survey of Canada map (1:100,000), Open file 1783.
1988b: Great Slave Lake Shear Zone, Canadian Shield: reconstructed vertical profile of a crustal-scale fault zone; Tectonophysics, vol. 149, p. 245-264.
**Hanmer, S. and Lucas, S.B.**
1985: Anatomy of a ductile Transcurrent Shear, The Great Slave Lake Shear zone, District of Mackenzie, N.W.T. (preliminary report); in Current Research part B, Geological Survey of Canada Paper 85-1B, p. 121-131.
**Hanmer, S., Bowring, S., van Breemen, O., and Parrish, R.**
in press: Great Slave Lake Shear Zone, NW Canada: Mylonitic press Record of Early Proterozoic Continental Convergence, Collision and Indentation; Journal of Structural Geology.
**Hoffman, P.F.**
1987: Continental transform tectonics: Great Slave Lake shear zone (ca. 1.9 Ga), northwest Canada; Nature, vol. 15, p. 785-788.
**van Breemen, O., Bostock, H.H. and Loveridge, W.D.**
1992: Geochronology of granites along the margin of the northern Taltson Magmatic Zone, (TMZ) and western Rae Province; in Radiogenic Age and Isotopic Studies: Report 5, Geological Survey of Canada Paper 91-2.
**Wright, G.M.**
1951: Second Preliminary Map, Christie Bay, Northwest Territories, Geological Survey of Canada Paper 51-25, p. 1-10.

---

Geological Survey of Canada Project 850005

# Local geological investigations in Hill Island Lake area, District of Mackenzie, Northwest Territories

**H.H. Bostock**
**Continental Geoscience Division**

*Bostock, H.H., 1992: Local geological investigations in Hill Island Lake area, District of Mackenzie, Northwest Territories; in Current Research, Part C; Geological Survey of Canada, Paper 92-1C, p. 217-223.*

***Abstract***

*Local reconnaissance mapping about Hill Island Lake suggests that the sinistral shear zone which follows the east shore of that lake extends north at least as far as Thekulthili Lake and south beyond the Saskatchewan border. Metamorphic grade rises to upper greenschist-lower amphibolite facies along the shear zone.*

*A body of metagabbro, 7 by 2 km, west of Thoa River, ranges in composition from hornblendite to anorthositic metagabbro. A smaller body 10 km north of Hill Island Lake shows less variation. Both bodies predate major deformation, metamorphism and granite intrusion. Mixed gneiss between these bodies has an increased proportion of mafic components including remnants of metagabbro.*

*Nonacho-like conglomerate and siltstone have been found in a faulted outlier along a sinistral shear zone at the south end of Shark Lake.*

***Résumé***

*La cartographie de reconnaissance locale autour du lac Hill Island indique que la zone de cisaillement senestre qui suit la rive est de ce lac s'étend vers le nord, au moins jusqu'au lac Thekulthili et vers le sud au-delà de la frontière de la Saskatchewan. Le long de la zone de cisaillement, le degré de métamorphisme se situe entre le faciès supérieur des schistes verts et le faciès inférieur des amphibolites.*

*La composition d'un massif de métagabbro de sept sur deux km de dimensions, situé à l'ouest de la rivière Thoa, varie de la hornblendite au gabbro anorthositique. Un autre massif plus petit situé à 10 km au nord du lac Hill Island présente une composition moins variée. Les deux massifs sont antérieurs à des événements importants de déformation, de métamorphisme et d'intrusion granitique. Les gneiss mélangés entre ces massifs contiennent une proportion accrue de composantes mafiques, dont des résidus de métagabbro.*

*Un conglomérat et un siltstone de type Nonacho ont été découverts dans un lambeau de recouvrement faillé longeant une zone de cisaillement senestre à l'extrémité sud du lac Shark.*

## INTRODUCTION

This report covers a part of the western half of the Hill Island Lake sheet (75C) some 130 km east-northeast of Ft. Smith (Fig. 1). Geologically it lies along the western margin of Rae Province and encompasses some of the north-south faulting that borders Taltson Magmatic Zone nearby to the west.

The Hill Island Lake sheet is covered by a coloured map with marginal notes at 1 inch to 4 miles (Mulligan and Taylor, 1954). The area about Hill Island Lake was later examined by Bostock (1984). This report provides a summary of reconnaissance mapping in 1991 along the east margin of the area mapped in 1984. The work is presented on two maps: Fig. 2 entitled, Thoa River area, covering the area north and northeast of Hill Island Lake; and Fig. 3 entitled, Tatse Lake area, covering the area immediately south of Hill Island Lake. Although the map (Fig. 2) extends eastward to the 110th meridian, only the rocks investigated during 1991 are described.

### *Acknowledgment*

The writer was ably assisted by Ronald Scott during the 4 weeks spent on this work.

## GENERAL GEOLOGY

### *Mixed gneiss*

The oldest rocks in the project area, east of Hill Island Lake, are probably found among the components of the mixed gneiss. This gneiss consists primarily of fine- to medium-grained, foliated, granitic rocks of syenogranite to dioritic composition within which massive to schistose remnants of more mafic rocks are preserved. Near the east margin of mapping, zones within the gneiss are slightly rusty and contain remnants of sillimanite and garnet indicating a sedimentary origin. Textures in these zones of paragneiss range from banded to schistose or nebulitic.

The mixed gneiss is mostly comparable to that farther northwest where zircons from the granite phases have been dated in the range 2.27-2.44 Ga (Bostock and Loveridge, 1988; Bostock et al., 1991; van Breemen et al., 1991). North of Shark Lake the proportion of foliated quartz dioritic rocks may warrant a distinct gneiss unit.

### *Metagabbro and associated gneiss*

The Thoa metagabbro is a complex body some 7 km long by 2 km wide that occurs within the mixed gneiss just west of Thoa River (Fig. 2). The rock ranges from medium-fine to coarse grained and different parts are gneissic, foliated or massive. Composition ranges from hornblendite through hornblende gabbro to anorthositic metagabbro. The coarser feldspathic phases contain feldspar which ranges from grey to white but none of the original mafic mineralogy appears to be preserved. Biotite is a significant component in some parts.

Structures within the Thoa metagabbro are best exposed at the north end of the unit where the surface has recently been burned over. Elsewhere, structural detail is obscured by organic cover. In the north, structures range from massive to chaotic. Although several phases may be present in a given outcrop, contacts are commonly curved and interdigitated. Metagabbro is intruded by irregular dykes of anorthositic metagabbro, by more mafic metagabbro or by amphibolite. Southerly trending mafic gneiss penetrates the metagabbro locally, probably along ductile faults. Similar gneiss wraps around the northern end of the intrusion. An isolated ridge of metagabbro, north of the main body, is cut up by small irregular bodies of pink granite.

Farther south where the Thoa metagabbro is less well exposed, it is clear that compositional variations are equally diverse though individual outcrops appear more homogeneous. Along the west margin of the intrusion metagabbro is bordered by a mafic, biotite-hornblende mixed gneiss which locally contains metagabbro inclusions or cross-cutting metagabbro. Zones of similar gneiss occur within the metagabbro, and small bodies of granite locally cut it.

A smaller and less well exposed body of metagabbro is present about 10 km north of Hill Island Lake. It consists mostly of medium-grained hornblende gabbro and is substantially less varied than the Thoa metagabbro.

The mixed gneiss which lies between the metagabbro bodies (Fig. 2), is particularly heterogeneous having a higher proportion of mafic rocks than other parts of the mixed gneiss unit. In places the unit ranges in composition from amphibolite and metagabbro to granite with little evident foliation. Elsewhere the rocks are hornblende and/or biotite gneiss grading to granite, as at the north end of the Thoa metagabbro.

The metagabbro bodies are older than the latest phase of granite intrusion and they predate major metamorphism. A granite from the mixed gneiss terrain about 12 km north-northeast of the smaller metagabbro has given a U/Pb zircon age of 2.39 Ga (van Breemen et al., 1991) and other granites in similar mixed gneisses farther northwest have given ages in the range 2.3-2.4 Ga. The gabbro bodies were likely emplaced during or before this range of ages.

These mafic bodies extend along the east side of a major fault zone, west of which granites of the Taltson Magmatic Zone appear (1.9-2.0 Ga; Bostock et al., 1987; Bostock and Loveridge, 1988); van Breemen et al., 1991). Xenoliths of similar mafic metamorphic rocks including Cr-Ni-rich talc-actinolite inclusions have been reported along a comparable boundary associated with dextral faulting east of Rutledge Lake (Fig 1; Bostock 1989). This distribution raises the question whether the western edge of Rae Province could have been a rifted plate margin before Taltson magmatism (Bostock, 1989).

### *Greywacke-schist*

The greywacke-mudstones of the Hill Island Lake area are described by Bostock (1984). West of Hill Island Lake (Fig. 2) they rise from sub-greenschist facies to lower amphibolite

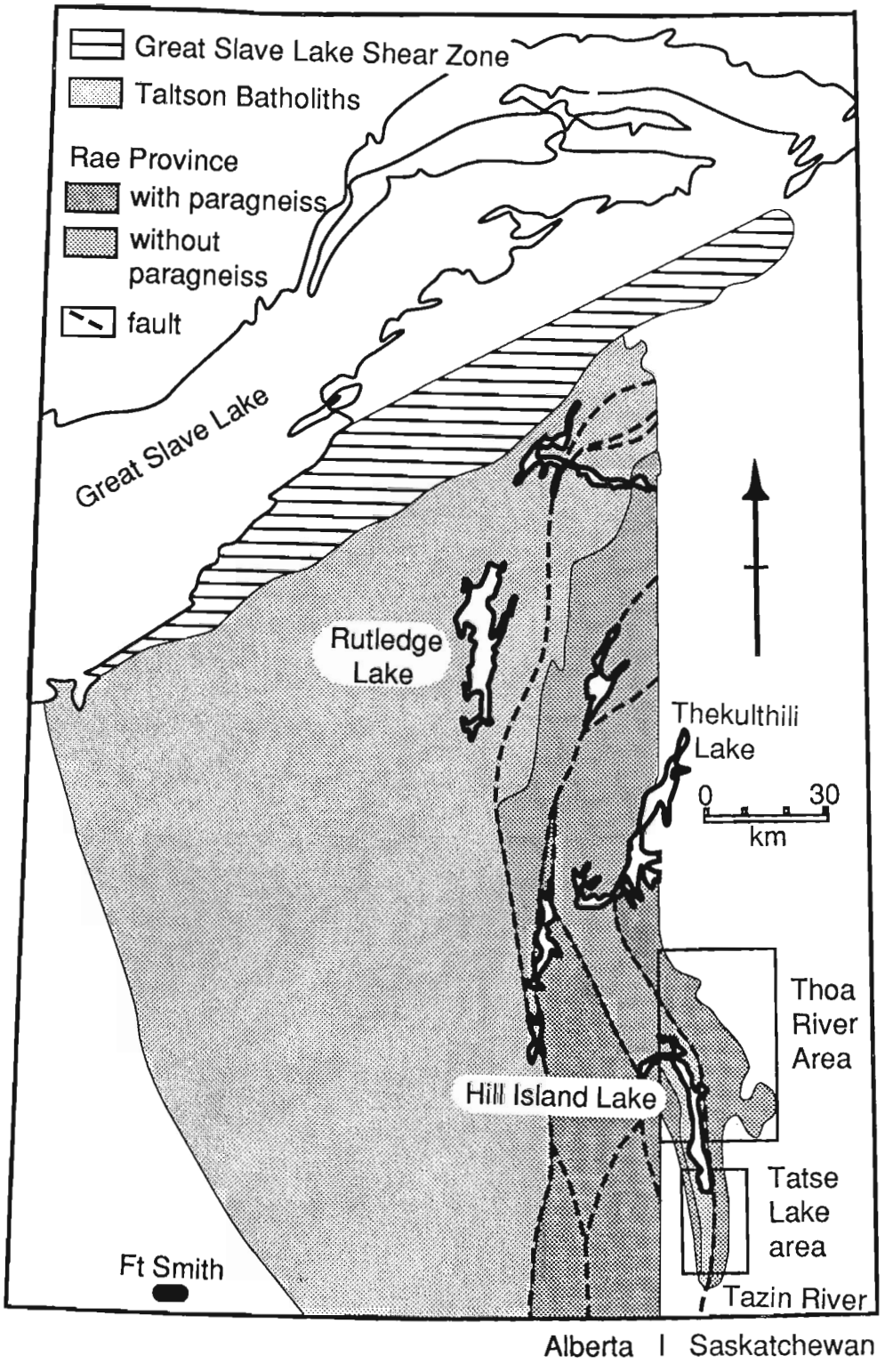


**Figure 1.** Map showing the location of the Hill Island Lake area and of the areas covered by Thoa River and Tatse Lake map figures.

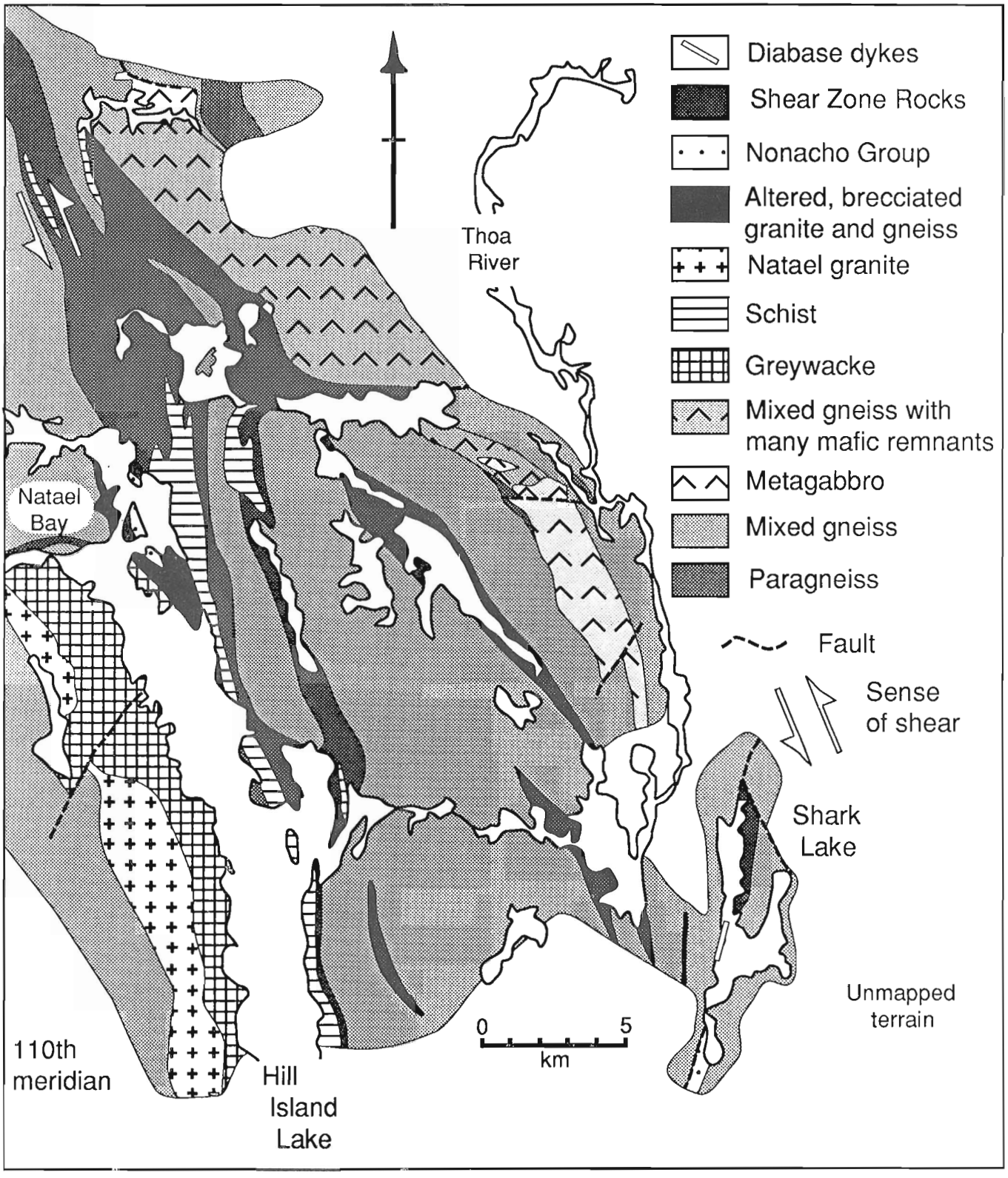


**Figure 2.** Thoa River area, geological map.

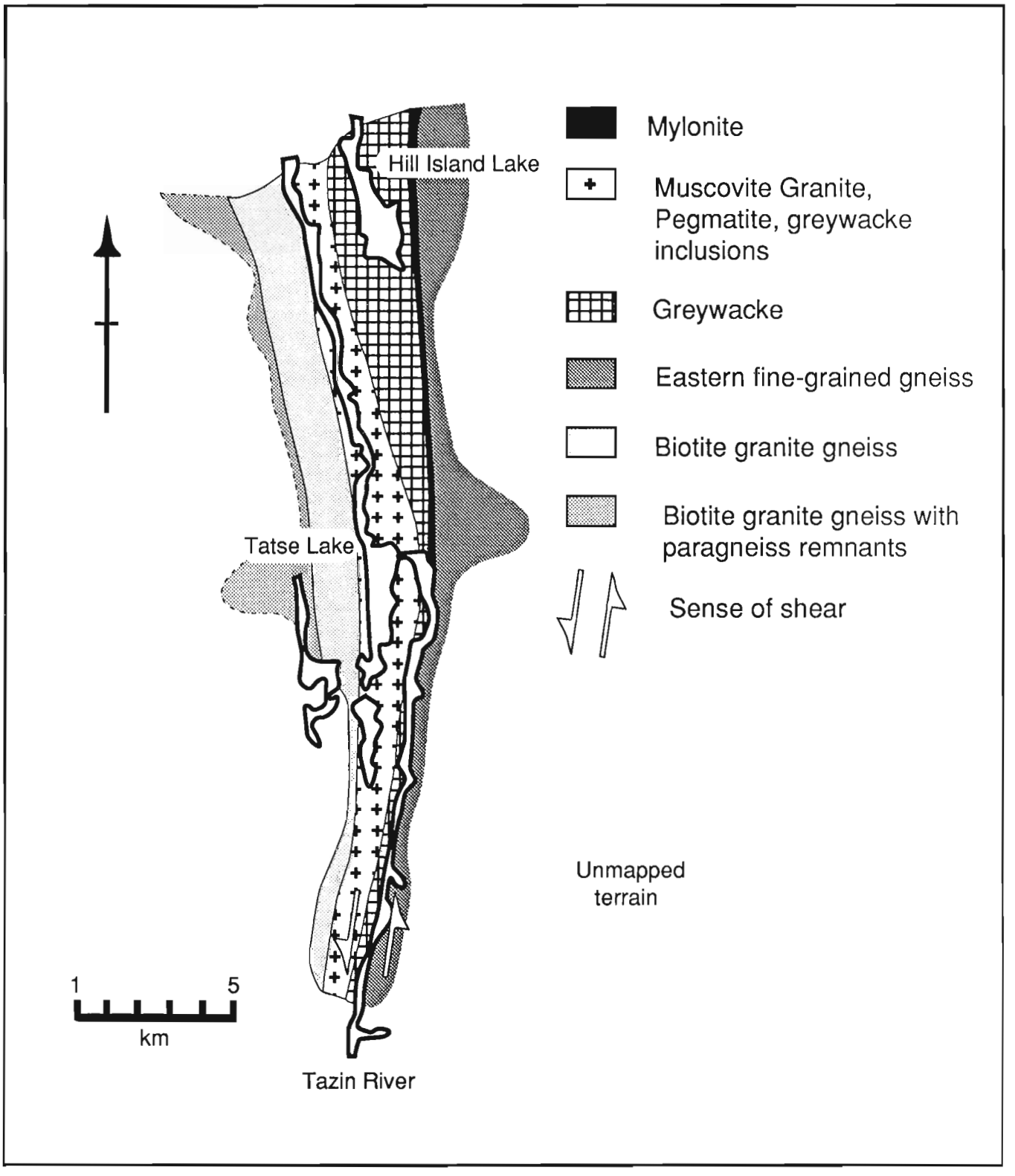


**Figure 3.** Tatse Lake area, geological map.

facies as indicated by the presence of cordierite near Natael granite. Andalusite-, garnet- and staurolite-bearing schists have developed locally in the same rocks along the east side of Hill Island Lake where the unit has been affected by the Thekulthili-Tazin River shear zone.

Slivers of schist similar to those on the east side of Hill Island Lake are present along the shear zone north of Hill Island Lake as far as the 110th meridian. Like the Hill Island Lake schists, but unlike the paragneiss-schist to east and west, the schist slivers are locally andalusite-bearing. Upper greenschist-lower amphibolite conditions of metamorphic grade therefore occurred this far north along the shear zone. South of Hill Island Lake the schist along the east margin of the greywacke-mudstones pinches out and low grade mudstones are exposed within a few tens of meters of the bounding shear zone.

Field relations of the greywacke-mudstones to adjacent units have been obscured by faulting along their eastern and northern contacts, and also along the western one where they have been intruded by Natael granite (1935 +/-3 Ma; Bostock et al., 1987). Earlier mapping (Mulligan and Taylor, 1954) and examination of air photographs suggested that the Natael granite might pinch out south of Tatse Lake (Fig. 3) where greywacke-mudstone and older gneisses appeared to be in contact. Outcrops in the area indicate a tectonic mix of abundant schistose lenses of greywacke-mudstone in muscovite granite at the contact with the western gneiss. Muscovite granite veins emplaced within the gneisses west of the contact suggest that it is a faulted intrusive contact and not an unconformity at this point.

### *Nonacho Group*

A small outlier of conglomerate of the Nonacho Group (Fig. 2) occurs near the north end of Hill Island Lake (Mulligan and Taylor, 1954; Bostock, 1984). A second outlier of this group has been tentatively identified near the south end of Shark Lake.

The Shark Lake Nonacho outlier along the west shore of the small lake immediately south of Shark Lake consists of buff, schistose, sericitic siltstone with granite cobble conglomerate in the hills behind. Scattered ovoid pebbles of granite and of white vein quartz occur locally in the siltstone, whereas the conglomerate to the west consists of up to 50% pink, near round to ovoid granite clasts up to 35 cm in length in a sandy chloritic matrix. Larger granite bodies, partly obscured by lichens, are likely talus slabs. Still farther west moss-covered outcrops become increasingly granitic making the precise position and nature of the western contact uncertain.

Although the siltstone-conglomerate at the south end of Shark Lake appears lithologically similar to basal rocks of the Nonacho Group (Aspler 1985; Bostock, 1987), the correlation is tentative because these rocks have been mapped as part of a belt of sediments extending north beyond the sixty-first parallel which is included in the same map unit with the greywacke-mudstones at Hill Island Lake (Mulligan and Taylor, 1954). The belt includes minor conglomerate in a somewhat different sedimentary assemblage north of Thoa River (Bostock, 1980), but very little is known of the intervening area. On the other hand, the putative Nonacho outlier at Shark Lake may lie in a graben or half graben along the fault through Stark Lake, the type of environment which commonly controlled the distribution of Nonacho deposition farther northwest (see Aspler, 1985).

### *Fault zone lithologies*

Mylonite, schist, saccharoidal gneiss and augen gneiss form a suite of mostly fine-grained tectonites which occupy the fault zone east of Hill Island Lake (Bostock, 1984). The rocks are characterized by sinistral strike slip cleavage intersections in the schists and greywacke-turbidites on either side of the Lake. Current work on the northern and southern projections of this zone better defines its limits and the sense of movements along it. An additional north-south fault zone with associated mylonite was found farther east at Shark Lake.

North and south of Hill Island Lake (Figs. 1, 2 and 3) the fault zone contracts but is recognizable as a fault lineament as far north as the south shore of Thekulthili Lake. North of the lake sinistral shear bands within the zone are compatible with sinistral shear sense as interpreted at Hill Island Lake. South of Hill Island Lake the fault zone along the east side of the lake projects southward across a drift covered area to intersect Tazin River just east of Tatse Lake (Fig. 3). A 150m wide section of mylonite is exposed in an isolated ridge just north of the intersection, and a smaller section is exposed on an island in the river about 12 km farther south. The same lineament continues south beyond the Saskatchewan border. Subhorizontal stretching lineations are evident in the mylonite, and sinistral shear bands were found in the adjacent greywacke-mudstones and between boudins in the inclusion-rich muscovite granite farther west.

### *Diabase*

A single brown weathering, dark grey, fine-grained diabase dyke was mapped at Shark Lake. The dyke is 2.5 m thick and trends north 20 degrees east, dipping 60 degrees west parallel to banding in the enclosing mixed gneiss. Similar but more abundant dykes are present about Hill Island Lake.

## CONCLUSIONS

Mapping during 1991 in the Hill Island Lake area suggests that the fault zone immediately east of Hill Island Lake projects northward as far as Thekulthili Lake and southward beyond the Saskatchewan border, a distance of over 100 km. Additional data support sinistral strike slip movement sense. Metamorphic grade over a substantial section of the fault zone is upper greenschist-lower amphibolite facies.

Two mappable metagabbro bodies which predate the latest granitic rocks and major deformation occur within the mixed gneiss on the northeast side of the northern part of the Hill Island Lake shear zone. The larger Thoa metagabbro is

compositionally varied with plagioclase-rich and hornblende-rich phases. Mixed gneiss between these bodies appears enriched in mafic components.

An outlier of Nonacho-like conglomerate and siltstone is preserved along a north-south fault zone with sinistral strike slip through Shark Lake.

## REFERENCES


**Aspler, L.B.**
1985: Geology of Nonacho Basin (Early Proterozoic) N.W.T.; unpublished, Ph.D. Thesis, Carleton University, 384 p.

**Bostock, H.H.**
1980: Reconnaissance geology of the Fort Smith-Hill Island Lake area, Northwest Territories; in Current Research, Part A, Geological Survey of Canada Paper 80-1A, p. 153-155.
1984: Preliminary geological reconnaissance of the Hill Island Lake and Taltson Lake areas, District of Mackenzie; in Current Research, Part A, Geological Survey of Canada, Paper 84-1A, p. 165-170.
1987: Geology of the south half of the Taltson Lake map area District of Mackenzie; in Current Research, Part A, Geological Survey of Canada, Paper 87-1A, p. 443-450.
1989: The significance of ultramafic inclusions in gneisses along the eastern margin of the Taltson Magmatic Zone District of Mackenzie, N.W.T.; in Current Research, Part C, Geological Survey of Canada, Paper 89-1C, p. 49-56.

**Bostock, H.H., van Breemen, O., and Loveridge, W.D.**
1987: Proterozoic geochronology in the Taltson Magmatic Zone, N.W.T.; in Radiogenic Age and Isotopic Studies: Report 1, Geological Survey of Canada, Paper 87-2, p. 73-80.

**Bostock, H.H., van Breemen, O., and Loveridge, W.D.**
1991: Further geochronology of plutonic rocks in northern Taltson Magmatic Zone, District of Mackenzie, N.W.T.; in Radiogenic Age and Isotopic Studies: Report 4, Geological Survey of Canada, Paper 90-2, p. 67-78.

**Bostock, H.H. and Loveridge, W.D.**
1988: Geochronology of the Taltson Magmatic Zone and its eastern cratonic margin, District of Mackenzie; in Radiogenic Age and Isotopic Studies: Report 2, Geological Survey of Canada, Paper 88-2, p. 59-65.

**Mulligan, R and Taylor, F.C.**
1954: Hill Island Lake; Geological Survey of Canada Map 1203A with marginal notes.

**van Breemen, O., Bostock, H.H. and Loveridge, W.D.**
1991: Geochronology of granites along the margin of the northern Taltson Magmatic Zone (TMZ) and western Rae Province; in Radiogenic Age and Isotopic Studies: Report 5, Geological Survey of Canada, Paper 91-2.



Geological Survey of Canada Project 850005

# Magnetite deposits in metasiltstones of the Snare Group at Hump Lake, Northwest Territories

**S.S. Gandhi**
**Mineral Resources Division**

*Gandhi, S.S., 1992: Magnetite deposits in metasiltstones of the Snare Group at Hump Lake, Northwest Territories; in Current Research, Part A; Geological Survey of Canada, Paper 92-1A, p. 225-235.*

***Abstract***

*Two stratabound massive magnetite-hematite deposits and several smaller occurrences in the Hump Lake area of the southern Great Bear magmatic zone, are hosted by metasiltstones of the Aphebian Snare Group. The host sequence includes some quartzo-feldspathic and calc-silicate beds, and is tightly folded and trends northwest. It is metamorphosed to lower amphibolite facies. It is intruded by a foliated dacitic porphyry body, and by post-deformation plutons of quartz monzonite and leucogranite related to the Great Bear magmatic activity.*

*Magnetite and hematite in the metasiltstones occur as granoblastic aggregates with quartz, feldspar, diopside, amphibole and epidote. The stratiform distribution of the iron oxides, quartzo-feldspathic character of the host siltstones, and close association of the dacitic feldspar porphyry, indicate a sedimentary origin in volcanic environment. These occurrences represent a metallogenic event older than the one that formed the magnetite-rich polymetallic veins and breccias in the Great Bear volcano-plutonic settings.*

***Résumé***

*Deux gisements massifs de magnétite-hématite limités par des strates et plusieurs venues minéralisées de moindre importance situés dans la région de Hump Lake, gisant dans la partie sud de la zone magmatique de Great Bear, sont contenus dans des métasiltstones du groupe de Snare (Aphébien). La séquence encaissante contient quelques lits quartzo-feldspathiques et calco-silicatés, est déformée par des plis serrés, et présente une direction générale nord-ouest. Elle est métamorphisée dans le sous-faciès inférieur des amphibolites et traversée par un corps intrusif schisteux composé de porphyre dacitique, et par des plutons de monzonite quartzifère et de leucogranite postérieurs à la déformation et associés à l'activité magmatique de l'épisode de Great Bear.*

*Dans les métasiltstones, la magnétite et l'hématite se présentent sous forme d'agrégats granoblastiques accompagnés de quartz, de feldspath, de diopside, d'amphibole et d'épidote. La distribution stratiforme des oxydes de fer, le caractère quartzo-feldspathique des siltstones encaissants et l'étroite association avec le porphyre feldspathique de composition dacitique, indiquent une origine sédimentaire dans un milieu volcanique. Ces venues minéralisées correspondent à un événement métallogénique plus ancien que celui qui a généré les filons et brèches polymétalliques riches en magnétite dans les milieux volcano-plutoniques de Great Bear.*

## INTRODUCTION

Recent metallogenic studies in the southern Great Bear magmatic zone (Fig. 1) have led to the recognition of potential for large magnetite-rich Cu-U-Au-Ag-REE deposits in volcano-plutonic settings, comparable to the Olympic Dam deposit in South Australia (Gandhi, 1988, 1989; Gandhi and Bell, 1990). Continuation of the studies involved geological appraisal of two strong airborne magnetic anomalies in the Hump Lake area, which were further defined by ground magnetic survey carried out by Noranda Exploration Company Limited in 1979 (Bryan, 1981a, b). Magnetite-rich outcrops were located, but no detailed geological mapping was done on them, and the nature of the deposits remained obscure. The present study was undertaken to bring it to light.

## GEOLOGY OF THE HUMP LAKE AREA

### *General geology*

The Hump Lake area is situated in the southern Great Bear magmatic zone close to the eastern boundary marked by the Wopmay fault zone (Fig. 1). Regional mapping by Lord (1942) recognized Archean rocks east of the fault zone, which are overlain unconformably by the Aphebian Snare Group. This group comprises conglomerate, sandstone, siltstone, shale, dolomite, and mafic to intermediate volcanics. Strata of this group are affected by deformation and metamorphism, and are intruded by the Hepburn suite of granitic plutons, which are late Aphebian in age (Frith et al., 1977). Lithologically similar, northwest-trending metasedimentary beds west of the Wopmay fault zone, including those at Hump Lake, have been regarded by Lord (1942), McGlynn (1968, 1977, 1979), and Gandhi and Lentz (1990), as part of the Snare Group. Detailed stratigraphic correlations between the strata on two sides of the fault zone have not yet been made.

Rhyolitic volcanic rocks of the magmatic zone overlie unconformably the metasediments of the Snare Group at Lou Lake 10 km west of Hump Lake. (Fig. 1), and are intruded by quartz monzonite (Gandhi and Lentz, 1990). Lithologically similar quartz monzonite underlies a large part of the Hump Lake area (Fig. 2), and contains numerous xenoliths of metasediments and a few of rhyolitic rocks. Gneissic granite-granodiorite in southwestern part of the area (Fig. 2), however, may be equivalent of the Hepburn suite.

### *Lithological units*

#### Snare Group

The metasedimentary rocks of this group are mainly siltstones, interbedded with subordinate sandstone, argillaceous sandstone, calcareous beds, and some magnetite-hematite-rich layers and lenses. Zones dominated by various lithologies are shown in Figures 2, 3 and 4.

The siltstones are thin bedded (on centimetre scale), and the beds are pale pink, cream and grey and greenish grey. The lighter coloured beds are quartzo-feldspathic, and the darker ones contain a relatively greater proportion of magnetite, hematite, clinopyroxene, amphibole, biotite, garnet, epidote and chlorite. The relative proportion of minerals varies greatly. The magnetite-hematite deposits and occurrences discussed later, are essentially beds containing more than 50 per cent iron oxides. Most of the siltstones contain some disseminated magnetite, which in grey beds exceeds 3 per cent. The texture is typically equigranular and granoblastic, with subhedral to euhedral iron oxides. Feldspars include lamellar twinned albitic plagioclase, cross-hatched microcline, string perthite and untwinned alkali feldspar.

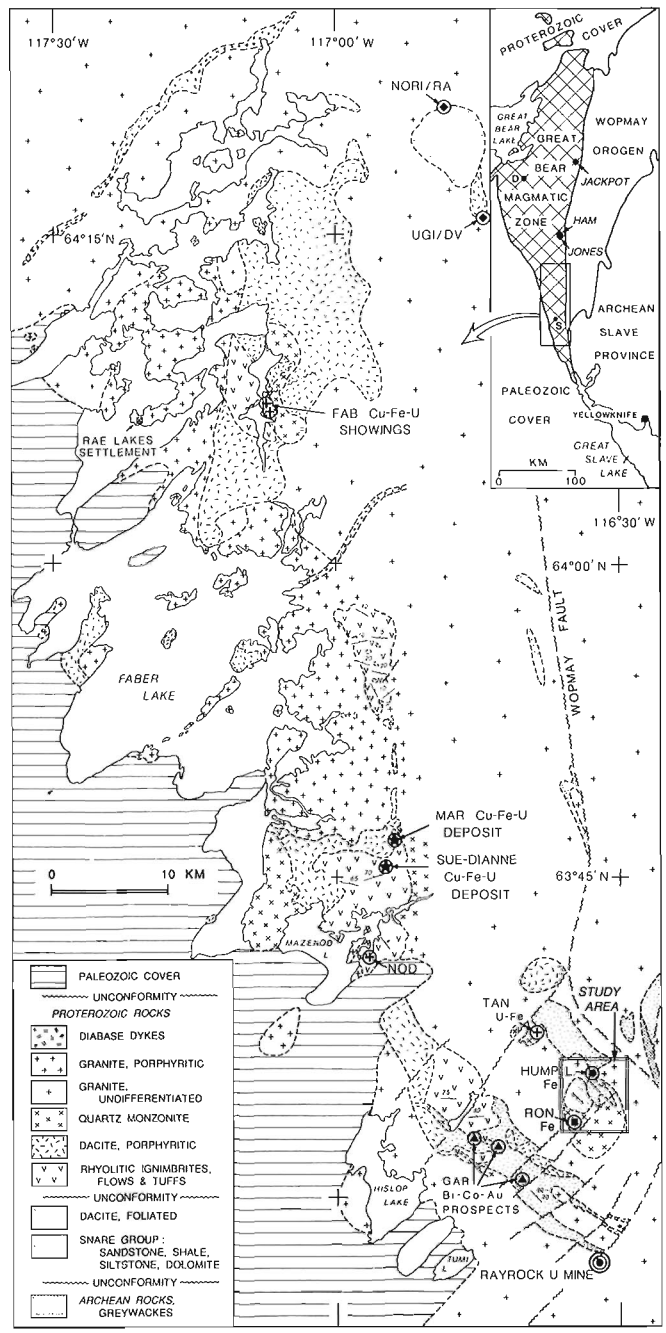


**Figure 1.** General geology of the southern Great Bear magmatic zone and location of Hump Lake area, Northwest Territories.

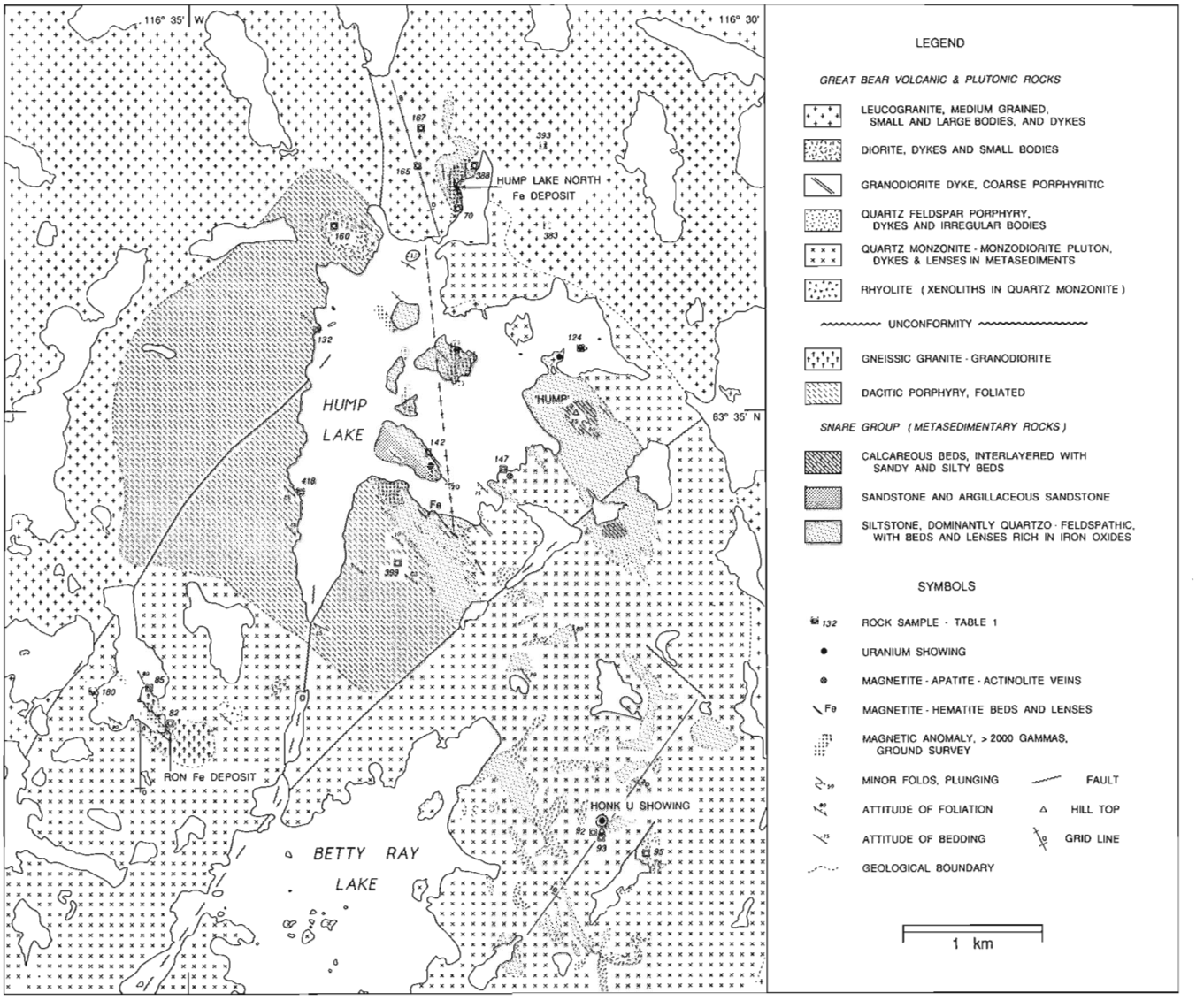


**Figure 2.** Geology and mineral occurrences of the Hump Lake area.

Some plagioclase crystals are zoned near their margin, and most are cloudy due to sericitization. Chlorite and epidote are mafic alteration (or retrograde metamorphic) minerals. Coarser aggregates rich in amphibole, epidote and or chlorite, occur in some beds. Epidote-rich veinlets are common. Bedding is well preserved even in tightly folded zones. Some of the quartzo-feldspathic beds are thick, ranging up to a few metres. In small exposures, some of these resemble leucogranitic dykes or rhyolite.

Quartz-rich beds are massive, grey, medium to fine grained, and contain some biotite and magnetite. They are interbedded with, and in places grade into, thin, biotite-rich argillaceous beds. The main exposures are on the south island of Hump Lake. Highly contorted biotitic quartzo-feldspathic zones occur at many places on islands and shore of Hump Lake. These have boudin-like mafic lenses and layers, and resemble migmatite (Fig. 5). Some of the layers are garnetiferous, and some others are amphibole-rich.

The calcareous beds occur on the hilltop of the 'Hump' of the Hump Lake near the east shore (70 m high hill; Fig. 2). They may be present on a smaller hill to the southeast along the strike zone, and some of the metasedimentary xenoliths on the hill of the Honk uranium showing contain calc-silicate (Bond and Rockel, 1976). The calcareous white beds on the Hump are a few centimetres thick, and are interbedded with thinner, greenish silty beds and thicker sandy beds. They dip steeply to northeast and minor folds in them plunge moderately to the southeast (Fig. 6). Mineral phases associated with calcite in the calcareous beds are clinopyroxene, garnet and sylvite, which were identified by x-ray diffraction.

**Table 1.** Whole-rock chemical analyses of selected igneous rocks from the Hump Lake area, Northwest Territories.

| Analysis # | | 1 | 2 | 3 | 4 | 5 | 6 | 7 | 8 | 9 | 10 | 11 | 12 | 13 | 14 | 15 | 16 | 17 | 18 | 19 |
|---|---|---|---|---|---|---|---|---|---|---|---|---|---|---|---|---|---|---|---|---|
| Sample # | | 85 | 132 | 399 | 418 | 70 | 82 | 92 | 93 | 124 | 147 | 393 | 95 | 142 | 160 | 180 | 165 | 167 | 383 | 388 |
| SiO2 | % | 65.10 | 58.30 | 64.90 | 58.40 | 58.10 | 55.90 | 62.60 | 51.00 | 52.30 | 59.70 | 60.90 | 72.00 | 64.30 | 53.70 | 55.10 | 71.30 | 67.10 | 73.60 | 66.50 |
| Al2O3 | " | 15.80 | 15.00 | 16.60 | 16.70 | 17.80 | 14.50 | 15.20 | 13.50 | 16.40 | 16.50 | 16.00 | 14.40 | 14.80 | 15.70 | 15.70 | 13.80 | 15.70 | 13.30 | 14.40 |
| TiO2 | " | 0.37 | 0.75 | 0.56 | 0.76 | 0.61 | 0.81 | 0.61 | 1.39 | 1.12 | 0.63 | 0.62 | 0.19 | 0.79 | 0.63 | 1.45 | 0.22 | 0.43 | 0.02 | 0.49 |
| FeO | " | 3.00 | 3.30 | 0.06 | 3.70 | 2.50 | 6.00 | 2.20 | 6.40 | 5.70 | 2.80 | 3.30 | 0.50 | 2.60 | 5.30 | 6.10 | 0.70 | 0.90 | 0.20 | 2.20 |
| Fe2O3 | " | 1.10 | 3.50 | 3.90 | 2.60 | 2.40 | 1.90 | 2.20 | 5.40 | 3.10 | 2.00 | 1.70 | 0.70 | 2.20 | 2.20 | 2.90 | 1.90 | 2.90 | 1.60 | 2.20 |
| MnO | " | 0.07 | 0.12 | 0.01 | 0.11 | 0.08 | 0.16 | 0.08 | 0.14 | 0.14 | 0.06 | 0.07 | 0.01 | 0.04 | 0.12 | 0.13 | 0.03 | 0.02 | 0.00 | 0.07 |
| MgO | " | 1.51 | 3.20 | 0.87 | 2.87 | 2.40 | 6.00 | 2.40 | 7.21 | 4.62 | 2.90 | 2.63 | 0.42 | 1.79 | 6.27 | 3.55 | 0.28 | 0.35 | 0.15 | 1.32 |
| CaO | " | 1.82 | 3.76 | 3.00 | 5.02 | 3.44 | 3.85 | 2.83 | 6.91 | 7.40 | 3.70 | 3.46 | 0.92 | 2.57 | 7.25 | 4.73 | 0.43 | 1.69 | 0.41 | 0.69 |
| Na2O | " | 2.70 | 4.80 | 3.60 | 2.80 | 3.10 | 3.50 | 3.50 | 2.70 | 3.00 | 4.00 | 3.00 | 4.20 | 2.90 | 3.20 | 3.10 | 1.70 | 2.80 | 3.80 | 3.30 |
| K2O | " | 6.16 | 3.37 | 4.45 | 4.33 | 5.95 | 3.10 | 5.44 | 1.95 | 3.18 | 4.64 | 5.25 | 5.68 | 5.07 | 2.57 | 2.90 | 7.83 | 6.19 | 5.44 | 6.16 |
| P2O5 | " | 0.18 | 0.21 | 0.16 | 0.21 | 0.22 | 0.27 | 0.18 | 0.53 | 0.38 | 0.20 | 0.19 | 0.05 | 0.26 | 0.13 | 0.64 | 0.04 | 0.10 | 0.04 | 0.12 |
| H2O | " | 1.80 | 1.80 | 0.70 | 1.50 | 2.10 | 2.90 | 1.40 | 2.60 | 1.60 | 1.60 | 1.60 | 0.60 | 0.90 | 2.00 | 2.40 | 0.60 | 0.50 | 0.40 | 1.20 |
| CO2 | " | 0.20 | 0.00 | 0.00 | 0.10 | 0.30 | 0.20 | 0.10 | 0.10 | 0.20 | 0.20 | 0.00 | 0.10 | 0.10 | 0.40 | 0.20 | 0.10 | 0.20 | 0.00 | 0.10 |
| S | " | 0.00 | 0.01 | 0.00 | 0.00 | 0.01 | 0.06 | 0.01 | 0.07 | 0.10 | 0.04 | 0.00 | 0.08 | 0.05 | 0.02 | 0.13 | 0.00 | 0.06 | 0.00 | 0.00 |
| Total | " | 99.81 | 98.12 | 98.81 | 99.10 | 99.01 | 99.15 | 98.75 | 99.90 | 99.24 | 98.97 | 98.72 | 99.85 | 98.37 | 99.49 | 99.03 | 98.93 | 98.94 | 98.96 | 98.75 |
| Ba | ppm | 678 | 858 | 860 | 878 | 1203 | 741 | 961 | 786 | 807 | 957 | 1039 | 602 | 812 | 367 | 911 | 649 | 1191 | 621 | 1308 |
| Be | " | 3.2 | 3 | 2.5 | 2.8 | 2.9 | 3.3 | 3.7 | 2 | 2.4 | 3 | 3 | 3.2 | 3.1 | 2.1 | 2.9 | 2.1 | 2.8 | 2.8 | 1.8 |
| Co | " | 9 | 19 | 4 | 16 | 12 | 29 | 12 | 33 | 26 | 15 | 12 | 2 | 11 | 26 | 22 | 4 | 4 | 1 | 7 |
| Cr | " | 16 | 54 | 18 | 49 | 24 | 210 | 46 | 150 | 96 | 47 | 48 | 5 | 20 | 140 | 43 | 4 | 7 | 2 | 6 |
| Cu | " | 7 | 82 | 3 | 43 | 35 | 66 | 65 | 36 | 66 | 17 | 38 | 9 | 48 | 14 | 50 | 3 | 5 | 7 | 12 |
| La | " | 33 | 39 | 38 | 43 | 40 | 35 | 42 | 32 | 43 | 48 | 47 | 71 | 100 | 21 | 60 | 71 | 52 | 20 | 34 |
| Nb | " | 16 | 12 | 13 | 6 | 5 | 13 | 18 | 5 | 19 | 7 | 11 | 20 | 27 | 9 | 24 | 18 | 15 | 16 | 16 |
| Ni | " | 7 | 18 | 6 | 21 | 8 | 83 | 19 | 53 | 35 | 15 | 14 | 0 | 10 | 45 | 26 | 0 | 0 | 0 | 0 |
| Rb | " | 230 | 100 | 180 | 160 | 230 | 130 | 180 | 65 | 130 | 180 | 190 | 160 | 200 | 100 | 82 | 350 | 290 | 200 | 200 |
| Sr | " | 160 | 280 | 330 | 430 | 530 | 200 | 220 | 340 | 560 | 350 | 390 | 130 | 320 | 310 | 530 | 48 | 75 | 68 | 22 |
| V | " | 28 | 85 | 37 | 90 | 60 | 120 | 59 | 220 | 140 | 69 | 65 | 1 | 43 | 140 | 97 | 1 | 21 | 0 | 30 |
| Y | " | 18 | 22 | 18 | 23 | 21 | 22 | 23 | 28 | 16 | 23 | 25 | 29 | 40 | 18 | 28 | 36 | 26 | 18 | 31 |
| Zn | " | 12 | 74 | 0 | 58 | 40 | 200 | 82 | 82 | 58 | 23 | 35 | 2 | 8 | 44 | 100 | 0 | 0 | 0 | 20 |
| Zr | " | 180 | 200 | 210 | 200 | 200 | 120 | 320 | 100 | 290 | 230 | 250 | 330 | 340 | 86 | 290 | 220 | 270 | 73 | 210 |

Notes: 1) Sample locations in Figures 2, 3 and 4; sample series GFA-'90.
2) Lithology : Analysis # 1 - Gneissic granodiorite; # 2, 3 & 4 - Foliated dacitic porphyry; # 5, 6, 7, 8, 9, 10 & 11 - Quartz monzonite; # 12 - Feldspar porphyry; # 13 - Granodiorite dyke; # 14 & 15 - Diorite; # 16, 17, 18 & 19 - Leucogranite.
3) Analyses by the Analytical Chemistry Section, Mineral Resources Division, Geological Survey of Canada, Ottawa.
4) All analyses by x-ray fluorescence method except FeO, H2OT, CO2T and S by rapid chemical methods.
5) Fe2O3 is calculated using formula : Fe2O3 + Fe2O3(xrf) - 1.11134 X FeO(volumetric).

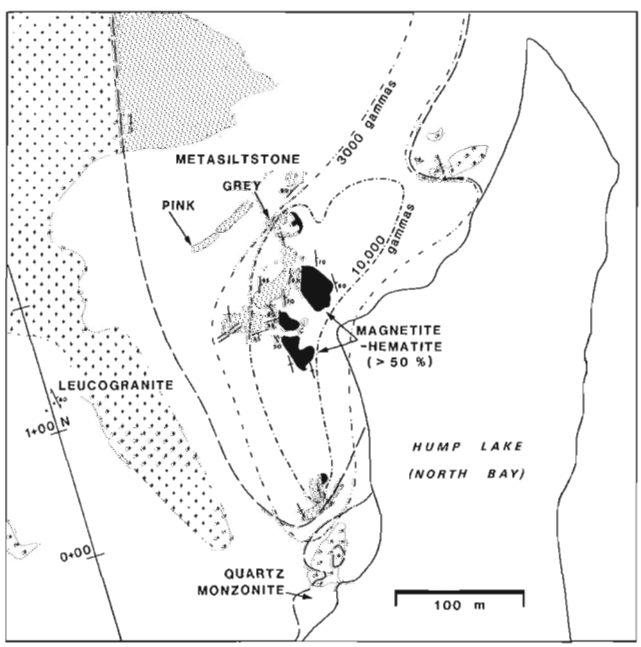


**Figure 3.** Geology of the Hump Lake North magnetite-hematite deposit.

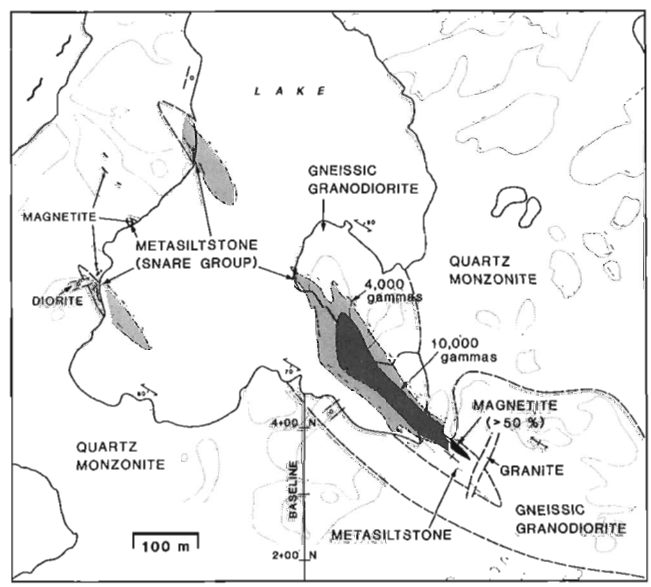


**Figure 4.** Geology of the Ron magnetite-hematite deposit, Hump Lake area.

The dacitic porphyritic unit has a well developed penetrative foliation (Fig. 7), which dips steeply and trends consistently to the northwest parallel to the regional structural trend of the Snare Group strata. The rock unit is uniform in the outcrops examined along the west shore, and south of Hump Lake, and its contact with the siltstones is sharp and interfingering, due in part at least, to the tight minor folding (Fig. 8). The rock has phenocrysts of plagioclase (~An30), set in quartz-feldspar matrix with abundant well aligned flakes of biotite. It contains small phenocrysts of hornblende, streaky aggregates of quartz and of mafic minerals, disseminations of iron oxide with sphene, accessory apatite and rare zircon, and alteration minerals sericite, chlorite and epidote.

## *Syntectonic intrusion*

### Gneissic granite-granodiorite

Outcrops of weakly to strongly foliated granite-granodiorite occur in the vicinity of Ron deposit (Fig. 2; Table 1). The northwest-trending foliation is defined by biotite, which is altered to chlorite and epidote. Phenocrystic plagioclase occurs in medium to coarse aggregate of quartz, microcline and perthitic feldspar. Accessory minerals are apatite, zoned zircon, and oxides.

## *Great Bear magmatic rocks*

The Great Bear magmatic activity is represented in the Hump Lake area by large intrusions of quartz monzonite and leucocratic medium grained granite, and smaller bodies and dykes of granodiorite, diorite, quartz feldspar porphyry and aplite. Volcanic rocks are represented only by what appear to be xenoliths of porphyritic rhyolite in quartz monzonite between the Ron deposit and Betty Ray Lake. Quartz and feldspar phenocrysts in rhyolite are up to 3 mm long, and the rock has faint banding trending northwest.

### Quartz monzonite

Quartz monzonite is dominant east of Betty Ray Lake, where it was mapped as syenite/mafic syenite by Bond (1975) and Bond and Rockel (1976). Chemical and petrographic data show, however, that the rock is quartz monzonite (Table 2). Numerous xenoliths of metasediments occur in the inrusion, in particular southeast of Hump Lake. Their contacts are sharp. The boundary of the intrusion is an irregular zone marked by numerous concordant sheets, wedges, and lens-like bodies of quartz monzonite along bedding of the metasediments (Fig. 9). Locally, the concordant injections impart a lit-par-lit character. In such injections, the intrusive material commonly has crude to well developed alignment of mafic streaks parallel to bedding in the metasediments. Dykes and veins of quartz monzonite are also present, but these are scarce.

Quartz monzonite is typically massive, coarse with feldspar crystals 0.5 to 1 cm long, and hornblende and quartz that commonly make up to 25 and 10 per cent of the rock respectively. Proportion of these minerals vary and the rock grades locally into monzodiorite-diorite (Table 1), e.g. near Honk uranium showing. Hornblende is the principal mafic silicate, but in some places it is accompanied by a notable amount of biotite. Clinopyroxene remnants were seen in the core of hornblende crystals in one sample (#124, Table 1; Fig. 2). Feldspars are mainly plagioclase, and subordinate microcline and perthite. The latter dominate over plagioclase in felsic varieties. Accessory minerals are iron oxide, apatite, sphene and zircon. Chlorite and epidote are common alteration minerals. Alteration is intense in many places.

**Table 2.** Spectrometer readings of K, U and Th in a magnetite-hematite deposit and other rocks of Hump Lake, Northwest Territories.

| Location : Hump Lake grid, ln m | eK % | eU ppm | eTh ppm |
|---|---|---|---|
| Iron oxide-rich (>50 %) beds | | | |
| 189 E, 007 N | 1.6 | 0.4 | 4.6 |
| 195 E, 100 N | 2.2 | 0.7 | 1.8 |
| 203 E, 105 N | 1.6 | 2.1 | 3.2 |
| 195 E, 128 N | 4.2 | 3.5 | 13.5 |
| 185 E, 143 N | 6.4 | 1.4 | 12.8 |
| 228 E, 155 N | 2.5 | 3.1 | 13.3 |
| 232 E, 146 N | 1.6 | 1.5 | 7.2 |
| 220 E, 133 N | 1.3 | 0.9 | 7.8 |
| 190 E, 114 N | 0.5 | 1.2 | 3.2 |
| 170 E, 134 N | 5.1 | 0.2 | 16.0 |
| Metasiltstone, gray | | | |
| 181 E, 008 N | 1.9 | 1.0 | 8.1 |
| 167 E, 017 S | 2.0 | 3.2 | 15.4 |
| 177 E, 015 S | 3.3 | 2.9 | 18.3 |
| 178 E, 151 N | 5.1 | 2.4 | 11.9 |
| 191 E, 159 N | 2.3 | 6.7 | 1.4 |
| 194 E, 155 N | 4.1 | 58.3 | 18.1 |
| 198 E, 155 N | 3.3 | 2.4 | 11.6 |
| 208 E, 169 N | 2.4 | 3.6 | 13.8 |
| 211 E, 182 N | 5.7 | 4.6 | 14.8 |
| 215 E, 158 N | 1.9 | 1.5 | 13.1 |
| 214 E, 148 N | 1.7 | 3.2 | 12.0 |
| 210 E, 197 N | 5.7 | 2.0 | 11.0 |
| 225 E, 205 N | 2.9 | 0.9 | 12.2 |
| Metasiltstone, pale pink | | | |
| 208 E, 127 N | 1.3 | 5.5 | 23.1 |
| 150 E, 140 N | 5.6 | 1.7 | 14.3 |
| 165 E, 150 N | 1.2 | 9.6 | 13.4 |
| 202 E, 207 N | 0.6 | 11.7 | 7.5 |
| 238 E, 233 N | 0.6 | 3.6 | 9.9 |
| 213 E, 244 N | 0.4 | 2.8 | 12.8 |
| Metasediments, biotitic | | | |
| 040 W,1900S | 1.0 | 7.6 | 13.2 |
| 060 W,1980S | 0.3 | 4.6 | 10.7 |
| 070 W,1900S | 1.7 | 5.3 | 18.3 |
| 100 W,1900S | 1.9 | 1.5 | 10.7 |
| 150 W,1870S | 1.3 | 3.1 | 15.4 |
| 150 W,1809S | 4.3 | 4.6 | 15.3 |
| 150 W, 1842S | 1.1 | 5.3 | 16.8 |
| 150 W, 1795S | 5.8 | 2.8 | 18.6 |
| 093 W, 1802S | 5.9 | 4.4 | 18.8 |
| 130 W, 1900S | 1.1 | 28.8 | 14.0 |
| Foliated dacitic porphyry | | | |
| 825 W, 2550S | 3.6 | 4.4 | 18.5 |
| 850 W, 2550S | 4.2 | 4.5 | 22.7 |
| 1075 W,1950S | 3.7 | 4.0 | 19.0 |
| 1085 W,1955S | 3.8 | 4.0 | 20.7 |
| Quartz monzonite | | | |
| 185 E, 035 S | 4.4 | 5.0 | 10.7 |
| 178 E, 043 S | 4.8 | 4.9 | 18.6 |
| 1050 E, 1225S | 2.9 | 2.8 | 9.7 |
| 1050 E, 1230S | 3.1 | 1.7 | 11.6 |
| Granodiorite | | | |
| 075 W, 1815S | 4.7 | 13.0 | 40.5 |
| 110 W, 1800S | 4.4 | 5.1 | 45.2 |
| 165 W, 1702S | 4.3 | 5.2 | 45.8 |
| 160 w, 1705S | 4.1 | 5.7 | 43.1 |
| Leucogranite | | | |
| 187 E, 012 S | 4.6 | 2.8 | 18.1 |
| 197 E, 003 S | 5.0 | 3.1 | 16.3 |
| 190 E, 091 N | 6.4 | 3.4 | 16.7 |
| 082 E, 000 N | 5.3 | 2.8 | 23.4 |
| 092 E, 000 N | 5.6 | 4.1 | 3.7 |
| 102 E, 000 N | 6.5 | 4.1 | 3.9 |
| 337 E, 210 N | 5.9 | 5.3 | 18.0 |
| 357 E, 214 N | 5.2 | 4.3 | 19.1 |
| 373 E, 210 N | 5.2 | 4.2 | 21.4 |
| 345 E, 234 N | 5.3 | 4.3 | 19.0 |
| 030W,1950S | 7.0 | 4.6 | 26.9 |
| Granitic dykes & metasediments | | | |
| 090 W, 1850S | 6.1 | 37.7 | 42.3 |
| 070 W, 1980S | 2.0 | 111.7 | 35.7 |
| 138 W, 1891S | 7.0 | 348.4 | 70.4 |
| 150 W, 1890S | 11.6 | 365.9 | 41.2 |

Note : Readings taken with Exploranium GRS-256 Spectrometer, by S.S. Gandhi during July-August 1990.
Hump Lake grid baseline in Figures 2 and 3.

### Porphyries

A number of feldspar porphyry and quartz-feldspar porphyry dykes and irregular bodies intrude the foliated dacitic porphyry and quartz monzonite southeast of Hump Lake. Phenocrysts of plagioclase and perthitic feldspar are up to 8 mm long, and are set in fine to medium grained matrix of microcline, perthite,

**Figure 5.** Plastic deformation in a metasedimentary unit of the Snare Group, near sample site 147 (Fig. 2).

**Figure 6.** Plunging folds in calcareous beds at top of the 'Hump', Hump Lake (Fig. 2). Looking southeast.

**Figure 7.** Foliated dacitic porphyry, west shore of Hump Lake, Sample site 418 (Fig. 2). Looking southeast.

**Figure 8.** Tightly folded contact between metasiltstone and foliated dacitic porphyry, near sample site 399 (Fig. 2).

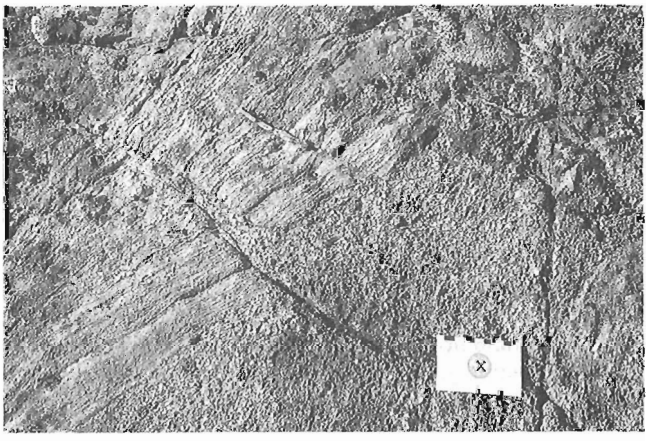

**Figure 9.** Contact between metasiltstone and concordant sheet of quartz monzonite. Note an offshoot dykelet. South shore of Hump Lake.

**Figure 10.** Massive magnetite-hematite zone, Hump Lake North deposit; 210 N, 225 E (Fig. 3). Note faintly defined lamination.

plagioclase, quartz and hornblende. Apatite, magnetite, and zircon occur as accessory minerals. Chemical analysis of a feldspar porphyry is presented in Table 1.

### Granodiorite

A dyke of of coarse feldspar porphyritic granodiorite is exposed on the shore of south island and in outcrops at the southeast corner of Hump Lake. It cuts quartz monzonite and metasediments, but its relationship to quartz feldspar porphyry is not known. The dyke is 14.5 m wide on the island, and trends east-southeast. It contains plagioclase phenocrysts up to 5 cm long in coarse granitic matrix, in which plagioclase predominates over alkali feldspar, and biotite over hornblende, and the rock has a small excess of potash over soda (Table 1). Other minerals present are quartz, apatite, zircon, sphene, and iron oxide.

### Diorite

Diorite dykes and small bodies intrude quartz monzonite and metasediments, but their relation to other Great Bear intrusions is not certain. They form a cluster or a stockwork in some places. Many of them are too small to show in Figure 2. They are commonly massive, grey and medium grained, and contain a few scattered phenocrysts of plagioclase (~An30). Matrix contains subhedral plagioclase and interstitial hornblende, biotite, alkali feldspar, quartz, iron oxide, apatite, zircon and sphene. Plagioclase is zoned. Chlorite and epidote are alteration minerals. Dyke margins are fine grained or chilled. A coarse phase occurs in the body at the northwest corner of Hump Lake, where some very coarse hornblende-feldspar pegmatoid patches are also seen. Analyses of a sample of the coarse phase (#160) and of a dyke (#180) are given in Table 1.

### Leucogranite

Leucocratic granite is well exposed north of Hump Lake, and numerous small bodies and dykes of more typical granitic and aplitic composition occur throughout the area. North of the lake, it is generally medium grained, equigranular to seriate, with anhedral aggregate of quartz, microcline, perthitic feldspar and plagioclase. Some coarse subhedral plagioclase and anhedral quartz grains or aggregates of grains occur in places, and locally the rock is coarse grained. In some zones, the rock is weakly sheared. Mafic minerals are mostly biotite and magnetite, and make up less than 5 per cent of the rock. Other minerals present in trace amounts are muscovite, apatite, zircon and sphene. Chlorite and traces of epidote occur as alteration product of the mafic minerals. The unit is highly potassic as seen from the chemical analyses and spectrometer readings (Tables 1 and 2).

## MINERAL OCCURRENCES

### *Hump Lake North deposit*

This deposit was mapped in detail during the present study (Fig. 3). A magnetic survey of the area on grid lines 100 m apart was carried out earlier by Noranda Exploration Company Limited (Bryan, 1981b). Contour of 10 000 gammas from this survey outlines a zone containing over 50 per cent iron oxides (Fig. 3). The zone is several metres wide in outcrops (Fig. 10). It is a stratiform zone comprised of iron oxide-rich thin beds and lamellae interlayered with oxide-poor quartzo-feldspathic beds. The boundary of the deposit with adjacent siltstone is abrupt to interbedded over a metre or so. The siltstones are weakly to moderately magnetic, and have magnetic response in the 1000 to 4000 gammas range, in comparison with about 500 gammas for the granitic area. The siltstones and the deposit are tightly folded as seen from v-shaped minor folds on metre scale. More open minor folds occur in the middle part where there is a change in strike from general north-northwest direction to the south-west, and the plunge of these folds is moderate to the southeast. The deposit is cut by a few leucogranitic veins (Fig. 11).

Petrographic study revealed granoblastic texture, with well preserved bedding and lamination (Fig. 12). Magnetite predominates over hematite, but in some layers hematite is predominant. Twin lamellae are seen in many hematite crystals (Fig. 12). Some thicker beds of iron oxides show layers of relatively coarser crystals parallel to bedding. In such coarser beds, hematite is generally more abundant than magnetite. Coarse aggregates and veinlets in disrupted parts of beds contain mostly hematite. Replacement of magnetite by hematite along margins and cracks is seen in a few grains, and many of the magnetite crystals are partially or wholly replaced by hematite, with well preserved crystal form of magnetite. Microprobe analyses of selected grains in 4 samples from this deposit revealed composition close to the end member for both magnetite and hematite (analyses 1 to 22, Table 3). Calculated molecular proportions of ulvospinel in magnetite and of ilmenite in hematite are less than 2 and 3 percent respectively, and petrographic and x-ray diffraction studies did not reveal any separate titaniferous oxide phase. Some of the magnetite analyses (17 to 20) may reflect a mixture of magnetite and hematite. Feldspar is more abundant than quartz, and it is mainly potash feldspar and perthite. Apatite and zircon are sparsely distributed. Epidote and clinopyroxene occur in some layers close to the boundary with siltstone. Spectrometer readings indicated very low U and Th (Table 2). The K content reflects the feldspathic component. Copper minerals were not found in this deposit nor in other similar stratiform occurrences to the south, during the present study. Bryan (1981a, b) reported traces of copper minerals, but it is likely that some iridescent colours developed on the iron oxide aggregates exposed to weathering may have been mistaken as being due to the presence of copper minerals.

### Ron deposit

This deposit is poorly exposed, and the magnetic data indicate most of it lies under a small lake (Fig. 4). Its main exposure at the southeast end of the lake contains more than 50 per cent magnetite and is up to 22 m wide. On the west shore of the lake, there are a few smaller exposures which have bands and disrupted patches of massive magnetite, ranging from 0.5 m to a few metres wide. A thin-bedded siltstone occurs adjacent to the magnetite zone. It has a northwest trend, steep dips, and

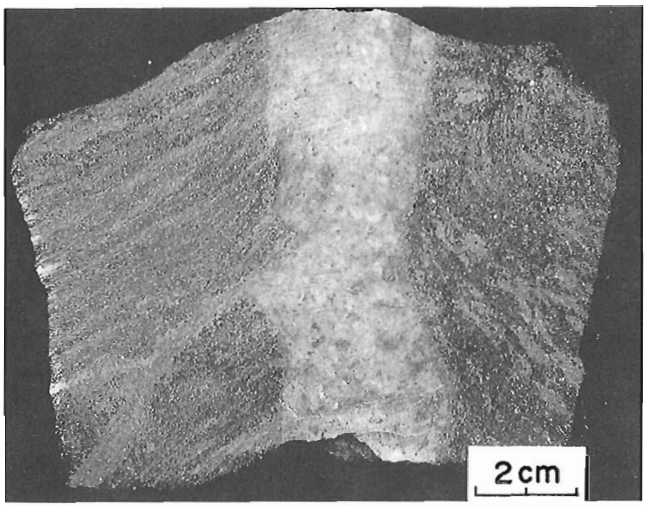


**Figure 11.** A sawed specimen from Hump Lake North deposit, showing a granitic dyke cutting laminated magnetite-hematite zone; 007 N, 189 E (Fig. 3).

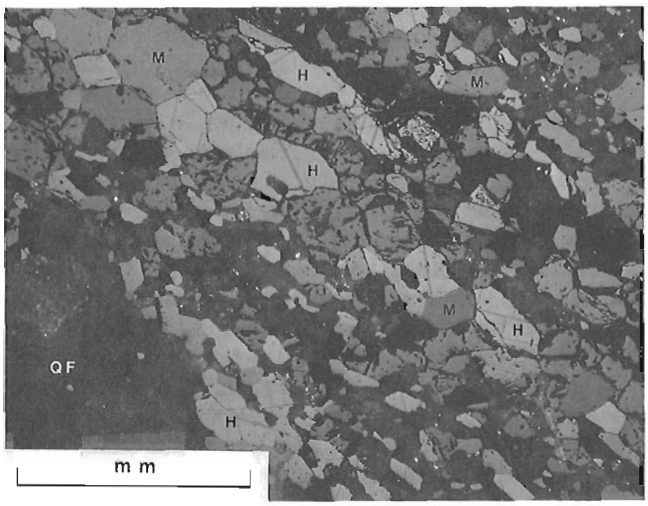


**Figure 12.** Magnetite-hematite-rich rock, Hump Lake North showing; 2+20 N, 2+30 E (Fig. 3). Reflected light, crossed nicols. Note lamellae in hematite (H). Magnetite (M).

**Figure 13.** Folded magnetite-bearing siltstone, Ron deposit, 625 N, 300 W (Fig. 4). Looking south-southeast.

locally minor folds plunging moderately to the southeast (Fig. 13). The lighter coloured beds in the siltstone contain lamellar twinned plagioclase, untwinned feldspar, diopside and/or amphibole, and scattered magnetite. The darker beds and aggregates contain relatively more magnetite (over 25 per cent), and some apatite. Quartz monzonite truncates the boundary between the magnetite zone and siltstone at the southeastern shore, and on the west shore it has intruded them and contains xenoliths of magnetite (Fig. 14). Epidote is common at both places, and is paragenetically late, occurring as veins and irregular patches in magnetite that predate quartz monzonite. In addition, there are epidote veins younger than quartz monzonite.

Magnetite is the predominant iron oxide, and is replaced by hematite along margins and cracks. A few crystals are completely replaced by hematite. The proportion of hematite, however, is very small, in contrast to that in the Hump Lake North deposit. Microprobe analyses of magnetite and hematite in two samples from the deposit show little or no titanium (analyses 31 to 42, Table 3), and the minerals are essentially pure end members of their respective oxide groups. In the southeastern exposure of the Ron deposit, the central part of magnetite zone has prismatic crystals of altered pyroxene up to 5 cm long (Fig. 15, 16). X-ray diffraction determination of the unaltered core and altered zone showed them to be clinopyroxene and talc. Microprobe analyses gave the following composition range for the pyroxene from three separate spots in terms of mole per cent wollastonite, enstatite and ferrosilite: i) Wo 47.02, En 43.86, Fs 3.04, ii) Wo 46.76, En 39.90, Fs 6.98, and iii) Wo 43.78, En 28.89, Fs 17.01. In addition to talc, the presence of tremolite is suggested from petrographic observations (Fig. 16). The rock contains trace amounts of apatite and chlorite, and veinlets of actinolite with sphene.

### Other mineral occurrences

Occurrences similar to the deposits described above, but smaller in size, are found at a few localities, and are indicated by magnetic anomalies (Fig. 2). The one near the

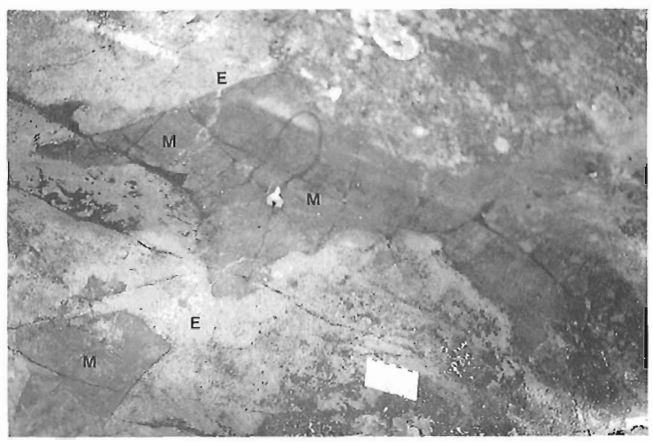


**Figure 14.** Photograph of xenoliths of massive magnetite-hematite (M) in quartz monzonite, Ron deposit, 650 N, 300 W (Fig. 4). Light coloured area is highly epidotized (E).

southeast shore of Hump Lake is a bed about 0.5 m thick containing over 75 per cent iron oxides, and is exposed discontinuously over several tens of metres, in a sequence of siltstones. The bed contains abundant magnetite in oxide-rich layers, and mostly hematite in oxide-poor layers. Microprobe analyses of these show composition similar to those of magnetite and hematite in the Hump Lake North deposit. The associated siltstones commonly have quartz-albite layers interbedded with darker layers that contain abundant diopside (confirmed by x-ray diffraction), magnetite, hematite and minor hornblende.

On the large central island of the lake, there is a shore exposure of magnetite pods and veins, several metres in length, in quartzite-metasiltstone beds. The veins are discordant to bedding, and are cut by a granitic dyke. Quartz, amphibole and apatite are associated with magnetite in veins.

Apatite amounts to over 5 per cent in some places, and occurs as small and coarser crystals in medium grained matrix. Traces of pyrite are present locally. Another occurrence of actinolite-apatite-magnetite veins, up to 5 cm

**Table 3.** Microprobe analyses of magnetite and hematite in samples from the Hump Lake North and Ron deposits, southern Great Bear magmatic zone.

| Analysis # | FeO | Al2O3 | TiO2 | MnO | V2O3 | Total | Molecular % end member |
|---|---|---|---|---|---|---|---|
| | | | | | | | Hump Lake North deposit |
| 1 | 94.0 | 0.1 | 0.0 | 0.2 | 0.1 | 94.7 | Mgn. 98.59, Ulv. 0.08 |
| 2 | 94.1 | 0.1 | 0.1 | 0.2 | 0.2 | 94.9 | Mgn. 98.29, Ulv. 0.16 |
| 3 | 93.6 | 0.1 | 0.0 | 0.1 | 0.1 | 94.1 | Mgn. 98.81, Ulv. 0.00 |
| 4 | 94.6 | 0.0 | 0.0 | 0.2 | 0.0 | 95.2 | Mgn. 98.71, Ulv. 0.12 |
| 5 | 94.4 | 0.0 | 0.0 | 0.1 | 0.1 | 94.8 | Mgn. 99.26, Ulv. 0.09 |
| 6 | 93.9 | 0.0 | 0.0 | 0.1 | 0.1 | 94.5 | Mgn. 98.98, Ulv. 0.05 |
| 7 | 95.0 | 0.2 | 0.1 | 0.2 | 0.2 | 96.0 | Mgn. 97.88, Ulv. 0.14 |
| 8 | 89.3 | 0.5 | 1.7 | 0.1 | 0.4 | 92.3 | Hem. 96.85, Ilm. 2.94 |
| 9 | 95.0 | 0.1 | 0.0 | 0.0 | 0.2 | 95.7 | Mgn. 98.68, Ulv. 0.11 |
| 10 | 89.0 | 0.5 | 1.8 | 0.0 | 0.4 | 91.9 | Hem. 96.65, Ilm. 3.19 |
| 11 | 90.1 | 0.6 | 1.5 | 0.0 | 0.3 | 92.6 | Hem. 97.11, Ilm. 2.84 |
| 12 | 89.0 | 0.7 | 1.8 | 0.0 | 0.3 | 92.1 | Hem. 96.69, Ilm. 3.05 |
| 13 | 94.1 | 0.5 | 0.0 | 0.1 | 0.3 | 95.4 | Mgn. 97.75, Ulv. 0.00 |
| 14 | 94.2 | 0.3 | 0.0 | 0.1 | 0.1 | 95.0 | Mgn. 98.39, Ulv. 0.02 |
| 15 | 94.3 | 0.1 | 0.1 | 0.1 | 0.2 | 95.1 | Mgn. 98.50, Ulv. 0.16 |
| 16 | 94.2 | 0.2 | 0.0 | 0.1 | 0.1 | 94.8 | Mgn. 99.13, Ulv. 0.04 |
| 17 | 91.3 | 0.3 | 0.6 | 0.1 | 0.3 | 92.6 | Mgn. 96.87, Ulv. 1.75 |
| 18 | 91.0 | 0.4 | 0.3 | 0.0 | 0.2 | 92.2 | Mgn. 97.48, Ulv. 0.83 |
| 19 | 91.5 | 0.3 | 0.3 | 0.0 | 0.2 | 92.2 | Mgn. 97.51, Ulv. 0.89 |
| 20 | 91.8 | 0.3 | 0.3 | 0.0 | 0.0 | 93.0 | Mgn. 97.48, Ulv. 0.74 |
| 21 | 93.6 | 0.1 | 0.0 | 0.2 | 0.1 | 94.3 | Mgn. 98.49, Ulv. 0.11 |
| 22 | 93.9 | 0.1 | 0.0 | 0.1 | 0.2 | 94.6 | Mgn. 98.72, Ulv. 0.00 |
| | | | | | | | Hump Lake South showing |
| 23 | 93.2 | 0.0 | 0.0 | 0.9 | 0.1 | 94.6 | Mgn. 95.53, Ulv. 0.07 |
| 24 | 90.2 | 0.2 | 0.7 | 0.0 | 0.1 | 91.5 | Hem. 98.59, Ilm. 1.21 |
| 25 | 90.1 | 0.3 | 0.8 | 0.1 | 0.1 | 91.5 | Hem. 98.54, Ilm. 1.41 |
| 26 | 93.5 | 0.0 | 0.0 | 0.4 | 0.0 | 94.2 | Mgn. 98.49, Ulv. 0.09 |
| 27 | 93.0 | 0.1 | 0.0 | 1.1 | 0.0 | 94.4 | Mgn. 96.05, Ulv. 0.12 |
| 28 | 94.0 | 0.1 | 0.1 | 0.8 | 0.1 | 95.2 | Mgn. 96.62, Ulv. 0.13 |
| 29 | 90.2 | 0.2 | 1.3 | 0.0 | 0.1 | 91.9 | Hem. 97.64, Ilm. 2.31 |
| 30 | 89.1 | 0.1 | 1.5 | 0.0 | 0.0 | 90.9 | Hem. 97.41, Ilm. 2.46 |
| | | | | | | | Ron deposit |
| 31 | 88.4 | 0.1 | 0.1 | 0.1 | 0.1 | 89.2 | Hem. 99.70, Ilm. 0.00 |
| 32 | 92.3 | 0.1 | 0.1 | 0.1 | 0.1 | 93.2 | Mgn. 98.20, Ulv. 0.39 |
| 33 | 91.6 | 0.2 | 0.2 | 0.0 | 0.0 | 92.1 | Mgn. 98.59, Ulv. 0.56 |
| 34 | 89.6 | 0.1 | 0.0 | 0.1 | 0.0 | 90.2 | Hem. 99.70, Ilm. 0.00 |
| 35 | 89.2 | 0.2 | 0.1 | 0.0 | 0.1 | 90.5 | Hem. 98.74, Ilm. 0.30 |
| 36 | 92.4 | 0.4 | 0.2 | 0.1 | 0.1 | 93.6 | Mgn. 98.61, Ulv. 0.62 |
| 37 | 88.9 | 0.3 | 0.3 | 0.1 | 0.0 | 89.9 | Hem. 99.60, Ilm. 0.00 |
| 38 | 91.7 | 0.1 | 0.1 | 0.1 | 0.0 | 92.6 | Mgn. 98.07, Ulv. 0.41 |
| 39 | 92.2 | 0.3 | 0.2 | 0.1 | 0.0 | 93.0 | Mgn. 97.91, Ulv. 0.45 |
| 40 | 94.5 | 0.2 | 0.3 | 0.2 | 0.0 | 95.3 | Mgn. 98.00, Ulv. 0.80 |
| 41 | 95.1 | 0.0 | 0.0 | 0.0 | 0.0 | 95.6 | Mgn. 99.34, Ulv. 0.05 |
| 42 | 94.3 | 0.3 | 0.2 | 0.3 | 0.0 | 95.2 | Mgn. 97.80, Ulv. 0.58 |

Notes :

1) Contents of MgO, CaO, SiO2, NiO, Cr2O3, ZnO, CoO and SO3 are less than 0.2per cent, except for the analysis 15-1A which showed 0.22 per cent MgO and the analysis 14-1A which showed 0.23 per cent CoO. The total figure includes these 8 elements.

2) End members :
Mgn.: Magnetite, Ulv.: Ulvospenel, Hem.: Hematite, Ilm.: Ilmenite.

3) Location of samples analyzed as follows :
Analyses 1 - 6 : GFA-'90-66; 132 m N, 220 m E (Fig. 3).
" 7 - 14 : GFA-'90-404; 100 m N, 195 m E (Fig. 3).
" 15 - 22 : GFA-'90-60; 7 m N, 189 m E (Fig. 4).
" 22 - 30 : GFA-'90-396; 2350 m S, 10 m W (Fig. 2).
" 31 - 39 : GFA-'90-79; 392 m N, 198 m E (Fig. 4).
" 40 - 42 : GFA-'90-179; 610 m N, 310 m W (Fig. 4).

4) Analyses by J. Stirling, Geological Survey of Canada, Ottawa.

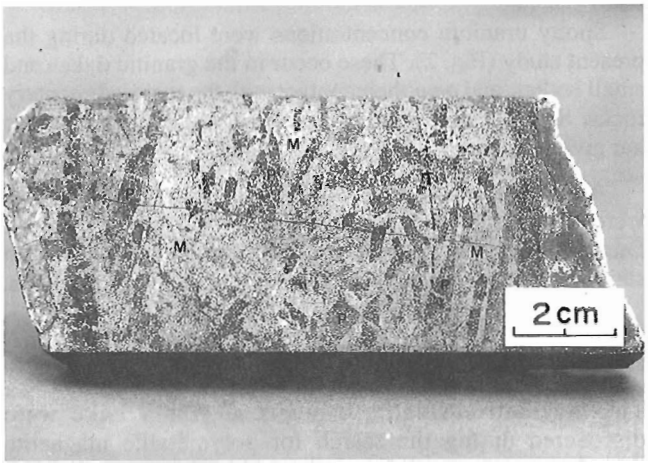


**Figure 15.** Magnetite-hematite-rich sample, Ron showing: 385 N, 212 E (Fig. 4). Note altered coarse pyroxene crystals (P), up to 5 cm long, in magnetite-rich matrix (M); polished surface.

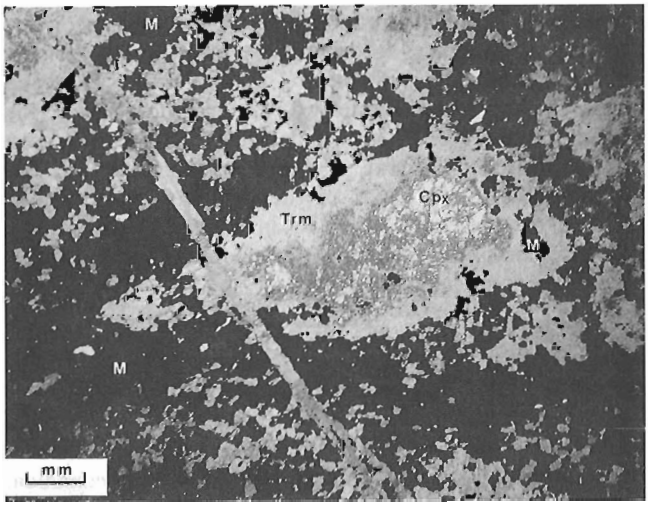


**Figure 16.** Thin section of the rock shown in Figure 17. Note clinopyroxene (Cpx) altered to tremolite (Trm) and containing magnetite (M) inclusions. Plane polarized light.

wide, is in quartz monzonite on the east shore of lake (near sample 147, Fig. 2). It is typical of the veins associated with these intrusions of the Great Bear magmatic zone.

The Honk uranium showing is located on a hill top, at the contact of calc-silicate xenolith in quartz monzonite (Bond, 1975; Bond and Rockel, 1976). Pitchblende veins, aggregates and disseminations occur mainly in pyroxene-rich rock over a zone 100 m long and 15 m wide. Pitchblende veinlets have yielded samples containing up to 0.55 per cent U. Coarse, acicular actinolite crystals occur locally along fractures in the mineralized zone. Chalcopyrite and pyrite, partially replaced by pitchblende, occur locally in fracture-fillings in diopside-microcline-sphene-magnetite rock. The pitchblende is thus a late phase, and may be much younger than the 'skarn' type mineralization at the time of quartz monzonite intrusion, as visualized by Bond and Rockel (1976).

Spotty uranium concentrations were located during the present study (Fig. 2). These occur in the granitic dykes and small bodies, and near their contact with the metasedimentary rocks. Spectrometer readings on some of these occurrences are given in Table 2.

A few occurrences of chalcopyrite in small quartz veins were reported in the Hump Lake area by Bryan (1981a, b). During the present study, one quartz veinlet with malachite stain was encountered on the southeast shore of Hump Lake.

## DISCUSSION

The magnetite-hematite deposits at Hump Lake were discovered during the search for polymetallic magnetite deposits occurring as veins and breccia fillings in the Great Bear volcano-plutonic settings as exemplified by the Sue-Dianne and Mar deposits (Bryan, 1981a and 1981b; Gandhi, 1989). They are, however, older than and different from the veins and breccia fillings.

The stratiform character of magnetite-hematite concentrations in the deposits, presence of the notable amounts of these oxides in the the host siltstones, and imprints of later deformation and metamorphism on the deposits, point to a synsedimentary deposition of the iron oxides in the Snare Group. The composition of the magnetite and hematite close to the end members of the oxide groups (Table 3), may in part reflect the composition of the source material, and are consistent with the metamorphosed character of the deposits (see Rumble, 1976, for discussion of iron oxides in metamorphosed rocks). Partial to complete replacement of magnetite by hematite is apparently post-metamorphic.

The host quartzo-feldspathic siltstones are clastic, probably tuffaceous in part at least. The dacitic porphyry unit is most likely a part of the magmatic activity that supplied the volcaniclastic material, including magnetite. These features indicate a sedimentary origin in an active volcanic environment. Concentration of iron may be mechanical (placer-type) or chemical. The latter is favoured here. A metasomatic origin (skarn-type) is considered unlikely as this would require very selective, large scale replacement of siltstones, instead of the more reactive calcareous beds which are associated with them.

Magnetite occurs in varying proportions in the Snare Group outside the study area, e.g. in the siltstones and argillaceous siltstones at Lou Lake (Gandhi and Lentz, 1990). Furthermore, there are several uraniferous magnetite occurrences in paragneiss believed to be derived from the Snare Group. Six such occurrences, namely the Jones, HAM, NORI/RA, JLD and UGI/DV, and Jackpot to the north (Fig. 1, and inset), were studied for U-Pb geochronology by Miller (1982). He described these occurrences as 'meta-placer deposits', and suggested that these placers in arkosic sediments were formed in desert environment or along marine beach. The writer examined these occurrences in 1982, and concurred with Miller in that the magnetite concentrations are essentially concordant to layering in paragneiss, with local discordances induced by later deformation. He noted, however, that they lack features commonly associated with fluvial and marine placers e.g. pebbles, cross-bedding, and various heavy minerals, and that the preponderance of siltstones indicates a rather low energy environment of deposition, such as the lacustrine environment.

Miller (1982) obtained U-Pb dates on uraninites from the occurrences in the range of 1880 to 1840 Ma. On the basis of these, he proposed that the source of the detrital magnetite and uraninite is the region of the ca 1890 Ma old Hepburn intrusive suite, the uplift of which provided the 'molasse' sediments. This requires, however, that the host sediments are much younger than the Snare Group, and have undergone deformation and metamorphism after the Wopmay orogeny, but prior to the post-orogenic Great Bear magmatic activity that occurred from 1875-1840 Ma (Hildebrand et al., 1987). It is more likely, in the writer's opinion, that the radiometric dates reflect an isotopic re-equilibration of uraninite formed earlier during emplacement of intrusions coeval with the Hepburn suite and/or the Great Bear magmatic activity. Some of the uraniferous magnetite occurrences mentioned above, also contain other minerals, e.g. chalcopyrite, pyrite, molybdenite and tourmaline, which are evidently later additions. Some isotopic reequilibration in uraninite may have occurred at the later stages of the Great Bear magmatic activity. At Hump Lake, the magnetite-rich metasediments of the Snare Group are not uraniferous, but spotty radioactivity is noted in them where they are in contact with, or very close to, granitic intrusions or dykes.

The presence of older stratabound iron deposits in many districts where magnetite-apatite-actinolite deposits occur in volcano-plutonic settings, was noted by Park (1972). It is clear that the Great Bear magmatic zone is no exception in this regard. A possibility that the older deposits could be remobilized on a large enough scale during magmatism to yield ultimately younger magnetite deposits has been suggested by Park (1972). Local remobilization on small scale is noted in the occurrences at Hump Lake and elsewhere. Whether it occurred on a much larger scale to yield veins and breccia-fillings hosted by the volcanics and related plutons of the Great Bear magmatic zone, remains speculative.

## CONCLUSIONS

Magnetite-hematite deposits at Hump Lake are stratiform concentrations in quartzo-feldspathic siltstones of the Snare Group, and were deformed and recrystallized with the host beds. They are older than, and metallogenically distinct from the magnetite-rich monometallic and polymetallic veins and breccia fillings, associated with the felsic volcanic rocks and quartz monzonitic plutons related to the Great Bear magmatic activity.

## ACKNOWLEDGMENTS

Tony Apple of the Ray Lakes settlement assisted the writer during the early part of fieldwork. Cominco Limited exploration team of Alex Nikolajevitch and Andrew Davies, accompanied the writer in the field for a few days, and generated stimulating discussions. X-ray diffraction identifications and microprobe analyses were done by Andrew Roberts and John Stirling, respectively, of the Geological Survey of Canada. Richard Bell, also of the Geological Survey of Canada, critically read the manuscript.

## REFERENCES

**Bond, K.**
1975: Geological and assessment report, Honk claims (NTS 85N-10); Uranerz Exploration and Mining Company Limited; Department of Indian and Northern Affairs Document 080192, 5 p.

**Bond, K. and Rockel, E.R.**
1976: Betty Ray Lake Project 71-24, 1975 Final Report; Uranerz Exploration and Mining Company Limited; Department of Indian and Northern Affairs Document 061469, 22 p.

**Bryan, D.**
1981a: Report on a magnetometer survey and prospecting program performed on the Noranda owned Ron 1 claim group, Hump Lake area (NTS 85N/10); Department of Indian and Northern Affairs, Document 081163, 5 p.
1981b: A magnetometer survey and prospecting program performed on the Noranda owned Ron 4 and Ron 5 claim groups, Hump Lake area (NTS 85N/10); Department of Indian and Northern Affairs, Document 081164, 7 p.

**Frith, R., Frith, R.A., and Doig, R.**
1977: The geochronology of the granitic rocks along the Bear-Slave Structural Province boundary, northwest Canadian Shield; Canadian Journal of Earth Science, v.14, p.1356- 1373.

**Gandhi, S.S.**
1988: Volcano-plutonic setting of U-Cu bearing magnetite veins of FAB claims, southern Great Bear magmatic zone, Northwest Territories; in Current Research, Part C, Geological Survey of Canada, Paper 88-1C, p. 177-187.
1989: Rhyodacite ignimbrites and breccias of the Sue-Dianne and Mar Cu-Fe-U deposits, southern Great Bear magmatic zone, Northwest Territories; in Current Research, Part C, Geological Survey of Canada, Paper 89-1C, p. 263-273.

**Gandhi, S.S. and Bell, R.T.**
1990: Metallogenic concepts to aid exploration for the giant Olympic Dam-type deposits and their derivatives; in Program with Abstracts, 8th IAGOD Symposium, International Association of on the Genesis of the Ore Deposits, August 12-18, 1990, Ottawa, Canada; p. A7.

**Gandhi, S.S. and Lentz, D.R.**
1990: Bi-Co-Cu-Au-As and U occurrences in the Snare Group metasediments and felsic volcanics of the southern Great Bear magmatic zone, Lou Lake, Northwest Territories; in Current Research, Part C, Geological Survey of Canada, Paper 90-1C, p.239-253.

**Hildebrand, R.S., Hoffman, P.F. and Bowring, S.A.**
1987: Tectono-magmatic evolution of the 1.9-Ga Great Bear magmatic zone, Wopmay orogen, Northwestern Canada; Journal of Volcanology and Geothermal Research, v. 32, p. 99-118.

**Lord, C.S.**
1942: Snare River and Ingray Lake map-areas, Northwest Territories; Geological Survey of Canada, Memoir 235, 35 p.

**McGlynn, J.C.**
1968: Tumi Lake, District of Mackenzie; Geological Survey of Canada, Map 1230A, scale 1 : 63 360.
1977: Geology of Bear-Slave Structural Provinces, District of Mackenzie; Geological Survey of Canada, Open File 445, scale 1:1 000 000.
1979: Geology of the Precambrian rocks of the Riviére Grandin and in part of the Marian River map areas, District of Mackenzie; in Current Research, Part A, Geological Survey of Canada, Paper 79-1A, p. 127-131.

**Miller, R.G.**
1982: The geochronology of uranium deposits in the Great Bear batholith, Northwest Territories; Canadian Journal of Earth Sciences, v. 19, no. 7, p. 1428-1448.

**Park, C.F.**
1972: The iron ore deposits of the Pacific basin; Economic Geology, v. 67, no. 2, p. 339-349.

**Rumble, D.**
1976: Oxide minerals in metamorphic rocks; in Oxide Minerals, (ed.) D. Rumble, Mineralogical Society of America Short Course Notes, v. 3, p. R-1 to R-21.

---

Geological Survey of Canada Project 715-7510

# Magnetite-rich breccia of the Mar deposit and veins of the Nod prospect, southern Great Bear magmatic zone, Northwest Territories

**S. S. Gandhi**
**Mineral Resources Division**

*Gandhi, S.S., 1992: Magnetite-rich breccia of the Mar deposit and veins of the Nod prospect, southern Great Bear magmatic zone, Northwest Territories; in Current Research, Part C; Geological Survey of Canada, Paper 92-1C, p. 237-249.*

***Abstract***

*Magnetite breccia-filling of the Mar deposit and magnetite-apatite-actinolite veins of the Nod prospect in Mazenod Lake area, are hosted by rhyolitic rocks of the 1870-1840 Ma old Great Bear magmatic zone. The Mar breccia zone is pipe-like in form, approximately 100 m in diameter, and straddles the contact between, and contains fragments of, rhyolitic rocks and a diorite intrusion. Epidote, hematite and some chalcopyrite, pyrite and pitchblende occur with abundant magnetite. Veins exposed at the Nod prospect contain abundant coarse actinolite, and veins in a nearby overburden-covered zone, explored by percussion drilling, are magnetite-rich and contain chalcopyrite and pyrite.*

*The breccia zone and veins are regarded as products of volatile-charged magmatic fractions generated at depth. Escaping volatiles created the openings that were subsequently filled by deposition from remaining fractions. The magnetite-epidote assemblage probably represents an early stage of mineralization, and the magnetite-apatite-actinolite assemblage was deposited from later more evolved fluids.*

***Résumé***

*Le remplissage bréchique de magnétite dans le gisement de Mar, et les filons de magnétite, apatite et actinolite dans la zone d'intérêt de Nod dans la région du lac Mazenod, sont contenus dans des roches rhyolitiques de la zone magmatique de Great Bear vieille de 1 870 à 1 840 Ma. La zone bréchique de Mar a la forme d'une cheminée d'environ 100 m de diamètre, enjambe le contact entre des roches rhyolitiques et une intrusion de diorite, et contient également des fragments de ces roches. L'épidote, l'hématite et de petites quantités de chalcopyrite, de pyrite et de pechblende accompagnent la magnétite abondante. Des filons qui affleurent dans la zone d'intérêt de Nod contiennent de l'actinolite grossière en abondance, et des filons présents dans une zone recouverte de morts-terrains à proximité, explorée au moyen de méthodes de forage à percussion, sont riches en magnétite et contiennent de la chalcopyrite et de la pyrite.*

*La zone bréchique et les filons sont considérés comme les produits de fractions magmatiques générées en profondeur et chargées de matières volatiles. Ces dernières, en s'échappant, ont créé les ouvertures qui ont par la suite été remplies par l'accumulation des fractions restantes. L'assemblage à magnétite et épidote représente probablement une étape précoce de la minéralisation, et l'assemblage à magnétite, apatite et actinolite s'est accumulé à partir de fluides ultérieurs plus évolués.*

## INTRODUCTION

The Mar deposit and Nod prospect are hosted by felsic volcanic rocks of the Great Bear magmatic zone (Fig. 1). This 1870-1840 Ma old zone is dominated by continental felsic volcanic rocks, and is located on the west side of the Wopmay orogen that culminated ca 1900 Ma ago (Hildebrand et al., 1987). The magnetite-rich breccia of the Mar deposit and the magnetite-apatite-actinolite veins of the Nod prospect exemplify two styles of mineralization that characterize the Great Bear magmatic zone. These breccia deposits, containing U and Cu, have been compared with the giant Olympic Dam Cu-U-Au-REE-Fe deposit in South Australia, and the vein-type occurrences have been compared with the Kiruna deposits in northern Sweden (Hildebrand, 1986; Gandhi, 1989; Gandhi and Bell, 1990). This paper presents observations, made during 1990, on the Mar deposit and Nod prospect, in terms of their geological setting and metallogenic linkage.

## PREVIOUS WORK

Regional mapping in the southern Great Bear magmatic zone was carried out by Lord (1942) and McGlynn (1968; 1979). An airborne radiometric survey by the Geological Survey of Canada in 1974 led to the discovery of the Sue-Dianne breccia deposit in 1975 (Gandhi, 1989), and further exploration of the region by Noranda Exploration Company Limited led to the discovery of the Mar deposit and the Nod prospect (Prest, 1977a, b). The latter two were explored by detailed geological mapping, and ground magnetic surveys. In addition, a ground scintillometer survey was carried out over the Mar deposit, and an induced polarization survey was conducted at the Nod prospect. The well exposed Mar deposit was tested by one diamond drill hole 137 m long, and the Nod magnetic anomaly, covered mostly by overburden, was tested by 9 percussion drill holes totalling 205 m in length (Bryan, 1979, 1981).

## GEOLOGY OF THE MAZENOD LAKE AREA

The southern part of the Great Bear magmatic zone is characterized by felsic volcanic rocks, which were deposited unconformably on the metasedimentary rocks of the Snare Group (Lord, 1942; McGlynn, 1968, 1979; Gandhi and Lentz, 1990). The Mazenod Lake area is underlain by a thick and extensive pile of rhyodacite-rhyolite flows and ignimbrites (Fig. 1). Their aggregate thickness is more than 5 km (Gandhi, 1989). These volcanic rocks have been intruded by porphyritic dacite, diorite, and granodiorite-quartz monzonite intrusions that form part of the Great Bear magmatic zone, and younger diabase dykes. Quartz veins and stockworks are found along major brittle faults and their subsidiary fractures.

### *Snare Group*

Metasedimentary rocks in small exposures north of the Mar deposit represent the Snare Group in the study area (Fig. 1). They include laminated grey and light grey siltstone-mudstone and white to buff coloured calcsilicate rocks. Bedding in them dips steeply, and trends northwesterly, and is thus parallel to the regional trend of other larger zones of metasedimentary rocks of the Snare Group to the south in the Tumi Lake area (McGlynn, 1968). Outcrops of the rocks north of the Mar deposit are in a low swampy terrain, and their contacts with other rocks in the region are not exposed.

### *Great Bear magmatic zone*

#### Volcanic sequence

Stratigraphic and structural relations of the volcanic sequence are complex, and work to date has not been adequate to resolve them. However, a brief overview of the sequence is presented below in terms of lithology, structure and petrochemistry.

*Lithology:* The volcanic sequence includes some thick ignimbrite units, and its aggregate thickness is estimated as 5 km or more (Gandhi, 1989). Flowage or compaction foliation and layering are well developed in the lower parts of these units. In some places these show undulations and minor folds and contortions developed during flowage. The middle parts of the units are relatively massive, and tops of some units are marked by an abundance of lithic fragments. Lithic fragments also occur in other parts of the units, and many were stretched or streaked during deposition, welding and flowage. Tuffaceous siltstone, and fragmental beds and lenses are relatively minor components of the sequence. Current bedding and graded bedding are observed in some of the siltstone beds (Fig. 2).

*Structure:* Units of the sequence have variable attitudes. In the south and east, the units strike northerly and have steep dips towards the east, but in the remainder of the area the trend is easterly and dips are moderate to the north. Units in the easterly trending domain are considered tentatively to form an older part of the volcanic sequence, relative to the units in the remainder of the area. Abrupt changes in strike east of the Sue-Dianne deposit and in the northeast arm of Mazenod Lake are attributable to faults. Local variations in attitude within each domain are apparently due to changes in attitudes inherent in a volcanic pile of this type and later gentle folding.

Units in the older part of the sequence in the Dianne Lake area have been described, and chemical data on them presented by Gandhi (1989). Extension of their boundaries to the west is not well known, but the structural data from McGlynn (1979) and airphotos indicate that they extend 8 km west of Dianne Lake. They dip gently or moderately to the north. Their aggregate thickness is more than 3 km (Gandhi, 1989).

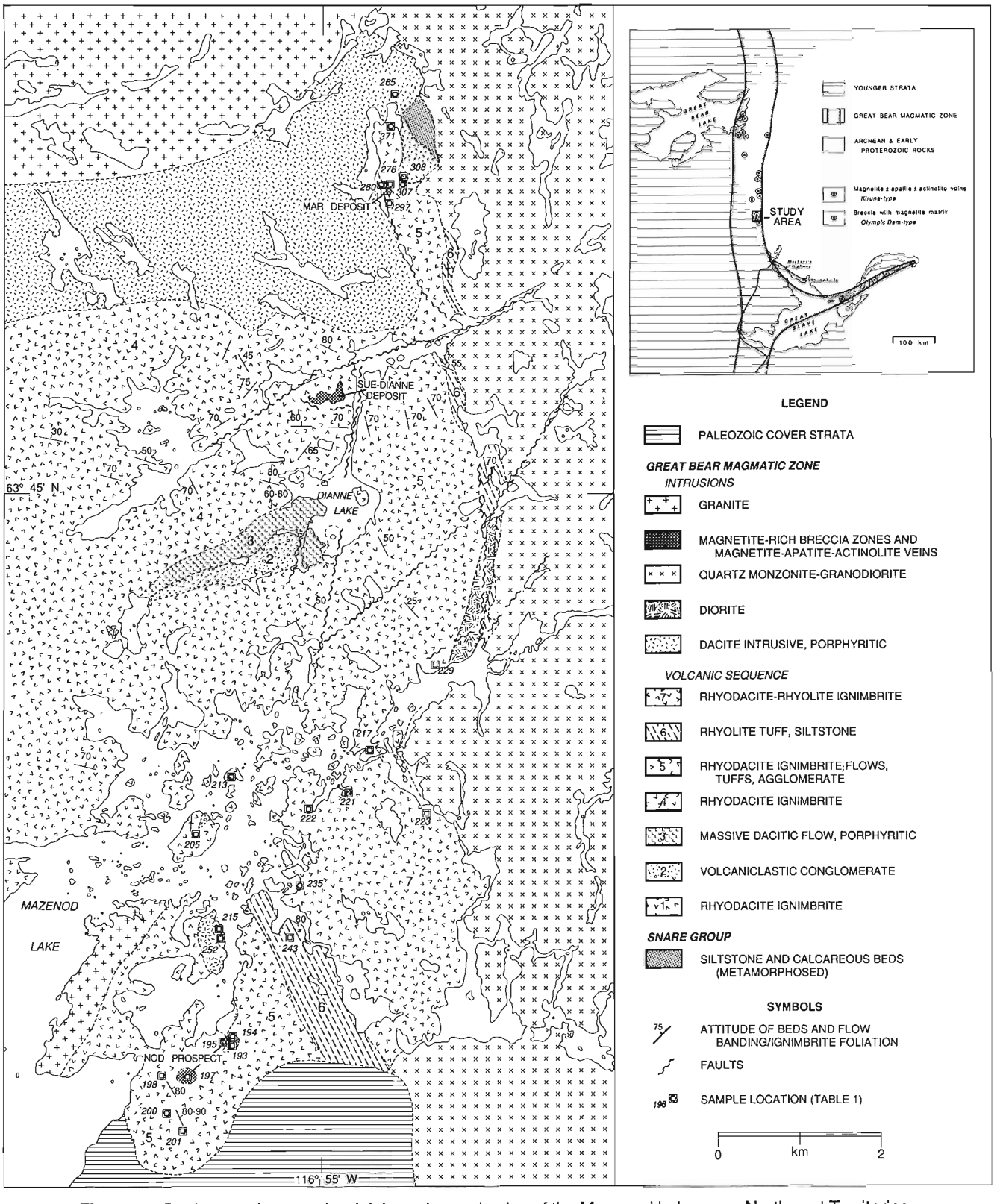


**Figure 1.** Geology and magnetite-rich breccias and veins of the Mazenod Lake area, Northwest Territories.

The units exposed on the south side of Mazenod Lake are commonly massive, and are characterized by abundant phenocrysts of feldspar and quartz. Ignimbritic texture, however, is seen in them at many places. They resemble texturally the upper units in the Lou Lake area 15 km to the south-southeast, which have been described in detail by Gandhi and Lentz (1990), and are located on the regional north-northwest trend of the latter. The area between Mazenod Lake and Lou Lake has not been mapped in detail, and outcrops there are scarce. It is suggested here, however, that some of the larger units at Mazenod Lake are correlatable with those at Lou Lake.

The felsic volcanic units exposed north of the Mar deposit have variable attitudes, although an east-northeast trend is the most common one. The main unit here resembles more siliceous rhyolitic units east of Dianne Lake and on the south side of Mazenod Lake. Hence it is regarded here as one of the younger units of the sequence.

*Petrochemistry:* The petrochemical data for rocks collected during 1990 are reported in Table 1. These data and those reported earlier from the Dianne Lake area (Gandhi, 1989), show that the volcanic sequence is calc-alkaline, with a marginally alkaline character. In general, potash dominates over soda, although there is a considerable variation in the proportions of soda and potash. Some of the rocks have undergone alkali metasomatism and hydrothermal alteration. The compositional range is from mafic dacite to siliceous rhyolite. One unit in the Dianne Lake area, which is highly altered with epidote veins, was previously regarded as a probable andesitic flow (Gandhi, 1989, p. 265, 267), but is now considered an altered diorite intrusive from its comparison with a dioritic dyke at the Mar prospect (Fig. 1). It may be noted here that the volcanic sequence in the southern Great Bear magmatic zone lacks basalts and andesites that are typical of calc-alkaline sequences, such as the LaBine Group in the northern Great Bear magmatic zone (Hildebrand et al., 1987).

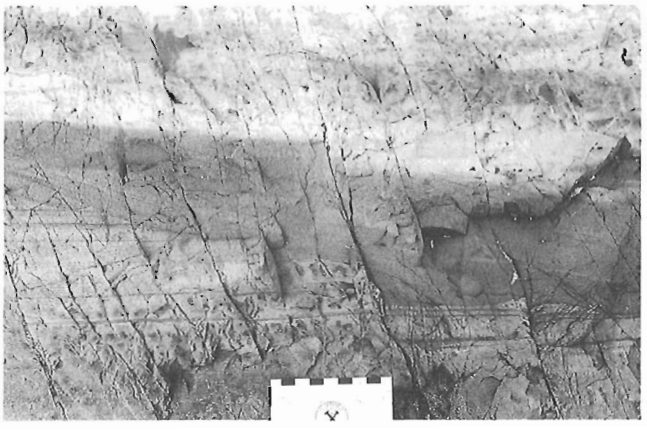

**Figure 2.** Cross bedding in siltstone, 2 km northeast of the Nod prospect, south end of a bay (Fig. 1). Looking down on northeast-facing, nearly vertical beds in a minor S fold. GSC 205341-B

### Intrusive rocks

The volcanic sequence has been intruded by dacite, diorite and granite-granodiorite bodies. Dacite is generally uniformly massive with abundant phenocrysts of feldspar and some quartz in an aphanitic pale pink to cream matrix. It forms dykes and irregular bodies, which are regarded as subvolcanic intrusions (McGlynn, 1979). A massive, fine to medium grained diorite, containing a few scattered phenocrysts of feldspar, was recognized during the present study at the Mar deposit. It is characterized by numerous thin veinlets of epidote. It is a thick dyke-like body, which trends north-northwest and transects the easterly trending volcanic units in the area. It has chilled margins against the volcanic units. This diorite intrusion is situated on the strike from the north-south body of the altered diorite near Dianne Lake mentioned above (Fig. 1). The relative age of the diorite and the porphyritic dacite is not known, because the two have not been observed in contact with each other. They host magnetite-rich breccia and veins, which are genetically related to the Great Bear magmatic activity. Hence the diorite is also a product of this magmatic activity. The large plutons of quartz monzonite-granodiorite in the area mark the final phase of the magmatic activity. These are commonly feldspar porphyritic, coarse grained, massive rocks.

## MAR DEPOSIT

*Geological Setting:* The Mar deposit is a pipe-like breccia body straddling the contact between a rhyolitic sequence and a large diorite dyke (Fig. 1). The breccia contains abundant magnetite as matrix, and angular to subrounded fragments of rhyolitic rocks and of diorite. It contains minor amounts of copper and uranium. It is similar in many respects to the larger Sue-Dianne breccia deposit located 2.5 km to the southwest, which has approximately 8 million tonnes of material averaging 0.8 per cent copper, and 100 to 150 ppm uranium, and erratically distributed small values in gold (Gandhi, 1989). The surface area of the Mar deposit is nearly half that of the Sue-Dianne deposit. One difference is that there is no diorite at the Sue-Dianne deposit.

*Host Rocks:* The host volcanic sequence is dominated by feldspar(± quartz) porphyritic rhyolite and siliceous rhyolite units (Fig. 3). Ignimbritic texture is observed in outcrops east-northeast of the deposit. The units to the southeast include rhyodacitic volcanic and fragmental rocks, and associated volcaniclastic sediments. The trend of the volcanic units varies between northeast and southeast, and dips are moderate to steep. The sequence has been intruded by quartz-feldspar porphyritic dacite, and diorite in the vicinity of the deposit. The diorite forms a prominent north-northwest trending ridge along the east shore of the lake. It contains sparsely distributed small phenocrysts of feldspar, and in some places of amphibole as well, in a fine to medium grained matrix. It is massive, moderately magnetic and rusty weathering, and is traversed by numerous thin veinlets of epidote. Epidote veins also occur in the dacite west of the Mar deposit, and these may be related either to the mineralization of the Mar deposit or to faults along the length of Mar Lake.

*Deposit characteristics:* The core of the Mar breccia zone contains several irregular and dyke-like bodies of massive magnetite with some epidote. These bodies are as much as 8 m wide, and contain numerous angular and subrounded fragments of rhyodacite/rhyolite (Fig. 4, 5, 6 and 7). Stockworks of magnetite-rich veins extend outwards from these bodies into the rhyolitic host rock. Various stages of brecciation are observed in the host rock, and fragments range from angular with little relative movements to the randomly distributed and subrounded (Fig. 6 and 7). The rhyolitic fragments are commonly a few millimetres to a few tens of centimetres long. Fragments of other lithologies in this size range are rare, but several large blocks of diorite, several metres in length, occur in the east central part of the deposit. These have sharp contacts with magnetite-matrix breccia, and some of them are surrounded by the breccia (Fig. 3). Diorite encountered in the drill hole (see Fig. 10) may also be a large fragment.

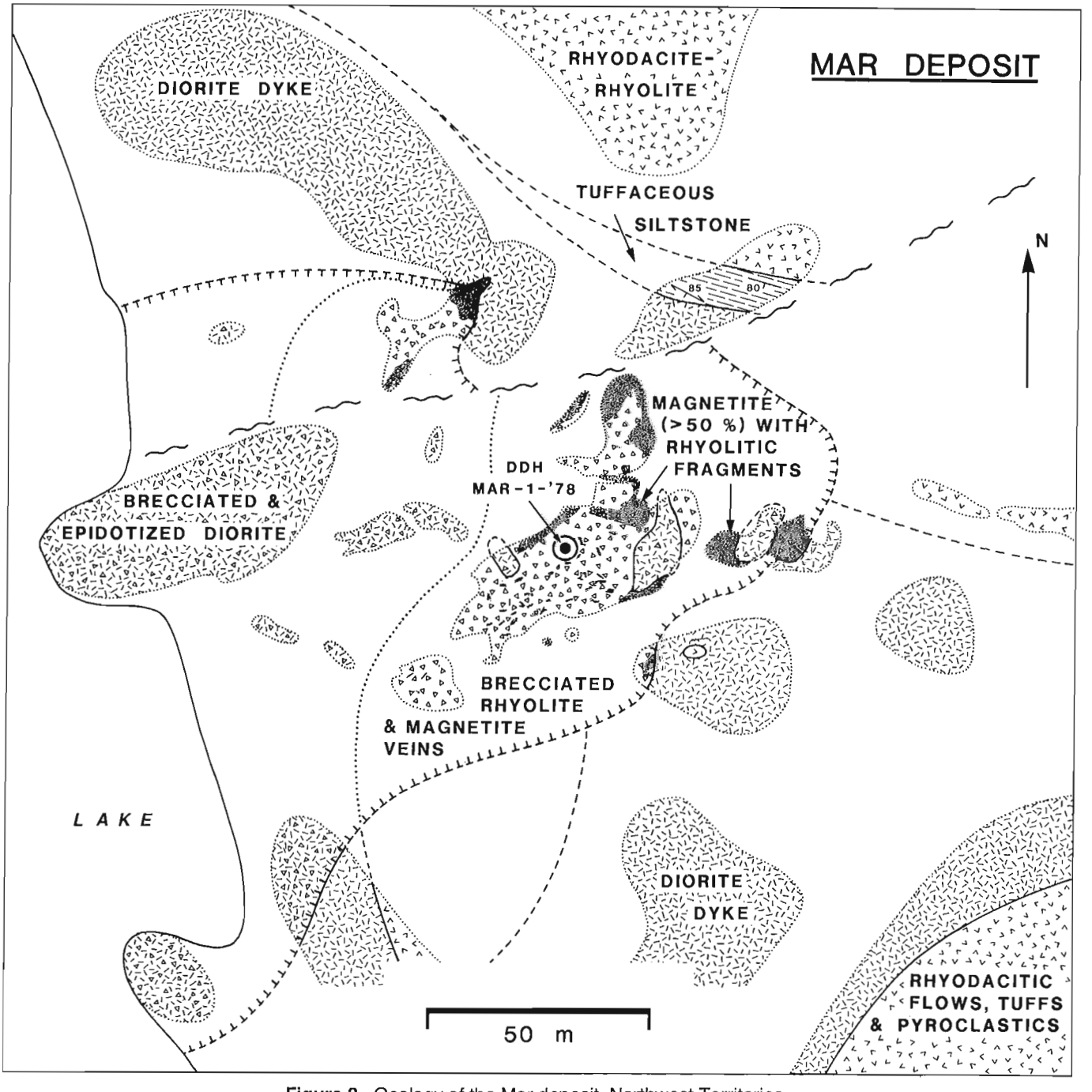


**Figure 3.** Geology of the Mar deposit, Northwest Territories.

In the northwestern part of the deposit, the magnetite-matrix breccia is in sharp contact with the large body of diorite. Locally in this part, the breccia has discernable layering, which is steeply dipping and has northeasterly strike. This layering indicates flowage of the breccia material in a semi-viscous state, at least locally. In several other magnetite-rich parts of the deposit, a more subtle flowage feature is can be detected upon close examination.

On the west side of the deposit, the diorite body is strongly brecciated and epidotized. The brecciated diorite contains angular to subrounded fragments of diorite in fine grained epidote-rich matrix (Fig. 8) The subrounded character of many of the fragments is attributable to progressive alteration towards the core of the fragments. An alteration rim, as much as a few millimetres wide, is conspicuous in some of the fragments.

**Figure 6.** Brecciated rhyolite with magnetite fracture-fillings, Mar deposit. 14 m east and 15 m north of drill hole Mar-1-'78 (Fig. 3). GSC 205328

**Figure 4.** Magnetite-rich zone 8 m north of drill hole Mar-1-'78 (Fig. 3). Looking east. GSC 205339-G

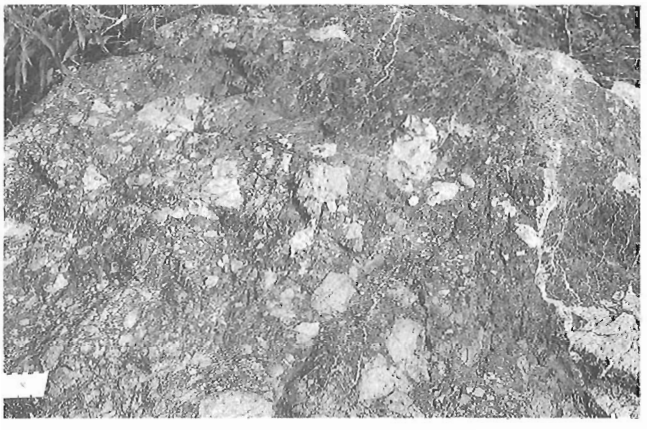

**Figure 7.** Loose block from the Mar deposit, located 51 m west and 23 m south of drill hole Mar-1-'78 (Fig. 3). Rhyolite fragments (pale grey/white) in magnetite (dark grey), cut by epidote veins and patches (white). GSC 205340

**Figure 5.** Epidote patches (medium grey) between rhyolite fragments (light grey/white) and magnetite matrix (dark grey). 35 m east of drill hole Mar-1-'78 (Fig. 3). GSC 205339-C

**Figure 8.** Brecciated and epidotized diorite on the west side of the Mar deposit. 65 m west and 25 m south of drill hole Mar-1-'78 (Fig. 3). Looking down towards east-southeast. GSC 205337

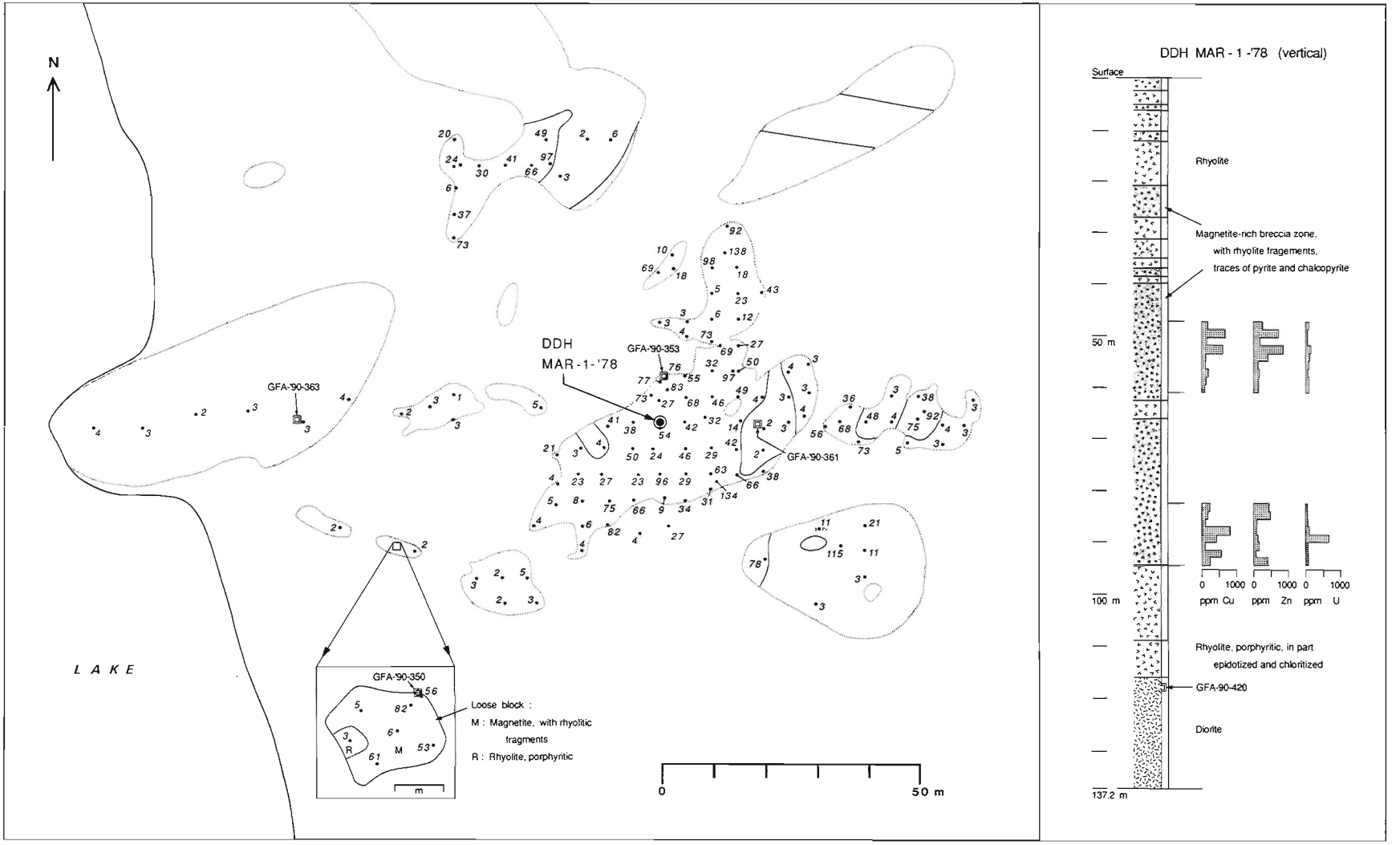


**Figure 9.** Map of the Mar deposit showing uranium concentrations, in parts per million eU, obtained by Exploranium GRS-256 spectrometer (Table 2), and a section of drill hole Mar-1-'78 with selected core assays (Bryan, 1979).

*Mineralogy:* Magnetite is the dominant mineral in the deposit, and associated minerals include hematite and epidote, and minor to trace amounts of pyrite, chalcopyrite, quartz, pitchblende/uraninite, chlorite and amphibole. Magnetite forms coarse aggregates. The crystals range in size from a fraction of a millimetre to a centimetre. Coarser magnetite crystals and aggregates are commonly surrounded by finer grained magnetite. This texture suggests more than one stage of magnetite formation. Microprobe analyses of magnetite in two polished sections of a typical sample (GFA-'90-350, Fig. 3) showed the molecular proportion of magnetite to be between 98.4 and 99.4 per cent for 4 grains. Contents of oxides of Ti, V, Al, Mn, Ni, Co, Cr, and Zn are below detection limits. Three additional grains contained significant amounts of $SiO_2$ (1.7 to 7.5 %), MgO (0.4 to 0.9 %) and CaO (0.7 to 1.7 %), indicating epidote as an impurity with the grains. Hematite is present in small amounts, mainly as an alteration product of magnetite, and also as specularite laths in some parts of the deposit. Chalcopyrite and pyrite are sparsely and irregularly distributed in magnetite aggregates. They are fine to medium grained, and occur mainly as small clusters of grains. Assay results on drill core showed as much as 0.08 per cent copper over 1.5 m (Fig. 10), although some shorter intervals are richer. Weak to moderately anomalous radioactivity was noted over the deposit during a scintillometer survey conducted during initial exploration, and uranium contents as much as 0.07 per cent over 1.5 m have been reported for the drill hole (Prest, 1977a; Bryan, 1979). No visible pitchblende has, however, been identified in the deposit. A spectrometer survey during the present study revealed 25 to 125 ppm eU and 10 to 30 ppm eTh through much of the magnetite-rich portions of the breccia zone (Fig. 9; Table 2). Autoradiographs of relatively more radioactive samples showed that the radioactive mineral is fine grained and sparsely distributed interstitially in magnetite aggregates (Fig. 10 a, b). Preliminary data from microprobe analysis indicate that the mineral is uranium oxide, viz. pitchblende or uraninite (J. Stirling, personal communication, 1991). Autoradiographs of a few drill core samples showed that in some places the uranium mineral is relatively more strongly concentrated in mafic silicates, mainly chlorite and actinolitic hornblende, which occur in small amounts in the deposit.

*Alteration:* The chemical alteration of the rhyolitic fragments in magnetite matrix is minimal, as can be seen from the comparison of the analysis for one of the fragments (sawn from a sample; Table 1, Analysis 21), with the analyses for the rhyolitic rocks in the host sequence (Table 1). The boundaries of fragments are commonly sharp, but in some places the fragments are epidotized, and locally epidotization is intense. Epidote is the main late stage mineral associated closely with magnetite. It occurs as irregular patches, frequently between magnetite aggregates and rhyolitic fragments (Fig. 5), and it also occurs as irregular veinlets in the aggregates (Fig. 7), and in the surrounding host rocks. Minor amounts of quartz are associated with epidote, and locally quartz-rich veins cut the epidote veins. The brecciated diorite is intensely epidotized (Fig. 8), and irregular patches of fine grained epidote, up to a few metres long, are common.

## NOD PROSPECT

Two strong magnetic anomalies occur in the Nod prospect area, one at the north end of a rhyodacite ridge and the other in the low overburden-covered area to its northeast explored by drilling (Fig. 11). A small outcrop of rhyodacite ignimbrite in the low ground has magnetite-actinolite veins containing minor amounts of chalcopyrite. A ground magnetic survey conducted by Noranda Exploration Company Limited outlined a magnetic zone 1000 m long and 250 to 500 m wide, with readings up to 41 000 gammas above background. An induced polarization survey revealed a coincident anomaly. The zone was tested by 205 m of percussion drilling in 9 holes (Bryan, 1981).

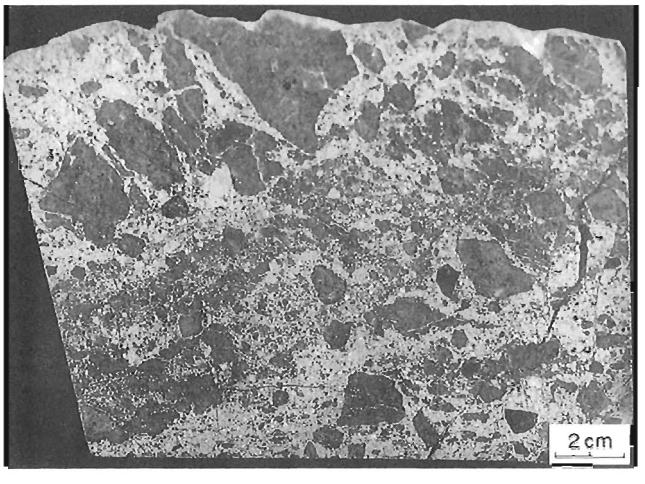


**Figure 10a.** Photograph of a polished slab of magnetite (white/light grey) with rhyolite fragments (grey), sample GFA-'90-350 (Fig. 9 inset). GSC 205427-F

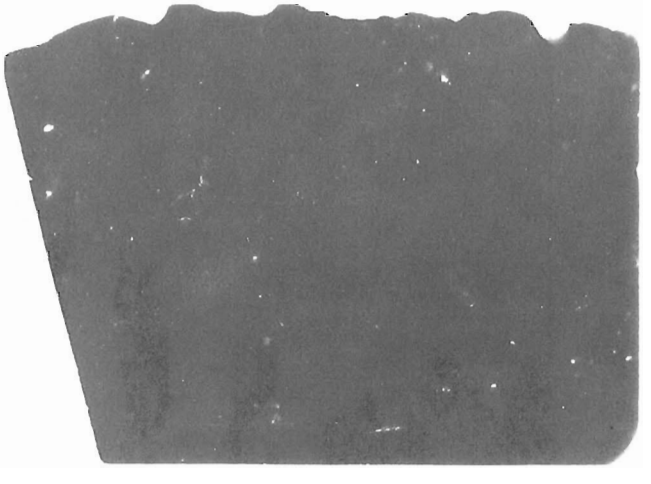

**Figure 10b.** Autoradiograph of the slab above, showing the distribution of uranium oxide (pitchblende or uraninite) as small grains interstitial to magnetite crystals. Film exposure: 4 days.

**Table 1.** Analyses of rocks and an actinolite separate from the volcanic sequence and intrusions in the Mazenod Lake-Mar deposit area, Northwest Territories

| Analysis # | 1 | 2 | 3 | 4 | 5 | 6 | 7 | 8 | 9 | 10 | 11 | 12 | 13 | 14 | 15 | 16 | 17 | 18 | 19 | 20 | 21 | 22 | 23 | 24 | 25 | 26 | 27 | 28 | 29 |
|---|---|---|---|---|---|---|---|---|---|---|---|---|---|---|---|---|---|---|---|---|---|---|---|---|---|---|---|---|---|
| Lithology | Rhyo. | Rhyo. | Rhyo. | Rhda. | Rhyo. | Rhda. | Rhda. | Rhda. | QFrh. | QFrh. | Rhyo. | Rhyo. | Rhtl | Da.fl? | Daci. | Dac.alt. | Daci. | Actino. | Rhyo. | Rhyo. | Rhy.br. | Rhda. | Daci. | Daci. | Dior. | Dior. | Dior. | Dior. | Dio.br. |
| Sample # | 201 | 200 | 198 | 194 | 195 | 252 | 205 | 213 | 221 | 222 | 223 | 229 | 243 | 235 | 215 | 217 | 193 | 197 | 276 | 307 | 353 | 371 | 308 | 265 | 280 | 297 | 361 | 420 | 363 |
| SiO2 % | 69.20 | 70.50 | 72.20 | 65.20 | 70.80 | 65.10 | 66.90 | 62.00 | 62.50 | 63.20 | 72.00 | 69.30 | 67.60 | 60.40 | 68.80 | 59.30 | 68.70 | 52.30 | 67.60 | 70.80 | 72.00 | 64.20 | 68.10 | 62.90 | 55.60 | 56.40 | 55.00 | 55.50 | 51.60 |
| TiO2 | 0.29 | 0.30 | 0.30 | 0.44 | 0.26 | 0.53 | 0.31 | 0.57 | 0.54 | 0.57 | 0.28 | 0.39 | 0.29 | 0.80 | 0.34 | 0.93 | 0.35 | 0.03 | 0.31 | 0.27 | 0.27 | 0.54 | 0.36 | 0.79 | 0.68 | 0.73 | 0.66 | 0.69 | 0.65 |
| Al2O3 | 14.50 | 14.80 | 14.50 | 16.60 | 15.10 | 15.20 | 15.20 | 15.20 | 15.30 | 15.40 | 14.00 | 15.40 | 15.90 | 17.00 | 15.20 | 16.50 | 15.30 | 1.00 | 14.20 | 13.20 | 13.20 | 15.00 | 15.20 | 16.60 | 17.70 | 18.30 | 17.10 | 17.70 | 17.40 |
| Fe2O3 | 0.60 | 0.00 | 0.30 | 1.00 | 0.60 | 2.30 | 1.90 | 2.50 | 2.30 | 1.90 | 1.40 | 0.40 | 2.20 | 4.60 | 1.40 | 2.60 | 0.70 | 2.80 | 3.80 | 1.60 | 1.60 | 3.30 | 1.30 | 4.10 | 4.10 | 3.80 | 2.10 | 4.20 | 4.50 |
| FeO | 0.90 | 1.50 | 0.90 | 2.30 | 0.80 | 2.70 | 1.10 | 3.40 | 3.30 | 3.20 | 1.00 | 0.30 | 1.10 | 1.00 | 2.00 | 4.20 | 2.00 | 19.00 | 1.10 | 1.00 | 0.50 | 1.90 | 1.20 | 1.00 | 3.10 | 4.90 | 4.70 | 4.40 | 3.20 |
| MnO | 0.01 | 0.01 | 0.04 | 0.03 | 0.01 | 0.10 | 0.03 | 0.05 | 0.09 | 0.09 | 0.06 | 0.04 | 0.01 | 0.05 | 0.06 | 0.12 | 0.02 | 0.42 | 0.00 | 0.02 | 0.02 | 0.06 | 0.01 | 0.05 | 0.18 | 0.11 | 0.12 | 0.22 | 0.25 |
| MgO | 0.44 | 0.45 | 0.44 | 1.20 | 0.49 | 1.22 | 0.62 | 2.55 | 3.16 | 2.45 | 0.65 | 0.23 | 0.93 | 2.08 | 0.93 | 2.18 | 0.85 | 10.10 | 0.16 | 0.47 | 0.37 | 1.31 | 0.92 | 0.76 | 2.84 | 3.39 | 4.21 | 3.13 | 3.07 |
| CaO | 0.28 | 0.28 | 0.72 | 1.46 | 0.94 | 3.88 | 0.09 | 1.43 | 1.82 | 3.42 | 0.57 | 1.91 | 0.25 | 2.41 | 0.99 | 2.93 | 1.30 | 12.30 | 0.46 | 1.01 | 0.65 | 1.74 | 2.37 | 3.18 | 5.91 | 1.73 | 6.45 | 3.56 | 10.40 |
| Na2O | 2.00 | 2.00 | 8.20 | 9.40 | 8.40 | 3.00 | 0.80 | 2.50 | 2.30 | 2.60 | 2.40 | 3.80 | 2.80 | 1.90 | 2.10 | 2.90 | 7.90 | 0.20 | 2.00 | 2.00 | 4.80 | 2.90 | 3.30 | 3.90 | 3.30 | 4.80 | 2.80 | 4.80 | 2.60 |
| K2O | 9.44 | 9.50 | 0.22 | 0.28 | 0.36 | 4.66 | 10.60 | 6.44 | 4.77 | 3.74 | 6.20 | 6.71 | 6.23 | 4.93 | 7.15 | 5.42 | 0.57 | 0.09 | 9.14 | 8.12 | 4.01 | 5.99 | 5.45 | 5.30 | 3.90 | 3.06 | 4.16 | 2.69 | 3.57 |
| H2OT | 0.40 | 0.60 | 0.50 | 0.70 | 0.60 | 1.20 | 1.10 | 1.50 | 2.40 | 2.30 | 1.20 | 0.60 | 1.50 | 2.30 | 1.40 | 2.20 | 0.80 | 1.90 | 0.40 | 0.70 | 0.60 | 1.30 | 0.90 | 1.10 | 2.00 | 2.80 | 1.90 | 2.20 | 1.50 |
| CO2T | 0.20 | 0.10 | 0.10 | 0.20 | 0.30 | 0.10 | 0.10 | 1.20 | 1.50 | 1.10 | 0.00 | 0.70 | 0.10 | 2.10 | 0.20 | 1.00 | 0.30 | 0.00 | 0.10 | 0.10 | 0.30 | 0.50 | 0.10 | 0.10 | 0.10 | 0.10 | 0.10 | 0.10 | 0.10 |
| P2O5 | 0.07 | 0.07 | 0.07 | 0.10 | 0.07 | 0.13 | 0.08 | 0.14 | 0.13 | 0.14 | 0.07 | 0.09 | 0.08 | 0.26 | 0.09 | 0.23 | 0.09 | 0.01 | 0.07 | 0.06 | 0.07 | 0.14 | 0.09 | 0.25 | 0.16 | 0.16 | 0.16 | 0.16 | 0.16 |
| S | 0.01 | 0.25 | 0.01 | 0.11 | 0.00 | 0.00 | 0.00 | 0.03 | 0.00 | 0.03 | 0.00 | 0.00 | 0.01 | 0.00 | 0.11 | 0.01 | 0.05 | 0.00 | 0.00 | 0.00 | 0.02 | 0.02 | 0.00 | 0.00 | 0.00 | 0.00 | 0.00 | 0.00 | 0.04 |
| Total | 98.3 | 100.4 | 98.5 | 99.0 | 98.7 | 100.1 | 98.8 | 99.5 | 100.1 | 100.1 | 99.8 | 99.9 | 99.0 | 99.8 | 100.8 | 100.5 | 98.9 | 100.2 | 99.3 | 99.4 | 98.4 | 98.9 | 99.3 | 100.0 | 99.6 | 100.3 | 99.5 | 99.4 | 99.0 |
| Ba ppm | 1700 | 1700 | 30 | 60 | 110 | 820 | 1900 | 850 | 870 | 770 | 850 | 1700 | 690 | 450 | 880 | 890 | 130 | 70 | 2200 | 1600 | 460 | 890 | 940 | 960 | 930 | 580 | 650 | 920 | 430 |
| Be | 2.6 | 1.0 | 1.8 | 3.2 | 2.6 | 2.6 | 1.6 | 2.9 | 2.6 | 2.7 | 2.4 | 2.1 | 2.3 | 2.3 | 2.6 | 3.0 | 3.0 | 13.0 | 1.2 | 1.2 | 1.0 | 2.7 | 2.9 | 3.1 | 2.3 | 2.3 | 2.1 | 2.6 | 2.3 |
| Co | 11 | 64 | 1 | 5 | 2 | 11 | 5 | 23 | 13 | 14 | 6 | 3 | 5 | 7 | 7 | 17 | 4 | 14 | 4 | 6 | 9 | 10 | 5 | 7 | 19 | 24 | 20 | 30 | 21 |
| Cr | 14 | 9 | 11 | 26 | 3 | 31 | 11 | 31 | 24 | 29 | 10 | 14 | 17 | 7 | 7 | 2 | 9 | 0 | 12 | 11 | 13 | 29 | 8 | 8 | 15 | 15 | 37 | 43 | 12 |
| Cu | 130 | 300 | 5 | 310 | 16 | 6 | 2 | 19 | 14 | 22 | 24 | 7 | 5 | 4 | 52 | 110 | 13 | 14 | 3 | 29 | 150 | 4 | 9 | 11 | 34 | 3 | 7 | 9 | 290 |
| La | 27 | 40 | 5 | 27 | 47 | 39 | 13 | 36 | 40 | 38 | 58 | 8 | 26 | 46 | 59 | 44 | 40 | 0 | 70 | 37 | 980 | 38 | 55 | 51 | 29 | 44 | 30 | 30 | 30 |
| Nb | 14 | 6 | 23 | 22 | 20 | 9 | 4 | 12 | 10 | 12 | 15 | 7 | 19 | 25 | 13 | 18 | 21 | 14 | 6 | 8 | 23 | 15 | 11 | 14 | 8 | 12 | 13 | 13 | 16 |
| Ni | 0 | 0 | 4 | 10 | 4 | 13 | 2 | 15 | 16 | 16 | 3 | 0 | 6 | 5 | 4 | 6 | 6 | 48 | 1 | 0 | 1 | 14 | 2 | 1 | 11 | 9 | 18 | 16 | 14 |
| Rb | 270 | 260 | 5 | 7 | 23 | 170 | 330 | 310 | 170 | 140 | 260 | 230 | 210 | 160 | 250 | 160 | 38 | 0 | 300 | 270 | 120 | 260 | 160 | 250 | 180 | 180 | 180 | 98 | 150 |
| Sr | 54 | 60 | 19 | 23 | 35 | 220 | 60 | 140 | 210 | 280 | 91 | 140 | 74 | 97 | 130 | 170 | 54 | 0 | 52 | 49 | 26 | 130 | 190 | 210 | 240 | 130 | 250 | 210 | 120 |
| V | 13 | 2 | 5 | 31 | 1 | 61 | 20 | 66 | 61 | 64 | 13 | 13 | 27 | 35 | 17 | 94 | 16 | 160 | 27 | 12 | 0 | 64 | 18 | 40 | 130 | 110 | 130 | 120 | 120 |
| Y | 16 | 11 | 16 | 23 | 17 | 18 | 13 | 17 | 20 | 19 | 20 | 11 | 20 | 31 | 23 | 27 | 23 | 9 | 16 | 21 | 7 | 17 | 26 | 28 | 19 | 17 | 19 | 20 | 19 |
| Zn | 0 | 0 | 0 | 0 | 0 | 9 | 5 | 17 | 100 | 82 | 35 | 0 | 0 | 2 | 34 | 41 | 0 | 91 | 0 | 2 | 58 | 17 | 0 | 8 | 47 | 46 | 47 | 130 | 50 |
| Zr | 190 | 190 | 190 | 270 | 270 | 190 | 190 | 180 | 180 | 200 | 170 | 210 | 190 | 310 | 210 | 250 | 240 | 6 | 190 | 160 | 170 | 200 | 220 | 300 | 140 | 150 | 140 | 140 | 140 |

Notes :

1) Location of samples in Figures 1, 9 and 11; sample numbers are of GFA-'90 serires.
2) Sample 197 is an actinolite separate from a coarse crystalline actinolite-magnetite-apatite vein at the north end of the ridge in Nod prospect area (Fig. 11).
3) Analyses by the Analytical Chemistry Section, Mineral Resources Division, Geological Survey of Canada, Ottawa.
4) All analyses by x-ray fluorescence method except FeO, H2OT, CO2T and S by rapid chemical methods.
5) Fe2O3 is calculated using formula : Fe2O3 + Fe2O3 (xrf) - 1.11134 X FeO (volumetric).

Core chips from most of the holes revealed the presence of traces of chalcopyrite and malachite with magnetite, occurring in veins cutting rhyodacite ignimbrite. In the easternmost hole NP-2, however, a 6 m zone of massive magnetite was intersected near surface (Fig. 11). It occurs in tuffaceous argillitic rock, which had been logged as part of Snare Group that is flat-lying. Tuffaceous sedimentary beds occur, however, to the north and east, and are steeply dipping (Fig. 1). They are regarded here as part of the volcanic sequence of the Great Bear magmatic zone. The copper values encountered were low. The best intersection was in hole NP-4 which contained an average of 0.14 % Cu, 11 ppm Co, 65 ppb Au and 3.8 ppm U over 3 m (Bryan, 1981). Disseminated pyrite is common in the veins and in the host rocks, which explains the induced polarization anomaly. The northern drill holes intersected some porphyritic dacite, which occurs as a an irregular intrusive body in the outcrop at drill hole NP-7 (Fig. 11), and also in larger outcrops to the north.

The rhyodacite ridge is 45 m high and has steep slopes. Numerous actinolite-magnetite-apatite veins are exposed at the north end of the ridge. In some places they form a stockwork (Fig. 12). Actinolite dominates in the veins. It forms coarse prismatic crystals up to 5 cm long. These contain inclusions of magnetite and apatite. Magnetite forms small crystals and aggregates as much as a centimetre in diameter. Apatite is irregularly and sparsely distributed. Traces of pyrite and chalcopyrite occur in some places. None of the veins examined by the writer was radioactive. In addition to these veins, the rhyodacite ignimbrites in the central part of the ridge contain disseminated pyrite, and fractures lined with pyrite. Trace amounts of chalcopyrite are associated with pyrite in some places. This mineralization is thus different from the actinolite-magnetite-apatite veins.

Chemical analysis of an actinolite separate from the Nod prospect is given in Table 1 (Analysis 18). This separate is pale green under a binocular microscope. Initially, it contained a small proportion of pale brown hornblende, identified by x-ray diffraction method. Repeated magnetic and heavy liquid separations were required to separate the two phases. Recalculation of the actinolite analysis in terms of 24 oxygen atoms yields the following formula:

$$\{Na_{0.03}Ca_{1.97}\}\ \{Mg_{2.25}Fe^{+2}_{2.37}Mn_{0.05}Fe^{+3}_{0.31}Ca_{0.01}\}$$
$$Si_8O_{22}\ \{O_{0.11}OH_{1.89}\}$$

## METALLOGENIC ASPECTS

An important metallogenic feature of the Great Bear magmatic zone is the presence of numerous magnetite ± apatite ± actinolite veins associated spatially and temporally with quartz monzonitic intrusions, which are among the early plutons of the magmatic zone (Badham and Morton, 1976; Badham, 1978; Hildebrand, 1986; Gandhi and Prasad, 1982; Reardon, 1990). Hence a genetic relation between the quartz monzonitic intrusions and the veins is apparent, although the process of formation involved has been a subject of considerable debate. The processes invoked include liquid immiscibility (Badham and Morton, 1976), hydrothermal circulation (Hildebrand, 1986), and volatile fractionation (Gandhi and Bell, 1990). Distribution of the veins in the roof zones and margins of the plutons, and their crystallization in

**Table 2.** Spectrometer readings on the Mar magnetite deposit, southern Great Bear magmatic zone, Northwest Territories

| Location, m from DDH-M-1-78 | eK % | eU ppm | eTh ppm | Location, m from DDH-M-1-78 | eK % | eU ppm | eTh ppm |
|---|---|---|---|---|---|---|---|
| 111 W, 1 S | 5.9 | 4.0 | 9.5 | 5 E, 8.5 N | 4.5 | 54.8 | 20.3 |
| 100 W, 1 S | 5.4 | 2.6 | 9.9 | 5 E, 16.5 N | 4.5 | 4.0 | 11.4 |
| 90 W, 1.5 N | 4.3 | 2.3 | 10.7 | 5 E, 19.5 N | 4.7 | 2.9 | 11.5 |
| 80 W, 2.5 N | 2.0 | 2.8 | 10.9 | 0 E, 19.5 N | 5.7 | 2.6 | 10.5 |
| 69 W, 1 E | 4.2 | 2.9 | 11.6 | 0 E, 29.5 N | 2.2 | 68.8 | 10.9 |
| 60 W, 4 N | 4.6 | 4.0 | 12.9 | 3 E, 32.5 N | 3.9 | 109.9 | 10.1 |
| 50 W, 2 N | 4.8 | 2.1 | 12.9 | 3 E, 32.5 N | 3.4 | 18.3 | 9.4 |
| 40 W, 0 N | 4.1 | 3.3 | 10.5 | 10 E, 30 N | 2.7 | 97.6 | 7.0 |
| 22 W, 3 N | 5.1 | 4.9 | 11.1 | 15 E, 30 N | 3.5 | 17.9 | 9.4 |
| 10 W, 1 S | 4.4 | 40.5 | 23.5 | 13.5 E, 33 N | 2.4 | 91.7 | 12.6 |
| 0 E, 1 S | 2.9 | 53.5 | 12.8 | 13 E, 29 N | 3.4 | 137.8 | 7.5 |
| 9 E, 1 N | 7.6 | 32.4 | 22.8 | 10.5 E, 25 N | 6.2 | 4.7 | 11.4 |
| 20 E, 1 S | 3.3 | 1.8 | 10.6 | 15 E, 25 N | 4.2 | 22.8 | 10.6 |
| 28 E, 1 N | 5.7 | 3.5 | 10.3 | 20 E, 25 N | 1.7 | 42.9 | 14.6 |
| 40 E, 0 N | 4.9 | 48.0 | 9.9 | 10 E, 20 N | 3.9 | 6.4 | 10.7 |
| 50 E, 0.5 N | 2.0 | 75.3 | 9.7 | 15 E, 20 N | 5.8 | 12.3 | 11.2 |
| 51 E, 2 N | 1.3 | 92.4 | 8.1 | 10 E, 15.5 N | 5.1 | 72.6 | 16.5 |
| 59 E, 1 S | 2.8 | 3.1 | 10.7 | 11 E, 15 N | 6.9 | 69.2 | 17.1 |
| 75 E, 1 S | 3.0 | 1.6 | 9.6 | 15 E, 15 N | 6.5 | 26.9 | 26.2 |
| 100 E, 6 N | 3.2 | 3.5 | 10.7 | 10 E, 10 N | 7.2 | 31.8 | 23.6 |
| 110 E, 6 N | 3.1 | 3.4 | 9.8 | 15 E, 10 N | 5.1 | 49.6 | 16.4 |
| 120 E, 1 N | 2.9 | 3.5 | 10.9 | 14 E, 10 N | 4.7 | 96.6 | 16.3 |
| 130 E, 0.5 W | 4.6 | 2.7 | 12.2 | 16 E, 0 N | 2.9 | 13.5 | 32.6 |
| 138 E, 2 N | 1.6 | 3.0 | 11.3 | 5 E, 4.5 S | 7.1 | 45.5 | 20.5 |
| 149 E, 0 N | 1.4 | 3.6 | 10.8 | 5 E, 9.5 S | 4.5 | 29.2 | 20.7 |
| 150 E, 18 N | 5.8 | 4.6 | 22.2 | 5 E, 15 S | 6.3 | 34.2 | 14.2 |
| 150 E, 47.5 N | 5.1 | 6.1 | 28.5 | 10 E, 5 S | 3.9 | 28.8 | 24.0 |
| 170 E, 70 N | 6.5 | 7.4 | 28.0 | 10 E, 10 S | 5.4 | 62.5 | 10.8 |
| 170 E, 90 N | 6.7 | 6.6 | 29.1 | 10 E, 13 S | 5.2 | 30.8 | 22.2 |
| 170 E, 95 N | 5.5 | 7.1 | 30.5 | 11.5 E, 11.5 S | 3.5 | 134.4 | 10.9 |
| 172 E, 102 N | 5.0 | 7.0 | 29.5 | 15 E, 10 S | 3.1 | 65.7 | 22.0 |
| 170 E, 113 N | 4.4 | 6.8 | 27.6 | 15 E, 5 S | 2.2 | 41.6 | 17.8 |
| 160 E, 55 N * | 1.8 | 4.5 | 25.6 | 19. 5 E, 5 S | 3.8 | 2.3 | 12.9 |
| 160 E, 55 N * | 1.9 | 6.2 | 23.5 | 20 E, 5 N | 3.9 | 4.0 | 10.9 |
| 1 W, 5 S | 6.9 | 23.8 | 26.0 | 20 E, 9.5 S | 3.8 | 38.3 | 18.2 |
| 0 E, 10 S | 2.4 | 95.6 | 13.6 | 24.5 E, 0 S | 2.7 | 3.0 | 9.9 |
| 1 E, 14.5 S | 7.3 | 9.0 | 14.7 | 25 E, 5 N | 2.7 | 2.8 | 10.4 |
| 1.5 E, 20 S | 3.9 | 27.3 | 14.3 | 25 E, 10 N | 5.9 | 3.6 | 11.2 |
| 5 W, 15 S | 2.8 | 66.0 | 24.9 | 29 E, 11 N | 3.8 | 3.2 | 10.2 |
| 4 W, 10 S | 8.0 | 23.2 | 26.2 | 29.5 E, 6 N | 5.8 | 3.4 | 10.1 |
| 5 W, 5 S | 3.0 | 50.1 | 18.6 | 15 E, 5 N | 3.6 | 48.0 | 17.5 |
| 5 W, 0 S | 1.4 | 37.5 | 25.6 | 10 E, 5 N | 5.4 | 47.2 | 18.0 |
| 4 W, 20 S | 4.8 | 3.9 | 11.4 | 35 E, 0 N | 1.0 | 67.6 | 9.5 |
| 11 W, 10 S | 2.7 | 26.5 | 17.1 | 32.5 E, 1 S | 2.9 | 55.6 | 16.3 |
| 11 W, 5 S | 5.0 | 3.5 | 11.4 | 36 E, 3.5 N | 2.5 | 36.4 | 34.7 |
| 10 W, 15 S | 3.1 | 75.1 | 8.9 | 38.5 E, 4 S | 2.6 | 73.1 | 11.1 |
| 16 W, 10 S | 3.4 | 22.7 | 16.7 | 45 E, 1 N | 4.3 | 4.2 | 9.4 |
| 1.5 W, 5 S | 4.1 | 3.2 | 10.9 | 45 E, 7.5 N | 3.5 | 2.6 | 9.4 |
| 20 W, 6.5 S | 5.6 | 21.2 | 11.4 | 50 E, 5 N | 2.7 | 38.0 | 12.8 |
| 20 W, 12 S | 5.7 | 3.8 | 11.5 | 48 E, 4 S | 5.3 | 4.6 | 11.9 |
| 20 W, 16 S | 8.7 | 4.6 | 11.7 | 55 E, 1 S | 3.2 | 3.8 | 10.8 |
| 15 W, 15 S | 4.8 | 8.2 | 9.7 | 55 E, 5 S | 2.8 | 3.4 | 12.7 |
| 15 W, 20 S | 7.4 | 5.6 | 11.7 | 61 E, 4.5 N | 3.4 | 2.6 | 11.4 |
| 15 W, 25 S | 6.1 | 4.1 | 11.5 | 40 E, 20 S | 3.8 | 21.4 | 9.2 |
| 10 W, 20 S | 5.6 | 81.9 | 13.5 | 40 E, 25 S | 3.7 | 11.0 | 10.4 |
| 24.5 W, 20 S | 7.7 | 4.1 | 12.3 | 40 E, 31 S | 4.3 | 3.1 | 10.5 |
| 25.5 W, 30 S | 4.8 | 4.5 | 10.7 | 35 E, 24 S | 4.2 | 115.2 | 8.8 |
| 30.5 W, 30 S | 6.0 | 2.1 | 11.4 | 32 E, 21 S * | 4.0 | 10.5 | 7.1 |
| 35.5 W, 30 S | 8.4 | 2.9 | 13.5 | 30 E, 35 S | 4.4 | 2.5 | 11.1 |
| 30 W, 35 S | 8.7 | 1.8 | 13.5 | 22 E, 30 S | 4.6 | 78.1 | 6.2 |
| 24.5 W, 35 S | 8.9 | 3.3 | 10.8 | 44 W, 3 N | 3.5 | 2.5 | 9.1 |
| 47.5 W, 25 S | 6.7 | 2.0 | 12.5 | 40 W, 5 N | 5.9 | 14.0 | 9.8 |
| 62 W, 20 S | 4.0 | 2.0 | 9.6 | 40 W, 36 N | 2.3 | 73.3 | 9.0 |
| 51 W, 23 S ** | 1.3 | 60.5 | 6.2 | 40 W, 40 N | 2.6 | 37.3 | 11.8 |
| 51 W, 23 S ** | 3.0 | 82.1 | 9.8 | 40 W, 45 N | 5.5 | 5.6 | 12.2 |
| 51 W, 23 S ** | 2.4 | 56.5 | 8.8 | 38.5 W, 50 N | 4.4 | 23.6 | 9.5 |
| 51 W, 23 S ** | 1.2 | 53.3 | 1.7 | 40 W, 54 N | 3.9 | 19.8 | 8.6 |
| 51 W, 23 S ** | 3.4 | 63.2 | 12.1 | 35 W, 48 N | 4.6 | 30.2 | 8.7 |
| 51 W, 23 S ** | 2.8 | 55.0 | 11.9 | 29 W, 50 N | 3.8 | 41.1 | 9.7 |
| 51 W, 23 S ** | 6.5 | 29.7 | 23.1 | 25 W, 50 N | 4.0 | 66.2 | 7.8 |
| 0 E, 4.6 N | 4.9 | 26.5 | 22.5 | 22 W, 54 N | 4.6 | 49.1 | 8.7 |
| 0 E, 8.2 N | 1.3 | 76.6 | 2.4 | 19 W, 48.5 N | 3.4 | 3.1 | 10.1 |
| 1 E, 8.5 N | 2.2 | 75.5 | 8.6 | 21 W, 50 N | 3.9 | 97.2 | 5.2 |
| 1.25 E, 7 N | 2.8 | 83.4 | 12.2 | 15 W, 54 N | 4.0 | 2.2 | 8.6 |
| 1.5 W, 6 N | 2.6 | 72.5 | 7.9 | 10 W, 54 N | 6.0 | 5.9 | 11.4 |
| 5 E, 0 N | 2.9 | 42.1 | 17.5 | 10 E, 150 N | 8.2 | 6.5 | 29.6 |
| 5 E, 5 N | 2.1 | 67.7 | 13.1 | 13 E, 154 N | 8.6 | 7.8 | 30.7 |

Note: * Magnetite-rich veins; ** Loose block of magnetite-rich breccia.

tensional fractures, indicate either volatile-streaming or hydrothermal deposition. There is little wall rock alteration associated with the veins. This suggests that no large scale circulation of hydrothermal solutions involving meteoric waters, was operative. Instead, the mineralizing fluids appear to have been charged with volatiles, the escape of which formed the openings in which the remainder of the fraction deposited the minerals, as suggested by Gandhi and Bell (1990).

The veins at the Nod prospect are similar to most of the veins elsewhere in the magmatic zone, except that no quartz monzonite intrusion is exposed at this prospect. Quartz monzonite-granodiorite intrusions, however, occur in the Mazenod Lake region (Fig. 1; McGlynn, 1979; Gandhi, 1989). It may, therefore, be postulated that such a pluton occurs at depth in the Nod prospect area, and was the source of the veins.

Breccia zones of the Mar and Sue-Dianne deposits differ from the veins of the Nod prospect mainly in that they contain notable amounts of uranium and copper, and epidote $\{Ca_2(Al,Fe^{+3})_3(SiO_4)_3(OH)\}$, instead of the actinolite and apatite typical of the veins. The polymetallic character, however, is not restricted to the breccia-type deposits, because examples of polymetallic veins are known elsewhere in the Great Bear magmatic zone. In the southern part of the magmatic zone are the U-Cu-bearing Fab showings, located 25 km north-northwest of the Mar deposit (Gandhi, 1988). These are mineralogically similar to the Mar deposit. Monometallic magnetite ± apatite ± actinolite veins occur, however, within a few kilometres of the Fab polymetallic

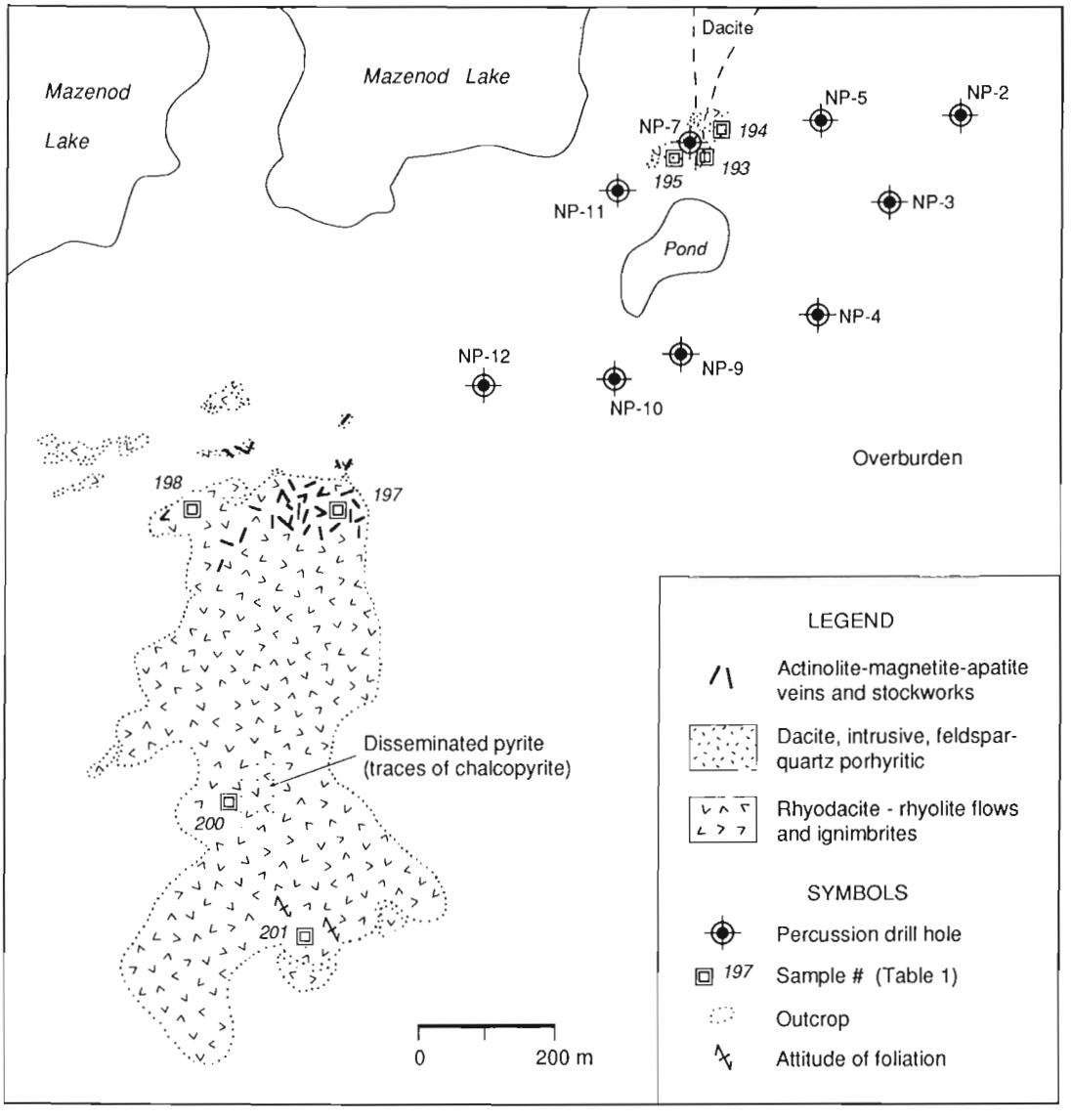


**Figure 11.** Geology and drill holes of the Nod prospect, Mazenod Lake.

**Figure 12.** Photograph of a stockwork-like cluster of actinolite-magnetite-apatite veins in rhyodacite ignimbrite, 10 m southwest of sample GFA-'90-197 (Fig. 11). GSC 205349

veins, but these are not seen in the vicinity of the larger Mar and Sue-Dianne polymetallic deposits. The study of the veins and of the Sue-Dianne deposit led Gandhi (1989) to suggest that there is some sort of lateral and vertical zonation in this group of magnetite occurrences. The present study of the Mar and Nod occurrences supports this suggestion. The precise controls of such a zonation remain obscure, as the variations seen in the group as a whole are not observed within a single occurrence. In the writer's opinion, a generalization may, however, be made that the polymetallic breccia zones, like the Sue-Dianne and Mar deposits, represent the deeper and higher temperature parts of a system, which grade upwards at lower temperature into the polymetallic veins, and finally to the monometallic magnetite ± apatite ± actinolite veins. The latter are considered to have formed at the lowest temperatures and relatively more distal from the source. Further studies are required to constrain the temperature and pressure conditions for deposition of the mineral assemblages in the group, and also the compositions of the mineralizing fluids and the source magma.

## GUIDES TO EXPLORATION

The implications of the above generalization to mineral exploration are that the clusters of monometallic veins, which in themselves are economically not attractive, may indicate the presence of polymetallic breccia deposits in the vicinity, and that the polymetallic veins and breccia deposits like the Mar deposit, which contain relatively small amounts of U and Cu, may grade at depth into, or indicate a presence in their vicinity of, larger and richer deposits containing significant amounts of U, Cu, Au, and possibly other metals like Co, Ni, and rare earth elements.

## CONCLUSION

Magnetite-rich polymetallic breccia deposits and clusters of magnetite ± apatite ± actinolite veins, exemplified by the Mar deposit and Nod prospect, respectively, are genetically linked to the intermediate to felsic magmas that dominated the Great Bear volcano-plutonic zone. The differences in the mineral assemblages, in particular the abundance of paragenetically late epidote in the breccia deposit and the abundance of actinolite in the veins, is primarily a function of the initial composition and evolution of the mineralizing fluids as they moved along the openings created by escaping volatiles.

## ACKNOWLEDGMENTS

Fieldwork at and near the Nod prospect was done with the co-operation of the Cominco Limited exploration team of Alex Nikolajevitch and Andrew Davies. Their help and geological observations have been very valuable. X-ray diffraction identification and microprobe analyses were done by Andrew Roberts and John Stirling, respectively, of the Geological Survey of Canada. The manuscript benefitted from critical reviews by R.T. Bell and R.I. Thorpe of the Geological Survey of Canada.

## REFERENCES

**Badham, J.P.N.**
1978: Magnetite-apatite-amphibole uranium and silver-arsenide mineralizations in the lower Proterozoic igneous rocks, east arm, Great Slave Lake, Canada; Economic Geology, v. 73, p. 1474-1491.

**Badham, J.P.N. and Morton, R.D.**
1976: Magnetite-apatite intrusions and calc-alkali magmatism, Camsell River, N.W.T.; Canadian Journal of Earth Sciences, v. 13, p. 348-354.

**Bryan, D.**
1979: Geological Report on a diamond drilling program performed on the Noranda owned Mar-1 claim group, Mazenod Lake area, District of Mackenzie (85-N-15); Department of Indian and Northern Affairs Document 081030, 2 p.
1981: Report on a percussion drilling program performed on the Noranda owned Nod claim group, Mazenod Lake area, District of Mackenzie (NTS 85N/10); Department of Indian and Northern Affairs Document 081282, 5 p.

**Gandhi, S.S.**
1988: Volcano-plutonic setting of U-Cu bearing magnetite veins of FAB claims, southern Great Bear magmatic zone, Northwest Territories; in Current Research, Part C; Geological Survey of Canada Paper 88-1C, p. 177-187.
1989: Rhyodacite ignimbrites and breccias of the Sue-Dianne and Mar Cu-Fe-U deposits, southern Great Bear magmatic zone, Northwest Territories; in Current Research, Part C; Geological Survey of Canada, Paper 89-1C, p. 263-273.

**Gandhi, S.S. and Bell, R.T.**
1990: Metallogenic concepts to aid exploration for the giant Olympic Dam-type deposits and their derivatives; Program with Abstracts, 8th IAGOD Symposium, International Association on the Genesis of the Ore Deposits, August 12-18, 1990, Ottawa, Canada; p. A7.

**Gandhi, S.S. and Lentz, D.R.**
1990: Bi-Co-Cu-Au-As and U occurrences in the Snare Group metasediments and felsic volcanics of the southern Great Bear magmatic zone, Lou Lake, Northwest Territories; in Current Research, Part C; Geological Survey of Canada, Paper 90-1C, p. 239-253.

**Gandhi, S.S. and Prasad, N.**
1982: Comparative petrochemistry of two cogenetic monzonitic laccoliths and genesis of associated uraniferous actinolite-apatite-magnetite veins, east arm of Great Slave Lake, District of Mackenzie; in Uranium in Granites, (ed.) Y.T. Maurice; Geological Survey of Canada, Paper 81-23, p. 81-90.

**Hildebrand, R.S.**
1986: Kiruna-type Deposits: Their Origin and Relationship to Intermediate Subvolcanic Plutons in the Great Bear Magmatic Zone, Northwest Canada; Economic Geology, v. 81, no. 3, p. 640-659.

**Hildebrand, R.S., Hoffman, P.F. and Bowring, S.A.**
1987: Tectono-magmatic evolution of the 1.9-Ga Great Bear magmatic zone, Wopmay orogen, Northwestern Canada; Journal of Volcanology and Geothermal Research, v. 32, p. 99-118.

**Lord, C.S.**
1942: Geological Map, Snare River, District of Mackenzie, Northwest Territories; Geological Survey of Canada Map 690, scale 1:253,440.

**McGlynn, J.C.**
1968: Tumi Lake, District of Mackenzie, Geological Survey of Canada Map 1230A, scale 1:63,360.
1979: Geology of the Precambrian rocks of the Riviére Grandin and in part of the Marian River map areas, District of Mackenzie; in Current Research, Part A; Geological Survey of Canada, Paper 79-1A, p. 127-131.

**Prest, S.E.**
1977a: Geological and geophysical investigations of the Nod claim group, District of Mackenzie, N.W.T. (NTS 85 N 10); Noranda Exploration Company Limited; Department of Indian and Northern Affairs Document 080643, 10 p.
1977b: Geological and geophysical investigations of the Mar claim group, District of Mackenzie, N.W.T. (NTS 85 N 15); Noranda Exploration Company Limited; Department of Indian and Northern Affairs Document 080646, 10 p.

**Reardon, N.C.**
1990: Altered and mineralized rocks at Echo Bay, N.W.T., and their relationship to the Mystery Island intrusive suite; in Current Research, Part C; Geological Survey of Canada, Paper 90-1C, p 143-150.

Geological Survey of Canada Project 715-7510

# Geological reassessment in parts of the Laughland Lake area (Prince Albert Group) for Mineral and Energy Resource Assessment of the proposed Wager Bay National Park, Northwest Territories

**C.W. Jefferson and Mikkel Schau[1]**
**Mineral Resources Division**

*Jefferson, C.W. and Schau, Mikkel, 1992: Geological reassessment in parts of the Laughland Lake area (Prince Albert Group) for Mineral and Energy Resource Assessment of the proposed Wager Bay National Park, Northwest Territories; in Current Research, Part C, Geological Survey of Canada, Paper 92-1C, p. 251-258.*

***Abstract***

*This resource assessment involves mapping, prospecting and geochemical sampling of the western end of the proposed Wager Bay national park. Orientation studies in 1991 outlined major geological domains to be studied next year. From 92° to 92°20'W, variably strained tonalitic and granitic gneisses of several ages trend NE and are cut by massive granite. From 92°20' to 92°40'W northerly trending lenses of spinifex-bearing komatiites are fault-bounded by gneisses, have NE apophyses, and merge to the south with metasediments including quartzite and iron formation. These continue, around the south end of a large gneiss oval (basement?), into multiply deformed komatiites, metasediments and hill-forming quartzites of the Prince Albert Group (PAG). A deformed and recrystallized layered anorthosite pluton centred at 66°15'N / 92°30'W cuts all but granite gneiss and granite units. Mineral potential is yet to be assessed.*

***Résumé***

*Cette évaluation des ressources comprend la cartographie, la prospection et l'échantillonnage géochimique de l'extrémité ouest du parc national proposé de la baie Wager. Les études d'orientation de 1991 ont permis de délimiter les principaux domaines géologiques à étudier au cours de la prochaine année. Entre 92° et 92°20' W, les gneiss tonalitiques et granitiques, dont l'âge et le degré de déformation varient, sont orientés au nord-est et sont recoupés par un granite massif. Entre 92°20' et 92°40' W, des lentilles de komatiites à spinifex orientées vers le nord sont limitées par des gneiss, comportent des apophyses au nord-est et fusionnent au sud avec des métasédiments, notamment de la quartzite et de la formation ferrifère. Ceux-ci se transforment à l'extrémité sud d'un gneiss oval (socle ?) en komatiites déformées de façons diverses, en métasédiments et en quartzites formant colline dans le groupe de Prince Albert. Un pluton d'anorthosite stratifié déformé et recristallisé, centré à 66°15'N/92°30' W, recoupe toutes les unités, sauf celles de gneiss granitique et de granite. Le paysage et la géologie offrent un intérêt pour les visiteurs du parc, mais le potentiel minéral reste encore à évaluer.*

[1] Continental Geoscience Division

## INTRODUCTION

Parks Canada (1978) first proposed a national park centred on the head of Wager Bay (Fig. 1). The landscape and geology here are of interest to potential park visitors. Additional planning led to a Mineral and Energy Resource Assessment (MERA) survey of a terrestrial area east of 92° by Jefferson et al. (1991) who indicated moderate to low potential for metallic minerals in highly deformed and metamorphosed Archean tonalitic and supracrustal gneisses which are transected by the Wager Shear Zone (Henderson et al., 1991b; Henderson and Broome, 1990; Broome, 1990; LeCheminant et al., 1987) and high potential for oil shales in lower Paleozoic strata on Southampton Island.

Continuing studies by Canadian Parks Service have suggested including the marine waters of Wager Bay and the headwaters of the Brown River west of 92°. Additional MERA field studies began in 1991 for these areas. An Open File resource assessment report is expected to be released by March 1993. The park establishment process includes on-going public and internal government consultations at local, community, territorial and national levels. The report will contribute to the public information base for these consultations.

The GSC is considering methods for assessing the marine part of the Wager Bay park proposal, for which limited information is available. Published bathymetric information is a single line of soundings from the mouth of Wager Bay to Douglas Harbour.

## REGIONAL GEOLOGIC SETTING

The Laughland Lake area has been partially mapped at scales of 1:250,000 by Schau (1982) and 1:1,000,000 by Heywood (1961). Two weeks of field studies in August 1991 set up the logistical and geological framework for a 1:50,000-scale 1992 survey of 56K1, 56K2 and adjacent areas (Fig. 1). Our 1991 observations on tonalitic gneisses, komatiites, quartzites, iron formations, anorthosites, granite gneisses and granites are reported here.

The expression of various map units in the Laughland Lake area is distinctive on the magnetic anomaly map (Geological Survey of Canada, 1984). Such data were not available in the study area in the early 1970s.

In the study area (Fig. 2), iron formations are characterized by linear extreme highs (500 to 1500 gammas), flanked by extreme lows (-300 gammas). The komatiites correspond to moderate highs (50 to 250 gammas) flanked by lows, reflecting magnetite generated by breakdown of iron-bearing magnesian silicate minerals to low-grade metamorphic minerals such as serpentine. The magnetite in some flows affects the compass at ground level. Broad -300 gamma lows are not distinctive by themselves because they correspond variably to gneiss, pelite and quartzite.

The NE structural trends of the magnetic patterns, parallel to measured gneissossities and compositional layering, lend credence to their use in regional mapping and are particularly useful in tracing PAG map units from upper greenschist metamorphic facies toward higher grade rocks along strike to the NE, especially beneath thick surficial deposits.

The units are discussed below from oldest to youngest; all locations are in Figure 2.

## BROWN RIVER GNEISS COMPLEX

Gneisses interpreted as basement to the PAG (Schau, 1982) are located NE and NW of the Laughland Lake Anorthosite Complex. Primary layering in the contained and adjacent PAG is generally at angles to the surrounding gneissossity, and metamorphic grade in PAG tends to be lower than that of the gneisses (ibid.). The PAG is in fault contact with the inferred basement gneisses (ibid.) in most places. Northerly structural trends in the centre of the study area define the North-South Fault zone (Schau, 1982, p. 9), strands of which border the thin komatiite belt. Localities "x", "y" and "z" on the western contact between komatiites and gneiss are linked by a high strain zone. At site "w" the eastern contact of the komatiites is a 1 m covered interval between east-facing flows and relatively undeformed tonalite gneiss, suggesting a brittle fault.

A critical re-examination of a proposed unconformity between gneisses and conglomerates to sandstones (Schau, 1982, p.11) at locality "x" showed it to be a mylonite (straight gneisses, mica phyllonites and mylonitic komatiites) and fault gouge zone containing boudins of a distinctive local aplite dyke. The suggestion of an unconformity remains at locality "y", a few kilometres south of "x". Here, steeply dipping S-striking protomylonitic tonalite on the NW is separated by a one-metre NE-trending covered interval from a moderately SE-dipping komatiite flow with spinifex textures suggesting facing to the SE. The covered contact zone truncates the gneissosity. The great differences in strain and metamorphic grade, and the lack of on-strike continuity of the ductile shear fabric, so well developed in the protomylonite but absent in the serpentinized komatiite, suggest that the contact is an unconformity. The high ductile strain elsewhere along this contact (see description of locality "z" below) and the possibility of superimposed brittle faults require that this hypothesis be tested by future mapping.

## PRINCE ALBERT GROUP (PAG)

The PAG includes metakomatiites, layered greenschists and phyllites, pelites, quartzites, and iron formations. Intensity of metamorphism and deformation is low enough to permit a provisional measured section NW of Laughland Lake (Schau, 1982, table 4).

### *Komatiites*

Within the thin komatiite belt ("w x y z"), north-trending ice-sculpted outcrops expose abundant spinifex texture and moderate NE- to SE-dipping flows. Easterly stratigraphic tops are indicated by gradation, from massive orange-weathering cumulate zones with abrupt basal

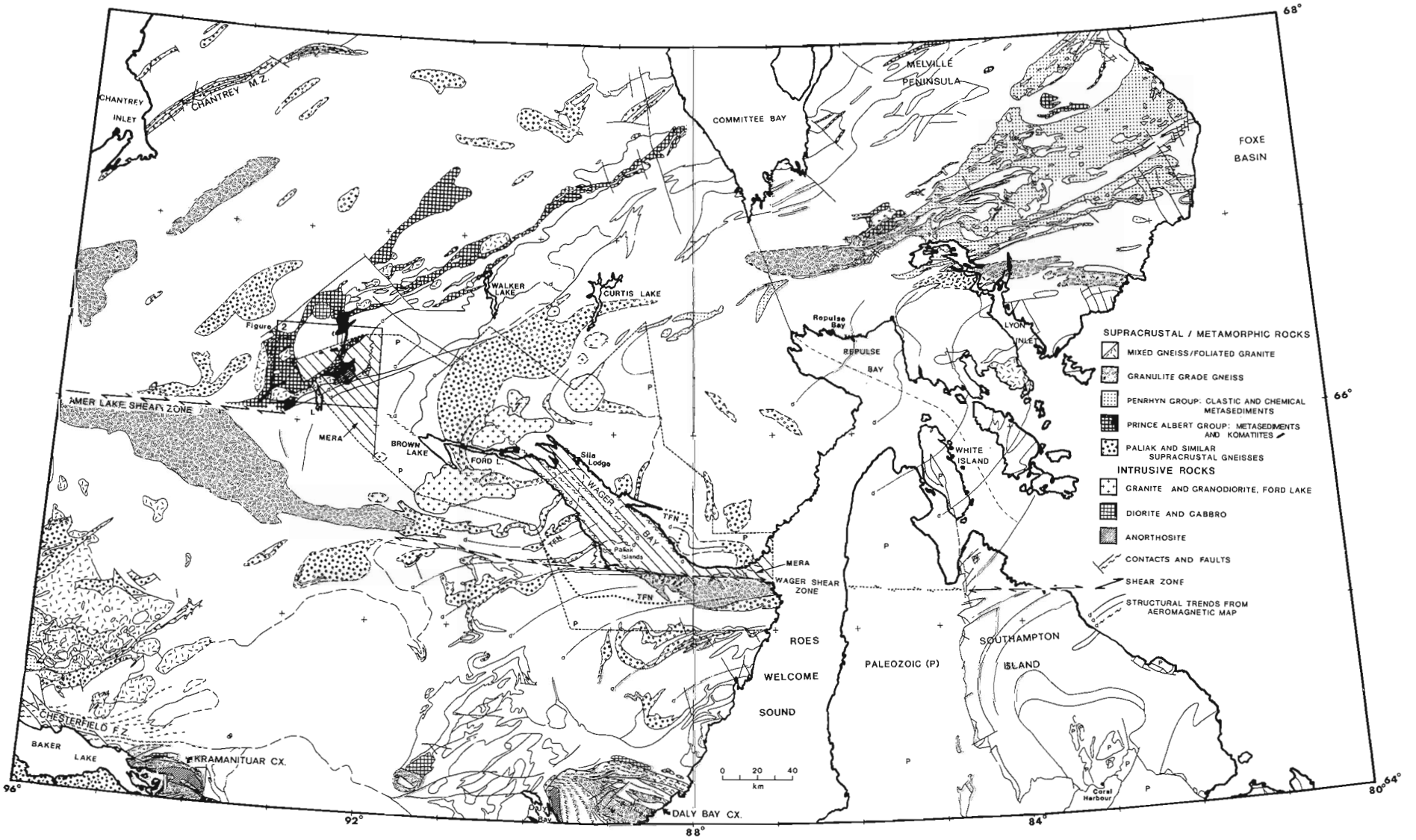


**Figure 1**. Geological setting of the Wager Bay region and location of Figure 2, modified after Broome (1990). "P": proposed national park boundaries as of March 1991, "TFN": lands selected by the Inuit, March 1991, "MERA": areas which require resource assessment by this study. In the event of park establishment, provision has been made for potential northern and southern access corridors between Wager Bay and the hinterland, subject to environmental assessment, legislation and regulations, and public consultations. Access across Inuit land would be subject to the terms of their agreements with the Government of Canada.

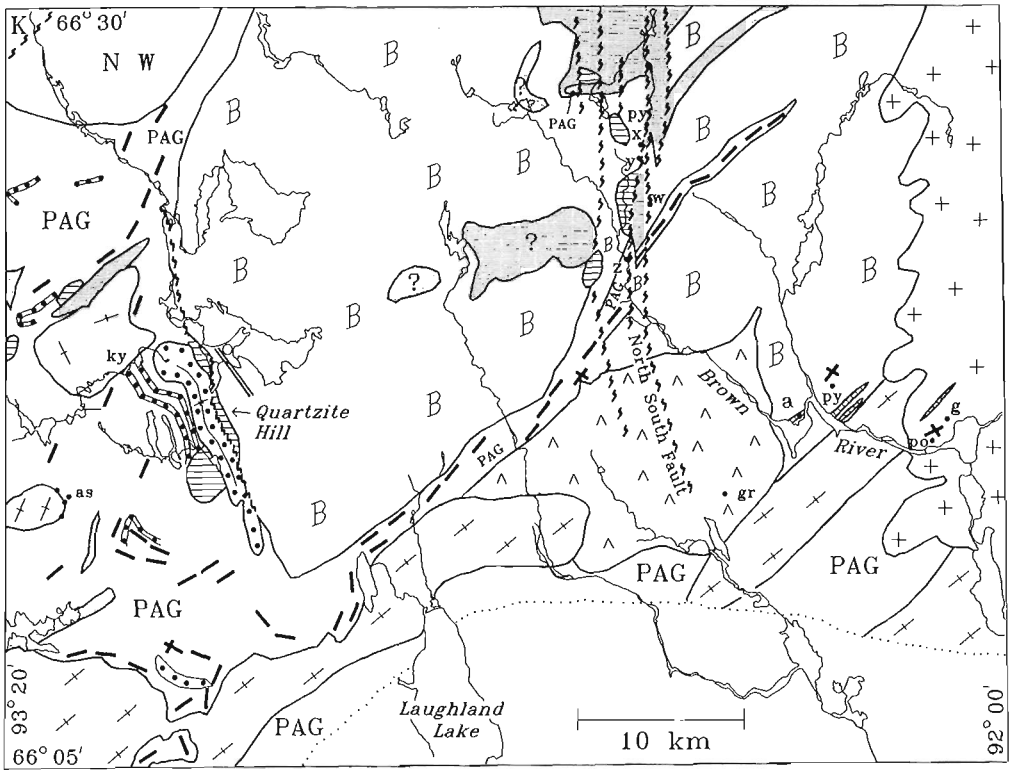


**Figure 2.** Geological sketch of Laughland Lake study area; most gneiss and granite contacts are interpreted from aeromagnetic data (see Regional Geologic Setting and unit descriptions in text), extrapolated from outcrop data of Schau (1982) and this study. Areas shaded as komatiites and denoted by "?" are identified solely by aeromagnetic highs, as are all but four of the iron formation symbols. Quartzites, mafic intrusions, the central komatiites and the Laughland Lake Anorthosite are delineated by outcrop data. Mineral abbreviations are as follows: as - arsenopyrite, gr - graphite, ky - kyanite, po - pyrrhotite, py - pyrite. Drainage modified after digital data from Surveys and Mapping Sector of EMR.

contacts, into green-weathering finer-to-coarser spinifex. Some outcrops are bounded by recessive highly foliated ultramafic schists whose fabrics dip steeply and trend N-S, truncating the layering. Deformation is less severe in wider western exposures of the PAG, where layering can be traced continuously along strike. The anatomy of the large komatiite complex north of locality "x" will be studied next season.

### *Quartzites*

The quartzites form mappable units, tens of metres to 2 km wide and are continuous along strike on the order of kilometres. On "Quartzite Hill" the true stratigraphic thickness is at most 1 km because of folds. A series of varicoloured quartzite outcrops 10 to 50 m wide parallels the edge of Quartzite Hill about 500 m west of the white quartzites, separated by pale to dark, variably rusty, pyrrhotitic chloritic quartzites and some metavolcanic rocks. Compositional changes at the boundaries of the quartzite units are gradational.

Rare cross-bedded quartzites in the PAG are illustrated by Schau (1982). In 1991 we observed numerous large cross beds and variations in bedding thickness from centimetre to metre scale. Vitreous quartzites display clearly detrital textures on glacially polished surfaces. Tabular and cross beds are accentuated by 0.5-2 mm. black heavy mineral laminae and muscovitic partings. The planar or gently concave, low-angle (10-15°) fore-sets are 1-2 m high and generally. Rare high angles suggest synsedimentary deformation of the foresets.

A 100 m-thick fining-upward stratigraphic sequence with cross beds defines the core of the isoclinal syncline on Quartzite Hill. The thick-bedded, massive- to cross-bedded,

LEGEND

PROTEROZOIC
- Mafic dykes

PROTEROZOIC/ARCHEAN
- SOUTHERN WALKER LAKE GNEISS

ARCHEAN
- A' GRANITE GNEISS
- K — KUAGNAT GNEISS COMPLEX
- N W — NORTHERN WALKER LAKE GNEISS
- LAUGHLAND ANORTHOSITE COMPLEX
- Amphibolite dyke
- Metagabbroic stocks

PRINCE ALBERT GROUP
- PAG — Undivided
- Metakomatiites
- Quartzite
- Magnetite iron formation from aeromagnetic data
- Iron formation outcrop
- B — BROWN RIVER GNEISS
- Approximate geological contacts
- Faults
- Limit of mapping
- . y,gr — Locality, mineral occurrence discussed in text
- Syncline

vitreous-white quartzarenites grade inward to tabular, decimeter-bedded quartzarenites with millimetre-centimetre thick muscovitic partings every 5-10 cm. These in turn grade inward to thinly bedded very fine-grained, laminated muscovite green and hematitic red quartzites which form the core of the syncline. The thinly laminated beds, more prone to deformation than the vitreous white quartzites, are intensely crenulated and contain lenticular mylonitic laminae.

The red hematitic zone along the syncline axis is most intense in the thin bedded, fine grained and muscovitic upper stratigraphic units. Thinly laminated strata here are hematitic in layers several metres thick. In tabular bedded strata near the axis, alternating intense red and white coloration outlines layers a few cm thick parallel to the thin bedding. A fainter red hematitic coloration is disseminated in thicker, more vitreous quartzite layers in the same vicinity. Some hematite is earthy and postdates the metamorphic micas. It may be a product of alteration during late, more brittle stages of deformation which preferentially affected thinner bedded strata.

### *Iron Formation*

Iron formations that underlie the intense aeromagnetic anomalies were noted as outcrop in two places by Schau (1982) but were not investigated in 1991. Schau described them as alternating quartz and iron mineral laminae. Thin iron formations with negligible aeromagnetic signatures were sampled at two localities in this study. NE of locality "a" a few metres of alternating quartz and magnetite laminae are in a highly strained lens of garnet-biotite paragneiss, within Brown River Gneiss. Iron formation at locality "g" is also a few metres thick, is concordant with the SE margin of a kilometre-long xenolith of dark green fine-grained metabasalt, and is gossanous, including both magnetite-quartz laminae and disseminated pyrrhotite in medium-grained biotite schist.

Large lenses and elongate extensions of PAG iron formations, komatiites and quartzites project into the Brown River Gneiss across splays of the North South Fault from the central komatiite belt. They may represent structural keels as they are continuous with larger areas of PAG. Other lenses of PAG-like rocks located in the A′ granite and eastern Walker Lake Gneiss are clearly xenoliths.

### *Paleogeography*

Schau (1982) and Schau and Ashton (1988) ascribed a regional continental and subaerial environment to the PAG. Prolonged and/or severe weathering would have been required to produce the quartzites. The pelites and abundant iron formations record subaqueous environments in much of the area. NW of Laughland lake, komatiites are interbedded with sediments (Schau, 1982, fig. 8) but as noted in the above discussion on Brown River Gneiss, no sedimentary rocks are documented in the N-S-trending central komatiite belt.

## LAUGHLAND LAKE ANORTHOSITES AND RELATED GABBROIC INTRUSIONS

The sugary white Laughland Lake Anorthosite Complex, comprising a locally layered anorthosite with a thin, thinly layered border phase of leucogabbro and gabbro, is exposed in rugged white hills NNE of Laughland Lake and underlies about 150 km$^2$. Schau (1982, p.19) suggested that it cuts the Brown River Gneiss and the PAG, is complexly deformed, and is Archean. We have observed that it is cut by the A′ granites and affected by their later deformation. It contains local shear zones parallel with both the N-S trends so common to the north and with the NE trends so common to the east of the Complex. At locality "gr" graphite nodules several cm across are contained in sugary coarse-grained anorthosite.

Other coarser grained resistant amphibolite bodies appear to be lenticular metagabbro dykes that intrude Brown River Gneiss and PAG lenses in NE-trending high-strain zones which are inferred to be regional. Large amphibolite pods close to the Laughland Lake Anorthosite Complex are interpreted to be part of its marginal phase. At location "a" a 10 x 30 m pod is massive in its core, foliated on its margins, and forms an isoclinal hook which is open to the NNE and truncated on its west side by a sequence of annealed mylonitic granodiorite and biotite-hornblende phyllonite. The core of the hook preserves biotite-hornblende schist. The hook is interpreted as a large inclusion in a ductile shear zone.

### *A′ GRANITES*

A′ granites were described west of the study area as foliated granites (Schau, 1982). The foliated granites in the eastern part of the study area probably are part of the same suite, but have undergone more deformation. Heywood's (1961) mapping shows that the granite intrudes PAG correlatives to the south, consistent with the inclusions or roof appendages seen in the granite.

The locally megacrystic orthogneiss component of the A′ granite ranges from tonalite to quartz monzonite in composition, with biotite- and hornblende-rich phases. The structure ranges from non-layered to conspicuously layered, most layering having the appearance of intrusive contacts that are transposed parallel to the strong biotite-hornblende foliation. Lenticular xenoliths within the orthogneisses, metres to kilometres in length, comprise biotite fels and amphibolite with local iron formation, garnetiferous layers and disseminated pyrrhotite. Xenoliths and their contained fabrics are oriented sub-parallel to the gneissossity and foliation.

## UNDEFORMED GRANITIC PLUTONS AND THE WALKER LAKE GNEISS COMPLEX

The A′ granite orthogneiss and its contained xenoliths are discordantly intruded on the east by locally red stained, equigranular granite characterized by weak foliation, minor

biotite and local muscovite, accessory magnetite and fluorite. The granite contains polygonal blocks and lenses, metres to kilometres in scale, of all above-described units. For example the metabasalt with concordant iron formation at locality "g" is intruded on the NW by gneissic white tonalite (a phase of the A′ granite?), intruded to the SE by gneissic pink porphyritic granite (A′), and all are invaded by the equigranular granite. No obvious metamorphic aureole exists in the adjacent granitoid orthogneisses and the gneissossities are undeformed by the granite, suggesting that the pluton stoped into the host gneisses during the late stages of regional metamorphism.

The presence of muscovite and absence of hornblende suggest the equigranular granite may be related to the muscovite-bearing granites to the north (Schau, 1982), but the rock textures and accessories are quite different. The undeformed nature and red staining of this granite are similar to those of the $1805^{+10}/_{-5}$ Ma Base Camp Granite south of Paliak Islands (Henderson et al., 1991b). Circular to elliptical plutons of similar Proterozoic hornblende-biotite granites, which locally contain fluorite (LeCheminant et al., 1987), extend from south of Brown Lake, NE to Curtis Lake. Late red-stained granitic plutons which have been mapped to the north generally contain biotite, hornblende, accessory tourmaline, sphene and magnetite (Schau, 1982).

The small area of granite mapped this summer corresponds to one of a series of aeromagnetic highs in the order of 750 gammas which cover a broad north-trending belt, part of which is shown in the eastern edge of Fig. 2. Only about 3 km of the sharp western contact of the granite has been mapped in outcrop west of locality "g". The remainder of the irregular contact of the eastern granite (mapped as Southern Walker Lake Gneiss on Fig. 2) was extended to the north and south by tracing the western edges of the series of small aeromagnetic highs which characterize the belt.

The Southern Walker Lake Gneiss Complex (Schau, 1982, p. 22) is characterized by gneissic granite and/or granodiorite, and inclusions or septa of almost flat-lying biotite-rich layers containing large porphyroblastic K-feldspar crystals. Rocks assigned to the southern part of the Walker Lake Gneiss Complex by Schau (1982) may be more deformed counterparts of the A′ granites and Brown River Gneiss which are abundantly intruded by late granites. For convenience, and until these relationships are resolved by ground observations, the mixture of tonalitic gneisses and late granites is shown undivided in Fig. 2 as the Southern Walker Lake Gneiss Complex.

## STRUCTURE OF THE ARCHEAN ROCKS

### *NE Shear Zones*

In the eastern part of the study area, regional foliation, gneissic layering, ductile shear zones, and orientations of supracrustal xenoliths and keels trend NE with steep NW dips. Gneissossity is folded about gently NE-plunging axes, locally showing subhorizontal attitudes (e.g. A′ Granite between localities "a" and "g"). NE-trending ductile shear fabrics characterize the A′ granite orthogneiss. Two zones of more intensely deformed, and locally sulphidic lenses and keels of PAG are shown by the exposed iron formation symbols between localities "a" and "g".

### *North-South Fault Zone*

A north-south zone of deformation transects the central komatiite belt and Brown River Gneiss, through localities "w" to "z" and appears to extend into the Laughland Lake Anorthosite Complex. The protracted deformation zone possibly represents the site of feeders to the PAG komatiites, the gabbro stocks (Schau, 1982, p. 32) and the Laughland Lake Anorthosite Complex, and includes west-side-down and sinistral shear. Several structural discontinuities of this zone, especially the tectonic east and west boundaries of the narrow central komatiite belt, are figured by Schau (1982) and modified in Fig. 2. Fault boundaries trend N-S, whereas komatiite flows dip easterly with strikes varying from NE to NW.

The eastern boundary of the central komatiite belt is constrained to a covered interval a few metres wide. Here, no north-south fabric is developed in either gneiss or PAG, therefore this contact is interpreted as a brittle fault, west-side-down. Along strike to the north, apophyses of PAG extend across this fault, and within the study area aeromagnetic anomalies interpreted as iron formation and komatiites cross the projected faults with little apparent displacement.

The western contact of the narrow central komatiite belt is also faulted, probably resulting from both an east-side-down brittle component (not exposed), and an earlier development of mylonitic fabrics, with subhorizontal extension lineation, at or near contacts of both Brown River Gneiss and the komatiites. Along part of the contact finely laminated mylonites of felsic to ultramafic parentage are seen. Gossans are developed in overburden and outcrop along this contact; pyrite is locally abundant in both mylonitic tonalite and laminated felsic mylonite. At locality "z" the eastern boundary of the komatiite belt extending from the south is marked by a steeply dipping, north-south striking tectonic melange tens of metres thick, comprising interleaved mylonitic gneiss, amphibolite, and ultramafic schist that contains isolated spheroidal tectoclasts of gneiss and amphibolite.

Another mylonite zone, within the gneiss about 200 m SW of locality "y", trends NW and contains a vertical extension lineation. Local C-S fabrics and minor folds suggest dominant NE-side-down movement, with no obvious offset of the nearby komatiite-gneiss contact.

### *Multiple stages of Folding*

Complex folds of at least two generations are exposed in PAG NW of Laughland Lake (Schau, 1982). An older fold generation is isoclinal, exemplified by the syncline coring Quartzite Hill. A mineral foliation sub-parallel to bedding is most intense along the syncline axis, in a laminated quartzite phyllite, and on the west side of the hill in similar phyllites,

possibly the anticlinal complement. The fabric is weak in thick bedded quartzites and metavolcanic rocks in the same vicinity. The fabrics clearly predate a NE-trending steeply dipping crenulation cleavage. A stepped, subhorizontal mineral lineation is developed only on the surfaces of thicker quartzite beds and is possibly related to flexural slip during folding (kinematics require investigation). A steeply SW-plunging mineral lineation penetrates both the vitreous quartzites and the laminated rocks.

Relatively younger, more open folds in the Quartzite Hill area trend NE, refolding the earlier structures and forming Type 2 interference patterns at the north end of Quartzite Hill. These steeply plunging folds are associated with locally intense zones of NE-striking, sub-vertical crenulation cleavage.

## SURFICIAL GEOLOGY

The surficial geology of the Laughland Lake area has been mapped by Thomas (1981), and the adjoining area to the east by Smith (in Jefferson et al. 1991). The region is covered by till and glacio-fluvial deposits. Glacial striae, sculpted bedrock landforms and glacial-constructional landforms all record NE ice-flow directions.

Most outcrops are in glacial meltwater channels, a lesser number in Recent fluvial systems, and a few at heights of land. Systems of kames, eskers and meltwater channels indicate that meltwater flowed SE.

A train of angular debris in the valley immediately west of "a", on the SE side of the Laughland Lake Anorthosite, terminates abruptly at its SE end and is associated with a kame-esker system. Large blocks of anorthosite sit on Brown River Gneiss and were derived from the W-NW. The debris is interpreted as deposited by a SE-directed mass flow, possibly originating from a broken ice dam.

Large fields of rounded boulder deposits, several metres thick with little or no fine-grained matrix, are spatially associated with meltwater channels, preserve very large channel forms visible from the air, and are interpreted as the beds of large meltwater streams which removed sand and clay from till, leaving extensive boulder fields as lag deposits.

Recent high-velocity winter winds have been reworking the finer sand deposits, particularly along the Brown River system, creating large blow-outs and sand flats trending toward the SSE.

## MINERAL POTENTIAL

Little mineral exploration activity has been recorded since Schau (1982) summarized the mineral potential of the Laughland Lake area. He listed reports of mining companies who have worked in the area, and cited Laporte's (1974) summary of nickel and copper exploration in komatiitic terrains. Eckstrand (1975) and Schau (1982) listed several similarities among the komatiitic rocks of the PAG, and ultramafic rocks of the Abitibi Belt (Canada), Yilgarn and Pilbara blocks (Australia). These similarities suggest potential for nickel, copper and chromium deposits in the PAG.

A key attribute of the ultramafic-hosted Ni-Cu deposit model to consider in this resource assessment is contamination of the ultramafic magmas by sulphidic supracrustal rocks (R. Eckstrand, pers. comm., 1991). Assimilation of crustal sulphur related to such deposits probably occurred at depth, rather than by thermal erosion of footwall rocks as the komatiite lavas flowed across the seafloor (Duke, 1990). In the Laughland Lake area, most komatiite is concentrated in the central belt which is bounded by gneisses and lacks exposed intercalations of metasediments. All flows observed are tabular, some as thin as 20 cm, and none are pillowed, therefore the environment seems to have been subaerial. From these observations, it seems that the central komatiite is less favoured for Ni-Cu deposits. Attention will be focussed on komatiites overlying or intercalated with thicker portions of PAG metasedimentary rocks.

Showings of pyrrhotitic iron formations of the PAG were investigated several decades ago by Aquitaine Company of Canada Ltd. The showings are near the intrusive contact of the Laughland Lake Anorthosite with the PAG, within the proposed park boundaries. A pyrrhotitic biotite schist is preserved as part of a xenolith in the southern Walker Lake Gneiss Complex at locality "g". NE of locality "a", densely disseminated pyrite is in granitoid gneiss on the SE side of the magnetite-chert iron formation outcrop.

West of the proposed park area, Comaplex Resources International Ltd. investigated arsenopyrite showings previously reported by Schau (1982) at the contact between PAG and A′ granite (Fig. 2).

Prospectors report that specimen grade piedmontite is present in the Laughland Lake Anorthosite Complex (A.R. Miller, pers. comm. 1989).

Exploration for gold has intensified to the SW along strike of the PAG. Metasomatic gold trapped in sulphidic parts of iron formation (Henderson et al., 1991a; Armitage et al., 1991) and komatiites (Annesley et al., 1991) has been found in the Woodburn Lake Group, an equivalent of PAG to the SW (Schau and Ashton, 1988). Targets could be magnetically invisible primary sulphide-facies iron formations such as Lupin, in sulphidized parts of magnetically prominent oxide-facies iron formation (Kerswill, 1990), or in structurally controlled late metasomatic veins (Armitage et al., 1991).

Sedimentary-exhalative sulphides containing either lead-zinc (sedex of Carne and Cathro, 1982) or the newly recognized association of zinc-nickel-platinum-group-elements (Hulbert et al., 1990) also should be considered for the PAG. Further investigation of this possibility is planned for metasedimentary rocks of the belt.

Roscoe (pers. comm. 1990) has proposed to study the potential of PAG quartzites for paleoplacer gold and uranium. Scintillometers recorded only background radioactivity over dark heavy mineral laminae and all other parts of the

quartzites which we traversed in a two day period. No pyrite was found in the sedimentary laminae. Future testing of this exploration possibility should concentrate on basal and conglomeratic units of the quartzites.

## ACKNOWLEDGMENTS

We thank Polar Continental Shelf Project for helicopter support; aircrew George Fawcett and Lana Voll for reliable service; Canadian Parks Service and Elizabeth Seale for support and collaboration; DIAND for support through the MERA process; Baker Lake Lodge and Liz Kotelowitz for local logistics and radio communication; GSC administrative staff Geneviève Allen and Bonny Rankin, and Supply and Services Canada for efficiently implementing logistics; Joe Angotingoar and Bill Crawford for reliable fuel emplacement; and Kelli Powis for efficient and cheerful assistance in office and field.

Bert Struik and co-workers at G.S.C. Vancouver are thanked for the use of their GEOF program, which allowed us to enter field notes on the outcrop into our digital database. Deborah Lemkow lent her Autocad expertise at short notice.

Critical review by Subhas Tella much improved an earlier version of the manuscript.

## REFERENCES

**Annesley, I.R., Madore, C., Mudry, P., and Balog, M.**
1991: Gold Mineralization in altered metakomatiites of the Woodburn Group, Amer Lake, North West Territories (abstract); in Program with Abstracts; Geological Association of Canada, Mineralogical Association of Canada, Society of Economic Geologists, Joint Annual Meeting, v. 16, p. A3.

**Armitage, A. and James, R. and Goff, S.**
1991: Auriferous Iron Formation, Third Portage Lake Area, Keewatin District, N.W.T.; in Program with Abstracts; Geological Association of Canada, Mineralogical Association of Canada, Society of Economic Geologists, Joint Annual Meeting, v. 16, p. A4.

**Broome, H.J.**
1990: Generation and interpretation of geophysical images with examples from the Rae Province, northwestern Canadian Shield; Geophysics, v. 55, p. 977-997.

**Carne, R.C. and Cathro, R.J.**
1982: Sedimentary exhalative (sedex) zinc-lead-silver deposits, northern Canadian Cordillera; Canadian Mining and Metallurgy Bulletin, v. 75, No. 840, pp. 66-78.

**Duke, J.M.**
1990: Mineral deposit models: Nickel sulphide deposits of the Kambalda type; Canadian Mineralogist, v. 28, p. 379-388.

**Eckstrand, O.R.**
1975: Nickel Potential of the Prince Albert Group, N.W.T.; in Report of Activities, Part A, Geological Survey of Canada, Paper 75-1A, p. 253-255.

**Geological Survey of Canada**
1984: Magnetic anomaly map, Quoich River; Geological Survey of Canada, Map NQ 15-16-17-M, scale 1:1,000,000.

**Henderson, J.R. and Broome, H.J.**
1990: Geometry and kinematics of Wager shear zone interpreted from structural fabric and magnetic data; Canadian Journal of Earth Sciences, v. 27, p. 590-604.

**Henderson, J.R., Henderson, M.N., Pryer, L.L., and Creswell, R.G.**
1991a: Geology of the Whitehills-Tehek area, District of Keewatin: an Archean supracrustal belt with iron-formation-hosted gold mineralization in the Central Churchill Province; in Current Research, Part C, Geological Survey of Canada, Paper 91-1C, p. 149- 156.

**Henderson, J.R., Jefferson, C.W., Henderson, M.N., Coe, K. and Derome, I.**
1991b: Geology, Wager Bay region, District of Keewatin, N.W.T. (parts of 46E and 56H), 2 sheets, 1:100,000; Geological Survey of Canada, Open File 2383.

**Heywood, W.W.**
1961: Geological notes, northern District of Keewatin; Geological Survey of Canada, Paper 61-18, 9 p.

**Hulbert, L., Gregoire, C., Pactunc, D., Abbot, G. and Cathro, R.**
1990: Sedimentary hosted nickel-zinc mineralization in the Selwyn Basin, Yukon (abstract); in Program with Abstracts, Minerals Colloquium, Geological Survey of Canada, Ottawa, p. 23.

**Jefferson, C.W., Smith, J.E.M. and Hamilton, S.M.**
1991: Preliminary account of the resource assessment study of proposed national park, Wager Bay - Southampton Island areas, District of Keewatin; Geological Survey of Canada, Open File 2351, 47 p. and pocket map.

**Kerswill, J.A.**
1990: Models for iron formation-hosted gold deposits; in Program with Abstracts, 8th IAGOD Symposium, International Association on the Genesis of Ore Deposits, August 12-18, p. A270.

**Laporte, P.J.**
1974: North of 60 Mineral Industry Report 1969 and 1970, v. 2, N.W.T. East of 104° West Longitude; Indian and Northern Affairs Canada, EGS 1974-1, 191 p.

**LeCheminant, A.N., Roddick, J.C., Tessier, A.C. and Bethune, K.M.**
1987: Geology and U-Pb ages of early Proterozoic calc-alkaline plutons northwest of Wager Bay, District of Keewatin; in Current Research, Part A, Geological Survey of Canada, Paper 87-1A, p. 773-782.

**Parks Canada**
1978: Wager Bay - a natural area of Canadian significance; Parks Canada, 13 p.

**Schau, Mikkel**
1982: Geology of the Prince Albert Group in the parts of Walker Lake and Laughland Lake Map Areas, District of Keewatin; Geological Survey of Canada Bulletin 337, 62 p. and map in pocket.

**Schau, Mikkel and Ashton, K.**
1988: The Archean Prince Albert Group, northeastern Canada; Evidence for crust with extension with a 2.9 G.a. Continent; in Abstracts with Programs, Geological Society of America, p. A50.

**Thomas, R.D.**
1981: Surficial geology, Laughland Lake, District of Keewatin; Geological Survey of Canada, Map 5-1981, scale 1:250,000.

Geological Survey of Canada Project 840003

# Reconnaissance of the stratigraphy and structure of the Basler Lake area, southern Wopmay Orogen, Northwest Territories[1]

**Beverly Z. Saylor[2]**

*Saylor, B.Z. and Grotzinger, J.P., 1992: Reconnaissance of the stratigraphy and structure of the Basler Lake area, southern Wopmay Orogen, Northwest Territories; in Current Research, Part C; Geological Survey of Canada, Paper 92-1C, p. 259-268.*

***Abstract***

*In the Basler Lake area of southern Wopmay Orogen, N.W.T., Early Proterozoic sedimentary rocks of the Snare Group are exposed in a north-trending belt of outcrop with Archean basement on both sides. The Snare Group consists of a siliciclastic sequence that was deposited on a shallow marine shelf, and an upward-shallowing carbonate slope and shelf sequence. Long wavelength basement-involved folds and superimposed shorter wavelength folds within the Snare Group accommodated shortening in the Basler Lake area. The structure of the north is dominated by a tight basement syncline which is split by a wrench fault. In the east arm of the syncline, more than 700 m of Snare Group siliciclastic rocks thin to zero northward in less than 15 km. The thick succession might have been cut-out by a second wrench fault. Alternatively, syn-Snare block faulting and erosion can account for the rapid northward thinning.*

***Résumé***

*Dans la région du lac Basler, dans le sud de l'orogène de Wopmay (T.N.-O.), les roches sédimentaires du groupe de Snare, datées du Protérozoïque précoce, affleurent selon une zone de direction générale nord, bordée de chaque côté par des roches granitiques archéennes. Le Groupe de Snare se compose d'une séquence silicoclastique, qui s'est accumulée le long du littoral dans un milieu marin peu profond, et d'une séquence carbonatée de talus et de plate-forme continentaux, à couches formées dans des profondeurs d'eau progressivement décroissantes vers le haut. Des plis de grande longueur d'onde ayant impliqué le socle, et des plis superposés de plus courte longueur d'onde, dans le Groupe de Snare, ont accommodé le raccourcissement survenu dans la région du lac Basler. La structure du nord se caractérise principalement par un étroit synclinal formé dans le socle et divisé par une faille de décrochement. Du côté est du synclinal, le rapide amincissement en biseau, vers le nord, de plus de 700 m de roches silicoclastiques du groupe de Snare s'est fait sur moins de 15 km. L'épaisse succession peut avoir été découpée par une deuxième faille de décrochement. Autrement, le morcellement par failles et l'érosion contemporains au groupe de Snare auraient causé l'amincissement rapide vers le nord.*

[1] Contribution to the Canada-Government of Northwest Territories Mineral Development Agreement, 1991-96.

[2] Massachusetts Institute of Technology, Cambridge, Massachusetts 02139 U.S.A.

## INTRODUCTION

During 1991 a reconnaissance study of the Basler Lake area in southern Wopmay Orogen, N.W.T. (Fig. 1), was undertaken to evaluate the potential for detailed stratigraphic study of the Proterozoic Snare Group. Traverses were chosen, based on the geologic maps of Ross and McGlynn (1965), and Lord (1942), in order to examine the lateral variation in stratigraphic and structural style. Detailed analysis could be applied to reconstruct the depositional history of the Snare Group, determine its relation to tectono-stratigraphic units of northern Wopmay Orogen, and constrain the structural evolution of southern Wopmay Orogen.

The Proterozoic Snare Group consists of a basal siliciclastic unit and an upper carbonate unit. It is exposed in a band of outcrop which extends from Basler Lake, 100 km northward along the Emile River (Lord, 1942; Ross and McGlynn, 1965). The Snare Group unconformably overlies Archean basement composed of the Yellowknife Supergroup and intrusive granitic rocks. In the Basler Lake area, the band of Snare outcrop is in depositional contact with Archean basement on both its east and west side. Basement and cover rocks were deformed during the Calderian orogeny and possibly the younger Fish River event.

## ARCHEAN BASEMENT ROCKS

Archean basement rocks are widely exposed on both sides of Basler Lake (Fig. 1). The basement consists of granitic plutons intruded into metasedimentary rocks of the Yellowknife Supergroup.

The Yellowknife sedimentary rocks consist of mostly fine grained, quartzofeldspathic sandstone and dark gray argillite, which is regionally metamorphosed to chlorite grade with local development of cordierite and andalusite near granite intrusions (Ross and McGlynn, 1965). Exposures of Yellowknife rocks on the east side of Basler Lake retain some traces of original bedding (fining upward turbidite cycles), but on the west side of the lake, where deformation is more intense, no traces of bedding were found. Rocks of the Yellowknife Supergroup underwent Archean deformation and metamorphism as well as Proterozoic overprinting after deposition of the Snare Group (Ross and McGlynn, 1965). Yellowknife rocks are distinguished from siliciclastic rocks of the Snare Group by their overall finer grain size, higher metamorphic grade, and the common occurrence of pods and stringers of leucogranite and pegmatite.

The granitic rocks are fine- to coarse-grained, often porphyritic or pegmatitic. The granite porphyries commonly contain feldspar phenocrysts, and the pegmatites contain megacrysts of quartz, feldspar, and muscovite. The granitic rocks intrude the Yellowknife rocks but are unconformably overlain by siliciclastic rocks of the Snare Group (Ross and McGlynn, 1965). Depositional contacts between the Snare Group and the granitic basement are exposed on both the east and west side of Basler Lake (Fig. 2).

## SNARE GROUP

The Proterozoic Snare Group consists of a siliciclastic (Unit 5 of Lord, 1942) and overlying carbonate (Unit 6 of Lord, 1942) succession deposited on the granitic and

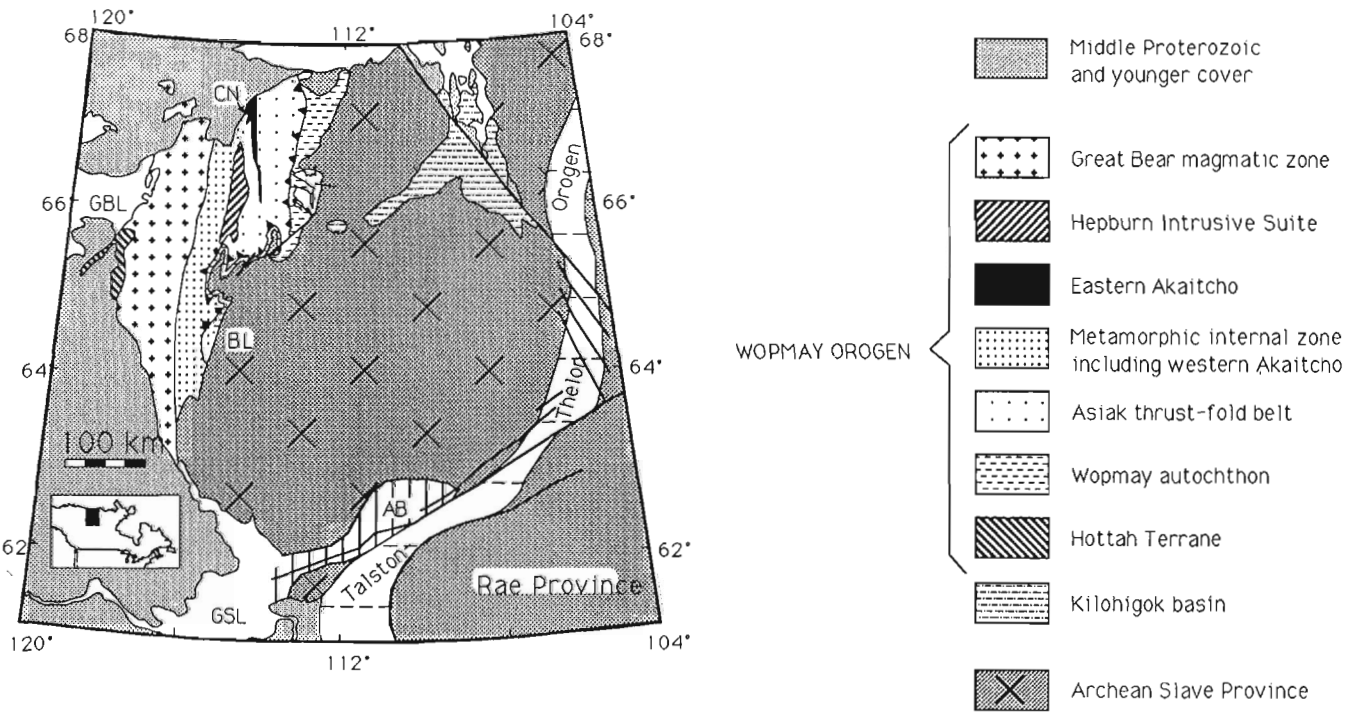


**Figure 1.** Simplified tectonic map of the northwestern Canadian Shield showing the location of Basler Lake relative to major elements of the early Proterozoic Wopmay Orogen. BL-Basler Lake; GBL-Great Bear Lake; GSL-Great Slave Lake; CN-Cloos Nappe (From Bowring and Grotzinger, in press).

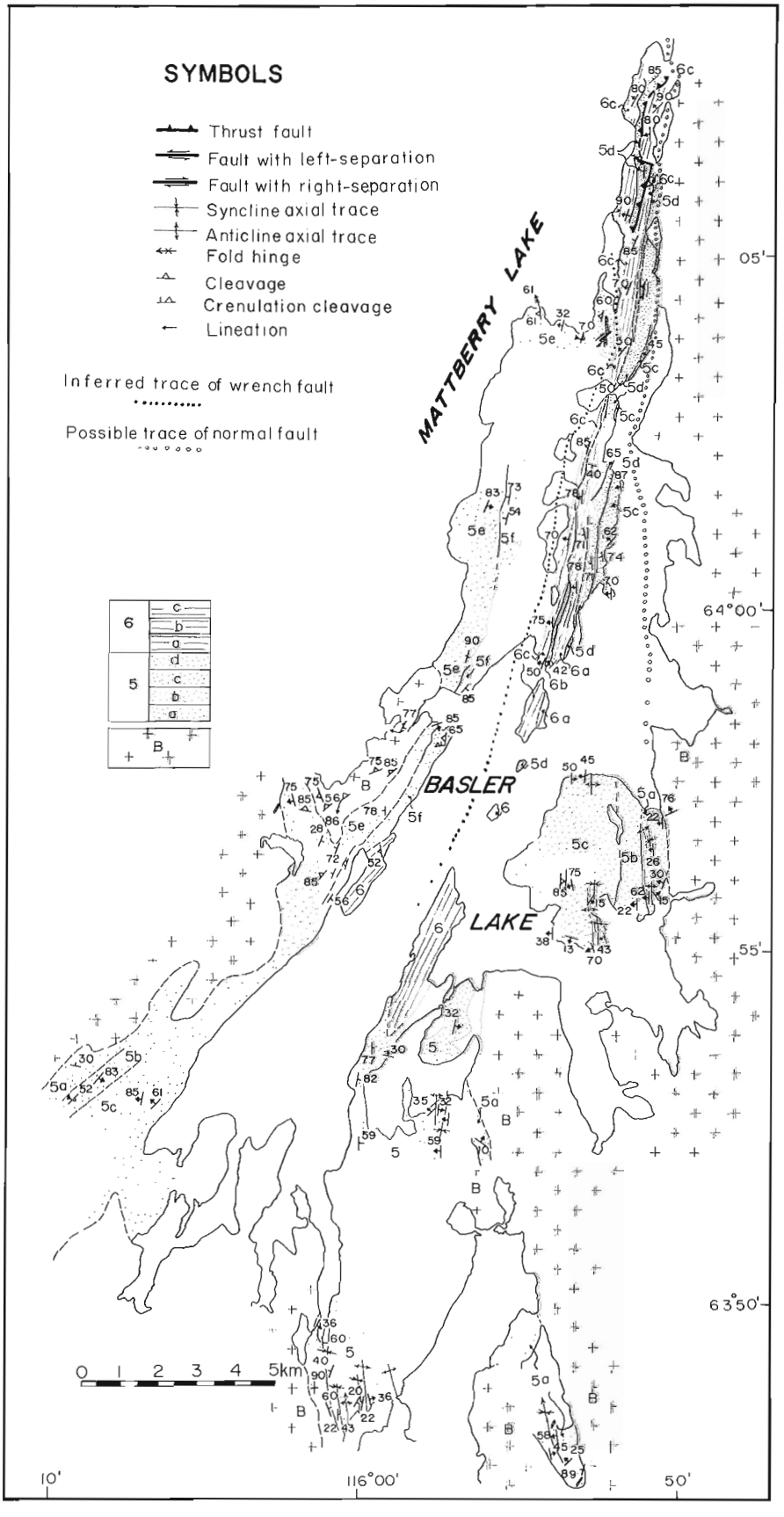


**Figure 2.** Preliminary geologic map of the Basler Lake area. Rock units are described in the text and in Figure 3.

metasedimentary basement rocks (Fig. 3). The siliciclastic rocks of the Snare Group crop out along the southern, eastern, and western margins of Basler Lake, but the carbonate rocks are restricted to a band in the northern half of the lake (Fig. 2). On both the east and west sides of the band of carbonate rocks, depositional contacts between Snare Group siliciclastic rocks and the basement rocks are exposed. A lag conglomerate, composed of centimetre-scale clasts of the basement rock, is characteristic of the contact.

### *Siliciclastic sequence (Unit 5)*

The siliciclastic portion of the Snare Group is composed predominantly of medium- to coarse-grained sandstone with subordinate mudstone, siltstone, and carbonate. Lithology and thickness vary significantly from north to south and east to west in the Basler Lake area. On the east and west sides of the carbonate band, dominantly trough cross-stratified sandstone and subordinate carbonate compose the lower half of Unit 5. However, the upper half of the unit consists dominantly of wavy and plane parallel laminated sandstone on the east side, and dark gray, fine grained argillite on the west side. In the east, Unit 5 thins to zero northward, so that at the northern tip of Basler Lake, the carbonate rocks are in covered contact with Yellowknife basement. Unfortunately, because of tight folding and covered intervals, it is not possible to walk out the lateral changes.

In the central part of Basler Lake, the siliciclastic sequence is almost complete and deformation relatively minimal permitting more detailed stratigraphic and sedimentalogic analysis. There Unit 5 is at least 700 m thick (Fig. 3) and consists of a basal argillite, overlain by trough cross-stratified sandstone, which grades upward into a mixed siliciclastic and carbonate unit. Dolarenite becomes increasingly important in the uppermost part of Unit 5, and a karstic breccia is developed at the top.

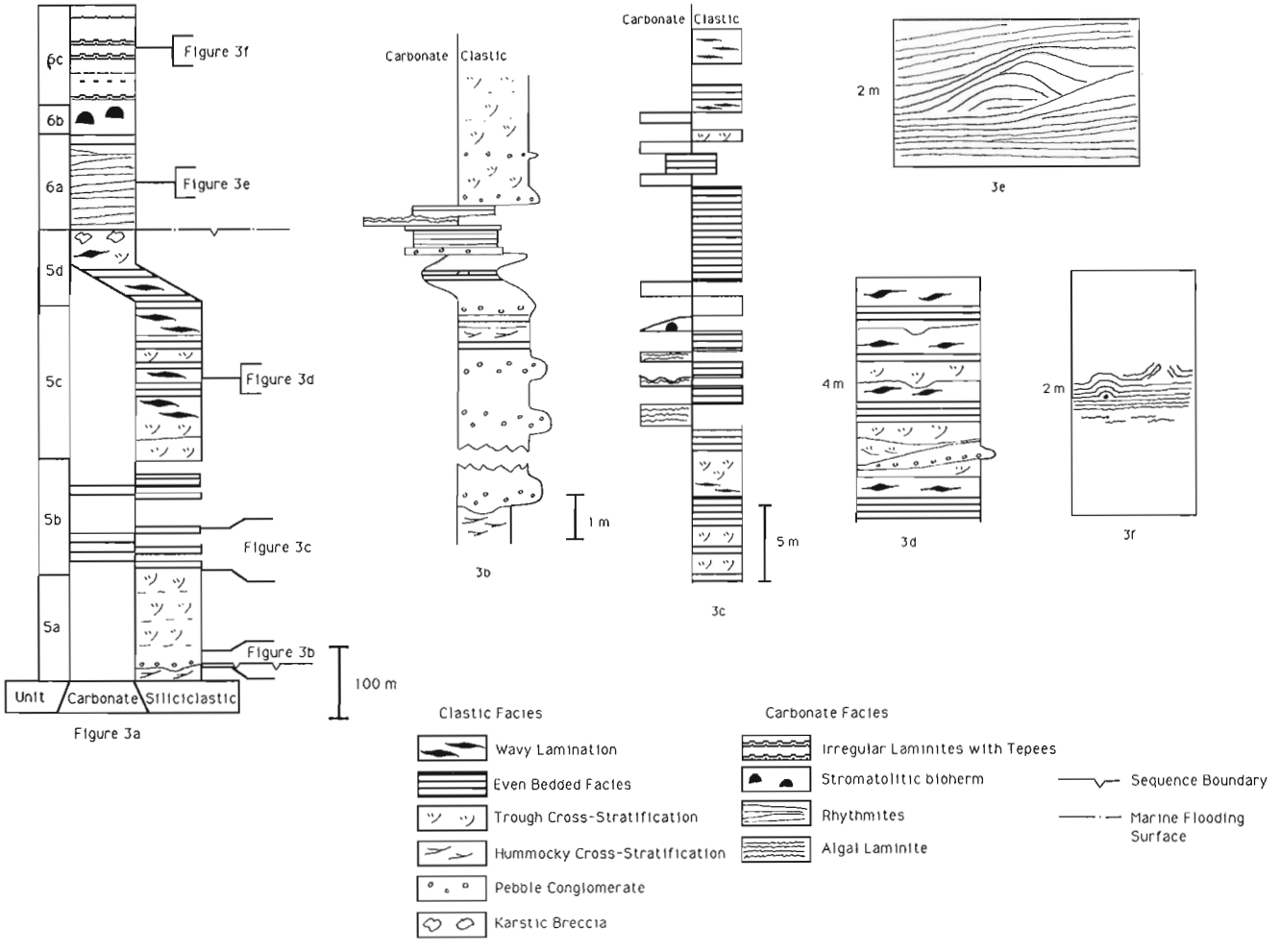


**Figure 3.** Simplified, composite stratigraphic column and sketches of sedimentary facies in the Snare Group on the east side of Basler Lake.

## Unit 5a

*Basal argillite*

The base of Unit 5a is characterized by several metres of thinly laminated, dark gray argillite and hummocky cross-stratified, fine grained sandstone. The top is scoured and is overlain by coarse pebble conglomerate.

The basal argillite is marine in origin and is the deepest water facies of Unit 5. It is separated from overlying pebble conglomerate and trough cross-stratified sandstone by a sequence boundary.

*Trough cross-stratified sandstone*

Approximately 15 m of interbedded pebbly and medium coarse-grained sandstone overlie the basal argillite. The pebbly sandstone, in turn, is overlain by approximately 10 m of thinly interbedded (tens of centimetres) planar stratified quartz and dolarenite, stromatolitic dolomite, and possible hummocky cross-stratified sandstone (Fig. 3b). This mixed interval grades vertically into a 100 m thick interval of dominantly trough cross-stratified sandstone.

The basal pebble conglomerate contains subrounded to subangular centimetre scale clasts of quartz and subordinate feldspar in a medium coarse-grained matrix. The planar stratified arenites are medium coarse-grained and often contain vertically aligned intraclasts.The trough cross-stratified sandstone consists of amalgamated stacks of 7-15 cm thick sets of cross-strata. Millimetre scale mud drapes form partings every few metres. Wave ripples are preserved below the mud drapes.

The basal interbedded pebble conglomerate and sandstone is probably fluvial in origin. Marine flooding is recorded by the development of hummocky and planar cross-stratified sandstone and stromatolitic dolomite. The thick succession of wave rippled, trough cross-stratified sandstone may record wave-washed fluvial and deltaic sedimentation.

## Unit 5b

*Mixed siliciclastic-carbonate facies*

At least 75 metres of mixed siliciclastic and carbonate rocks occur above the trough cross-stratified unit. This mixed unit is composed of intervals of interstratified dolomite and sandstone that alternate with intervals of amalgamated trough cross-stratified sandstone.The trough cross-stratified sandstone intervals are several to tens of metres thick. The sandstone-dolomite packages are also tens of metres thick and contain metre-scale interbeds of pure dolomite and even bedded sandstone (Fig. 3c).

Dolomite beds range from 10 to 50 centimetres in thickness and contain both clastic and algal lamination. The clastic dolomite beds consist of finely laminated dolomite mud and silt. The algal dolomite beds are sometimes composed of small stromatolite bioherms and pinch out laterally. The dolomite beds often contain rip up clasts of sandstone and have scoured tops.

The even-bedded sandstone consists of thin, plane parallel bedded, medium- to coarse-grained sandstone. Individual beds, 1 to 3 cm thick, occur in sets 10 to 100 cm thick. Often the even-bedded sandstone is carbonate cemented, causing ridgy weathering.

The mixed siliciclastic and carbonate rocks are interpreted as tidal flat deposits. The trough cross-stratified sandstone intervals may have been deposited by delta lobes migrating onto the tidal flat, possibly during times of increased siliciclastic sourcing, or lowered sea level.

## Unit 5c

*Wavy and planar laminated sandstone*

In the upper half of the siliciclastic sequence, trough cross-stratified sandstone, although still present, is less common and smaller in scale than in the lower half. Even-bedded sandstone and wavy- to flaser-bedded sandstone/mudstone are more important. The three facies are interbedded on a metre scale (Fig. 3d). The upper contact of the wavy bedded sandstone/mudstone is usually sharp and often scoured. Mud cracks are common. Rip up clasts of mudstone from the wavy bedded facies are incorporated in the overlying sandstone. Transitions between trough cross-stratified and even-bedded sandstone and the bases of the wavy bedded sandstone/mudstone are usually more gradational.

Unit 5c is also interpreted as tidal flat deposits. It probably originated in slightly deeper water than unit 5b so that thick intervals of fluvial or deltaic trough cross-stratified sand were not deposited.

## Unit 5d

*Dolarenite unit*

The uppermost part of Unit 5 contains increasing amounts of carbonate cement and dolarenite. Locally, dolarenite is interbedded with quartz arenite or with argillite. The grain size, composition, and sedimentary structures of the dolarenites are similar to those of the quartz arenites. Trough cross-stratified, even bedded and wavy bedded facies are all developed.

The similarity of sedimentary facies between the dolarenites and the underlying quartz arenites suggest similar depositional environments, i.e., tidal flat. The increase in the carbonate content may record a change in the sediment source. Alternatively, as has been suggested by Grotzinger et al. (1987) for a similar transition in Rifle Formation, it could record early carbonate cementation during progressive subaerial exposure.

*Karstic breccia*

The top of the dolarenite is fractured into metre-scale blocks which remain approximately in place, and smaller blocks which appear to have been ripped up and transported. Pure carbonate mud infills the cracks between, and forms the matrix around, the sandstone blocks. Locally, the breccia is as much as 15 or 20 m thick. In southern exposures, the breccia is overlain directly by rhythmites of the carbonate sequence. In northern exposures however, quartz arenite lies depositionally between the breccia and the rhythmites.

The breccia is interpreted as a karstic surface which developed during prolonged subaerial exposure. It marks a sequence boundary. Where it is overlain by deeper water carbonate rhythmites the sequence boundary corresponds to a flooding surface.

### Units 4e and 4f (western side of Basler Lake only)

Siliciclastic rocks in the west are too deformed for detailed sedimentalogic study. Dominantly trough cross-stratified sandstone with minor dolomite grades upward into dominantly fine grained sandstone and argillite. The trough cross-stratified sandstone is probably correlative with trough cross-stratified fluvial and shallow marine deposits on the east. The overlying argillite is probably the basinward equivalent of the eastern tidal flat deposits.

## UNIT 5: CARBONATE SEQUENCE

Three units were broken out of the carbonate sequence. These are a basal rhythmite unit, a middle stromatolitic bioherm unit, and an upper irregularly laminated unit with tepee structures. The carbonate sequence is approximately 300 metres thick in its southern exposures. Like the siliciclastic sequence, it thins toward the north.

### Unit 6a

*Rhythmites*

Rhythmites form the lowest unit of the carbonate sequence. In southern exposures the rhythmite unit is composed of pure dolomite mud, and the contact with the underlying karstic breccia is abrupt. In the north however, the transition is gradational. Quartz sandstone lies between the breccia and the rhythmites; there is a significant sand component in the rhythmites which decreases upward. Also northward, the rhythmite unit thins and stratigraphically pinches-out.

The rhythmites consist of buff to gray, thickly laminated dolomite mudstone. Slump folds developed in the rhythmites vary from several centimetres to a metre across and display low angle truncation surfaces (Fig. 3e).

Similar rhythmites have been described in slope deposits of the Rocknest carbonate platform (Grotzinger, 1986a, b). They were interpreted as carbonate ooze derived from the shelf margin. The slump folds and truncation surfaces developed during slope failure. A similar interpretation is proposed here for the origin of the rhythmite unit of the Snare Group.

### Unit 5b

*Stromatolitic bioherms*

Stromatolite mounds are commonly found above the rhythmite unit. In the south, the transition from rhythmites to stromatolites is gradational. The rhythmites become less well developed and more convoluted upward. The chert content, which appears to have formed along algal laminae, also increases upward. Small stromatolites are superimposed on silicified algal laminae. In the north, the rhythmite unit is missing and the stromatolite unit is in sharp depositional contact with carbonate cemented sandstone of the siliciclastic sequence.

The stromatolites occur in a fairly laterally continuous biostromes that are 10 to 30 metres thick. Stromatolites vary from 6 centimetres to 1.5 metres across and have 4 to 60 cm of synoptic relief. The larger stromatolites occur in the northern exposures.

The stromatolitic bioherms are interpreted as shallow reef complexes that developed on a carbonate ramp. The reefs prograded over the deeper water rhythmites.

### Unit 5c

*Irregularly laminated, cherty dolomite*

The upper unit of the carbonate sequence consists of 1 to 3 m thick sets of massive dolomite mudstone capped by irregularly laminated cherty dolomite. It is the most ubiquitous of the carbonate units. At the northern tip of Basler Lake, where neither the rhythmites nor the stromatolitic bioherms are developed, irregular laminates lie depositionally on carbonate cemented sandstone of the siliciclastic sequence.

The massive dolomite mud infills irregularities in the surface of the laminated dolomite. The laminations are generally subparallel but undulatory. Laminae drape over and magnify irregularities in underlying laminae to form small convexities. The convexities range from 3 to 15 centimetres across. They occur individually and in chains, and although usually concentric, they can be asymmetric. The laminae occasionally contain mud chips and are broken by tepee structures.

The evenly draped laminations, which produce convexities and are broken by tepee structures, are interpreted as the product of constant, fine carbonate precipitation in a restricted shallow water environment. They are similar to incipient tufas of the Rocknest Platform (Grotzinger, 1986a, b) and probably record the shallowest water environment of the carbonate sequence. The massive mud bases may record episodic input of carbonate mud by storms or during sea level rise.

### *Depositional environment and history*

The Snare Group was deposited on a shallow, open marine shelf (Fig. 4). The deepest water siliciclastic facies occurs at the base of the unit and is separated by a sequence boundary from overlying, fluvial, pebble conglomerate and sandstone. The sequence may deepen gradually upward from dominantly fluvial to dominantly tidal flat deposits in the east and deeper water argillites in the west. The top of the sequence was subaerially exposed and a karstic breccia developed. After subaerial exposure and subsequent flooding, siliciclastic input to the area recurred for a brief interval to form a south-tapering wedge. Carbonate rhythmites on-lapped the clastic sediments along a flooding surface. Stromatolitic reefs and the overlying peritidal, irregularly laminates prograded across the slope rhythmites.

## STRUCTURE

### *Northern Basler Lake*

The structure of the northern half of Basler Lake is dominated by what is interpreted as a single basement involved syncline (Fig. 2). The axis of the syncline trends approximately north-south and plunges gently to the north. Sedimentary contacts between granitic basement and Snare Group siliciclastic rocks are exposed in both the eastern and western limbs of the syncline. The Snare Group carbonate rocks are confined mostly to the eastern limb. There is an abrupt change in structural style between the eastern and western limbs of the syncline such that the two limbs define distinct structural domains.

The eastern limb of the syncline contains the complete section of the Snare Group. The Unit 5 siliciclastic rocks are openly folded on north-trending, generally shallowly plunging axes. The axial planes are near vertical. The carbonate rocks are homoclinal and dip steeply.

Snare siliciclastic rocks in the western limb of the syncline are isoclinally folded. Cleavage and bedding in the Snare siliciclastic rocks are near vertical and subparallel, and are also subparallel to cleavage in the Yellowknife and granitic basement (Fig. 5). Snare carbonate rocks occur only in the southernmost part of the western limb.

A fault is inferred to account for the juxtaposition of the different structural styles in the east and west arms of the syncline, and the cut-out of carbonate rocks in the northern part of western arm (Fig. 1, 6a). Steep cleavage and down-dip lineations in the quartzites of the western arm are consistent a steep dip. The throw on the fault must be at least 300 metres, enough to place siliciclastic rocks of the western limb on carbonate rocks of the eastern limb. Throw decreases towards the south and eventually reverses direction, exposing intensely deformed carbonate rocks in the southern part of the western limb (Fig. 6b). Thus, the syncline is split by a wrench fault which accommodated differential compression from north to south.

Reverse faults, that are subparallel to steep bedding, are developed in the eastern limb of the syncline (Fig. 2). They repeat the Unit 5-Unit 6 contact. Because the hanging wall of the synclinal wrench fault is much more intensely deformed than the hanging walls of the east arm reverse faults, the wrench fault is inferred to pass to the west of the reverse faults. However, the reverse faults are subparallel to, and may

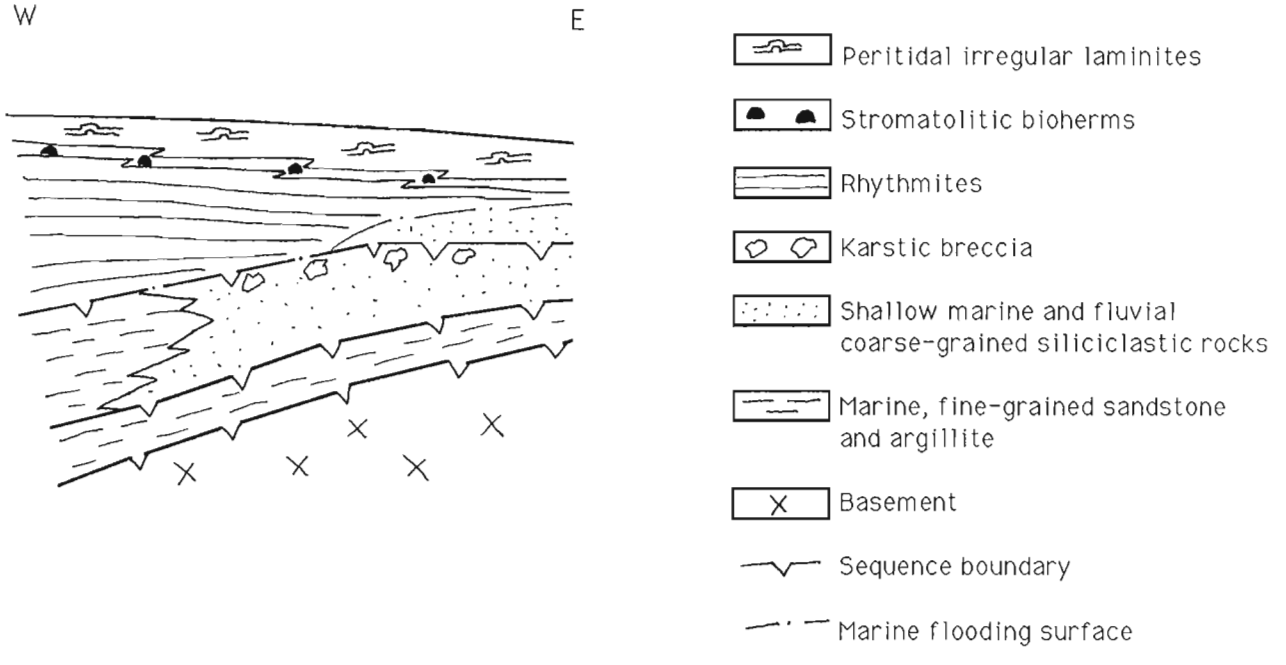


**Figure 4.** Possible cross-section of Snare Group shelf stratigraphy. Not to scale.

be coeval with, the wrench fault. Alternatively, the reverse could have originated as low angle thrust faults and been rotated to steeper dips during formation of the syncline.

### *Southern Basler Lake*

Although detailed mapping of southern Basler Lake has not been completed, preliminary investigations indicate that the structural style is different from that of the north. Rather than a single, tightly folded and wrench-faulted syncline, several open folds produce a gently undulatory basement-cover contact. No reverse faults were found. As in the north, shorter wavelength folds in the siliciclastic cover are superimposed on the basement folds. The east to west structural change from open to isoclinal folds also occurs, but is more gradual.

## DISCUSSION

Structure and stratigraphy vary from south to north in the Basler Lake area. More than 700 m of siliciclastic sediment in the east arm of the syncline thin to zero in less than 15 km. The rapid cut out of the thick Snare siliciclastic rocks corresponds to a thinning of the carbonate sequence, and a northward change in structural style from a gently undulating basement-cover contact to the single, tightly folded, wrench-faulted syncline.

The change in structural style may be the result of rheologic differences arising from the northward change in basement-cover contact. Without the thick siliciclastic sequence, the basement-cover contact could be more tightly folded. These rheologic difference could cause differential compression along the syncline and subsequent wrench faulting. Alternatively, the structural change could reflect the southward exposure of deeper structural levels of the fold-belt.

Structural cut-out of the siliciclastic rocks by a normal fault has been suggested by Helmstedt (unpublished report) to explain relations between carbonate and basement rocks just north of the map area. This normal fault might truncate the eastern side of the syncline and thus account for both the cut-out of the siliciclastic rocks in the east arm and the continued thickness of siliciclastic sediments in the west arm (Fig. 7a). The normal fault would strike approximately north, and would dip steeply to the west. Greater amounts of the siliciclastic sequence would be exposed toward the south where throw on the normal fault decreases (Fig. 7b, c).

The normal fault maight be coeval with the wrench fault which splits the syncline and reverse fault within the east arm of the syncline. These faults are subparallel to each other and show a similar southward decrease in throw.

Another possible explanation for the rapid northward thinning of the siliciclastic rocks is syn-Snare block faulting and erosion. Snare siliciclastic rocks could have been eroded prior to deposition of the carbonate rocks. One possible scenario is presented in Figure 8. After block faulting, the siliciclastic rocks on the uplifted block could have been completely eroded, while those on the down dropped block were not. Siliciclastic rocks in the hanging wall that lie

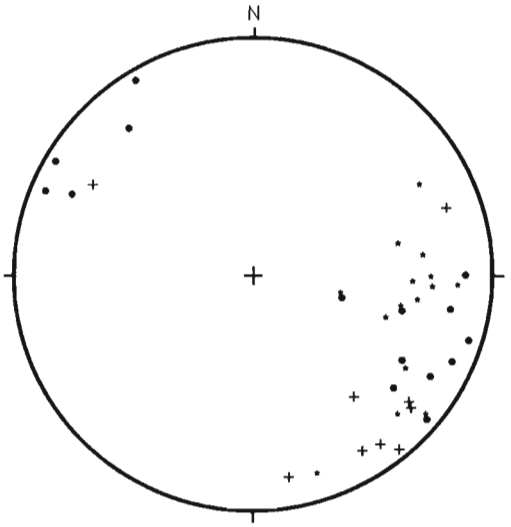


**Figure 5.** Bedding and cleavage relationships in the Snare Group and cleavage in the basement plotted on and equal area stereonet. Note steep, subparallel dips of bedding and cleavage.

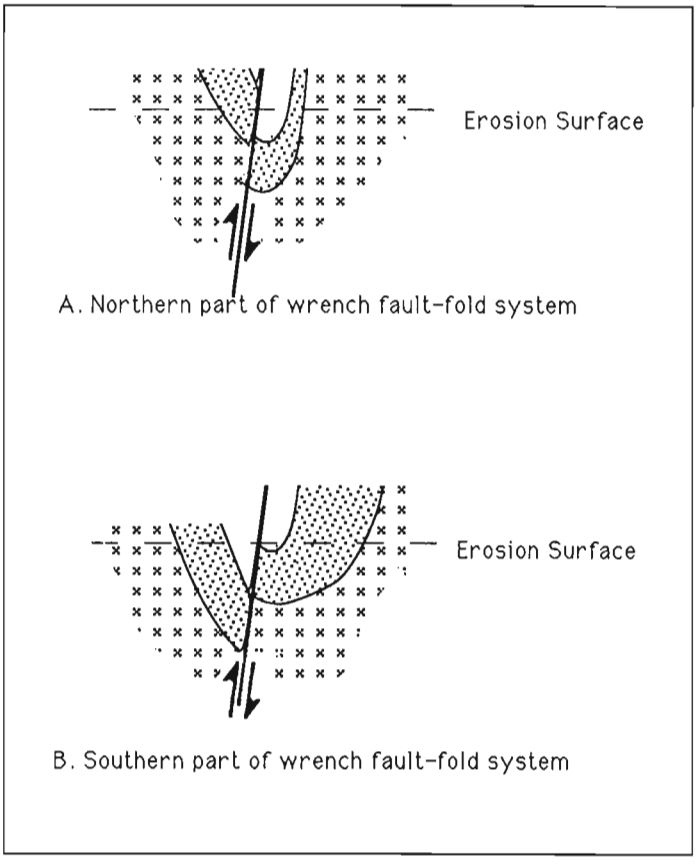


**Figure 6.** Scematic diagram of the wrench fault-fold system which dominates the structure of northern Basler Lake.

depositionally above the karstic breccia and below the rhythmites may have been sourced from the eroding, uplifted footwall block. After flooding, the rhythmites pinched out against uplifted block, but the shallow water carbonates prograded over it.

At the south end of the Emile River belt at Snively Lake, a breccia which is composed of clasts of dolarenite and is similar to the Basler Lake breccia, is found in contact with basaltic rocks. According to the map of Ross and McGlynn (1965) basalts are also found interbedded with carbonate rocks just south of Basler Lake. Basaltic eruptions are commonly associated with block faulting during rifting and may be consistent with the hypothesis of syn-Snare block-faulting.

In addition, at Cloos Nappe in the northern part of Wopmay Orogen (Fig. 1), arkosic grit, mafic volcanic rocks and stromatolitic dolomite are thought to stratigraphically underlie the Epworth Group (Bowring and Grotzinger, in press; Hoffman and Pelletier, 1982). The rocks at Cloos Nappe are thought to be a possible rift sequence (Mellville Group) for the development of the passive margin represented by the Epworth Group. The presence of quartz sand in the carbonates, the associated mafic volcanic and carbonate rocks, and possible evidence for syn-Snare block faulting suggest that the Snare Group is a rift sequence that is correlative with the Melville Group rather than the Epworth Group passive margin sediments.

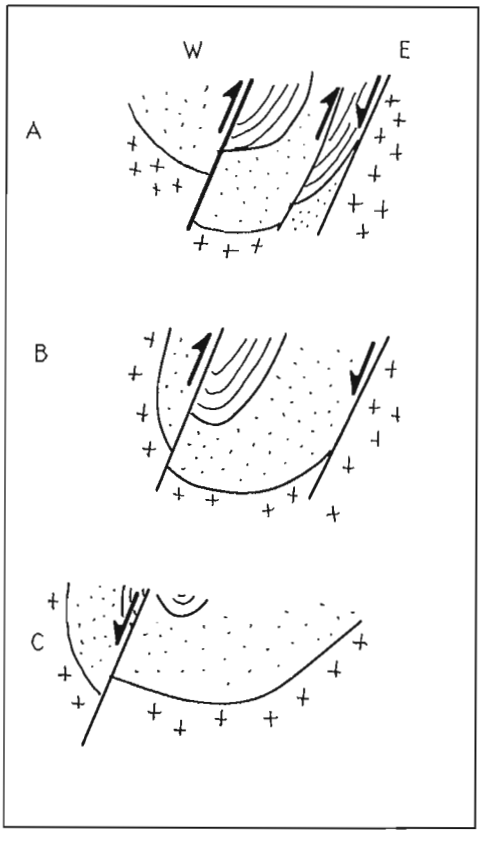


**Figure 7.** **A**) Possible cross-section of the northern tip of Basler Lake showing post-Snare structural cut-out of the Snare siliciclastic rocks. 7**B**) and **C**) show progressively smaller smaller and possible reversal of offset toward the south. Crosses are basement, stipples are siliciclastic rocks, and lines are carbonates.

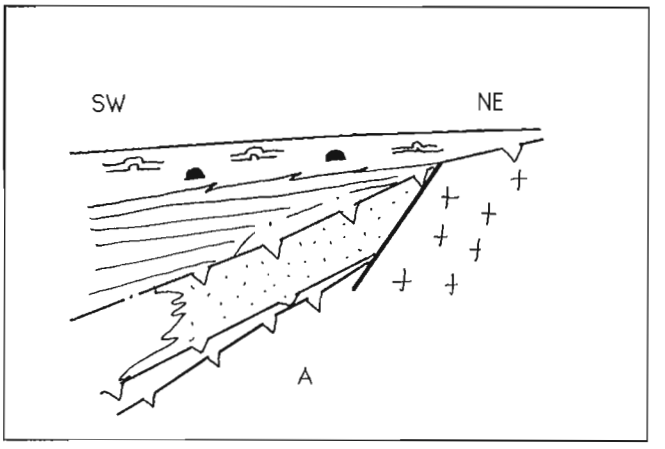


**Figure 8.** Possible cross-section of the Snare Group shelf showing syn-Snare block-faulting and erosional cut out of the Snare siliciclastic rocks. Same symbols as Figure 4.

## CONCLUSIONS

In the Basler Lake area of southern Wopmay Orogen, Early Proterozoic sedimentary rocks of the Snare Group are exposed in a north-trending band, bordered on the east and west sides by Archean granitic and metasedimentary basement rocks. The granitic rocks intrude the Yellowknife metasedimentary rocks, but are unconformably overlain by the Snare Group.

Study of the Snare Group shows that it consists of a siliciclastic succession that was deposited on a shallow marine shoreline. A sequence boundary and marine flooding surface separates the siliciclastic sequence from overlying shoaling upward carbonate platform rocks.

Long wavelength basement involved folds and superimposed high frequency folds within the Snare Group siliciclastic rocks accommodated compression in the Basler Lake area. The structure of the northern end of the Basler Lake is dominated by a tight, basement involved syncline. A wrench fault splits the fold. At the southern end of Basler Lake, the basement folds are more gentle than in the north, and the basement-cover contact undulates.

From south to north in the Basler Lake area more than 700 metres of Snare siliciclastic rocks thin to zero in less than 15 km. The rapid thinning may be the result of structural cut-out by a series of wrench faults developed at the northern tip of Basler Lake. Block faulting and erosion of the siliciclastic rocks prior to the deposition of the carbonate rocks provides an alternative interpretation. Given the lithologic similarities syn-Snare block-faulting and volcanism, the Snare Group might be interpreted as a rift sequence equivalent to lithologically similar rocks underlying the Epworth Group at Cloos Nappe.

## ACKNOWLEDGMENTS

This research was supported in part by a grant from the Geological Society of Canada and a Mineral Development Agreement contract awarded to Paul Hoffman. Bill Padgham and Sam Bowring provided additional logistical support. I would like to thank Paul Hoffman, Sam Bowring and John Grotzinger for valuable discussions and John Grotzinger for reviewing the manuscript.

## REFERENCES

**Bowring, S.A. and Grotzinger, J.P.**
in press: Implications of new chronostratigraphy for tectonic evolution of Wopmay Orogen, northwest Canadian Shield; American Journal of Science.

**Grotzinger, J.P.**
1986a: Cyclicity and paleoenvironmental dynamics, Rocknest platform, northwest Canada; Geological Society of America Bulletin, 97, p. 1208-1231.

1986b: Evolution of early Proterozoic passive-margin carbonate platform: Rocknest Formation, Wopmay Orogen, N.W.T., Canada; Journal Sedimentary Petrology, 56, p. 831-847.

**Grotzinger, J.P., McCormick, D.S., and Pelechaty, S.M.**
1987: Progress report on the stratigraphy, sedimentology, and significance of the Kimerot and Bear Creek groups, Kilohigok Basin, District of Mackenzie; in Current Research, Part A; Geological Survey of Canada, Paper 87-1A, p. 219-238.

**Hoffman, P.F. and Pelletier, K.S.**
1982: Cloos Nappe in Wopmay Orogen: significance for stratigraphy and structure of the Akaitcho Group, and implications for opening and closing of an early Proterozoic continental margin; in Current Research, Part A; Geological Survey of Canada, Paper 82-1A, p. 109-115.

**Lord, C.S.**
1942: Snare River and Ingray Lake map-areas, N.W.T.; Geological Survey of Canada, Memoir 235.

**Ross, J.V. and McGlynn, J.C.**
1965: Snare-Yellowknife relations, District of MacKenzie, N.W.T.; Canadian Journal of Earth Science, v. 2, p. 118-130.

Geological Survey of Canada Project 810021

# Patterned ground on lake shores in northeastern Abitibi, Quebec

**J.J. Veillette and C.L. Prévost[1]**
**Terrain Sciences Division**

*Veillette, J.J. and Prévost, C.L., 1992: Patterned ground on lake shores in northeastern Abitibi, Quebec; in Current Research, Part C; Geological Survey of Canada, Paper 92-1C, p. 269-275.*

***Abstract***

*Patterned ground consisting of mudboils and large and small polygons was observed at three locations on the shores of Lac Olga and Lac aux Goélands, in late summer 1990 and 1991. Patterned ground in subarctic Québec found under similar site specific conditions suggests that the features at both locations may have developed in a nonpermafrost environment or, less likely, represent relict permafrost. Features at a site on Lac Olga, interpreted as beach cusps by an earlier investigator, were found to be partially submerged polygons.*

***Résumé***

*Des cryosols comprenant des polygones de petite et de grande taille et des ostioles ont été découverts à la fin des étés 1990 et 1991, sur les rivages des lacs Olga et aux Goélands. Ces formes, comparées à d'autres du Québec subarctique présentant des caractéristiques de terrain semblables à celles de l'Abitibi, se sont probablement développées dans un environnement sans pergélisol. Il est aussi possible, bien que moins probable, que ces formes représentent du pergélisol fossile. Une ligne de rivage de forme inusitée (en forme de corne) du lac Olga, dont la formation avait été attribuée à l'action érosive des vagues lors de recherches précédant celles-ci, n'est en fait qu'un réseau de polygones partiellement submergés.*

[1] Canadian Museum of Nature, 1505 Laperrière, Ottawa, Ontario K1Z 7T1

## INTRODUCTION

Patterned ground consisting of polygons and mudboils was observed at three locations on the shores of Lac aux Goélands and Lac Olga in northeastern Abitibi (Fig.1), during late summer in 1990 and 1991. Patterned ground developed on lake shores and bottoms is widespread in subarctic regions (north of 54° N) of central Québec (Dionne, 1974), but had not been reported south of 50°N in Abitibi. Our observations, added to possible evidences of fossil and/or active patterned ground reported in recent years in other parts of southern Abitibi, raise the question of the processes involved in the formation of these features. Are they relict features of widespread or scattered permafrost in Abitibi formed some time following the retreat of Lake Ojibway about 8000 years ago or are they the product of seasonal freeze and thaw cycles at specific sites with favourable conditions? This note presents an overview of the literature pertaining to patterned ground in the Abitibi area and a brief description of the features under investigation. An attempt is made to assess their reliability as former permafrost indicators in Abitibi. Abitibi here refers to the general area bounded by latitude 48°N and 50°N and longitude 76°W and 80°W (Fig.1).

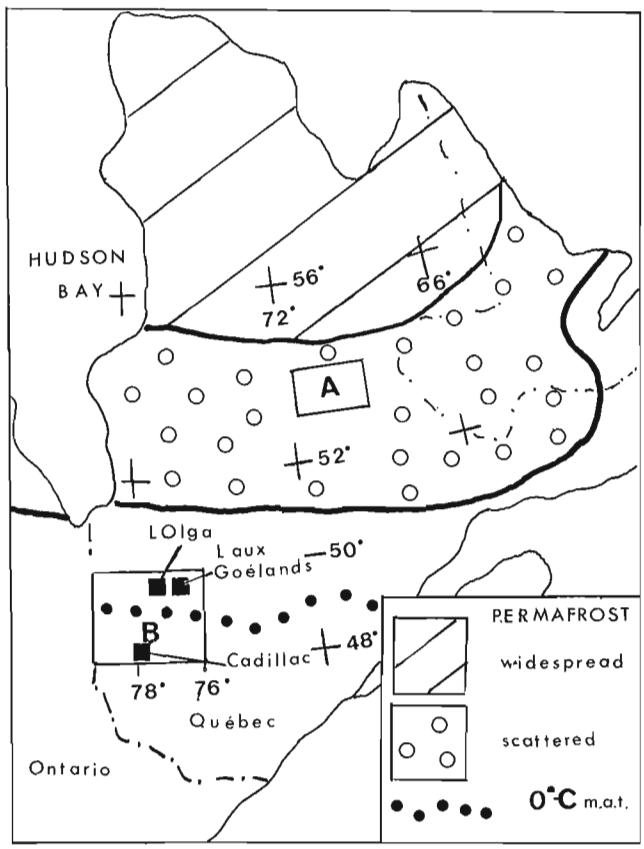


**Figure 1.** Distribution of permafrost in Québec (adapted from The National Atlas of Canada, 1973) and generalized location of (**A**) lakeshore patterned ground described by Dionne (1974) in subarctic regions and (**B**) the Lac Olga and Lac aux Goélands and the Cadillac (Brown and Gangloff, 1980) areas. The 0°C mean annual temperature isotherm is from Wilson (1971).

## PREVIOUS WORK

Clear evidence for widespread former periglacial conditions south of 50°N is lacking in Abitibi. Hamelin (1958), considered *les cours d'eau à berges festonnées,* in some brooks along Bell river of northeastern Abitibi, to be a bankform possibly inherited from the presence of ground ice lenses some time in the past. Dionne(1978) felt, however, that other factors such as flooding can produce similar forms since cuspate banks are all located along meandering streams where flooding occurs both from natural and artificial causes. Lagarec (1973), from airphoto analysis, attributed a postglacial permafrost origin to polygonal patterns observed in bogs filling former lake basins, and to some meanders thought to represent streams flowing along polygon trenches. He also considered cuspate-banked rivers and beaded streams with closely spaced small ponds in alluvial sediment as evidence of former periglacial conditions. The first detailed field work on patterned ground in Abitibi is from Brown and Gangloff (1980) who reported features considered to be evidence of fossil, as well as active, patterned ground in the vicinity of Cadillac in southern Abitibi, just north of 48°N (Fig.1). They assumed that permafrost could once have been widespread in Abitibi following the retreat of Lake Ojibway on the basis that some of the stone circles found in their study area had a diameter greater than 2 m. Features of such dimensions require a permafrost environment to develop (Goldthwait, 1976), and a mean annual temperature somewhere between -2°C to -10°C, depending on local conditions, to initiate cracking (Washburn, 1985). String bogs, also characteristic of subarctic regions, are relatively abundant in northern Abitibi and are also present south of 49°N in several other parts of Québec and even south of 47°N in Cape Breton (Dionne, 1978). String bogs are well developed at a few locations in upper (south of 48°N) Témiscamingue (Veillette, 1990).

Surficial geology mapping programs involving airphoto interpretation at 1:40 000 scale and systematic field inspection of hundreds of borrow pits, roadcuts, and natural exposures along lakes and rivers conducted in recent years in Témiscamingue and Abitibi by the senior author and other GSC and MERQ mappers in the last twenty years have failed to reveal satisfactory indicators of former widespread periglacial activity. But in central subarctic Québec (Fig.1), Dionne (1974) reported well developed patterned ground in the Lac Le Grand area, nearly 4° latitude north of the area discussed here, on gently sloping shores and on lake bottoms with a thick mantle of till. Although the distance between the two areas is considerable, Dionne described site characteristics similar to those reported in this note.

## LOCATION AND SITE DESCRIPTION OF SMALL POLYGONS AND MUDBOILS

Small polygons were observed at one location on the shores of Lac aux Goélands in 1990 and mudboils were observed at one location on the shores of Lac Olga in 1991.

### *Lac aux Goélands site*

This site was the object of a brief visit in mid-August 1990. It is located at the northeast point of an island exposed to the north winds over a stretch of several kilometers of open water (Fig. 2 site A). The island consists of till in excess of 2 m thick masked by glaciolacustrine clays, except on its periphery where it has been eroded by wave action. Several de Geer moraines, apparently composed of bouldery till, protrude through the clays. The patterned ground of Lac aux Goélands consists of a patch, only a few tens of square metres of small polygons 2-4 m in diameter covered with a carapace of cobbles and coarse gravel and separated by oversized (15-30 cm deep) troughs. The polygons were partially submerged even at low water level. Their surfaces had been considerably levelled by seasonal ice and ice-pushed debris which are particularly abundant at the site. Due to high waves and rain at the time of the visit, photographs could not be taken.

### *Lac Olga site*

The Lac Olga mudboils are located at the eastern tip of a peninsula on the west shores of Lac Olga (Fig. 2 site B ). The site was visited in mid-August 1991 at a time of exceptionally low lake levels. The features occupy a nearly flat surface in till, slightly above lake level but well below the high water line, and would be covered by water in a normal year (Fig. 3A). The absence of vegetation in mid-August indicates that the period of subaerial exposure was limited to late summer. Rock outcrops in the vicinity suggest that the mudboils occur in till pockets resting on bedrock at shallow depth. About twelve roughly circular or elongated mudboils with long diameters varying between 1 and 5 m were found within an area of about 1000 $m^2$ (Fig. 3B). A test pit dug in one of the mudboils showed a pebbly mud in the centre containing both subrounded and angular pebbles of different lithologies with a mean diameter less than 3 cm. The surface of the feature was essentially flat, its central portion covered with scattered small pebbles, and the periphery with cobbles and small boulders generaly less than 20 cm in diameter. A few centimetres underneath this cobbly ring the till matrix consists of silty sand with little fines.

## THE LAC OLGA POLYGONS, LOCATION AND DESCRIPTION

The polygons occupy the gently sloping eastern shores of Lac Olga near the mouth of Waswanipi River, in a shallow bay at the western tip of a peninsula exposed to the prevailing winds from the northwest (Fig. 2 site C), and constitute the most spectacular example of patterned ground ever described south of 50°N (Fig. 4). Discovery of the site results from a follow-up to an obscure report (Butler, 1937) suggesting that unusual beach cusps composed essentially of boulders occur

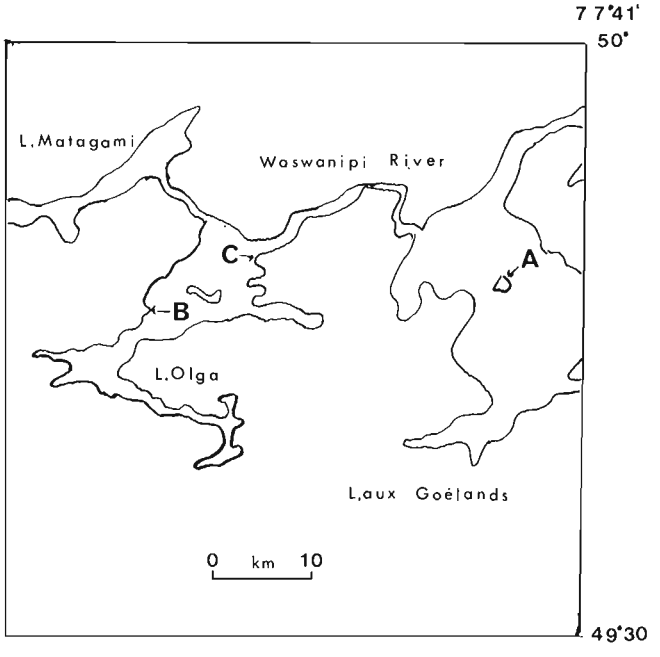


**Figure 2.** Location of the small polygons of Lac aux Goélands (**A**), the mudboils of Lac Olga (**B**), and the well developed polygons of Lac Olga (**C**).

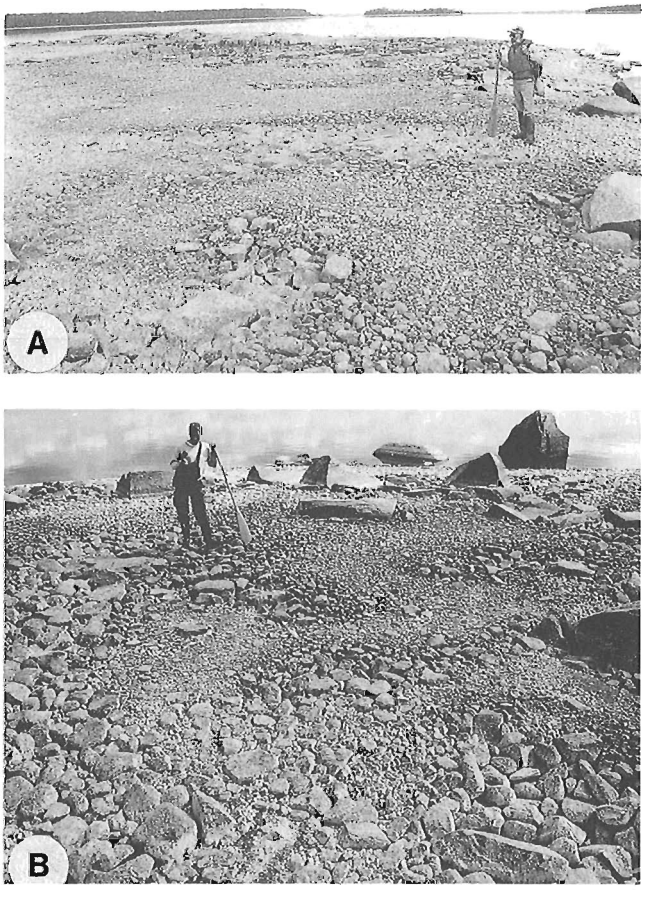


**Figure 3.** The Lac Olga mudboils (sorted circles). (**A**) Till flat below the high water mark (GSC 1991-586 H). (**B**) Elongated mudboils (GSC 1991-586 I).

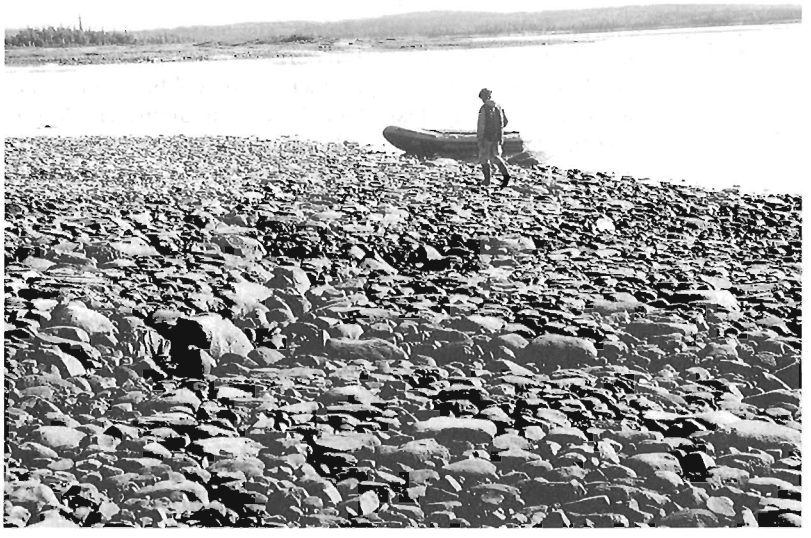

**Figure 4.** Close view of the Lac Olga polygons (GSC 1991-578 F).

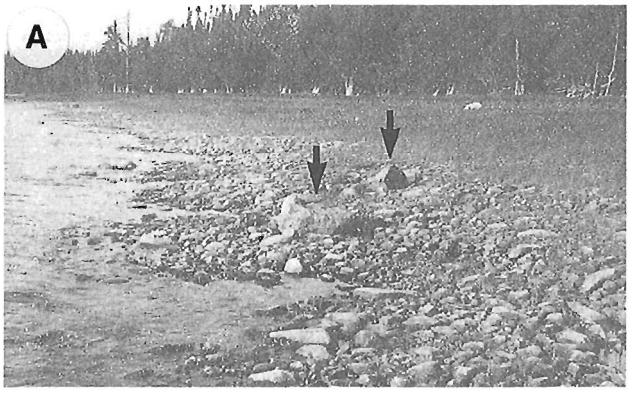


**Figure 5.** Comparison of 1935 and 1991 photographs of Lac Olga polygons. (**A**) South to north view of "beach cusps" photographed by Butler (1935), arrows point to boulders (GSC 1991-582). (**B**) Close-up view taken in 1991 showing the large boulders seen in A (GSC 1991-578 J). (**C**) South to north view of beach photographed in 1991 (GSC 1991-578 H).


at this location. Butler was intrigued by the morphological and compositional characteristics of the Lac Olga "beach cusps". In trying to reconcile the current models on the formation of beach cusps elsewhere in the world with those of Lac Olga, he was led to conclude that the cumulative effect of the swash by small waves produced extremely selective erosion of bouldery glacial drift in the shapes of cusps. Our field investigation however, clearly revealed that polygonal ground due to frost action is what Butler saw.

The exceptionally low water level of Lac Olga in mid-August 1991, combined with the interest awakened by Butler's report, prompted a visit to the site, the location of which was poorly indicated on a small scale map. A photograph taken by Butler during summer 1935, compared to others taken in mid-August 1991, clearly demonstrates that both parties were exactly at the same location (Fig. 5A, B and C). Individual boulders can be identified in Figure 5B and 5C, taken 56 years after Figure 5A.

Polygonal ground is well developed in a section of beach stretching approximately 100 m along the shore line and extending 35 m inland. It is located entirely below the high water mark and is devoid of vegetation except for a narrow fringe covered with grasses near the forested shore (Fig.5B).

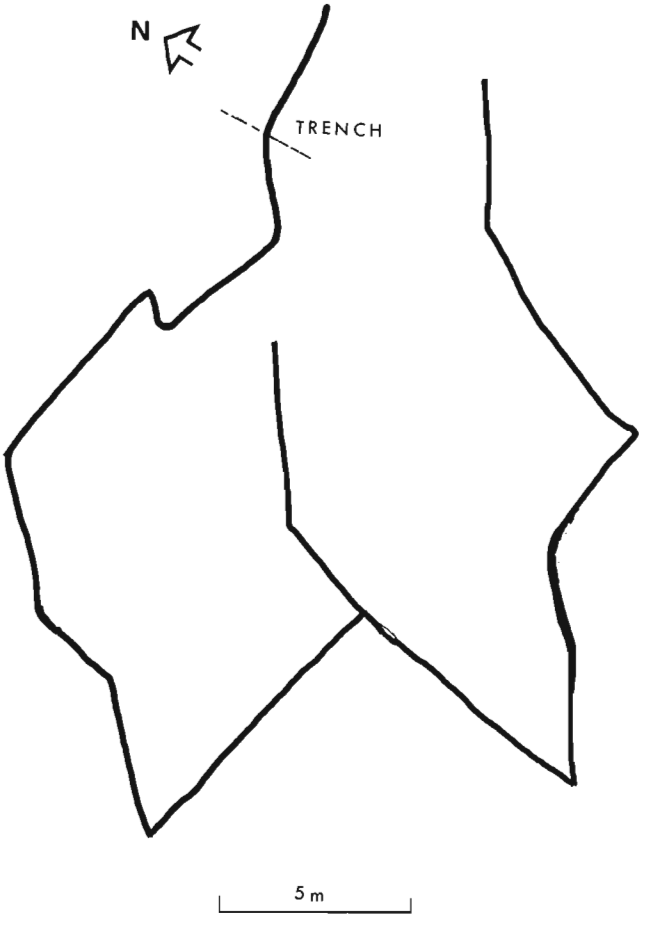


**Figure 6.** Part of the Lac Olga polygon field drawn to scale showing elongated polygons toward the lake (bottom of sketch) and position of the trench.

Polygons have diameters reaching 8 to 9 m, are elongated lakeward, and are separated by troughs 0.1 to 0.8 m wide with depths between 0.10 and 0.30 m (Fig.6). At junction points between some troughs, depressions up to 0.9 m deep and twice as large as the width of the troughs could represent former ice-rich zones or points of maximum thermal expansion. The troughs, probably due to their position in the swash zone, have not been infilled by sediment. The surface of the polygons consists of a cobbly and bouldery carapace, levelled by the action of seasonal ice-pushed floes and smoothed by wave action. The levelling action of the ice may explain the near disappearance of some troughs. Isolated large ice-rafted boulders are scattered at the surface.

A trench dug across one of the troughs revealed a sand wedge extending downward and disappearing below the floor of the trench at 0.8 m depth. It consists of a well sorted massive sand showing sharp contacts with undisturbed moderately stony, sandy, silty till on each side. The pervious sand, saturated with water because of a high water table, prevented digging below 0.8 m (Fig.7 ).

### *Beach cusps or polygons?*

Close inspection of Figure 5 clearly shows that the level of Lac Olga was considerably higher at the time of Butler's visit in 1935 than in late summer 1991. Given the gentle slope of the beach, this difference in water level (estimated at about 60 cm between the two visits) means that an additional horizontal distance of up to 20 m was under water at the time of Butler's visit. Since all the observed patterned ground is less than 35 m from the 1991 shore line, several troughs were under water in 1935 producing the cuspate shore line shown on Fig.5A. The cuspate pattern was emphasized by the elongated polygons in a lakeward direction (Fig.6), a pattern also observed by Dionne (1974) on the shores of large lakes in subarctic central Québec. These site-specific conditions explain Butler's interpretation of the features. Had he seen


**Figure 7.** Sand wedge in till observed in a trench dug across a trough (GSC 1991-586 A).

the site at very low lake level, his conclusions as to the origin of the patterned ground might have been different. It should also be taken into consideration that the study of periglacial phenomena was then much less advanced than it is now and was restricted to a handful of specialists.

## DISCUSSION

The patterned ground features discussed here, normally found in a periglacial environment, constitute the second reported occurrence in Abitibi (Brown and Gangloff, 1980, documented the first case) that includes detailed field measurements and observations. However, the fundamental question as to whether the features represent relict permafrost from a period of widespread or sporadic permafrost in Abitibi or result from freeze and thaw seasonal cycles triggered by favourable site-specific conditions in a nonpermafrost environment remains unanswered. McGreevy (1981, p. 56) in an overview of frost shattering processes comments on the paucity of field measurements and "the very lack of knowledge concerning the operation of freezing processes in high latitude and high altitude areas." Similar observations at each site, such as the presence of thick (1m or more) till, the position of the features in the range between the annual maximum and minimum lake levels, the absence of vegetation, the gentle lakeshore slopes, the high water table, and the exposure to wind, may indicate that the combination of all or some of those factors can produce periglacial forms by seasonal frost action alone. Active sorted and nonsorted circles have been reported from several nonpermafrost environments around the world (Washburn, 1985), and active nonsorted circles have been described by Brown and Gangloff (1980) in glaciolacustrine clays of southern Abitibi, nearly 2° latitude to the south of the Lac aux Goélands and Lac Olga sites. Dionne (1974) found abundant examples of patterned ground (sorted circles and polygons, and stone nets) along lake shores north of 54°N, but no evidence of permafrost in the lacustrine basins or in the depressions where the patterned ground was found. It then appears likely, given the position of the 0°C mean annual temperature isotherm in Abitibi (Fig.1) and the similarity of site conditions in the regions studied by Dionne to the north and by us in Abitibi, that seasonal cryoturbation processes could explain all or at least some of the features discussed in this note. Wind-swept beaches devoid of vegetation, with little snow cover, and underlain by saturated till with a frost susceptible fine sand and silty matrix, such as that of the regional till, would favour maximum frost penetration in the fall and subsequent cracking. On the other hand, the size and the level of development of the large Lac Olga polygons and the presence of sand wedges underneath the bouldery carapace in the troughs argue for a permafrost origin. Ice-wedge polygons are the most reliable permafrost indicators. To this day frost cracks have been reported only north of 52°N (Dionne, 1978). But, as noted in Washburn (1985 p. 177) " ...estimates of the temperature required for cracking depend upon the rate of temperature drop as well as upon the actual ground temperature as influenced by soil conditions and the insulating effect of snow and vegetation." Given the highly specific site conditions of the lake shore polygons of Abitibi and subarctic Québec, the possibility that relatively large soil-wedge polygons (if not ice-wedge polygons) could have formed in the absence of permafrost must be retained. Little is known about the occurrence of active soil-wedge polygons in nonpermafrost environments (Washburn, 1985). The Lac Olga site offers an interesting potential for the study of patterned ground involving cracking in a nonpermafrost environment. If, on the other hand, the polygons are relict permafrost features then they could date from an earlier and pronounced phase of lower lake level. This is, however, very speculative since patterned ground is concentrated on lake shores in subarctic central Québec, an area, like that of northern Abitibi, still undergoing significant isostatic rebound. Consequently, as pointed out earlier by Dionne (1974), lake shore patterned ground is probably relatively young, its age being possibly tied up to the rate of subaerial exposure (uplift) of the beach.

It is improbable, given the lack of sufficient reliable indicators such as ice-wedge casts, that widespread permafrost ever existed in Abitibi in postglacial time. As noted earlier, systematic field inspection associated with surficial geology mapping programs failed to produce the necessary evidence. But the polygonal patterns observed on large scale (1:15 840) airphotos and attributed to relict permafrost in central Abitibi (Lagarec, 1973), must be taken into consideration. The airphoto interpretation done to date within the framework of the current mapping projects is from small scale (1:40 000) airphotos, and may have failed to detect the polygons described by Lagarec. Time of year of photography and differences in soil moisture conditions, among other factors, can also explain why well developed polygons may be visible in one year and not in the next, as demonstrated by Morgan (1982) in southern Ontario.

Finally, there is no palynological evidence for tundra conditions in Témiscamingue and in central Abitibi where forest cover is believed to have closely followed the retreat of the large proglacial lakes Barlow and Ojibway (Richard, 1979; Richard et al., 1989). This situation differs from that near the periphery of the retreating Laurentide Ice Sheet to the south where at least partially developed tundra conditions prevailed. The youngest periglacial structures formed on the margins of glacial Lake Whittlesey are about 13 000 years old (Morgan,1982). Based on the presence of fossil indicators of periglacial conditions, Dionne (1975) has suggested that a discontinuous permafrost zone may have existed in lowland areas near the margin of the retreating Laurentide Ice Sheet in southern Québec between 13 000 and 11 000 years BP.

Establishing the absolute age of the lakeshore patterned ground of Abitibi would allow correlation with known cooling events (such as The Little Ice Age) and facilitate the determination of its origin. Alternatively, detailed surveys of lake shores at low water levels in late summer and early fall followed by late fall and winter visits of instrumented sites, could determine if the processes are active or not.

## ACKNOWLEDGMENTS

Assistance in the field was provided by J.-S. Pomarès and A. Watelet. The manuscript was critically reviewed by L.A. Dredge.

## REFERENCES

**Brown, J.-L. and Gangloff, P.**
1980: Géliformes et sols cryiques dans le sud de l'Abitibi, Québec; Géographie physique et Quaternaire, vol. 34, nº 2, p. 137-158.

**Butler, J.W., Jr.**
1937: Boulder beach cusps, Lake Olga, Québec; American Journal of Science, v. 33, p. 442-453.

**Dionne, J.-C.**
1974: Cryosols avec triage sur rivage et fond de lacs, Québec central subarctique; Revue de Géographie de Montréal, vol. 28, nº 4, p. 323-342, 11 fig., 3 tableaux.
1975: Paleoclimatic significance of Late Pleistocene ice wedge casts in southern Québec, Canada; Paleogeography, Paleoclimatology, Paleoecology, v. 17, p. 65-76.
1978: Formes et phénomènes périglaciaires en Jamésie, Québec subarctique; Géographie physique et Quaternaire, vol. 32, nº 3, p. 187-247.

**Goldthwait, R. P.**
1976: Frost sorted patterned ground, a review; Quaternary Research, v. 6, no. 1, p. 27-36.

**Hamelin, L.-E.**
1958: Les cours d'eau à berges festonnées; Canadian Geographer, nº 12, p. 20-25, 1 fig.

**Lagarec, D.**
1973: Postglacial permafrost features in eastern Canada. In Permafrost; in North American Contribution to the Second International Conference, National Academy of Sciences, Washington, D.C. p. 126-131.

**McGreevy, J. P.**
1981: Some perspectives on frost shattering; Progress in Physical Geography, v. 5, no. 1, p. 56-75.

**Morgan, A.V.**
1982: Distribution and probable age of relict permafrost features in southern Ontario; in Proceedings, Fourth Canadian Permafrost Conference, (ed) H.M. French; Climate and Permafrost, p. 91-100.

**National Atlas of Canada**
1973: Permafrost Map of Canada; Geological Survey of Canada, modified from Permafrost in Canada, Map 1246A, prepared by R.J.E. Brown.

**Richard, P.**
1979: Histoire postglaciaire de la végétation au sud du lac Abitibi, Ontario et Québec; Service de la recherche en analyse pollinique, Rapport de recherche pour la Commission archéologique du Canada, 50 p.

**Richard, P., Veillette, J.J. et Larouche, A.C.**
1989: Palynostratigraphie et chronologie du retrait glaciaire au Témiscamingue: évaluation des âges $^{14}C$ et implications paléoenvironnementales; Journal canadien des sciences de la terre, v. 26, nº 4, p. 627-641.

**Veillette, J.J.**
1990: Le dernier glaciaire au Témiscamingue; Thèse de doctorat non publiée, Département des sciences de la terre et de l'environnement, Faculté des sciences, université Libre de Bruxelles, 344 p.

**Washburn, A.L.**
1985: Periglacial problems; in Field and Theory, Lectures in Geocryology, (ed.) M. Church and O. Slaymaker; University of British Columbia Press, Vancouver, p. 166-199.

**Wilson, C.V.**
1971: Le climat du Québec; Atlas climatique, Service météorologique du Canada, Etudes climatologiques, nº 11, 67 figs.

Geological Survey of Canada Project 860020

# AUTHOR INDEX

## NOTE TO CONTRIBUTORS

Submissions to the Discussion section of Current Research are welcome from both the staff of the Geological Survey of Canada and from the public. Discussions are limited to 6 double-spaced typewritten pages (about 1500 words) and are subject to review by the Chief Scientific Editor. Discussions are restricted to the scientific content of Geological Survey reports. General discussions concerning sector or government policy will not be accepted. All manuscripts must be computer word-processed on an IBM compatible system and must be submitted with a diskette using WordPerfect 5.0 or 5.1. Illustrations will be accepted only if, in the opinion of the editor, they are considered essential. In any case no redrafting will be undertaken and reproducible copy must accompany the original submissions. Discussion is limited to recent reports (not more than 2 years old) and may be in either English or French. Every effort is made to include both Discussion and Reply in the same issue. Current Research is published in January and July. Submissions should be sent to the Chief Scientific Editor, Geological Survey of Canada, 601 Booth Street, Ottawa, Canada, K1A 0E8.

## AVIS AUX AUTEURS D'ARTICLES

Nous encourageons tant le personnel de la Commission géologique que le grand public à nous faire parvenir des articles destinés à la section discussion de la publication Recherches en cours. Le texte doit comprendre au plus six pages dactylographiées à double interligne (environ 1500 mots), texte qui peut faire l'objet d'un réexamen par le rédacteur scientifique en chef. Les discussions doivent se limiter au contenu scientifique des rapports de la Commission géologique. Les discussions générales sur le Secteur ou les politiques gouvernementales ne seront pas acceptées. Le texte doit être soumis à un traitement de texte informatisé par un système IBM compatible et enregistré sur disquette WordPerfect 5.0 ou 5.1. Les illustrations ne seront acceptées que dans la mesure où, selon l'opinion du rédacteur, elles seront considérées comme essentielles. Aucune retouche ne sera faite au texte et dans tous les cas, une copie qui puisse être reproduite doit accompagner le texte original. Les discussions en français ou en anglais doivent se limiter aux rapports récents (au plus de 2 ans). On s'efforcera de faire coïncider les articles destinés aux rubriques discussions et réponses dans le même numéro. La publication Recherches en cours paraît en janvier et en juillet. Les articles doivent être envoyés au rédacteur en chef scientifique, Commission géologique du Canada, 601, rue Booth, Ottawa, Canada, K1A 0E8.

Geological Survey of Canada Current Research, is now released twice a year, in January and in July. The four parts published in January 1992 (Paper 92-1, parts A to D) are listed below and can be purchased separately.

Recherches en cours, une publication de la Commission géologique du Canada, est publiée maintenant deux fois par année, en janvier et en juillet. Les quatre parties publiées en janvier 1992 (Étude 92-1, parties A à D) sont énumérées ci-dessous et vendues séparément.

Part A, Cordillera and Pacific Margin
Partie A, Cordillère et marge du Pacifique

Part B, Interior Plains and Arctic Canada
Partie B, Plaines intérieures et région arctique du Canada

Part C, Canadian Shield
Partie C, Bouclier canadien

Part D, Eastern Canada and national and general programs
Partie D, Est du Canada et programmes nationaux et généraux

Part E (this volume)
Partie E (ce volume)